Author:
Auler, Augusto Sarreiro

Title:
Karst evolution and paleoclimate of eastern Brazil.

KARST EVOLUTION AND PALAEOCLIMATE OF EASTERN BRAZIL

Augusto Sarreiro Auler

A thesis submitted to the University of Bristol in accordance with the requirements of the degree of Ph.D. in the Faculty of Science

University of Bristol
School of Geographical Sciences

November 1999

ABSTRACT

This thesis considers geochronology of cave deposits in the cratonic area of eastern Brazil. Magnetostratigraphic and especially U-series dating are used to constrain timescales of cave development and provide information of timing of distinctive episodes of palaeoclimate in the area. Magnetostratigraphy of cave sediments in eastern Brazil showed low rates of fluvial incision, compatible with other published rates of denudation for cratonic areas. Geomorphological studies in the Una Group carbonates of semi-arid northeast Brazil show that cave development is controlled mostly by sulphuric acid dissolution due to pyrite oxidation. This shallow hypogenic mode of development is responsible for very extensive cave systems that display many but not all of the features described for deep-seated hypogenic caves. Sulphide oxidation in the Una Group is also corroborated by hydrochemical and sulphur isotope data. Cave development through paragenesis appears to predominate over much of the area, regardless of lithology and climatic setting. A denudational model of cave development in cratonic settings is proposed, in which areas with low denudation rates (and thus low rates of water table lowering) display dominance of paragenetic caves, given availability of sediment. In such areas, any given phreatic passage will remain for longer time in the phreatic zone, and thus is more likely to develop through paragenesis towards the water table. Phreatic conduits in areas with high rates of denudation, such as in tectonically active or mountainous regions, are likely to be drained before substantial paragenetic development has taken place. This denudational model should have a global application but needs to be tested in other similar geomorphic settings.

Travertines, subaqueous calcite and vertebrate fossils, which indicate wetter climate conditions in semi-arid northeast Brazil than present, were dated by the U-series method. The data shows that the last glacial maximum in the area was wetter and more forested than at present. Travertine deposits grew between 21 - 9 ka and around 400 ka, while the water table was 13 ± 1 m above present levels at the LGM, and still higher during the penultimate glacial maximum. Dating of fossil remains, especially fossil bat guano, and abundant plant imprints in the younger travertines point toward an environment with much more abundant vegetation. A wet LGM in the Brazilian northeast is in contrast with evidence of an arid LGM derived from numerous pollen records from Amazonia and southeastern Brazil. This difference in climatic conditions is not depicted in any GCM simulations and demonstrates the importance of intraregional variability in past climatic patterns.

ACKNOWLEDGEMENTS

This thesis was made possible by a doctoral scholarship awarded to me by the Brazilian Research Council (CNPq). My thanks to Pete Smart for the thorough supervision and availability during the four years of this project. His contributions to the project during the two week field trip in Brazil were especially invaluable.

Field trip for this thesis involved over 40,000 km of travelling in the Brazilian backlands. Through all of this I was accompanied by friends who, besides enduring the not so pleasant field conditions, also cheerfully helped me with sampling and geological observations. My sincere thanks to Arnaldo Carvalho, Helena David, Andy Farrant, Murilo Valle, Georgete Dutra and Luciano Barbosa. Special thanks to José d'Ávila for help in many trips and Aloísio Cardoso (Baiano) for his hospitality and help in Seabra.

Many people have helped by sending critical bibliography from Brazil, by providing scientific discussions and information, and for giving a hand during field work. With apologies for forgetting someone, thanks to Chico Bill, Fernando Laureano, Luis Beethoven Piló, Roberto Valadão, Aroldo Misi, Ivo Karmann, Soraya Ayub, Maria Giovanna Parizzi, Joel Rodet, Ezio Rubbioli, Myrian Paiano, Castor Cartelle and Rodrigo Lopes. SEE from Ouro Preto allowed the use of their unpublished cave maps, and CPRM and CERB from Salvador kindly authorised the use of unpublished geological and hydrochemical data. Osmar, the geologist from CISAFRA (Campo Formoso) provided interesting geological information and ECOLAB (Belo Horizonte) lent water bottles for hydrochemical sampling. Initial forays on pollen analyses and oxygen isotopes were performed by Paulo de Oliveira (USP) and Roberto Ventura Santos (UnB).

The never ending U-series laboratory work at Bristol had the collaboration of the helpful staff from the School of Geographical Sciences, Richard Newman, Bob Isles, Dave King and Chris Norris. Additional thanks to Jenny Mills for dionex and atomic absorption analyses. At the palaeomagnetism laboratory at the University of Plymouth, thanks to Peter Davies, Don Tarling and Antony Morris and at the sulphur isotope laboratory at the University of Leeds, I acknowledge the help and interest of Simon Bottrell and the lab staff. David Richards of the School of Geographical Sciences at Bristol University helped during U-series analysis and data interpretation.

Field work was made easier by the always friendly collaboration of land owners and local people. Thanks to Lima and Eduardo of Lapa Doce and Torrinha caves, and the people of Laje dos Negros.

Some of the ideas presented in this thesis originated during caving trips along the years with friends of Grupo Bambui de Pesquisas Espeleologicas. I acknowledge the continuous cooperation, and the use of the club extensive map library.

My parents, as usual, supported in every way my three years abroad. My final thanks to Adriana, my wife, for coming to Bristol in the first place and helping during all the stages of the project, especially drawing figures, and formatting the thesis.

This thesis is the original work of the candidate except where acknowledgement is given and has not been submitted previously for a higher degree in this or any other university.

Augusto S. Auler

October, 1999

TABLE OF CONTENTS

LIST OF FIGURES

LIST OF TABLES

CHAPTER 1
INTRODUCTION

1.1. KARST GEOMORPHOLOGY OF EASTERN BRAZIL

1.1.1. Cave geomorphology and global geomorphic processes

Knowledge of geomorphic processes in the tropical areas of South America is still in its infancy. In particular, the relationship between rates and modes of landscape formation and tectonic processes is extremely important in understanding the generation of planation surfaces on the continental scale, one of the most controversial and less understood macroscale geomorphological features. Such surfaces predominate in much of the Southern Hemisphere ancient continental domains such as interior South America, Africa and Australia. Efforts have been made by several researchers (King, 1967, Gilchrist and Summerfield, 1990, 1991) over nearly half century to provide a global geomorphic model that links (now accepted) global tectonics with denudational processes. The advent of both reliable dating methods and computer modelling, together with a much improved understanding of the Earth's endogenic processes, have enabled a quantum leap in the current understanding of the planetary scale geomorphic processes, although many questions remain to be answered.

Early cave genesis studies have followed the general trends of geomorphic thought. One of the first comprehensive theories of karst and cave evolution (Davis, 1930) was an extension of the influential geographical cycle model of landscape evolution (Davis, 1899). Since Davis, the link between global geomorphic processes and cave genesis has been somewhat neglected. There have been attempts to build a unified model of landscape evolution based on tectonic processes (Summerfield, 1991a), but this has not been extended to karst areas. This thesis will consider how global tectonics and macro scale geomorphic processes can control speleogenetic processes, using case studies from the cratonic interior of eastern Brazil.

1.1.2. Influence of lithology on subsurface carbonate dissolution

In contrast with the limited progress made in linking global geomorphology and cave processes, substantial advances have been made regarding the chemistry of carbonate dissolution since the pioneering studies in the 50's and 60's (Trombe, 1952, Corbel, 1957, Bogli, 1964). Studies of the kinetics of carbonate dissolution have allowed the modelling of conduit initiation in karst settings (White, 1977, 1984, Dreybrodt, 1990, Palmer, 1991, Dreybrodt, 1996 and Siemers and Dreybrodt, 1998). These studies have suggested that timescales of conduit initiation can be too long to be explained by dissolution by the H_20-CO_2 system alone (Worthington, 1991).

A separate avenue of research has been pursued by cave geomorphologists in analysing the speleogenesis and mineralogy of some long and complex cave systems such as Jewel and

Wind Caves, and Carlsbad Caverns in the Unites States (Bakalowicz et al., 1987, Hill, 1987). This has demonstrated that meteoric derived carbonic acid is not the dominant acid in some karst settings, where sulphuric acid or carbonic acid of deep-seated origin is more important. This finding represented a major departure from the paradigm of climatic geomorphology as applied to karst, championed by Corbel (1957) and later by Smith and Atkinson (1976). If climate (controlling runoff and dissolution rates) is not the sole determinant of karst and cave evolution, a hitherto unrecognised relationship between endogenic geological processes and karst geomorphology could be established. The growing recognition of the importance of non-carbonate dissolution in the generation of caves (Hill, 1990, Ball and Jones, 1990, Lowe, 1992, Worthington and Ford, 1995) represents a novel approach to the study of dissolution processes and cave development in karst terrains. In this thesis the role of lithology-controlled acidity represented by sulphide minerals, in promoting karst formation will be examined. Its importance for karst geomorphology in drylands, where traditional meteoric dissolution is very limited, will be reassessed.

1.1.3. Palaeoclimate in eastern Brazil

Continental palaeoclimate studies have traditionally been concentrated near major centres of research in the Northern Hemisphere. Major global efforts have been made to integrate the world's dataset of palaeoclimate data but extensive "blank" areas exist in the Southern Hemisphere, notably in South America. One such area is eastern Brazil, where only recently have pollen studies drawn the first preliminary picture of the climate during the late Quaternary. The need for reliable global data is ever increasing, as modelling efforts need to be constrained by field evidence. No such information exists for large areas of South America, and particularly for the semi-arid zone of northeastern Brazil, where lakes or swamps suitable for pollen analysis are largely absent. An alternative approach is to use calcite cave deposits, which have the potential to provide reliable palaeoclimate data and can be dated by Uranium series methods. In this thesis, the first integrated record for late Quaternary climatic changes has been obtained from cave deposits and subaerial travertines in northeastern Brazil. This research challenges previous conceptual palaeoclimatic interpretations for the area, illustrating the important regional variability that can derive from topographic factors.

The geomorphic impact of climatic changes have been examined in a number of geomorphic systems, such as slopes and river systems (Bull, 1991). Caves provide an unusually good environment for such studies because much sediment trapped in them is intercalated with calcite deposits that can be dated. Caves have been used as recorders for aggradation/erosion cycles in rivers, or slope disaggregation/retention cycles in studies dealing with entrance facies deposits mostly in sites of archaeological significance (Campy and Chaline, 1993, Brain, 1995a). In this thesis such relationship will be explored in detail for a number of caves in distinct climatic settings.

The objectives of this thesis are thus: (1) To generate broad models of cave evolution that should be applicable in similar climatic settings that can help explain major differences in the style and morphology of karst terrains in dry, stable cratonic settings. (2) To provide the first late Quaternary palaeoclimate data for the semi-arid northeastern Brazil, and to consider its influence on the generation of surface carbonates and clastic cave deposits.

1.2. THE STUDY AREA

The broad term "eastern Brazil" used throughout this thesis should be understood as the inland portion of Brazil comprised within the São Francisco Craton (see Fig. 3.2), running approximately from latitude 10 to 20° S (Fig. 1.1). The area is limited in the east and west by the more elevated zones of the fold belts that mark the limit of the craton, comprising mostly quartzites, sandstones and igneous rocks of varied age. This very extensive area corresponds roughly with the limits of other regional studies on Brazilian geomorphology such as that of King (1956a) and Valadão (1998). Approximately the same region has been loosely termed the "Brazilian Highlands" (Burton, 1869, Clapperton, 1993a) when referring to the characteristic plateaux usually above 600 m, "South America Lowlands" (Servant et al., 1993, Ledru et al., 1998) when the Andes is taken as a relative comparison, or "Central Brazil" (Ledru, 1993, Ledru et al., 1998, Salgado-Labouriau et al., 1998). While the limits of such areas differ according to the author, they nearly always include the lower (southern portion) of the thesis study area. The northeastern sector of the thesis study area, which comprises the semi-arid zone, is usually not included in most of these studies due to its distinct climate.

Detailed geomorphic and palaeoclimate research was performed in four karst areas located roughly in a north-south latitudinal gradient. These areas, namely the Campo Formoso, Iraquara, Santa Maria da Vitória and Lagoa Santa, were chosen because of differences in climate and lithology which could provide comparative data on the relative importance of such parameters for cave and karst landscape development. Furthermore, these areas are among the very few Brazilian karst areas where basic speleological research has been conducted, regional surveys and cave maps are therefore available.

1.2.1. Climate and vegetation

Eastern Brazil is located entirely in the Tropical Zone. In such settings, air flows towards the Intertropical Convergence Zone (ITCZ) which migrates in position north and south with the annual passage of the overhead sun (Clapperton, 1993a). High rainfall is usually associated with the ITCZ and the migration of the ITCZ determines the seasonal character of the climate in eastern Brazil. In January the ITCZ moves southward and remains near the centre of the study area, inducing over 80% of the annual rainfall during the (Southern Hemisphere) summer months (October to March) (Ledru, 1993). In July it moves northwards, towards Amazonia (Ledru, 1993), and the winters in eastern Brazil are markedly dry.

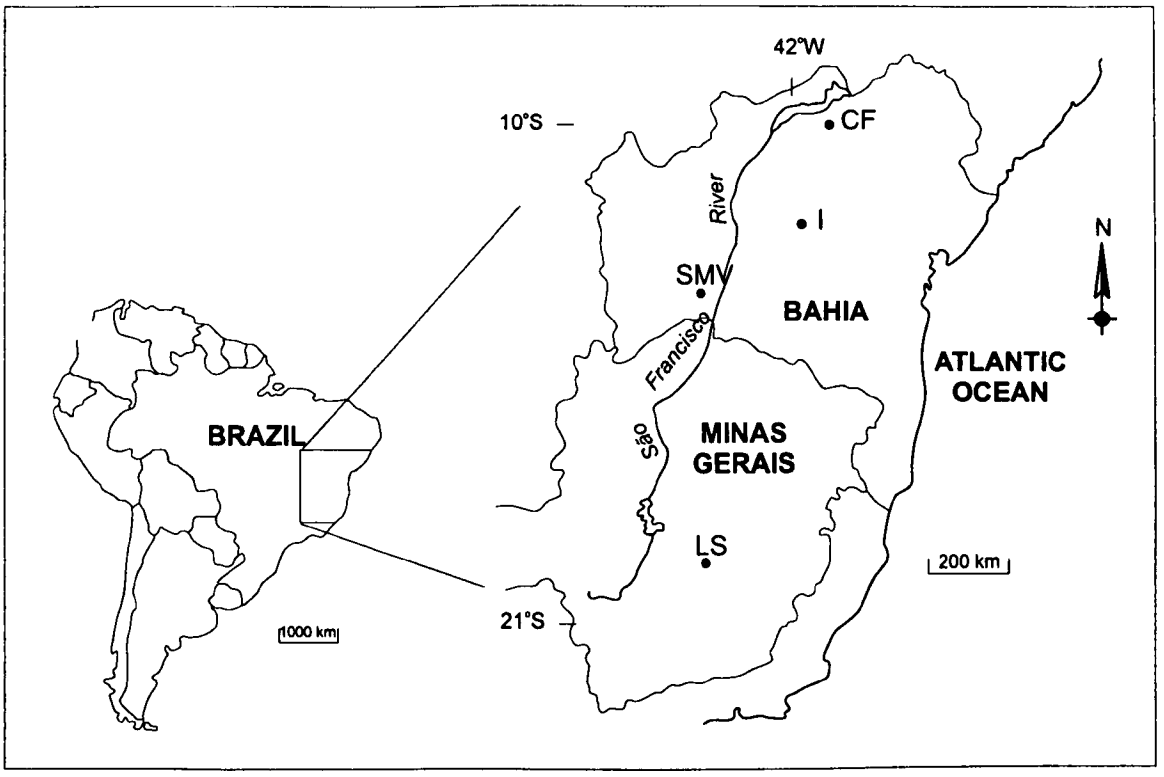

Figure 1.1. Thesis area in the states of Bahia and Minas Gerais and location of studied sites. CF - Campo Formoso; I - Iraquara; SMV - Santa Maria da Vitória; LS - Lagoa Santa. Adapted from Valadão (1998).

There is a gradual decrease in annual precipitation towards the north (Fig. 1.2) and the northern portion of the study area is semi-arid. This northern area also differs markedly from the southern zone due to the extreme interannual variability of rainfall (Roucou et al., 1996), which can be as much as 40% between years (Cadier, 1996). In the semi-arid northeast the rainy season is usually delayed in relation to the wetter southeast, not starting until February and ending in May (Harzallah et al., 1996). The unusual presence of a semi-arid zone at such a latitude is probably caused by a strong influence of dry and stable southeasterly anticyclonic air masses coming from the Atlantic Ocean (Niewolt, 1977). Drought and wet years are apparently caused by regional changes in the positioning of the ITCZ (Harzallah et al., 1996, Roucou et al., 1996).

Regional vegetation patterns in eastern Brazil change according to the climatic gradient (Fig. 1.3). In the wetter southern portion, cerrado (savanna) predominates. The southernmost Lagoa Santa area lies near to the southern limit of the cerrado, close to where forest starts to predominate. Going northwards cerrado gradually gives place to caatinga, a low arboreal deciduous scrubland vegetation that lies dormant and leafless for much of the year (Clapperton, 1993a).

1.3.THESIS OUTLINE

The thesis has been divided in two major sections, related to the geomorphology and to the palaeoclimate of eastern Brazil. Chapter 2 describes the methodology, detailing the alpha spectrometric uranium series method of dating carbonates, and the principles of

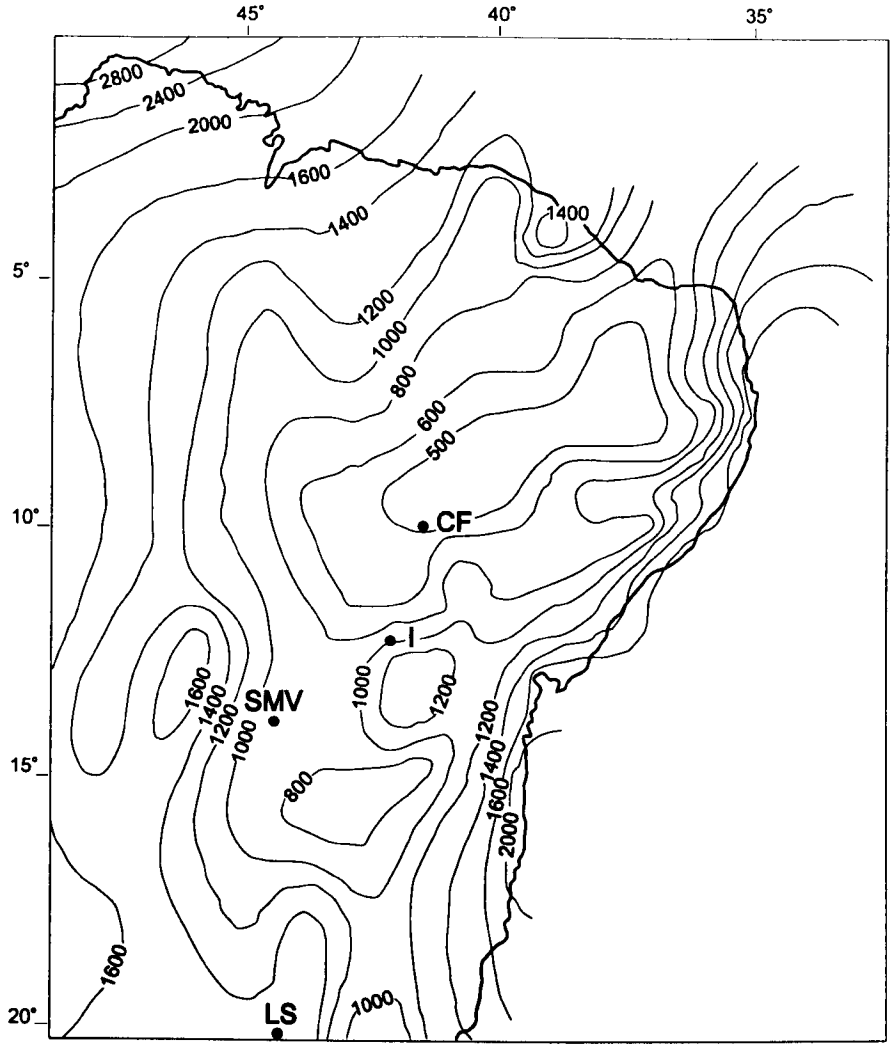

Figure 1.2. Annual mean precipitation in millimetres for the period 1931-1960 as compiled by Strang (1972). Adapted from Ramos (1975). CF - Campo Formoso; I - Iraquara; SMV - Santa Maria da Vitória; LS - Lagoa Santa.

magnetostratigraphy. Other techniques utilised in this thesis are also described.

Chapter 3 reviews the geomorphology of continental passive margins, and denudation rates in cratonic areas. Fluvial incision rates are deduced from magnetostratigraphy at Gruta do Padre, a cave within the Santa Maria da Vitória Karst.

Chapter 4 addresses the importance of non-meteoric carbonate dissolution in arid lands. The geomorphology of the semi-arid Campo Formoso Karst is described, and a shallow hypogenic model of speleogenesis is proposed for the area.

Chapter 5 studies the cave geomorphology of three karst areas, the Iraquara, Caatinga and Lagoa Santa. The role of paragenesis in the speleogenesis of the cave systems is discussed. The chapter closes with a general model of cave development in stable cratonic areas which takes into account the relationship between rates of denudation and rates of conduit development.

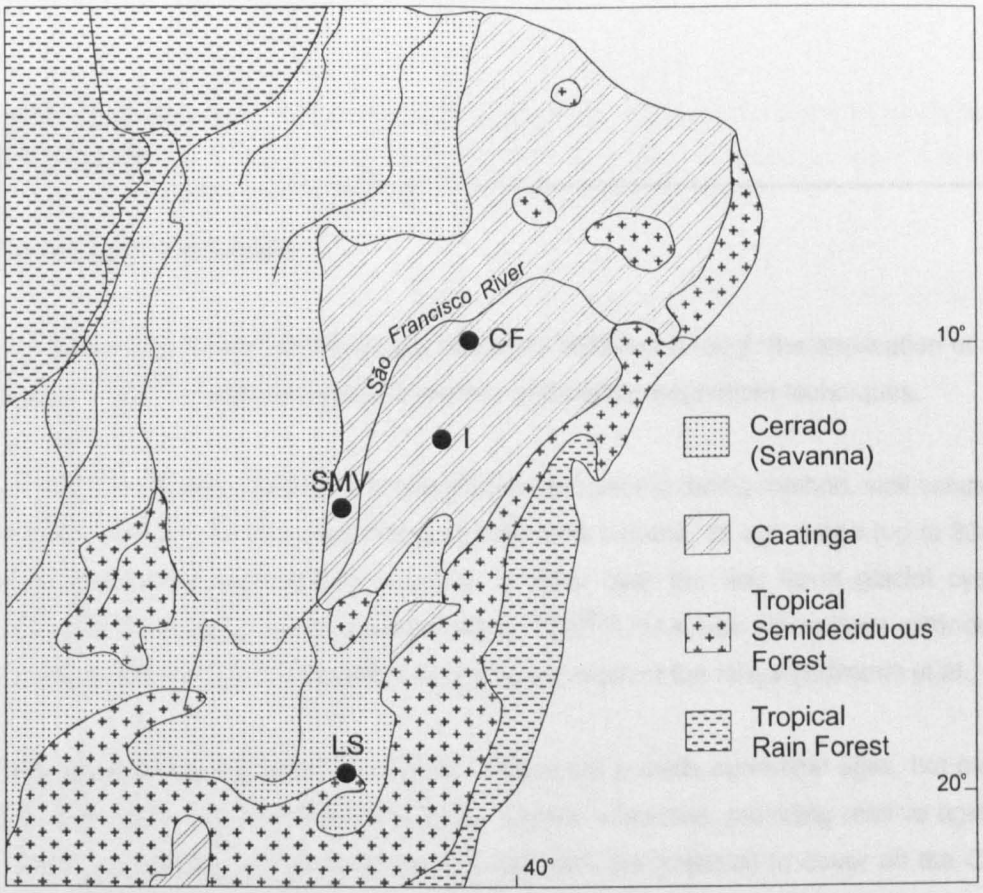

Figure 1.3. Vegetation types of eastern Brazil. From Clapperton (1993a).

Chapter 6 discusses palaeoclimate in the lowlands of South America with emphasis on eastern Brazil. The palaeoclimate of semi-arid northeastern Brazil is studied through dating and palaeoenvironmental reconstruction based on subaerial travertines, water table calcite and fossil deposits in caves. Results are compared with General Circulation Model simulations and palaeoclimate data based on pollen records from the wetter southern portion of the area.

Chapter 7 provides a link between cave geomorphology and palaeoclimate, addressing the geomorphic response to climatic change in terms of cycles of cave sediment emplacement and removal. The relationship between clastic sedimentation, carbonate dissolution (speleothem layers) and sediment removal is discussed based on the semi-arid northeast and the subhumid southeast karst areas, and a preliminary assessment of the correspondence between these processes in caves, and in slopes and fluvial systems is provided.

Chapter 8 gives the general conclusions for the thesis together with suggestions for future work.

CHAPTER 2
METHODS

2.1. DATING TECHNIQUES

The chronology presented in this thesis has been obtained through the application of two dating methods, $^{230}Th/^{234}U$ uranium series (U-series) and palaeomagnetism techniques.

The $^{230}Th/^{234}U$ U-series method is a quantitative radiometric dating method, well established and well suited for dating calcite precipitates in limestone terrains. Its age range (up to 350 ka using alpha spectrometric techniques) is useful in work over the last three glacial cycles. More recently, developments in mass spectrometric $^{230}Th/^{234}U$ U-series dating have extended the age limit to about 500 ka, and increased precision over much of the range (Edwards et al., 1986).

Palaeomagnetism is a correlative method. It does not provide numerical ages, but can be used to match samples with a well-dated polarity reversal timescale, providing relative ages. A rough but useful chronology can then be constructed with the potential to cover all the Quaternary. Palaeomagnetism can be applied in both fine-grained sediments and calcite deposits, and is a useful complementary method to U-series techniques.

2.1.1. U-series dating of speleothems and fresh water carbonates

Measurements of the disequilibrium between the isotopes of uranium and its related radioactive daughters can provide ages for carbonate precipitates. Because of its high abundance, the determination of the ^{230}Th daughter of ^{234}U is most widely used, but ^{231}Pa, a daughter of ^{235}U, can be employed when U concentrations are high (Ivanovich and Harmon, 1992). Uranium is soluble in water, being transported in solution while thorium (and protactinium), on the other hand, have very low solubility and are absorbed strongly at mineral surfaces. On deposition a pure carbonate material should contain only uranium, and be free of thorium. The $^{230}Th/^{234}U$ method is based on the principle that the thorium found in a sample will be derived from the subsequent decay of uranium. The age of a sample is then determined using:

$$^{230}Th/^{234}U = 1 - e^{-\lambda 230 t} / (^{234}U/^{238}U) + [1 - 1/(^{234}U/^{238}U)]\, \lambda_{230}/(\lambda_{230} - \lambda_{234})[1 - e^{-(\lambda 230 - \lambda 234)t}]$$

(equation 2.1) (Ivanovich and Harmon, 1992)

where λ denotes de decay constant of a given isotope. The ^{230}Th half-life is of 75.38 ka, giving the $^{230}Th/^{234}U$ method a potential range of 350 ka. Note that a correction is applied for the presence of ^{238}U which may maintain the activity of ^{234}U, affecting the $^{230}Th/^{234}U$ ratio.

The uranium concentration of cave secondary carbonates is related to the geochemical cycle of the water that generates the precipitate. It is dependent (among others) on the U content of the

overlying bedrock, presence of shale units, residence time of ground water, availability of CO_2 and rate of degassing of the solution (Gascoyne et al., 1978). U content in speleothems can vary from less than 0.01 to more than 100 ppm (Ford and Williams, 1989).

Speleothems and particularly fresh water subaerial carbonates frequently have impurities present in the calcite matrix, made up of clay, silica and other non carbonate minerals. This introduces a problem in $^{230}Th/^{234}U$ dating, because ^{230}Th is frequently present on these impurities, thus increasing the initial $^{230}Th/^{234}U$ activity ratio of the sample. The relative contribution of detritally derived ^{230}Th may usually be determined from the presence of ^{232}Th, a long lived isotope which is the most abundant isotope of Th. As a general rule, it is assumed that a $^{230}Th/^{232}Th$ activity ratio > 20 indicates that a reliable age may be calculated. Values less than this indicate detrital contamination, and corrections are needed. Several correction procedures have been proposed (see Ivanovich et al., 1992). Many of these procedures involve multiple analysis and are time consuming. In this thesis, corrections were done for individual analysis by assuming an initial $^{230}Th/^{232}Th$ ratio of 1.7 suggested by Kaufman (1992) as suitable for an unstudied area, and correcting initial $^{230}Th/^{234}U$ ratios accordingly. This procedure introduces uncertainties on the corrected ages. Additional uncertainty is also introduced because isotopes of uranium may also be released from the detritus, but are not considered by the correction procedure.

In theory, the decay of ^{238}U into ^{234}U could be used in dating. However, it has been shown that initial $^{234}U/^{238}U$ activity ratios on deposition can vary between 1.0 to 30 (Osmond and Cowart, 1992). This fractionation is due to the fact that ^{234}U occupies a site that has been damaged by radiation emitted by ^{238}U, and is thus more readily released (Gascoyne et al., 1978). Changes in the Eh and pH of seepage water, which are controlled mostly by organic activity in the soil may also possibly affect the $^{234}U/^{238}U$ ratio (Osmond and Cowart, 1992). Since there is no way of knowing the initial $^{234}U/^{238}U$ ratio in a carbonate sample, this method cannot normally be used for dating, although Gascoyne et al. (1983) have suggested that broad age ranges may be inferred for samples of infinite $^{230}Th/^{234}U$ age if the range of initial $^{234}U/^{238}U$ is determined for the area using samples of finite age.

The $^{230}Th/^{234}U$ method is a well established dating technique and it is the main dating method used in this thesis.

2.1.1.1 Chemical procedures

The chemical extraction techniques for U-series analysis are well established (see Gascoyne, 1977). The method used at the U-series laboratory of the University of Bristol was derived from procedures adopted at the University of Bath, with some minor later modifications. Fig. 2.1 summarises the steps involved in the chemical extraction.

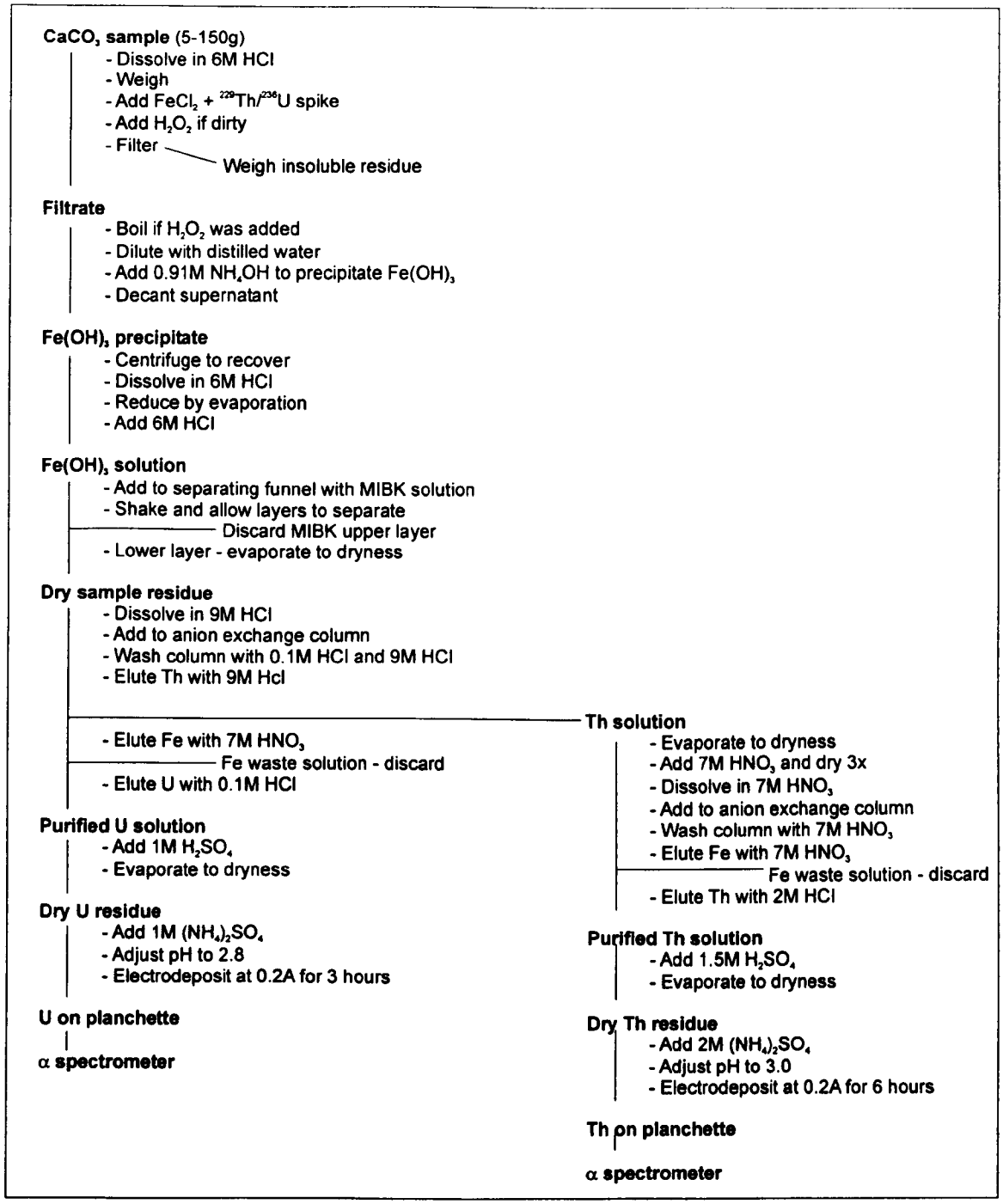

Figure 2.1. Chemical extraction of U and Th for alpha spectrometric determination.

After being sectioned, the sample was described and photographed. Sub-samples were then cut and weighed for analysis. The sample size used depended on the amount of uranium present in the sample. In general, each area studied tended to have a characteristic isotopic signature (Table 2.1) with U content varying from 0.02 up to 9 ppm. For the highest concentrations a sample mass of around 3 g was used, but low U material required a sample of over 100 g.

The sample is diluted in 6M HCl, and 5 ml of ferric chloride is added, together with an aliquot of 0.5-1.0 ml of $^{229}Th/^{236}U$ tracer. The tracer is used to monitor the final yield of the U and Th extraction. According to Ivanovich and Murray (1992) the $^{229}Th/^{236}U$ solution has the following advantages over other commonly used spikes, such as $^{228}Th/^{232}U$: (1) neither isotope occurs

naturally, (2) they undergo negligible decay losses because of their long half lives (3) they cause minimum recoil contamination of the detector (4) they require relatively simple corrections for spectral interference's. The spike solution used was prepared by P.A. Rowe (University of East Anglia) and calibrated by D.A. Richards (University of Bristol). The $^{229}Th/^{236}U$ activity ratio was 1.464 ± 0.013, ^{236}U = 8.78 dpm/g and ^{229}Th = 12.85 dpm/g, calibrated using uraninite solutions (Richards, 1995). Hydrogen peroxide is added to detritally contaminated or organically rich samples. The sample is then left to equilibrate.

Location/Lithology	U (ppm)	$^{234}U/^{238}U$ initial
Caatinga Limestone bedrock	0.638 ± 0.813	1.12 ± 0.09
Caatinga Limestone speleothems	0.121 ± 0.132	1.44 ± 0.23
Travertines	0.111 ± 0.103	4.80 ± 2.01
Iraquara Karst (Una Group)	0.719 ± 1.943	2.44 ± 0.62
Campo Formoso Karst (Una Group)	0.702 ± 1.886	2.66 ± 0.82
Lagoa Santa Karst (Bambuí Group)	0.098 ± 0.035	1.72 ± 0.38

Table 2.1. Mean uranium concentrations and $^{234}U/^{238}U$ values for U-series analyses in the study area.

The sample solution is filtered under vacuum through a Whatman GF/C filter, and the residue is weighed. The solution is then boiled to evolve hydrogen peroxide. After dilution to 4.5 litre with distilled water, ferric hydroxide is precipitated by the addition of 0.88 M NH_4OH solution to pH 7.5.

The solution is decanted and the precipitate is separated in a centrifuge. U and Th are then separated from most of the Fe by a liquid-liquid extraction using 4-Methylpentan-2-one equilibrated with 6 M HCl. The solution is dried and then redissolved in 9 M HCl.

A 1.5 cm diameter by 15 cm long column is prepared with Biorad AG1-X8 anion exchange resin, and washed with aliquots of 0.1 M and 9M HCl, prior to adding the sample. The sample is added and washed with successive aliquots of 9 M HCl (4x 5 ml and 20 ml). The effluent is collected in a teflon beaker for later Th extraction. A 50/50 solution of 9 M HCl and 7 M HNO_3 is added, followed by aliquots of 7 M HNO_3 (2x 5 ml and 20 ml). The effluent, which contains Fe, is discarded. Uranium is then eluted into a teflon beaker by adding 2x 5 ml and 25 ml of 0.1 M HCl. 2.5 ml of 1.5 M H_2SO_4 is added to the U solution before being evaporated to dryness.

The thorium solution from the previous column is dissolved twice into 10 ml 7 M HNO_3 and evaporated to dryness before being added to a second ion exchange column, prepared in the same way as the previous one, but washed with 2x 5 ml and 30 ml 7 M HNO_3. The sample is dissolved in 10 ml HNO_3 and washed with 4x 5 ml and 20 ml HNO_3. The effluent is discarded. Thorium solution is then collected in a teflon beaker, after addition of 2x 5 ml and 30 ml 2M HCl. Finally, 2.5 ml H_2SO_4 is added and the solution is evaporated to dryness.

The final stage of the analysis consists of separately electrodepositing the U and Th onto stainless steel planchettes. $(NH_4)_2SO_4$ electrolyte solution (two different strengths) is added to

the U and Th residues in a Teflon cell using a 0.2 amperes current for 3 hours (U) and 6 hours (Th). 2 ml of 0.88 M NH_4OH is added shortly before breaking circuit. The U and Th are then present as a thin film on the planchette. The planchette is washed in 0.2 M NH_4OH, distilled water and acetone, and dried on a hotplate, before being counted in the alpha spectrometer.

The efficiency of the chemical procedure depends on many factors, some of which, due to the number of steps involved, are difficult to determine. Samples analyses prior to June 1997 gave very low recoveries, producing low precision results and even total losses. A series of experiments were performed and it was determined that the losses were probably occurring during the electroplating stage. Changes in material and reagent quantities improved significantly the U and Th yields, although low recoveries occasionally occur, probably caused by some unknown chemical interference associated with the composition of specific samples.

2.1.1.2. Alpha spectrometry

The U and Th planchettes are counted separately using surface barrier detectors in a four channel Canberra 7404 alpha spectrometer interfaced with a Canberra series 35 plus multichannel analyser via a mixed/router (Canberra 8222). Alpha particles resulting from the decay of each of U and Th nuclide have a range of characteristic energies (Table 2.2) which are determined by the detectors and converted to corresponding electronic pulses.

isotope	energy (MeV)	abundance (%)
^{238}U	4.19	77
	4.15	23
^{236}U	4.49	74
	4.44	26
^{234}U	4.77	72
	4.72	28
^{232}Th	4.01	69
	3.95	24
^{230}Th	4.68	76
	4.61	24
^{229}Th	5.05	7
	4.97	10
	4.90	11
	4.84	69

Table 2.2. Alpha energy of uranium and thorium isotopes of interest. From Quinif (1989) and Ivanovich and Murray (1992)

The one standard deviation error determined for each age is based solely on counting statistics, determined by propagation of the counting uncertainty for each isotope. This uncertainty is derived from the square root of the total counts for the respective isotope, and is dependent on counting time, chemical yield, sample size and uranium content. Usually between 4,000 and 10,000 counts were obtained for each sample (equivalent to uncertainties of 1.6 and 1%). Background for each detector was determined for the energy range of each isotope and subtracted from the counts obtained. Errors derived from background determination were also included in the determined age. The backgrounds were always very low, less than 0.01 counts per minute. Efficiency of the detectors varied in the range of 21%.

Because of the proximity of the energy levels of ^{230}Th and ^{229}Th, samples with thick Th sources tended to have overlap of the tail of the ^{230}Th peak into ^{229}Th peak. This was corrected by extrapolation of the tail of ^{230}Th, and subtraction of the counts in the ^{229}Th region of interest. This procedure will cause further uncertainty in the resulting age. Tail overlapping was present in 3% of the spectra and tended to be characteristic of some particular sampling sites.

A second problem dealt with during interpretation of the spectra was the presence of some uranium breakthrough into the thorium spectra. This is caused by poor separation during the first column stage of the chemical analysis, related mostly to an attempt to use less resin in the columns. Given the ratio of uranium isotopes known from the U spectrum, and the magnitude of the ^{234}U peak in the Th spectrum, corrections could be applied to the determined ^{230}Th and ^{229}Th counts. Uranium breakthrough occurred in 9% of the analysis.

Isotopic ratios and the final age were obtained through the use of an Excel spreadsheet developed by the Minnesota Isotope Laboratory.

2.1.1.3. Sample dating criteria and age validity

For an age to be reliable a series of criteria must be met. The first assumption is that the sample must have behaved as a closed system, with no addition or migration of Th and U isotopes since it was deposited. Open system conditions occur when the sample is porous, undergoes recrystallisation, redissolution or weathering. All four possibilities can affect samples in the study area. The very warm and dry atmosphere both inside and outside caves favours the deposition of porous calcite, due to evaporation. Recrystallisation was also observed to occur. A change from calcite to aragonite, probably due to changes in the cave microclimate (from cooler and humid to drier and warmer) has been observed. The presence of abundant guano deposits in the caves may cause a series of chemical reactions with the speleothem calcite, producing phosphate crusts (usually whitlockite and hydroxylapatite), which were observed on the outside of several speleothems (Fig.2.2a). Schwarcz (1980) has pointed out that PO_4^{-3} ions can form strong complexes with uranium which inhibit ion absorption on the resin columns and cause insoluble precipitates with thorium. This may explain why all samples associated with phosphate crusts presented total or near total U and Th losses during extraction, rendering determination of any age impossible.

Redissolution and weathering can occur due to reflooding of the area, when acidic water can dissolve the sample. But in the study area, it is due mainly to condensation-corrosion, a dissolution process that occurs in the cave atmosphere probably due to high levels of CO_2. Condensation-corrosion can turn crystalline speleothem calcite into an opaque milky sugar textured material unsuitable for dating (Fig. 2.2b). Such samples were avoided although at most sites good quality calcite could be found below the weathered surface layers.

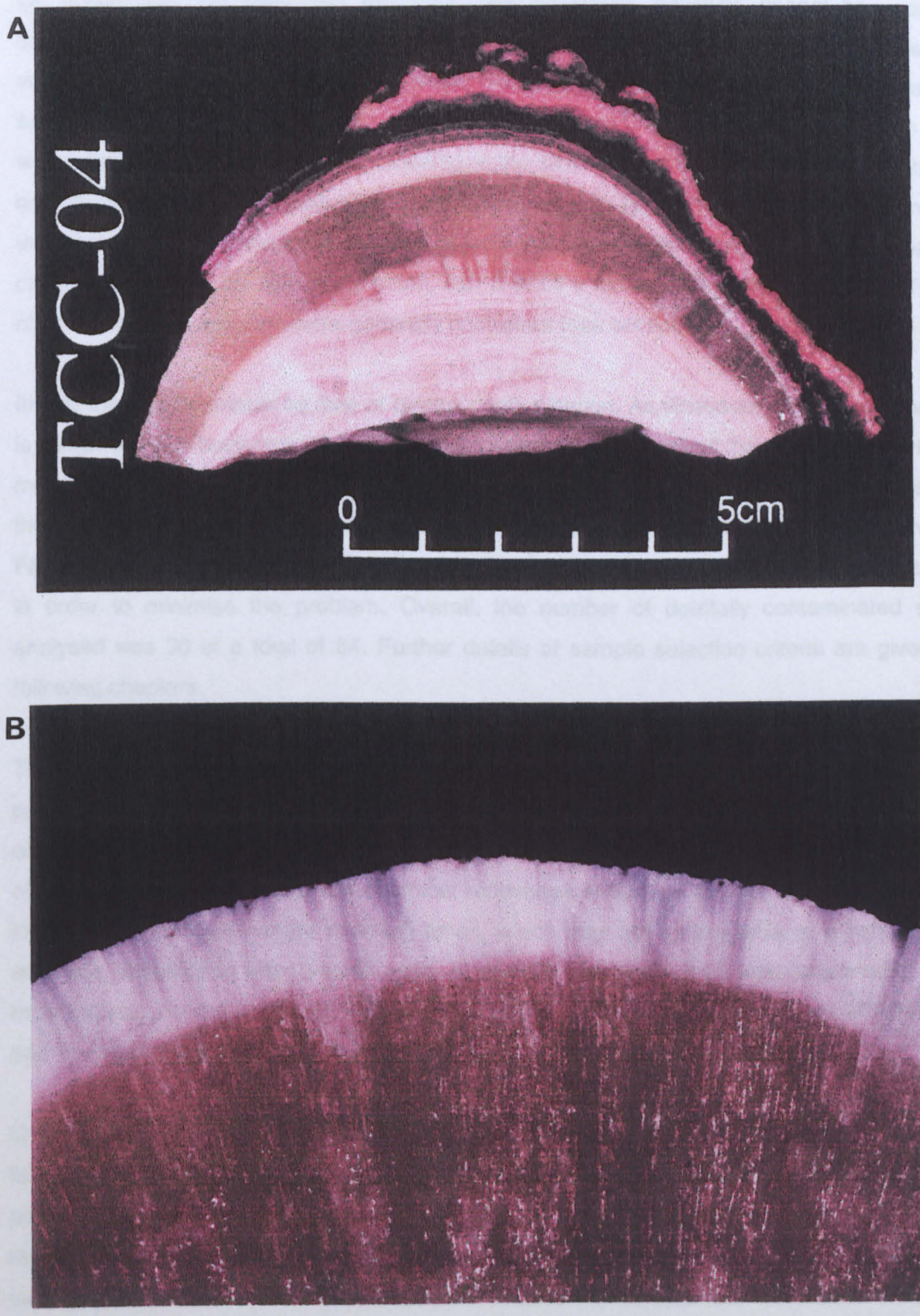

Figure 2.2. A- Phosphate layer overlying stalagmite. B- Detail of condensation-corrosion rind over stalagmite sample TBV-41.

Open system conditions may cause the age either to increase or decrease. Sometimes this can be detected after analysis, due to abnormal activity ratios, such as $^{230}Th/^{234}U > 1.5$. But when the isotopic migration occurs within the boundaries of normal activity ratios, inaccurate ages can be produced which will pass unnoticed. There is no straightforward way to check on this. Whenever possible it should be observed if there is stratigraphically consistency between ages,

i.e., basal ages are older than top ages. This procedure, however, cannot be used for all samples due to limitations on laboratory time, and is in any case limited by the growth span separating the two ages and the analytical precision. Furthermore, some samples cannot be subdivided, such as thin calcite films overlying fossil bones. The stratigraphic test, when applied, was able to detect 4 age inversions, leading to the discarding of these ages. However, the test is not fail proof, because small isotopic variations due to open system conditions can still go undetected. Separate samples generated by the same geomorphic event, such as subaqueous calcite produced under a flooding event, can provide a further check on age validity. The ages obtained for such samples were generally consistent (see section 6.6).

Ideally the sample should be free of detrital contamination. As discussed before, extraneous Th is introduced with such impurities, tending to increase the true age of the material. Unfortunately, many of the sites did not contain secondary carbonates with clean calcite. This was especially the case when dealing with speleothems inter-layered with sediments and subaerial travertines. For such samples, careful sub-sample selection, and further cleaning during cutting were used in order to minimise the problem. Overall, the number of detritally contaminated samples analysed was 30 of a total of 84. Further details of sample selection criteria are given in the following chapters.

The minimum U content of calcite for successful dating by alpha spectrometry should be 0.01 ppm (Ford and Williams, 1989). All samples analysed contained more than this amount, although in general the U content was quite low (Table 2.1), probably due to the shallow nature of the karst systems. Ideally, the chemical recoveries should be as high as possible, because low recoveries require longer counting times, which may not be available at a tight laboratory schedule, resulting in less precise ages. U and Th chemical yields were reasonably good in most cases, showing that the chemical procedure is efficient. Mean yields were 47% for both U and Th. Samples with recoveries below 10% were generally discarded.

Overall, it is not easy to ascertain the reliability of the ages obtained. In the majority of cases they do pass the stratigraphic test, and are within expected ranges for similar geomorphic or palaeoclimatic events. The laboratory procedure also seems to be sound, because the recoveries are good and the method has been used successfully for over 15 years. I believe that the ages are mostly reliable and possible undetected outliers will not affect the general interpretation.

2.1.2. Palaeomagnetism dating

The Earth's magnetic field has undergone several polarity reversals in the past, when the magnetic north reversed and was at the south pole. Through studies of the ocean floor and of terrestrial lavas, a detailed chronology of these reversals has been developed (Fig. 2.3) (Mankinen and Dalrymple, 1979). The last reversal, marked by the Matuyama-Brunhes

boundary occurred 778 ka ago (Tauxe et al., 1996), although several excursions have been suggested when brief field reversals may have occurred. The rationale behind the use of magnetostratigraphy is that polarity reversals found in sediments can be matched with the palaeomagnetic time scale. However, the reversal episodes cannot be distinguished between each other, so a modern datum should be established, with sufficient sample density to allow correlation with each successive reversal in the sequence.

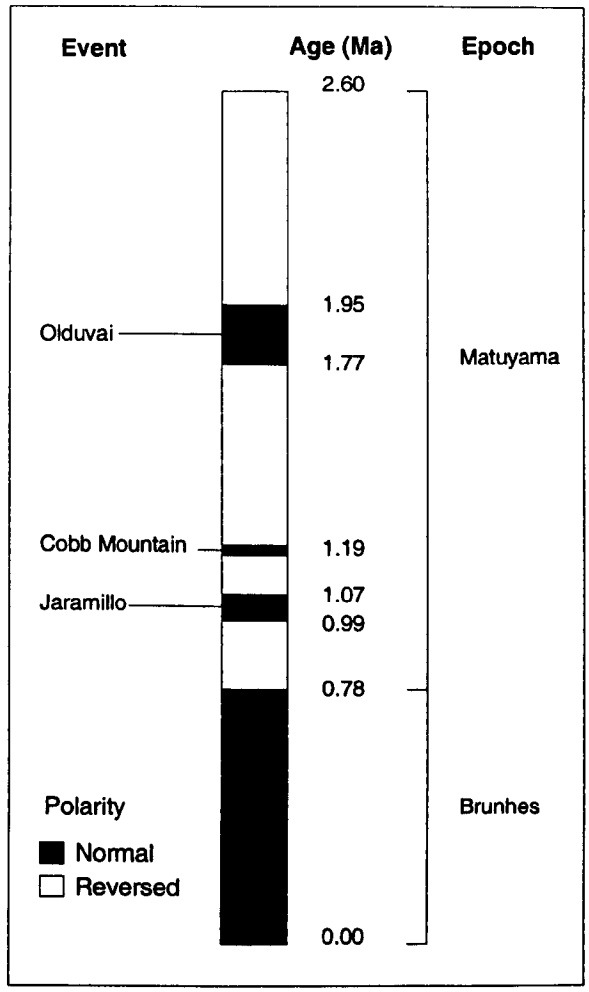

Figure 2.3. Magnetic polarity timescale. Ages from Shackleton et al. (1990)

In fluvial systems, as in cave passages, this datum comprises the alluvial sediments associated with the present base level river. These modern sediments will have normal polarity (the present polarity). The polarity will eventually change with successively higher levels. In this way, a crude but consistent local chronology can be constructed. Magnetostratigraphy has the potential to determine a cave chronology well into the Pleistocene, considerably extending the age range of the $^{230}Th/^{234}U$ method.

Caves are particularly suitable for palaeomagnetic studies because previously deposited sediments are protected from surficial erosion or weathering. Potentially damaging effects such as bioturbation are also minimised (Noel, 1986). As fine-grained sediments settle out from suspension, magnetic grains (usually magnetite) will become oriented according to the ambient

magnetic field, acquiring a primary magnetisation. Later, due to diagenetic effects associated with changes in fluid composition, temperature, pressure, or to weathering, the sediment can acquire a magnetic overprint (Tarling, 1983). This overprint is called secondary magnetisation, and will tend to mask the original magnetic orientation. In many cases the overprint can be isolated in laboratory, and the original magnetic field can be determined.

2.1.2.1. Sampling and analytical techniques

Fine-grained sediments are best suited for palaeomagnetic analysis. In the field, suitable sites were identified, and a set of 6 duplicate samples was collected at each. The sampling technique consisted in horizontally pushing a 2.5 cm diameter plastic cylinder 2.1-2.2 cm deep into the mud. The base of the cylinder was marked, and the azimuth of the insertion was measured with a Suunto compass. Dip and strike of the sediment layer were also recorded with a compass and clinometer (measurement precision is ± 2°). If the sediment was too hard to allow the insertion of the cylinder, a larger block of sediment on which magnetic north was marked was collected and carefully stored to avoid disturbance. These larger blocks were subsequently cut into smaller samples in the laboratory. The position of each sampling site was marked in a map of the cave, and its elevation in relation to the base level could be inferred later from the cave survey. In the study area cave survey elevations are known with an uncertainty which is probably less than 5 m.

Samples were analysed at the magnetically shielded Palaeomagnetism Laboratory at the University of Plymouth. Samples were demagnetised using stepwise alternating field demagnetisation. A weak alternating field is applied to the specimen, causing the magnetisation of grains of low coercivity to be randomised, leaving after successive steps only the more stable primary magnetisation. Fields up to 75 mT were applied. After each successive step, the magnetisation was measured in a Molspin fluxgate spinner magnetometer. The majority of samples had initial intensities within the detection limit of the instruments. The data was treated either in the DATAIN program devised by D.Tarling (pers. comm.) or in the MOLDEV program devised by A. Morris (pers. comm). Fisher statistics allowed the polarity to be determined. Details on statistic parameters and sample reliability are presented in Chapter 3.

2.1.3. Age correction procedures

Radiocarbon ages are quoted throughout the thesis. These ages, unless noted otherwise, have been calibrated in order to enable a direct comparison with the U-series ages obtained on this thesis. Uncalibrated ages up to 8.5 ka were calibrated using the dendrochronology curves of Stuiver and Becker (1993). Ages from 8.5 ka up to the limit of the radiocarbon method were calibrated using the procedure of Bard et al. (1993). Due to the limited number of calibration points, calibration of ages older than 25 ka carry a large uncertainty, possibly at least ±1.5 ka (Arz et al., 1998).

2.2. OTHER TECHNIQUES

2.2.1. X-ray diffraction

The mineralogy of a series of samples was determined through X-ray diffraction techniques, performed in the Department of Geology, University of Bristol. The sample was initially ground in an agate pestle and mortar, until < 63 μm. It was then slightly wetted, and a small amount was spread as a thin layer on a glass slide. The samples were run in a Phillips Automatic PW 1840 Diffractometer, and a print out of the diffractogram peaks was produced. The mineralogy was identified by matching the measured diffraction patterns (series of peaks) with a set of standard patterns in the Powder Diffraction Index for minerals. In most cases, identification was straightforward, although in samples with multiple minerals, minor constituents were difficult to determine.

2.2.2. Anion and cation analysis

Anions (Cl^-, NO_3^-, SO_4^{2-}) and cations (Ca^{+2}, Mg^{+2}, Na^+, K^+, Fe) concentrations of twenty-four samples of ground water collected from wells, springs and caves were determined on a Dionex 4000i ion chromatograph and a Pye Unicam SP9 Atomic Absorption Spectrophotometer by the technician Jenny Mills.

Ion chromatographic analysis was used for anion determinations. New eluants were degassed with He at 10 psi for about 5 mins. Detection limits are around 0.5 μeq/l. Several blanks (deionised water) were analysed prior to the start of each sample run. Blank samples were also included in each run. A standard was run every 6 samples and recalibration was carried out after every 15 samples. Standards were prepared from stock solutions. The standards span the range of concentrations expected in the samples and were used to calibrate the ion chromatograph. Samples with very high concentrations were diluted and the analysis was repeated.

Cations were analysed by atomic absorption spectrophotometry. The oxidant gas (air or nitrous oxide) flows into the nebuliser and creates a vacuum. The solution sample is then aspirated into the nebuliser via a plastic capillary tube and, together with the oxidant, is converted into an aerosol. This mixture is then forced into the flame which is of a sufficient high temperature to cause the atomisation of the analyte element. The free atoms thus formed absorb radiation from the hollow cathode lamp. Since the cathode is constructed of the analyte element (or an alloy of it) the radiation will be specific to that element only. The radiation will enter the monochromator which allows only a narrow region of the spectrum, typically 0.5 nm centred on the preselected wavelength of the resonance line for the analyte element to pass into the photomultiplier. The resulting signal is then presented as a digital display. For each cation, a calibrated solution containing a known concentration of the element of interest was run prior to analysis.

2.2.3. Sulphur isotope analysis

Samples of sulphate-rich ground water, gypsum speleothems and pyritiferous limestone were collected for $^{34}S/^{32}S$ analysis. The determinations were performed by myself at the Department of Earth Sciences of the University of Leeds, under supervision of Dr. Simon Bottrell.

Immediately after collection ground water samples were filtered and left standing under the sun to be warmed. $BaCl_2$ was added to precipitate the sulphate. The samples were then left to stand for about 48 hours, before the precipitate was filtered off using a Whatman slow filter paper and stored in sterile plastic bags. In the laboratory the sulphate was reacted at 930°C with $Na_3(PO_3)_3$ to yield SO_3, which was reduced to SO_2 on heated Cu. The gas was cryogenically purified and analysed in a VG SIRA 10 mass spectrometer. Errors for the $BaSO_4$ precipitates are ± 0.2‰. Sulphide samples followed similar procedures after sulphide concentration from the rock sample. Sulphide and sulphate standards were run previous to each day's analysis.

CHAPTER 3
DENUDATION RATES IN CRATONIC AREAS

3.1. REGIONAL GEOLOGY AND TECTONICS

The continent of South America is composed of a collision margin on its western border, represented by the Pacific littoral zone and the Andes Mountains, a passive margin on the eastern Atlantic zone, developed since the breakup of the Gondwana continent in the Mesozoic, and the continental interior which comprises a number of ancient geotectonic unities, or shields. These shields are composed mostly of Archaean and Palaeoproterozoic medium grade metamorphic rocks (Misi and Veizer, 1998), and can be separated into the Guyana, Brazilian and Atlantic shields (Fig. 3.1) (Schobbenhaus and Campos, 1984).

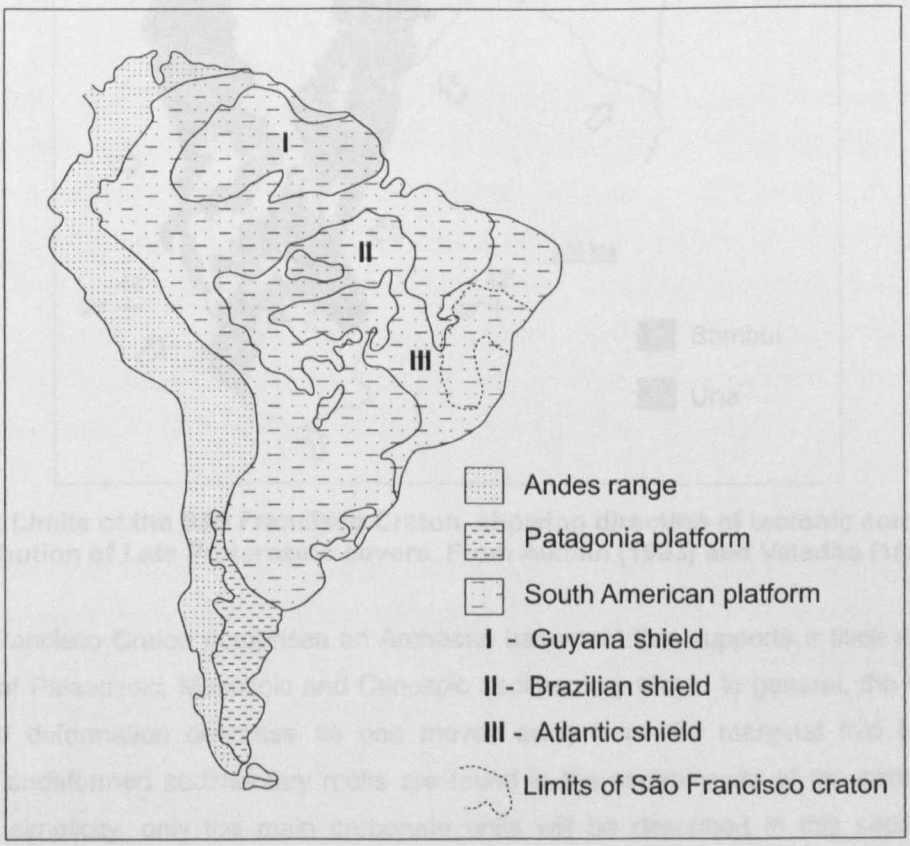

Figure 3.1. Geotectonic framework of South America. From Schobbenhaus and Campos (1984).

South America experienced a common tectonic history with Africa until Mesozoic rifting and separation. During the Brasiliano/Pan-African orogenic event (450-700 Ma), oblique collision between the West African and the Congo-São Francisco Cratons (Harman et al., 1998) created the present structure of the São Francisco Craton. The São Francisco Craton is surrounded by several fold belts of Brasiliano age and is internally composed of several small archaean cratonic blocks, separated by intracratonic mobile belts (Harman et al., 1998). The São Francisco Craton split from the Congo Craton during the continental breakup, and its

northeastern limit now coincides with the Atlantic platform. The present configuration of the São Francisco Craton is illustrated in Fig. 3.2.

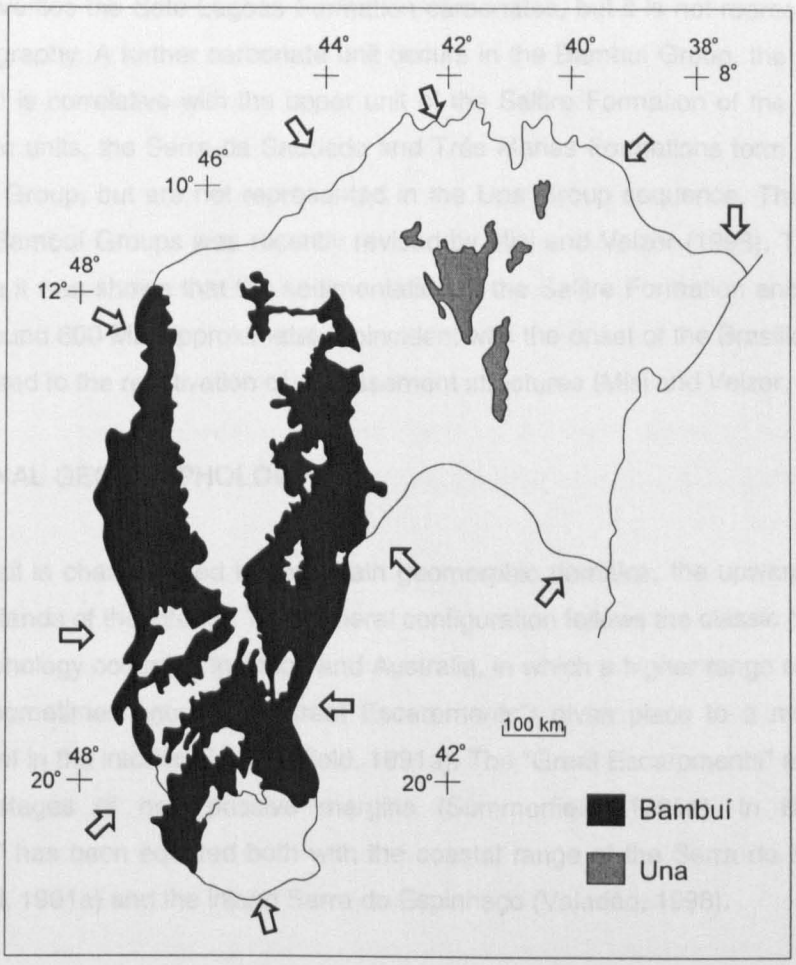

Figure 3.2. Limits of the São Francisco Craton, showing direction of tectonic compression and distribution of Late Proterozoic covers. From Alkmin (1993) and Valadão (1998).

The São Francisco Craton comprises an Archaean basement that supports a thick and varied sequence of Palaeozoic, Mesozoic and Cenozoic sedimentary rocks. In general, the degree of folding and deformation decrease as one moves away from the marginal fold belts, and essentially undeformed sedimentary rocks are found in the central parts of the craton. In the interest of simplicity, only the main carbonate units will be described in this section. More detailed geological information will be included in the description of each study area.

Among the sedimentary units that overlie the São Francisco Craton, there are extensive Proterozoic carbonate deposits. These units can be grouped into the Bambuí Group, which occurs in the southern parts of the São Francisco Craton, and the Una Group, prevalent in its northern parts (Fig. 3.2). The Una and Bambuí Groups have been considered as correlative units (Misi and Veizer, 1998), and share a similar tectonic and stratigraphic history. They occupy an area of approximately 300,000 km^2 (Misi and Kyle, 1994). Following Dardenne (1978) both sequences start with a glaciogenic conglomerate known as the Jequitaí Formation in the Bambuí Group, or as the Bebedouro Formation in the Una Group. Overlying the Jequitaí

Formation, follows a carbonate unit, the Sete Lagoas Formation which is correlative with the basal units of the Salitre Formation in the Una Group. A pellitic unit, the Serra de Santa Helena Formation overlies the Sete Lagoas Formation carbonates, but it is not represented in the Una Group stratigraphy. A further carbonate unit occurs in the Bambuí Group, the Lagoa do Jacaré Formation. It is correlative with the upper unit of the Salitre Formation of the Una Group. Two further pellitic units, the Serra da Saudade and Três Marias Formations form the upper part of the Bambuí Group, but are not represented in the Una Group sequence. The age of the Una Group and Bambuí Groups was recently revised by Misi and Veizer (1998). Through Sr and S isotopic data it was shown that the sedimentation of the Salitre Formation and correlative units occurred around 600 Ma, approximately coincident with the onset of the Brasiliano orogeny, and possibly related to the reactivation of old basement structures (Misi and Veizer, 1998).

3.2. REGIONAL GEOMORPHOLOGY

Eastern Brazil is characterized by two main geomorphic domains, the upwarped coastal zone and the highlands of the interior. This general configuration follows the classic pattern of passive margin morphology occurring in Africa and Australia, in which a higher range of mountains near the coast (sometimes known as "Great Escarpments") gives place to a more subdued but elevated relief in the interior (Summerfield, 1991a). The "Great Escarpments" are created during the rifting stages of new passive margins (Summerfield, 1991a). In Brazil the "Great Escarpment" has been equated both with the coastal range of the Serra do Mar (Ollier, 1985, Summerfield, 1991a) and the inland Serra do Espinhaço (Valadão, 1998).

An attempt to explain the intraplate evolution of passive margins such as eastern Brazil has been made by Gilchrist and Summerfield (1990, 1991). In this model, denudation in the coastal escarpment is higher than in the low relief interior. Flexural isostasy thus causes a more marked uplift of the escarpment than the interior, maintaining, or actually increasing the elevation difference between these areas (Summerfield, 1991a).

3.2.1. Planation surfaces

One of the most characteristic geomorphological features of passive margin interiors are planation surfaces. They are widespread in Africa, Australia and South America, and have received extensive treatment in the literature (see Adams, 1975). However, their genesis and evolution (and even their mere existence) remain controversial (Ollier, 1991). Even the number of surfaces have been subject to debate, as evident in well studied areas such as Australia (Young, 1992) and Africa (Partridge and Maud, 1987).

L.C. King, in a series of papers (King, 1956b, 1967, 1976, 1983) developed a model of landscape evolution based on escarpment retreat in response to episodic uplift. King envisaged a landscape in which a suite of erosion surfaces limited by scarps would evolve on a global

basis, following planetary scale uplift events. Correlation between the world's erosion surfaces has been proposed by King (1967) and Melhorn and Edgar (1975). One basic premise in King's model is that episodic uplift is needed in order to produce a new set of erosion surfaces. Thus, King (1983) proposed that uplift episodes in the early Cretaceous (breakup of continents), mid Cretaceous, late Oligocene, late Miocene and late Pliocene would be responsible for the worldwide development of erosion surfaces. Central to King's theory of planation is the concept of episodic and rapid uplift. This view has been challenged by Gilchrist and Summerfield (1991), who suggest that over the timescale of landscape evolution, isostatic compensation is continuous, depending on the flexural rigidity of the crust and the wavelength of applied loads. Modelling of passive margins by Gilchrist and Summerfield (1991) suggests that maximum active tectonic uplift occurs in a single major event associated with the breakup of the continents. Subsequently, isostatic rebound will tend to match the denudation rate, and the evolution of the landscape could proceed for long periods without apparent change in elevation (Summerfield, 1991a). If the Gilchrist and Summerfield (1990, 1991) model of continuous isostatic uplift is correct, several interpretations of macroscale geomorphology in passive margins will need to be revised.

In eastern Brazil, the most influential study on the ubiquitous planation surfaces was performed by King (1956a), who identified five major planation events, namely the Gondwana, Post Gondwana, Sul Americana, Velhas and Paraguaçú. According to King, the oldest planation surface, the Gondwana, evolved before the separation of the Gondwana supercontinent, and nowadays is preserved as restricted remnants in highlands. The Post Gondwana Surface followed the breakup of the continents, and was of mid Cretaceous age. Uplift in the mid Cretaceous prompted initiation of the Sul Americana Surface, the flattest and global index surface, also known as African or Moorland Surface. In Brazil the Sul Americana Surface was uplifted in the late Oligocene when a new cycle, represented by the Velhas Surface was initiated (King, 1956a). The Velhas Surface only reached the planation stage in the northern parts of eastern Brazil. Nowadays it is the most widespread planation cycle (King, 1956a). Following another uplift in the end of the Pliocene, the youngest cycle, named Paraguaçú in Brazil started developing, but did not reach the stage of planation, comprising mostly incised valleys in the main rivers. In later writings, King (1976) adopted global names for these surfaces, and subdivided the Velhas Cycle (also known as Post-African in Africa) into the Rolling and the Widespread Planation Surfaces (Fig. 3.3).

The cycles and planation surfaces of King have for many years formed a paradigm in macroscale geomorphic studies in Brazil. Although several authors have made minor contributions on the subject (Braun, 1971, Mabesoone and Castro, 1975, among others), the key scheme proposed by King remained essentially unchanged. A major revision of the long-term geomorphic evolution of eastern Brazil has now been proposed by Valadão (1998). Using remote sensing techniques, and a wealth of new stratigraphic data, Valadão has recognised only 3 major surfaces. The oldest of these surfaces can be correlated with the Sul Americana

Surface of King despite differences in areal distribution. It started forming after the continental breakup, and lasted for approximately 102 Ma. Following Miocene uplift, the Sul Americana I Surface evolved for about 8 Ma before being interrupted by another uplift event in the Pliocene which marked the beginning of the Sul Americana II Surface. Valadão (1998) found no evidence of the Gondwana and Post Gondwana Surfaces of King (1956a). Valadão's scheme, and its equivalence with King's surfaces are shown in Fig. 3.3.

The new set of geomorphic events proposed by Valadão (1998) has similarities with the scheme envisaged for Southern Africa by Partridge and Maud (1987). Critical chronological markers in both studies are provided by the breakup of the Gondwana continent and uplift events of the Miocene and Pliocene. The delimitation of such uplift events in Brazil is based, among other factors, on correlation with the influx of deep oceanic sediments (Davies et al. 1977). Summerfield (1991a) has warned on the potential problems in correlating deep ocean sedimentation rates with continental denudation, while in Australia, Bishop (1985) has demonstrated that accelerated denudation did not occur in the Miocene, as suggested by the oceanic data of Davies et al. (1977).

Recent apatite fission track analyses (AFTA) performed in the São Francisco Craton have not clarified the picture. AFTA cooling ages have the potential to record episodes of increased denudation (R. Brown et al. 1994). Amaral et al. (1997) studied three samples and found no evidence of increased denudation during the last 240 Ma, although samples from southeastern Brazil (outside the São Francisco Craton) indicate increased denudation at 60 Ma. In a more comprehensive study, Harman et al. (1998) analysed 20 samples from the São Francisco Craton (and a further 20 samples from the Guaporé Craton) and detected two episodes of enhanced denudation in both cratons, one associated with the breakup of the continents at 130 Ma and another during the late Cretaceous (80-60 Ma). No evidence either of the Miocene or Pliocene denudational episodes was found. Clearly, there is a need for further AFTA and both onshore and offshore sedimentological studies in the area in order to clarify the timing, relative importance and even the existence of uplift episodes in the region. For the timescale of concern in this thesis, there appears to be an agreement that no uplift, or tectonic related denudational episodes occurred during the Quaternary. Continuous isostatic rebound, as proposed by Gilchrist and Summerfield (1990, 1991) will apparently be the only major tectonic process acting upon the carbonate sequences of the São Francisco Craton since the late Tertiary.

3.3. DENUDATION RATES IN CRATONIC AREAS

Denudation rates can be calculated from several types of data, including the amount of sediment and solute removed from drainage basins, results of apatite fission track analysis, fluvial incision rates and from rates of sedimentation in oceanic basins (see review in Goudie, 1995). However, it is not entirely clear how well these denudation rates, derived by several distinct techniques, can be compared with each other. Rates derived from fluvial downcutting

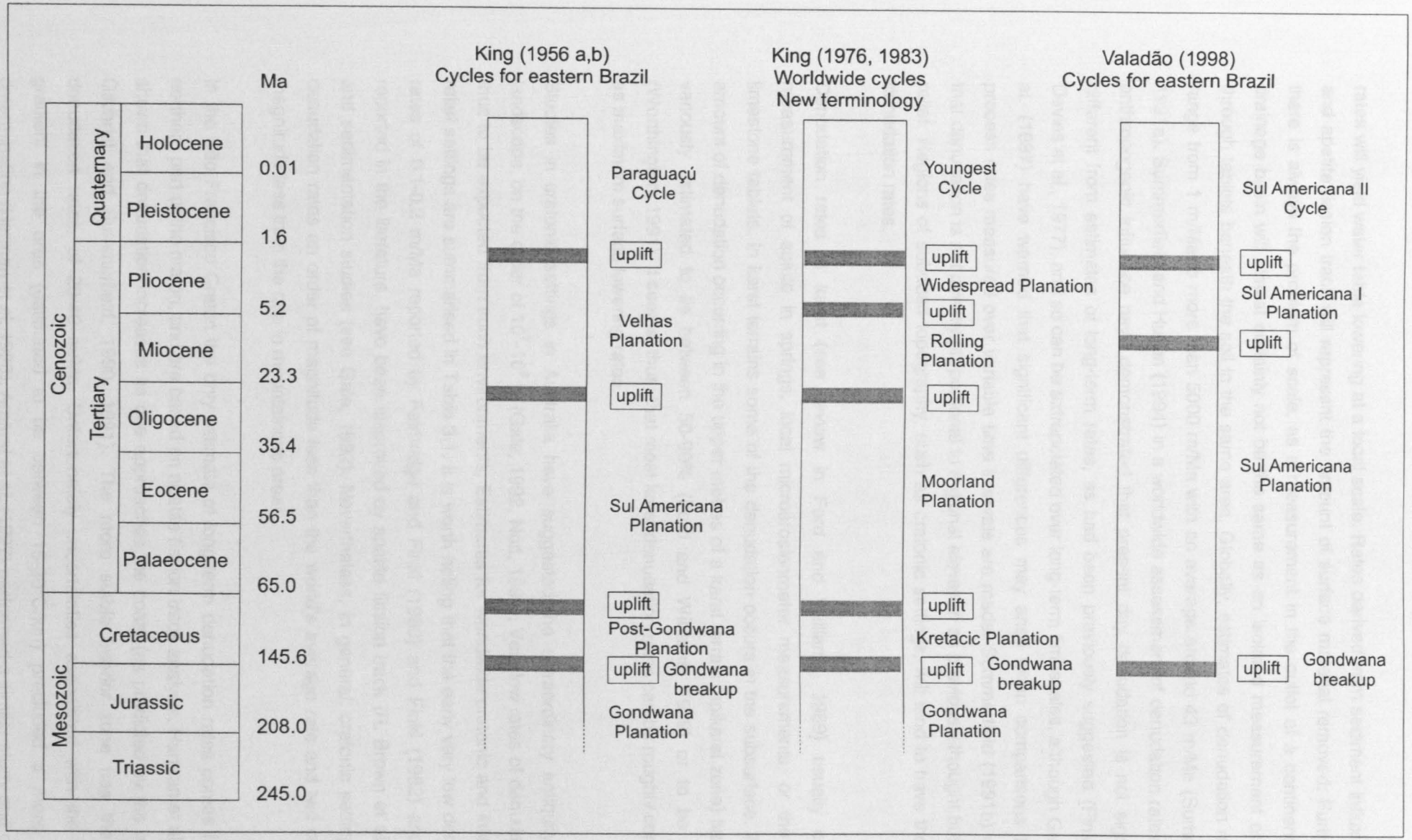

Figure 3.3. Correlation between the planation surface cycles proposed by L.C.King and the new scheme by Valadão (1998). Time intervals not to scale.

rates will yield water table lowering at a local scale. Rates derived from sediment influx in rivers and apatite fission track will represent the amount of surface material removed. Furthermore, there is always the problem of scale, as a measurement in the outlet of a continental scale drainage basin will almost certainly not be the same as an isolated measurement of erosion through tablets beneath the soil in the same area. Globally, estimates of denudation rates can range from 1 m/Ma to more than 5000 m/Ma with an average around 43 m/Ma (Summerfield, 1991a). Summerfield and Hulton (1994) in a worldwide assessment of denudation rates without anthropogenic influence have demonstrated that present day denudation is not significantly different from estimates of long-term rates, as had been previously suggested (Finkl, 1982, Davies et al., 1977), and so can be extrapolated over long-term timescales, although Gardner et al. (1987) have warned that significant differences may arise when comparisons between process rates measured over variable time intervals are made. Summerfield (1991b) stressed that denudation is not directly proportional to regional elevation as previously thought but to local relief. Regions of subdued topography, such as cratonic settings, will tend to have the lowest denudation rates.

Denudation rates in karst (see review in Ford and Williams, 1989) usually comprise measurement of solute in springs, local microerosionmeter measurements, or the use of limestone tablets. In karst terrains some of the denudation occurs in the subsurface. The total amount of denudation occurring in the upper metres of a karst terrain (epikarst zone) have been variously estimated to lie between 50-90% (Ford and Williams, 1989) or to be 98-99% (Worthington, 1991). It seems, thus, that most karst denudation rates can be roughly considered as maximum surface lowering rates.

Studies in cratonic settings in Australia have suggested the extraordinary antiquity of the landscape, on the order of 10^7-10^8 yr (Gale, 1992, Nott, 1995). Very low rates of denudation are thus to be expected from such environments. Estimates for worldwide cratonic and interior low relief settings are summarised in Table 3.1. It is worth noting that the early very low denudation rates of 0.1-0.2 m/Ma reported by Fairbridge and Finkl (1980) and Finkl (1982) and widely reported in the literature, have been disproved by apatite fission track (R. Brown et al., 1994) and sedimentation studies (see Gale, 1992). Nevertheless, in general, cratonic settings have denudation rates an order of magnitude less than the world's average rate and two orders of magnitude less than the rate in mountainous areas.

In the São Francisco Craton the only estimate of long-term denudation rates comes from the northern part of the craton, and are based on apatite fission track analysis. Harman et al. (1998) shows that denudation increases as one approaches the coast (as predicted by the model of Gilchrist and Summerfield, 1990, 1991). The more stable interior zone has the lowest denudation rates, of 20-40 m/Ma. Unfortunately uncertainties associated with the thermal gradient in the area (estimated to be between 15-30°C/km) precluded a more precise determination (Harman et al. 1998). Amaral et al. (1997) performed a similar study and deduced

a denudation rate of 18 m/Ma assuming a thermal gradient of 15°C/km. This result is considerably lower than that reported by Harman et al. (1998) because if a thermal gradient of 30°C/km had been adopted the average denudation would be around 9 m/Ma. These discrepancies need to be resolved in the light of new studies.

Location	Method	Rate m/Ma	Reference
West Australian Craton	Geomorphological criteria	0.1-0.2	Fairbridge and Finkl (1980)
Southeastern Australia	Incision rates	1-10	Bishop (1985)
Guyana Craton	Fluvial geochemistry	10	Edmond et al. (1995)
West African Craton	Cosmogenic	3-8	E.Brown et al. (1994)
Mount Roraima, Guyana Craton	Cosmogenic	1	E.Brown et al. (1992)
Southeastern Australia, Yilgarn	Weathering rates	1-2	Shoemaker et al. (1990)
Africa, Lake Chad	Fluvial geochemistry	8	Gac (1980)
SE Australia, Snowy River	AFTA	15-18	Kohn et al. (1999)
Southeastern Brazil, Paraná	AFTA	8	Gallagher et al. (1994)
Guaporé Craton, Brazil	AFTA	15-50	Harman et al. (1998)
Interior São Francisco Craton	AFTA	20-40	Harman et al. (1998)
Interior São Francisco Craton	AFTA	18	Amaral et al. (1997)
Global average rate		43	Summerfield (1991a)
Mountainous areas/highlands		500	Ollier and Pain (1996)

Table 3.1. Denudation rates for cratonic and low relief interior settings. Estimates extrapolated over diverse timescales. This list is by no means a complete list. AFTA – Apatite fission track analysis.

3.4. THE BAMBUÍ KARST

The carbonate rocks of the Bambuí Group occur over a vast area in the states of Minas Gerais, Bahia and Goiás (Fig. 3.2). The stratigraphy of the Bambuí Group following Branco and Costa (1961) and Dardenne (1978) comprises two main carbonate formations (Fig. 3.4), the Sete Lagoas Formation which is represented by limestone and dolomite with some clay/silt intercalations and the Lagoa do Jacaré Formation, compring oolitic and pisolitic limestone, usually dark and crystalline, with some silt/clay. The Serra de Santa Helena Formation, which separates the two carbonate units, corresponds to shales and siltites with minor limestone lenses.

Extensive karst landforms occur over the carbonate rocks of the Bambuí Group. The areal distribution of the carbonate rocks in relation to the surrounding topography forms several physiographic domains, imprinting distinct morphological patterns on the karst landforms. Preliminary descriptions of the major karst areas and their caves have been presented by Karmann and Sanchez (1979), Auler and Farrant (1996) and Piló (1998). In this thesis, two areas of the Bambuí Karst will be examined in detail, the Santa Maria da Vitória Karst (following section) and the Lagoa Santa Karst (section 5.5).

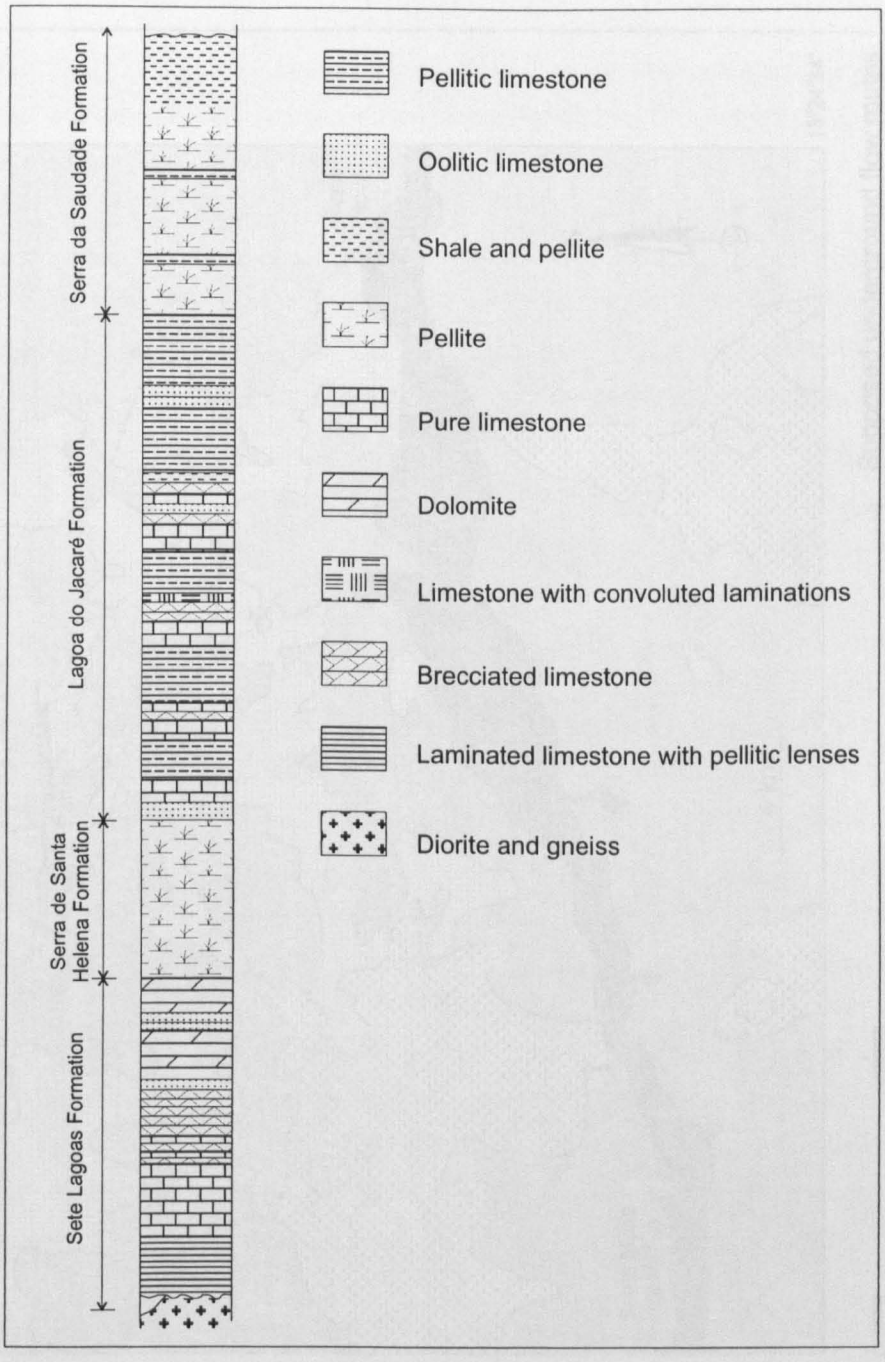

Figure 3.4. Stratigraphy of the Bambuí Group at the centre of the São Francisco Craton. Lower and upper formations are absent. From Dardenne (1978).

3.4.1. Santa Maria da Vitória Karst

3.4.1.1. Study area

Located away from the fold belts that surround the São Francisco Craton, the Santa Maria da Vitória Karst lies in an undeformed portion of the Bambuí Group sequence. Strata are horizontally bedded, and maximum dips in the area do not exceed 5° (Nascimento, 1990). Fig. 3.5 presents the stratigraphy and the geology of the area. The Bambuí Group at Serra do Ramalho, about 50 km to the south, comprises carbonates of the Sete Lagoas Formation, metapellitic rocks of the Serra de Santa Helena Formation and carbonates of Lagoa do Jacaré

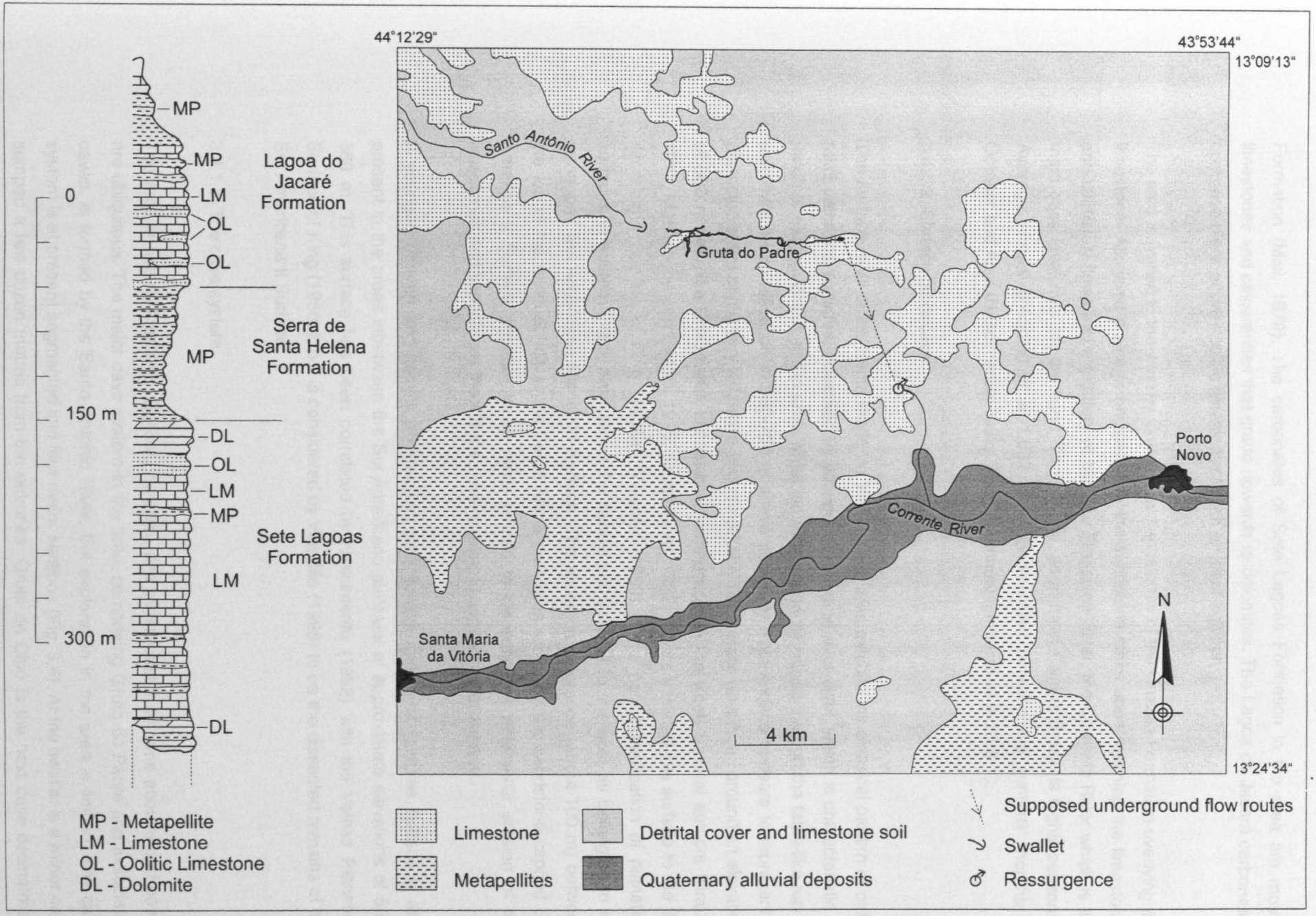

Figure 3.5. Geological map of Santa Maria da Vitória Karst. From Nascimento (1990, 1992). Stratigraphical column from nearby Serra do Ramalho by Misi (1979).

Formation (Misi, 1979). The carbonates of Sete Lagoas Formation in the area are mostly limestones and calcarenites that grade upwards to dolomites. The Lagoa do Jacaré carbonates comprise black or grey oolitic limestones which smell of sulphur.

The area is limited to the west by Cretaceous sandstones of the Urucuia Formation overlying the limestone. Allogenic drainage originating in the sandstone sinks upon reaching the limestone, and ultimately flows into a tributary of the São Francisco River, the Corrente River which is the main base level river for the karst. The climate, as in most Central Brazil, is highly seasonal. Average annual precipitation is 1,032 mm, concentrated between the summer months of October and April (Nascimento, 1992). Average annual temperature is 23.8 °C.

3.4.1.2. Surface landscape

The surface relief of the Santa Maria da Vitória karst area exhibits the classical pattern of older relict planation surfaces, dissected by younger surfaces at river level, which is characteristic of much of eastern Brazil. In the area, an older surface can be traced through the table-like top of relict hills, at an elevation of 660-700 m above sea level. This surface appears to represent a dissected stage of the very extensive and remarkably flat surface developed around an elevation of 800 m over the Cretaceous sandstones immediately to the west. Several authors (Braun, 1971, Mabesoone and Castro, 1975, Nascimento, 1992) have correlated this surface to the Sul Americana Surface of King (1956a). Valadão (1998) in his new classification of planation surfaces in eastern Brazil also places the sandstone uplands to the west as belonging to his remapped Sul Americana Planation Surface. The elevation difference (about 100 m) between the top of the residual hills in the Santa Maria da Vitória area and the sandstone capped Sul Americana Surface appears to be more related to dissection or differential erosion of the limestones and sandstones than to the development of another lower surface.

A younger, uneven and heavily pockmarked with dolines and karst features surface is also present in the areas inbetween the Sul Americana plateaux at approximate elevations of 550-580 m. This surface has been correlated by Nascimento (1992) with the Velhas Planation Surface of King (1956a), but is considered by Valadão (1998) to be the dissected remains of the Sul Americana II Surface.

3.4.1.3. The cave system

The area is heavily karstified. Dolines, swallets, and other karst landforms abound and caves are ubiquitous. The major cave system in the area, comprising Gruta do Padre and associated caves, is formed by the Santo Antonio River, but exploration in the area is limited. The cave system is at present segmented into four major sections (Fig. 3.6). At the swallet is a minor cave sumped a few dozen metres from the entrance. Gruta do Cipó is the next cave downstream from the swallet. It is a multilevel cave about 2.8 km long with an active lower level that ends in a

sump associated with breakdown. Gruta do Cipó floods to the ceiling and the majority of its sediments have been reworked in recent times. No sampling was performed in this cave. The underground drainage is seen again at Gruta do Padre, the major cave of the system. Downstream from Gruta do Padre there is a gap of 7 km in a straight line to the presumed resurgence of the system, Gruna da Bananeira, a short sumped cave near the Corrente River.

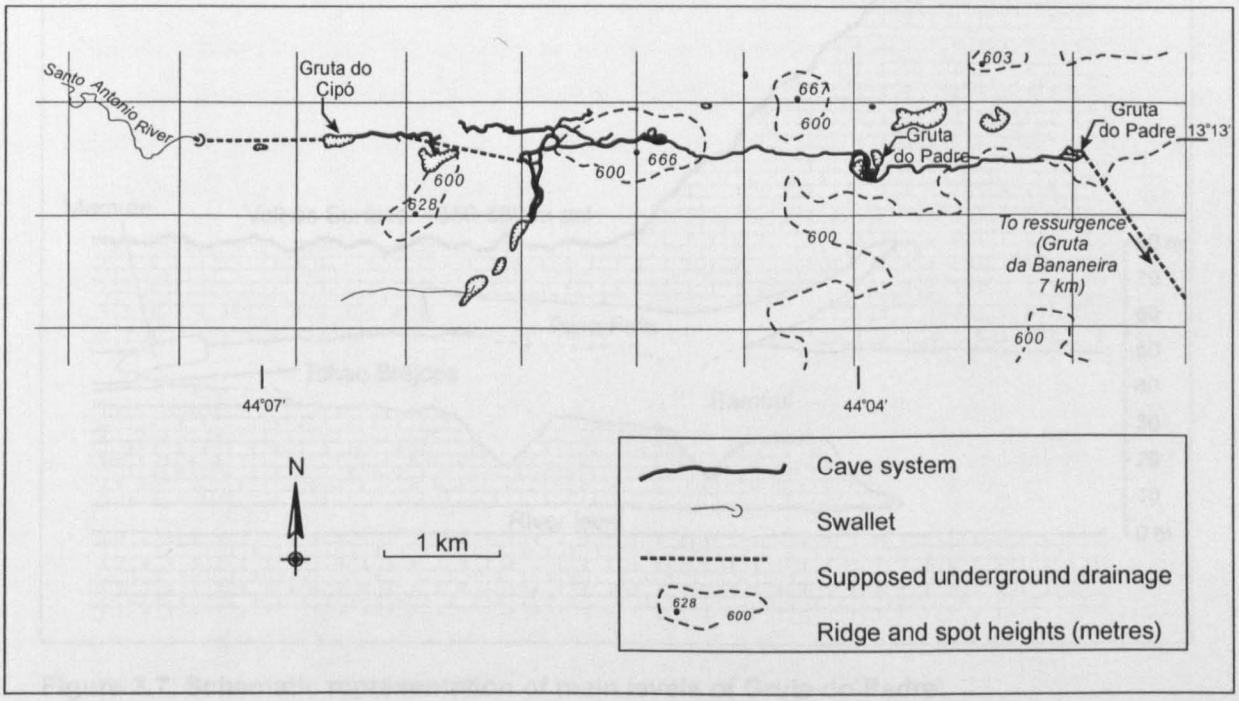

Figure 3.6. Plan map of Gruta do Padre. Survey BCRA 3C by Operação Tatus II.

Gruta do Padre is a 15.8 km long cave, comprised of 3 well defined subhorizontal levels, a major tributary passage and a few minor side passages. Fig. 3.7 schematically portrays the main levels of Gruta do Padre. The lowest level is represented by the Santo Antonio River. It can be followed for over 5 km and can be up to 40 m high where combined with passages of next level, but in many areas is less than 15 m high. The hydraulic gradient of the river passage from the cave survey is 0.0067. A few kilometres upstream from the main entrance, the river level splits into two levels. The Bambuí level (including Dunas Passage) is a massive dry passage lying about 45 m above the base level river. It follows almost perfectly the lower river passage in plan, being offset by a few tens of metres in places. The Bambuí level floor is highly irregular, due to breakdown and collapses into the lower level. Because of this, its elevations thus vary between 30 to more than 50 m above the cave stream.

The upper and older level is represented by the Terra Fofa Passage, a large passage fragmented and only accessible in two places. Its floor lies approximately 53 m above the cave stream and about 10 m above the Bambuí Passage. It does not appear to be genetically related to the Bambuí (or river) passages, having a different direction and being connected to it accidentally by breakdown. The upstream end of Terra Fofa Passage is blocked by flowstone and breakdown, but a very similar isolated high level passage (Mamute Passage) can be

entered some 400 m away, although it is somewhat lower in elevation (about 45 m above the river). Due to its direction and morphology, the Mamute Passage is interpreted as belonging to the same level as the Terra Fofa Passage.

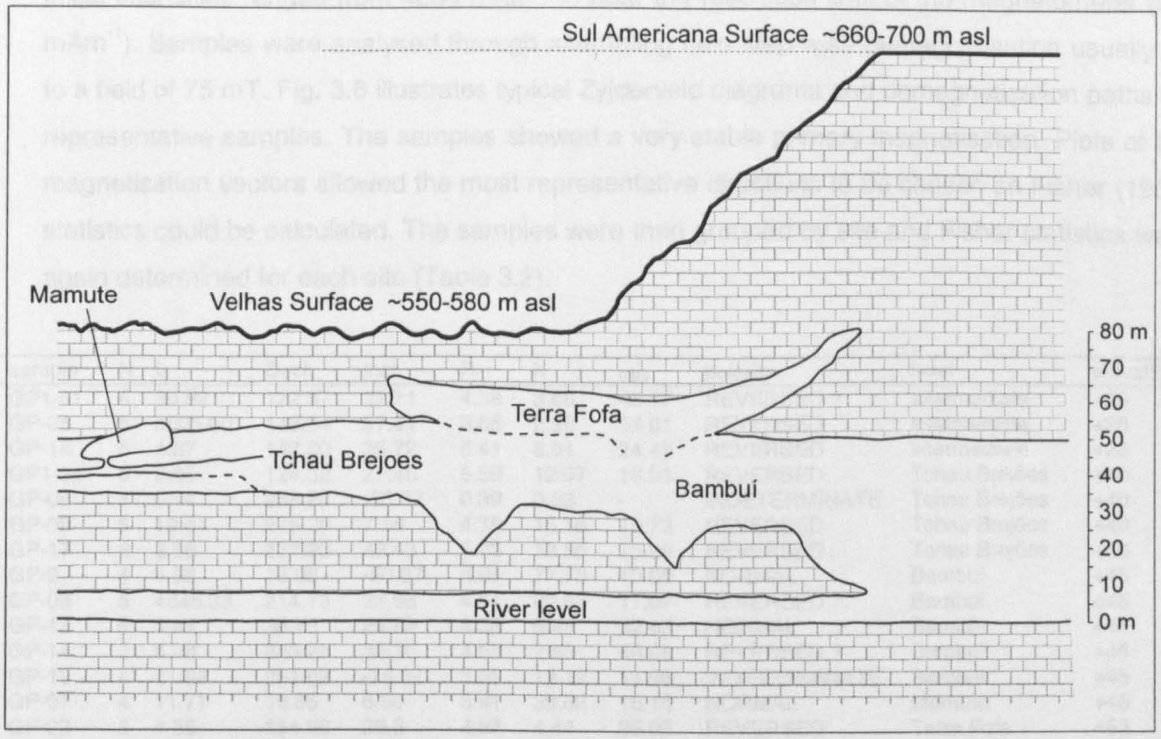

Figure 3.7. Schematic representation of main levels of Gruta do Padre.

The Tchau Brejões Passage is an important tributary of the Bambuí level at an elevation between 33-40 m abover river level. It is a narrow paragenetic passage with a sediment infill at least 6 m thick. Because the Tchau Brejões Passage is a tributary of the Bambuí level, and lies in general below it, it is interpreted as postdating it. It appears that the Bambuí level had already drained (at least in part) while the Tchau Brejões was still in the phreatic zone as its phreatic ceiling lies below the Bambuí ceiling.

The sequence of passages in Gruta do Padre has evolved largely under vadose conditions in response to incision of the Corrente River. Sediment deposition in the levels proceeded from the older upper passages represented by the Terra Fofa level (including Mamute) towards Bambui and Tchau Brejões up to the present river level.

3.4.1.4. Magnetostratigraphy of Gruta do Padre levels

Samples for palaeomagnetism dating were collected from the three main cave levels over a 53 m vertical range above the present cave stream. One hundred thirty seven oriented samples of clay and silt were collected from 19 sites. Of these, 4 sites (24 samples) had initial intensities (I_o) too low to be analysed. A further 10 samples were too desiccated to provide meaningful results and were discarded. A total of 103 samples from 15 sites were therefore analysed (see section

2.1.2 for methods). Elevations for the cave levels and sampling sites were determined from the cave survey, and relate to height above cave stream.

Initial intensities ranged from 4884 mAm^{-1} to near the resolution limit of the magnetometer (0.1 mAm^{-1}). Samples were analysed through alternating field step-wise demagnetisation usually up to a field of 75 mT. Fig. 3.8 illustrates typical Zyjderveld diagrams and demagnetisation paths for representative samples. The samples showed a very stable primary magnetisation. Plots of the magnetisation vectors allowed the most representative directions to be chosen so Fisher (1953) statistics could be calculated. The samples were then grouped by site and Fisher statistics were again determined for each site (Table 3.2).

sample	N	I_o	Decl.	Incl.	R	K	α_{95}	polarity	level	elevation
GP1-01	6	30.82	122.37	37.71	4.38	3.08	45.87	REVERSED ?	intermediate	+25
GP-05	5	3505.00	149.94	27.81	3.65	2.96	54.01	REVERSED	intermediate	+25
GP-18	6	4.87	142.60	35.72	5.41	8.54	24.43	REVERSED	intermediate	+25
GP1-04	6	2.05	124.32	27.46	5.59	12.07	19.98	REVERSED	Tchau Brejões	+40
GP-08	4	0.14	258.28	-53.57	0.39	0.83	-	INDETERMINATE	Tchau Brejões	+40
GP-09	5	19.61	216.25	7.16	4.75	16.16	19.73	REVERSED	Tchau Brejões	+40
GP-17	6	2.38	137.23	48.43	5.73	18.86	15.99	REVERSED	Tchau Brejões	+40
GP-2	4	8.98	18.98	-50.67	3.96	77.78	10.68	NORMAL	Bambui	+45
GP-06	5	4848.33	214.73	23.96	4.81	20.67	17.07	REVERSED	Bambui	+45
GP-13	5	1.41	36.73	23.89	4.38	6.45	32.63	NORMAL	Bambui	+45
GP-14	7	6.28	233.22	35.10	4.63	2.53	48.06	REVERSED ?	Bambui	+45
GP-19	4	21.98	281.62	-78.37	3.95	13.12	11.96	INDETERMINATE	Bambui	+45
GP-07	4	11.71	19.85	6.50	3.91	33.62	16.15	NORMAL	Mamute	+45
GP-03	6	4.55	154.66	26.3	4.87	4.44	35.95	REVERSED	Terra Fofa	+53
GP-10	6	2.61	147.85	41.91	5.18	6.13	29.54	REVERSED	Terra Fofa	+53

Table 3.2. Palaeomagnetic data from Gruta do Padre. Initial intensities (I_o) in mA/m, Declination, Inclination and α95 in degrees, elevation in metres above cave stream. α_{95} – 95% probability that the direction lies on that angle span, K- Fisher precision estimate which determines the dispersion of points, R- length of resultant vector.

Although individual samples tended to show good results, grouping the samples by site produced sometimes high α_{95} values, suggesting a low precision. Difficulties in determining the bedding orientation of the layers and slumping of some layers are believed to be largely responsible for high site α_{95}. Samples were usually taken as far as 1 m apart in a sediment section, and changes of bedding were observed in many sites. Lovlie et al. (1995) argues that further errors can be introduced by insertion of the sampling containers and compaction of sediments. Despite these limitations, polarity could be clearly established for most sites.

All part of the lowest cave level containing the river is within present flood range, and because the sediments in this area are subject to seasonal reworking they should belong to the present normal polarity Brunhes Epoch. Progressing upwards, a side passage at 25 m above river level yielded reversed polarity sediment from three closely spaced sites (Intermediate site in Table 3.2). The tributary passage of Tchau Brejões, at 40 m above base level was sampled at 4 sites. Three sites had reversed polarity, and one had very low initial intensity and showed scattered plots, being considered as indeterminate. The major Bambuí level was sampled at 5 sites. Two sites showed normal polarity, and one site had reversed polarity. A fourth site is also probably reversed. An additional sample (GP-19), clearly associated with a more recent invasion stream,

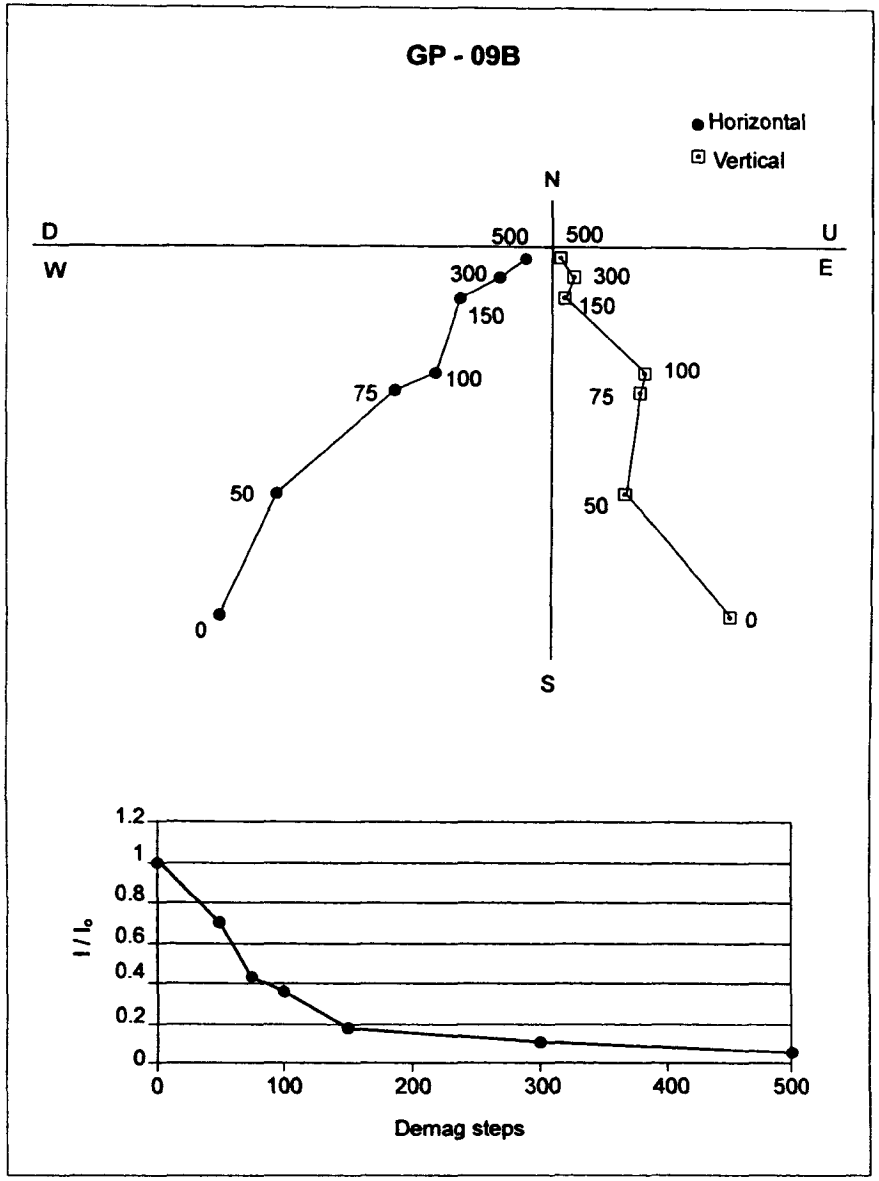

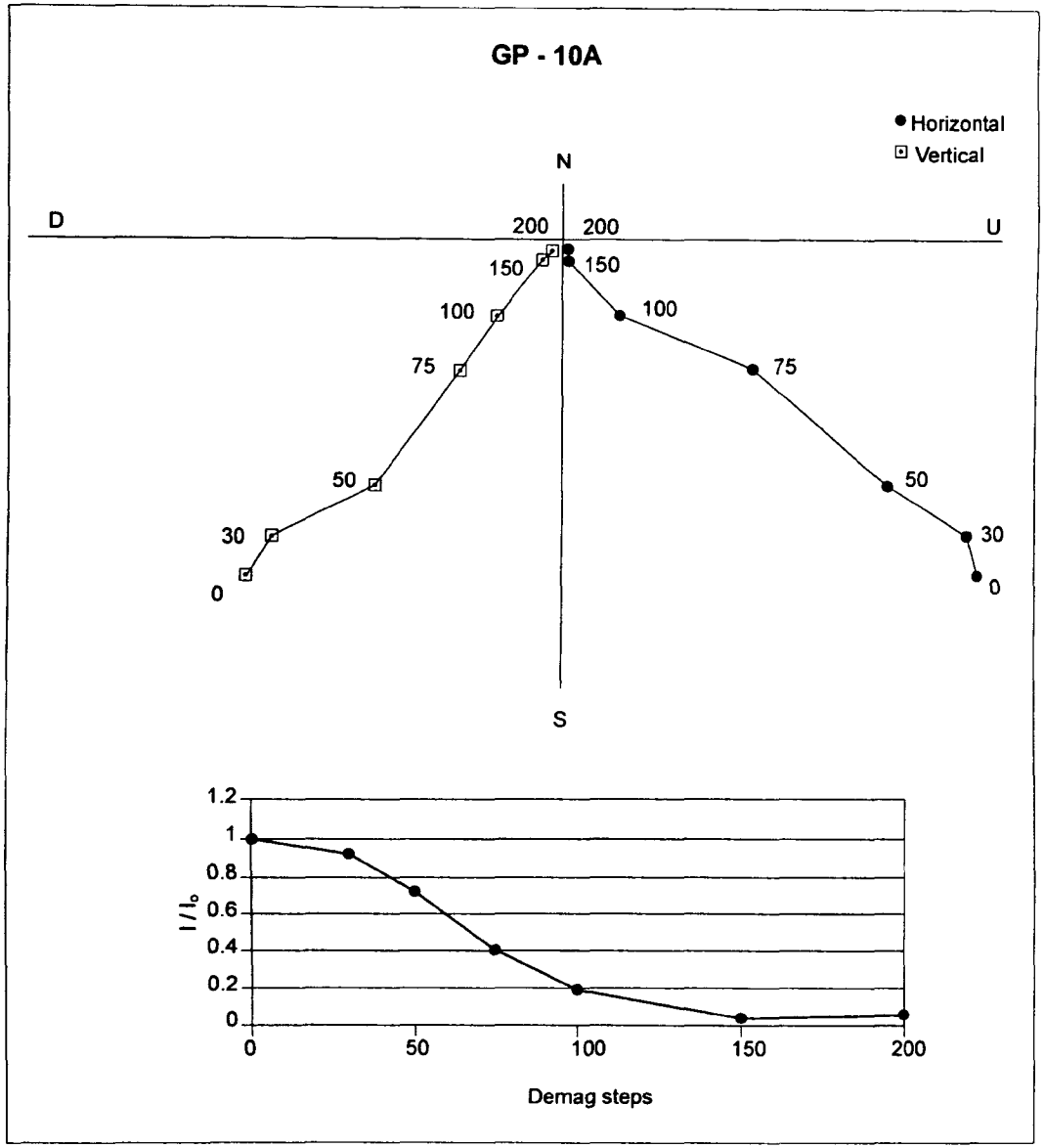

Figure 3.8. Zyjderveld plots and demagnetisation paths for selected samples from Gruta do Padre. I - Intensity. See Table 3.2 for details on samples.

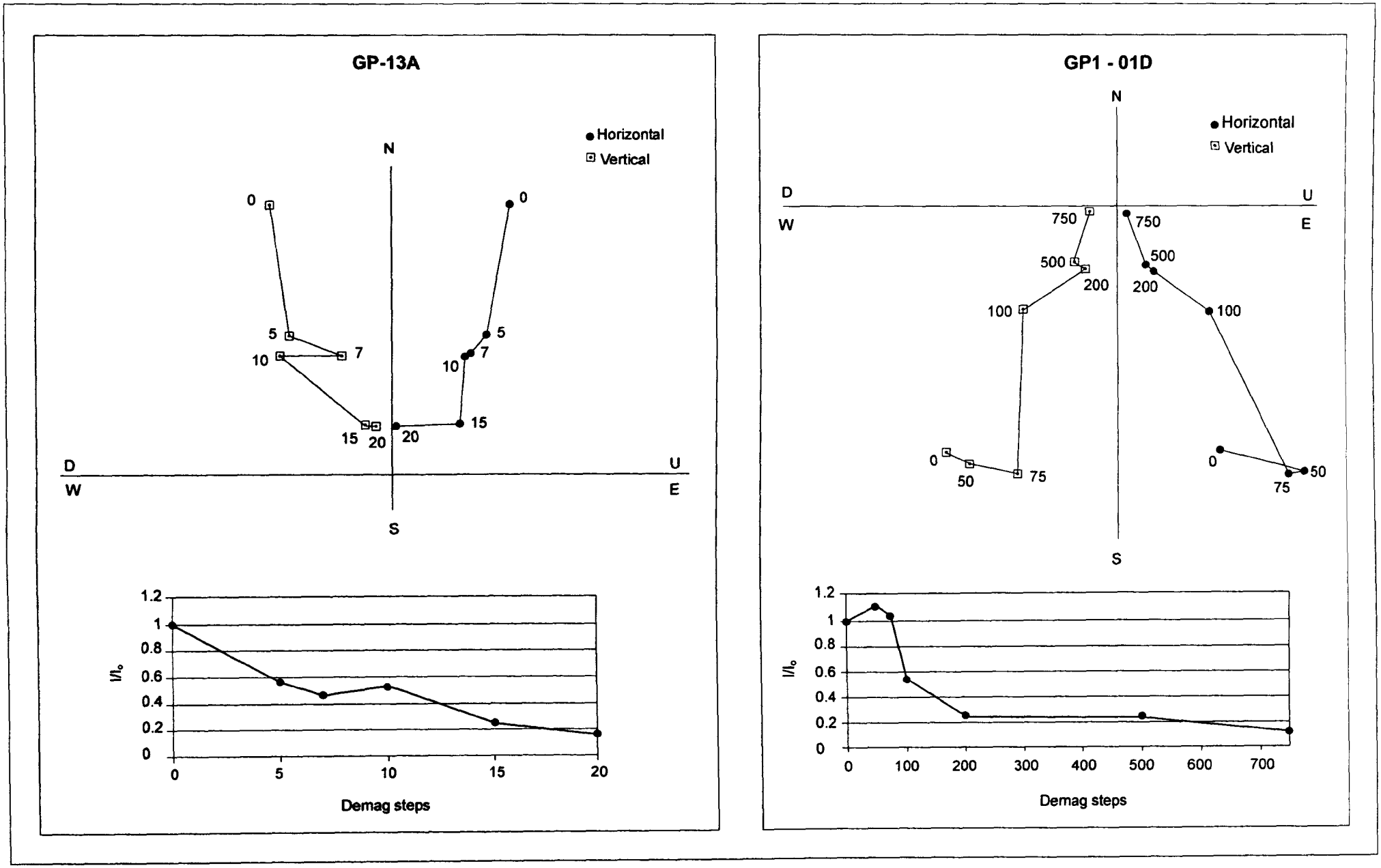

Figure 3.8. Cont.

was collected at the end of Bambui passage. Due to severe bioturbation, this sample yielded an indeterminate polarity. The highest and older level had normal polarity at the Mamute passage, and reversed polarity in two sites in Terra Fofa, 53 m above the cave stream.

3.4.1.5. Discussion

The presence of well defined levels in caves is generally accepted as caused by episodic response to external controls such as glacial erosion, rapid base level drop, or knickpoint recession (see review in Worthington, 1991) or lithological variations (Schmidt et al., 1984). Episodic uplift could also drain active levels and initiate lower ones. However, Worthington (1991) has pointed out that the development of cave levels can be primarily a function of aquifer length and stratal dip. Modern tectonic studies have suggested that uplift is continuous at the scale of denudational cycles and in stable cratonic areas occurs in response to denudational unloading (Summerfield, 1991a). Furthermore, the concept of long periods of erosion separated by abrupt uplift, as conceived by early geomorphologists such as King (1967) lacks critical support (Ollier, 1991, Summerfield, 1991a; but see Partridge and Maud, 1987), especially in tectonically stable areas. Therefore, we interpret the long term base level lowering at Gruta do Padre as having occurred at roughly constant rates, as assumed in other river incision studies (Sasowsky et al., 1995, Schmidt et al., 1984).

When trying to match the polarity changes in the cave sediment with the palaeomagnetic timescale, several possible alternatives exist. The assumption that downcutting rates were approximately constant in the timescale of cave development was applied in order to direct the data interpretation. Any interpretation that yielded wide variation in incision rates was discarded. Fig. 3.9 presents the preferred palaeomagnetic interpretation for Gruta do Padre levels. Going upwards from the zero datum of the river level, the reversed sediments present in the intermediate side passage at +25 m above the river are interpreted as belonging to the last reversed episode of the Matuyama Chron, between 0.99-0.70 Ma, giving base level lowering rates between 25-32 m/Ma. Assuming roughly constant rates, the reversal present at Tchau Brejões (+40 m) has to be placed in the reversed episode between 1.77-1.19 Ma, yielding incision rates between 26-34 m/Ma. Because the sediments at Tchau Brejões were deposited under phreatic conditions, at an unknown depth below the palaeo water table, the lower figure seems more likely. The Tchau Brejões reversal could not possibly be placed in more recent episodes because it would then imply much increased incision rates, which do not provide a reasonable match for the older normal polarity sites. In this interpretation the Jaramillo and Cobb Mountain subchrons have not been sampled in the cave. The Bambui level (+45 m) shows both reversed and normal polarity sediment, and can be correlated to the transition towards the Olduvai normal polarity subchron, at around 1.77 Ma, yielding an incision rate of around 25 m/Ma. The normal polarity site of the Mamute passage, of roughly similar elevation, is also placed in this subchron. The older Terra Fofa level (+53 m) is then correlated to the reversed episode that preceded the Olduvai Event, which ended at 1.95 Ma. This interpretation provides

approximately similar incision rates for all levels. Overall, the base level lowering rate at Gruta do Padre lies between 25-34 m/Ma, being likely that the true rate lies closer to the lower limit of this estimate. It is important to notice that any other interpretation (i.e., placing the Intermediate and Tchau Brejões levels in the same reversed subchron) would cause disparate incision rates in the sequence and thus were discarded.

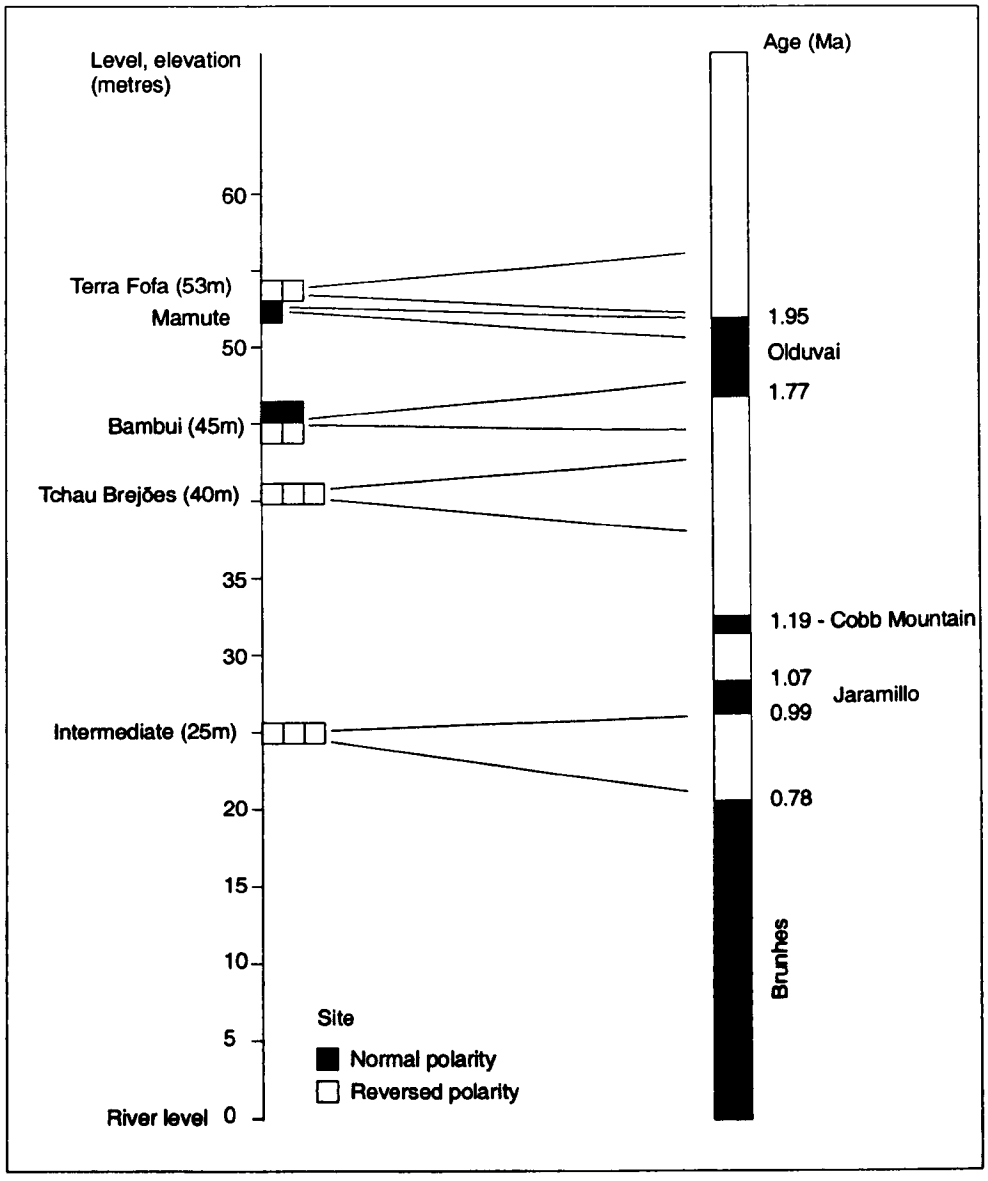

Figure 3.9. Preferred interpretation for palaeomagnetically dated levels of Gruta do Padre. Each site represents in average six samples.

A summary of incision rates in karst terrains is provided in Table 3.3. The base level lowering rates obtained in this study are in accordance with rates derived from similar geomorphic settings (see Table 3.1), and agree with denudation rates of 20-40 m/Ma inferred by apatite fission track for the São Francisco Craton since the breakup of South America and Africa (Harman et al., 1998). They are a little higher than the estimate of 18 m/Ma reported in another apatite fission track study by Amaral et al (1997). Considering the relatively low hydraulic gradients in the rivers in the area, the absence of knickpoints and the fact the major rivers levels are not perched above the water table, the fluvial incision rate of 25-34 m/Ma reported for Gruta

do Padre is likely to reflect the incision rate of the Corrente River, the base level river in the area, being probably also representative of the regional uplift rates.

Location	Rate (m/Ma)	Author
Cueva del Agua, Spain	c. 300	Smart, 1986
Nahanni River, Canada	< 800	Ford, 1973
Green River, Kentucky	70-90	Palmer, 1989
Matchlight Cave, Tasmania	< 100-200	Goede and Harmon, 1983
Exit Cave, Tasmania	< 60	Goede and Harmon, 1983
Yorkshire Dales, England	120	Waltham, 1986
	> 50 < 200	Gascoyne et al., 1983
Elwy Valley, Wales	120	Green, 1986
Creswell Crags, England	65	Rowe et al., 1989
Perlait River, Malaysia	8	Smart et al., 1988
Cheddar Gorge, England	190	Atkinson et al., 1978
	60	Smart et al., 1984
	200	Farrant, 1995
Crowsnest Pass, Canada	115-130	Ford et al., 1981
Bearjaw Cave, Canada	290-510	Ford et al., 1981
Castleguard Cave, Canada	50-130	Gascoyne et al., 1983
Arige Valley, France	120-210	Bakalowicz et al., 1984
Manifold Valley, England	55	Rowe et al., 1988
Derwent Gorge, England	< 190	Noel et al., 1984
Mammoth Cave, USA	40	Schmidt, 1982
Cheat River, USA	56-63	Springer et al., 1997
Buchan Karst, Australia	3-4	Webb et al., 1982
East Fork Obey River, USA	< 20	Sasowsky et al., 1998
Wee Jasper, Australia	26	Schmidt et al., 1984
Greenbrier River, USA	46	Selfridge, 1986
Santana Cave, Brazil	42	Karmann, 1994
Wyandotte Cave, USA	60	Pease et al., 1994
Clearwater Cave, Malaysia	190	Farrant et al., 1995

Table 3.3. Compilation of fluvial downcutting rates in karst terrains. Adapted from Atkinson and Rowe (1992) and Farrant (1995).

3.4.1.6. Implications for local landscape chronology

Two generations of planation surfaces have been identified above Gruta do Padre. The younger surface has elevations between 550 - 580 m immediately above the cave, tending to lower elevations as it approaches river valleys. This surface has been correlated with the Velhas Surface of King (1956a, 1967), or the Sul Americana II Surface of Valadão (1998). The age of the start of the Velhas Surface, through incision of an older surface, has not been chronologically constrained. Dating of the inception of planation surfaces has been traditionally associated with uplift events (King, 1967, Partridge and Maud, 1987). King (1956a) tentatively relates the beginning of the Velhas surface to a late Tertiary uplift, while Mabesoone and Castro (1975) believe that it could have started in the early Pleistocene. Valadão (1998) associates the start of the planation cycle related to the Sul Americana II surface with an uplift event in the Pliocene (3 Ma). No Tertiary uplift episodes were detected in apatite fission track studies of the São Francisco Craton (Harman et al., 1998, Amaral et al., 1997), making any relationship between (elusive) uplift episodes and planation surfaces uncertain.

An upper planation surface is now represented by flat topped residual hills at elevations of 660 - 700 m in the surroundings of the cave. These relict plateaux are remains of the extensive Sul

Americana Surface, created between late Cretaceous to early Miocene according to King (1956a). Other authors place the end of the Sul Americana pediplanation at the Oligocene (Mabesoone and Castro, 1975) or around the transition Miocene-Pliocene (Braun, 1971). In a recent review, Valadão (1998) interpreted that the Sul Americana Surface was the product of a long planation cycle between the Gondwana breakup (130 Ma) and a late Miocene uplift (10.8 Ma).

The relative elevation of the cave levels in relation to the surface, although known only with great uncertainty due to the non-existence of connection between the underground survey and topographical markers in the surface, suffice to allow a chronological relationship to be established. The river level is known to develop about 50 m below the cave entrance, which lies probably around 540 m in elevation. Through the cave survey and topographical map, it can be inferred that the oldest level, Terra Fofa, lies approximately at the 560 m elevation. Terra Fofa passage develops mostly below a plateau of the Sul Americana Surface, but its upstream end is below the Velhas/Sul Americana II plain (Fig. 3.7). Considering that Terra Fofa Passage is over 10 m high in places, whenever below the Velhas planation, it must lay very close to the surface, probably no more than 20 metres below it. In fact, several collapse dolines can probably be attributed to the surface interception of Terra Fofa level cave passages.

Terra Fofa level certainly predates the Velhas/Sul Americana II Surface, because when hydrologically active, it would have been located much deeper below ground. The underground river lies between 50 - 80 m below the Velhas/Sul Americana II plain at present. The depth to the phreatic zone is likely to have remained approximately in the same figures in the past due to the constant rates of uplift/denudation. This suggests that at the time of genesis of the upper levels of Gruta do Padre, the Velhas/Sul Americana II Surface was not present in the immediate vicinity of the cave, at least not in its present level and configuration. The early stages of Gruta do Padre are likely to have been generated entirely below the Sul Americana Surface, before the local generation of the Velhas/Sul Americana II Surface by scarp retreat. Since Terra Fofa Passage has been assigned a minimum magnetostratigraphical age of 1.95 Ma, the development of the present planation level of the Velhas/Sul Americana II Surface above the cave should postdate it. It is possible that the Velhas/Sul Americana II denudational cycle in the immediate surroundings of the cave occurred entirely within the Quaternary.

Unfortunately, although these planation surfaces have been traced through much of eastern Brazil, no chronological extrapolation can be done for other areas. This is because planation surfaces evolve by scarp retreat, the sections close to the residual plateaux of older surfaces being younger than those further away (Ollier, 1991). Furthermore, planation surface can also undergo vertical denudation, the resulting dissected surface being somewhat lower than the original surface. In fact, Valadão (1998) has mapped the Sul Americana II Surface in the area as being largely dissected, the original elevation being preserved only on fluvial divides. Considering that the Gruta do Padre site lies in the edge between the Velhas/Sul Americana II

and a previous planation surface, the Velhas/Sul Americana II Surface could be significantly older in other regions of Brazil.

CHAPTER 4
KARST GEOMORPHOLOGY OF SEMI-ARID NORTHEASTERN BRAZIL

4.1. KARST IN SEMI-ARID/ARID DOMAINS

Relatively little is known about karst landscapes in hot arid/semi-arid domains (Jennings, 1983, Ford and Williams, 1989) as this environment has been neglected in comparison with better studied temperate and humid tropical areas. This is probably due to the less than spectacular surface karst landforms displayed in these areas, and the assumed paucity of caves.

Solutional processes in karst terrains are largely driven by the H_2O-CO_2-$CaCO_3$ (meteoric) system. In this system, water runoff is the major factor in enhancing karst denudation rates (Smith and Atkinson, 1976, Gunn, 1986). Areas with little precipitation will tend to have poorly developed soils and little associated vegetation, with consequent low levels of biogenic CO_2. This is especially true for hot arid areas, where evaporation will decrease the effectiveness of the precipitation (Jennings, 1985).

In dry areas precipitation tends to be concentrated in short events that favour rapid surface runoff. In limestones, gullies tend to replace solution dolines (Sweeting, 1972) and with little solvent activity the limestone tends to behave as a resistant rock giving rise to structural relief (Jennings, 1983). Furthermore, mechanical weathering is likely to dominate net erosion, inhibiting the generation of typical karst landforms (Palmer, 1990). Smaller landforms such as karren tend to be infrequent and more poorly developed (Jennings, 1983). However, extensive deep phreatic circulation is known to occur in desert areas resulting in some of the world's largest springs (Ford and Williams, 1989, Jennings, 1983). Speleogenesis in dry lands will tend to be more limited, the major types of caves being vadose shafts and simple cut-off caves that capture the rapid runoff (Ford and Williams, 1989).

In summary, current wisdom claims that the limited availability of rainfall in arid areas will necessarily result in poorly developed surface and underground karst landforms. However, this does not appear to be the case in many of the dry karst areas of the world, where well developed underground karst features are known to occur. In fact, some of the world's most extensive caves are located in arid domains. Good examples are Jewel and Wind Caves (respectively 193 and 134 km long) located in the semi-arid temperate Black Hills area, northeastern United States (mean annual precipitation between 360-420 mm/yr) and Lechuguilla and Carlsbad Caves (162 and 50 km long) situated in the Guadalupe Mountains in the hot Chihuahuan Desert of southwestern United States (362 mm/yr) (Bakalowicz et al., 1987, Brook et al., 1990).

Many of the well developed karst landscapes now in dry lands can be ascribed to past wetter periods. These relict karst areas are widespread, and good examples are known from most the continents, for example at Kalahari Desert, Botswana (Brook et al., 1990). Such karst areas go through cyclic periods of development and "dormancy" related to pluvial/arid phases. On the other hand, many karst areas, although containing well developed caves, do not appear to have undergone major recent palaeoclimatic changes, for example the Nullarbor Karst in Australia (Lowry and Jennings, 1974, Goede et al., 1990). In other areas, although significant climate changes have occurred in the past, the caves appear not to be related to any past period of increased rainfall, as exemplified by the caves in the Black Hills and Guadalupe Mountains.

In meteoric karst systems, dissolution will tend to occur mostly near the surface. Ford and Williams (1989) have calculated that between 50-90% of the total dissolution will be concentrated in the uppermost 10 m of limestone. These figures have been revised by Worthington (1991) who claims that around 99% of the total dissolution will occur in the epikarst/surface zone. From these calculations it is clear that underground dissolution is responsible for a relatively minor amount of dissolution in relation to the surface. The immediate conclusion to be derived from these rates is that any meteoric karst that presents well developed endokarst features (caves) will also present widespread surface landforms.

In recent years there has been a growing awareness that non-biogenic CO_2-driven karst dissolution can play a major role in many karst systems. Non-meteoric acidity can be derived from subsurface processes that generate H_2CO_3 or H_2SO_4 through redox reactions or igneous activity (Palmer, 1991). Karst landforms where this type of process predominates have been termed Hypogenic Karst (Ford and Williams, 1989). The somewhat more restrictive term "Sulphuric Acid Karst" (Hill, 1990) has been proposed for karst systems where sulphide-oxidation driven mechanisms predominate. Hypogenic karst exhibits a series of diagnostic features on the scale of cave systems that will be discussed in detail in the following sections. At the scale of karst landscapes, however, the most obvious distinction between hypogenic and epigenic (meteoric) karst will be the disparity between the degree of development of surface and underground features. In a hypogenic karst, dissolution will occur solely in the subsurface, normally away from the epikarst zone, and no surface features (except subsurface related forms such as collapse dolines) will result. In the arid/semi-arid realm, where superficial landforms are subdued, a very contrasting style of karst terrain should evolve where the relatively poor development of surface karst features contrast markedly with well developed underground features. The lack of climate dependency enables hypogenic karst to be more easily recognised in arid lands, where the relative importance of these processes is greater (Fig. 4.1). In more humid regions, invading vadose streams tend to modify and mask hypogenic caves, making their recognition difficult (Palmer, 1991).

A strong contrast between the degree of development of surface and underground landforms is apparent in several karst regions of the world now known to have been largely generated by

hypogenic processes such as the Guadalupe Mountains (Hill, 1990, 1995), Black Hills (Bakalowicz et al., 1987, Palmer and Palmer, 1989), Namibia (Martini and Marais, 1996), Big Horn Basin, Wyoming (Egemeier, 1981), Central and Southern Italy (Galdenzi and Menichetti, 1995, Galdenzi, 1997), Buda Hills, Hungary (Dublyansky, 1995) among others. However, hypogenic caves are unrelated to surface features and tend to remain largely inaccessible from the surface, unless a fortuitous interception of the passages occurs by a surface valley or collapse. Our current sampling of hypogenic caves could therefore be strongly biased, the relative quantitative importance of hypogenic processes being probably greater than the 10% estimated by Palmer (1991) from present cave exploration and mapping. Similar conclusion was reached by Worthington and Ford (1995) based on a worldwide survey of sulphate and bicarbonate levels in karst springs.

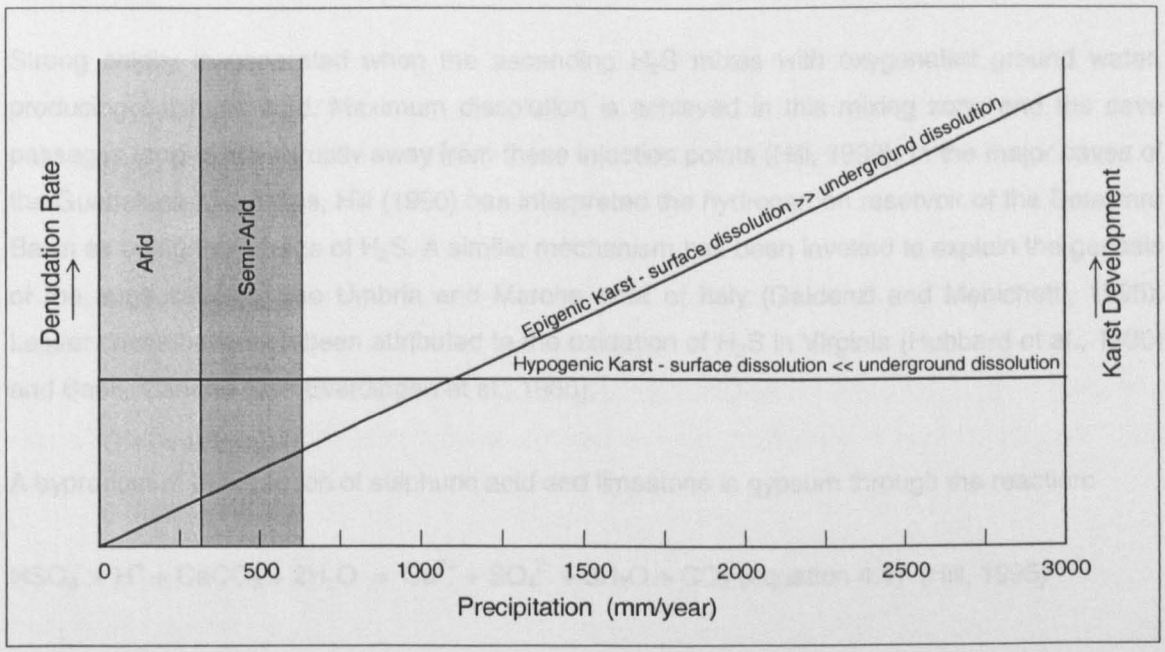

Figure 4.1. Schematic representation of the relative importance of hypogenic and epigenic components in several climatic settings. Hypogenic karst, if present, will predominate in arid / semi-arid domains. In humid climates meteoric dissolution will overwhelm hypogenic dissolution. Epigenic curve based loosely on Smith and Atkinson (1976).

4.2. MODES OF HYPOGENIC KARST DEVELOPMENT

Hypogenic caves can be classified according to the main acid involved in the carbonate dissolution. Two large groups are represented by hydrothermal caves generated by ascending CO_2 and caves generated by sulphuric acid dissolution (Ford and Williams, 1989). CO_2-related hydrothermal caves occur when deep waters associated with volcanic settings, connate water, or even meteoric water heated by deep circulation, rise through the soluble rock (Ford and Williams, 1989). Among the best known examples, there are the caves in the Buda Hills, Hungary (Dublyansky, 1995) and the Black Hills (Bakalowicz et al., 1997, Ford, 1989). The caves generated by this process are usually tri-dimensional mazes which display distinctive hydrothermal mineralogy, such as well developed phreatic calcite precipitates coating the walls. Stable isotope and fluid inclusion analysis of such precipitates have supported a hydrothermal

genesis for these caves (Dublyansky, 1995, Bakalowicz et al., 1987). Hydrothermal caves generated by CO_2-rich water do not appear to be prevalent in the eastern Brazilian karst and will not be discussed further.

Sulphuric acid processes are now accepted to be responsible for the generation of many extremely large and long caves. Sources of acidity are normally attributed to deep-seated processes such as migration of either gaseous or aqueous H_2S from sedimentary basins (Egemeier, 1981, Hill, 1990) or volcanic emissions (Hose and Pisarowicz, 1999). Processes causing the production of H_2S-rich water can include slow migration of deep circulating meteoric water, compaction of sediments causing discharge of basin brines, convective circulation of fluids in thermal plumes produced by igneous activity, and release of deep-seated water and gases from overpressurised zones by hydraulic fracture or tectonic activity (Palmer, 1991).

Strong acidity is generated when the ascending H_2S mixes with oxygenated ground water, producing sulphuric acid. Maximum dissolution is achieved in this mixing zone and the cave passages tend to die abruptly away from these injection points (Hill, 1990). In the major caves of the Guadalupe Mountains, Hill (1990) has interpreted the hydrocarbon reservoir of the Delaware Basin as being the source of H_2S. A similar mechanism has been invoked to explain the genesis of the large caves in the Umbria and Marche area of Italy (Galdenzi and Menichetti, 1995). Lesser caves have also been attributed to the oxidation of H_2S in Virginia (Hubbard et al., 1990) and Banff, Canada (van Everdingen et al., 1985).

A byproduct of the reaction of sulphuric acid and limestone is gypsum through the reaction:

$HSO_4^- + H^+ + CaCO_3 + 2H_2O = Ca^{2+} + SO_4^{2-} + 3H_2O + CO_2$ (equation 4.1) (Hill, 1995)

In situ conversion of the limestone into gypsum can occur, and some small caves are thought to evolve through such "replacement-solution" mechanism (Egemeier, 1981).

The role of bacteria in sulphuric acid karst is still largely unknown. Bacteria will aid the production of H_2S from hydrocarbons (Palmer, 1990, Hill, 1995) and will possibly be involved in the oxidation of H_2S, and in the dissolution of limestone (Hill, 1995).

An alternative source of acidity is the oxidation of sulphide minerals, notably pyrite. Ball and Jones (1990), Worthington (1991) and Lowe and Gunn (1995) have suggested that the oxidation of sulphide minerals can provide the necessary acidity for the initial enlargement of underground flow paths. This process could predominate even in epigenic settings, to be later overwhelmed by carbonic acid dissolution. Sulphuric acid karst due to sulphide oxidation will be explored in detail in the following section.

4.2.1. Pyrite oxidation in carbonate systems

Pyrite (FeS_2) and marcasite are readily oxidisable in near neutral pH. Pyrite oxidation has traditionally been regarded as unimportant in large scale underground dissolution in karst areas, being of only secondary importance in relation to deep-seated H_2S processes. The reasons given for that include the relatively slow rate of pyrite oxidation (Palmer, 1990) and the low concentration and dispersed nature of these minerals in the carbonate sequences (Ball and Jones, 1990, Palmer, 1991). The genesis of some small caves have been attributed to this mechanism (Morehouse, 1968). However, Durov (1956 in Egemeier, 1981) claimed that a significant part of cave dissolution in the former Soviet Union was due to pyrite dissolution. Auler (1995a) has suggested that pyrite oxidation may be responsible for the large cave systems in the Una Group carbonates of northeastern Brazil.

Pyrite oxidation is a complex and poorly known process because it involves the transfer of 7 or 8 electrons per sulphur atom (Moses et al., 1987). This transfer involves several different steps in the reaction, involving sulphur species of intermediate oxidation states which are very difficult to measure (Toran and Harris, 1989, Moses et al., 1987). Furthermore, there is competition between biological and abiological pathways (Toran and Harris, 1989). Bacteria of the genus *Thiobacillus*, especially *Thiobacillus ferrooxidans* are known for their ability to oxidise ferrous iron and sulphides (Ball and Jones, 1990). *T. ferrooxidans* bacteria thrive best between pH levels of 2-4 (Nicholson et al., 1988), but can operate with reasonable efficiency up to pH 6 (Ball and Jones, 1990). Other *Thiobacillus* species can catalyse oxidation paths in neutral pH (Toran and Harris, 1989).

Pyrite is unstable in waters containing dissolved oxygen, and will be readily oxidised according to the general reaction:

$2FeS_2 + 7O_2 + 2H_2O = 2FeSO_4 + 2H_2SO_4$ (equation 4.2) (Ball and Jones, 1990)

Under normal conditions, this reaction can lower the pH to values around 1.0-2.0 (Jorgensen, 1983). However, in karst systems $CaCO_3$ promotes buffering of the solution, and the pH tends to remain circumneutral. This reaction is likely to proceed mostly abiotically (van Breemen, 1988). Sulphuric acid reaction with calcite is described by equation 1 and releases CO_2, which in itself causes further carbonate dissolution.

The ferrous sulphate produced in reaction 4.2 can then be further oxidised in the presence of oxygen and sulphuric acid, producing ferric sulphate:

$4\ FeSO_4 + 2H_2SO_4 + O_2 = Fe_2(SO_4)_3 + 2H_2O$ (equation 4.3) (Ball and Jones, 1990)

This reaction, if occurring abiotically, can be the limiting step in the sulphide oxidation process. However, *T. ferrooxidans* can speed up the process by 5 or 6 orders of magnitude (van Breemen, 1988), and generate steady state ferric iron concentrations for the succeeding steps of the process. Ferric iron (Fe^{+3}) is a very important oxidant at low pH (Nicholson et al., 1988) and will cause further oxidation of pyrite:

$7\ Fe(SO_4)_3 + FeS_2 + 8H_2O = 15FeSO_4 + 8H_2SO_4$ (equation 4.4) (Ball and Jones, 1990)

In near neutral pH, typical of carbonate systems, ferric iron will be largely insoluble, and its role as an oxidant has been considered to be small (Nicholson et al., 1988).

The redox process will only be interrupted when one of the reagents is entirely consumed. This is likely to be the pyrite if it is present in small amounts. However, as the carbonate is dissolved, more pyrite is exposed and the entire chain of reactions can proceed. Another limiting factor in the pyrite oxidation reaction may be the availability of dissolved oxygen in the water. Ground water, especially in closed systems, has a low O_2. This is especially true of deep flow paths, where the contact between the ground water and the atmosphere is limited, and O_2 may be completely consumed by reaction along the flow path. In shallow karst settings (as in eastern Brazil) true closed systems are unlikely, and enough dissolved oxygen to drive the oxidation reaction may be present.

Sulphuric acid production through pyrite oxidation is a very effective carbonate dissolution reaction. In addition to the oxidation itself, CO_2 produced in equation 4.1 will cause further dissolution of the carbonate. The byproducts of this chain of reactions include sulphate, calcium and bicarbonate ions, and iron hydroxide.

4.3. HYDROCHEMICAL EVIDENCE OF HYPOGENIC KARST

Bicarbonate (HCO_3^-) is the main byproduct of epigenic karst dissolution. Hypogenic karst, on the other hand, will yield both HCO_3^- and SO_4^{2-}. The ratio between these two anions in karst springs should be a reliable tool in discriminating between epigenic and hypogenic karst. Worthington and Ford (1995) surveyed 404 karst springs around the world, and found that thermal springs, which comprised 25% of the sample, had median bicarbonate and sulphate concentrations of 292 and 135 mg/l, while the remaining non thermal springs had median concentrations of 187 and 13 mg/l. Based on this dataset, Worthington and Ford (1995) suggested that the thermal springs could represent active hypogenic systems, which would thus correspond to more than 10% of the total number of caves as had been suggested from a cave morphological survey by Palmer (1991). It should be noted that sulphate concentrations in springs do not unequivocally indicate sulphuric acid dissolution, because gypsum and anhydrite are highly soluble common constituents in many carbonate sequences and yield sulphate anions on dissolution. A more definite proof of hypogenic karst is the presence of H_2S dissolved in the ground water. This has

been demonstrated for a number of sites (Hubbard et al., 1990, Egemeier, 1981). However, it can not be applied in pyrite oxidation-driven hypogenic karst.

Worthington and Ford (1995) and Lowe and Gunn (1995) suggested that the initial enlargement of karst conduits is due mostly to dissolution by the sulphuric acid reaction. High levels of sulphate should be expected in the spring flow at this stage. As the breakthrough from laminar to turbulent flow occurs, more carbonate will be dissolved by carbonic acid and the relative importance of sulphate anions will decrease. Lowe and Gunn (1995) also hypothesised that there should also be a major change in the relative importance of bicarbonate during the transition from phreatic to vadose flow.

The hydrochemistry of hypogenic karst should also respond in a distinct way to seasonal climate variations. Morehouse (1968) suggested that sulphate levels should remain constant per unit discharge, regardless of rainfall variations, while bicarbonate levels, which are dependent on CO_2 productivity in the soil and vegetation, should tend to decrease during dry seasons. This hypothesis has not however been evaluated with field data.

4.4. CAVE MORPHOLOGICAL EVIDENCE OF HYPOGENIC KARST

As stressed earlier, a major distinction between hypogenic and epigenic karst should be the comparative disparity in the degree of development between surface and underground karst. At the scale of the cave system and cave passages there will be a series of diagnostic features which will aid in distinguishing between hypogenic caves and their epigenic counterparts:

1. Lack of relationship with the surface (Egemeier, 1981). Epigenic caves develop synchronously with the surface, through inputs from swallets and closed depressions (Palmer, 1991). Hypogenic caves, on the other hand, need not relate in any way to the surface geomorphology. Entrances are created by chance interception of passages by surface lowering, valley downcutting or collapse.

2. Ramiform pattern (Palmer, 1991). This type of cave pattern is characterised by irregular rooms and galleries that wander three-dimensionally outward from focal points of development. Branchwork patterns typical of epigenic caves are absent.

3. Abrupt variation in cross sections (Bakalowicz et al., 1987). In epigenic caves passage cross section changes relatively slowly, but in hypogenic caves narrow passages can suddenly become large chambers. There is also no easy distinction between main passages and the smaller tributary side passages observed in epigenic caves.

4. Large passages may end abruptly in the bedrock (Hill, 1990). This is probably due to the neutralisation of the acid by bedrock away from the input point. Passages in epigenic caves usually end in sediment plugs, breakdown or lead to an entrance.

5. Levels of passages, when present, have developed simultaneously (Bakalowicz et al., 1987). In epigenic caves, higher levels represent former active passages that have been drained due to water table lowering, and can be significantly older than lower levels.

6. Lack of fluvial sediments (Dublyansky, 1980 in Bakalowicz et al., 1987). Some sort of fluvial sedimentation is present in nearly all epigenic caves. In hypogenic caves, they will be present only if later invasion streams have intercepted the cave system.

7. Lack of scallops or other directional marks (Palmer, 1991). Hypogenic caves lack the ubiquitous scallop marks so common in river caves. The identification of the direction of flow in hypogenic cave is not straightforward.

8. Condensation-corrosion features (Palmer, 1991). CO_2 produced by equation 4.1 will dissolve subaerial limestone surfaces, producing features such as cupolas, domes, blind pockets and residual dolomitic sand (although some of these features may be generated during the cave forming process).

9. Presence of blowholes on the surface (Lowry and Jennings, 1974). Many entrances to hypogenic caves are relatively small openings into vast cave systems. These limited openings discharge air from the substantial cave void in response to changes in the external air pressure and temperature, flowing being out during the day and in at night.

10. Frequent gypsum deposits (Hill, 1987). Gypsum will be produced by equation 4.1 and it is likely to predominate over normal carbonate speleothems. In some caves it can form massive deposits several tons in weight and it can also precipitate on the walls or can replace the limestone (Egemeier, 1981). Other sulphur related minerals, such as alunite, can also be present (Polyak et al., 1998).

11. Presence of acid clay minerals (Hill, 1990). Minerals such as endellite are generated under very acidic conditons in sulphuric acid environments (Hill, 1990). Endellite is derived by sulphuric acid attack on montmorillonite clays, and may indicate a hypogenic origin (Hill, 1990).

12. Presence of bacterially produced filaments (Cunningham et al., 1995). Unusual speleothems containing organic filaments, related to bacterial activity occur in some hypogenic caves. These biogenic formations may represent the primary producers in a subterranean ecosystem unique to these caves.

All of the criteria listed above have been described from deep seated hypogenic caves. Their existence in "shallow" hypogenic settings related to metal sulphide oxidation has not been adequately assessed. It is believed, however, that many of them should apply in these caves.

4.5. UNA KARST

4.5.1. Geology and geomorphology

The Neoproterozoic carbonate rocks of the Una Group occur in the northern half of the state of Bahia (Fig. 4.2), and comprise a series of separate basins divided by quartzite mountain ranges. The sequence starts with a basal glaciogenic unit, known as the Bebedouro Formation (Misi and Veizer, 1998) which is composed largely of diamictites overlain by arkosic quartzites (Fig. 4.3). The upper part of the Una Group comprises the Salitre Formation, a marine carbonate sequence over 300 m thick (Fig. 4.3). Of particular interest is the presence of rich sulphide and phosphatic strata which mostly occur in unit B1 of the Salitre Formation. Massive subsurface sulphides have been described in detail at only one site, but iron sulphide (both disseminated and in lenses) is known to occur in several areas, and a strong sulphur smell commonly issues after striking many of the outcrops of the Salitre Formation, for instance unit A1 (Negrão, 1987). The occurrence of further major sulphide deposits in the Una Group is possible given the sparse geological work performed in the area. The Una Group is underlaid largely by the Mesoproterozoic quartzites and pellites of the Chapada Diamantina Group.

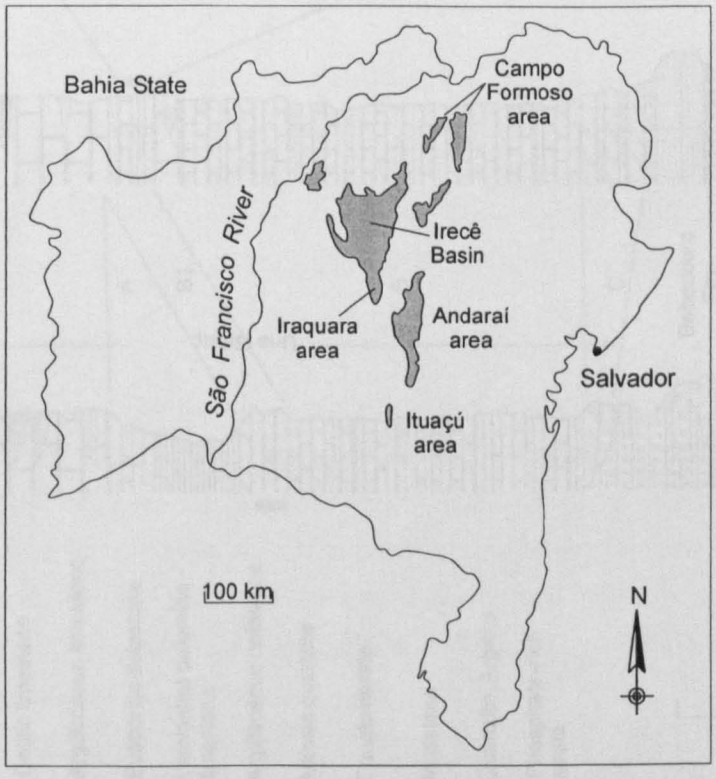

Figure 4.2. Areal distribution of the Una Group. From Schobbenhaus (1981).

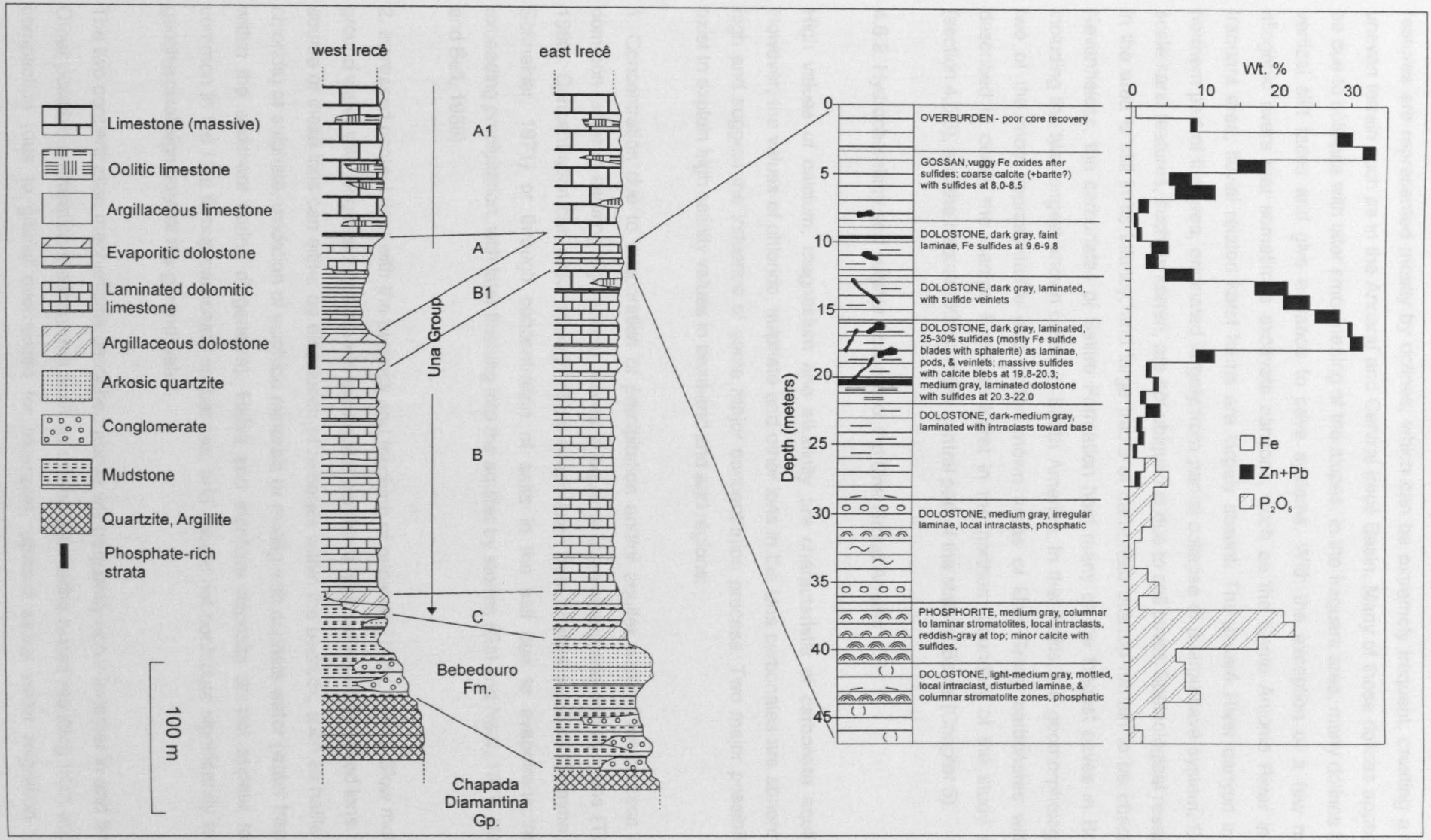

Figure 4.3. Stratigraphy of the Una Group in the Irecê Basin, and detailed geological column of the sulphide/phosphorite deposit of unit B1 at Três Irmãs area. From Misi and Kyle (1994).

Most of the carbonate bedrock surface is covered by a thick soil sequence. Surface karst features are represented mostly by dolines, which can be extremely frequent, creating a very uneven terrain such as in the Andaraí and Central Irecê Basin. Many of these dolines appear to be due to collapse with later smoothening of the slopes. In the Iraquara area, many dolines have vertical cliff faces and give entrance to cave systems. With the exception of a few major allogenic rivers that sometimes excavate canyons, such as the Santo Antonio River in the Iraquara area, fluvial related karst forms are largely absent. The Jacaré River canyon in the northern part of the area, originated largely from partial collapse of a large cave system. Small scale karst features, such as karren, are not ubiquitous due to soil cover. Speleological research in the area is still in its infancy, and large tracts of carbonate outcrop remain to be checked. Nevertheless, the carbonates of Salitre Formation host many of the longest caves in Brazil, including the two longest known caves in South America. In this thesis, the geomorphology of two of the most representative and better known areas of Una Group carbonates will be described in detail, the Campo Formoso Karst in the northern boundary of the study area (section 4.5.3), and the Iraquara Karst in the central part of the state of Bahia (Chapter 5).

4.5.2. Hydrochemistry and sulphur isotopes of the Una Group Aquifer

High values of calcium, magnesium and alkalinity are characteristic of carbonate aquifers. However, the values of chloride, sulphate and other ions in the Una carbonates are abnormally high and suggest the influence of some major concentration process. Two major possibilities exist to explain high salinity values in semi-arid and arid regions:

1. Concentration due to evaporation of precipitation and/or aquifer water. This process is a common factor in causing high salinity values in aquifers in semi-arid and arid domains (Todd, 1980). Concentration can occur through direct evaporation from shallow aquifers (Swayne and Schneider, 1971) or through concentration of salts in the soil due to evapotranspiration exceeding precipitation, with later flushing into the aquifer by storms (Gat and Naor, 1979, Hamill and Bell, 1986).

2. Increased contact time with the bedrock and leaching of minerals (Todd, 1980). Slow moving ground water with long residence time in the aquifer can have high values of dissolved ions. The source of these ions can either be dissolution of minerals within the bedrock, such as halite (for chloride) or sulphate, oxidation of sulphide minerals or mixing with connate water (water trapped within the sediment during diagenesis). Halite and sulphate deposits do not appear to be common in the Una Group carbonate sequences, and should not contribute significantly to the geochemical signature of the ground water.

The two concentration mechanisms described above will frequently occur together in arid lands. Other possible salinisation mechanisms such as mixing with saline brines resulting from aquifer compaction (due to glacial overburden for example), upward saline water migration from

hydrocarbon rich basins (Domenico and Schwartz, 1998), or hydrothermal brines associated with volcanic activity must be rejected for the study area on geological grounds.

Early work on the ground water hydrochemistry of the Una Group carbonates has demonstrated a high salinity for these waters (Siqueira, 1978). A compilation of available hydrochemical data from wells, springs and vadose water for the Salitre carbonates (Appendix 1) was performed based on data from CERB (1983), Siqueira (1978), Martins (1986) and CERB (unpublished data). A summary of these values is given in Table 4.1. It should be noted that the hydrochemical data derived from the literature is of uncertain quality. Techniques for sampling, preservation and analysis are often not specified, and the geological control on the sampling site is poor or non-existant. Even the location of some sites cannot be determined with precision. It is thus likely that some sampling sites represent water with contributions from non-carbonate sources. The quality of the hydrochemical data reported in the literature was tested through ion balance in all analyses. Major parameters (usually alkalinity or nitrates) are lacking in many of the reported analyses, precluding the application of this technique. In the 122 analyses where all major parameters had been reported, only 56 (46%) had an ion balance error below 5%. These samples were labelled as reliable (Good), while samples with error above 5% were labelled "Poor". Incomplete samples are the ones in which the analysis lacks at least one major ion.

A. All data

	n	mean	maximum	minimum
SO_4^{2-}	191	1.64	20.63	0.02
Cl^-	191	12.17	535.97	0.11
HCO_3^-	166	4.82	9.10	0.62
Ca^{+2}	191	6.60	248.25	0.61
Mg^{+2}	191	4.63	293.22	0.20
Na^+	169	6.70	377.64	0.28
K^+	169	0.30	16.69	0.03
NO_3^-	167	1.90	193.52	0

B. Mean values divided in sectors

	n	SO_4^{2-}	Cl^-	HCO_3^-	Ca^{+2}	Mg^{+2}	Na^+	K^+	NO_3^-
northern sector	20	1.25	14.80	5.13	4.04	3.65	8.42	0.55	0.38
southern sector	30	0.63	3.91	2.92	4.83	2.71	0.79	0.10	0.06
ocean	mean	28.21	545.84	2.32	9.98	53.06	468.03	10.20	-

C. Student's t test for northern and southern samples

	t-test
SO_4^{2-} (north) vs SO_4^{2-}(south)	t = 2.22, p = 0.033
Cl^- (north) vs Cl^- (south)	t = 2.93, p = 0.008

Table 4.1. Summary of the hydrochemical data for Una carbonate aquifer. Values in mmol/l. Northern sector data includes samples Sali-1 to 20 plus UNA-21 and 22. Southern sector data comprises samples Iraq-1 to 22 plus UNA-1 to 10. See appendix 1 for analyses. Ocean data from Drever (1997).

Mean annual precipitation in the Una Group region ranges from around 1100 mm in the southern part of the Iraquara area (Cruz Jr., 1998) to around 400 mm in the northern Campo Formoso Karst area (Martins, 1986). Evapotranspiration exceeds precipitation over the entire

area. Water deficit can range from 100 mm in the southern areas (Cruz Jr., 1998) to over 1700 mm in the drier northern portion (Martins, 1986). Evaporative concentration therefore has the potential to be important in controlling the chemical signature of ground waters in the study area. On the other hand, frequent occurrences of sulphide in the carbonates can provide another source of sulphate ions. The geomorphological consequences of evaporative processes will be restricted to the generation of surface deposits such as calcrete or travertine, while sulphide oxidation, if present, can be a major process in creating secondary porosity in the carbonates. The following section will consider the relative importance of these two processes.

4.5.2.1. Hydrochemistry

Major ions analysis of ground water in the Una carbonates show a great spread in the data (Table 4.1). In a sense this is to be expected considering the very large extent of the area and local changes in climate and geology. Furthermore, samples come from wells that tap the aquifer at distinct depths, and may therefore represent the waters derived from different lithological horizons. Due to considerable scatter in the data, values that presented high standard deviations and high leverage were eliminated during regression analysis. These data are believed to represent erroneous chemical analysis.

Sources of sodium and chloride are absent in the Una Group carbonates, and the high values of these parameters are suggestive of evaporative concentration. Fig. 4.4. shows the relationship between sodium and chloride. There is a good correlation in all sets of data (good, poor, incomplete, overall data R^2 = 0.74), indicating that evaporative concentration from an atmospheric source is responsible for the high Na and Cl values as suggested by Siqueira (1978) and Negrão (1987). Unfortunately, the chemistry of rainfall is not known for the area, as data reported by Tavares (1983) is believed to show contamination from dust from the soil (Guerra, 1986). However, the slope of the trend line for all values (0.79) is close to what would be expected from dilution from sea water, suggesting that rainfall derived from the ocean can be the ultimate source of these ions.

Sulphate, calcium and magnesium values are also high in the Una Group aquifer, and can be derived either from evaporation, or from reactions within the bedrock. Sulphate values, in particular, can indicate pyrite oxidation and sulphuric acid dissolution. The relative importance of sulphuric acid dissolution in relation to carbonic acid can be assessed through molarity balance (Table 4.2). Limestone and dolomite dissolution by sulphuric acid will yield a $(Ca+Mg)/HCO_3$ molar ratio of 1, while the ratio in carbonic acid reactions will be 0.5. In ideal conditions, where there is no other source of these ions, this ratio should never exceed 1. However, the histogram in Fig. 4.5 shows that the majority of the analyses (regardless of quality), show ratios above 1. This effect can be caused either by consistent underdetermination of alkalinity, e.g. due to degassing prior to determination, or by addition of Ca and Mg from another source. One possibility is the concentration in soil of rainfall derived from predominantly oceanic sources

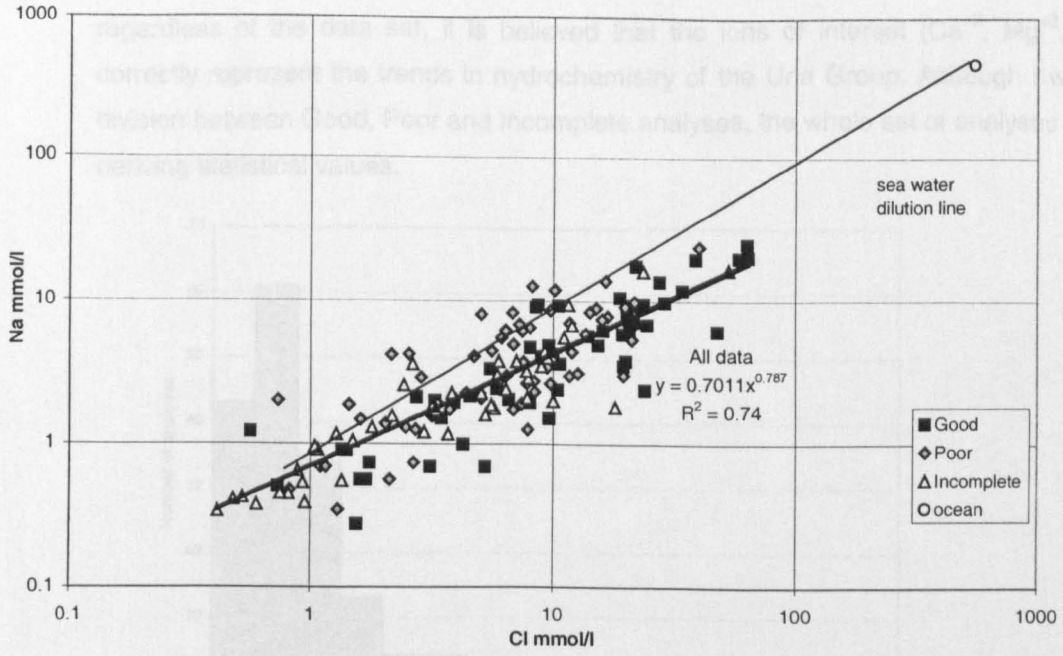

Figure 4.4. Correlation between sodium and chloride and sea water dilution line.

H_2SO_4

Reaction	(Ca+Mg)/HCO_3 (moles)	(Ca+Mg)/SO_4
Limestone $2CaCO_3 + H_2SO_4 = 2Ca^{+2} + SO_4^{2} + 2HCO_3$	(2+0)/2 = 1	(2 + 0)/1 = 2
Dolomite $Ca,Mg(CO_3)_2 + H_2SO_4 = Ca^{2+} + Mg^{2+} + SO_4^{2} + 2HCO_3$	(1 + 1)/2 = 1	(1 + 1)/1 = 2

H_2CO_3

Limestone $CaCO_3 + H_2CO_3 = Ca^{2+} + 2HCO_3^-$	(1 + 0)/2 = 0.5	-
Dolomite $Ca,Mg(CO_3)_2 + 2H_2CO_3 = Ca^{+2} + Mg^{+2} + 4HCO_3^-$	(1 + 1)/4 = 0.5	-

Table 4.2. Molarity balance of sulphuric acid and carbonic acid reactions.

(cyclic salts). (Ca+Mg)/HCO_3 ratios in sea water are very high (27.1), and could provide a possible source for the excess Ca and Mg. However, analysis of (Ca+Mg)/SO_4 molar ratios show a distinct picture. From Table 4.2, one should expect for the area values around 2 if bedrock sulphide is the sole source of acidity. The overall ratio for Una Group groundwater is 6.85, which demonstrates that carbonic acid dissolution is actively occurring in the area. The (Ca+Mg)/SO_4 molar ratio for sea water is 2.23 is thus sea water does not appear to be a major source of these ions. This data suggests that alkalinity values are probably underestimated. Alkalinity is a sensitive parameter and measurement should be performed as soon as possible after collection. According to notes on the analysis reports, laboratory analysis was performed several days (or even weeks) after sampling. I believe that many of the alkalinity values reported in the analysis are unreliable and should not be used as an aid to interpret the hydrochemistry of the area. In carbonate aquifers, alkalinity values are an important component of the ionic budget. As such, the ionic balances performed in the analyses should fail to truly represent the reliability of the analyses. Considering that the sodium and chloride regression showed a good correlation

regardless of the data set, it is believed that the ions of interest (Ca^{+2}, Mg^{+2}, SO_4^{2-}) should correctly represent the trends in hydrochemistry of the Una Group. Although I will maintain the division between Good, Poor and Incomplete analyses, the whole set of analyses will be used for deriving statistical values.

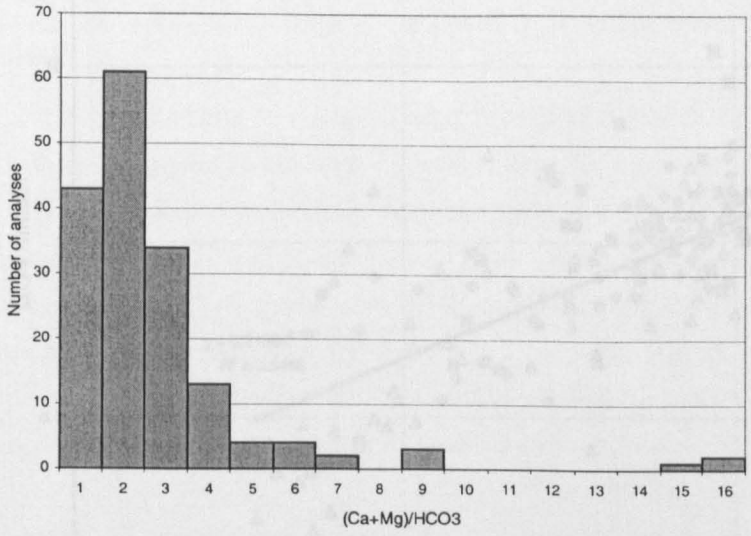

Figure 4.5. Histogram of (Ca+Mg)/HCO_3 ratios.

Fig. 4.6 plots sulphate and chloride values for all analyses and indicates a good correlation (R^2 = 0.55) between these parameters, suggestive of evaporative concentration. Values above the trend line show excess sulphate that could originate from bedrock sources, in which case sulphate should correlate with an excess in Ca^{+2} and Mg^{+2} which are cations also derived from bedrock reactions. In order to test this hypothesis, a plot of (Ca + Mg) against chloride was produced (Fig. 4.7). Because sea water (a possible source of the ions) has an excess in magnesium (Ca/Mg molar ratio = 0.19), magnesium values were "corrected" according to the following scheme:

$$Mg_{corrected} = Mg_{gw} - [Cl_{gw} \times (Mg/Cl)_{sw}] \quad \text{(equation 4.5)}$$

where sw - sea water
gw - ground water
all values in mmol/l

Any excess in Ca + Mg values in Fig. 4.7 (analyses above the trend line) should represent either Ca and Mg derived from bedrock (dolomite or limestone) or derived from atmospheric dust (non related to sea water rainfall), and in the later case there should be no correlation between excess sulphate and excess Ca + Mg. This correlation was tested using a χ^2 test on a 2x2 contingency matrix (Table 4.3). The χ^2 test suggests a highly significant association (χ^2 = 7.455, significant at the 99% confidence interval) between sulphate and Ca + Mg, indicating that sulphate is being produced by reactions within the bedrock.

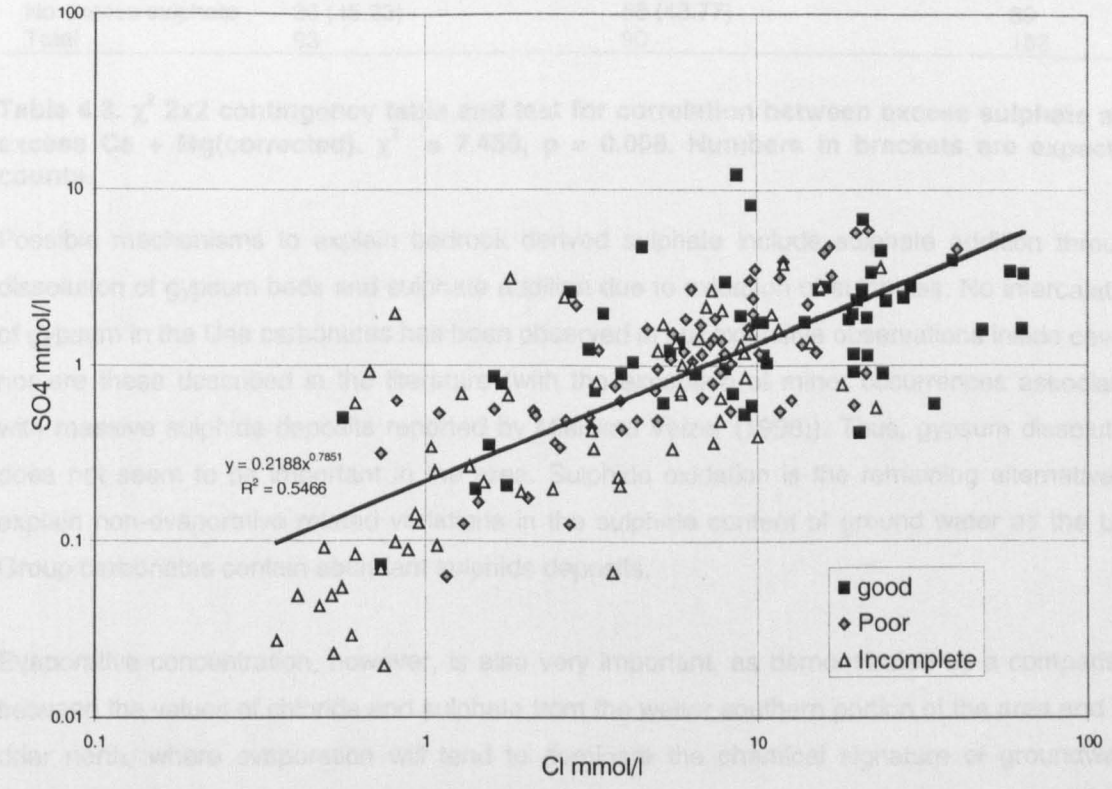

Figure 4.6. Plot of sulphate and chloride and trend line.

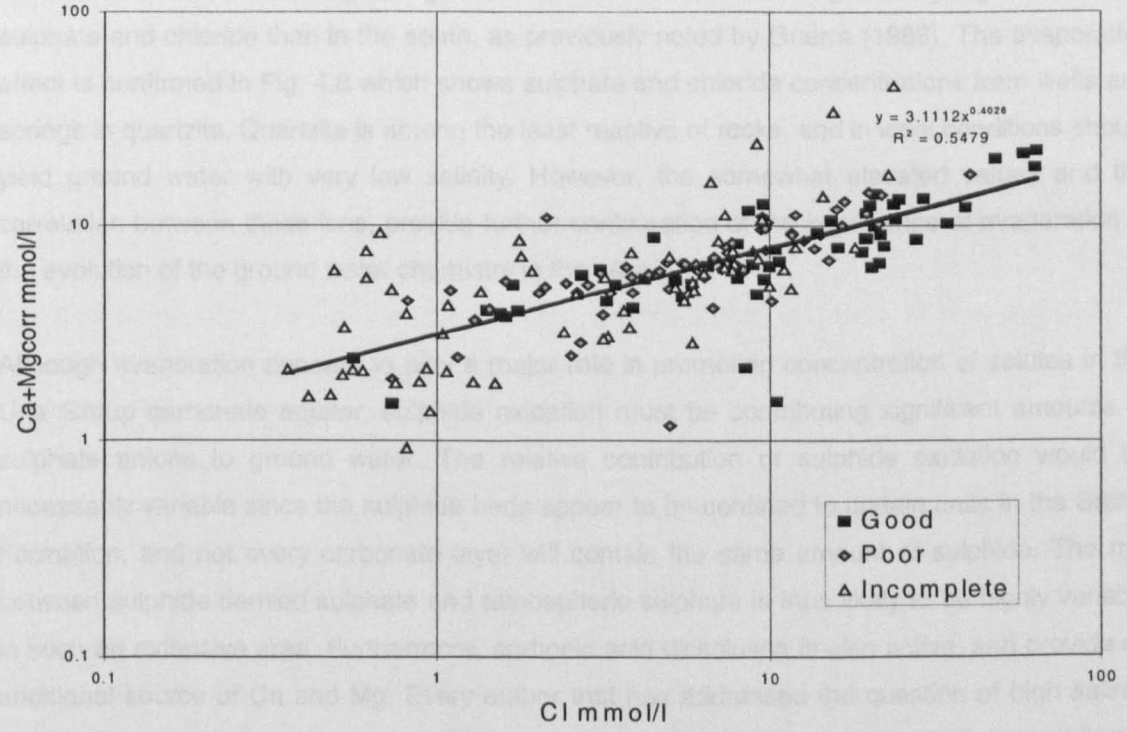

Figure 4.7. Plot of calcium + magnesium (corrected) and chloride.

	Excess Ca + Mg(corrected)	No excess Ca + Mg (corrected)	Total
Excess sulphate	57 (47.77)	37 (46.23)	94
No excess sulphate	36 (45.23)	53 (43.77)	89
Total	93	90	183

Table 4.3. χ^2 2x2 contingency table and test for correlation between excess sulphate and excess Ca + Mg(corrected). χ^2 = 7.455, p = 0.006. Numbers in brackets are expected counts.

Possible mechanisms to explain bedrock derived sulphate include sulphate addition through dissolution of gypsum beds and sulphate addition due to oxidation of sulphides. No intercalation of gypsum in the Una carbonates has been observed in our extensive observations inside caves, nor are these described in the literature (with the exception of minor occurrences associated with massive sulphide deposits reported by Misi and Veizer (1998)). Thus, gypsum dissolution does not seem to be important in the area. Sulphide oxidation is the remaining alternative to explain non-evaporative related variations in the sulphate content of ground water as the Una Group carbonates contain abundant sulphide deposits.

Evaporative concentration, however, is also very important, as demonstrated by a comparison between the values of chloride and sulphate from the wetter southern portion of the area and the drier north, where evaporation will tend to dominate the chemical signature of groundwater (Table 4.1). Student's t test shows that chloride values between the two areas are significantly different at 99% confidence interval, while sulphate values are significantly different at 95% confidence interval, indicating that groundwater in the north have significantly higher values of sulphate and chloride than in the south, as previously noted by Guerra (1986). The evaporative effect is confirmed in Fig. 4.8 which shows sulphate and chloride concentrations from wells and springs in quartzite. Quartzite is among the least reactive of rocks, and in ideal conditions should yield ground water with very low salinity. However, the somewhat elevated values and the correlation between these ions, provide further confirmation of the importance of evaporation in the evolution of the ground water chemistry in the area.

Although evaporation appears to play a major role in promoting concentration of solutes in the Una Group carbonate aquifer, sulphide oxidation must be contributing significant amounts of sulphate anions to ground water. The relative contribution of sulphide oxidation would be necessarily variable since the sulphide beds appear to be confined to certain units in the Salitre Formation, and not every carbonate layer will contain the same amount of sulphide. The mix between sulphide derived sulphate and atmospheric sulphate is thus likely to be highly variable in such an extensive area. Furthermore, carbonic acid dissolution is also active, and provide an additional source of Ca and Mg. Every author that has addressed the question of high salinity levels in the Una carbonate aquifer (Siqueira, 1978, Guerra, 1986, Negrão, 1987) has attributed the high sulphate levels to pyrite oxidation. The data here presented suggests that, while sulphide oxidation is an important process within the Una aquifer, evaporative concentration plays a major role especially in the drier areas to the north.

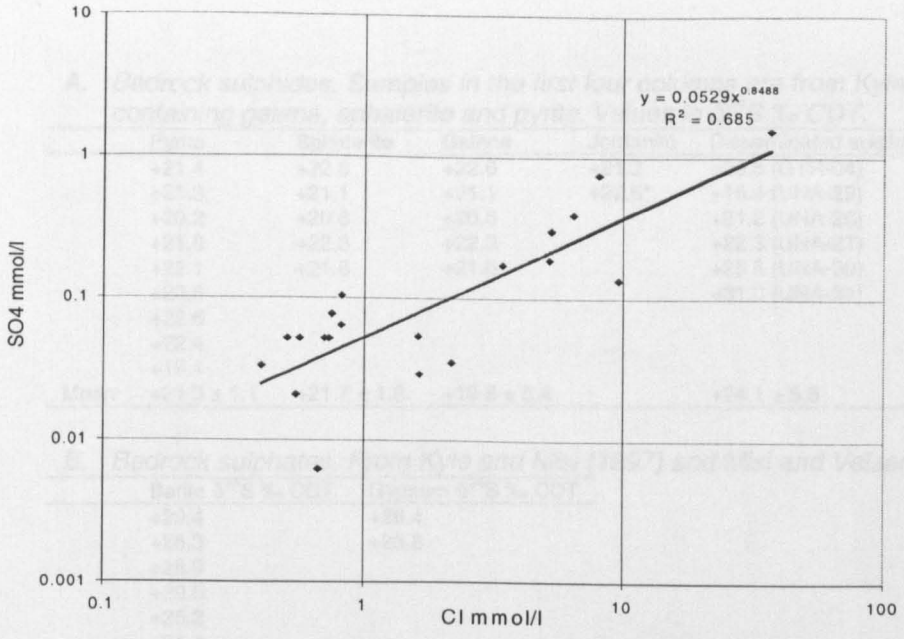

Figure 4.8. Sulphate and chloride correlation for quartzite ground water.

4.5.2.2. Sulphur isotopes

Sulphur isotope studies, when coupled with hydrochemical analysis, can be a useful tool for inferring sources of sulphate and providing information on the geochemical evolution of ground water (Rightmire et al., 1974, Rye et al., 1981, Krothe and Libra, 1983, Sacks et al., 1995). In karst systems, this technique has been applied to determine sources of sulphate in cave precipitates (Yonge and Krouse, 1987), sources of acidity in hypogenic settings (Hill, 1990, van Everdingen et al., 1985), in coastal mixing-zone areas (Bottrell et al., 1991) and in thermokarst settings (Lauritzen and Bottrell, 1994).

Table 4.4 presents $\delta^{34}S$ data for ground water, carbonate bedrock sulphide and sulphate, and cave precipitates in the Una sequence, and Fig. 4.9 shows location of sampling sites. The values for sedimentary sulphur are in agreement with the global estimates of Claypool et al. (1980) and Strauss (1993), and match isotopic values reported from the correlative Bambuí carbonates to the south (Iyer et al., 1992).

The hydrochemical data discussed in the previous section suggests that sulphate in Una carbonate ground waters derives from both atmospheric-derived sulphate (through evaporative concentration) and oxidation of bedrock sulphide. Bedrock sulphide displays $\delta^{34}S$ values of +21.8 ± 3.6‰. Ground water sulphate $\delta^{34}S$ values are significantly lower, (+14.8 ± 3.7‰) an average depletion of 7‰. Rain water $\delta^{34}S$ has not been analysed in the area but Rightmire et al. (1974) reported global values between +19.4 and -1.5‰. Isotopically heavy atmospheric sulphate is derived from marine aerosols, while lighter values (-1.5 to +6‰) characterise remote continental areas. A value between +5 to +8‰ may be close to the actual $\delta^{34}S$ rainfall value for the study area. No sulphur isotope fractionation usually occurs during sulphide oxidation (Nakai and Jensen, 1964, Toran and Harris, 1989), and thus sulphate derived from sulphide should

*A. Bedrock sulphides. Samples in the first four columns are from Kyle and Misi (1997). *sample containing galena, sphalerite and pyrite. Values in $\delta^{34}S$ ‰ CDT.*

	Pyrite	Sphalerite	Galena	Jordanite	Disseminated sulphide (This study)
	+21.4	+22.6	+22.6	+21.2	+29.5 (GTR-04)
	+21.3	+21.1	+21.1	+22.5*	+15.4 (UNA-29)
	+20.2	+20.8	+20.8		+21.2 (UNA-26)
	+21.8	+22.3	+22.3		+22.3 (UNA-27)
	+22.1	+21.6	+21.6		+25.5 (UNA-30)
	+20.6				+31.0 (UNA-31)
	+22.6				
	+22.4				
	+19.1				
Mean	+21.3 ± 1.1	+21.7 ± 1.8	+19.8 ± 5.4	-	+24.1 ± 5.8

B. Bedrock sulphates. From Kyle and Misi (1997) and Misi and Veizer (1998).

	Barite $\delta^{34}S$ ‰ CDT	Gypsum $\delta^{34}S$ ‰ CDT
	+29.4	+26.4
	+25.3	+25.8
	+25.9	
	+29.6	
	+25.2	
	+31.4	
	+30.9	
	+32.8	
	+32.8	
	+29.1	
	+31.9	
Mean	+29.5 ± 2.9	+26.1 ± 0.4

C. Sulphate in ground water (this study)

Sample	Type	$\delta^{34}S$ ‰ CDT
UNA-05	well	+15.5
UNA-07	well	+22.3
UNA-10	well	+13.2
UNA-11	well	+17.6
UNA-12	well	+15.2
UNA-13	well	+20.0
UNA-14	well	+15.0
UNA-15	well	+11.9
UNA-17	well	+13.1
UNA-18	well	+11.9
UNA-19	well	+15.4
UNA-20	well	+17.0
UNA-21	well	+6.8
UNA-23	rimstone dam (vadose)	+14.2 (north)
UNA-24	rimstone dam (vadose)	+12.6 (north)
Mean		+14.8 ± 3.7

D. Sulphate in cave secondary deposits (this study)

Sample	Cave	Type	$\delta^{34}S$ ‰ CDT
TUB-01	Toca da Umburana	gypsum flower	+28.3 (south)
GDM-01	Gruta Diva de Maura	gypsum flower	+22.2 (south)
BST-01	Buraco da Santa	gypsum crust	+22.8 (south)
GTR-02	Gruta da Torrinha	gypsum needles	+26.3 (south)
GLB-01	Gruta do Labirinto	gypsum crust (with phosphate)	+14.0 (south)
TCC-02	Toca do Calor de Cima	gypsum crust (with phosphate)	+17.3 (north)
TBV-05	Toca da Boa Vista	gypsum/bassanite chandelier	+14.8 (north)
TBV-08	Toca da Boa Vista	gypsum crust (with dolomite)	+15.1 (north)
Mean			+20.1 ± 5.5

Table 4.4. Summary of $\delta^{34}S$ analyses for bedrock sulphide, bedrock sulphate, ground water sulphate and speleothems for the Una Group. Location in Fig. 4.9.

exhibit $\delta^{34}S$ values similar to sulphide values. If ground water sulphate is derived from both sources, its $\delta^{34}S$ values should fall within these limits. Fig. 4.10 shows that such is the case. The uncertainty associated with the lack of rain water isotopic values for the area precludes a more thorough interpretation of the data. As discussed in the previous sections, bedrock sulphates are

an unlikely sulphate source for the ground water because of its relative low concentration in the carbonate. This is also suggested by the isotopic data since the majority of the ground water or speleothem samples do not show values close to the $\delta^{34}S$ values of bedrock sulphate (mean +29.0 ± 2.9‰).

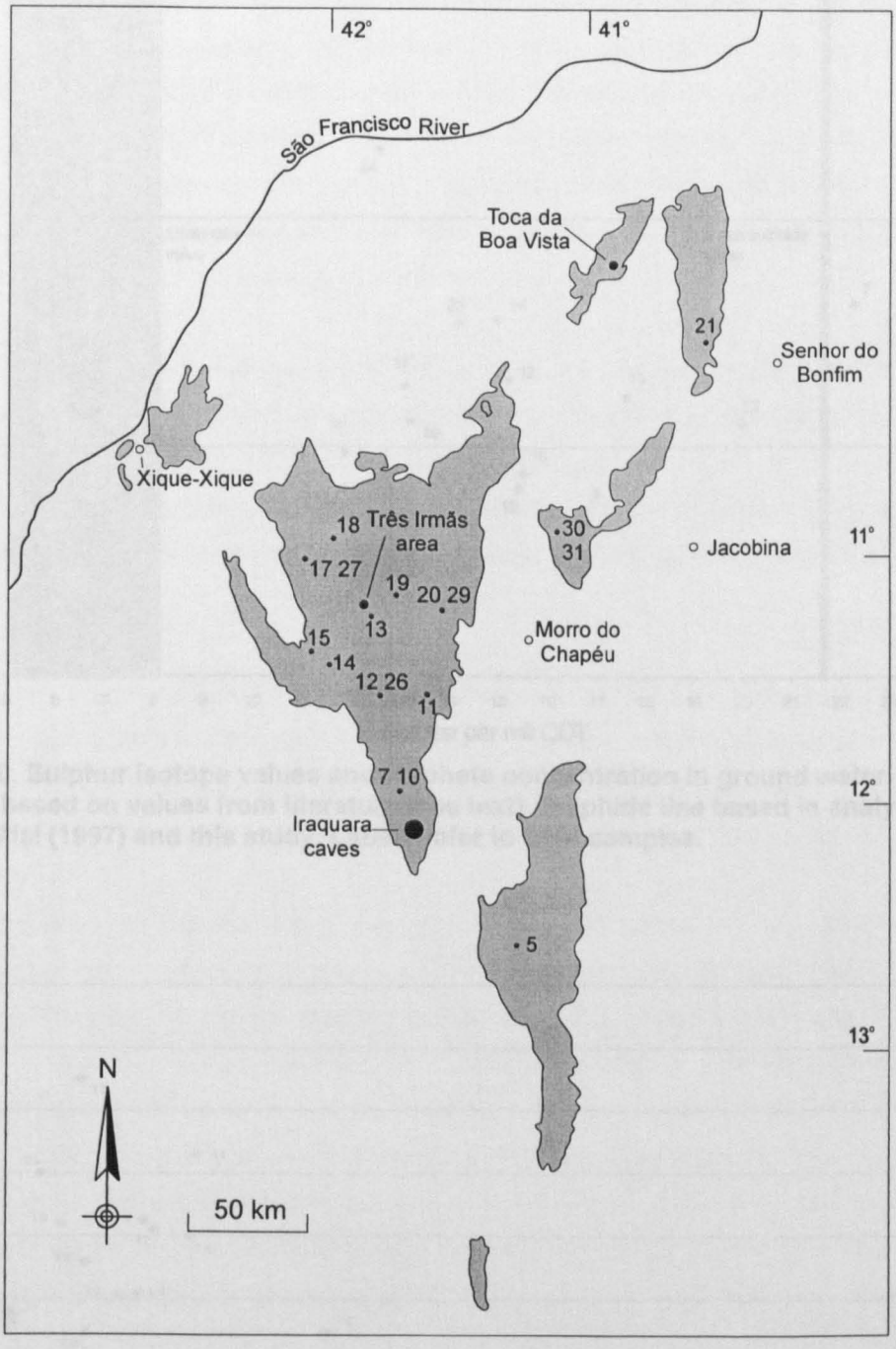

Figure 4.9. Location of sulphur isotope samples from Una Group (shaded). Numbers refer to ground water samples (UNA samples). Samples TUB-01, GDM-01, BST-01, GTR-02, GTR-04 and GLB-01 are from the Iraquara caves area. Samples from Kyle and Misi (1997) and Misi and Veizer (1998) are from the Três Irmãs area. Samples UNA-23, UNA-24, TCC-02, TBV-05 and TBV-08 were collected in Toca da Boa Vista area.

Areas where evaporative concentration predominates should show lighter $\delta^{34}S$ values in ground waters while waters with predominance of sulphide oxidation should display $\delta^{34}S$ values related to sulphide values, and should show correspondent higher SO_4/Cl ratios (Fig. 4.11). The majority of isotope values (with the exception of sample UNA-7) shows considerable scatter and not a

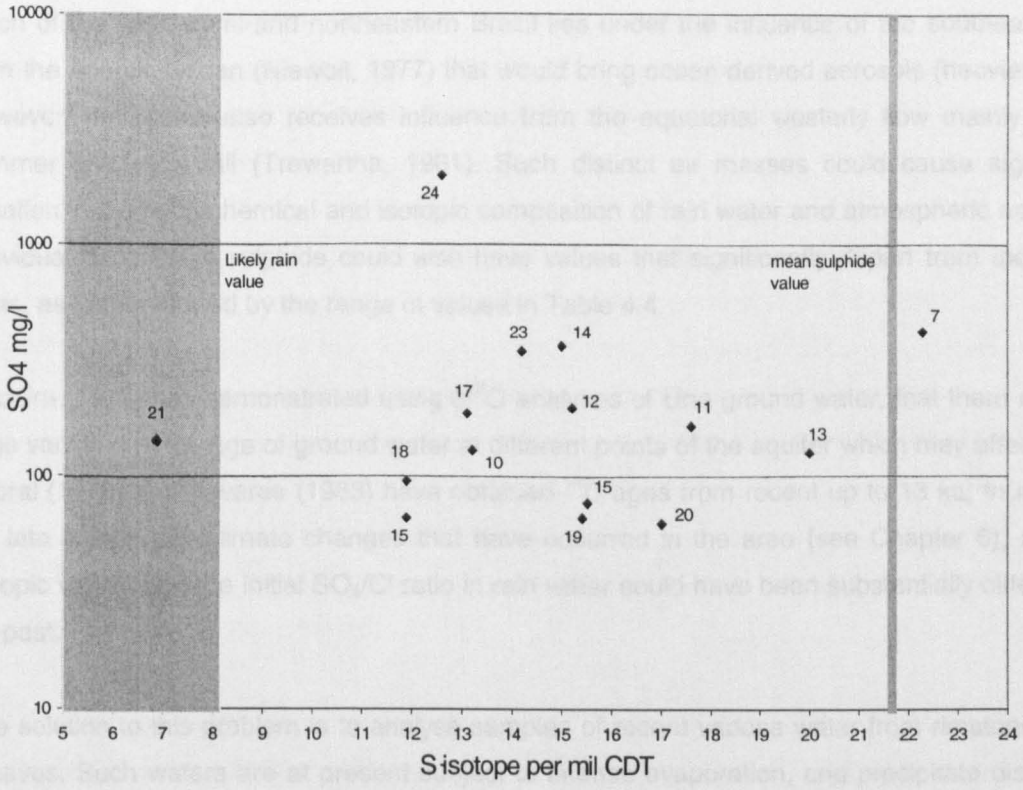

Figure 4.10. Sulphur isotope values and sulphate concentration in ground water. Rain water line based on values from literature (see text). Sulphide line based in analyses by Kyle and Misi (1997) and this study. Labels refer to UNA samples.

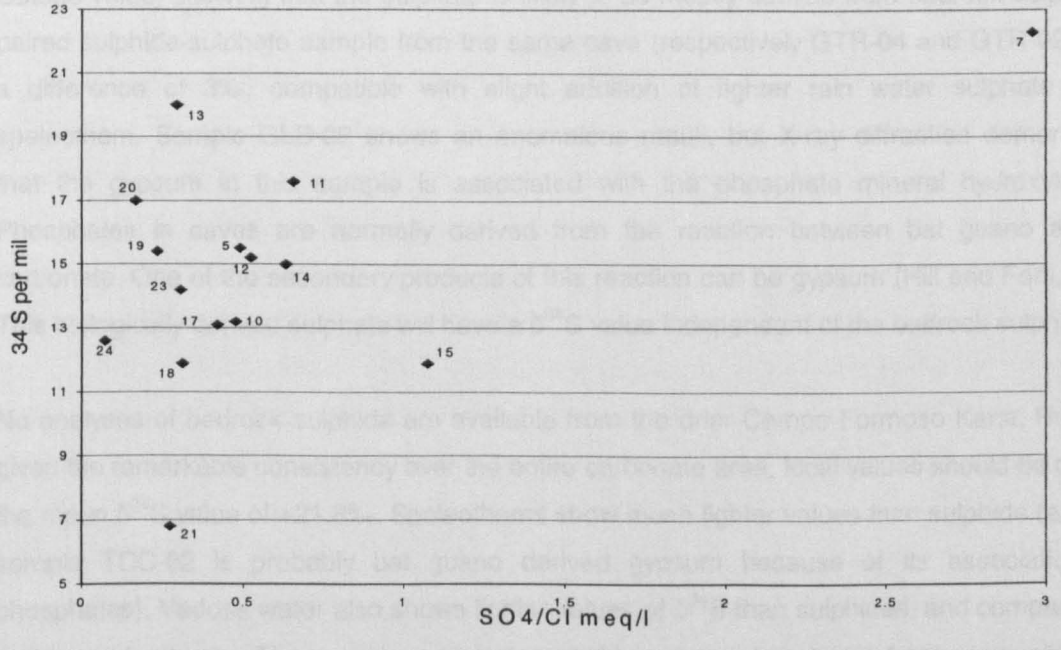

Figure 4.11. Sulphur isotopes in relation to SO_4/Cl ratio.

very clear dependency on relative changes of sulphide- or atmosphere-derived sulphate. A possible explanation for such scatter could lie on isotopic values of local rain water, which could have a large spread, depending on the source of atmospheric aerosols and precipitation. Over much of the year, semi-arid northeastern Brazil lies under the influence of the southeasterlies from the Atlantic Ocean (Niewolt, 1977) that would bring ocean derived aerosols (heavier $\delta^{34}S$). However, the region also receives influence from the equatorial westerly flow mainly during summer and early fall (Trewartha, 1961). Such distinct air masses could cause significant variation in the hydrochemical and isotopic composition of rain water and atmospheric aerosols. Individual deposits of sulphide could also have values that significantly depart from the mean value, as demonstrated by the range of values in Table 4.4.

Siqueira (1978) has demonstrated using $\delta^{18}O$ analyses of Una ground water, that there may be large variation of the age of ground water at different points of the aquifer which may affect $\delta^{34}S$. Cabral (1978) and Tavares (1983) have obtained ^{14}C ages from recent up to 13 ka, thus given the late Quaternary climate changes that have occurred in the area (see Chapter 6), sulphur isotopic values and the initial SO_4/Cl ratio in rain water could have been substantially different in the past.

One solution to this problem is to analyse samples of recent vadose water from rimstone pools in caves. Such waters are at present subject to intense evaporation, and precipitate distinctive subaerial sulphate speleothems. Both vadose waters and sulphate speleothems have been analysed from the southern Iraquara area and the northern Campo Formoso Karst (Table 4.4)

In the Iraquara area the sulphate speleothems show $\delta^{34}S$ values similar to the rock sulphide isotope value, showing that the sulphate is likely to be mostly derived from bedrock sulphide. A paired sulphide-sulphate sample from the same cave (respectively GTR-04 and GTR-02) show a difference of 3‰, compatible with slight addition of lighter rain water sulphate in the speleothem. Sample GLB-02 shows an anomalous result, but X-ray diffraction demonstrates that the gypsum in this sample is associated with the phosphate mineral hydroxylapatite. Phosphates in caves are normally derived from the reaction between bat guano and the carbonate. One of the secondary products of this reaction can be gypsum (Hill and Forti, 1997). This biologically derived sulphate will have a $\delta^{34}S$ value independent of the bedrock sulphide.

No analyses of bedrock sulphide are available from the drier Campo Formoso Karst. However, given the remarkable consistency over the entire carbonate area, local values should be close to the mean $\delta^{34}S$ value of +21.8‰. Speleothems show much lighter values than sulphide (although sample TCC-02 is probably bat guano derived gypsum because of its association with phosphates). Vadose water also shows lighter values of $\delta^{34}S$ than sulphides, and comparable to that in speleothems. These vadose waters probably represent recharge from unusually heavy thunderstorms because the high temperature and low humidity of the caves (section 4.5.3.3.6.1) cause rapid evaporation, and any slow recharge would be quickly evaporated before filling the

pool. Sequential ground water analysis of the UNA-24 rimstone pool showed an increase in sulphate from 544 mg/l in January 1994 to 1,980 mg/l in March 1997. Chloride levels were significantly above 18,000 mg/l in March 1997. These waters, and the speleothems derived from it probably show a high proportion of isotopic lighter sulphate derived from evaporatively concentrated sulphate in the soil. The limited sampling of vadose water thus supports the model of a dominance of evaporation over sulphide oxidation as a source of ground water salinity in the drier northern part of the study area.

The geochemistry of Una Group carbonate ground waters appears to be complex. Further research is needed in order to clarify the relative importance of the two distinct sources of sulphate. Systematic isotopic and hydrochemical measurements of rain water, together with a more careful sampling of wells, would help constrain the several variables that appear to be involved in the Una aquifer geochemistry. Nevertheless, it appears clear that sulphide oxidation plays an important role in the area, and that acidity generated by this process could be a major factor in generating secondary porosity in the carbonates.

4.5.3. The Campo Formoso Karst

The Campo Formoso Karst area is located in northern Bahia State, mainly within the municipality of Campo Formoso. The carbonates of the Una Group outcrop in two distinct zones, separated by the younger Caatinga Limestone (Fig. 4.2 and 4.12). The large area to the east is poorly known. To the west, the area near Laje dos Negros contains some of Brazil's most extensive caves. Intensive exploration in the last 12 years has yielded over 100 km of mapped passages. Further data presented in this thesis will refer mostly to the karst area in the surroundings of Laje dos Negros.

The area has recently been mapped by the Brazilian Geological Survey (CPRM, unpublished data), who have adopted a different subdivision of the Salitre Formation than that of Misi (1979) used in this thesis. The Laje dos Negros carbonates have been placed in the Gabriel Unit, which is described as predominantly calcosiltites (sometimes dolomitised) with local dolomitic calcarenites (CPRM, unpublished data). The correlation of the Gabriel Unit with the stratigraphy by Misi (1979) (Fig. 4.3) is not clear. Apparently the sulphide rich horizons belonging to unit B1 of Misi (1979) are interpreted as being immediately below the Gabriel Unit in the CPRM scheme, the Gabriel Unit being the possible correlative of the units A or A1 of Misi (1979). This would place the B1 sulphide-rich unit of Misi (Lapão Facies of CPRM) in the subsurface in the study area.

The carbonates are bounded in the northwest by hills composed of Mesoproterozoic quartzites of the Chapada Diamantina Group. The southeastern limit of the carbonates is marked by the extensive deposits of the freshwater Caatinga Limestone along the Salitre River. Also overlying the limestone are detrital fans of Tertiary-Quaternary age, and recent talus and alluvial deposits.

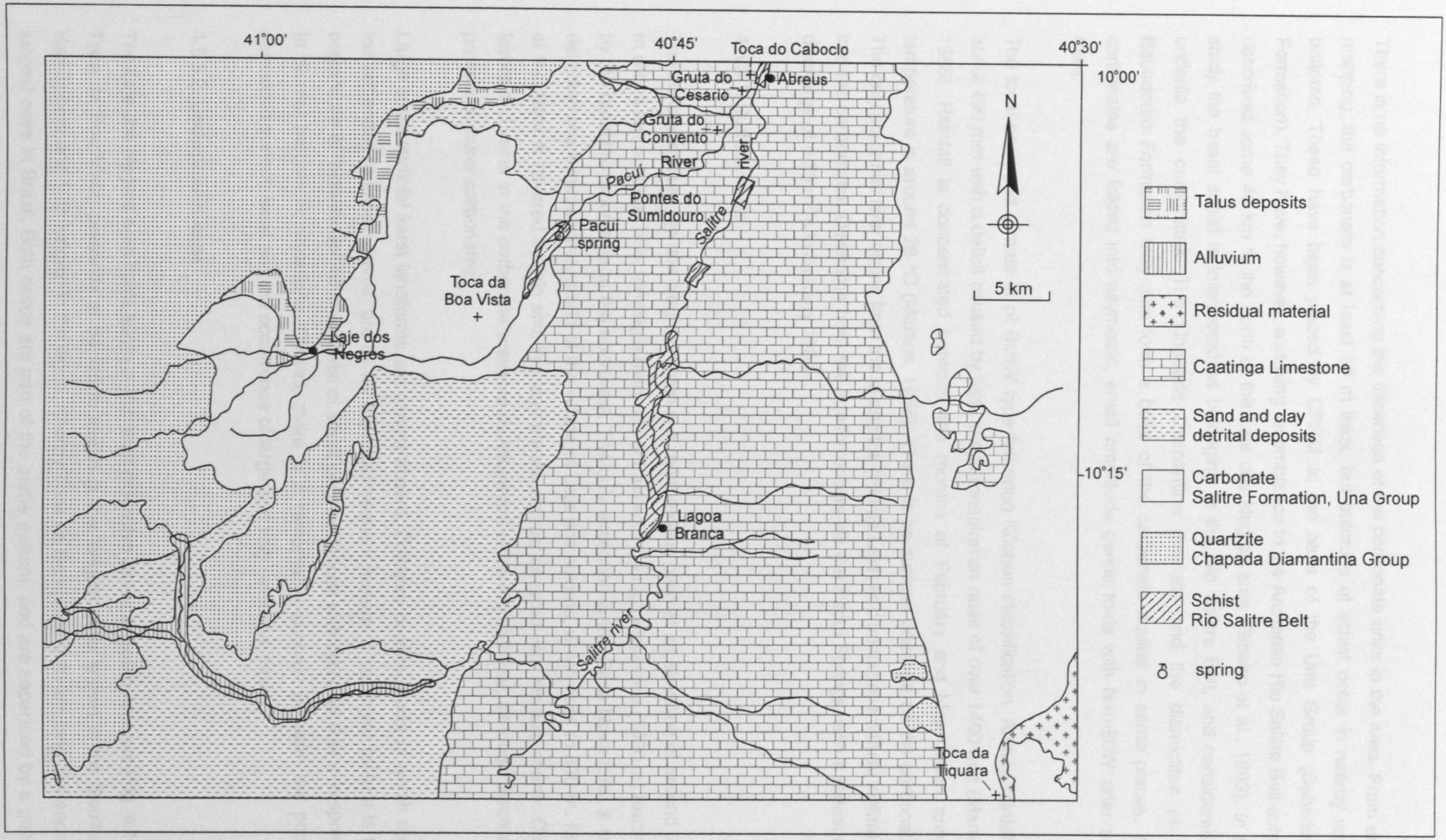

Figure 4.12. Geology of the Campo Formoso Karst. Adapted from CPRM (Unpublished data).

There is no information concerning the thickness of the carbonate units in the area. From cave mapping, the carbonate is at least 50 m thick, but outcrops of schist occur in nearby valley bottoms. These have been placed by CPRM at the base of the Una Group (Bebedouro Formation). They have, however, a striking resemblance to the Archaean Rio Salitre Belt schists described some 40 km to the north of the Laje dos Negros area (Ribeiro et al., 1993). In this study the basal schist is interpreted as belonging to the Rio Salitre Belt, and considered to underlie the carbonates. The Chapada Diamantina quartzite and the diamictites of the Bebedouro Formation may also form a base of the carbonate aquifer in some places. The carbonates are folded into asymetric, small amplitude gentle folds with N40-90W orientated axes.

The local semi-arid climate is of BshW type following Köppen classification. Annual rainfall is about 490 mm with a deficit caused by high evapotranspiration rates of over 1400 mm (Martins, 1986). Rainfall is concentrated between the months of February and May. Mean annual temperature is around 26 °C (Martins, 1986). There is no surface drainage on the carbonates. The only perennial river drains from the quartzites (Rio da Laje) and undergoes diffuse infiltration into the carbonates. Discharge from the aquifer occurs via the Pacuí Springs, with a measured discharge of 0.23 m^3/s in January 1994.

4.5.3.1. Surface karst

The surface of the Laje dos Negros region is a monotonous plain at an elevation of around 600 m with a few subdued hills, forming a marked contrast with the high elevations (1000 m) reached by the quartzite mountains to the northwest. The only exception is the Casa Nova Hills, a fault delimited block immediately south of the village of Laje dos Negros, which rises to 830 m. Most of the karst is covered by thin soil, in many places entirely covered with residual cherts. Chert layers and veins in the carbonate prevents development of karren features, although these are present on purer carbonates.

Large scale surficial karst landforms are almost absent. Collapse dolines, some of which mark the entrances to known caves, are by far the most frequent feature. A particular feature is the occurrence of "blow-holes" which consist of small cave entrances with cyclic air flow in response to diurnal barometric variations. Overall, there is a remarkable contrast between the poorly developed surface karst and the occurrence of large and very extensive caves.

4.5.3.2. Underground karst

The Laje dos Negros area hosts some of the most extensive caves in South America (Fig. 4.13). Toca da Boa Vista, presently at 84 km in length is the longest cave known in the Southern Hemisphere and 16th longest in the world. Nearby Toca da Barriguda is 20 km long, the second longest cave in Brazil. Both caves are part of the same system, and are separated by a gap of

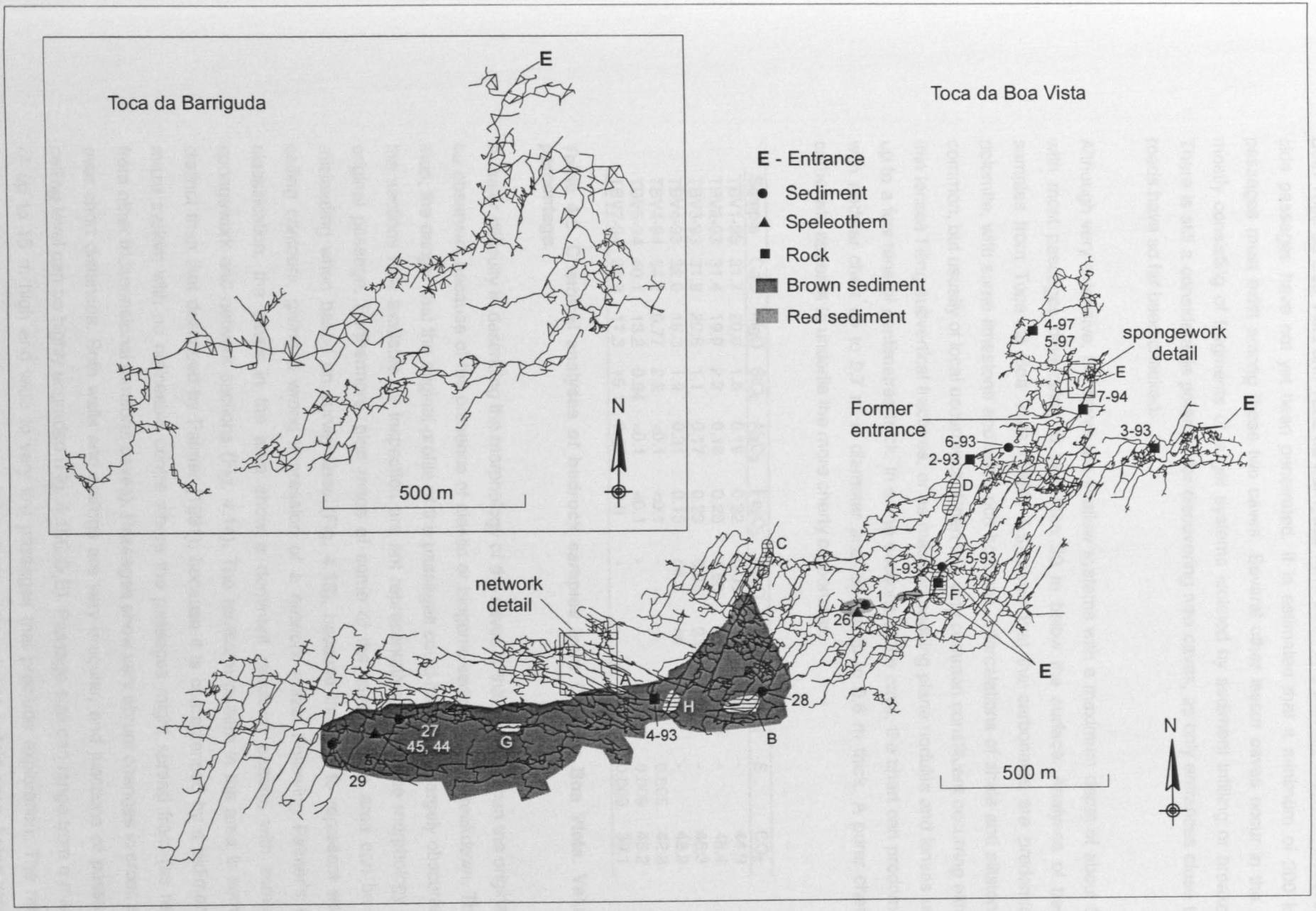

Figure 4.13. Survey of Toca da Boa Vista and Toca da Barriguda, showing sampling sites and location of sites discussed in Figs. 4.14 and 4.15. Survey by Grupo Bambuí de Pesquisas Espeleológicas.

less than 1 km. A connection between these caves is a very likely possibility in the near future. Both Toca da Boa Vista and Toca da Barriguda have been only partially explored. Hundreds of side passages have not yet been penetrated. It is estimated that a minimum of 200 km of passages must exist among these two caves. Several other lesser caves occur in the area, mostly consisting of fragments of larger systems isolated by sediment infilling or breakdown. There is still a considerable potential for discovering new caves, as only entrances close to the roads have so far been checked.

Although very extensive, the caves are shallow systems with a maximum depth of about 50 m, with most passages developing at less than 30 m below the surface. Analyses of bedrock samples from Toca da Boa Vista (Table 4.5) show that the carbonates are predominantly dolomite, with some limestone and silica rich horizons. Intercalations of shale and siltstone are common, but usually of local occurrence. Chert is a very common constituent occurring either as thin lenses filling subvertical fractures, or as massive bedding plane nodules and lenses usually up to a few tens of centimetres thick. In some sections of the cave, the chert can predominate, with nodular chert up to 0.7 m in diameter and lenses up to 0.6 m thick. A purer chert-free carbonate appears to underlie the more cherty carbonates.

Sample	CaO	MgO	SiO_2	Al_2O_3	Fe_2O_3	Na_2O	K_2O	P_2O_5	S	CO_2
TBV1-93	31.7	20.0	1.8	0.19	0.32	0.05	0.05	0.13	-	44.9
TBV2-93	31.4	19.9	2.2	0.18	0.23	0.66	0.04	0.33	-	45.4
TBV3-93	31.9	20.6	1.1	0.17	0.29	0.04	0.07	0.19	-	45.3
TBV4-93	32.0	19.3	1.9	0.31	0.15	nil	nil	nil	-	45.9
TBV4-94	54.2	0.77	2.2	<0.1	<0.1	-	-	-	0.005	42.3
TBV5-94	40.1	13.2	0.94	<0.1	<0.1	-	-	-	0.009	45.2
TBV7-94	26.9	17.3	15.1	0.57	0.6	-	-	-	0.009	39.1

Table 4.5. Chemical analyses of bedrock samples from Toca da Boa Vista. Values in percentage.

A major difficulty in describing the morphology of the caves is that nowhere can the original floor be observed, because of the presence of clastic or biogenic sediments, or breakdown. There is thus, the danger that the original profile of the passages could have been largely obscured, and the sections now available for inspection are not representative of the true morphology of the original passage. Furthermore, plan maps of some of the caves in the area can be highly misleading when based on survey lines (Fig. 4.13), because they fail to represent wall and ceiling contours, giving a wrong impression of a network maze. Following Palmer's (1991) classification, the caves in the area show a dominant ramiform pattern, with some local spongework and network sections (Fig. 4.14). The ramiform pattern in the area is somewhat distinct than that described by Palmer (1991), because it is characterised by a bidimensional maze system with no noticeable centre where the passages might spread from (as reported from other tridimensional ramiform caves). Passages show very abrupt changes in cross section over short distances. Both walls and ceilings are very irregular, and junctions of passages at ceiling level can be highly ungraded (Fig. 4.15C,D,E). Passage size can range from a maximum of up to 15 m high and wide to very low passages that preclude exploration. The ramiform pattern predominates where passages follow the bedding planes or fold axes, being developed

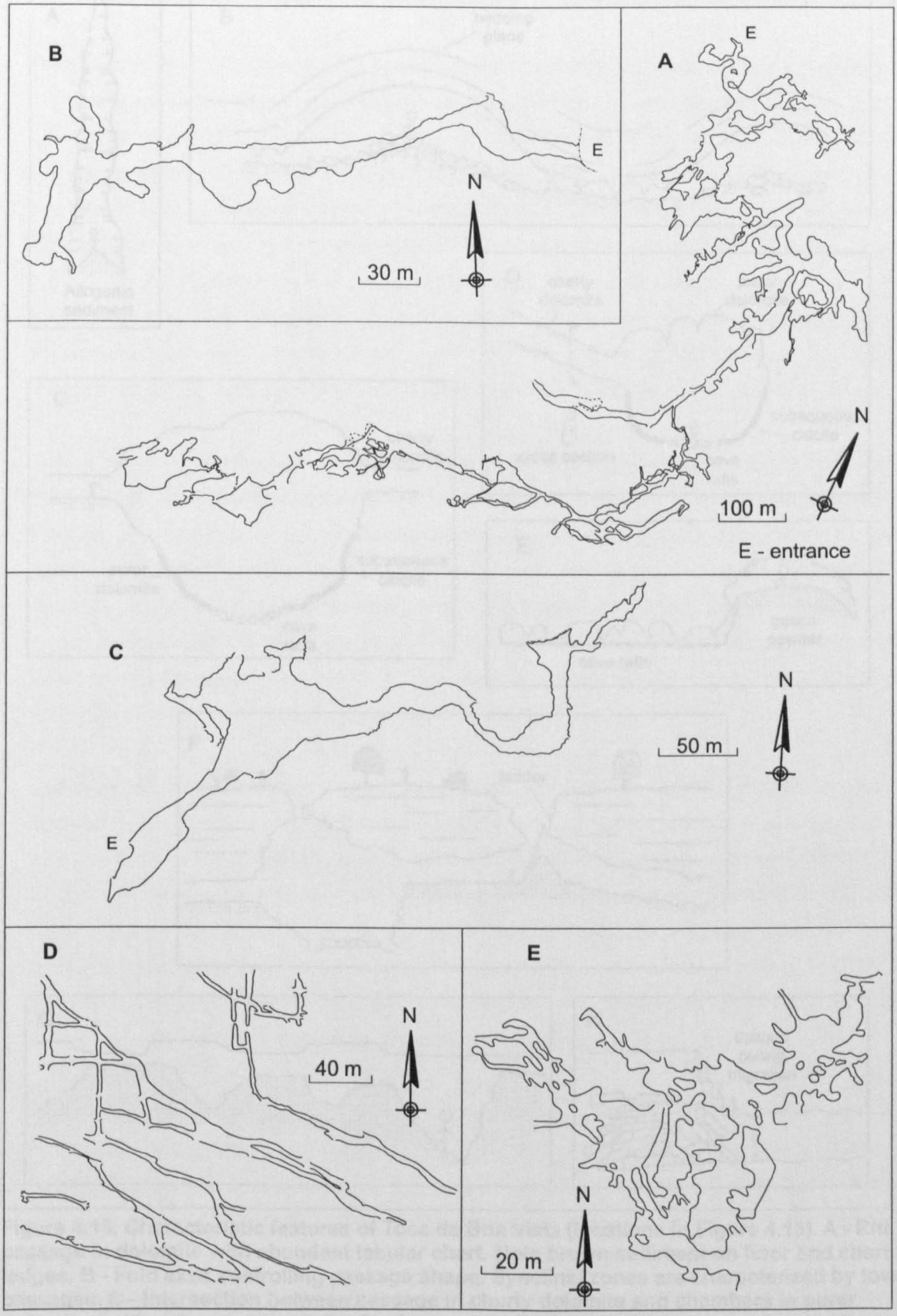

Figure 4.14. Pattern of caves in the Campo Formoso Karst. Ramiform pattern: A - Toca da Barriguda, B - Toca do Morrinho (segmented ramiform), C - Toca da Pedra (segmented ramiform). Network pattern: D - sector of Toca da Boa Vista. Spongework pattern: E - sector of Toca da Boa Vista. Location of sectors D and E are marked in Figure 4.13. Maps by Grupo Bambuí de Pesquisas Espeleológicas.

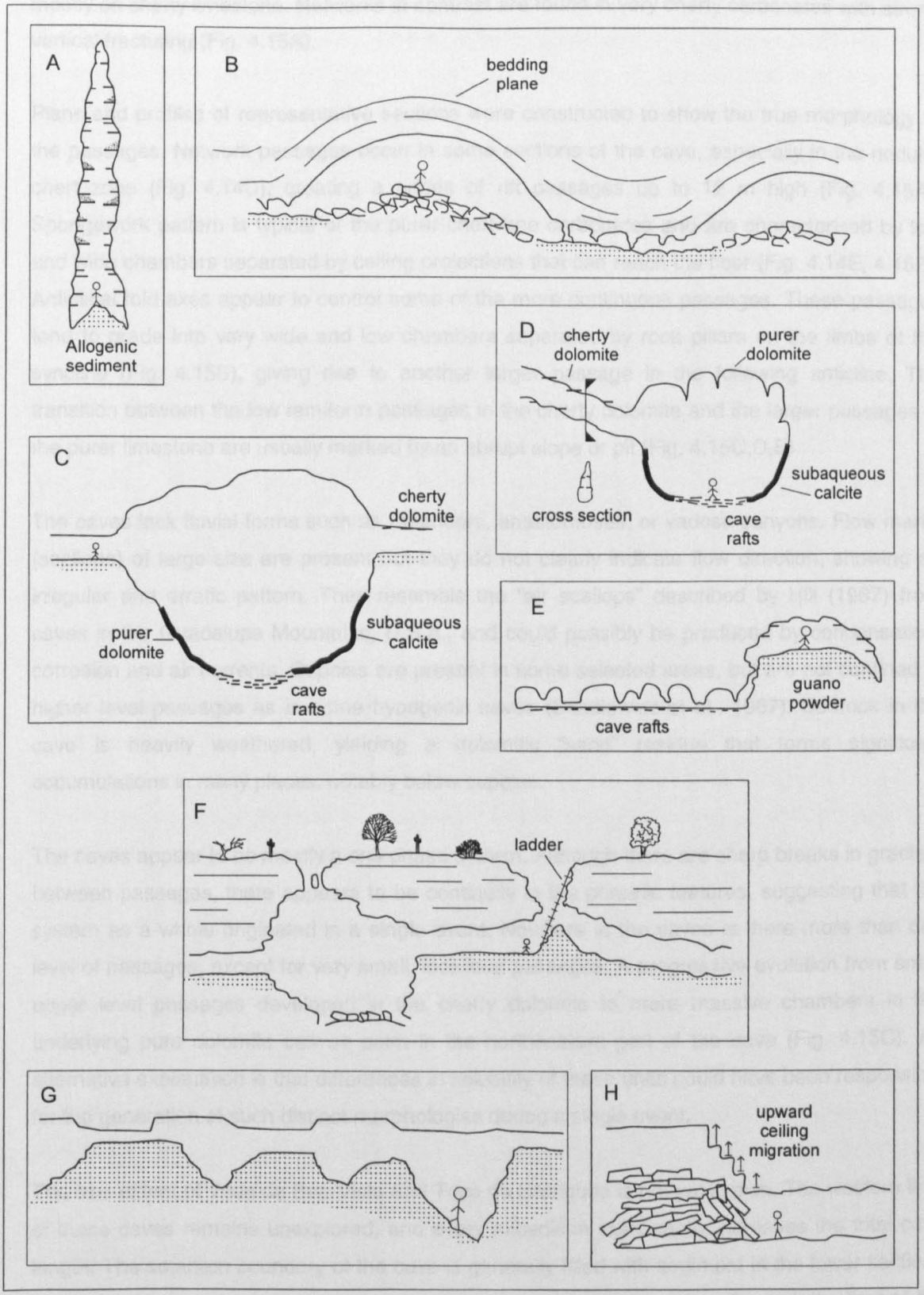

Figure 4.15. Characteristic features of Toca da Boa Vista (locations in Figure 4.13). A - Rift passage in dolomite with abundant tabular chert. Note brown sediment on floor and chert ledges. B - Fold axes controlling passage shape. Synclinal zones are characterized by lower passages. C - Intersection between passage in cherty dolomite and chambers in purer dolomites with subaqueous calcite. D - Same as C. E - Contact between passage in cherty dolomite and lower spongework area. F - Entrancee collapses. G - Internal collapse in brown sediment causing great variation in passage profile. H - Change of passage level caused by upward migration of ceiling due to slab breakdown. Schematic sketches are not to scale.

mostly on cherty limestone. Networks in contrast are found in very cherty carbonates with strong vertical fracturing (Fig. 4.15A).

Plans and profiles of representative sections were constructed to show the true morphology of the passages. Network passages occur in some sections of the cave, especially in the nodular chert zone (Fig. 4.14D), creating a series of rift passages up to 12 m high (Fig. 4.15A). Spongework pattern is typical of the purer chert-free carbonates and are characterised by low and wide chambers separated by ceiling projections that can reach the floor (Fig. 4.14E, 4.15E). Anticlinal fold axes appear to control some of the more continuous passages. These passages tend to grade into very wide and low chambers separated by rock pillars on the limbs of the syncline (Fig. 4.15B), giving rise to another larger passage in the following anticline. The transition between the low ramiform passages in the cherty dolomite and the larger passages in the purer limestone are usually marked by an abrupt slope or pit (Fig. 4.15C,D,E).

The caves lack fluvial forms such as meanders, anastomoses, or vadose canyons. Flow marks (scallops) of large size are present but they do not clearly indicate flow direction, showing an irregular and erratic pattern. They resemble the "air scallops" described by Hill (1987) from caves in the Guadalupe Mountains, U.S.A., and could possibly be produced by condensation-corrosion and air currents. Cupolas are present in some selected areas, but are not confined to higher level passages as in some hypogenic caves (Bakalowicz et al., 1987). Bedrock in the cave is heavily weathered, yielding a dolomitic "sand" residue that forms significant accumulations in many places, notably below cupolas.

The caves appear to be mostly a one phase system. Although there are sharp breaks in gradient between passages, there appears to be continuity in the phreatic features, suggesting that the system as a whole originated in a single event. Nowhere in the caves is there more than one level of passages, except for very small, localised passages. A progressive evolution from small upper level passages developed in the cherty dolomite to more massive chambers in the underlying pure dolomite can be seen in the northeastern part of the cave (Fig. 4.15C). An alternative explanation is that differences in solubility of these units could have been responsible for the generation of such distinct morphologies during a single event.

The true extent of Toca da Boa Vista and Toca da Barriguda is not yet known. The western limit of these caves remains unexplored, and every expedition significantly increases the total cave length. The southern boundary of the cave is generally filled with sediment in the lower sections or breakdown. In the northern section, the large rounded chambers usually mark the limit of the known cave. Overall, sediment plugs and breakdown commonly mark the end of passages. The present water table is reached in only a few places, usually on the bottom of narrow fissures.

The caves of the Laje dos Negros area bear no genetic relation to the surface. The entrances are either passages that were intercepted by surface lowering or fortuitous collapses into shallow

passages (Fig. 4.15F). The irregular profile of the caves appears to be largely controlled by bedding horizons in the dolomite. The passages at Toca da Boa Vista waves from the terrain surface elevation near the entrances to about 50 m in depth in the western section (Fig. 4.16). Observations near the entrance of Toca da Barriguda show that phreatic features are recognisable in the walls and ceiling near the entrance, and the upward inclination of the passages towards the surface demonstrates that the cave system originally extended above the present level of the terrain. Breakdown is extremely common but largely confined to the cherty limestone, and consists of slabs of carbonates and chert clasts. Upward passage migration due to breakdown is common in many sections of the cave (Fig. 4.15H) as the chert layers tend to favour slab breakdown.

4.5.3.2.1. Sediment deposits

The caves in the area have abundant sediment deposits. These are represented by autogenic deposits consisting of breakdown, chemical precipitates, biogenically derived sediments, carbonate weathering residues, and detrital allogenic deposits. Chemical precipitates, and weathering residues will be discussed in later sections.

Allogenic sedimentation is abundant in some sections of the cave but absent in others. Two major suites of sediments can be recognised. A suite comprising red fine grained and laminated silt/clay deposits usually up to 1 m thick are preserved as remnants in a few selected sites in upper passages near the vertical entrance of Toca da Boa Vista (Fig. 4.13). This sediment shows thin horizontal laminations suggesting a low energy depositional environment. This sediment will henceforth be referred to as red sediment.

The second sediment is much thicker and more abundant. It is a massive brown indurated clay that occurs in lower passages in the western portion of the cave (Fig. 4.13), filling some passages almost entirely. This sediment is composed mostly by silica (38%) and aluminium (12%) but includes significant calcium (10%), manganese (9%) and iron (7%). The deposits are at least 5 m thick in some places, although its total thickness can significantly exceed this figure since the base of the thicker sequences is never exposed. It is highly possible that there is more than one sequence of brown sediment but detailed stratigraphical mapping was not performed. In many places the brown sediment has been partially washed by a latter vadose event. Subsidence due to funnelling into lower passages is responsible for creating local breaks in the sediment sequence (Fig. 4.15G). The brown sediment at present is intensively fragmented due to shrinkage (mud cracks), sometimes very dry and indurated, but locally retaining some moisture.

A few sites in the caves contain other types of sediment that appear to be more of a local importance. An older and friable laminated beige clay/silt sediment is observed filling one passage in the western end of the passage (sample TBV-29 in Fig. 4.13). This sediment

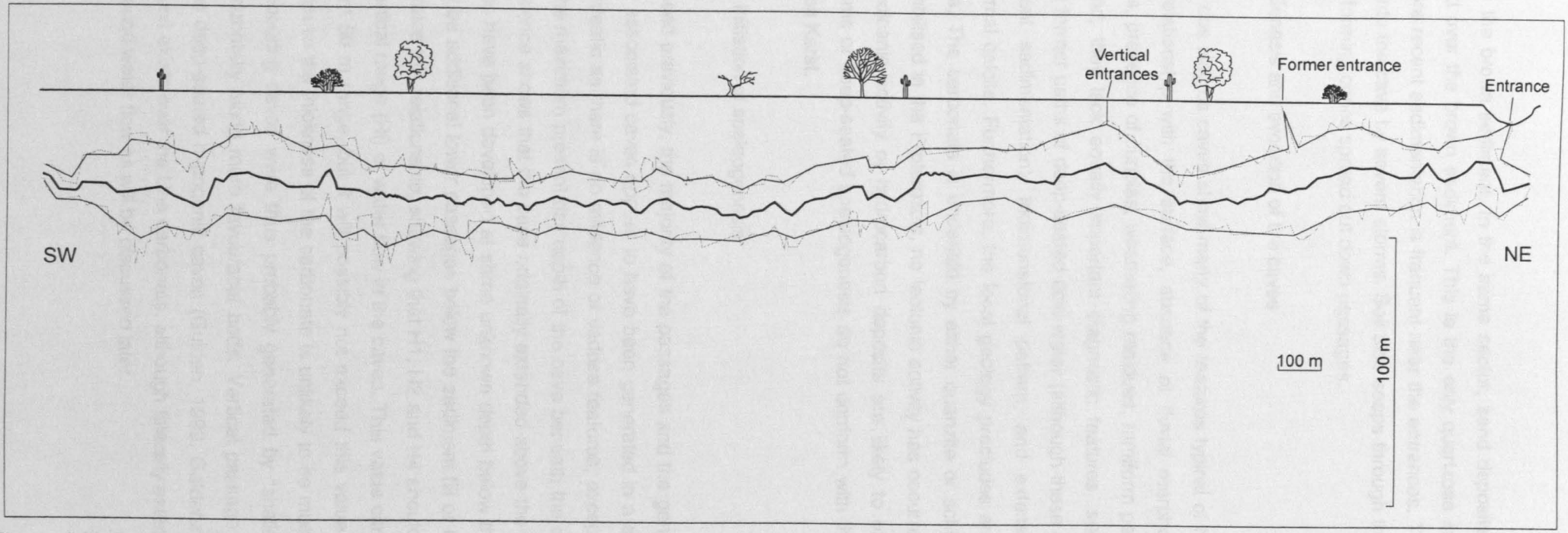

Figure 4.16. Profile of Toca da Boa Vista showing depth variation of passages. Note vertical exaggeration. Thicker line represents average elevation of passages (line goes through elevation with the highest density of passages). Upper and lower lines represent higher and lower limits of passage development (smoothed).

underlies the brown sediment. In the same sector, sand deposits, clearly a later event, were deposited over the brown sediment. This is the only quartzose sand deposit observed in the cave. More recent sedimentation is frequent near the entrances. This sediment consists of soil washed into the cave by severe storms. Soil also seeps through the fissures in a few places in the cave forming cones spread out down passages.

4.5.3.3. Genesis and evolution of the caves

The Laje dos Negros caves show many of the features typical of hypogenic caves, including a lack of relationship with the surface, absence of fluvial morphological features and fluvial sediments, presence of cupolas, weathering residues, ramiform pattern, among others. On the other hand, they lack equally important diagnostic features, such as ascending passages indicating former paths of deep-seated acid water (although these could have been masked by the present sedimentation), tridimensional pattern, and extensive sulphate deposition or hydrothermal calcite. Furthermore, the local geology precludes any possibility of deep-seated processes. The carbonate is underlaid by either quartzite or schist, the area is located in a craton stabilised in the Proterozoic, no tectonic activity has occurred since the Early Cambrian and no volcanic activity or hydrocarbon deposits are likely to exist in the area. Traditional mechanisms of deep-seated speleogenesis do not conform with the field evidence in the Laje dos Negros Karst.

4.5.3.3.1. Initiation of speleogenesis

As discussed previously, the majority of the passages and the general pattern of Toca da Boa Vista and associated caves appear to have been generated in a single event. This event was entirely phreatic as there is no evidence of vadose features, except for localised later invasion events. The maximum present day depth of the cave beneath the surface lies at approximately 50 m. Evidence shows that the cave originally extended above the present surface elevation. It should also have been developed at some unknown depth below the water table. Furthermore, there may be additional lower passages below the sediment fill or the present water table. Fig. 4.17 illustrates this relationship, showing that H1, H2 and H4 should be added to determine the original vertical range (Ht) of water flow in the caves. This value can be significantly higher than the present 50 m range, but it will possibly not exceed this value in more than three or four times, because the thickness of the carbonate is unlikely to be much larger. Toca da Boa Vista and neighbouring caves were thus probably generated by "shallow" ground water flow that flowed horizontally along more favourable beds. Vertical passage ranges of over 400 m are common in deep-seated hypogenic caves (Gulden, 1999, Galdenzi and Menichetti, 1995). No confining unit exists over the Una carbonate, although laterally extensive chert layers can locally confine ground water flow as will be discussed later.

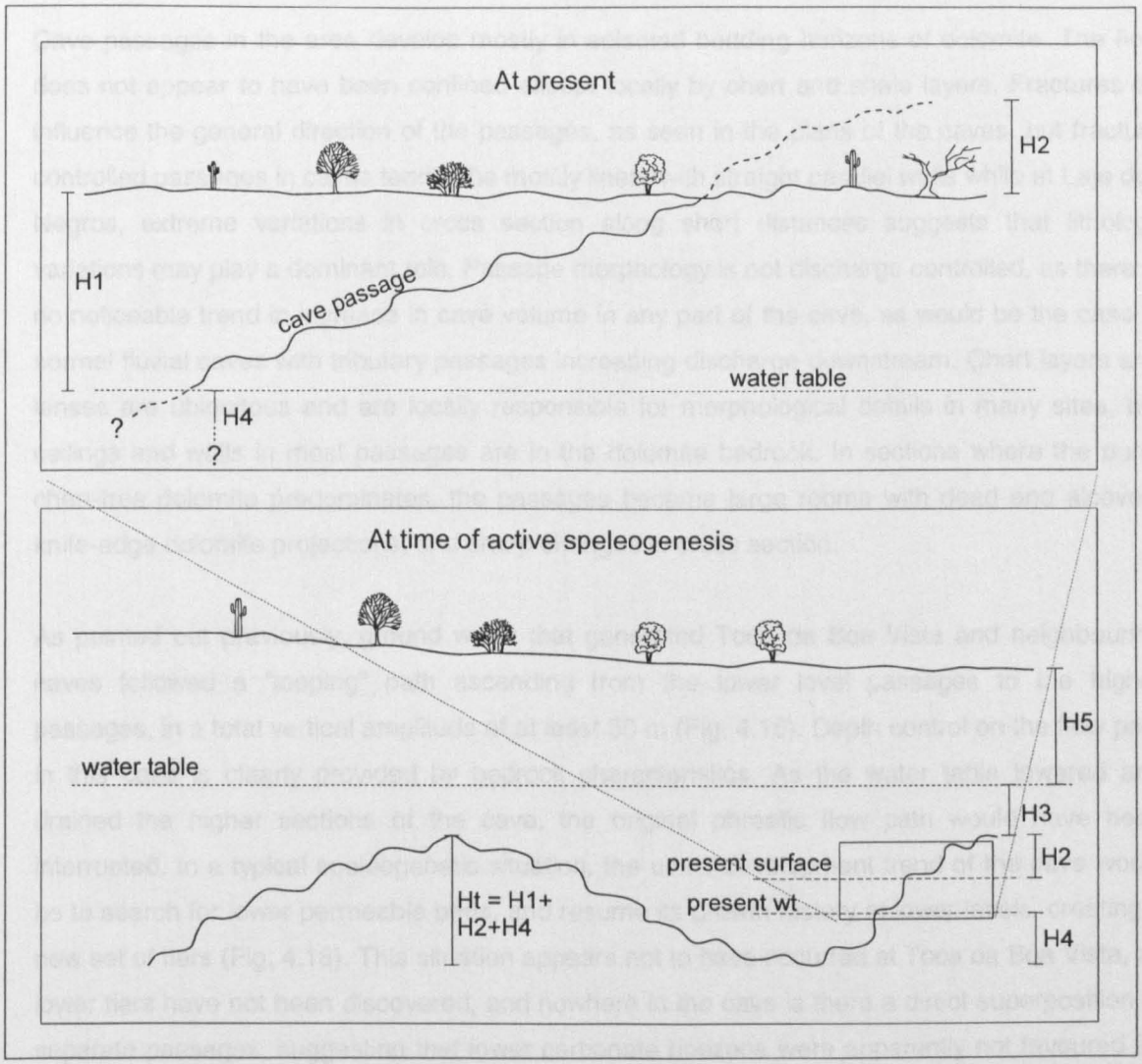

Figure 4.17. Schematic profile showing amplitude of passages above the water table at present (H1), elevation that the cave used to extend above the present surface (H2), depth below the palaeowater table that the cave initiated (H3), possible present extension of passages below the water table (H4) and depth of palaeowater table below the palaeosurface (H5), and vertical range of water flow (Ht).

The ground water flow velocities during speleogenesis were very slow, as attested by large flow marks (0.3 to 1 m long), presence of fragile small boxwork-like chert projections, and the ramiform/network/spongework pattern of the caves. It should be noted, however, that air flow and weathering (condensation-corrosion?) processes could have played a role in generating apparent flow marks and boxwork. Flow marks in the cave do not allow the recognition of the general flow direction. The overall pattern of the caves is equally uninformative. Assuming that the hydraulic gradient at the time of cave genesis had the same direction as today, a flow roughly towards the east (or south) is assumed. This is supported by the fact that the quartzite hills that bound the area in the north and west are the natural recharge areas for the carbonate, and would as today have formed an elevated area.

4.5.3.3.2. Controls on the early development of the flow path

Cave passages in the area develop mostly in selected bedding horizons of dolomite. The flow does not appear to have been confined except locally by chert and shale layers. Fractures do influence the general direction of the passages, as seen in the plans of the caves, but fracture controlled passages in caves tend to be mostly linear with straight parallel walls while at Laje dos Negros, extreme variations in cross section along short distances suggests that lithology variations may play a dominant role. Passage morphology is not discharge controlled, as there is no noticeable trend in increase in cave volume in any part of the cave, as would be the case in normal fluvial caves with tributary passages increasing discharge downstream. Chert layers and lenses are ubiquitous and are locally responsible for morphological details in many sites, but ceilings and walls in most passages are in the dolomite bedrock. In sections where the purer chert-free dolomite predominates, the passages became large rooms with dead end alcoves, knife-edge dolomite projections, and sharp changes in cross section.

As pointed out previously, ground water that generated Toca da Boa Vista and neighbouring caves followed a "looping" path ascending from the lower level passages to the higher passages, in a total vertical amplitude of at least 50 m (Fig. 4.16). Depth control on the flow path in this case is clearly provided by bedrock characteristics. As the water table lowered and drained the higher sections of the cave, the original phreatic flow path would have been interrupted. In a typical speleogenetic situation, the usual development trend of the cave would be to search for lower permeable beds, and resume its growth history at lower levels, creating a new set of tiers (Fig. 4.18). This situation appears not to have occurred at Toca da Boa Vista, as lower tiers have not been discovered, and nowhere in the cave is there a direct superposition of separate passages, suggesting that lower carbonate horizons were apparently not favoured for conduit inception. Abrupt changes in passage elevation do occur but these represent continuous, if sharp, breaks in roof height due to lithological variations, such as the transition between the cherty and the purer dolomite. However, it may still be possible that situation A in Fig. 4.18 is occurring at present, with a new independent tier being formed much deeper below the water table. Evidence of deep flow is provided by the Pacuí Springs, the sole outlet for the carbonate aquifer. The temperature of this spring is in average 2.5°C warmer than the phreatic water inside the cave. Thermal gradients in the area are not known, but assuming a range between 15-30°C/km, a flow depth of 80-170 m is suggested. This range is probably close to the maximum thickness of the carbonate, and indicates that active flow is occurring at depth. Evidence thus suggests that lithology is the major controlling factor in determining the position and shape of the cave passages in the area.

Ground water flow that generated the caves at Laje dos Negros area occurred mostly under closed system conditions in respect to CO_2, due to the absence of concentrated recharge points in the surface, although the shallow nature of the flow would have favoured occasional input of waters with distinct pCO_2. Under such conditions, water can quickly become saturated.

However, a decrease of dissolution reaction order occurs in normal H_2O-CO_2-$CaCO_3$ systems, allowing the water to prolong its dissolution potential, resulting in the slow growth of conduits over long distances (Palmer, 1991). The lack of conduit development in other carbonate horizons, and the possible presence of metal sulphides in the dolomite suggests, however, that dissolution may have been controlled by bedrock sources of acidity. Sulphide oxidation could considerably boost the dissolution potential of the ground water, speeding up conduit growth rates. Additional CO_2 produced by reaction 4.1 would further enhance dissolution. Such process would be "lithology controlled" and thus sharp changes in dissolution rates would occur due to variable availability of sulphides, resulting in abrupt morphological changes in cave passages.

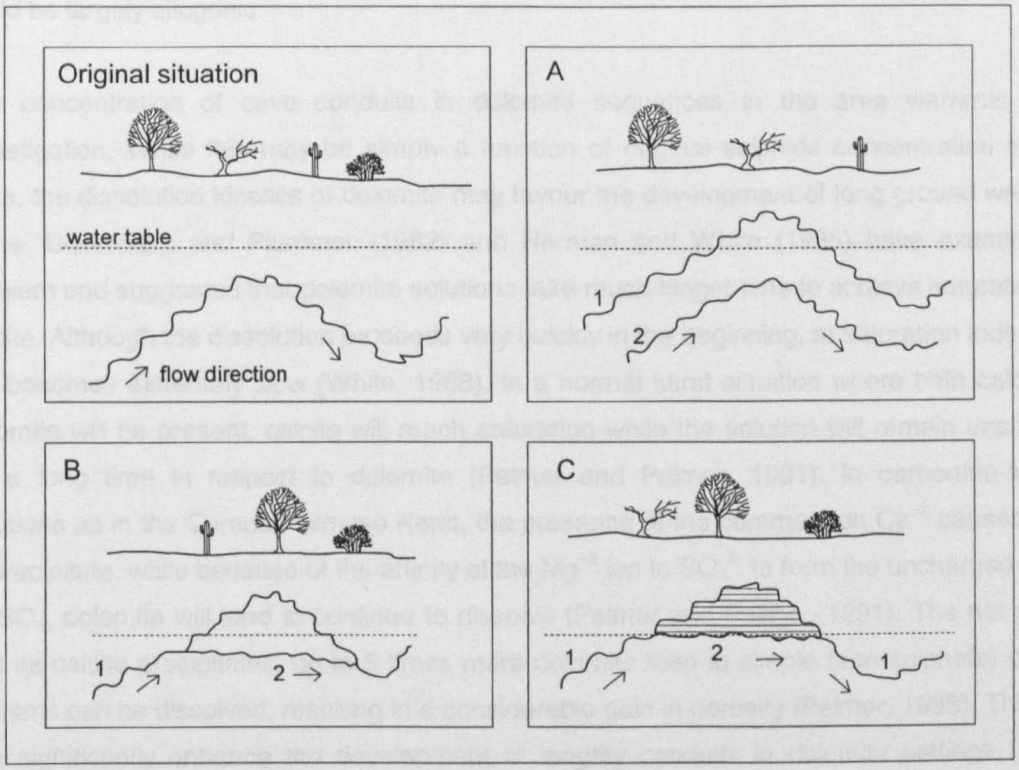

Figure 4.18. Possible effects of water table lowering on a phreatic system. A - An entire new set of passages develop at lower levels. B - A bypass at some depth below the water table (or close to it) develops. C - Vadose entrenchment of the drained section.

The importance of sulphuric acid speleogenesis for initial conduit development has been stressed in previous studies (Ball and Jones, 1990, Lowe and Gunn, 1995, Worthington and Ford, 1995). The role of sulphuric acid dissolution is considered to be dominant by these authors only during enlargement of the initial fracture aperture until turbulent flow takes place. The later history of the cave and its growth to human dimension would then be dominated by normal carbonic acid, and the final morphology of these caves could show no imprint of the early sulphuric acid processes. I believe that sulphuric acid dissolution was a major process during the entire period of cave development in the Laje dos Negros caves and that the present morphology, where not masked by later modification processes, is derived wholly from this hypogenic phase.

Bedrock sulphide would be consumed during the dissolution process, and this may explain why major sulphide occurrences cannot be seen in the cave walls. Whether the process acted on disseminated pyrite, or on massive metre thick sulphide beds such as the ones described in the Una Group of the Três Irmãs area is unclear, but any sulphide-rich bed would certainly develop into an avenue for concentrated ground water flow. The byproducts of sulphide oxidation are dissolved sulphates and iron hydroxides. If sulphate concentrations are very high gypsum may precipitate. Gypsum is frequent as a vadose speleothem in the area, but does not commonly occur as crust on cave walls. However, later active weathering of the cave walls would almost certainly have precluded the preservation of such precipitates. The sink for eventual iron hydroxides in the area is not yet clear. Sediment deposits in the caves are iron-rich, but they could be largely allogenic.

The concentration of cave conduits in dolomite sequences in the area warrants further investigation. While this may be simply a function of original sulphide concentration in these beds, the dissolution kinetics of dolomite may favour the development of long ground water flow paths. Busenberg and Plummer (1982) and Herman and White (1985) have examined the problem and suggested that dolomite solutions take much longer time to achieve saturation than calcite. Although the dissolution proceeds very quickly in the beginning, at saturation indexes of -2 it becomes extremely slow (White, 1988). In a normal karst situation where both calcite and dolomite will be present, calcite will reach saturation while the solution will remain unsaturated for a long time in respect to dolomite (Palmer and Palmer, 1991). In carbonate-sulphate solutions as in the Campo Formoso Karst, the presence of the common ion Ca^{+2} causes calcite to precipitate, while because of the affinity of the Mg^{+2} ion to SO_4^{2-} to form the uncharged ion pair $MgSO_4$, dolomite will tend to continue to dissolve (Palmer and Palmer, 1991). The net result is that as calcite precipitates, up to 5 times more dolomite than in simple (non-sulphate) dolomite systems can be dissolved, resulting in a considerable gain in porosity (Palmer, 1998). This effect can significantly enhance the development of lengthy conduits in dolomite settings (Palmer, 1998), and could be important in the Campo Formoso Karst.

4.5.3.3.3. Origin of conduit morphology

While the general pattern and distribution of underground features both in the scale of cave systems and individual passages appears to be due to lithological variations in the bedrock as seen in previous sections, there are a series of particular features that deserve special analysis.

Rift passages are abundant in the western section of the cave (Fig. 4.15A) and are in marked contrast with the surrounding lower passages that display a ramiform pattern. The presence of penetrative major joints in this section is probably the reason for the development of the network pattern. As water was forced upwards it eventually met laterally continuous chert layers. In normal conditions, these thick layers would behave as local confining units restricting upward migration of the flow. However, the joints in dolomite in the area cut across the chert layers. The

breaching of successive chert layers would cause the development of a series of rift passages (Fig. 4.19). The head of the ground water would control the maximum limit of upward migration of the rift. Absence of penetrative joints would preclude rift development.

Well developed dissolution pockets, named cupolas, occur at a few sites in the caves. They do not necessarily develop along joints, and seem to concentrate in areas with well developed bedrock weathering. In deep-seated hypogenic caves, cupolas are interpreted as the result of convectional solution (Ford and Williams, 1989) and occur usually in the highest passages. In the caves of the study area they are not related to passage elevation. The origin of these features in a shallow non thermal setting cannot be due to convection, and can be tentatively attributed to condensation-corrosion processes.

The massive sediment deposition that occurred in many of the passages is likely to have influenced passage morphology. Large parts of the western sector of Toca da Boa Vista appear to have been filled up to the ceiling by the brown sediment. This sediment could have caused upward dissolution of the ceiling, generating paragenetic features. However, due to the abundance of chert in the walls, and the local occurrence of confining chert layers, morphological evidence of paragenesis has been largely masked and none of the typical features (see Chapter 5) are recognisable. I believe that the sedimentary infilling was a later process, and its influence on cave genesis was localised. Indeed, most of the higher passages in the eastern section of Toca da Boa Vista do not contain sediment. The upper levels of Toca da Barriguda also do not show evidence of sediment infilling. Paragenesis, if indeed present, was confined to the lower levels of these caves.

The maximum thickness of the brown sediment is unknown, but appears to be variable along the passages. The presence of sediment residues near the ceiling suggests that the sediment originally used to completely plug the passages. The current void between the sediment and the ceiling appears in many cases to be due to shrinkage and volume reduction during drying of the sediment. This effect is more apparent where two sediment-filled passages meet, the variation in floor elevation suggesting differential volume reduction due to variation in sediment thickness (Fig. 4.20). Not much can be said about the older red sediment due to the very fragmentary nature of its deposit.

The generation of such massive amount of brown sediment would undoubtedly require substantial weathering of a non-carbonate rock. A search for the source rock must discard not only the pure quartzites that mark the northern limit of the area but also any of the carbonate beds which do not appear to have sufficient insoluble residues. One possible alternative that remains are the schists of Rio Salitre Belt. These rocks are easily weathered as observed in road cuts, and could have provided both iron and weathered clay minerals. Nowadays these rocks underlie the Caatinga Limestone in the south of the area (Fig. 4.12). Input of sediment

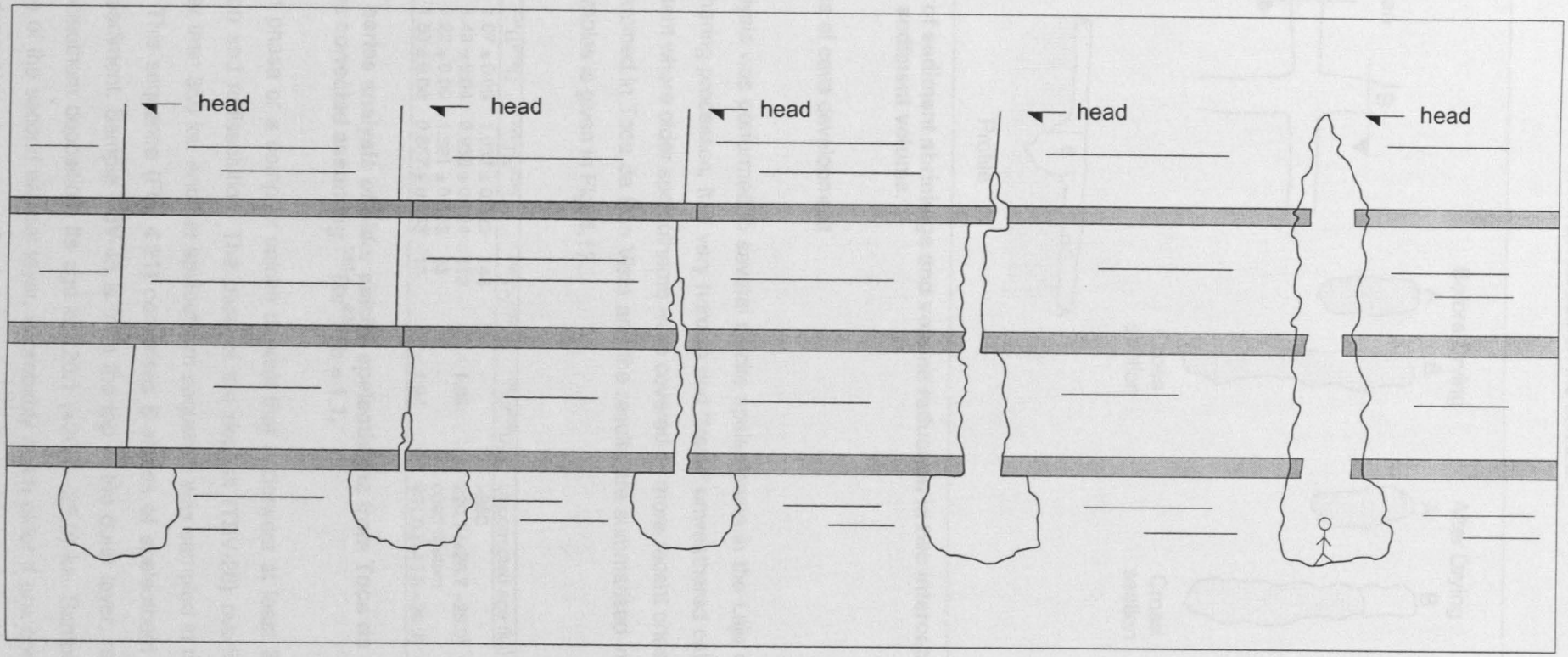

Figure 4.19. Hypothetical scheme for the development of phreatic rift passages. Chert layers (shaded beds) confine the ground water in the passage. Penetrative master joints form a possible route through the chert, due to higher permeability along the joint. Maximum height of rift is given by local head of ground water.

thus possibly occurred from the south, through palaeoswallets, the Caatinga Limestone now occupying the denuded fluvial catchment developed on the schists.

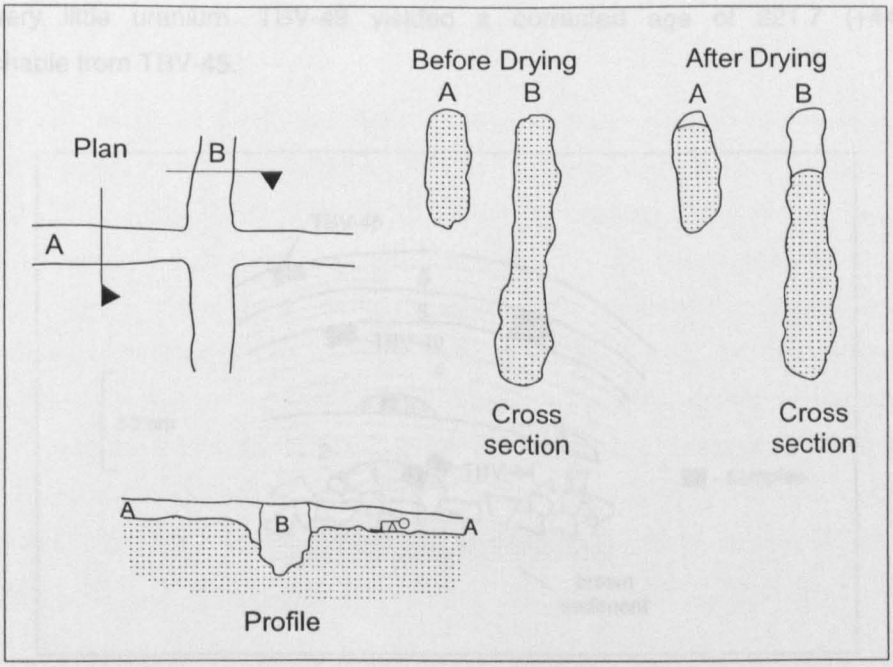

Figure 4.20. Effect of sediment shrinkage and volume reduction in two intercepting passages with distinct initial sediment volume.

4.5.3.3.4. Timescales of cave development

Uranium series analysis was performed in several calcite speleothems in the Laje dos Negros caves. Due to weathering processes, it is very hard to find "fresh" unweathered calcite. These are usually only present where older speleothems were covered by more recent ones. Two such sequences were examined in Toca da Boa Vista and the results are summarised in Table 4.6. Location of these samples is given in Fig. 4.13.

Sample	U (ppm)	$^{234}U/^{238}U$	$^{230}Th/^{234}U$	$^{230}Th/^{232}Th$	$^{234}U/^{238}U_{t=0}$	Uncorrected age (ka)	Corrected age (ka)
TBV-26	0.093 ± 0.002	1.07 ± 0.03	1.037 ± 0.029	146	-	>350	-
TBV-45	0.072 ± 0.002	1.48 ± 0.04	0.939 ± 0.024	113	1.89	220.1 (+26.7 –25.0)	-
TBV-44	0.017 ± 0.001	1.22 ± 0.09	1.321 ± 0.073	13	-	open system	-
TBV-49	0.016 ± 0.001	1.50 ± 0.06	0.957 ± 0.033	15	1.94	231.0 (+45.8 –39.3)	221.7 (+44.2 –33.1)

Table 4.6. Uranium series analysis of older calcite speleothems from Toca da Boa Vista. Errors are ±1σ. Ages corrected assuming $^{230}Th/^{232}Th = 1.7$.

TBV-26 is the oldest phase of a complex calcite deposit that underwent at least 3 stages of speleothem deposition and redissolution. The base of the deposit (TBV-26) overlies the red sediment, and is older than 350 ka. Another speleothem sequence was sampled in the western section of the cave. This sequence (Fig. 4.21) comprises 6 stages of speleothem deposition overlying the brown sediment. Sample TBV-45 is from the top of the outer layer, representing the final stage of speleothem deposition. Its age is 220.1 (+26.7 –25.0) ka. Sample TBV-44, belonging to the base of the second earliest layer, is probably much older if one considers the time involved in the deposition of each of the following calcite layers and the existence of five

periods of interruption of calcite deposition. Unfortunately, TBV-44 contains very low uranium sample, and shows evidence of post depositional radionuclide migration. Another sample, TBV-49, belongs to one of the intermediate phases and besides being detritally contaminated, it also contains very little uranium. TBV-49 yielded a corrected age of 221.7 (+44.2 -33.1), indistinguishable from TBV-45.

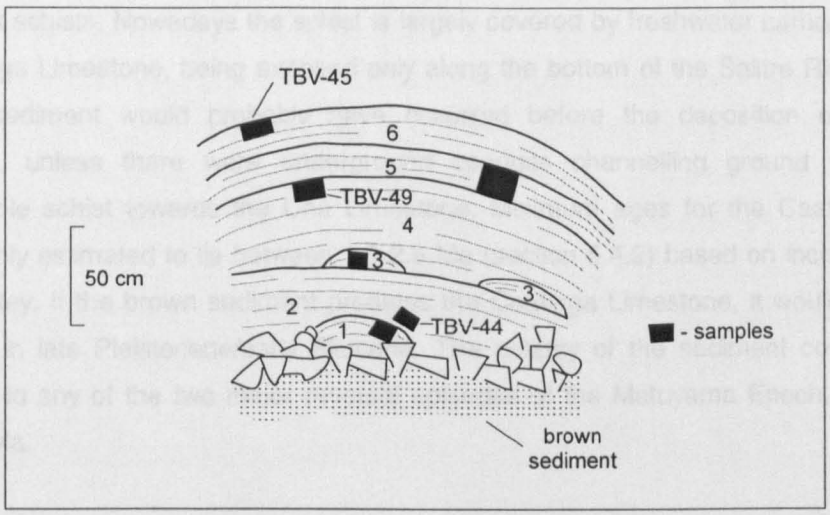

Figure 4.21. Sketch of speleothem sequence near station XL03, Toca da Boa Vista. The entire sequence was exposed following undermining of the brown sediment by flowing water. More recent speleothems overlie phase 6.

Both of the above mentioned speleothem sequences overlie sediments, giving a minimum age of 350 ka for the red sediment and 222 ka for the brown sediments. Samples from these sediments were analysed for remanent magnetisation (Table 4.7). Samples from the red sediment (TBV-1) show reversed polarity and the sediment is thus at least 778 ka old. Two samples were collected from the brown sediment. TBV-28 comprised very indurated, desiccated and cracked sediment. This sample showed a clear reversed polarity. TBV-27 was sampled in the western sector of the cave and did not allow clear identification of the polarity (possibly normal). Analysis of subaqueous speleothems elsewhere in Toca da Boa Vista has demonstrated that the cave underwent at least two major episodes of palaeoclimate controlled water table rise (section 6.6). The passage where sample TBV-27 was collected falls within this elevation range, and thus could have experienced major magnetic disturbance. The more reliable sample TBV-28 allows the establishment of the Brunhes/Matuyama reversal at 778 ka as a lower age limit for the brown sediment.

Sample	Sediment	N	I_o	Decl.	Incl.	R	K	α_{95}	Polarity
TBV-1	red	6	4.93	204.88	22.06	5.95	104.65	6.73	REVERSED
TBV-27	brown	6	2.92	50.86	-62.35	5.94	79.30	7.38	NORMAL?
TBV-28	brown	5	4.41	194.12	15.31	4.93	55.16	10.21	REVERSED
TBV-29	older local	6	1.70	64.26	-80.85	5.19	6.21	29.32	INDETERMINATE

Table 4.7. Palaeomagnetic data for Toca da Boa Vista sediments. Intensities (I_o) in mA/m, Declination, Inclination and α95 in degrees. α_{95} – 95% probability that the direction lies on that angle span, K- Fisher precision estimate which determines the dispersion of points, R- length of resultant vector.

Sample TBV-29 was from a friable clay/silt sediment found in only one passage. It underlies the brown sediment. A consistent polarity could not be determined for this sample, probably because of disturbance due to the friable nature of the sediments.

As discussed previously the brown sediment is likely to be derived by weathering of the Rio Salitre Belt schists. Nowadays the schist is largely covered by freshwater carbonate deposits of the Caatinga Limestone, being exposed only along the bottom of the Salitre River valley. Such input of sediment would probably have occurred before the deposition of the Caatinga Limestone, unless there were underground conduits channelling ground water over the impermeable schist towards the Una Limestone. Minimum ages for the Caatinga Limestone were roughly estimated to lie between 1.3-2.6 Ma (section 5.4.2) based on incision rates of the Salitre Valley. If the brown sediment predates the Caatinga Limestone, it would probably have deposited in late Pleistocene/early Pliocene. The polarity of the sediment could probably be correlated to any of the two major reversal episodes of the Matuyama Epoch, at 1.19-1.77 or 1.95-2 .6 Ma.

The red sediment lies higher in elevation than the brown sediment. It is probably higher than the base (and perhaps the top) of the Caatinga Limestone. If this sediment also originated from weathering of the Rio Salitre Belt schist, it would necessarily have predated the deposition of the Caatinga Limestone. However, the deposits are very fragmentary, and the small volume of sediment now present in the cave could have been deposited from a more local source, although its elevation and more eroded nature suggests that it is older than the brown sediment.

Only minimum ages for the caves of the Laje dos Negros area are provided by Uranium series and palaeomagnetism in secondary carbonates and sediments, because these deposits could significantly postdate the main phase of speleogenesis. An alternative way of providing possible timescales of speleogenesis is to estimate the total amount of water table lowering since the time the caves were active. As water table lowering can be correlated with surface lowering, regional denudation rates could be applied to provide a rough estimate of the age of the caves. Fig. 4.17 suggests that some sections of the cave originally developed at a significant depth below the water table. The upper passages, the first to be drained, now have been dissected by surface denudation. In Fig. 4.17, H1 (total elevation of drained passages accessible at present), H2 (original elevation of the caves above present surface) and H3 (original depth of upper passages below the water table) should be added to account for the total amount of denudation that has occurred following initial draining of the cave. The water table depth below the present surface (H1) is known and amounts to about 50 m. There is no reasonable way to estimate H2 and H3. Minimum values for H2 and H3 could be around 5 and 10 m, but they might be significantly higher (especially H3), because the cave could have been initiated deeper within the aquifer. This is supported by the geothermally heated water at the Pacuí Springs, which indicates present groundwater flow depths in the range 80-170 m.

The minimum denudation that has occurred is thus 50 m (draining of known system), but the total amount of water table lowering in the area since time of cavern genesis may have been much greater, probably at least 100 m. Denudation rates for the São Francisco Craton have been deduced from apatite fission track analysis and palaeomagnetism. Harman et al. (1998) working with some apatites sampled near the Campo Formoso Karst estimated a denudation rate between 20-40 m/Ma, somewhat higher than the 18 m/Ma rate derived by Amaral et al. (1997). The magnetostratigraphy of cave sediments for the Santa Maria da Vitória Karst (section 3.4.1) yielded minimum incision rates between 25-34 m/Ma. If a range of denudation rates of 30 ± 10 m/Ma is applied, the minimum age of the cave assuming a water table lowering of 50 m would be 1.2 Ma. However, assuming higher values for total amount of water table lowering, it appears more reasonable to suppose that the cave could have started forming as early as 5 Ma, and that the sediments could therefore be Tertiary or early Pleistocene in age. Without better control on long term rates of denudation or improved dating methods with extended range (eg. cosmogenic techniques) it is not possible to better constrain the age of the cave.

4.5.3.3.5. Later modification processes

The early morphology of the caves at Laje dos Negros is often masked by later processes that have modified the original passage configuration. Among these, detrital and chemical sedimentation and breakdown are of paramount importance. The caves have probably been re-flooded several times in the past. At least two of these episodes, related to times of wetter palaeoclimate, have been identified through dating of subaqueous calcite deposits (section 6.6). Removal of sediment by water flow took place in some areas of the cave. The speleothem deposit that comprise samples TBV-44 and TBV-45 (Fig. 4.21) show evidence of water corrosion, indicating that water flow occurred in the site after about 220 ka. Elsewhere in the cave, several sites present evidence of later invasion flow. The high water table event related to the deposition of the Caatinga Limestone would necessarily have affected the cave in some way, but due to uncertainties in the dating of this episode, it is not possible at present to ascertain the role of this major event.

Other lesser processes have also operated and may be responsible for some of the peculiar features now observed in the cave. Condensation-corrosion and bat guano weathering processes have acted upon the bedrock and speleothem surfaces dissolving away the original material. While these processes do not appear to be of major importance at the scale of the cave system, they are relevant at the smaller scale of individual cave features. Condensation-corrosion, because it has been frequently associated with hypogenic caves, will be discussed in the following section.

4.5.3.3.6. Condensation-corrosion

Water vapour contained in warm air that rises from deep passages may condense as it meets colder air or colder bedrock. During the condensation process, the water vapour can acquire either CO_2 or H_2S, and become quite acidic. Bedrock and speleothems will be attacked by such solutions resulting in weathered outer surfaces. The condensation-corrosion effect is considered to be particularly effective in deep-seated hydrothermal caves because of their greater depth and existence of warm water bodies that will enhance the thermal gradient and provide a source for water vapour (Palmer and Palmer, 1989). Acidity is also high due to abundance of CO_2 and H_2S (Palmer and Palmer, 1989). However, according to these authors, the process can occur in any cave where air movement between entrances is subdued, regulation of temperature by inflowing surface water is absent and thermal convection is enhanced by large vertical range. The caves at Laje dos Negros show restricted air flow in many areas, and lack any major input of surface water, although they have only a limited vertical range. Condensation-corrosion is also thought to play a major role in the development of solutional littoral caves (Tarhule-Lips and Ford, 1998). In the Guadalupe Mountains Karst the process has been shown to be bacterially mediated (Cunningham et al., 1995).

In the Laje dos Negros caves, weathering rinds up to 5 cm thick occur on both bedrock dolomite and speleothem surfaces (Fig. 2.2b). The bedrock frequently disintegrates into a carbonate sand that accumulates at the base of walls or in solution pockets. Thin section analysis shows that much of the original structure of the dolomite is still present in the weathered rind. Table 4.8 shows that the composition of the sand is essentially the same as the bedrock, and the residue can be described as a dolomitic sand.

Sample	CaO	MgO	SiO_2	Al_2O_3	Fe_2O_3	P_2O_5	CO_2
TBV5-93	30.7	19.1	4.2	1.1	0.48	0.59	42.3
TBV6-93	32.3	19.1	1.5	0.21	0.1	nil	45.9
Bedrock (mean)	32.2	18.4	3.8	0.25	0.28	0.16	44.3

Sample	Main mineral	Other minerals
TBV-07	dolomite	quartz
TBV-06	dolomite	quartz

Table 4.8. Chemical and X-ray diffraction mineralogical analyses of bedrock "sand" residues. Chemical values in percentage by weight.

Such type of carbonate sand has been attributed to condensation-corrosion processes in many hypogenic settings including Hungary (Dublyansky, 1995), Iowa, Illinois and Wisconsin area (Howard, 1960), the Black Hills (Palmer and Palmer, 1989) and Romania (Sarbu and Lascu, 1997). The process follows a dedolomitisation path (Palmer and Palmer, 1991, Bar-Matthews et al., 1991), in which weathering appears to occur through selective corrosion of the edges of dolomite grains, allowing the rock to disintegrate (Palmer and Palmer, 1989). A similar dissolution process occurs in speleothems, except that they do not disintegrate presumably due to the interlocking of the much larger crystals, but change to a milky white opaque porous

calcite. Condensation-corrosion processes in the Laje dos Negros area appear to be somehow lithology controlled because the process do not occur in the Caatinga Limestone caves, located in the same climatic setting, although the latter have a different morphology and microclimate.

4.5.3.3.6.1. Cave meteorology

Condensation-corrosion processes in caves are driven by moisture availability in the air (humidity), the thermal gradient within the cave which induces air flow, and cave atmosphere CO_2 content. At Toca da Boa Vista, the process is more noticeable in the deeper parts of the cave, away from the entrances, suggesting either increased volumes of condensation or higher acidity of the condensation water. Alternatively, the zonation may be due to the predominance of guano derived weathering that tends to overwhelm condensation-corrosion processes near the major guano deposits close to the entrances.

A general meteorological survey was performed in the caves (Table 4.9). Fig. 4.22 illustrates the location of meteorological measurements. The survey was performed in two separate days. Measurements 18 to 29 at Toca da Boa Vista were made during a single trip in 1992, using a hygrometer for obtaining temperature and humidity and did not include CO_2 measurements. The remaining measurements were performed in November 1995 with a sling psychrometer and a Drager CO_2 pump. Measurements 1 to 9, comprising sites on the western part of Toca da Boa Vista, were performed on the order displayed in Table 4.9, i.e., during a trip out of the cave. Measurements 10 to 17, related to the sector between the entrances, were performed in another day, as were the measurements at Toca da Barriguda and Toca do Calor de Cima. The measurement outside the cave was taken at night. Temperature during the day was observed to reach as much as 37.5°C. It is not clear if intrasite differences between the two sets of data (from 1992 and 1995) as in measurements 16 and 25, reflect seasonal variations of the cave atmosphere, or, more likely, differences in measurement techniques and equipment.

Temperatures are on average very high, actually higher than the annual mean temperature of the area (26°C) described by Martins (1986). Relative humidity values show a wide variation but in general are much lower than usually observed in caves where they tend to approach 100%. Fig. 4.22 shows that temperature, humidity and CO_2 levels increase away from the entrance zone towards the western sector of the cave. It appears, however, that there is no continuous trend, but rather a sharp break at certain areas of the cave (as in between measurements 6 and 7). This effect, long observed by the cave explorers, suggest some type of atmosphere zoning, probably associated with changes in passage elevation. A weak but perceptible air flow occurs in many areas of the caves. Sites located away from the main air flow routes apparently retain higher values of temperature and humidity, even when close to entrances, such as in the sites in the northeastern portion of the cave (measurements 14, 15, 23, 24).

Carbon dioxide levels agree with levels in other caves around the world (Ek and Gewelt, 1985), and the results tend to support the assertive that higher values are found away from the entrances, although some of the higher values at Toca da Barriguda and Toca do Calor de Cima are from sites close to the entrance. According to Ek and Gewelt (1985) the primary factor in affecting the concentration of CO_2 in caves is the amount of biomass above the cave. Caves in semi-arid domains were supposed by these authors to contain limited amount of CO_2. This does not appear to be the case in the study area, despite the limited biomass in soils in the area. A possible major source of CO_2 for the local caves is carbon dioxide produced by equation 4.1. At Toca da Boa Vista some of the areas where the condensation-corrosion effect is better displayed have high temperature, humidity and CO_2 levels. This is especially the case at the western end of the cave.

Number	Survey Station	Temperature °C	Relative humidity %	CO_2 ppm
Measurements at Toca da Boa Vista				
1	XM6	28.5	98	2000
2	XO2	28.1	76	1800
3	XJ105	28.3	99	-
4	XJ65	27.9	90	1500
5	ZG13	27.8	95	-
6	DD4	27.9	89	1200
7	MQ9	27.9	69	1000
8	CL18	27.5	65	-
9	MN9	27.5	62	1200
10	PERD	27.1	61	1000
11	WL27	28.0	59	1200
12	MJ7	27.5	57	1300
13	OPAC	27.3	79	1400
14	CX71	27.6	94	1500
15	MG8	28.0	84	1100
16	TEL	26.9	57	1000
17	AD19	27.0	60	1000
18	-	27	59	-
19	-	27	62	-
20	-	27	64	-
21	-	27.5	64	-
22	-	27.5	70	-
23	-	29	77	-
24	-	28.5	81	-
25	-	29	53	-
26	-	29	66	-
27	-	28	73	-
28	-	28	81.5	-
29	-	27	65	-
30	outside	24.9	63.6	800
Toca da Barriguda				
31	fossil	28.4	79.8	3000
32	fossil	28.6	92.7	4500
33	fossil	28.6	91.6	4600
Toca do Calor de Cima				
34	chamber	28.5	97.8	2500

Table 4.9. Meteorological measurements at the Laje dos Negros caves.

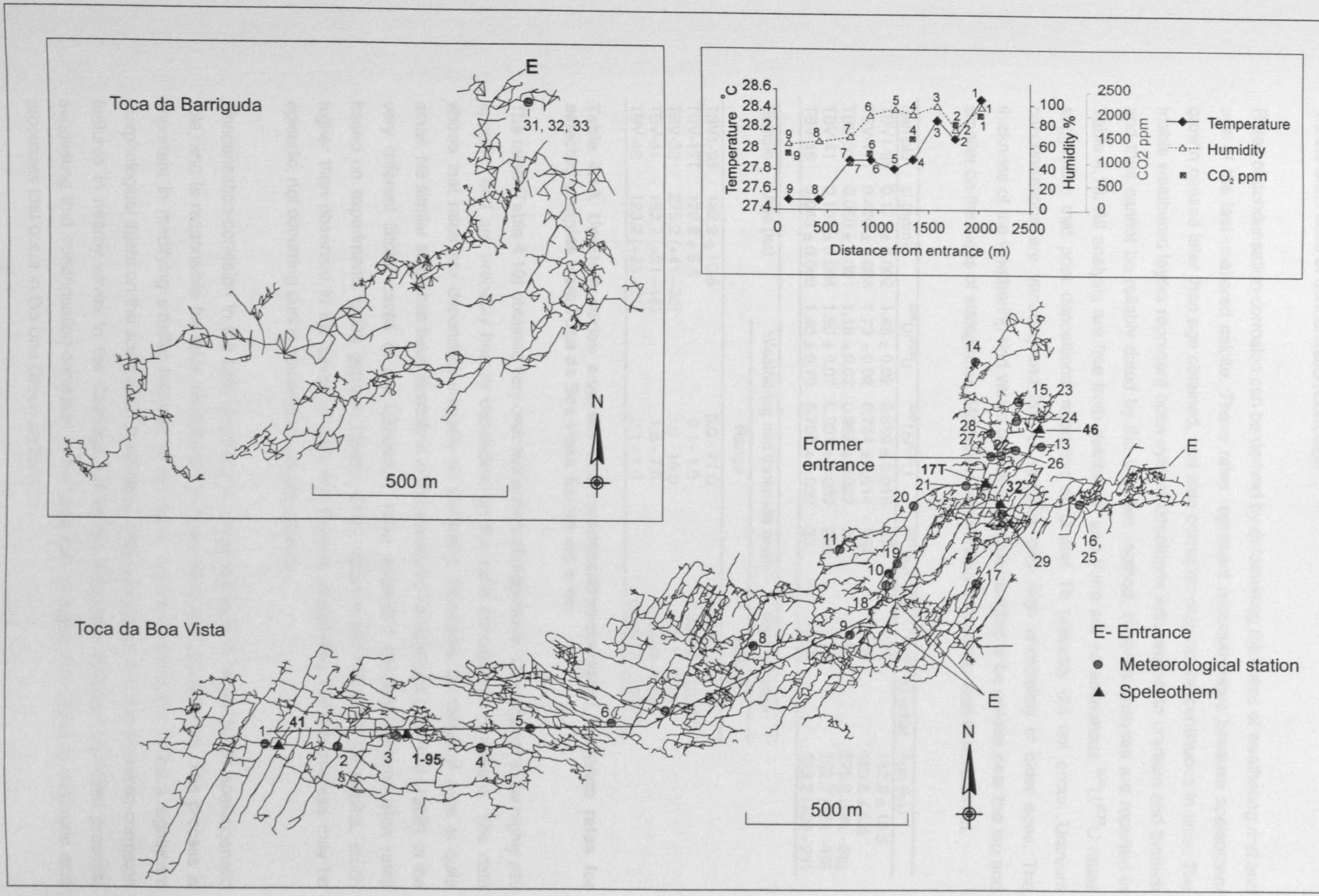

Figure 4.22. Location of meteorological measurements, sampling sites for condensation-corrosion speleothems, and graph showing temperature, humidity and CO_2 variations along the western sector of the cave towards the entrance (see line on map).

4.5.3.3.6.2. Rates of condensation-corrosion

Rates of condensation-corrosion can be derived by determining thickness of weathering rind and age of the last unaltered calcite. These rates represent minimum rates because speleothem growth ceased later than age obtained, and also corrosion may not be continuous in time. The friable weathered layers represent open system conditions with respect to uranium and thorium and thus cannot be reliably dated by the U-series method. U-series analyses are reported in Table 4.10. All analysis are free from detrital Th and there are no anomalous $^{234}U/^{238}U$ ratios suggesting that post depositional migration of U and Th probably did not occur. Uranium concentrations are variable, and low U samples give high uncertainty in older ages. The thickness of the weathering rind varies across a sample, tending to be greater near the top and smaller on the sides of stalagmites. Maximum and minimum thickness was thus obtained.

Sample	U (ppm)	$^{234}U/^{238}U$	$^{230}Th/^{234}U$	$^{230}Th/^{232}Th$	$^{234}U/^{238}U$ initial	Age (ka)
TBV1-95	0.171 ± 0.002	1.46 ± 0.02	0.869 ± 0.016	57	1.76	182.9 ± 10.5
TBV-17T	0.420 ± 0.006	1.73 ± 0.02	0.744 ± 0.014	754	2.06	129.8 ± 5.5
TBV-32	0.050 ± 0.001	1.18 ± 0.02	0.962 ± 0.022	24	1.39	275.2 (+41 –38)
TBV-41	0.103 ± 0.004	1.50 ± 0.07	0.801 ± 0.030	206	1.76	152.7 (+21 –19)
TBV-46	0.043 ± 0.003	1.40 ± 0.10	0.707 ± 0.039	33	1.56	123.2 (+25 –21)

Sample	Age (ka)	Weathering rind thickness (mm)	Rate (mm/ka)
		Range	Range
TBV1-95	182.9 ± 10.5	5.0 - 71.0	0.027 - 0.39
TBV-17T	129.8 ± 5.5	0.1 - 1.0	0.00077 - 0.0077
TBV-32	275.2 (+41 –38)	3.0 - 16.0	0.011 - 0.058
TBV-41	152.7 (+21 –19)	1.5 - 7.0	0.0098 - 0.046
TBV-46	123.2 (+25 –21)	0.1 - 1.0	0.00077 - 0.0077

Table 4.10. Uranium series analyses and condensation-corrosion minimum rates for selected samples from Toca da Boa Vista. Errors are ± 1σ.

The rates (Table 4.10) obtained vary over two orders of magnitude. They appear to be highly site specific, and are probably heavily dependent on the local atmospheric conditions. The data shows that rates are dependent primarily on thickness measured, as range of ages is quite small. No similar study has been described in the literature. Tarhule-Lips and Ford (1998), in the very different littoral caves of the Caribbean, have estimated condensation-corrosion rates based on experiments using gypsum tablets. They report mean values of 24 mm/ka, much higher than observed in the caves of Laje dos Negros, suggesting that the process may be episodic, not occurring during speleothem growth phases.

Condensation-corrosion in the Laje dos Negros caves appears to play a minor speleogenetic role, and is responsible for later modification of cave walls and speleothems. The process is important in modifying smaller features in the cave, but does not seem to be a significant morphological agent on the scale of karst systems. The total absence of condensation-corrosion features in nearby caves in the Caatinga Limestone indicate a lithology controlled process, suggesting that condensation-corrosion in the area can probably be related to sulphuric acid processes that occur in the Una Group carbonates.

4.6. SHALLOW HYPOGENIC SPELEOGENESIS

Aquifer hydrochemistry and cave geomorphology in the semi-arid Campo Formoso Karst have demonstrated that sulphuric acid produced by metal sulphide oxidation can play a major role in speleogenesis. The influence of metal sulphide oxidation has not been previously recognised as able to generate large scale speleogenesis (Palmer, 1990, 1991). The data presented in this thesis suggests, however, that given the availability of significant deposits of sulphide in the bedrock, major caves can be generated.

Such "shallow hypogenic" caves display a stronger lithological control than either deep-seated or meteoric systems, because the source of acidity lies within specific carbonate units. Among the major differences between deep-seated and shallow hypogenic speleogenesis of the Una Group Karst are:

(1). Deep seated processes tend to be "point source" controlled, in the sense that the area of carbonate affected by the process will be confined to the environs of either hydrocarbon basins or volcanic hot spots. Although these can cover quite large areas, as seen in the Guadalupe Mountains (Hill, 1990) or in Italy (Galdenzi and Menichetti, 1995), they are not as areally extensive as the outcrops of the Una Group which cover tens of thousands of squared kilometres. Caves with hypogenic characteristics have been observed in many of the distinct carbonate basins that comprise the Una Group (Fig. 4.2). These basins were never joined together and are underlain and separated by older quartzite units. It appears unlikely that deep-seated process would act simultaneously in distinct depositional basins spread over such vast area.

(2). Shallow hypogenic caves are controlled by the geometry of the sulphide beds. If these are horizontally disposed along specific units of the carbonate the caves will tend to have a two dimensional pattern. Deep-seated caves are generated from below, by water injected under high hydraulic head. These caves will almost always display a tridimensional pattern, unless there is a major confining layer. Furthermore, there will be evidence of deep ascending passages that mark the vertical path of the acid source. These are absent in shallow hypogenic caves which form extensive two dimensional ramiform mazes which have not been described for deep-seated hypogenic caves.

(3). The classic ramiform pattern, as described by Palmer (1991), consists of passages that wander away from single points of acid injection. The ramiform pattern observed in the area does not show this point source effect.

(4). Ancient drained shallow hypogenic caves are unlikely to display the acidity source (sulphide beds) because these will be consumed during speleogenesis. Active deep-seated caves, on the

other hand, have been observed in several sites (Egemeier, 1981, van Everdingen et al., 1985, Hose and Pisarowicz, 1999).

(5). Deep-seated hypogenic caves can develop at any depth below the water table, and some appear to have originally developed quite deep. Shallow hypogenic caves, on the other hand, are limited by the lack of dissolved oxygen in deeper parts of the aquifer (Ball and Jones, 1990), and by the decreasing aperture (or existence) of joints deep within the bedrock. Such caves will necessarily be limited to the upper parts of carbonate units. This is supported by the existence of non-weathered sulphide deposits deep in carbonate formations.

(6). Massive subaqueous speleothem accumulations, either of hydrothermal calcite or gypsum, tend to be absent in shallow hypogenic caves, presumably because of the relatively low amount of acidity generated by the sulphide oxidation process when compared to the massive injections of H_2S that can occur in deep-seated hypogenic settings.

Hypogenic speleogenesis will tend to be overwhelmed by normal meteoric processes in more humid areas. The Una Group Karst presents an excellent setting in which to study the relative importance of both hypogenic and meteoric processes, because of both the rainfall range within the carbonate area, and differences in the extent of concentrated allogenic recharge. The Iraquara Karst area, in the wetter southern portion of the Una Group display different features that will be discussed in the next chapter. Additionally, the occurrence of the Caatinga Limestone, a very distinct carbonate in which hypogenic processes do not occur, in the same semi-arid area as the Campo Formoso Karst, allows the study of the role of lithology in controlling speleogenesis. This shallow hypogenic model of speleogenesis should occur in other pyritiferous carbonate sequences, being evident under arid or semi-arid climate.

CHAPTER 5
CAVE DEVELOPMENT IN THE STABLE CRATONIC AREA OF EASTERN BRAZIL

5.1. INTRODUCTION

Cave geomorphological observations in a regional scale have allowed the recognition of a distinctive pattern of cave development in the São Francisco Craton. The influence of bedrock acidity in generating caves has been described in Chapter 4. In this chapter, three areas within the São Francisco Craton will be analysed. Despite differences in lithology, present climate, and geomorphic and hydrological settings, all areas display many of the features typical of paragenetic caves. The role of denudation rates in promoting cave development will be assessed based on observations in caves in eastern Brazil, and a global speleogenetic model for this type of tectonic setting will be presented.

5.2. PARAGENESIS

Paragenesis is a phreatic mode of cave development that occurs when the base of the conduit is armoured with impermeable sediment that inhibits dissolution of the floor, the passage thus develops by upward dissolution of the ceiling. The velocity of the water flowing in the conduit is kept in equilibrium, as any increase in it will cause sediment removal and a consequent increase in the cross-sectional area for flow, reducing the velocity below the threshold of sediment transport, and causing deposition and a return to the equilibrium cross-section. The conduit grows upwards until it reaches the water table (Fig. 5.1). The term paragenesis was introduced by Renault (1968) to distinguish this kind of passage from the syngenetic type, which is the classic vadose canyon that develops by fluvial downcutting.

The influence of sediment on the morphology of dissolution features in caves was recognised long ago. Bretz (1942) attributed the genesis of pendants to dissolution between sediment and the ceiling. He even attributed the genesis of a particular passage to paragenesis, but discarded it as a major cave forming process. Renault (1958) was probably the first to propose that evolution of caves can occur by paragenesis, a concept further developed in a later paper (Renault, 1968). Pasini (1967, 1975) also described the process, mostly from gypsum caves near Bologna, and referred to it as "antigravitational erosion".

Paragenesis has received a sketchy and poor treatment, especially in the English language karst literature. Most recent reviews have given it only a very brief treatment (White, 1988, Ford and Williams, 1989), and it has mostly been described as a process modifying previously syngenetic caves (Lauritzen, 1982, Webb et al., 1992, Springer et al., 1997, Hercman et al., 1997). There seems to be a number of reasons for such neglect. First, in contrast to vadose incision which is frequent in river caves, the process itself cannot be observed directly except by

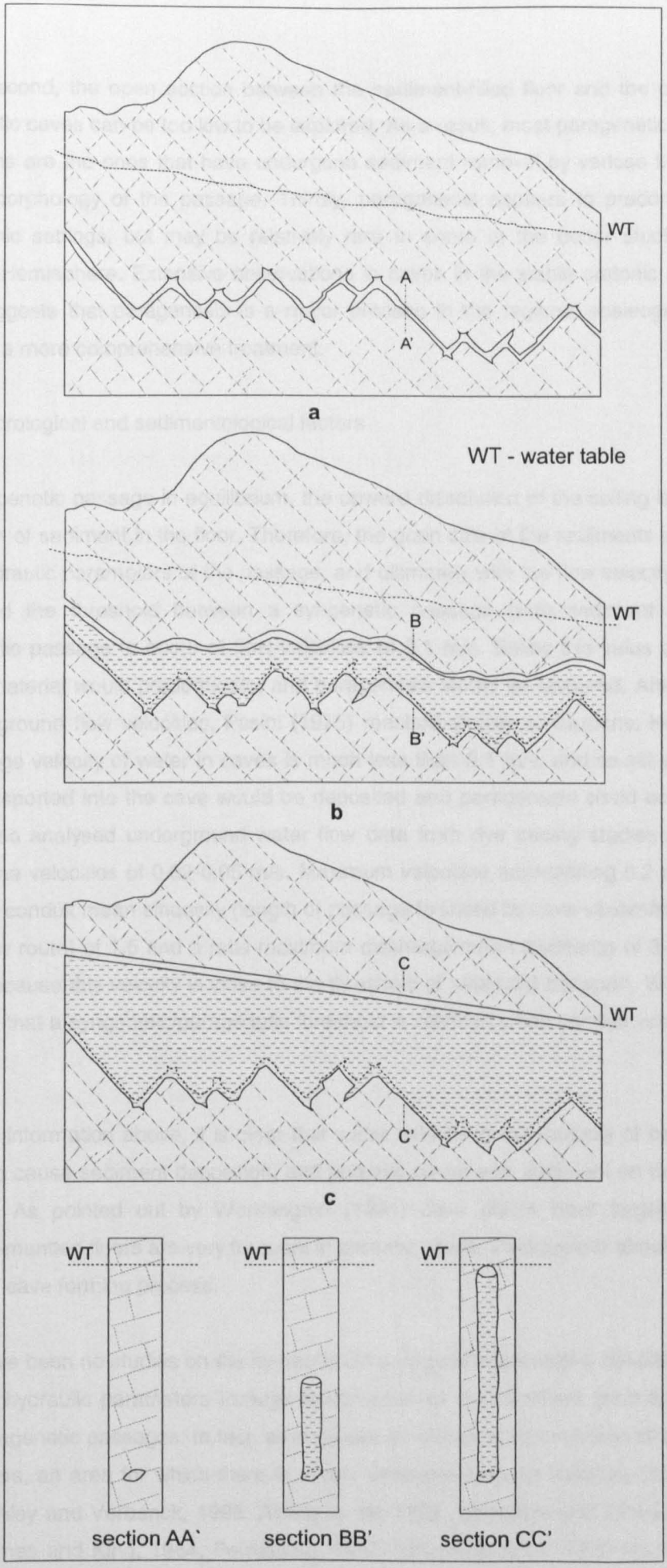

Figure 5.1. Evolution of a paragenetic passage. From Pasini (1967).

divers. Second, the open section between the sediment-filled floor and the ceiling in inactive paragenetic caves can be too low to be explored. As a result, most paragenetic caves enterable by humans are the ones that have undergone sediment removal by vadose flow, masking the original morphology of the passage. Thirdly, paragenesis appears to predominate in certain geomorphic settings, but may be relatively rare in some of the better studied areas of the Northern Hemisphere. Extensive observations in caves in the stable cratonic areas of eastern Brazil suggests that paragenesis is a major process in the regional speleogenesis, and thus deserves a more comprehensive treatment.

5.2.1. Hydrological and sedimentological factors

In a paragenetic passage in equilibrium, the upward dissolution of the ceiling is matched by the deposition of sediment in the floor. Therefore, the grain size of the sediments should be related to the hydraulic parameters of the passage, and ultimately with the flow velocity. Renault (1968) interpreted the threshold between a syngenetic passage (with sediment removal) and a paragenetic passage to occur at flow velocities of 0.1 m/s. Below this value deposition of fine grained material would predominate, and paragenesis would be favoured. After reviewing data on underground flow velocities, Pasini (1975) reached similar conclusions. He concluded that the average velocity of water in caves is much less than 0.1 m/s, and so silt and clay deposits once transported into the cave would be deposited and paragenesis could occur. Worthington (1991) also analysed underground water flow data from dye tracing studies and found mean straight line velocities of 0.02-0.05 m/s. Maximum velocities approaching 0.2 m/s were derived based on conduit mean sinuosity (length of passage followed by cave stream/straight line length of the flow route) of 1.5 and a ratio maximum discharge/mean discharge of 3-12 (Worthington, 1991). Because this velocity is close to the threshold of sediment transport, Worthington (1991) proposed that a syngenetic/paragenetic threshold is reached when conduit velocity drops below 0.2 m/s.

From the information above, it is clear that water velocity in the majority of caves can be slow enough to cause sediment deposition, and phreatic caves with sediment on the floor should be common. As pointed out by Worthington (1991) cave divers have largely confirmed that sediment-mantled floors are very frequent in phreatic caves. Paragenesis should therefore be an important cave forming process.

There have been no studies on the hydraulics of paragenetic passages, despite it being possible to obtain hydraulic parameters through examination of the sediment grain size and sorting in fossil paragenetic passages. In fact, analogy can be drawn to transmission of sediment in pipes and sewers, an area for which there is a very extensive body of literature (Acaroglu and Graf, 1968, Ashley and Verbanck, 1996, Ashley et al., 1992, Condolios and Chapus, 1963, Craven, 1953, James and King, 1984, Perrusquía, 1992, Skipworth et al., 1996 among others). Using laboratory experiments performed in perfectly circular pipes an order of magnitude smaller than

caves, several equations have been deduced to calculate the critical velocity for erosion (the velocity necessary to start moving a bed of sediment) or the critical transport velocity (the velocity needed to overcome settling of particles once suspended) (Durand, 1953, Robinson and Graf, 1972, Mayerle et al., 1991, Nalluri et al., 1994). The major problem in applying these equations to paragenetic passages is the difficulty in locating an undisturbed paragenetic sedimentary sequence. As pointed out before, most original paragenetic passages were probably too low for human penetration and sediment removal and reemplacement appears to have been extremely common. No unequivocal paragenetic sediment was located during the work for this thesis.

5.2.2. Criteria for recognition of paragenetic passages

Although vadose and paragenetic passages evolve in very distinctive ways, there has been little progress in setting reliable and foolproof criteria to distinguish between the two. As would be expected, most criteria deal with the morphology of abandoned passages. The following diagnostic features have been suggested in the literature:

1. Presence of pendants (Fig. 5.2a) (Bretz, 1942, Renault, 1968). These forms are created at the interface between the sediment and rock, and demonstrate that dissolution has occurred above the sediment. However, pendants can occur in vadose caves that are filled with later sediments.

2. Presence of anastomoses or half tubes (Fig. 5.2b,c) (Bretz, 1942, Renault, 1968). Both forms are created by an underfit stream flowing in the top of a sediment-filled (or near sediment-filled) passage. As with pendants, they can also occur in vadose caves.

3. Presence of parasitic wall tubes (Lauritzen and Lauritsen, 1995, Farrant, 1995). Wall tubes are similar to ceiling (half) tubes and develop between the sediment and the wall. Again these can also occur in sediment-filled vadose caves.

4. Presence of wall grooves (Farrant, 1995). These are rounded features similar to notches which develop on phreatic passages, representing zones of passage lateral enlargement on top of sediment fill. Wall grooves slope up and down parallel with the sediment fill.

5. Lack of guiding fracture or bedding plane (Pasini, 1967). A paragenetic passage may start as a fracture controlled tube, but as it grows upwards it will tend to evolve independent of any fracture or bedding plane. Paragenetic passages usually cut through the bedding. This is a good criterion, although paragenetic passages can follow vertical fractures if present.

6. Lack of a precursor phreatic tube on the ceiling (Lauritzen and Lauritsen, 1995, Farrant, 1995). This follows from the previous criterion as syngenetic caves will start as a phreatic tube in

the ceiling. Although difficult to observe, especially in high passages or when the canyon and ceiling tube are of similar dimension, this is a sufficiently sound criterion that set apart paragenetic and vadose passages.

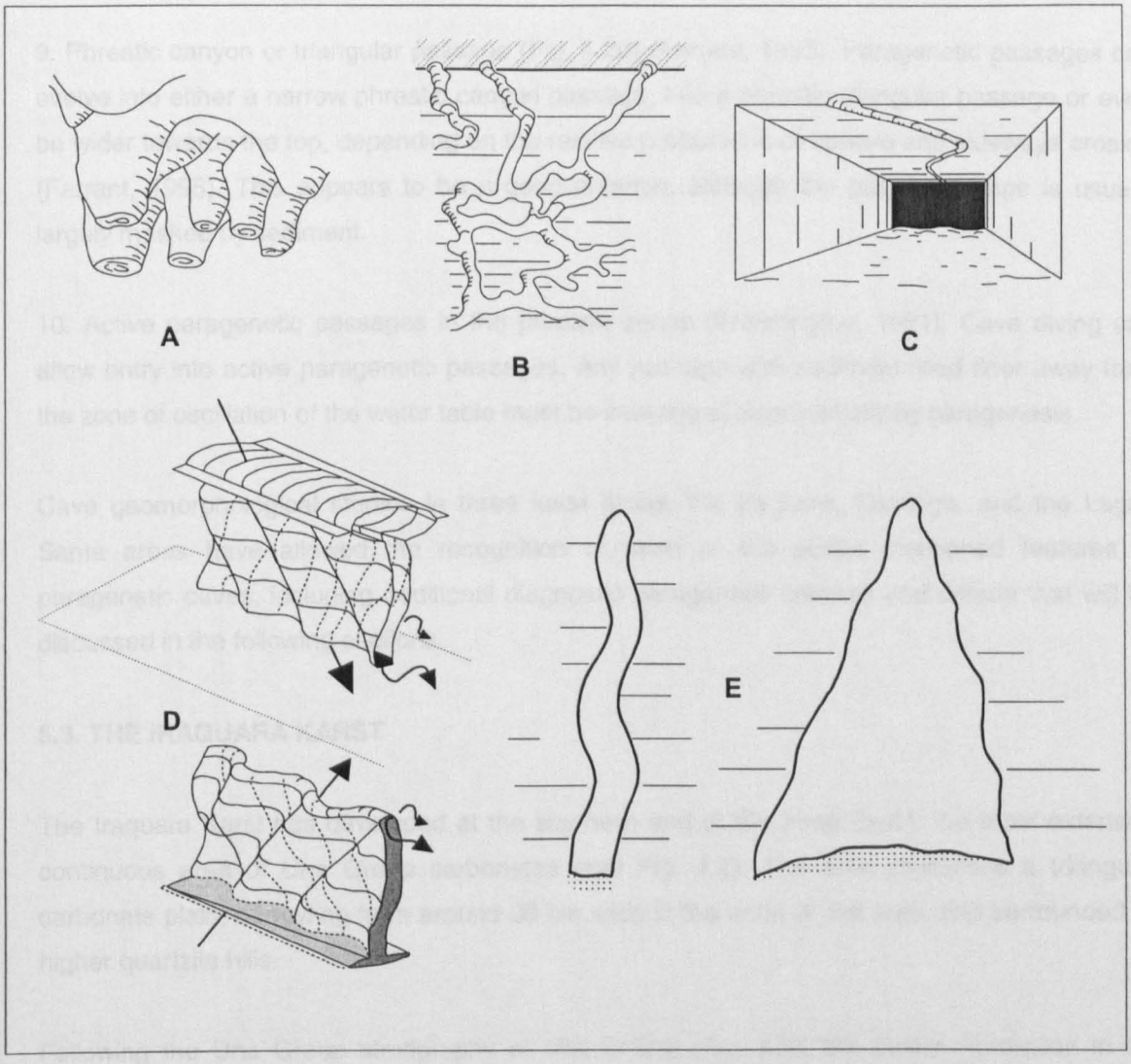

Figure 5.2. Some of the criteria used to recognise paragenetic passages. A. Presence of pendants (from Renault, 1968). B. Anastomoses (Renault, 1968). C. Ceiling (half) tubes (Bretz, 1942). D. Meander shift: upper - syngenetic; lower - paragenetic (Lauritzen and Lauritisen, 1995). E. Phreatic canyon or triangular passage (Farrant, 1995).

7. Evidence of total sediment fill (Farrant, 1995). A paragenetic passage may end up totally choked with sediment as the velocity of the stream drops, and fine-grained material deposits. In fact, many of the forms described above such as pendants, anastomoses and half-tubes originate due to dissolution in nearly choked passages. However, sediment-plugged vadose passages are extremely common, and Palmer (1987) has used total sediment infill as evidence against paragenesis in Mammoth Cave, Kentucky.

8. Downstream propagation of meanders (Fig. 5.2d) (Ewers, 1985). Meander bend axes progress downward in vadose canyons, while in paragenetic passages they progress upward. Lauritzen and Lauritsen (1995) have elaborated upon this criterion, and devised a method for

distinguishing between the two types by plotting scallop flow direction and meander shift direction in a stereonet. This is a sound criterion, although difficult to apply in low passages that contain sediment, or large passages which are wider than the meander offset.

9. Phreatic canyon or triangular passage (Fig. 5.2e) (Farrant, 1995). Paragenetic passages can evolve into either a narrow phreatic canyon passage, into a phreatic triangular passage or even be wider towards the top, depending on the relative proportions of upward and sideways erosion (Farrant, 1995). This appears to be a good criterion, although the passage shape is usually largely masked by sediment.

10. Active paragenetic passages in the phreatic zones (Worthington, 1991). Cave diving can allow entry into active paragenetic passages. Any passage with sediment-filled floor away from the zone of oscillation of the water table must be evolving at least partially by paragenesis.

Cave geomorphological studies in three karst areas, the Iraquara, Caatinga, and the Lagoa Santa areas have allowed the recognition of most of the above mentioned features of paragenetic caves, including additional diagnostic paragenetic features and criteria that will be discussed in the following sections.

5.3. THE IRAQUARA KARST

The Iraquara Karst has developed at the southern end of the Irecê Basin, the most extensive continuous area of Una Group carbonates (see Fig. 4.2). The area comprises a triangular carbonate plain, narrowing from around 30 km wide in the north of the area, and surrounded by higher quartzite hills.

Following the Una Group stratigraphy of Misi (1979) (Fig. 4.3), the Salitre Formation in the central portion of the area is composed by Units A1 and A, while Unit B occurs in the outer sectors (Fig. 5.3). Unit B1 is restricted to small patches inbetween units B and A. The carbonates are underlaid by the glaciogenic conglomerates and mudstones of the Bebedouro Formation, which form a narrow outcrop bordering the quartzite hills of the Chapada Diamantina Group. The Iraquara area lies in a major syncline with a north-south oriented axis. Dips on the carbonates are mostly horizontal, but can locally reach 30° (Cruz Jr., 1998). Analyses of carbonates from the area (Ferrari, 1990) shows average relative composition of CaO and MgO of 45.26 and 5.26%, denoting a dolomitic limestone. Depth of the carbonate sequence, as estimated from well logs, surpasses 150 m in the central portion of the area (Cruz Jr., 1998).

The Iraquara Karst has developed on a planation surface with an elevation between 700-750 m asl near the centre of the area, although numerous depressions of varied dimension and depth disrupt the plain. This surface was interpreted by King (1956, 1967) as belonging to the Paraguaçú Planation Cycle, the most recent cycle to act upon eastern Brazil, which started

developing after uplift at the end of the Pliocene (King, 1967). Later geologists (see review in Cruz Jr., 1998 and Laureano, 1998) have interpreted this same surface as belonging to the earlier Velhas Cycle of King (1956). Valadão (1998) in his recent review of eastern Brazil's planation surfaces has refrained from placing this area into any of his new planation surfaces. In view of the controversies regarding extent, distribution, timing and mechanism of initiation of planation surfaces in Brazil and the world (see review in section 3.2.1) it seems wise not to constrain any geomorphological interpretation on timescales derived from such planation cycles.

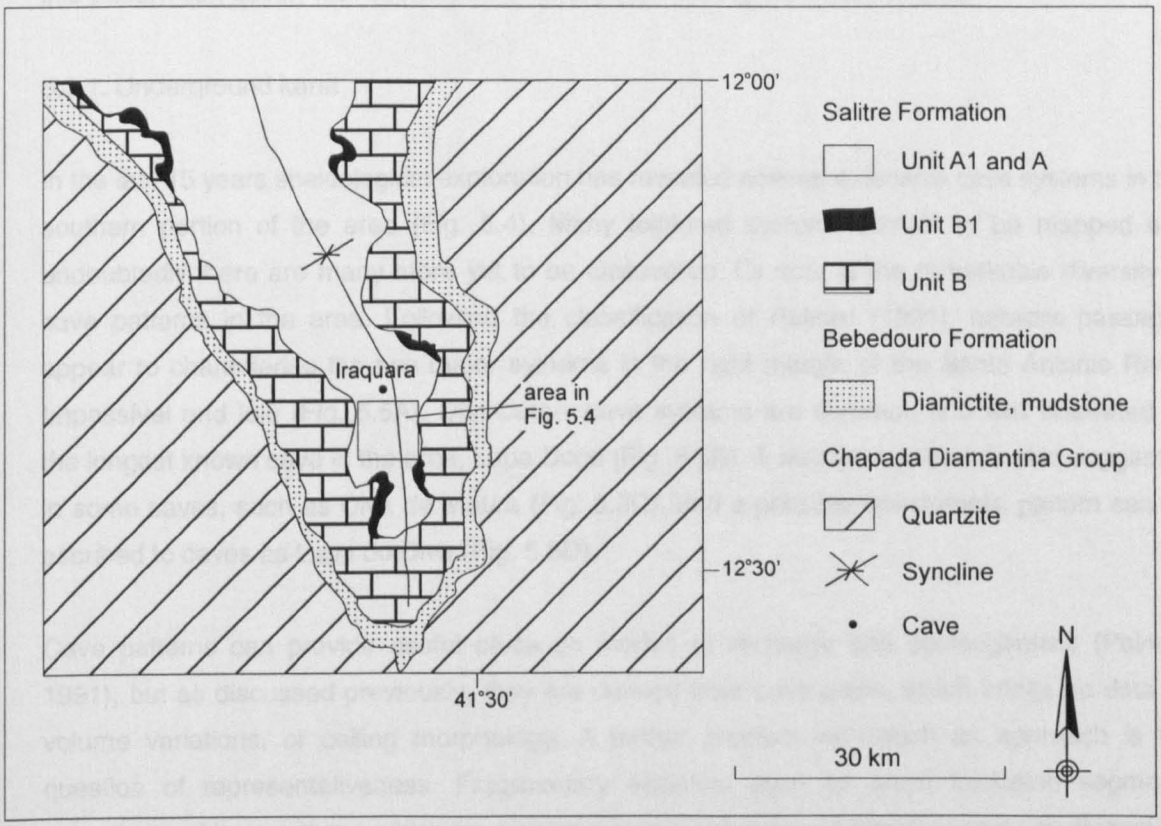

Figure 5.3. Geology of the Iraquara Karst area. From Misi and Kyle (1994).

Much of the karst surface is covered by soil, presumably derived from the carbonate sequence. Soil depths are highly irregular due to accumulation in dissolution hollows in the bedrock. Laureano (1998) has also recognised the significance of biogenic moulds (termite hills), residual silica crusts, and fluvial quartz conglomerates as important local constituents of the soil cover.

The surface hydrology is marked by ephemeral streams that sink into the limestone and only carry water after very intense rainfall. Some of these streams, such as the Água de Rega and Riacho das Almas, have their headwaters in the quartzite hills, while some minor others are entirely contained within the carbonate. The local base level is determined by the Santo Antonio River (Fig. 5.4), which derives from the quartzite hills to the south, and has excavated a wide meandering canyon up to 30 m high as it crosses the carbonates. The river is largely underfit in its wide valley and contains flowing water over much of the year. Several springs occur in the Santo Antonio River, and form an outlet for the extensive carbonate ground water catchment to

the north. Piezometric analysis has suggested that there is a ground water divide some 40 km north of Iraquara, between the Santo Antonio and Jacaré River ground water basins (Negrão, 1987).

Local climate is subhumid to semi-arid. Mean annual rainfall varies from 700 mm in the northwest of the area to around 1100 mm in the southwest (Cruz Jr., 1998). However, due to orographic influence of the elevated quartzite areas immediately to the south, departures from this pattern can occur, with occasional showers even during the driest months.

5.3.1. Underground karst

In the last 15 years speleological exploration has revealed several extensive cave systems in the southern portion of the area (Fig. 5.4). Many explored systems remain to be mapped and undoubtedly there are many more yet to be discovered. Of note is the remarkable diversity of cave patterns in the area. Following the classification of Palmer (1991), network passages appear to characterise the two major systems in the right margin of the Santo Antonio River, Impossível and Ioiô (Fig. 5.5A). Distributary cave systems are common and well illustrated by the longest known cave in the area, Lapa Doce (Fig. 5.5B). A ramiform pattern is also suggested in some caves, such as Diva de Maura (Fig. 5.5C), and a possible anastomotic pattern can be ascribed to caves as Lapa do Diva (Fig. 5.5D).

Cave patterns can provide useful clues on modes of recharge and speleogenesis (Palmer, 1991), but as discussed previously, they are derived from cave plans, which brings no data on volume variations, or ceiling morphology. A further problem with such an approach is the question of representativeness. Fragmentary systems, such as short truncated segments sometimes of large volume which are very common in the Iraquara Karst, cannot usually provide enough passage length to allow recognition of pattern. Although the major Iraquara Karst caves represented in Fig. 5.4 comprise several kilometres of passages, they still represent only small segments of much larger systems. For instance, some of the caves presented in Fig. 5.5 could actually belong to large scale anastomotic systems. Distributary systems, in particular, have not been recognised as a major cave pattern (Palmer, 1991), but are characteristic of some downstream sections of caves, usually near the discharge zone (Palmer, 1984). The possibility that some of the distributary caves in the area, such as Lapa Doce, could in fact represent massive truncated anastomotic systems, as suggested by Laureano (1998), has important speleogenetic implications as will be discussed later. Fragmentation of cave systems is particularly evident in the Iraquara area due to frequent surface collapse and sediment infilling. Superposition of distinct speleogenetic phases could also play a role in complicating the original cave pattern. In the following sections, studies will be concentrated in two of the most extensive caves in the area, Lapa Doce and Gruta da Torrinha, which represent isolated fragments of the same system. Additional data will be provided from Gruta Diva de Maura, a separate system.

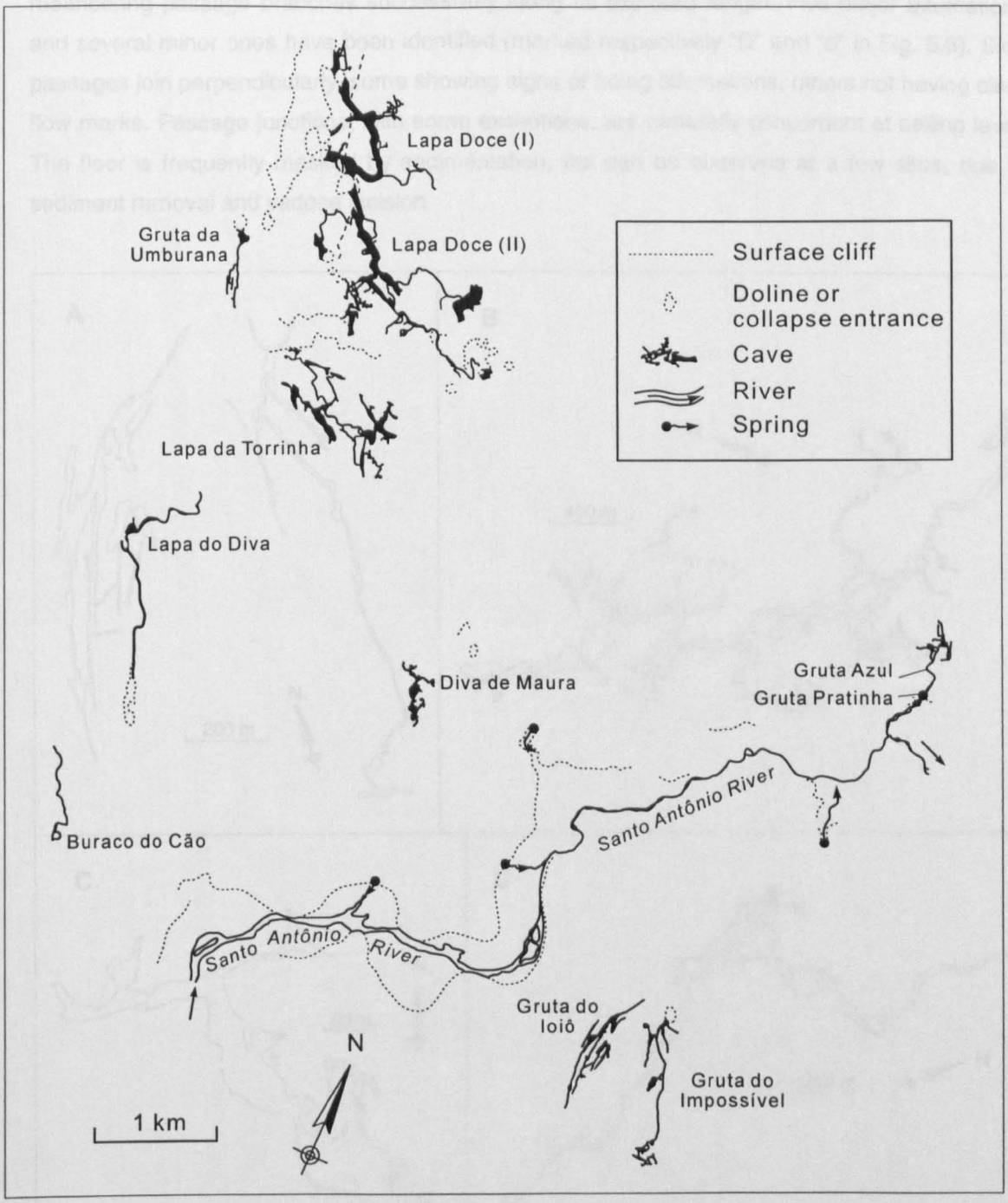

Figure 5.4. Main caves of the Iraquara Karst. From surveys by Grupo Bambuí de Pesquisas Espeleológicas, Groupe Meandres and Grupo de Explorações Espeleológicas do Ceará.

5.3.1.1. Morphology of caves

The morphology of Lapa Doce and Torrinha has been described in previous works (Ferrari, 1990, Cruz Jr., 1998, Laureano, 1998). Lapa Doce (Fig. 5.6) comprises a massive main passage in places over 40 m wide and 10 m high that starts in the swallet of the Água de Rega Canyon. The passage is bisected by a huge surface collapse that effectively divides the cave in two separate segments, Lapa Doce I and II, respectively 6.6 and 9.8 km long. The main

meandering passage branches successively along its explored length. Five major bifurcations and several minor ones have been identified (marked respectively "D" and "d" in Fig. 5.6). Side passages join perpendicularly, some showing signs of being bifurcations, others not having clear flow marks. Passage junctions, with some exceptions, are generally concordant at ceiling level. The floor is frequently masked by sedimentation, but can be observed at a few sites, due to sediment removal and vadose incision.

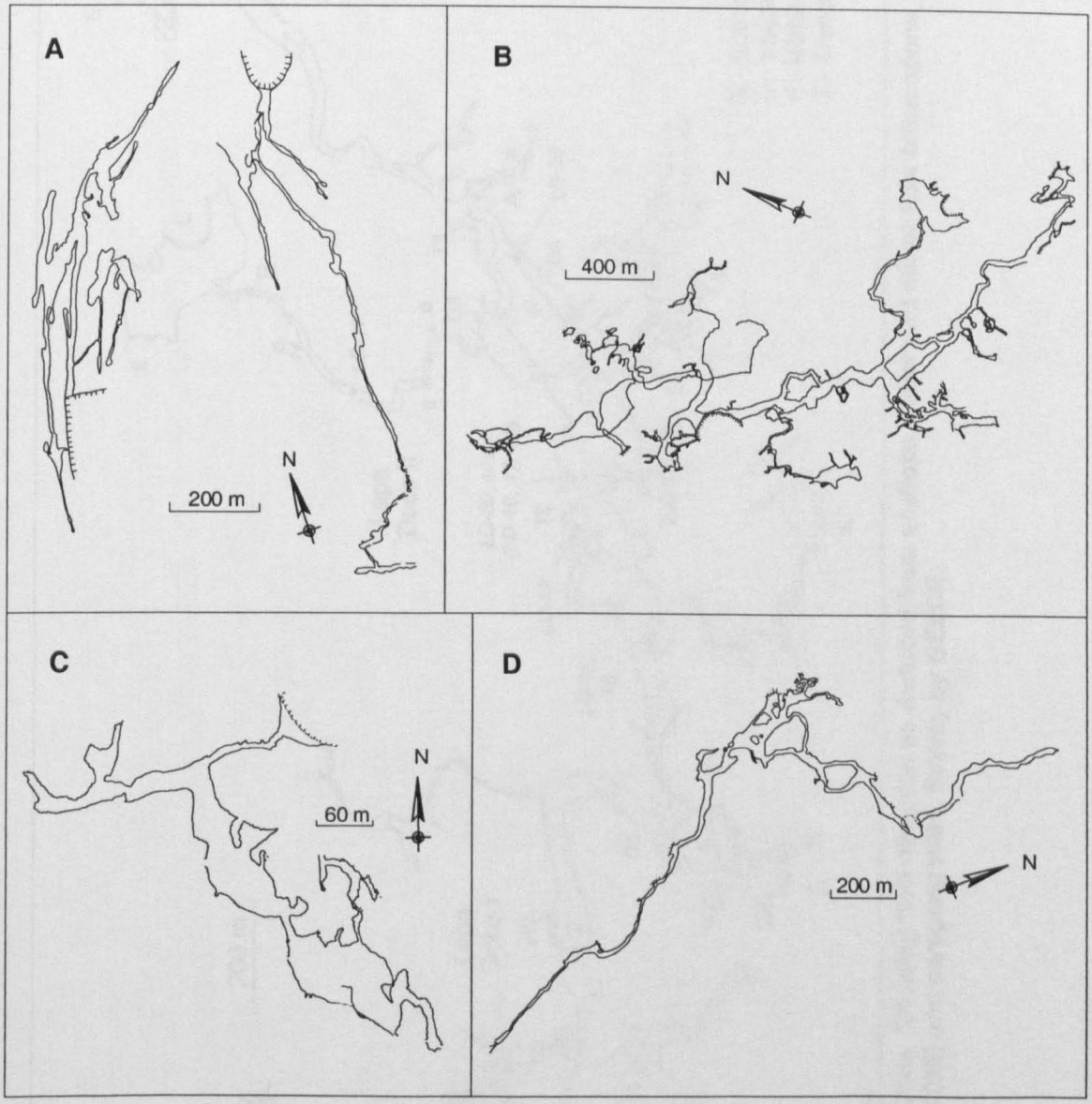

Figure 5.5. Cave patterns in the Iraquara Karst. A - Grutas Ioiô and Impossível (network?) (survey GBPE). B - Distributary (anastomotic?): Lapa Doce (survey GEECE). C - Ramiform: Gruta Diva de Maura (survey GBPE). D - Anastomotic (?): Lapa do Diva (survey GBPE).

Gruta da Torrinha, a 7.7 km long cave (Fig. 5.7) some 500 m to the south, displays some of the features of Lapa Doce without however conforming to its general layout. Its entrance is located in a major collapse doline, and is not related to any major swallet. Torrinha does not show a main trunk passage as in Lapa Doce, and there are abrupt transitions in ceiling level at passage junctions. The distributary pattern at Torrinha is also less conspicuous although it can be observed in places (e.g. downstream from T5, Fig. 5.7). The major distinguishing feature of

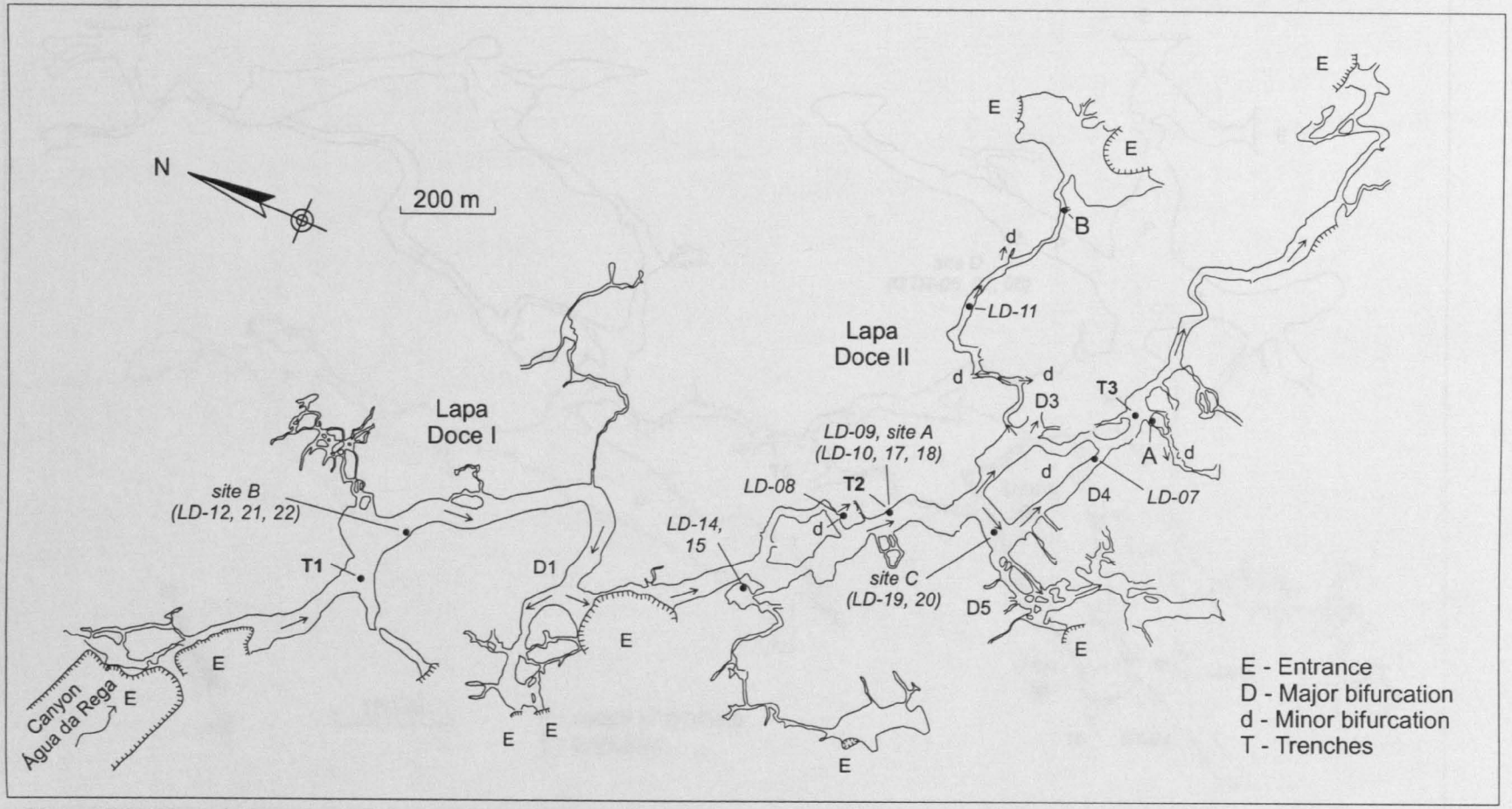

Figure 5.6. Plan of Lapa Doce. Showing flow direction as deduced from scallops, major and minor flow bifurcations, trenches described by Laureano (1998) and sampling sites. Survey by GEECE.

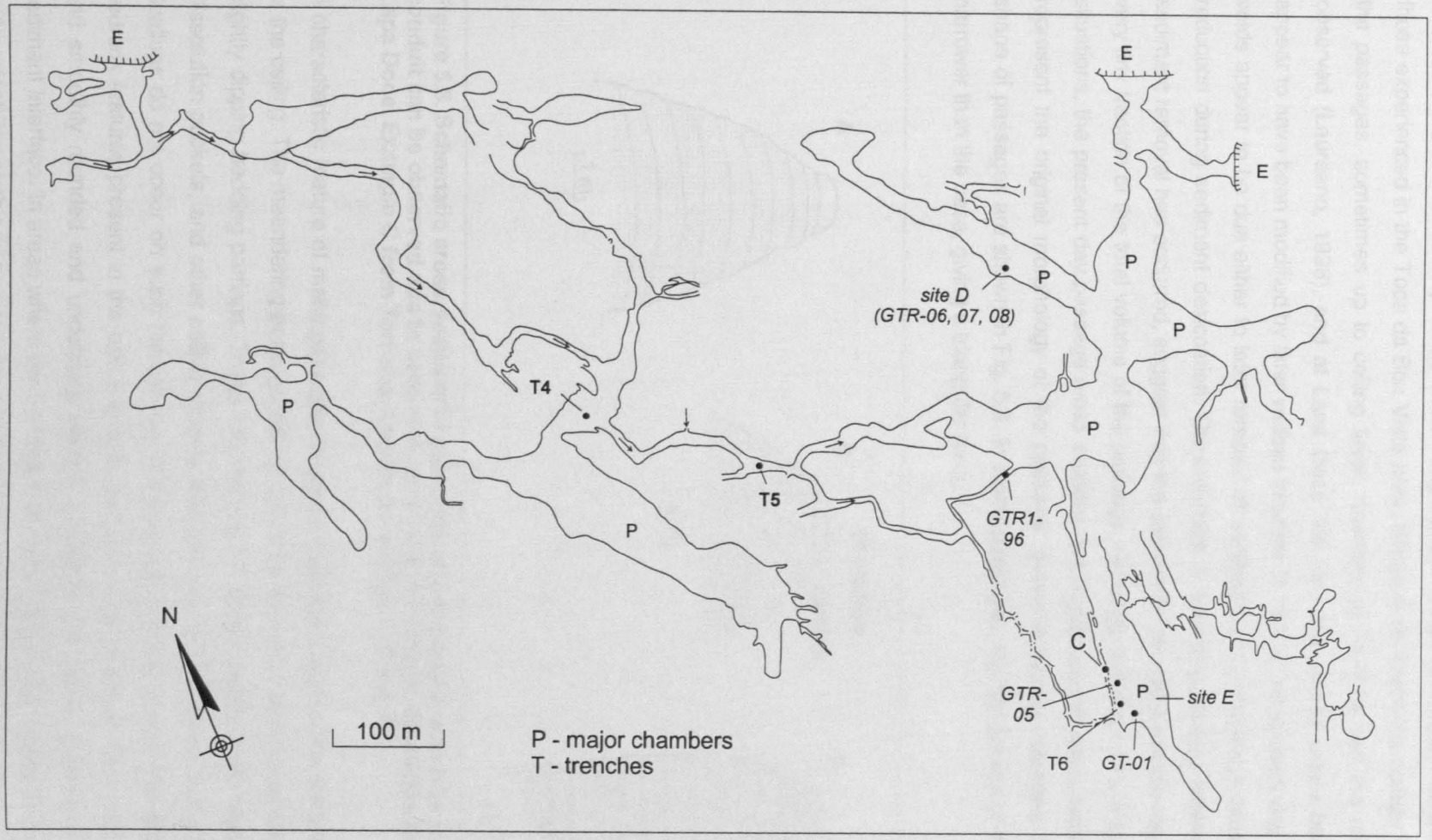

Figure 5.7. Plan of Gruta da Torrinha, showing flow directions as deduced from scallops, major chambers, trenches described by Laureano (1998), passage cross sections and sampling sites.

Torrinha is the existence of massive passages largely modified by breakdown (marked "P" in Fig. 5.7), which show no clear genetic relationship with the more continuous meandering passages. Flow marks in these larger passages have been obscured by breakdown.

The analysis of conduit morphology in the Iraquara caves carries inherent difficulties similar to those experienced in the Toca da Boa Vista area. Massive sediment fills occupy the majority of the passages, sometimes up to ceiling level. Nowhere at Torrinha can the original floor be observed (Laureano, 1998), and at Lapa Doce the very few places where bedrock is seen appear to have been modified by later vadose incision. In fact, all the present day sediment-free voids appear to be due either to later removal of sediment, or to shrinkage caused by volume reduction during sediment desiccation. Observations in several passages where shrinkage or sediment removal has occurred, suggest that the sediment-free upper section represents only a very tiny fraction of the total volume of the passage, generally less than 10% (Fig. 5.8). In such situations, the present day passage cross sections are highly uninformative, because it fails to represent the original morphology of the passage. Some schematic sections of the original shape of passages are shown in Fig. 5.8. In many passages, the top portion of the passage is narrower than the base, giving a triangular form.

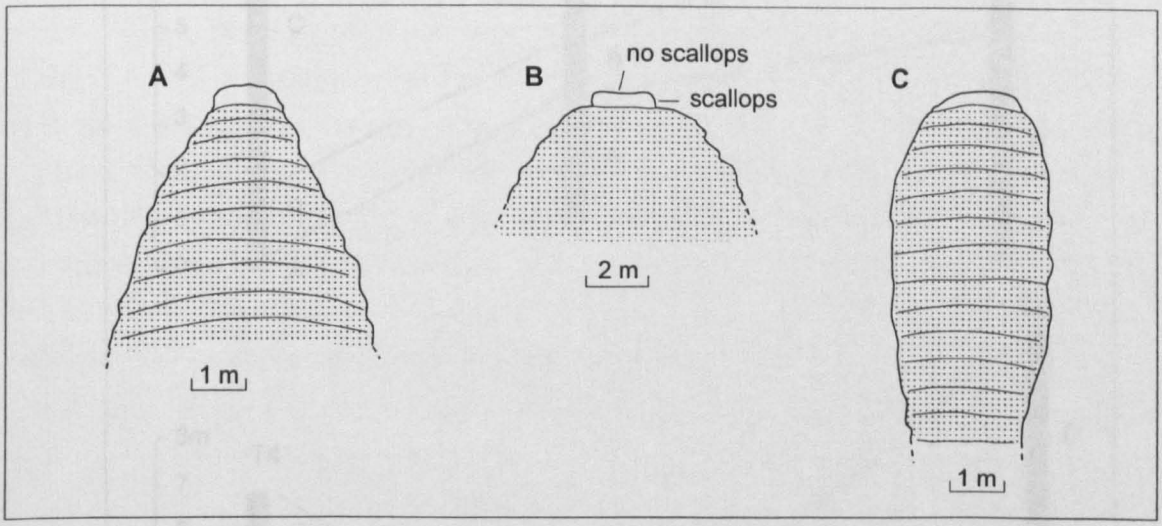

Figure 5.8. Schematic cross-sections of passages where the probable true shape of the conduit can be observed due to sediment removal or shrinkage. Examples A and B from Lapa Doce. Example C from Torrinha. Locations on Figs. 5.6 and 5.7.

A characteristic feature of many passages, especially at Lapa Doce, is the remarkable flatness of the ceiling. The meandering passage ceiling can often be seen to cut horizontally through the slightly dipping bedding partings. These flat ceilings are found usually in the higher passages. Dissolution pockets, and other ceiling phreatic features are largely absent in the higher levels. Scallops do not occur on such flat ceilings, but they are present on the side walls. Additional bedrock features present in the caves include pendants and pillars at lower ceiling undercuts and smoothly rounded and undulating vertical runnels in the walls, generated at the rock-sediment interface. In areas where the bedrock has been exposed by sediment removal, typical vadose features such as canyons occur, probably generated after sediment removal.

Lapa Doce and Torrinha present extensive sedimentation. All passages appear to have been filled (sometimes completely) with sediment. Laureano (1998) has performed a detailed description of this sediment, based on a series of trenches excavated at selected sites (T in Figs. 5.6 and 5.7). Three major facies associations have been distinguished (Fig. 5.9) which can be correlated both between the distinct trenches and in both caves (Laureano, 1998). Association A lies at the base of the sequence (bedrock has not been reached in any of the trenches) and comprises mostly mud and muddy sand with some minor sandy facies showing cross bedding and flat parallel bedding. Association B is characterised by sandy deposits with well marked erosive contacts between the units. The uppermost facies association C, is represented by muds which are concordant with the ceiling and appear in many places to have completely filled the passage. Sedimentary sequences in caves commonly terminate with such "mud caps" (Bull, 1981, Sasowski et al., 1995, Springer et al., 1997).

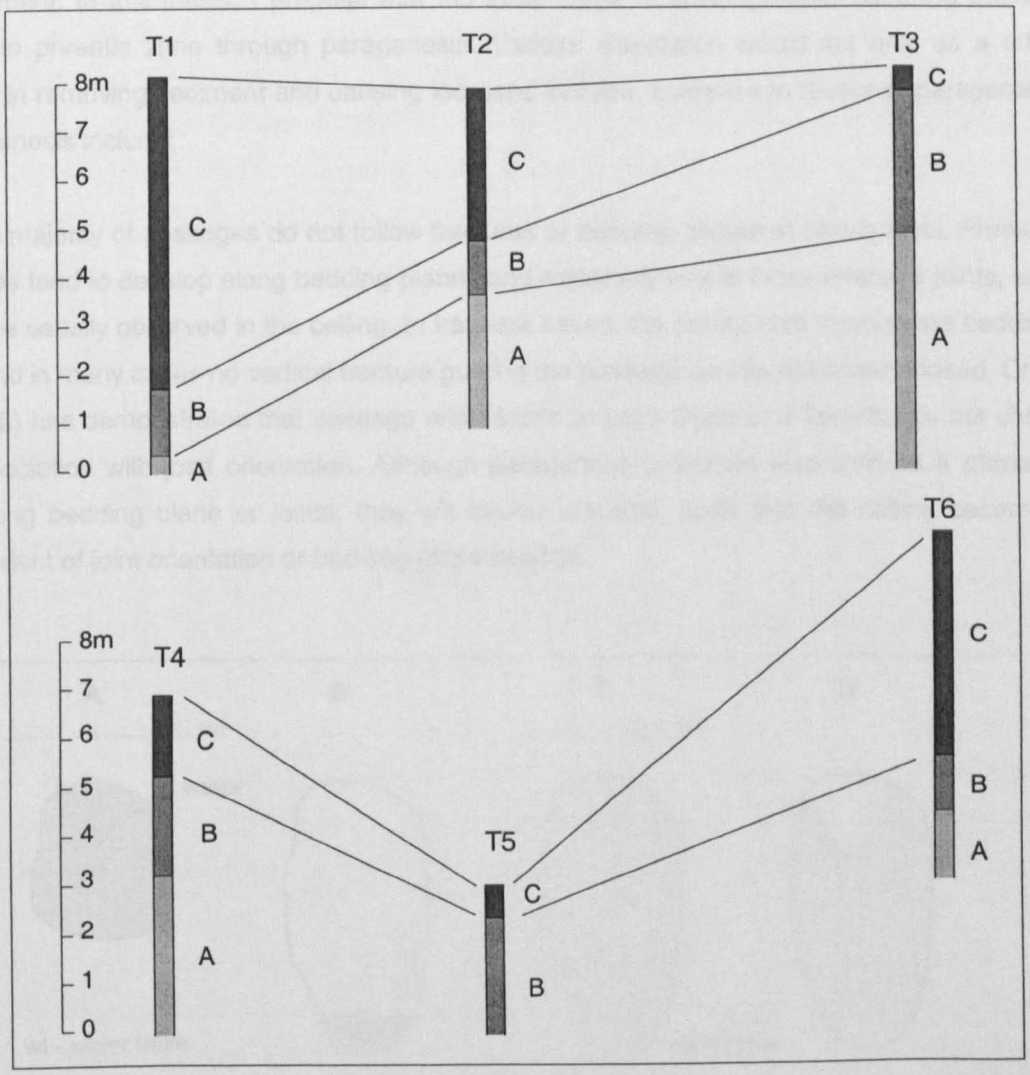

Figure 5.9. Correlation between facies associations in sediment trenches at Lapa Doce (T1 to T3) and Torrinha (T4 to T6). From Laureano (1998).

Sediment removal has been heterogeneous along the passages. The largest amount of removal has occurred along the present ephemeral course of the drainage coming from the Água de Rega Canyon. Many side passages (and one of the major distributaries of Lapa Doce, D3) still

preserve the entire sedimentary sequence. Abrupt changes in floor level along the passages, especially in Lapa Doce, are mainly due to variations in the amount of sediment removed.

5.3.1.2. Evolution of Lapa Doce and Torrinha

Ferrari (1990) has proposed an evolution model for Lapa Doce that comprises basically 4 stages (Fig. 5.10): (A) Generation of a phreatic passage, (B) vadose incision, (C) sediment infilling with possible dissolution at the sediment-rock interface, (D) removal of sediment. This model, which conforms with classical ideas, has been adopted by Cruz Jr. (1998) who has emphasised the role of paragenesis in promoting some ceiling dissolution and creating associated features. Cruz Jr. (1998) also believes that phase D was responsible for the opening of some minor passages. In this model, the present morphology of the cave would be largely due to vadose processes, the original phreatic tube (nowhere to be observed) having been masked by later paragenetic development. In this thesis, I propose that the initial stage of speleogenesis occurred entirely within the phreatic zone through paragenesis. Vadose dissolution would act only as a later process in removing sediment and causing localised incision. Evidence in favour of paragenetic speleogenesis include:

(1). The majority of passages do not follow fractures or bedding planes at ceiling level. Phreatic passages tend to develop along bedding planes and especially where those intersect joints, and these are usually observed in the ceiling. In Iraquara caves, the ceiling cuts through the bedding plane and in many cases no vertical fracture guiding the passage can be observed. Indeed, Cruz Jr. (1998) has demonstrated that passage orientations at Lapa Doce and Torrinha do not show any association with joint orientation. Although paragenetic passages also start as a phreatic tube along bedding plane or joints, they will evolve upwards, such that the ceiling becomes independent of joint orientation or bedding plane position.

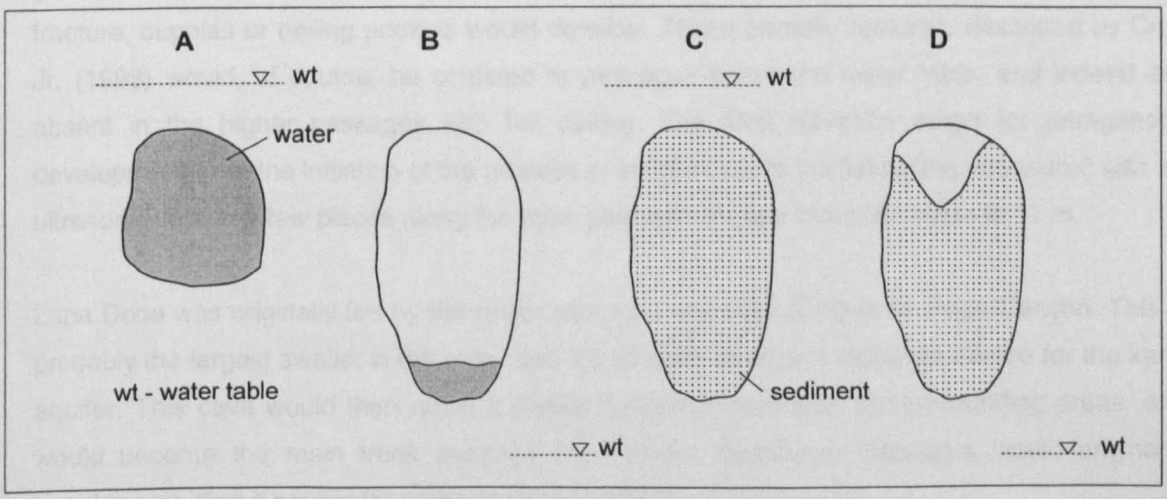

Figure 5.10. Mode of development of Lapa Doce proposed by Ferrari (1990). A - Generation of phreatic tube; B - Vadose incision; C - Sediment infill; D - Sediment excavation.

(2). Some passage cross sections show a triangular shape (Fig. 5.8a), suggestive of either active dissolution processes along the wall-sediment interface or declining flow with time as hydraulic head is reduced as passage nears the water table.

(3). Active caves in the area are evolving through paragenesis. Diving at Gruta Azul, an active spring, has showed that the cave is evolving paragenetically. The passage is wide and low, with fine grained sedimentation in the floor (a similar section to the now drained caves), and slow moving flow. These passages have been explored for several hundred metres up to a depth of 30 m.

(4). The overall pattern of the caves suggests phreatic flow. Caves that display several distributary (or anastomotic) branches and side passages are usually generated by phreatic flow, in situations where there is a wide fluctuation of discharge (Palmer, 1991). The typical anastomotic maze of Palmer, however, usually develops along a single major bedding plane, which is clearly not the case in the area. The main distributaries and side passages at the same level at Lapa Doce could have evolved synchronously because there is continuity at ceiling level. In such a situation it is difficult to explain the generation of such array of passages by flowing vadose streams splitting into dozens of distributary branches. This is not a common situation in vadose caves.

The flat ceiling typical of many passages, especially at Lapa Doce, suggests that in these passages the paragenetic process has progressed until the water table was reached. The essentially flat regional water table would represent the upward limit of paragenetic migration. The lack of scallops at the ceiling suggests restricted (or very slow) water flow at the ceiling, while faster ground water flow would occur immediately below, as indicated by the presence of scallops on the walls. Lower level paragenetic passages could either be synchronous, or generated after the higher passages had been drained. In places where the passage followed a fracture, cupolas or ceiling pockets would develop. These phreatic features, described by Cruz Jr. (1998) would, of course, be confined to passages below the water table, and indeed are absent in the higher passages with flat ceiling. The total elevation range for paragenetic development from the initiation of the process in the bedrock to the flat ceiling, measured with an ultrasonic tape in a few places along the main passage of Lapa Doce, amounts to 11 m.

Lapa Doce was originally fed by the major allogenic drainage of Água de Rega Canyon. This is probably the largest swallet in the area, and would work as a point recharge source for the karst aquifer. This cave would then retain a higher hydraulic head than the surrounding areas, and would become the main trunk passage from where distributary passages would originate, besides providing a source for some of the sediments.

The sediment sequence in Lapa Doce and Torrinha described by Laureano (1998) presents features such as cut and fill structures and erosive contacts that are characteristic of open

channel hydraulics, although it has not been shown that such features are absent in phreatic channels. The occurrence of fragments of speleothems near the base of one of the trenches (Laureano, 1998) is a strong argument in favour of a vadose origin of the sediment. However, although the sediment originated from a cave containing vadose passages, this does not preclude phreatic conditions at the point of deposition or during transport. Laureano (1998) has proposed an evolution sequence for vadose sedimentation that involves underground floodplains, ephemeral streams and lakes (Fig. 5.11). The data provided by Laureano (1998) indicates that the sedimentary sequence now occurring along the main passages at Lapa Doce and Torrinha probably does not represent the original paragenetic sediment, but belongs to a later phase of infilling.

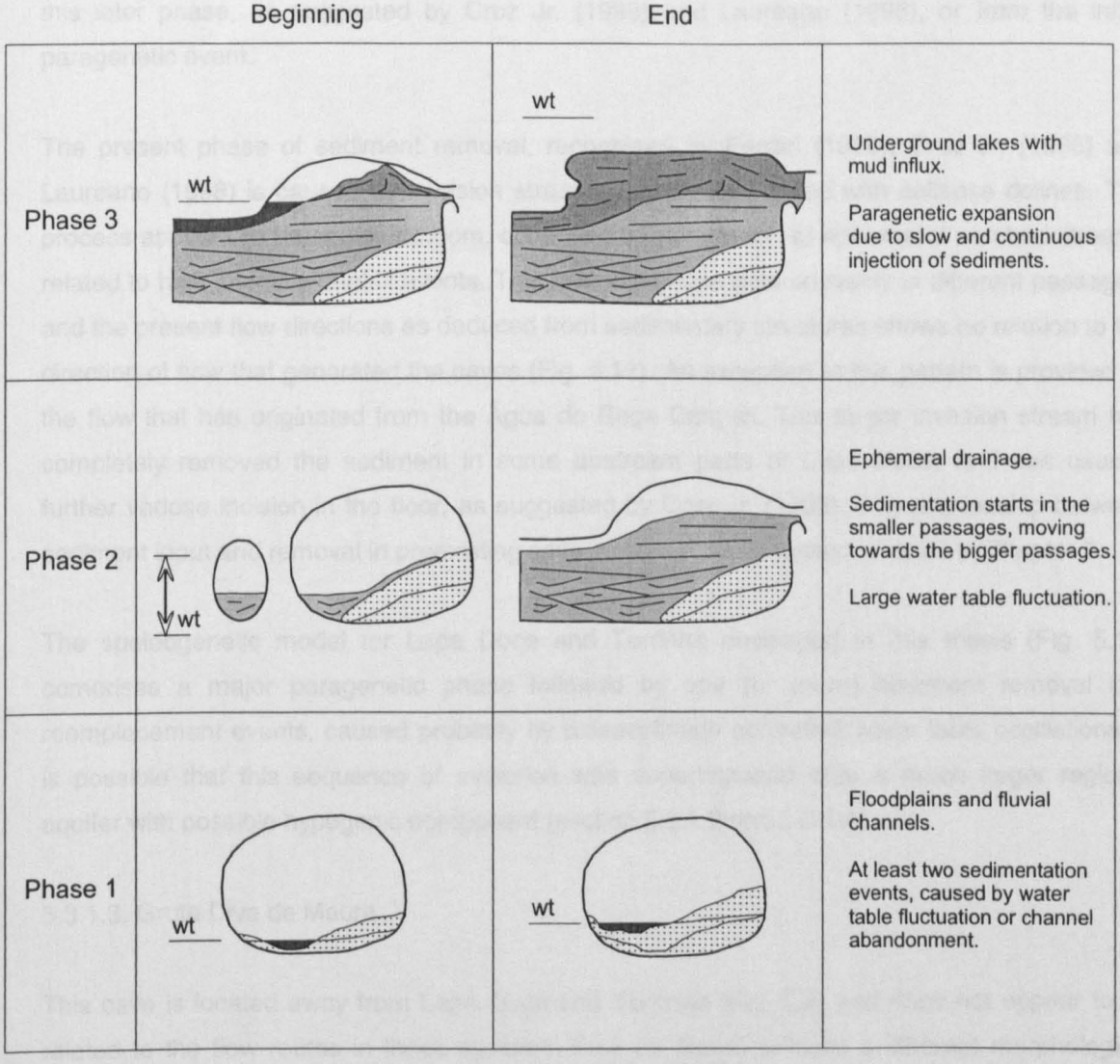

Figure 5.11. Infilling episodes according to Laureano (1998).

Major sediment input and removal episodes appear to be common phenomena in Brazilian caves (see Chapter 7). Accepting the present sedimentation as a later infill phase, it is necessary to account for the removal of the original paragenetic sediment. It is not clear if sediment removal has occurred equally in all passages. If the present stage of removal is taken as a model, a hypothetical future infilling phase would bring new sediment into now sediment

free voids, but would result in a complex mix with older sediment in filled or partially filled passages. It is thus possible that the sedimentary sequences in these caves are in fact diachronous. Until sedimentary sequence correlation includes other minor passages or detailed dating of the fills can be undertaken, these questions will remain unanswered.

The presence of speleothems dissolved by water flow in the ceiling demonstrates that upward (paragenetic) dissolution has occurred in a second development phase. But the fact that the speleothems were not completely removed suggests that this phase was of relatively minor importance, and unlikely to imprint major changes on the geometry of the passages. The numerous paragenetic forms found in these caves, such as pendants, could result either from this later phase, as suggested by Cruz Jr. (1998) and Laureano (1998), or from the initial paragenetic event.

The present phase of sediment removal, recognised by Ferrari (1990), Cruz Jr. (1998) and Laureano (1998) is caused by invasion streams usually associated with collapse dolines. The process appears to be largely random, controlled by percolation of ephemeral perched streams related to high intensity rainfall events. This invasion phase acts unevenly in different passages, and the present flow directions as deduced from sedimentary structures shows no relation to the direction of flow that generated the caves (Fig. 5.12). An exception to this pattern is provided by the flow that has originated from the Água de Rega Canyon. This larger invasion stream has completely removed the sediment in some upstream parts of Lapa Doce, and has caused further vadose incision in the floor, as suggested by Cruz Jr. (1998). The relationship between sediment input and removal in preexisting cave voids will be discussed in detail in Chapter 7.

The speleogenetic model for Lapa Doce and Torrinha envisaged in this thesis (Fig. 5.13) comprises a major paragenetic phase followed by one (or more) sediment removal and reemplacement events, caused probably by palaeoclimate controlled water table oscillations. It is possible that this sequence of evolution was superimposed onto a much larger regional aquifer with possible hypogenic component (section 5.3.1.3 and 5.3.1.4).

5.3.1.3. Gruta Diva de Maura

This cave is located away from Lapa Doce and Torrinha (Fig. 5.4) and does not appear to be related to the flow routes in these systems. Diva de Maura exhibits a different morphological pattern (Fig. 5.5C) resembling the ramiform pattern of Palmer (1991) (although the cave is relatively short (1.3 km long) and several passages remain to be mapped). A series of features, however, set it apart from Lapa Doce and Torrinha: (1) Lack of major meandering passages, (2) presence of large chambers connected irregularly, (3) presence of a series of small paragenetic tubes at ceiling level, (4) presence of a lower level, within the flood zone with another series of paragenetic tubes, (5) sediment deposits, although present, are distinct from the ones at Lapa Doce and Torrinha. They comprise mostly red coarse and fine grained sediment indurated and

sometimes cemented by calcite that do not infill passages to the ceiling, do not show extensive sandy units or widespread mud caps, and show no clear evidence of sediment removal by invasion streams, (6) display extensive condensation-corrosion features, including cupolas, and bedrock and speleothems are intensively weathered.

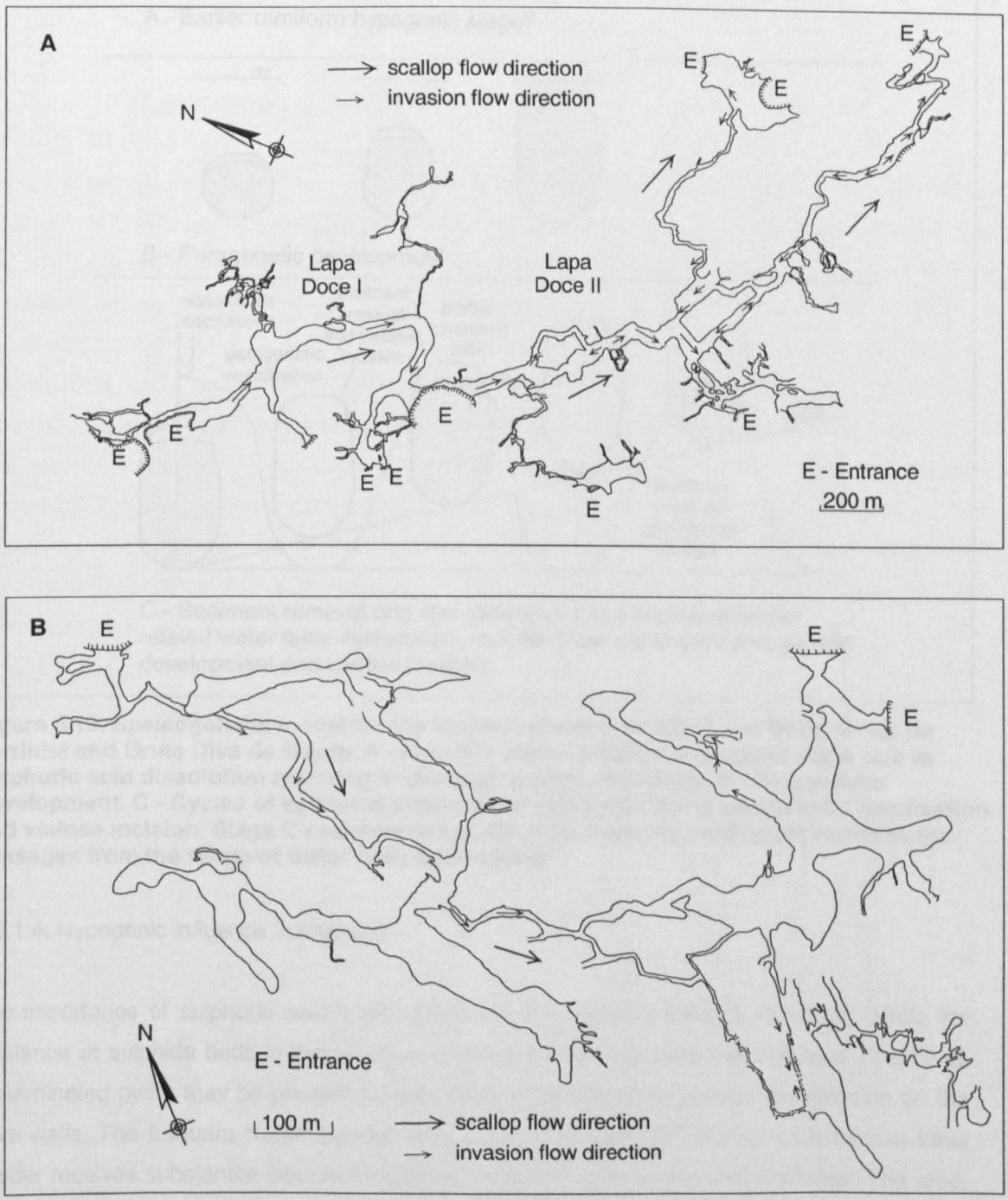

Figure 5.12. Flow directions of invasion streams as deduced from sedimentary structures. A - Lapa Doce (survey GEECE). B - Gruta da Torrinha (survey Groupe Meandres).

Although only a few of the paragenetic tubes at ceiling level have been explored, they appear to form a anastomotic maze above some of the chambers. Due to collapse of the ceiling, only half tubes are preserved in the present day roof of the chambers, but the tubes are observed to continue into the wall at the side of the chamber. Breakdown slabs in the chambers show

subaqueous dissolution features and water flow marks, suggesting that collapse has occurred in the phreatic zone. The genetic relationship between the paragenetic tubes and the large chambers is not clear. It is possible that they represent superimposed independent stages of development.

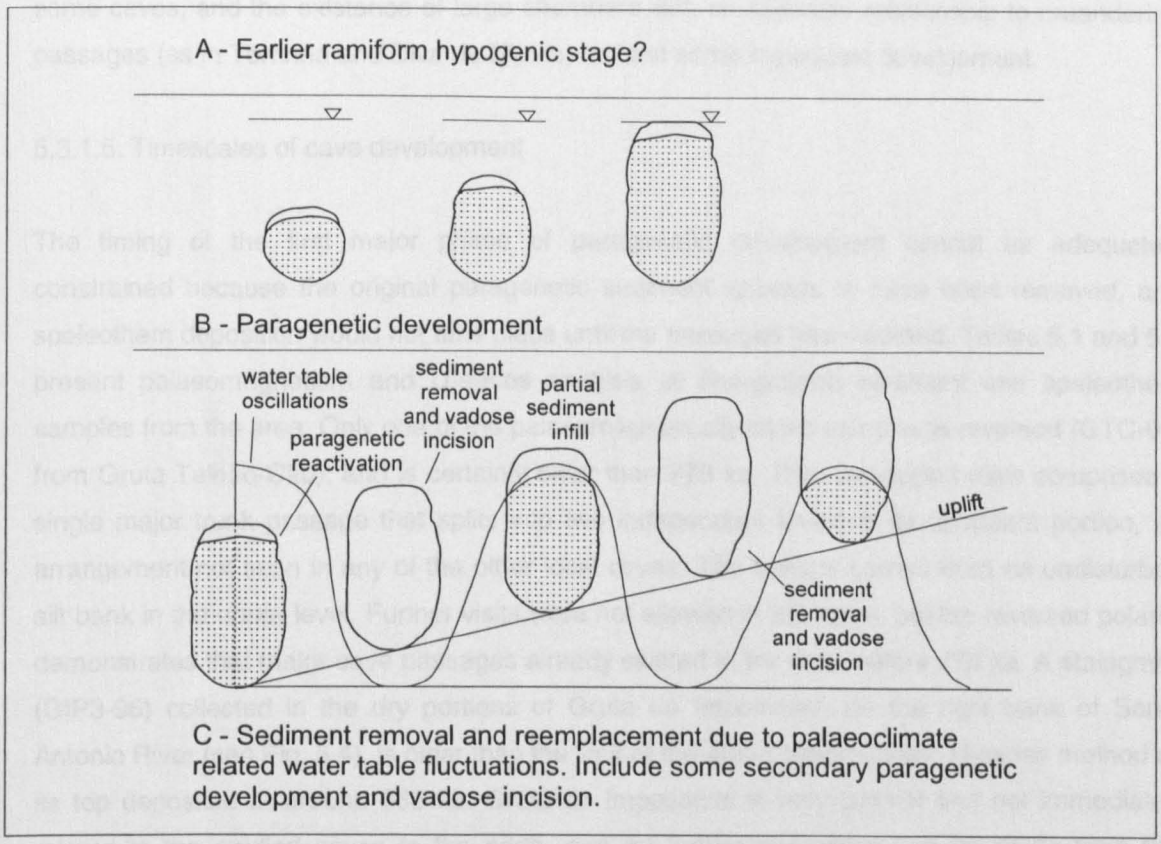

Figure 5.13. Speleogenetic model for the Iraquara Karst based on Lapa Doce, Gruta da Torrinha and Gruta Diva de Maura. A - Possible earlier shallow hypogenic stage due to sulphuric acid dissolution resulting in decoupled large chambers. B - Paragenetic development. C - Cycles of sediment removal and input with some paragenetic reactivation and vadose incision. Stage C ceases when water table lowering (and uplift) removes the passages from the range of water table oscillations.

5.3.1.4. Hypogenic influence in Iraquara?

The importance of sulphuric acid speleogenesis in the Iraquara Karst is not clear. While the existence of sulphide beds in the local units of the Salitre Formation has not been described, disseminated pyrite may be present as indicated by the extensive gypsum precipitation on the cave walls. The Iraquara Karst, besides lying in the downgradient zone of an extensive karst aquifer receives substantial input from allogenic streams running from the quartzites. The area, as it narrows towards the south, behaves as a ground water funnel, that channels the flow into a series of extensive cave systems. This type of hydrologic setting is absent in the Campo Formoso Karst, where slow moving flow predominates. Climate is also very different, the Iraquara area being considerably wetter. As pointed out in section 4.1, in such situation, normal meteoric processes will tend to overwhelm the hypogenic component.

Some evidence, however, suggest that sulphide oxidation may play a significant role in the generation of local caves. Hydrochemical data (section 4.5.2) shows that sulphide oxidation is an active ongoing process in the area. Furthermore, the presence of condensation-corrosion features in many caves, such as Diva de Maura, linked to the suggestive ramiform pattern of some caves, and the existence of large chambers with no apparent relationship to meandering passages (as in Torrinha and Diva de Maura) hints at some hypogenic development.

5.3.1.5. Timescales of cave development

The timing of the first major phase of paragenetic development cannot be adequately constrained because the original paragenetic sediment appears to have been removed, and speleothem deposition would not take place until the passages have drained. Tables 5.1 and 5.2 present palaeomagnetism and U-series analysis of fine-grained sediment and speleothem samples from the area. Only one of the palaeomagnetically dated samples is reversed (GTC-01, from Gruta Talhão-Cão), and is certainly older than 778 ka. This unmapped cave comprises a single major trunk passage that splits into two independent levels in its upstream portion, an arrangement not seen in any of the other local caves. The sample comes from an undisturbed silt bank in the upper level. Further visits were not allowed in this cave, but the reversed polarity demonstrates that major cave passages already existed in the area before 778 ka. A stalagmite (GIP3-96) collected in the dry portions of Gruta do Impossível, on the right bank of Santo Antonio River (see Fig. 5.4), is older than the limit of the alpha spectrometric U-series method as its top deposited at around 365 ka. Gruta do Impossível is very distinct and not immediately related to the studied caves to the north, and no further inferences can be made from this sample.

Sample	N	I_o	Decl.	Incl.	R	K	α_{95}	Polarity
GTC-01	6	1.90	157.34	26.61	5.45	9.09	23.49	REVERSED
LD-07	4	8.99	10.43	-57.74	3.93	45.47	14.19	NORMAL
LD-08	5	6.47	42.48	25.63	4.86	29.44	14.56	NORMAL
LD-09	4	1.06	9.49	-47.71	3.91	33.18	16.15	NORMAL
GT-01	6	1.67	350.86	23.39	5.94	91.29	7.38	NORMAL
GDM-03	7	3.01	24.74	-30.84	6.79	28.82	11.49	NORMAL
GDM-04	6	1.87	29.10	-41.87	5.66	14.94	18.07	NORMAL
GDM-05	3	2.11	27.51	-31.15	3.35	3.10	87.73	NORMAL?

Table 5.1. Palaeomagnetism data for Iraquara Karst caves. GTC (Gruta Talhão-Cão), LD (Lapa Doce), GT (Gruta Torrinha) and GDM (Gruta Diva de Maura). Intensities (I_o) in mA/m. Declination, inclination and α95 in degrees. α_{95} – 95% probability that the direction lies on that angle span, K- Fisher precision estimate which determines the dispersion of points, R- length of resultant vector.

Fig. 5.14 provides sketches of the major sites sampled in Lapa Doce and Torrinha. At several sites in Lapa Doce, speleothems at ceiling level have been redissolved by water. These indicate a phase of oscillation of the water table, with reactivation of the passage after a period of vadose conditions when speleothem was deposited. Such episodes may have reworked the sediment deposits. Speleothems belonging to this phase were sampled at two sites (Sites A and B, Fig. 5.14). At Site A, the redissolved speleothem (LD-17) started growing at around 167 ka and

Sample	U (ppm)	$^{234}U/^{238}U$	$^{230}Th/^{234}U$	$^{230}Th/^{232}Th$	$^{234}U/^{238}U_{t=0}$	Uncorrected age (ka)	Corrected age (ka)
GIP3-96B	0.382 ± 0.017	1.32 ± 0.06	1.132 ± 0.051	200	-	>350	-
GIP3-96T	0.444 ± 0.003	1.99 ± 0.01	1.133 ± 0.019	1065	3.79	365.4 (+31 –37)	-
LD-17	0.146 ± 0.004	1.97 ± 0.05	0.863 ± 0.023	5999	2.56	167.2 (+13.6 -13.4)	-
LD-18	0.042 ± 0.001	1.79 ± 0.05	0.716 ± 0.018	99	2.11	121.2 (+8.2 -8.0)	-
LD-10	1.135 ± 0.015	2.15 ± 0.01	0.208 ± 0.004	57	2.23	24.9 ± 0.5	-
LD-12	0.072 ± 0.001	1.68 ± 0.02	0.808 ± 0.015	72	2.04	151.7 ± 7.3	-
LD-21	0.065 ± 0.002	1.69 ± 0.05	0.767 ± 0.022	1912	2.01	137.7 (+11.7 -11.2)	-
LD-22	0.255 ± 0.007	1.48 ± 0.03	0.910 ± 0.026	851	1.85	203.4 ± 20.3	-
LD-19	0.057 ± 0.001	1.83 ± 0.04	0.127 ± 0.003	25	1.87	14.6 ± 0.57	-
LD-20	0.065 ± 0.002	1.95 ± 0.05	0.824 ± 0.022	37	2.46	153.0 (+12.7 -12.3)	-
LD-11	0.264 ± 0.006	2.95 ± 0.04	0.104 ± 0.003	8	3.01	11.8 ± 0.4	9.4 ± 0.3
LD-14	0.037 ± 0.001	1.90 ± 0.04	0.684 ± 0.014	115	2.23	111.7 (+5.7 -5.6)	-
LD-15	0.050 ± 0.002	1.61 ± 0.06	0.717 ± 0.023	37	1.86	123.1 (+12.6 -11.7)	-
GTR-07	0.097 ± 0.002	1.45 ± 0.04	1.008 ± 0.026	71	1.98	278.8 (+44.9 -41.9)	-
GTR-08	0.156 ± 0.007	1.63 ± 0.07	0.918 ± 0.041	656	2.11	200.9 (+36.8 -34.4)	-
GTR-06	0.081 ± 0.001	2.39 ± 0.03	0.146 ± 0.003	12	2.45	16.9 ± 0.4	14.7 ± 0.4
GTR-05	1.212 ± 0.018	3.28 ± 0.02	0.163 ± 0.003	2000	3.40	19.0 ± 0.4	-
GTR1-96	8.337 ± 0.146	3.56 ± 0.01	0.0007	10	3.56	Recent	-

Table 5.2. Uranium series analyses of speleothems from the Iraquara Karst. Ages corrected assuming $^{230}Th/^{232}Th$ = 1.7. Errors are ± 1σ.

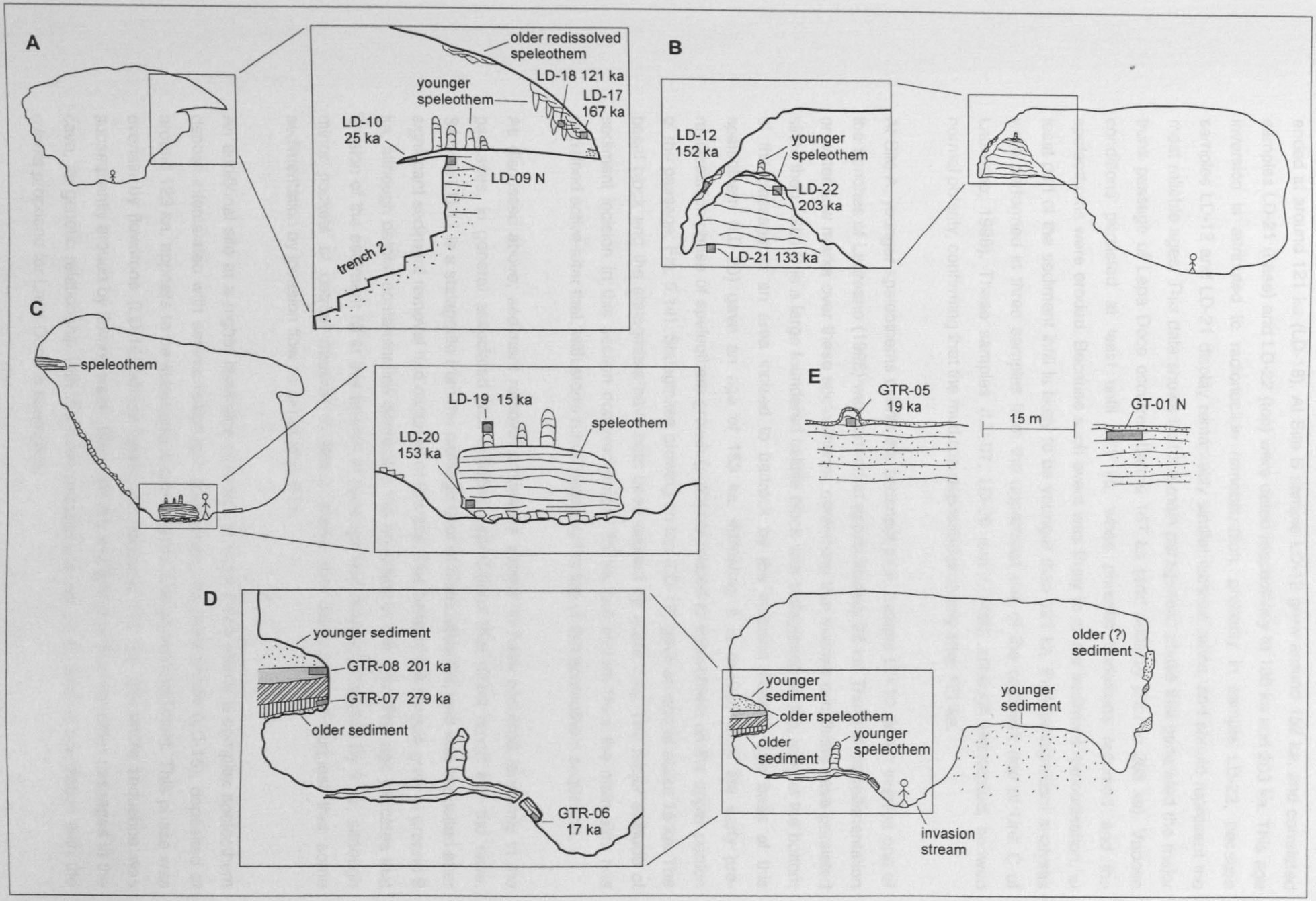

Figure 5.14. Sketch of sampling sites at Lapa Doce (sites A, B, and C) and Torrinha (sites D and E). Locations in Fig. 5.6 and Fig. 5.7.

ended at around 121 ka (LD-18). At Site B sample LD-12 grew around 152 ka, and correlated samples LD-21 (base) and LD-22 (top) were dated respectively to 138 ka and 203 ka. This age inversion is attributed to radionuclide remobilization, probably in sample LD-22, because samples LD-12 and LD-21 display remarkably similar isotopic ratios, and should represent the most reliable ages. This data shows that the main paragenetic phase that generated the major trunk passage of Lapa Doce occurred before 167 ka (and possibly prior to 203 ka). Vadose conditions persisted at least until 121 ka, when phreatic conditions resumed and the speleothems were eroded. Because such event was likely to cause sediment remobilisation, at least part of the sediment infill is likely to be younger than 121 ka. Palaeomagnetism analyses were performed in three samples from the uppermost unit of the sediment (top of Unit C of Laureano, 1998). These samples (LD-07, LD-08 and LD-09), although desiccated, showed normal polarity, confirming that the mud cap deposited probably after 121 ka.

At Site A, younger speleothems overlie the sediment infill. Sample LD-10, which overlies one of the trenches of Laureano (1998) was formed at approximately 25 ka. There is no sedimentation or water flow marks over these speleothems, confirming that vadose conditions have persisted since then. Site C is a large foundered calcite block with stalagmites on top, lying at the bottom of the passage in an area incised to bedrock by the invasion stream. The base of this speleothem (LD-20) gave an age of 153 ka, indicating it is derived from the early pre-redissolution phase of speleothem growth (probably related to speleothem on the upper portion of the passage; Fig. 5.14). Stalagmites growing on top (LD-19) gave an age of about 15 ka. The basal block and the stalagmites have both been eroded by water flow. The major episode of sediment incision in this section occurred before 15 ka, but stream from the main sink has remained active after that, with storm runoff reaching the top of this speleothem sequence.

As discussed above, sediment removal processes appear to have occurred randomly in the passages, in general associated with collapse depressions that direct runoff into the cave. Sample LD-11 is a stalagmite from the passage floor of distributary D2, and was deposited after significant sediment removal had occurred at this site. The base of the sample grew at around 9 ka, although detrital contamination decreases the accuracy of this age. This age indicates that erosion of the sediment fill in this branch of passage was largely completed by 9 ka, although minor pockets of detrital material in layers above the dated sample suggest that some sedimentation by invasion flow occurred after 9 ka.

An additional site at a higher level side chamber at Lapa Doce shows a complex speleothem deposit intercalated with sedimentation and breakdown. An older phase (LD-15), deposited at around 123 ka, appears to be subaqueous and overlies fine grained sediment. This phase was overlain by flowstone (LD-14) whose base was dated at 112 ka. The entire sequence was subsequently eroded by flowing water. Because this site is higher than the other passages in the cave, its genetic relationship with the main passages is not clear, and no correlation with the events proposed for Lapa Doce is attempted.

At Gruta da Torrinha, Site D (Fig. 5.14) lies in the Grand Gallerie, one of the massive side chambers of the cave. Three phases of speleothem deposition form a false floor on one wall and both overlie and are overlain by sediment. The last phase of sedimentation is represented by the major mud deposit that occurs throughout the chamber. The older speleothem layer (GTR-07) was deposited at around 280 ka, and the top of the sequence (GTR-08) was deposited at around 200 ka. These ages, when the associated errors are taken into account, overlap at the 1σ confidence interval (see Table 5.2), and thus should be considered as equivalent. These ages provide a minimum age for the passage itself, and for the older mud sedimentation. The entire speleothem sequence was then eroded by water flow and a younger phase of sedimentation followed. This phase had terminated by about 15 ka when the youngest set of speleothems (GTR-06), which are sediment free, was deposited. Some minor incision by an invasion stream had already occurred before the beginning of deposition of speleothem GTR-06 because the flowstone is draped into the channel created by removal of sediment. Further incision after 15 ka led to the deepening of the channel, and cracking of the speleothem.

Site E at Torrinha is in another large chamber that is paralleled by a series of narrower passages. A thick sequence of sediment, near one of the trenches of Laureano (1998), was sampled near the top for palaeomagnetism analysis (GT-01), yielding normal polarity. A stalagmite immediately above this mud layer (GTR-05) was dated at 19 ka. A thin veneer of mud overlies the stalagmite. The lower mud layer was probably deposited since 778 ka, but the topmost layer was deposited since 19 ka. Because the stalagmite shows no sign of water corrosion, it is believed that the younger mud layer was deposited by discrete injection of mud in a vadose setting. This area is the only one in all the caves where high humidity keeps the sediment moist, suggesting some recent water inflow. A further stalagmite sample (GTR1-96) comes from the middle of one of the lower meandering passages showing sandy invasion sediment. This sample is recent in age, and presents sand intercalations in several layers, suggesting that water flow was occurring during calcite deposition in very recent times.

Correlation of vadose and phreatic events between Lapa Doce and Torrinha is not straightforward because there are uncertainties concerning the genetic relationship between the passages, especially the large chambers at Torrinha, and between possible multiple phases of water table oscillation and sediment removal/deposition. It is clear from Site D at Torrinha that at least two major phases of mud deposition occurred. The older vadose phase indicated by speleothem deposition in sites A, B and D and the water flow episode responsible for their exposure could belong to the same interval, although more work is need to confirm this possibility. An alternative scenario is that the Grand Gallerie at Torrinha is an older passage and the sediment infilling phases in there predates the ones at Lapa Doce. Nevertheless, the absence of magnetically reversed samples and ancient speleothems suggests that the chemical and detrital sedimentation now present in the caves occurred during the Brunhes Epoch. The present water table lies around 15 m below the highest ceiling in these passages. Assuming

base level lowering rates typical for such cratonic setting (Table 3.1) it is indeed apparent that draining of the passages occurred since mid Quaternary times.

Palaeomagnetism analysis at sediments at Gruta Diva de Maura (GDM samples in Table 5.1) yielded normal polarity. Unfortunately the intense condensation-corrosion processes in this cave cause near total weathering of speleothems, precluding the application of Uranium-series dating. However, the palaeomagnetism data and the proximity to the water table also suggest draining during the Brunhes Epoch.

5.4. CAATINGA LIMESTONE KARST

The Caatinga Limestone is a carbonate unit occurring in northern Bahia State, along southerly tributary valleys of the São Francisco River. Caatinga Limestone Karst occurs in three separate regions, related to the main areas of outcrop of this unit (Fig. 5.15). These areas are drained by the Verde, Jacaré and Salitre Rivers, and are informally named after these rivers. The Salitre area is the best known region, and is the focus for most of the observations made in this thesis. The Verde area has been visited only briefly and does not appear to share the same extent of karst features as the Salitre area. The lesser Jacaré area has not been visited. All three areas occur in the semi-arid domain, and share the same climatic regimes already described for the Campo Formoso Karst.

5.4.1. Geology

The Caatinga limestone was first described by Branner (1910). He believed that the Caatinga Limestone and the more recent travertines found on valley sides (section 6.5) were distinct facies of the same deposit. Mello (1938) was the first to distinguish between the two carbonate units, although he believed that both had been formed during the Tertiary. A review of the early work on the Caatinga Limestone is provided by Penha (1994).

The carbonate unit comprises whitish limestone of varied degrees of consolidation, ranging from soft chalky limestone to crystalline indurated limestone that is quarried for decorative purposes. The thickness of the unit can reach up to 80 m but is on average 20 m (Suguio et al., 1980). The Caatinga limestone is usually found in contact with the older Precambrian limestone of Salitre Formation, Una Group, but can also be underlain by schists or quartzites. No tectonic events have acted upon the limestone. However, joints have been observed at some sites in the Salitre area, such as Gruta do Convento, and can probably be attributed to lateral unloading due to the stress release associated with the excavation of the Salitre Valley. The general character of the carbonate is massive, with bedding plane partings not being usually seen.

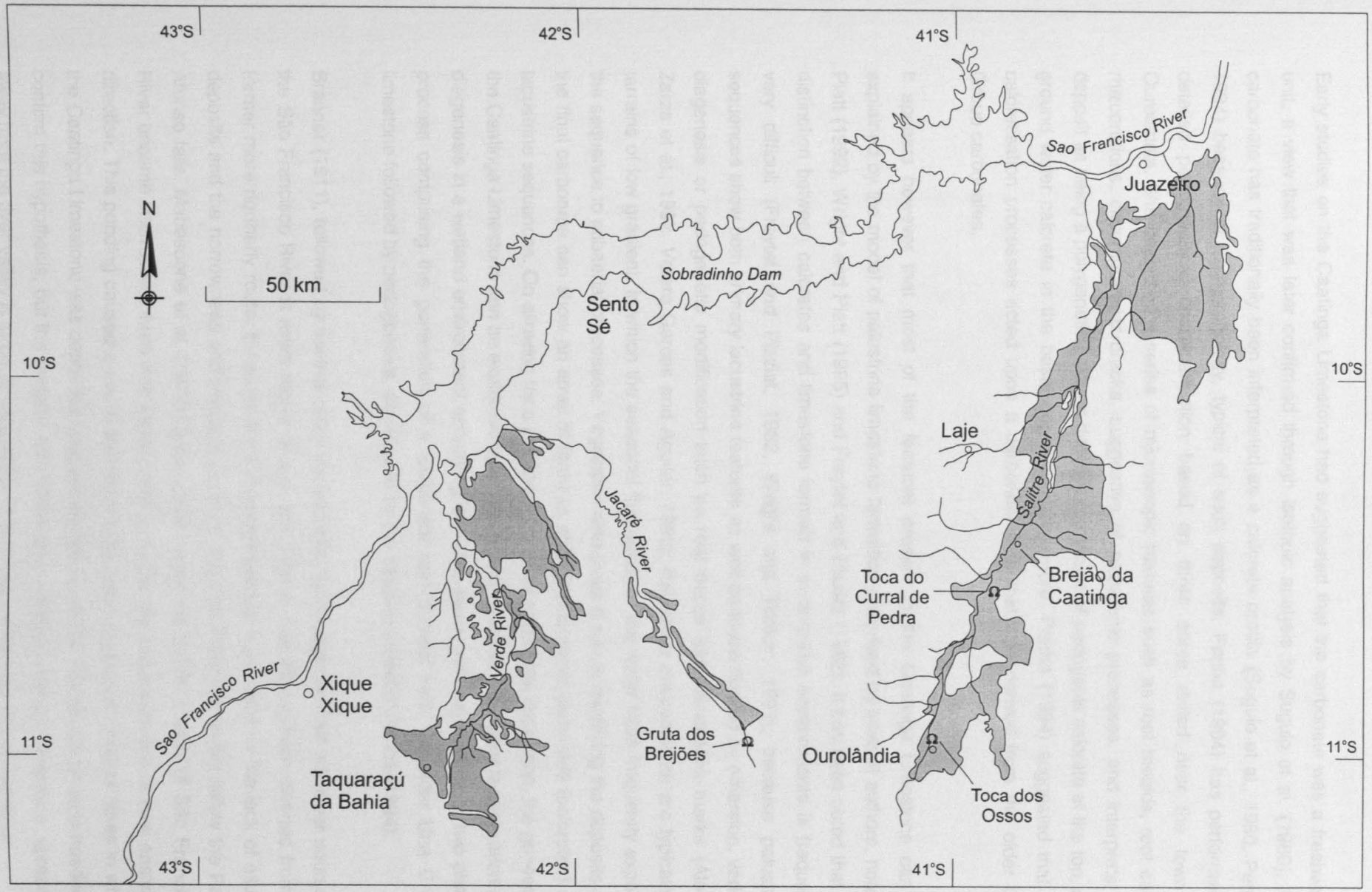

Figure 5.15. Outcrop areas of the Caatinga Limestone. From Bahia (1994).

5.4.1.1. Genesis and palaeoenvironment

Early studies on the Caatinga Limestone had suggested that the carbonate was a freshwater unit, a view that was later confirmed through isotopic analysis by Suguio et al. (1980). The carbonate has traditionally been interpreted as a calcrete profile (Suguio et al., 1980, Penha, 1994) because of its morphology, typical of such deposits. Penha (1994) has performed a detailed petrographical characterisation based on three cores drilled near the town of Ourolândia. She described a series of microscopic features such as root moulds, root casts, rhizocretions, circumgranular cracks, suggestive of pedogenic processes, and interprets the deposit as being a polygenetic calcrete deposit, composed of pedogenic calcrete at the top, and ground water calcrete in the basal portions. Furthermore, Penha (1994) suggested that the calcretisation processes acted upon a carbonate rock that was derived from the older Una Group carbonates.

It appears however that most of the features present in the Caatinga Limestone can be explained by the model of palustrine limestone formation described by several authors, notably Platt (1992), Wright and Platt (1995) and Freytet and Plaziat (1982). It has been noted that the distinction between calcretes and limestone formed in swamp-like environments is frequently very difficult (Freytet and Plaziat, 1982, Wright and Tucker, 1991), because palustrine sequences show both primary lacustrine features as well as those derived by emersion, vadose diagenesis or pedogenetic modification such as root traces and desiccation marks (Alonzo Zarza et al., 1992, Valero Garces and Aguilar, 1992). Palustrine environments are typically of terrains of low gradient, in which the seasonal fluctuation of the water table frequently exposes the sequence to subaerial processes. Vegetation also plays a role in modifying the deposits and the final carbonate can show an array of features of both pedogenic carbonate (calcretes) and lacustrine sequences. On allowing for a palustrine model of carbonate deposition, the genesis of the Caatinga Limestone can be explained by a "one phase" process of carbonate generation and diagenesis in a wetland environment occupying low-lying areas, without need for a "two phase" process comprising the generation of a carbonate unit derived from the older Una Group limestone followed by pedogenesis, as required by the calcrete model of Penha (1994).

Branner (1911), followed by several other researchers, has suggested that the lower course of the São Francisco River is more recent in age, the original river having been diverted from its former more northerly route. Evidence for a drainage change is provided by the lack of alluvial deposits and the narrowness and frequent rapids of the São Francisco valley below the Paulo Afonso falls. Mabesoone et al. (1977) believed that when the former course of São Francisco River became interrupted, there was some ponding before the water acquired its new eastward direction. This ponding caused a rise in the water table, creating several shallow lakes in which the Caatinga Limestone was deposited (Mabesoone et al., 1977). Further evidence is needed to confirm this hypothesis, but the general areal distribution of the Caatinga Limestone, spreading away from the river valley is strongly suggestive of damming of the São Francisco River.

Oxygen and carbon isotopic data for the Caatinga limestone have been reported by Suguio et al. (1980) and is reproduced in Fig. 5.16. Talbot (1990), in a review of freshwater carbonate isotopic signatures, has shown that in hydrologically closed lakes, carbon and oxygen isotopes will tend to be covariant with a correlation usually above 0.7 while open lakes will show little correlation between carbon and oxygen isotope data. The data from the Caatinga Limestone shows a lack of correlation between these isotopes (r = 0.415), suggesting an open lake environment, as would be expected if the water was ponded upstream of the São Francisco River. Furthermore, the isotope data is within the range for calcretes according to a worldwide survey by Talma and Netterberg (1983) although the carbon isotope values do not match those usually found in tropical regions.

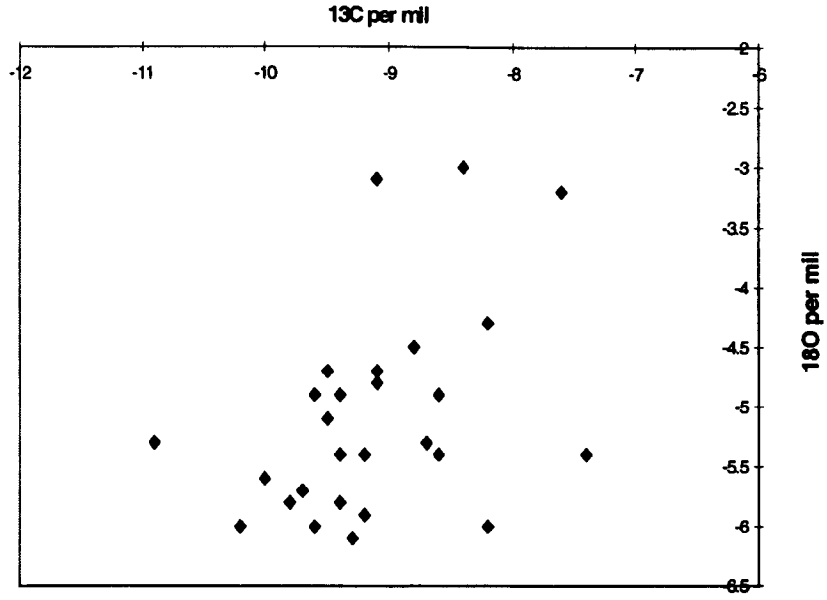

Figure 5.16. Carbon and oxygen isotope for Caatinga Limestone samples. Data from Suguio et al. (1980).

Few attempts have been made to assess the palaeoclimate significance of the Caatinga Limestone. Branner (1910) interpreted the deposits as being formed under a semi-arid climate. Suguio et al. (1980) found traces of montmorillonite and atapulgite in the carbonate, suggestive of deposition in an arid environment, as required by most calcrete deposits. However, palustrine limestones are not necessarily linked to arid zones. Modern analogues of the palustrine environment are the Everglades in Florida, USA (Wright and Platt, 1995). Seasonal fluctuation of the water table is needed in order to promote development of vadose features, but a high water table is a basic requirement. The event that caused the deposition of the Caatinga Limestone does not appear to be entirely palaeoclimatically controlled. If climate was the sole determinant on the formation of the deposit, one would expect to find similar carbonates generated in other climatic cycles. The Caatinga Limestone deposit is one of a kind, and no similar carbonate sequence has been identified in the area.

5.4.1.2. U-series analysis of the deposits

Various ages have been assigned to the Caatinga Limestone, mostly based on mollusc fossil identification. One major problem associated with these fossil-based chronologies is that it is not clear if the fossils were derived from the Caatinga Limestone itself, or from the much younger travertine deposits. Broad ages ranging from the Tertiary to the Quaternary have been assigned to the deposits (see review in Penha, 1994). Mabesoone et al. (1977) placed the ponding of the São Francisco River (and supposed associated limestone formation) in the Mindel Glaciation. Azevedo and Azevedo (1991) have dated samples from two of the cores described by Penha (1994) using the $^{230}Th/^{234}U$ method, and obtained ages ranging from 10 ka at the base to 250 ka at the top. This inverse age relationship suggests the results are not reliable, and therefore new analyses were conducted in this thesis.

Seven analyses of the Caatinga Limestone were undertaken (Table 5.3), and an additional three samples were discarded during the chemical extraction due to the large proportion of insoluble residues. The samples came from different elevations in the sequence, were collected over a wide area in both the Salitre and Verde drainage basins, and consisted of hard and compact limestone, free from friable material or obvious porous zones. During preparation, attempts were made to separate the carbonate matrix from the other constituents. However, this proved difficult because of the heterogeneous nature of the rock. The samples should therefore, be considered as an "average" of the usual constituents found in the limestone, with the exception of sample PDR-01 which consists of calcite in voids, similar to horizontal desiccation cracks described by Freytet and Plaziat (1982) or crystallaria of Wright and Tucker (1991).

Three of the seven samples analysed suffered from significant detrital contamination ($^{230}Th/^{232}Th < 20$). All samples showed $^{234}U/^{238}U$ ratios close to 1.0, but U concentration varied widely from 0.04 to 2.42 ppm. Only one infinite age was obtained, others ranging from 210 ka (uncorrected) and showing no clear relation between top and basal ages. An important test of the ages is given by dating of speleothems from caves excavated in the Caatinga Limestone (see below) and travertine deposits that overlie it (Table 6.2). The older suite of travertines sampled are close to the limit of the U series method, while some speleothems yield infinite ages. It therefore seems likely that the limestone has behaved as an open system, with postdepositional migration of uranium. The large variability of uranium content supports this assumption. The calcite infilling sample (PDR-01) could indeed represent a younger deposit. Such later calcite growth, when associated with the matrix, could tend to make the ages younger than the true date of deposition (Schwarcz, 1980). Recrystallisation of the matrix and resetting of the ages is also a possibility. Thus, the Caatinga Limestone represents an open system in respect to uranium isotopes, and cannot be reliably dated by the U-series method. The ages reported by Azevedo and Azevedo (1991) probably also reflect this postdepositional isotope migration and, together with their associated palaeoclimatic interpretation, should be regarded with caution.

Sample	Area	Location	U (ppm)	$^{234}U/^{238}U$	$^{230}Th/^{234}U$	$^{230}Th/^{232}Th$	$^{234}U/^{238}U_{t=0}$	Uncorrected age (ka)	Corrected age (ka)
PDR-01	Salitre	top	0.037 ± 0.001	1.06 ± 0.03	0.904 ± 0.025	8	1.10	242.2 (+49.3 –39.7)	219.5 (+39.5 –29.4)
GC1153	Salitre	base	0.271 ± 0.005	1.11 ± 0.01	0.979 ± 0.022	25	1.27	322.3 (+47.5 –54.9)	-
CLC-02	Salitre	top	0.633 ± 0.017	1.01 ± 0.01	1.031 ± 0.031	27	-	> 350	
CLC-03	Verde	top	0.469 ± 0.008	1.03 ± 0.02	0.956 ± 0.021	9	1.07	319.1 (+60.0 –61.8)	299.1 (+56.8 –40.5)
CLC-05	Salitre	mid	0.481 ± 0.008	1.05 ± 0.01	0.962 ± 0.022	53	1.12	322.4 (+53.2 –60.5)	-
CLC-06	Salitre	top	0.154 ± 0.002	1.05 ± 0.01	0.866 ± 0.017	6	1.09	211.1 (+17.2 –17.1)	181.0 (+13.2 –12.0)
CLC-08	Salitre	base	2.421 ± 0.061	1.02 ± 0.01	0.921 ± 0.027	25	1.04	271.4 (+33.0 –42.9)	-

Table 5.3. U-series analyses of Caatinga Limestone samples. Errors are ± 1σ. Ages corrected assuming $^{230}Th/^{232}Th = 1.7$.

5.4.2. Incision of the Salitre Valley

Three major river valleys are partially incised into the Caatinga Limestone, the Salitre, Verde and Jacaré. The Salitre was studied in detail and transverse profiles were made of the valley, starting where it leaves the quartzites and runs onto the Caatinga Limestone, and ending near the junction with the Pacuí River, in the middle course of the Salitre River (Fig. 5.17). The valley ranges from about 16 m deep in the upper course to up to 52 m near the junction with the Pacuí River. The latter appears to be close to the maximum depth of the valley, because it becomes shallower and less well marked in its lower course, where it runs mostly over non-carbonate rocks. Most of the Salitre Valley sections are entirely incised into the horizontally bedded Caatinga Limestone, but the basal schists are seen on several places. In fact, in some parts of the valley, the Caatinga Limestone appears to be quite thin, only a few tens of metres thick at best.

The beginning of the incision of the Salitre Valley necessarily postdates the deposition of the Caatinga Limestone. Since no reliable ages for the limestone could be obtained through U-series dating, an alternative method to provide a rough age for the deposit would be to take into account the incision rate of the valley developed in it. Assuming the denudation values of 30 ± 10 m/Ma of Harman et al. (1998), which is within range of the incision rates obtained for Gruta do Padre (section 3.4.1.5) of 25-34 m/Ma, as representative of the general denudation values in the area, and using the maximum valley depth of 52 m, a minimum age range of 1.3-2.6 Ma is estimated for the Caatinga Limestone. These figures should be taken only as a very crude approximation. The Caatinga Limestone is, therefore, at least 350 ka old, but was probably deposited at some point in early Pleistocene or late Pliocene.

5.4.3. Underground karst

Among the outcrop regions of the Caatinga Limestone, only the Salitre area has received proper speleological attention. Brief reconnaissance visits were paid to the Verde area, in which a few caves were examined. The following description of the underground karst of the Caatinga Limestone will thus be based on the Salitre area.

The extent and volume of the caves present in the Salitre area is quite remarkable considering that the Caatinga Limestone, although relatively extensive, is rather thin over most of the area. In several situations, a single cave passage represents over 50% of the total thickness of the sequence above the water table. It thus hardly remarkable that surface collapses are invariably associated with many of the cave passages.

Two characteristics of the carbonate rock represent important controls on speleogenesis: the almost complete lack of joints, and the heterogeneity of the deposits. The absence of bedding planes or tectonic joints means that ground water does not have a favourable initial route to

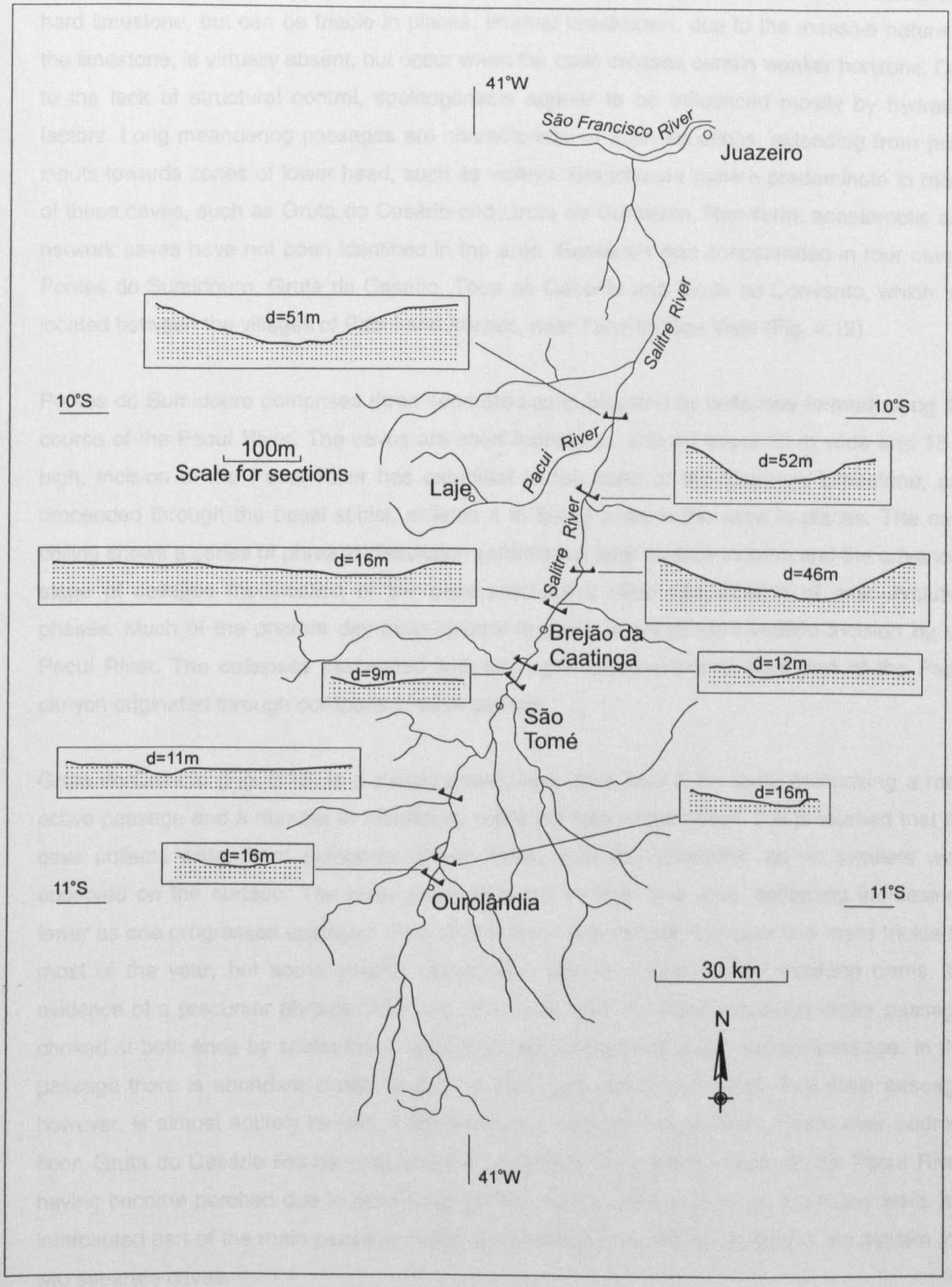

Figure 5.17. Sections along the Salitre River Valley. d = depth.

follow, but instead dissolves the limestone in a more diffuse way. Spongework passages tend to develop in this situation. Outstanding examples of spongework can be found in many caves of the area. Toca dos Ossos comprises probably over 10 km of passages (yet unmapped), most of it distributed in a complex spongework maze. The Caatinga Limestone is mostly a massive and hard limestone, but can be friable in places. Internal breakdown, due to the massive nature of the limestone, is virtually absent, but occur when the cave crosses certain weaker horizons. Due to the lack of structural control, speleogenesis appear to be influenced mostly by hydraulic factors. Long meandering passages are characteristic of such situations, extending from point inputs towards zones of lower head, such as valleys. Branchwork pattern predominate in many of these caves, such as Gruta do Cesário and Gruta do Convento. Ramiform, anastomotic and network caves have not been identified in the area. Research was concentrated in four caves, Pontes do Sumidouro, Gruta do Cesário, Toca do Caboclo and Gruta do Convento, which are located between the villages of Pacuí and Abreus, near Toca da Boa Vista (Fig. 4.12).

Pontes do Sumidouro comprises three separate caves bisected by collapses formed along the course of the Pacuí River. The caves are short tunnels (c. 100 m) about 30 m wide and 15 m high. Incision of the Pacuí River has extended to the base of the Caatinga Limestone, and proceeded through the basal schist, at least 4 m being seen in the cave in places. The cave ceiling shows a series of phreatic dissolution pockets but later vadose incision and the advanced stage of collapse modification of the cave preclude a clear identification of past evolution phases. Much of the present day cave volume appears to result from vadose incision by the Pacuí River. The collapses associated with this cave indicate that at least part of the Pacuí canyon originated through collapses of cave ceilings.

Gruta do Cesário (Fig. 5.18) is a classic branchwork cave near 2 km long, comprising a main active passage and a number of tributaries, some not fully explored yet. It is presumed that the cave collects water from autogenic diffuse inputs over the limestone, as no swallets were observed on the surface. The main passage is 2-3 m high and wide, becoming increasingly lower as one progresses upstream. The stream that flows through the cave is a mere trickle for most of the year, but some ponded areas exist due to obstruction by rimstone dams. No evidence of a precursor phreatic tube can been observed. An older and much larger passage, choked at both ends by speleothems and sediment, is bisected by the stream passage. In this passage there is abundant clastic sediments and speleothem deposition. The main passage, however, is almost entirely devoid of sedimentation, and the stream flows mostly over bedrock floor. Gruta do Cesário lies hanging about 15 m above the present bottom of the Pacuí River, having become perched due to differential valley erosion. Gully erosion on the valley walls has intercepted part of the main passage, splitting the terminal (southerly) portion of the system into two separate caves.

Toca do Caboclo (Fig. 7.6) is a small cave on a barren karren field located during this thesis field work. The cave has been largely filled with speleothem, and later partially reexcavated. Because

of the small extent of the cave, and of the few exposures of limestone it is difficult to ascertain the initial phase of development. This cave and the palaeoclimatic significance of the impressive speleothem fill will be discussed in Chapter 7.

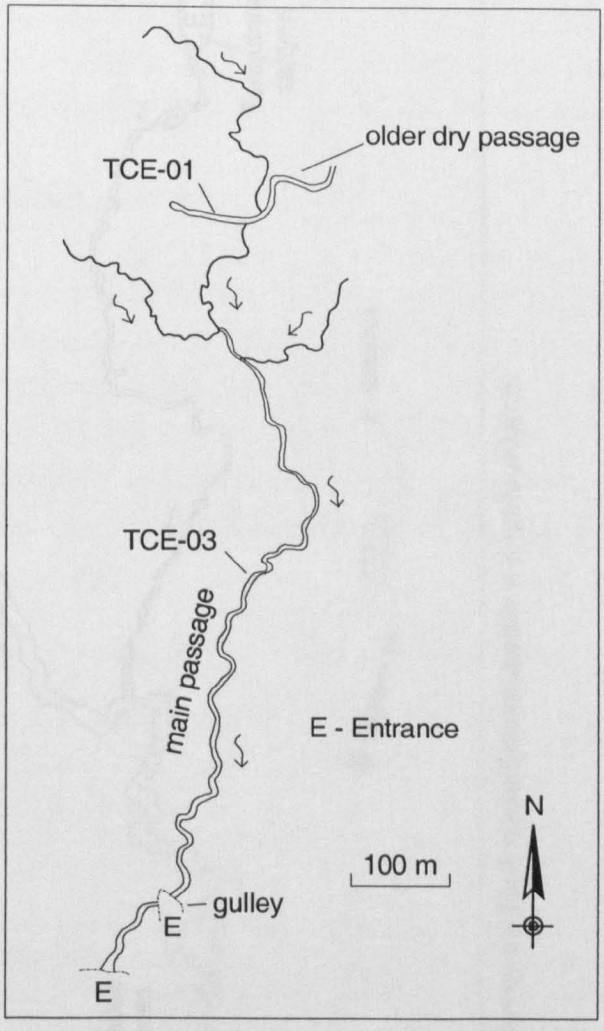

Figure 5.18. Plan map of Gruta do Cesário. Survey by Grupo Bambuí de Pesquisas Espeleológicas.

Gruta do Convento (Fig. 5.19) is the major known cave in the Caatinga Limestone. It is a 9.2 km long branchwork cave, with two major inlet points, associated with the swallets of the ephemeral streams Queixo D'Anta and Tanquinho. The major passage, the one associated with the Queixo D'Anta Canyon, is mostly over 30 m wide and 10-20 m high, being interrupted by major collapse dolines. Its downstream end is marked by a diversion into three "levels", characterised by distinct ceiling elevations, the original floor being masked by sedimentation. Downstream, these levels are either choked by sediments or by the collapse that marks the main entrance to the cave. Another cave, Gruta do Martiliano, located on the Pacuí Valley side appears to represent the former downstream end of Gruta do Convento.

The ceiling of the main passage of Convento maintains a roughly constant elevation but there is some irregularity associated with well developed ceiling pockets. In contrast, the ceiling of the middle level (see Fig. 5.20) displays no such features, being remarkably level. The longitudinal

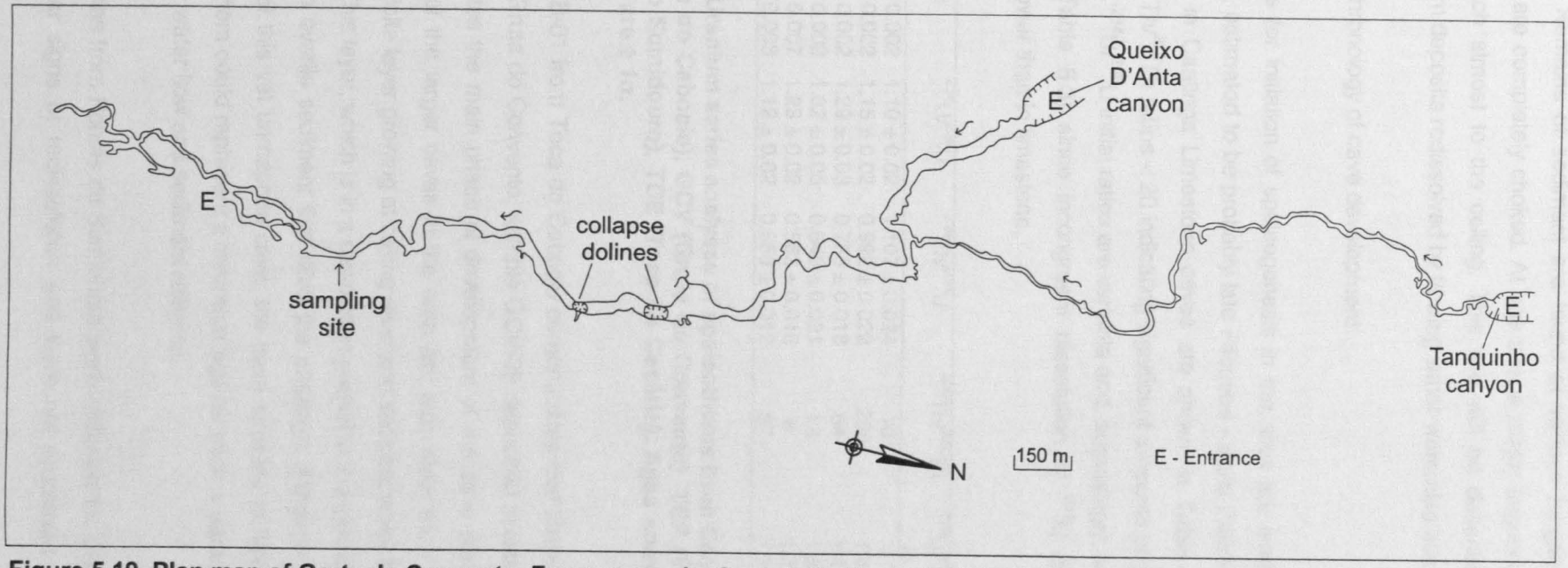

Figure 5.19. Plan map of Gruta do Convento. From survey by Sociedade Excursionista e Espeleológica.

profile in the lower level is very irregular, and in places the ceiling is shaped as a series of arches. As the cave lacks guiding joints, a precursor phreatic tube cannot be observed at roof level. Gruta do Convento presents evidence of having been nearly completely filled with sediment. Remains of sediment are found at various heights on the walls, and some side passages are completely choked. At one site, a major sequence of sediment and speleothem layers reach almost to the ceiling. This site will be described in detail in section 7.4.1.2. Speleothem deposits redissolved by flowing water were also observed at ceiling level.

5.4.3.1. Chronology of cave development

Timescales for initiation of speleogenesis in the area are limited by the age of the Caatinga Limestone, estimated to be probably late Pliocene - early Pleistocene. Uranium series analyses performed in Caatinga Limestone caves are shown in Table 5.4. Three out of six samples showed $^{230}Th/^{232}Th$ ratios < 20 indicating significant amounts of detrital Th, and corrections were performed. $^{234}U/^{238}U$ initial ratios are variable and, surprisingly, are higher than such ratios in the bedrock (Table 5.3) since incongruent dissolution of ^{234}U during speleothem formation is generally lower than in limestone.

Sample	U (ppm)	$^{234}U/^{238}U$	$^{230}Th/^{234}U$	$^{230}Th/^{232}Th$	$^{234}U/^{238}U$ t=0	Uncorrected age (ka)	Corrected age (ka)
TCB-01	0.149 ± 0.002	1.10 ± 0.02	1.107 ± 0.024	10	-	>350	-
GCV-09	0.102 ± 0.002	1.15 ± 0.02	0.992 ± 0.022	250	1.4	328.0 (+54.9 –57.6)	-
TCP-02	0.076 ± 0.002	1.29 ± 0.03	0.783 ± 0.018	54	1.4	151.7 (+11.5 -11.1)	-
PS-02	0.072 ± 0.002	1.62 ± 0.05	0.648 ± 0.021	12	1.8	104.6 (+8.5 -8.1)	95.7 (+7.8 -7.2)
TCE-03	0.268 ± 0.007	1.23 ± 0.02	0.582 ± 0.016	9	1.3	91.9 ± 5.1	79.2 ± 4.5
TCE-01	0.198 ± 0.003	1.12 ± 0.02	0.550 ± 0.012	87	1.1	85.7 ± 3.5	-

Table 5.4. Uranium series analyses of speleothems from Caatinga Limestone Karst caves. TCB (Toca do Caboclo), GCV (Gruta do Convento), TCP (Toca do Curral de Pedra), PS (Pontes do Sumidouro), TCE (Toca do Cesário). Ages corrected assuming $^{230}Th/^{232}Th$ = 1.7. Errors are ± 1σ.

Sample TCB-01 from Toca do Caboclo demonstrates that there were caves in the area before 350 ka. At Gruta do Convento, sample GCV-09 deposited at around 328 ka in a sediment bank that postdates the main phase of development of the cave (section 7.4.1.2). It seems certain that some of the larger caves in the area are also older than 350 ka. At Toca do Curral de Pedra, a calcite layer growing at ceiling level and showing water flow marks (TCP-02) was dated to 152 ka. This layer, which is in a dissolution pocket in the ceiling, probably represents a deposit that used to overlie sediment that filled the passage. Although no systematic study has been performed of this yet unmapped cave, the cave appears to have evolved paragenetically, and this speleothem could represent a minimum age for such a paragenetic phase, and a maximum age for later water flow and sediment removal.

A few samples from Pontes do Sumidouro were collected for U-series dating, but most of them showed clear signs of redissolution and were not processed. Sample PS-02 belongs to a

flowstone from the upper ledges of the passage, some 10 metres above the present river. It was dated at 96 ka, but probably considerably postdates the passage.

At Toca do Cesário, the older dry passage accidentally bisected by the smaller stream passage is certainly older than the main branchwork system. Sample TCE-01 represents a free hanging calcite false floor that used to overlie sediment in this chamber. It could possibly represent calcite deposition that preceded the formation of the lower passage. However, its age, around 84 ka is within error limits of the age of sample TCE-03 (79 ka) obtained from a flowstone in the walls of the main passage downstream from the older dry passage (see Fig. 5.17). This data proves that the main passage had already evolved by 80 ka, because the flowstone occupies over half of the entire height of the passage, and thus sample TCE-01 considerably postdates the development of the older chamber.

Gruta do Convento shows throughout the length of its passage evidence of an almost complete sediment fill. The lack of a defined phreatic tube and guiding joints in passage roof, suggest that paragenesis could have played a major role in its genesis. The present sediment in the cave is clearly a secondary infill, because it is frequently intercalated with stalagmitic layers which can only have formed under vadose conditions. The presence of redissolved speleothems in the ceiling also demonstrates that a second phase of water flow occurred, probably above a sedimentary fill. This may have generated some secondary paragenetic enlargement, but the incomplete removal of preexisting speleothems suggests that this modification was very limited. The overall sequence of events appears rather similar to the evolution model proposed for Lapa Doce and the paragenetic passages of Torrinha in the Iraquara Karst (section 5.3.1.2). The triple bifurcation at the downstream end of the cave (Fig. 5.20) might be explained by a classical vadose incision model, the upper passages being abandoned in favour of newly established lower routes. However, all three passages show evidence of near complete sediment infill (either paragenetic or secondary), and particularly the morphology of the middle passage (passage B) is highly suggestive of paragenesis. It is hypothesised that draining of the main passage A would cause ceiling collapse and paragenetic diversion to the middle level B, that would then represent basically a bypass route. Draining of both passages could then originate the lower passage C by a similar process. This passage appears to be a very low gradient one due to the absence of a well defined ceiling channel. All transitions at roof level between these three passages are very abrupt, suggesting that no phreatic flow occurred at ceiling level between these passages.

The Caatinga Limestone Karst, although relatively young, shows all typical features of a mature karst landscape. Styles of cave development such as paragenetic and branchwork systems, identified in cave systems in older carbonates are also present in the area, demonstrating that these processes can probably occur entirely within the time range of the Quaternary period, and are not dependent on shallow hypogene processes controlled by carbonate lithology (presence of sulphides).

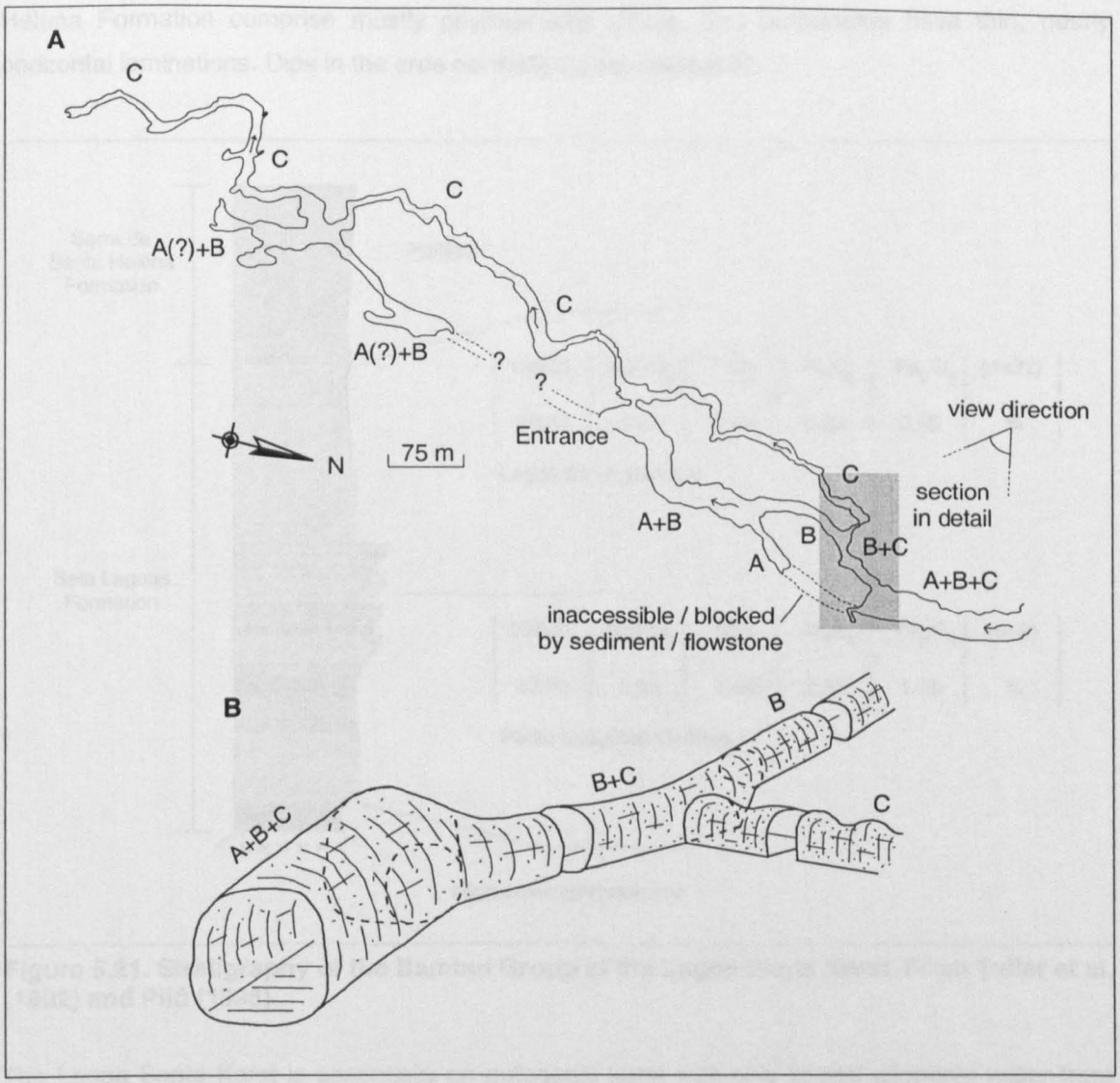

Figure 5.20. A - Plan of downstream end of Gruta do Convento showing passage diversions. B - Schematic view of the passage diversions. Plan based on map by Sociedade Excursionista e Espeleológica.

5.5. THE LAGOA SANTA KARST

The karst of Lagoa Santa is located in south central Minas Gerais State, about 30 km north of the state capital Belo Horizonte, encompassing the municipality of Lagoa Santa among many others. In the area, the three basal formations of the Bambuí Group are present. The conglomerates of the Jequitaí Formation have restricted occurrence and are locally known as Carrancas Formation. The carbonate rocks of the Sete Lagoas Formation and the pellitic Serra de Santa Helena Formation comprise most of the outcrops. Fig. 5.21 presents the stratigraphy of the area. Tuller et al. (1992) has separated the Sete Lagoas Formation into two members, the lower Pedro Leopoldo Member is characterised by impure limestone with intercalations of pellites and siltites, while the upper Lagoa Santa Member is of purer calcarenites and calcissiltites. Chemical analyses reported by Piló (1998) show a marked increase in silica and decrease in calcium carbonate in the lower Pedro Leopoldo Member. The Serra de Santa

Helena Formation comprise mostly phyllites and siltites. The carbonates have thin, nearly horizontal laminations. Dips in the area normally do not exceed 5°.

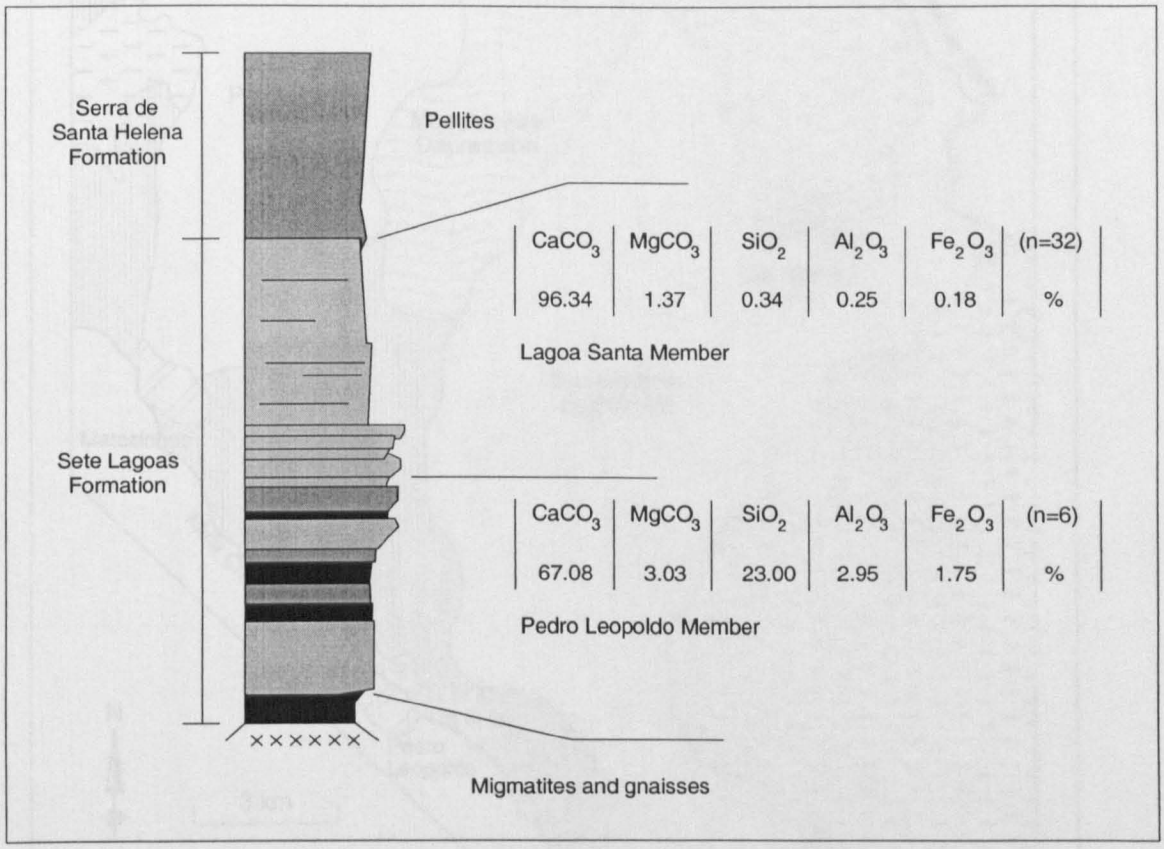

Figure 5.21. Stratigraphy of the Bambuí Group at the Lagoa Santa Karst. From Tuller et al. (1992) and Piló (1998).

The Lagoa Santa Karst is essentially an autogenic karst with only limited allogenic water from phyllite areas to the north. The area lies in an interfluvial zone between the Velhas and Mata Rivers. Discharge measurement in several springs have shown that around 88% of the karst ground water discharges towards the Velhas River, the remainder draining toward the Mata Creek (Auler, 1994). Six major physiographic domains have been identified in the area (Fig. 5.22). Karst landforms are concentrated in the High Plains which comprise two distinct areas drained by the Palmeiras and Samambaia Rivers both tributaries of Velhas River and the Mocambeiro Depression which separates these areas.

The average annual rainfall at the Pedro Leopoldo meteorological station reaches 1,284 mm (data from 1942-1990). Mean annual temperature at Lagoa Santa is 22.8°C (data from 1961-1970 and 1987-1990). The highest temperatures during summer are in the upper 30's and lowest temperatures during winter reach around 7°C. The original vegetation in the area has been largely modified since the arrival of the first settlers in the late 1600's. Nowadays, grasslands for cattle pastures predominate over most of the region, although the limestone outcrops, and some dolines still hold patches of forest.

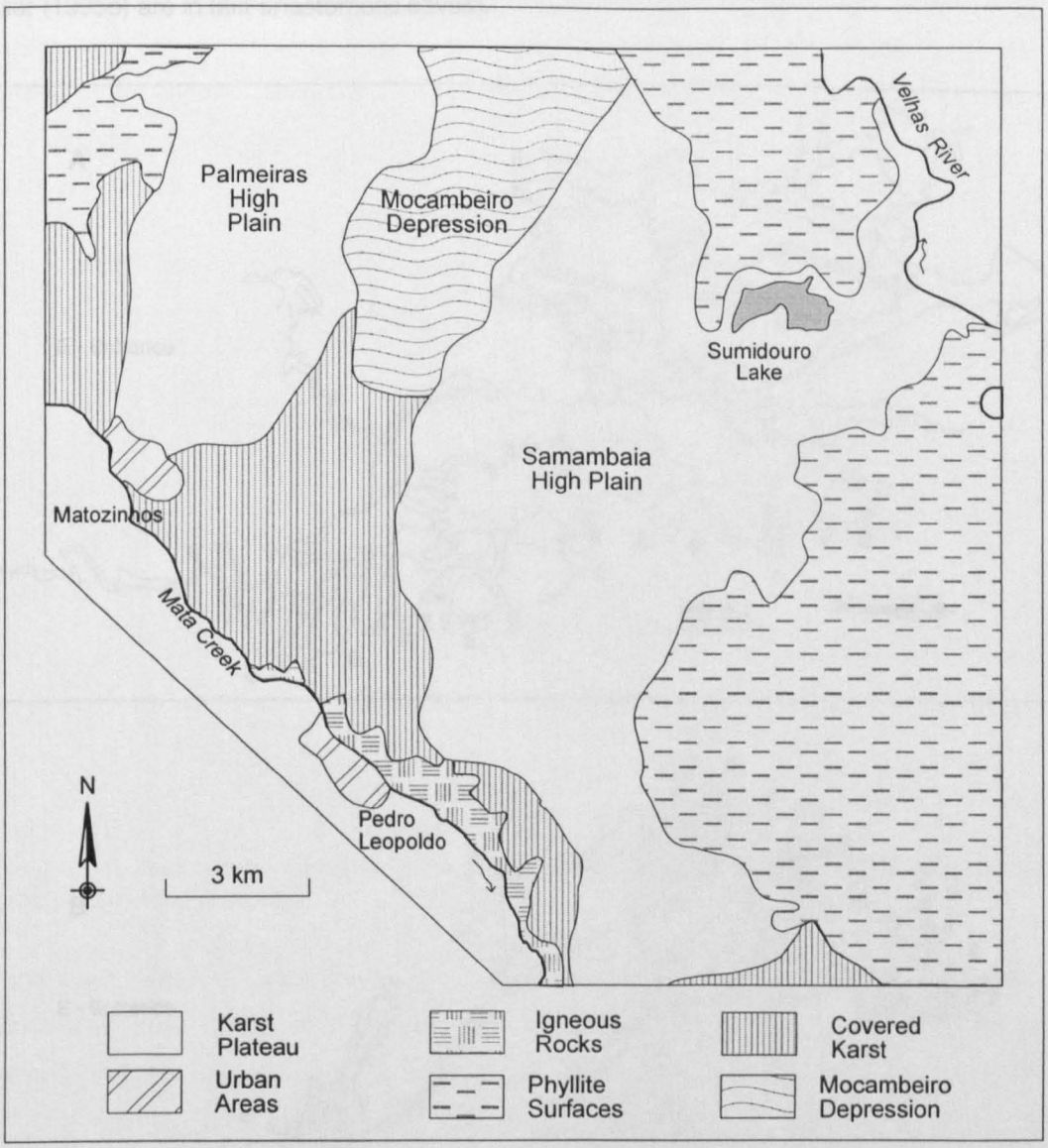

Figure 5.22. Physiographic domains in the Lagoa Santa Karst. From Auler (1994).

5.5.1. Underground karst

5.5.1.1. Morphology of the caves

Over 500 caves have been identified in the Lagoa Santa Karst. In general the caves are short sections of much longer systems that have been exposed or segmented by doline deepening and general surface and valley lowering. The majority of caves are dry passages occurring at the bottom of dolines or at the base of limestone cliffs. Network caves are frequent and usually associated with lakes (Auler, 1995b), but by far the most characteristic cave type in the area is anastomotic mazes (Fig. 5.23), comprising usually high and narrow meandering canyons with smooth walls that tend to intertwine with others of a similar kind. In plan, because of the short horizontal amplitude of the meanders, the series of anastomotic canyons can easily be mistaken

for network caves (indeed some of the caves defined as network in a previous sample of caves by Auler (1995b) are in fact anastomotic caves).

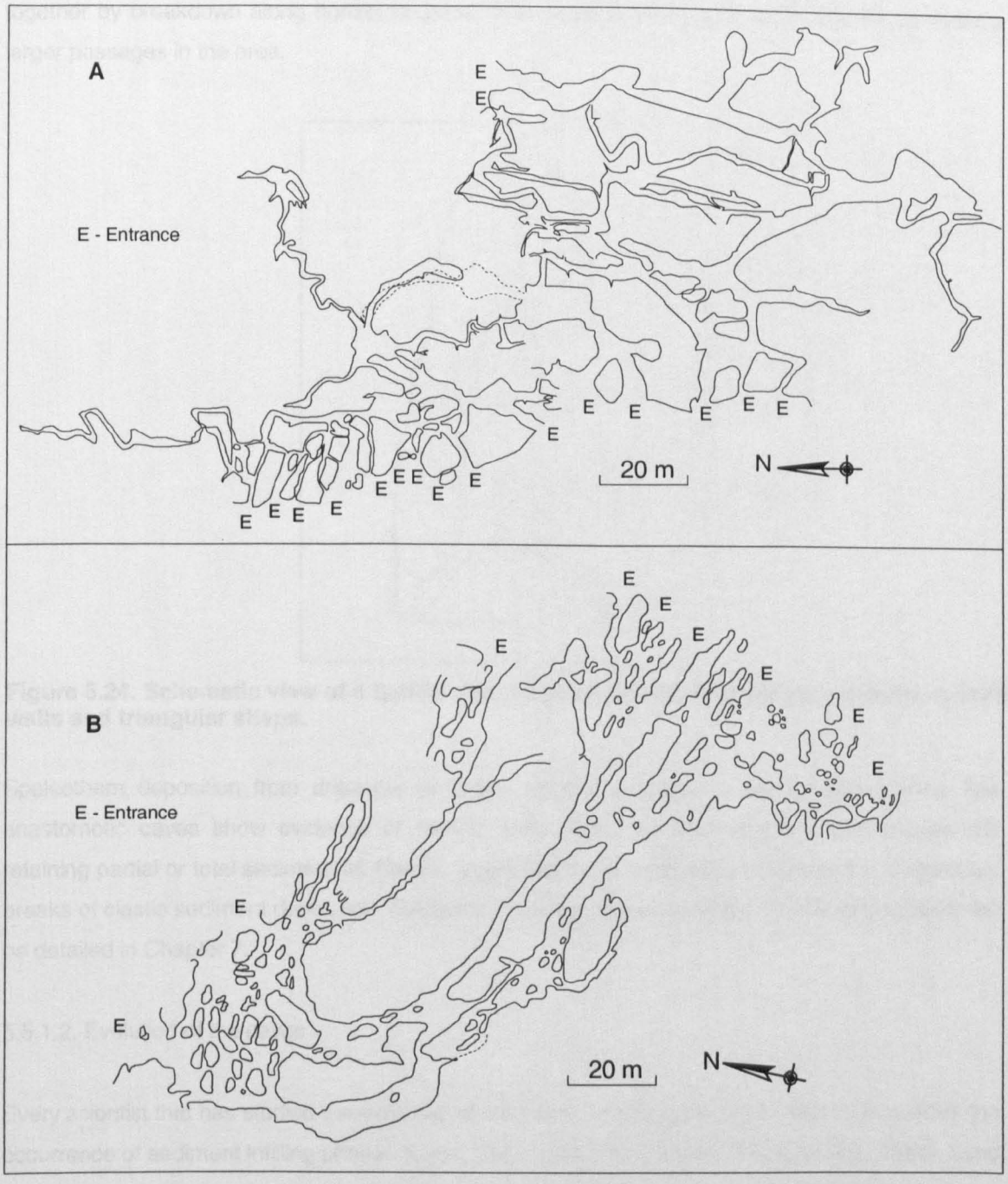

Figure 5.23. Plan of some anastomotic caves. A - Gruta de Escada (survey by Sociedade Excursionista e Espeleológica). B - Gruta do Baú (from Piló (1998)).

As with many of the caves in eastern Brazil, the bedrock floor is nearly always masked by sedimentation, precluding the determination of the true height and morphology of the passages. Based on the exposed sections, the canyon passages usually display a triangular shape, although they are much narrower at the base than passages in the Iraquara Karst. Canyon heights can reach up to 15 m, but are usually less than 10 m. The ratio of height/width of the passages is usually above 3 (but exceptions exist). Passage walls are very smooth and scallops are normally absent. The sinuosity due to meandering at the ceiling tends to be largely attenuated down along

the passage walls, and the meandering curves are usually not obvious at floor level. Smooth curved surfaces dominate the walls (Fig. 5.24). Pendants, parasitic wall tubes, and small anastomoses are common. In many caves, closely spaced meandering canyons can be joined together by breakdown along horizontal joints. This appears to be a common way of generating larger passages in the area.

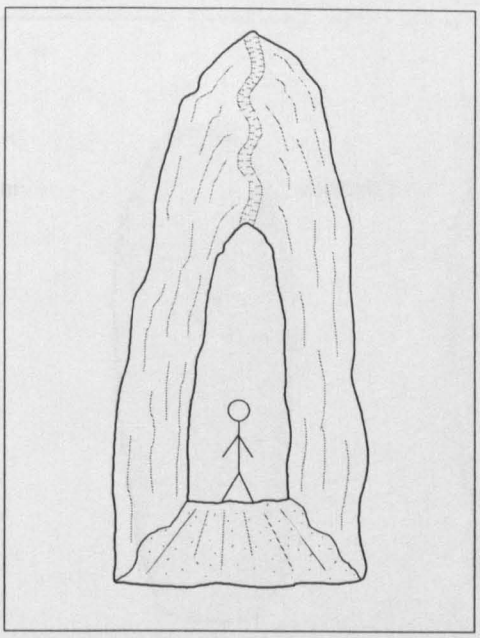

Figure 5.24. Schematic view of a typical canyon passage showing ceiling meander, smooth walls and triangular shape.

Speleothem deposition from dripwater is largely absent, except in a few localised sites. The anastomotic caves show evidence of having been infilled by sediment, some passages still retaining partial or total sediment fill. Calcitic layers within the sediment are frequent and represent breaks of clastic sediment deposition. Evidence of cyclical events in sediment infill and removal will be detailed in Chapter 7.

5.5.1.2. Evolution of the caves

Every scientist that has studied the evolution of the caves in the Lagoa Santa Karst has noticed the occurrence of sediment infilling phases (Lund, 1844, Liais, 1872, Lanari, 1909, Balázs, 1984). Lund (1844) was the first to develop a speleogenetic model for the area. He noticed that most caves showed remains of sediment attached to the walls and ceilings, demonstrating that the caves had been filled with sediment prior to the present time. Lund (1844) believed that the caves were formed by vertical percolation of acidic water with simultaneous infilling by clay from the bottom of dolines. In his model, doline formation was associated with cave genesis, although in a later stage, the sediment would be partially or totally removed by underground streams. Invasion streams would bring more recent sedimentation, and the final sediment deposits would be diachronous (Lund, 1844). Liais (1872) suggested that the caves were filled by sediment much later after their formation.

Coutard et al. (1978) proposed that many of the local caves had evolved through paragenesis. They recognised the high and narrow passages as paragenetic canyons and described typical paragenetic features such as ceiling channels and pendants. Piló (1998) proposed a different model based on Gruta do Baú, in which the canyons would be generated entirely in the phreatic zone, with no sedimentation, the passage being completely filled with sediment in a later stage, with evolution of some paragenetic features (Fig. 5.25).

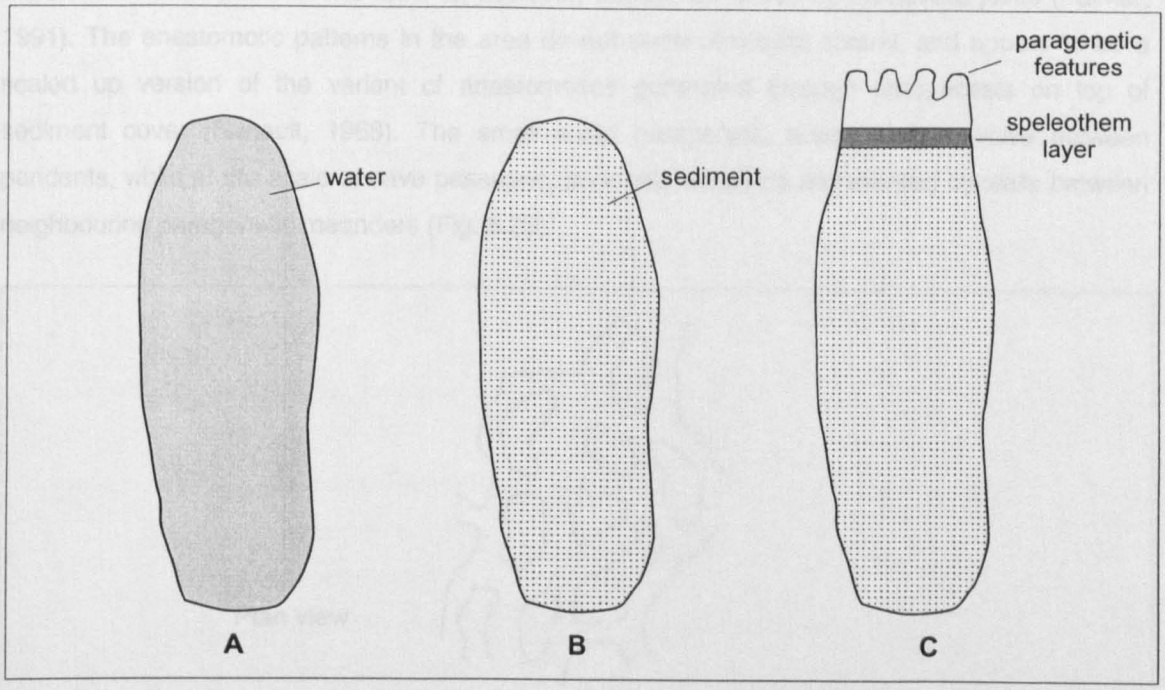

Figure 5.25. Evolution model of Piló (1998) based on Gruta do Baú. A - Generation of a canyon passage in the phreatic zone without participation of sediment. B - Complete sediment infill. C - Generation of paragenetic features above the sediment and deposition of speleothem layers.

Morphological evidence suggests, however, that the initial and major stage of speleogenesis involved paragenesis, as proposed by Coutard et al. (1978). The following evidence supports this hypothesis:

(1). In many cases there are no guiding joints in the roof, suggesting that the passage did not evolve initially at present day ceiling level. The generation of a vertically elongated phreatic canyon, as suggested by Piló (1998) would certainly require the existence of a guiding vertical joint. The same is true for the vertical percolation model of Lund (1844), because sediment infilling of caves from dolines would have to follow enlarged vertical joints at ceiling level.

(2). There is a meandering channel at the ceiling. This channel does not appear to be a later feature, because the entire canyon narrows uniformly towards the ceiling meander. Rift passages can be generated entirely by sediment free slow moving water in situations where there is a strong hydraulic head associated with the injection of unsaturated water, or due to uniform recharge through overlying permeable formations (Palmer, 1975). In fact, such a situation does occur in the

Lagoa Santa Karst due to the existence of caves generated by the numerous lakes in the area (Auler, 1995b). However, such phreatic rifts do not have meanders in the ceiling.

(3). The caves are not network systems, but anastomotic mazes. Small scale anastomoses can either develop along bedding partings (being the initial stage of competing proto conduits in some settings; White, 1988), or on a much larger scale as a passage element generating the anastomotic cave pattern. The latter is, however, usually controlled by favourable joints (Palmer, 1991). The anastomotic patterns in the area do not show structural control, and appear to be a scaled up version of the variant of anastomoses generated through paragenesis on top of sediment cover (Renault, 1968). The small scale paragenetic anastomoses evolve between pendants, while at the scale of cave passages, pendants would be represented by walls between neighbouring paragenetic meanders (Fig. 5.26).

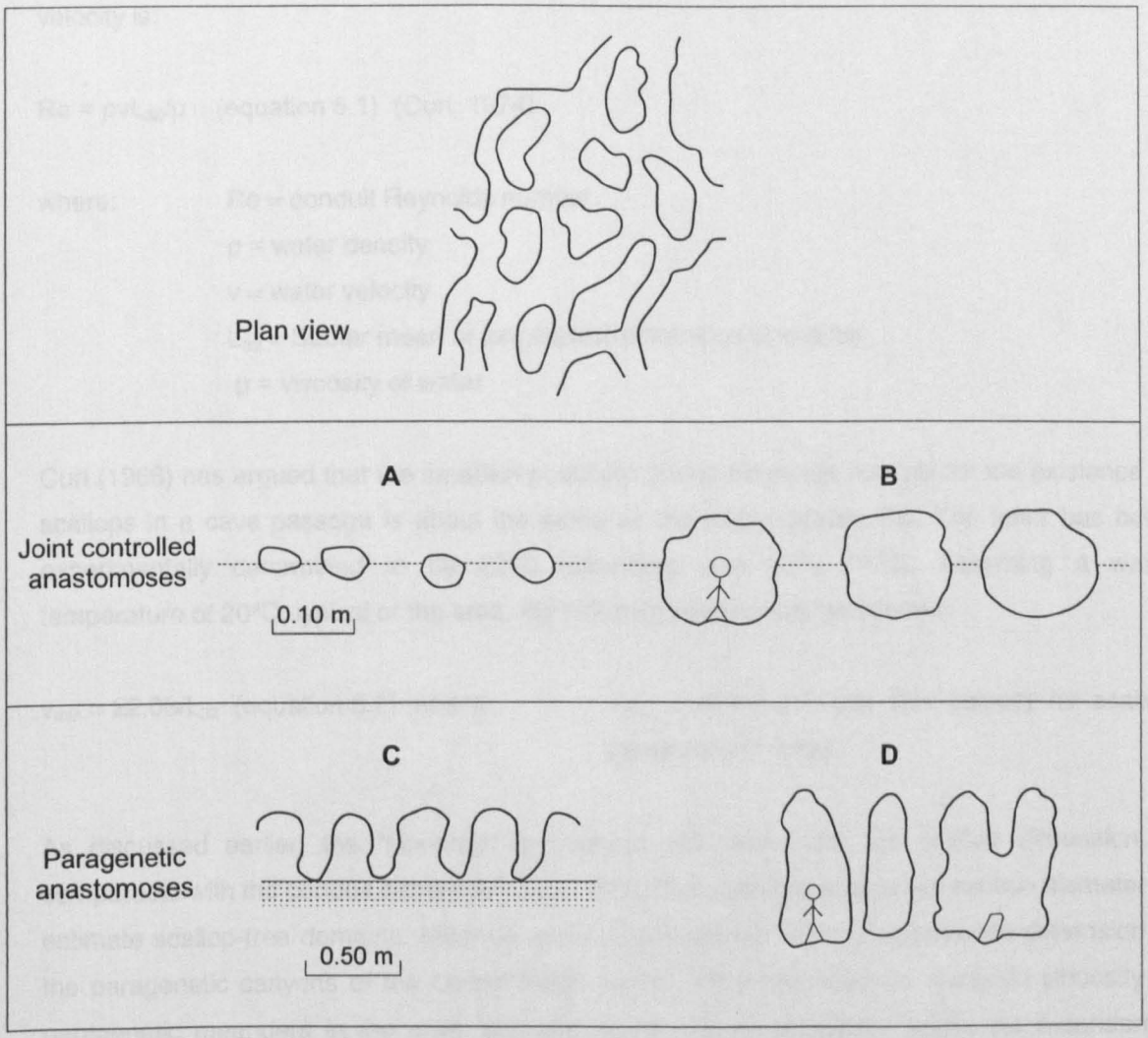

Figure 5.26. Types of anastomoses. A - Small scale protoconduit anastomoses. B - Anastomotic cave pattern. C - Pendants and small scale paragenetic anastomoses. D - Paragenetic canyons.

(4). Junctions between passages of distinct ceiling height are characterised by an "ascending meander" that links the meanders in both passages without loss of continuity. This feature indicates that water flow was occurring at ceiling level when both passages were active. The lower portion of

both connecting canyon passages had, thus, to be filled with sediment. Passage junctions at ceiling level between canyon passages of differing ceiling height in other phreatic and vadose situations do not display such feature (Fig. 5.27).

(5). There is a general lack of scallops on cave walls and ceiling meanders. Although dissolution at the sediment/rock interface can play a role in masking the scallops, a second possibility is that flow was sufficiently slow to preclude the generation of scallops. Theoretically, scallops should always be produced by dissolution by flowing water, but in very slow moving water scallops whose width and length are larger than the sinuosity of the passage will be generated, and will thus not be separable from bends in the conduit (Curl, 1966).

In a cave passage, the Reynolds number as determined from scallop size and average water velocity is:

$Re = \rho v L_{32}/\mu$ (equation 5.1) (Curl, 1974)

where: Re = conduit Reynolds number
ρ = water density
v = water velocity
L_{32} = Sauter mean of longitudinal dimension of scallop
μ = viscosity of water

Curl (1966) has argued that the smallest possible conduit Reynolds number for the existence of scallops in a cave passage is about the same as the stable scallop Re. The latter has been experimentally determined to be 2200 (Blumberg and Curl, 1974). Assuming a water temperature of 20°C, typical of the area, the following relation can be derived:

$v_{min} = 22.08/L_{32}$ (equation 5.2) where: v_{min} = minimum water flow velocity for scallop development (cm/s)

As discussed earlier, the "absence" of scallops will mean that the scallop dimension is comparable with the conduit dimension. Curl (1966) has used passage cross section diameter to estimate scallop-free domains. Meander wave length appear a more appropriate dimension in the paragenetic canyons of the Lagoa Santa Karst. There has been no study on sinuosity of paragenetic meanders in the area, and plan maps do not accurately depict the meandering curves at ceiling level. Assuming an average ceiling meander wavelength an order of magnitude of 5 m, paragenetic water velocities in the area would be in the range of 0.04 cm/s for non generation of scallops. Such minimum velocity is two orders of magnitude lower than the paragenetic maximum threshold velocities of 20 cm/s and 10 cm/s derived respectively by Worthington (1991) and Renault (1968) needed in order not to remove sediment in a conduit. It seems thus that flow velocities are slow enough to promote sediment deposition in scallop free

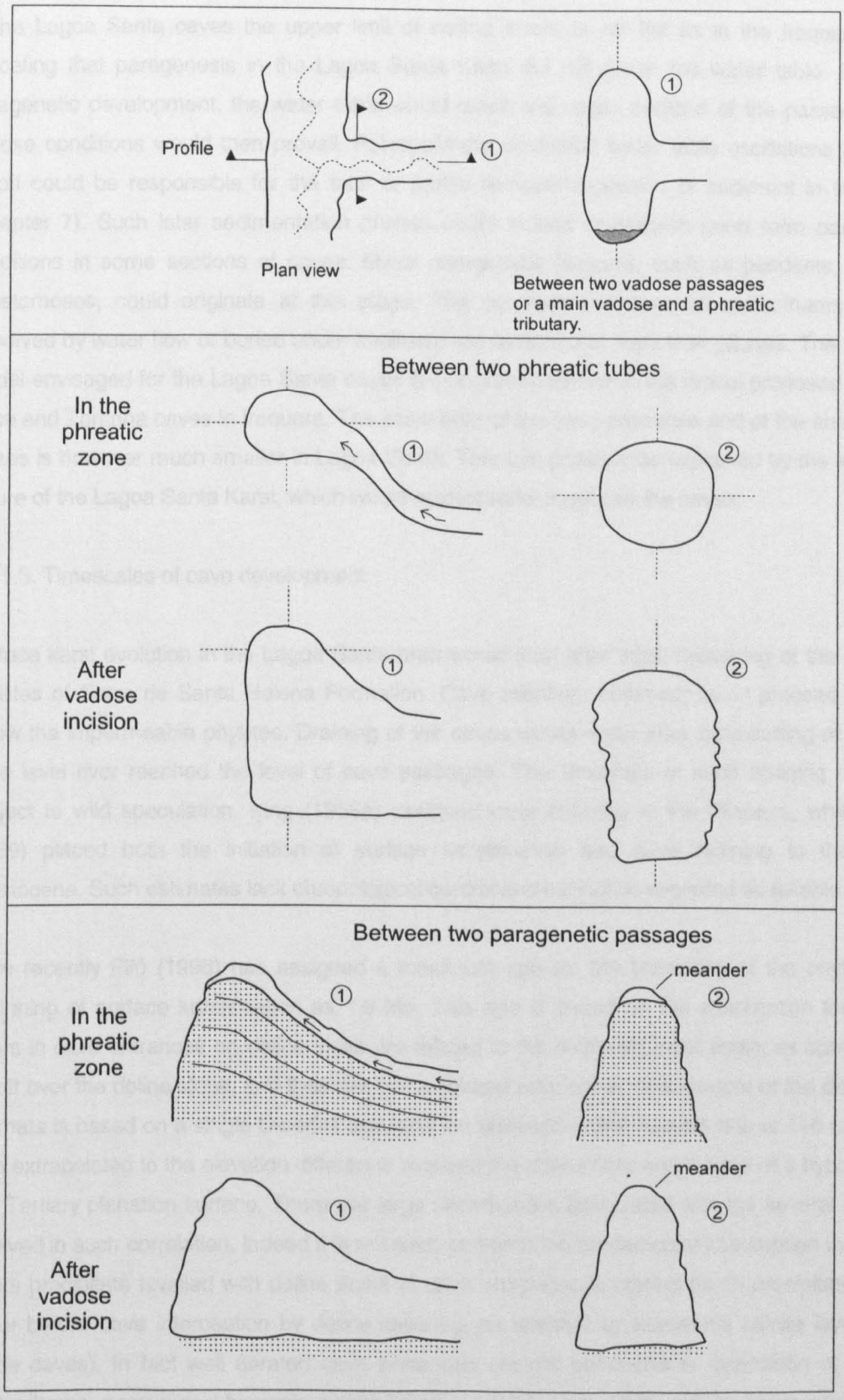

Figure 5.27. Morphology of passage junctions in vadose and phreatic situations when original ceilings are at distinct levels.

paragenetic passages. Together with other morphological criteria, absence of scallops can thus be used to infer paragenesis.

In the Lagoa Santa caves the upper limit of ceiling levels is not flat as in the Iraquara Karst, indicating that paragenesis in the Lagoa Santa Karst did not reach the water table. Following paragenetic development, the water table would reach the upper portions of the passages, and vadose conditions would then prevail. Palaeoclimate controlled water table oscillations or doline runoff could be responsible for the total or partial removal/deposition of sediment in the caves (Chapter 7). Such later sedimentation phases could indeed reestablish short form paragenetic conditions in some sections of caves. Minor paragenetic features, such as pendants, or small anastomoses, could originate at this stage. The common presence of speleothems partially dissolved by water flow or buried under sediment are evidence of such later phases. The evolution model envisaged for the Lagoa Santa caves is in essence similar to the model proposed for Lapa Doce and Torrinha caves in Iraquara. The scale both of the cave passages and of the anastomotic mazes is however much smaller in Lagoa Santa. This can possibly be explained by the autogenic nature of the Lagoa Santa Karst, which would restrict water input into the caves.

5.5.1.3. Timescales of cave development

Surface karst evolution in the Lagoa Santa area would start after initial breaching of the overlying phyllites of Serra de Santa Helena Formation. Cave initiation, however, could proceed at depth below the impermeable phyllites. Draining of the caves would occur after downcutting of the local base level river reached the level of cave passages. The timescale of such draining has been subject to wild speculation. King (1956a) assigned cave draining to the Pliocene, while Kohler (1989) placed both the initiation of surface karstification and cave draining to the middle Pleistocene. Such estimates lack chronological control and cannot be regarded as reliable.

More recently Piló (1998) has assigned a maximum age for the breaching of the phyllites and beginning of surface karstification as 1.9 Ma. This age is based on the assumption that calcite layers in cave entrances on doline sides are related to the sediment input episodes controlled by runoff over the doline slope, and thus can be correlated with former palaeofloors of the doline. The estimate is based on a single U-series age, and the deduced doline incision rate of 110 m/Ma was then extrapolated to the elevation difference between the doline floor and the top of a hypothesised late Tertiary planation surface. There are large uncertainties associated with the several variables involved in such correlation, indeed it is not even certain if the fundamental assumption that calcite layers precipitate levelled with doline floors at cave entrances is correct (such precipitation could occur before cave interception by doline lowering, as attested by numerous calcite layers deep inside caves). In fact well aerated cave entrances are not conducive to deposition of massive speleothems, porous and biogenic calcite being more frequent. Many calcite layers now present near cave entrances could in fact originally have been deposited deep inside caves, and be exposed by erosion. There is no firm evidence for the existence, let alone the elevation, of a former

planation surface in the area in the late Tertiary. Furthermore, the beginning of karstification would occur when incision reached the top of the carbonates, and the elevation difference between the top of the hypothetical planation surface and the limestone-phyllite contact (not doline bottom) should be used. Individual rates of doline deepening can vary significantly. Piló (1998) has reported two other rates deduced from calcite layers deep inside caves that show variations of over 100%. The doline incision rate reported by Piló appears to be too high when compared with surface denudation rates deduced from cratonic settings (Table 3.1).

An U-series age from a speleothem from Gruta Bauzinho de Ossos (Table 5.5) is older than the limit of the alpha spectrometric method and palaeomagnetism samples, although showing magnetic instability during the demagnetisation steps, appear to have normal polarity, precluding further interpretation (Table 5.5b). The samples reported in Table 7.2 are part of speleothem layers that were originally intercalated with sediment infilling deposits. They thus belong to the later cyclical episodes of sediment infilling/removal that can significantly postdate cave generation.

A

Sample	U (ppm)	$^{234}U/^{238}U$	$^{230}Th/^{234}U$	$^{230}Th/^{232}Th$	$^{234}U/^{238}U_{t=0}$	Age (ka)
GBO-03	0.098 ± 0.002	1.08 ± 0.03	1.012 ± 0.030	29	-	>350

B

Sample	N	I_o	Decl.	Incl.	R	K	α_{95}	Polarity
GMR-01	5	86.96	359.09	-62.75	4.87	31.77	14.01	NORMAL
GBO-01	4	815.28	37.73	-66.79	3.67	9.23	32.23	NORMAL?

Table 5.5. *A.* U-series analysis of speleothems from Gruta Bauzinho de Ossos in the Lagoa Santa Karst. *B.* Palaeomagnetism analyses of samples from Gruta do Morro Redondo (GMR) and Gruta Bauzinho de Ossos (GBO). Intensities (I_o) in mA/m, Declination, Inclination and α95 in degrees. α_{95} – 95% probability that the direction lies on that angle span, K- Fisher precision estimate which determines the dispersion of points, R- length of resultant vector.

Some of the caves in the area are now several metres above the water table. One of the paragenetic caves, Gruta do Morro Redondo, is known to be at least 75 m above the local water table. If the surface lowering rates of 30 ± 10 m/Ma reported for the São Francisco Craton by Harman et al. (1998) are applied to the above cave, minimum ages of draining between 3.7 and 1.9 Ma are obtained. Initial karstification would necessarily have predated cave draining because of the available volume of carbonate rock above the cave. This data demonstrates that cave development had started well within the Tertiary, and the beginning of cave draining and karstification occurred prior to the Pleistocene. The antiquity of the Lagoa Santa caves is further demonstrated by the fact that many caves are now mere remnants above karst towers, or represent decoupled hydrologic routes that do not bear any relationship with current ground water flow paths (Auler, 1998).

5.6. SUMMARY OF PARAGENETIC DIAGNOSTIC CRITERIA

Criteria for diagnosing paragenesis have been listed in section 5.2.2 and are summarised below:

1. Presence of pendants. 2. Presence of anastomoses or half tubes. 3. Presence of parasitic wall tubes. 4. Presence of wall grooves. 5. Lack of guiding fracture or bedding plane at ceiling level. 6. Lack of a precursor phreatic tube on the ceiling. 7. Downstream propagation of meanders. 8. Phreatic canyon or triangular passage cross section. 9. Active paragenetic passages in the phreatic zone.

Study of the Lagoa Santa, Caatinga and Iraquara Karst areas has allowed the recognition of the following additional distinctive features of paragenesis:

10. Lack of scallops. The velocity required for scallop length to match passage sinuosity (and thus become indistinguishable) is too slow to allow for sediment removal and should therefore favour paragenesis if there is sediment availability.

11. Meander junctions at ceiling level occur through an ascending meander. This feature demonstrates that water flow was occurring mostly at ceiling level at time of junction (Fig. 5.27).

12. Anastomotic canyons are the predominant type of cave pattern. In low dip situations this should be the prevalent type of paragenetic cave pattern. Variable passage cross section due to changes in sediment volume can keep several passages simultaneously competitive.

13. Presence of flat ceiling without phreatic dissolution features. When a paragenetic passage has reached the water table, the ceiling is determined by the elevation of the water table. Since the ceiling will mark the upper limit of the phreatic zone, no phreatic features can develop after this stage.

14. General absence of joint fed speleothems. When compared with vadose caves, paragenetic caves may exhibit less speleothem, because of the general absence of vertical joints at ceiling level. Furthermore, the overall volume of a paragenetic passage spends more time in the phreatic zone and under sediment cover than a typical vadose cave, restricting the chance of speleothem precipitation by water percolating through joints.

5.7. A MODEL OF CAVE DEVELOPMENT IN STABLE CRATONIC AREAS

Studies in three different areas (Iraquara, Caatinga and Lagoa Santa) along the São Francisco Craton have shown similar styles of cave development, despite major differences in lithology, hydrology and present climate. When not overwhelmed by the sulphuric acid effect, paragenetic processes are evident in the majority of caves examined. It will be proposed in this thesis that

the mode of conduit development after initiation is controlled by large scale denudation rates which are dependent on the tectonic setting. Later vadose processes frequently obliterate the original paragenetic features, and caves initially originated by paragenesis can pass undetected.

5.7.1. Controls on paragenetic development

5.7.1.1. Sediment availability

The first requisite for paragenesis is the availability of sediment for transport into the cave system. In eastern Brazil, bare bedrock floors are extremely rare, nearly all caves having their floor covered by sediment deposits usually of unknown thickness. There has been no worldwide survey on the frequency and extent of soil cover in karst areas, but covered karst predominates in most of the karst areas in the Americas, especially in eastern United States, northern Mexico, Central America and some islands of the Caribbean such as Cuba, and most of South America. Soil cover predominates in many karst areas of Europe, such as in England, parts of France and Italy, and in most of tropical Asia sites. It seems apparent that sediment derived from the soil is commonly available in most karst areas of the world.

White and White (1968) have been the only authors to discuss the possible role of sediments in the early initiation of cave conduits. They argue that flow velocities in the initial openings in the limestone would be too slow to exceed the threshold of sediment transport, but that after the threshold, when flow changes from laminar to turbulent, fine grained sediment may be transported. In fact, White and White (1968) have pointed out that a sedimentary layer on the floor of caves is the natural state of passages at all stages of development, and should be present as soon as the conduit size and flow velocity surpass the threshold for sediment entrainment. Possible exceptions to this situation would be very pure limestones in barren karst areas with very limited sediment supply such as in some alpine settings, mixing zone karst areas, or hypogenic settings where deep flow is not surface derived.

5.7.1.2. Proto conduits and the development of anastomotic systems

In the Iraquara and Lagoa Santa karst areas, an array of anastomotic channels of varying size seems to be the dominant pattern of conduit distribution. These paragenetic anastomotic systems can vary over two orders of magnitude from small centimetre wide anastomotic channels between pendants to large metre wide cave passages. These anastomoses are morphologically similar to anastomoses generated during the early development of cave systems and frequently found along bedding partings in some karst areas (Fig. 5.26). According to Ford and Ewers (1978) anastomoses occur (within 15° of the dip of the bedding) whenever the dip of bedding is less than 5°, single conduit proto tubes being produced if the dip is steeper. Such protoconduit anastomoses are believed to be evidence of the earliest stage of conduit development when competition between several passages have not yet produced a "victor" tube

which will capture most of the discharge (Ford and Williams, 1989). As such, remnants of such anastomotic arrays should be commonly observable in cave walls, and indeed, most textbooks on karst geomorphology provide examples of such features (Jennings, 1985, White, 1988, Ford and Williams, 1989). Although the majority of karst areas in eastern Brazil displays nearly horizontal carbonate bedding, precursor small scale anastomotic bedding plane systems have *never* been observed in the hundreds of caves examined in the Lagoa Santa and Iraquara areas. Because of paragenetic development, such networks (if they exist) in the area, would be located near the base of the passage which is nearly always masked by sedimentation. However, wherever vadose entrenchment allows the observation of the full height of the passage, no anastomotic precursor tubes can be observed. I believe that the small scale anastomoses commonly reported in the literature cannot be observed in eastern Brazil because they have evolved to become the cave passages themselves.

The initial stage of conduit generation involves small apertures (μm) that evolve under laminar flow, and dissolution follows the slow fourth order kinetic rate law (Dreybrodt, 1990). A threshold occurs when aperture becomes wide enough for the faster first order dissolution rates to become predominant and turbulent flow to take place (White, 1977). Such breakthrough is characterised by a large increase in discharge (Dreybrodt, 1990). Modelling has suggested that channels at breakthrough time are 1 - 10 cm wide (Dreybrodt, 1990), suggesting that sediment transport may start occurring at this stage (White and White, 1968). During the initial stages of conduit generation, there will be a dominant (or victor) tube which will tend to evolve faster and carry a larger discharge than neighbouring passages, as demonstrated in modelling experiments (Ford and Williams, 1989, Groves and Howard, 1994, Siemers and Dreybrodt, 1998). As breakthrough occurs, the dominant tube will discharge nearly all the flow in the initial system (Siemers and Dreybrodt, 1998). However, if the water input to this channel becomes restricted, for instance by sedimentation, and constant head conditions remain elsewhere, other competing channels can still evolve towards breakthrough (Siemers and Dreybrodt, 1998), and a series of competing anastomotic channels with turbulent flow would result.

During the evolution of competing channels, the larger aperture of the dominant passage causes a drop in hydraulic head, and neighbouring passages converge downgradient towards it (Ford and Williams, 1989, Palmer, 1991). In order for an anastomotic system to remain operative, there should be a limiting mechanism to keep the several passages simultaneously competitive. In paragenetic passages, an increase in discharge will lead to a higher flow velocity. This will cause sediment removal, and an increase of the cross sectional area which will ultimately result in a decrease in the water velocity. A dynamic equilibrium is thus established, and there will be no dominant passage, because all tubes can adjust the cross-sectional area to any given increment in discharge. This rapid hydraulic adjustment is a unique feature of paragenetic systems. There should therefore be no large variations of head between competing pathways, and an array of interconnected meandering channels could persist without noticeable convergence towards a single major tube.

5.7.1.3. Paragenesis as an early attribute of karst aquifers?

The scheme of early anastomotic development of paragenetic passages suggested for the horizontally bedded carbonates of eastern Brazil should be applicable to other carbonate settings. For areas with steeper dips, less interconnective primary anastomotic tubes will develop (Ford and Ewers, 1978). Steeply dipping bedding planes will favour looping passages, in which the prime areas for paragenetic development will be at the downward apex of loops, and the final tendency of the passage will be to match the water table contour (Fig. 5.1).

The realisation that paragenesis may be present from the early stages of turbulent flow conduit development can have interesting consequences for our understanding of karst aquifers. Current knowledge of conduit porosity in karst aquifers is largely based on dye tracing, spring hydrographs and analysis of cave patterns. Due to sediment infill, paragenetic caves when exposed at the surface are not readily explored. Observations at many sites in Brazil and the UK (Eldon Hill Quarry) suggest that many of the paragenetic anastomotic networks can be too small to be entered, but the density of such passages appears to be higher than in settings where vadose speleogenesis predominates. This bias in the existing sample of "observable" caves is apparent in the worldwide survey by Palmer (1991) in which anastomotic caves constitute only 3% of the observed caves, and 10% of the total passage length. In the karst areas of Lagoa Santa and Iraquara most passages are paragenetic.

The existence of anastomotic systems within karst aquifers can help explain why distributary flow paths are commonly detected during dye traces while at the same time appear to be rather uncommon in vadose settings or drained caves. Previous explanations for such phenomena involved the existence of overflow interbasin routes (Worthington, 1991) or delta type branching near springs (Palmer, 1987). It appears though that distributary conditions can occur even in low flow regimes and far from spring outlets. The onset of vadose conditions in a paragenetic system, to be detailed in section 5.7.5, will tend to restrict the number of active flow routes, somehow linearising existing flow paths. Water input points into the passages may be restricted to swallets, and therefore not all passages will carry a fluvial drainage. A high density array of small interconnecting paragenetic passages would represent a departure from the more conventional "conduit" flow system, where major passages carry large amounts of water through an otherwise impermeable carbonate aquifer.

5.7.1.4. Depth of conduit initiation

The depth at which a cave will originate below the water table has been subject to considerable debate in the past on conceptual grounds (see review in White, 1988) but even recently few quantitative advances have been made. The Four State Model of Ford and Ewers (1978) states that depth of conduit development is dependent on joint frequency. Horizontally bedded limestone will tend to carry water at shallow depths, unless strong joints can guide the water into

deeper paths. The Four State Model makes no attempt to quantify the effective depth of conduit initiation in karst aquifers. Palmer (1991) and Groves and Howard (1994) have suggested that initial aperture width is very important in guiding initial flow routes. Fissures with the least flow resistance will be preferred, even if this means following an indirect path towards the output point. Palmer (1991) has argued that, since fractures diminish in number and width downward in the bedrock, shallow flow should in general be more efficient. The possible presence of favourable horizons of more soluble material, termed inception horizons by Lowe (1992), that may foster initial speleogenesis by non carbonic acid processes, may however provide routes to ground water flow to greater depths (Worthington, 1991). Folding and faulting can also promote deeper ground water routes (Palmer, 1987). For the sake of simplicity, a homogeneous carbonate aquifer, without significant folding or faulting and without impermeable beds that can cause confined and artesian aquifers will be assumed. This is the common situation in the São Francisco Craton carbonate areas.

There are several ways of determining depth of present or past ground water circulation below the water table. Water temperature at spring outlets can be used, together with thermal gradients, to infer approximate maximum depths of water flow (review in Worthington, 1991 and Worthington and Ford, 1995). Borehole logging and packer testing frequently show the presence of dissolution openings at depths up to 3000 m (Ford and Williams, 1989), often with capacity for water circulation. These two approaches suggest that deep water flow, on the range of over 100 m below the water table are rather common. Direct observation of flooded passages by cave divers worldwide also confirm the common existence of deep flow routes in carbonate systems, to depths well in excess of 100 m below the water table (Farr, 1991). In the Iraquara Karst, flooded passages have been explored to a depth of 30 m below the water table. An alternative method of determining minimum flow depth of cave passages is provided by the vertical range of a paragenetic passage. This is represented by the elevation difference between the bedrock floor of the passage and the ceiling. Considering that some water table lowering must have occurred since the beginning of the paragenetic development, this parameter provides a minimum depth of initiation below the water table. Vertical paragenetic amplitudes up to 50 m have been reported in the literature (Renault, 1968). At Lapa Doce in the Iraquara Karst, the vertical paragenetic range is 11 m as measured at several sites with an ultrasonic tape. In the Lagoa Santa Karst, it may exceed 15 m in some caves.

Worthington (1991) has provided the only attempt to effectively determine flow depth in karst aquifers. Based on a somewhat small dataset, he suggested that flow depth is typically about 1% of the catchment length. A relationship between flow depth and catchment length in karst systems was derived:

$Dm = 0.11 (L_x \sin \theta)^{0.81}$ (equation 5.3) Worthington (1991)

where: Dm = mean depth of conduit flow

L_x = catchment length

θ = dip of strata

Fig. 5.28 presents a graphical solution for the above equation, showing the depths to be expected from typical (<10°) stratal dips found in the São Francisco Craton. The results are in the correct order of magnitude when compared to explored flooded conduits and paragenetic amplitudes in the Lagoa Santa and Iraquara areas.

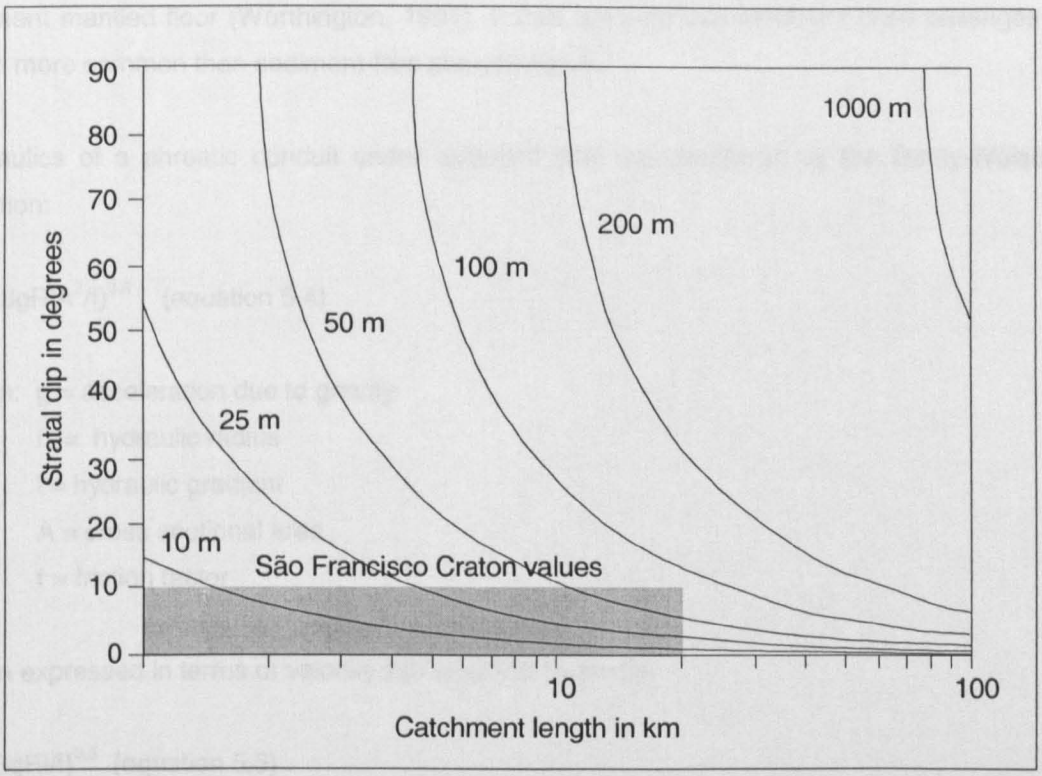

Figure 5.28. Depth of conduit initiation in relation to catchment length and stratal dip with range of values to be expected from the São Francisco Craton. From Worthington (1991).

It should be emphasised that conduit phreatic depth determinations by direct observation (cave diving), vertical paragenetic range and by the empirical relation of Worthington (equation 5.3) refer to depths of passages after breakthrough has occurred. This is because flooded passages can spend an extended time during the initial stages of slow order reaction and laminar flow, especially in low relief areas such as the São Francisco Craton (see Palmer, 1991 and Dreybrodt, 1990). Significant lowering of the water table could occur during this period. The initiation depth of cave passages would necessarily be significantly larger than the observed depths determined by the three techniques outlined above. In this thesis, conduit depth after breakthrough will be adopted throughout.

5.7.2. Rates of upward paragenetic evolution

After breakthrough has been achieved, provided the water table remains above the passage during the period of enlargement, there will be two alternatives for further development of a

flooded conduit. In a situation where there is no supply of sediment, or where water velocities are too high to allow for sediment deposition, a phreatic tube will develop. Such a tube will grow indefinitely until modified by breakdown or drained by water table lowering. Given the existence of flooded passages at great depths (in excess of 100 m) we should expect the common occurrence of very large phreatic tubes. Although White (1988) and Worthington (1991) have acknowledged the existence of phreatic tubes > 40 m in diameter, such very large passages appear to be more the exception than the rule. The second style of development is through paragenesis. Cave divers have commonly reported that phreatic caves normally have a sediment mantled floor (Worthington, 1991). It thus appears that sediment filled passages are much more common than sediment-free phreatic tubes.

Hydraulics of a phreatic conduit under turbulent flow are described by the Darcy-Weisbach equation:

$Q = (8gRiA^2/f)^{0.5}$ (equation 5.4)

where: g = acceleration due to gravity
R = hydraulic radius
i = hydraulic gradient
A = cross sectional area
f = friction factor

When expressed in terms of velocity this equation becomes:

$v = (8gRi/f)^{0.5}$ (equation 5.5)

Ground water flow velocities decrease with lower hydraulic gradients. In the subdued relief of eastern Brazil low hydraulic gradients should be expected, resulting in very low conduit velocities. Worldwide conduit dye tracing velocity data (reviewed in Worthington, 1991) are marked low, in average 0.02-0.05 m/s, below the threshold for sediment transport. Considering the nearly global availability of sediment in karst systems, the ubiquitous existence of input points linking sediment sources to underground passages, and the slow water flow velocities in subsurface conduits, paragenesis should be a common mode of cave evolution in the phreatic zone.

During paragenesis, the floor of a phreatic passage is armoured by sediment. Dissolution, if it occurs, is unlikely to be significant at the sediment-bedrock interface because it will be limited by replacement of reactant and evacuation of products. The sole section of bedrock available for conduit enlargement are the upper walls and ceiling. The cave will then evolve upwards towards the water table. Rates of upward conduit migration are an important component in determining the magnitude of vertical paragenetic range, the rate of loop elimination, and possibly the

development of flat water table roofs. There has been no previous study of this problem. However, if a paragenetic passage is considered to be half tube with a sediment floor, the relation of Palmer (1991) can be used

$S = 31.56\ Q\ (C - C_0) / p L \rho_r$ (equation 5.6)

where: S = rate of paragenetic upward migration

Q = discharge of water through the passage

C = solute concentration (C_0 = C at upstream end of passage)

p = wetted perimeter

L = passage length

ρ_r = rock density

Dreybrodt (1990) has estimated average rates of 100 m/Ma for conduit bedrock removal after breakthrough, but variations of an order of magnitude on either side are possible. Fig. 5.29 illustrates the rate of enlargement of a phreatic tube under closed system conditions and at water temperatures of 10°C. Taking into consideration discharges measured at the Lagoa Santa Karst (Auler, 1994) and estimated discharges for springs in the Iraquara Karst, a range between 0.05 - 2 m^3/s appears reasonable. Length of underground flow paths should be in the range 1 - 20 km, resulting in Q/L ratios below 20 cm^2/s. In Fig. 5.29 these values would represent enlargement rates at the upper limit of the curve, in the range of 1000 m/Ma. Typical maximum enlargement rates for karst systems averages about 100-1000 m/Ma (Palmer, 1991).

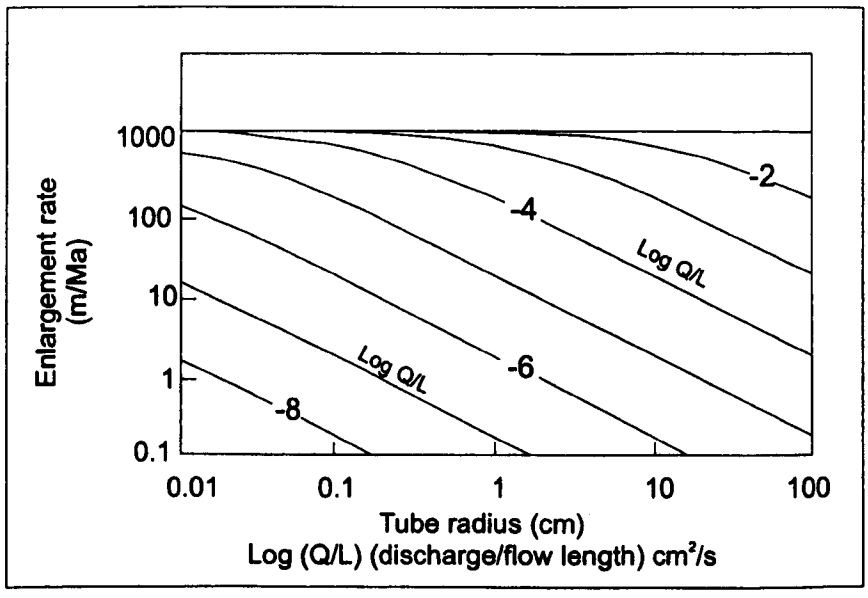

Figure 5.29. Enlargement rate for a phreatic tube under closed system and at water temperature = 10°C. From Palmer (1991).

5.7.3. Water table lowering rates in karst regions

The end of the phreatic regime in a cave system happens when the water table reaches the top of the passage, and dissolution becomes concentrated on the floor. It is thus important to quantify the rates of water table lowering, because these will determine the amount of time available for paragenesis. Water table lowering will be considered as a relative measure in relation to a fixed point in the bedrock (or a cave system within the bedrock). This is because tectonic uplift can rapidly change relative water table positions within the bedrock, while the water table elevation relative to a outside datum (such as sea level) could remain virtually unchanged.

Regional denudation rates in cratonic or low relief areas have been discussed in section 3.3 and data based mainly on apatite fission track were reported in Table 3.1. Denudation rates based on fluvial incision rates in karst have been presented in Table 3.3. In this thesis it is assumed that surface lowering rates are compatible with water table lowering rates. Furthermore, fluvial downcutting rates, together with other techniques of punctual measurements, are assumed to provide reasonable approximation of regional scale water table lowering rates.

The data demonstrate that denudation rates in cratonic or low relief areas are typically in the range 1 - 50 m/Ma, with several areas (mainly in the best studied sites in the plains of Australia) having values below 10 m/Ma. These data demonstrates that denudation rates in stable tectonic settings can be an order of magnitude lower than in mountainous or in tectonically active regions.

5.7.4. A denudational model of cave evolution

It has been demonstrated in the previous sections that conduits commonly carry sediment deposits. It has also been shown that ground water velocities, especially in low relief areas with low hydraulic gradients, may fall below the threshold of sediment transport. Under such conditions, the minimum requirements for the initiation of paragenetic development should be present in many if not most karst settings. Two further variables should be taken into account. Because paragenetic passages evolve upwards towards the water table, there should be enough vertical amplitude for a passage to develop, i.e., the deeper the passage is, the more "room" for upward paragenetic development there will be. Flow depth in karst systems appears to be controlled mostly by stratal dip (section 5.7.1.4), and thus areas with steeply dipping carbonate should in theory be more favourable for paragenetic development. However, a major control affecting this opportunity for upward development is the rates of water table lowering. The rate is very slow in eastern Brazil permitting an extended period for paragenesis, despite the shallow dip of the carbonate which limits depth of paragenetic development.

Water table lowering rates in mountainous or tectonically active areas are an order of magnitude higher than in stable cratonic settings. In the latter regions, caves would tend to remain for a much longer time in the phreatic zone. It has also been demonstrated that upward paragenetic migration rates should be at least an order of magnitude higher than water table lowering rates in tectonically stable, low relief areas, but should match these rates in mountainous settings. Fig. 5.30 illustrates these relationships. For any given initial conduit depth, the time available for upward paragenetic migration would be greatly increased in karst areas with low water table lowering rates. On the other hand in areas with very fast water table lowering rates, such as mountain ranges, the cave passage could be intercepted by the water table before significant paragenetic development had occurred.

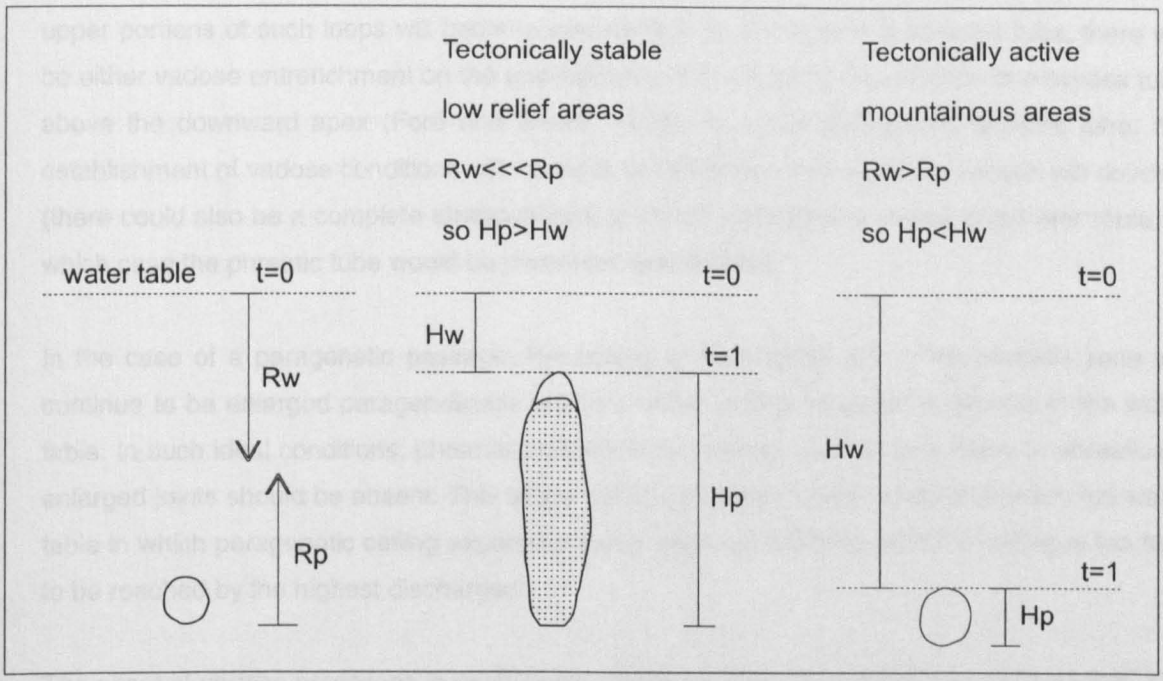

Figure 5.30. Model of cave development in relation to water table lowering rates. Rw = Rate of water table lowering; Rp = Rate of paragenetic upward migration; Hw = Amount of water table lowering between t=0 and t=1; Hp = Paragenetic vertical range.

From this denudational model of cave development, paragenetic caves should predominate where water table lowering rates are slow, such as in cratonic settings or in low relief continental interiors. Prime candidates are the ancient tablelands of interior South America, Africa and Australia. At the other extreme, areas with very high denudation rates, such as mountain ranges or areas with active tectonics, should show predominantly vadose passages and little paragenetic development. Many karst areas, however, fall between these extremes, and could display both paragenetic and syngenetic development styles, depending on initial flow depth, sediment availability and local geomorphic factors.

The above model, developed at a regional scale of cave systems, is also applicable to individual passages in caves. It has been suggested by Palmer (1991), Worthington (1991), Dreybrodt (1990) and others, that cave passages can play the role of local base levels for tributary conduits, in the same way that major rivers do for large cave systems. It is thus possible that a

tributary can evolve paragenetically towards a vadose trunk passage. This is supported by the observation of paragenetic passages within otherwise predominantly vadose caves, such as in Gruta do Padre, Brazil, Ogof Draenen, Wales, among others.

5.7.5. The onset of vadose conditions and post paragenetic modification

The final stage of phreatic development (either during phreatic tube enlargement or paragenesis) is marked by the lowering of the water table below the top of the passage. The upper portion of the conduit will become air-filled, and dissolution will proceed mostly on the floor under vadose conditions. Because phreatic passages often loop below the water table, the upper portions of such loops will become vadose first. In the case of a phreatic tube, there will be either vadose entrenchment on the upward apex of the loop, or the creation of a bypass tube above the downward apex (Ford and Ewers, 1978). In a non-paragenetic phreatic tube, the establishment of vadose conditions will cause floor dissolution and a vadose canyon will develop (there could also be a complete abandonment of the phreatic tube in favour of a lower route, in which case the phreatic tube would be preserved unmodified).

In the case of a paragenetic passage, the ceiling in the sectors still in the phreatic zone will continue to be enlarged paragenetically until the entire ceiling becomes horizontal at the water table. In such ideal conditions, phreatic features in the ceiling, such as bell holes or phreatically enlarged joints should be absent. This stage will be probably marked by oscillations in the water table in which paragenetic ceiling expansion would occur at intervals, until the ceiling is too high to be reached by the highest discharges.

The onset of vadose processes in paragenetic passages can result in two types of situation. The vadose water flow may remain in the original paragenetic passage, with progressive water table lowering leading to erosion of the sediment, and the overprinting of vadose features onto a canyon originally developed during paragenesis. By analogy with the terminology proposed by Ford and Ewers (1978) for phreatic tubes, such process will be termed "paragenetic drawdown". The onset of a drawdown paragenetic passage follows the same principles as a drawdown vadose passage, the most common type of active vadose cave and should thus be very common.

The paragenetic passage may also be abandoned, with its original preserved paragenetic sediment preserved (Pasini, 1967). Later surface drainage could by chance invade the passage modifying its sediment deposits. These "invasion" streams (Malott, 1937) could reestablish paragenetic conditions, bring new sediment or reexcavate existing deposits. In both the invasion and drawdown types, once the full thickness of the deposits has been removed, floor incision will take place and a true vadose trench may develop in the lower section of a paragenetic canyon. In the Iraquara Karst, the present sediment removal stage at Lapa Doce and Torrinha is of invasion type, mostly associated with doline input and reoccupation of the swallet by ephemeral

streams. These invasion streams are causing vadose incision in an otherwise paragenetic passage as in site D5 at Lapa Doce (Fig. 5.6). Lapa do Diva, a cave in the Iraquara Karst that contains a slow moving stream appears to be a typical paragenetic cave now undergoing a drawdown phase. In the Lagoa Santa Karst, sediment removal appears to be associated with doline deepening and slope runoff, being in this case of later invasion type.

Selective occupation of former paragenetic passages will often occur, especially when low dip situations favour anastomotic systems. Surface input into the subsurface karst is often concentrated at point input, usually swallets or dolines. Subsequent reoccupation of more favourable passages could occur, while other passages could remain decoupled from the vadose underground drainage system. This is illustrated in several passages at Gruta da Torrinha such as site C in Fig. 5.7, where only one passage carries an ephemeral stream, while several side passages remain filled with sediment. This linearisation of drainage during the transition from anastomotic paragenetic stage to vadose conditions will represent a shift from distributary flow systems in the phreatic zone towards a fluvial pattern more closely related to the surface drainage system.

A vadose flow in a paragenetic passage may not easily entrench the sediment beds. This is because of the abundance of cohesive fine grained material in the paragenetic sediments such as silt and clay facies (e.g. facies C, Fig. 5.9 in Iraquara). It is possible that some of these streams may become perched above the sediment bed, until a head is created by base level lowering and incision can take place (White and White, 1968).

A characteristic feature of vadose cave evolution is the existence of levels of independent passages. These levels are created by a number of processes (see review in Palmer, 1987) such as rapid base level lowering, stratigraphical perching or control, variations in discharge, among others. Worthington (1991) has developed the concept of flow field below existing passages. According to this hypothesis, there is always a flow field developing at depths determined by equation 5.3 below an active conduit. This lower passage will evolve and carry the available drainage as the upper level becomes drained. The development of lower levels could occur in a paragenetic passage, but because of its vertical amplitude, the development of a new level within the range of its amplitude would rather tend to reoccupy the same passage. In theory it is also possible that a lower paragenetic passage immediately below an older one could migrate upwards until a connection is achieved. Distinct levels of paragenetic passages have been observed at the Lagoa Santa Karst, where doline deepening have bisected more than one level. Overall, it appears that the creation of independent levels of cave development could be less favoured under paragenetic conditions.

One of the major difficulties in identifying paragenetic caves lies in the fact that later vadose modification will mask the original features. In a paragenetic passage occupied by an underfit stream, only partial sediment removal will occur, and the walls may still retain many of the

original paragenetic features. However, if the invasion stream is of large volume or occupies a relatively small paragenetic passage, vadose modification will occur over most of the passage section, and the final cave will resemble a typical vadose cave, the only section possibly retaining paragenetic features being the ceiling. Paragenetic caves are possibly much more common in nature than realised at present, but their identification may be very difficult where typical vadose processes predominate.

5.7.6. Secondary paragenetic processes

Secondary paragenesis is defined here as the processes occurring under sediment fill after the cave passage has become vadose. This may occur either during flooding due to impeded drainage under paragenetic conditions above the water table or due to episodic, localised or short lived palaeoclimate determined oscillations in the water table. These processes can create paragenetic features similar to the ones originated during a "primary" paragenetic stage. Secondary paragenesis can occur in a number of situations such as:

(1). Aggradation of base level. The water table may rise if aggradation of the surface river occurs, impeding the spring outlet and raising the base level. Flow velocities in cave passages will diminish and a ponding environment, suitable for sediment accumulation and paragenesis may occur. This situation was shown to occur in Clearwater Cave in Sarawak (Farrant, 1995).

(2). Episodic flooding in seasonal climates. Several karst areas, such as those of eastern Brazil, have a strongly seasonal climate regime, in which runoff is concentrated in a few low frequency high magnitude precipitation events. Many caves in such type of climate carry underfit streams, or streams that meander between sediment banks. During severe rainfall, the entire section of the passage is flooded. The dissolution potential of such "flash floods" which may comprise highly undersaturate quick flow waters is concentrated on the ceiling, as the floor is armoured by impermeable sediment. Such a situation is extremely frequent in the karst of eastern Brazil, where the large diameter of the gravel in the cave sediment shows transport by such flood events. This effect has been quantified by Meiman and Groves (1997) who demonstrated that 70% of the dissolution in a passage in Mammoth Cave, U.S.A., occurred during the 7% of time when the passage was filled to the ceiling. This is a type of paragenesis that can evolve by very fast moving water. The upper limit of such type of episodic paragenesis will be determined by the maximum hydraulic head of a series of flood events.

(3). Later invasion runoff. This situation, already discussed in section 5.7.5, comprises a later stream that removes and reemplaces sediments into a vadose or paragenetic drained passage. Such episodes of sediment input can originate paragenetic features in otherwise vadose caves, or can superimpose paragenetic features into "primary" paragenetic forms.

CHAPTER 6
PALAEOCLIMATE IN EASTERN BRAZIL

6.1. INTRODUCTION

In the past few decades, the realisation that the Earth has gone through a series of long and short term climatic changes has revolutionised our understanding of the planet dynamic atmospheric system. This alternation between glacial (or colder) periods and warmer intervals has had dramatic effects on geomorphic and biological processes. With the recognition that climatic changes are cyclic, there came an urgent need to better understand the processes and driving mechanisms behind these changes in order to enable prediction of the response of the Earth system to increasing human intervention.

The imprint of past climatic regimes is recognisable in many oceanic and continental records. Palaeoclimate records of global significance are traditionally derived from two main sources: ice cores (e.g. Jouzel et al., 1993) and ocean sediment cores (e.g. Shackleton and Opdyke, 1973). These records have the potential to span most of the Quaternary, although each one has its own specific limitations. Continental records (excluding glaciers) are available in several settings, but they are typically temporally non-continuous, although there are some notable exceptions such as the calcite record in Devils Hole (Winograd et al, 1992). Due to the proximity to major research centres, and to the existence of a larger scientific community, palaeoclimate research is strongly concentrated in the Northern Hemisphere, particularly in the higher latitudes. The density of palaeoclimate records is very low in South America (see review in Clapperton, 1993a), and especially poor in lowland areas, since the Andes has been the focus of most research. This is a very unsatisfactory situation, considering that the South American lowlands comprise the largest portion of the continent, and hold the highest biodiversity of world's ecosystem. Thus, there is an urgent need for gathering reliable palaeoclimate data from the tropical lowland areas of South America.

6.1.1. Global records

Ocean cores from several basins around the world have provided a chronology for climatic changes on a global scale. The SPECMAP marine record is a composite of several ocean core records of $\delta^{18}O$ in foraminifera (Imbrie et al., 1993) and has been used extensively. Unfortunately, these deep sea sediment records cannot normally be dated beyond the range of radiocarbon dating (c. 45 ka), and so the ages for the SPECMAP record are generated by "orbital tuning", i.e., matching the changes in $\delta^{18}O$ to variations in Earth's precession and obliquity (Imbrie et al., 1993). The only precisely dated points in the SPECMAP chronology are at 127 ka (from uranium series dating of high sea stand using corals), and the Brunhes/Matuyama palaeomagnetic reversal at 778 ka (Grootes, 1993). Nevertheless, the SPECMAP record provides striking support for the Milankovitch hypothesis, that the Earth's glacial-interglacial

cycles are driven by changes in solar insolation caused by orbital variations.

The cyclicity of climatic variations is also evident in ice cores, drilled initially in the high latitudes of the northern hemisphere (eg. GRIP members, 1993). Chronological control over longer timescales (0-100 ka) in these cores is usually provided by ice-sheet flow models, with the assumption that the sequential layering of the ice has not been disrupted (Dansgaard et al., 1993). The major isotopic shifts in the ice cores agree well with the orbital theory.

The Greenland record (Dansgaard et al., 1993) also showed that the Earth experienced a series of short and abrupt climatic changes during the last glacial period, known as Dansgaard-Oeschger cycles. These averaged a few thousand years in duration, and were characterised by abrupt jumps in temperature (Dansgaard et al., 1993, Broecker, 1994). The last of these cycles, named the Younger Dryas occurred immediately before the start of the Holocene. The Dansgaard-Oeschger cycles have been found to correlate with massive iceberg discharge events in the North Atlantic (Bond et al., 1993) known as Heinrich events. The fresh water produced during the melting of the huge iceberg armadas may have disrupted the production of North Atlantic Deep Water, shutting down the "conveyor belt" of oceanic circulation that carries heat to the North Atlantic (Broecker, 1994) and triggering more extensive climatic changes. Furthermore, the Greenland data has indicated that the last interglacial was also characterised by a series of severe cold periods that started abruptly and lasted from decades to centuries (GRIP members, 1993), while another Greenland record has shown abrupt switches of even shorter duration between 42 - 10 ka ago in the scale of 3 - 20 yr, when the climate changed from glacial to near interglacial conditions (Taylor et al., 1993).

The ice core records have demonstrated that a series of climatic shifts of varying intensity and duration have occurred since the penultimate glaciation. Although there is growing evidence that some of these events might have a global signature, the spatial extent of these shifts is still largely unknown, as the palaeoclimate database and record resolution in other parts of the world is still poor. The synchronicity of these shorter climatic cycles in lower latitudes continental areas is still subject to question.

6.1.2. Continental records - The Devils Hole calcite record and the United States "pluvial" lakes

Continental records have the potential to provide information on the regional expression of changes in global climate in the past (Grootes, 1993). However, due to erosion and to changes in environmental conditions, they tend to be fragmentary, although very good time resolution can be obtained in some of them, such as the Devils Hole record (Winograd et al., 1988, 1992).

The Devils Hole record was obtained from a well dated subaqueous speleothem from a submerged cave in southwestern U.S (Winograd et al., 1988). The record spans several glacial-interglacial cycles up to 500 ka in age, the limit of the mass spectrometric U-series dating

technique applied. Although the record agrees in general terms with the ocean and ice core records, there are some important differences regarding, the timing of the onset of the last interglacial, the 20 ka duration of the interglacials, increasing duration of the 100 ka cycle as one comes forward in time, and the occurrence of a well developed glacial cycle at 350-450 ka (Winograd et al., 1992). These disagreements led Winograd et al. (1992) to conclude that the Devils Hole record is inconsistent with the Milankovitch theory, but it is consistent with the concept that the glacial/interglacial cycles originated from internal non-linear feedbacks within the atmosphere-ice sheet-ocean system. Initially criticism was raised concerning the accuracy of the dating method (Edwards and Gallup, 1993, Shackleton, 1993) and the validity of the palaeoclimate interpretation (Johnson and Wright, 1989; Emiliani, 1993, Grootes, 1993, Imbrie et al., 1993, Crowley, 1994). However, the chronology of the Devils Hole record is now generally accepted to be accurate since it has also been dated by a second technique (Edwards et al., 1997), but the implications of the record are still subject to debate. Winograd et al. (1997) suggest that until all other records (SPECMAP, ice cores, high sea stands) are radiometrically dated with comparable precision, the exact duration of the last interglaciation, and the leads and lags present between the respective records will not be resolved.

Several lakes in non-glacial environments experienced increase in volume during glacial times. These lakes were termed "pluvial lakes" and were thought to be due to increased runoff in glacial times. In southwestern United States lakes reached their highest level at the Last Glacial Maximum (LGM) while at the same time there was widespread aridity in eastern United States (Dawson, 1992), and lakes at the United States northwest were low (COHMAP, 1988). Such spatial variability illustrates the complex pattern of responses to a given ocean glacial signal.

Continental records demonstrate the important role of regional climate patterns caused by displacement of currents, orographic effects, and other factors. Well-dated continental records are, thus, invaluable in giving regional detail to the general pattern of climatic change, and provide the necessary field data to test simulations of past climates generated using General Circulation Models.

6.1.3. The Southern Hemisphere perspective

The global significance of Northern Hemisphere climatic shifts was not confirmed until reliable ice core records became available for Antarctica. The Vostok ice core showed many of the general features present in the SPECMAP record (Jouzel et al., 1993), and also matched some of the features of the Devils Hole record such as the extended duration of the last interglacial (Winograd et al., 1997). More importantly, the Vostok record clearly confirms evidence of Milankovitch forcing, giving global signature to these events. It appears that interglacial events occurred in east Antarctica whenever those in Greenland lasted longer than 2 ka (Bender et al., 1994).

Research in the Andes and New Zealand have demonstrated that glacier advances were coeval with ice-rafting pulses in the North Atlantic, implying a global atmospheric signal rather than regional forcing mechanisms, and suggesting rapid propagation through the atmosphere of late Pleistocene climatic signals (Lowell et al., 1995). In particular, the Younger Dryas event has been identified in tropical areas away from the North Atlantic (Hughen et al., 1996), but its general presence in South American records, claimed by some to give it a global significance (Clapperton, 1993b, Kuhry et al., 1993) has received some criticism (Markgraf, 1989, 1993a). Overall, there seems to be agreement that the Southern Hemisphere climatic changes are in general coeval with the ones in the Northern Hemisphere although the magnitude of the changes appears to have been much smaller (Clapperton, 1993b).

6.2. PALAEOCLIMATE IN THE TROPICS

In comparison to temperate and high latitude areas of the globe, little is known on the behaviour of the continental tropical regions during the glacial stages (Beck et al., 1997) because of the paucity of palaeoclimate records.

In the late 1970's the CLIMAP (Climate: Long-Range Investigation, Mapping and Prediction) project generated an ambitious map of ice age Earth Sea Surface Temperatures (SST). CLIMAP (1976) concluded that oceans in the tropics and subtropics during the Last Glacial Maximum had SST as warm as, or slightly warmer than today. CLIMAP's data were used extensively in several GCM simulations, and the concept of tropical areas being unaffected by decreased temperature during ice ages permeated the literature.

SST are very important in climate dynamics because of their relationship with heat transfer in the atmosphere. Even small SST changes (0.5-1.0° C) can have large effects on the patterns of rainfall, storm tracks and intensities, and the overall atmospheric circulation pattern (Beck et al., 1997, Rind, 1990). Thus, SST in the tropics are an essential boundary condition for models attempting to simulate the behaviour of the Earth's climate during the glacial stages (Thompson et al., 1995). CLIMAP's prediction of no tropical cooling also led people to believe that the tropics might be spared any future warming caused by rising carbon dioxide levels, a concept with wide ranging consequences. However, GCM used by different groups in estimating the degree of global warming to be expected from increased levels of atmosphere CO_2 give results for the tropics that differ by a factor of 2 (Rind, 1990).

In the 1990's, detailed records obtained from tropical areas started to raise questions on the reliability of CLIMAP conclusions. Using two independent methods (Sr/Ca and oxygen isotope thermometry), Guilderson et al. (1994) estimated from studies in corals in Barbados that SST were 5° C colder than at present at 19 ka. Furthermore, the Barbados data showed that Western Tropical Atlantic is quite sensitive to climate change during deglaciation, as demonstrated by a 4° C shift between 13.7 - 12 ka (Guilderson et al., 1994). Beck et al. (1997), using Sr/Ca ratios

corals from Vanuatu (southwest Pacific Ocean) found that SST was depressed by as much as 6.5° C below modern levels at 10.35 ka..

The tropical and subtropical Atlantic Ocean exerts a major control on the temperature and humidity of airstreams affecting most of South America (Clapperton, 1993a). Because of this, any cooling of the Atlantic tropical SST during the LGM should have an impact also on continental climates. In fact, a cooling of 8 - 12° C was inferred from ice cores at Huascaran, in the Andes Mountains, translating to about 5 - 6° C cooling in the ocean (Thompson et al., 1995). In lowland northeast Brazil, noble gases in ground water indicate a 5.4° C cooling at the LGM (Stute et al., 1995).

These records suggest that the tropics were affected by climate changes during the glacial stages. If correct, views of ocean circulation during the ice ages may also need revision (Kerr, 1995). There is evidence that the key mechanism for carrying heat from the tropics to the far northern latitudes, the so-called "conveyor-belt" of currents, was not working strongly in glacial times (Kerr, 1995). The slowing of the conveyor seemed a plausible explanation for the warm tropics suggested by CLIMAP, but if the tropics cooled despite the failure of the conveyor belt, then another heat drain would need to be operating (Kerr, 1995).

Despite the increasing strength of data that seems to contradict the CLIMAP SST, the riddle is far from resolved because some oceanic data remain consistent with CLIMAP (Broecker, 1986), while others continue to reafirm the original conclusions (Thunnel et al., 1994). Broecker (1996) has also suggested that although most records indeed indicate a lowering of tropical temperatures, they tend not to agree with each other. In particular, while Sr/Ca in corals and noble gases suggest cooling in the range 4 - 6° C, foraminifera speciation, alkenone, and oxygen isotope data suggest a cooling of no more than 3° C (Broecker, 1996). More recent modelling results also suggest that the CLIMAP tropical SST may be only 1 - 2° C too warm (Pollard and Thompson, 1997), and ocean cores off the coast of northeastern Brazil indicate a cooling in the range of 2 - 3° C, a value intermediate between the CLIMAP predictions and SST estimates from corals and noble gases (Wolff et al., 1998).

The difference in tropical climate response is also illustrated by the recent results of Harris and Mix (1999) from an ocean core off the Amazon delta, which suggest that late Pleistocene climate extremes in Amazonia *preceded* Northern Hemisphere ice extremes. They suggest that tropical climate changes may affect, rather than respond to, global ice-age climate cycles.

6.2.1. Tropical ice ages, wet or dry?

While overall cooling of the globe occurred during ice ages, the regional response in terms of precipitation seems to be rather complex. In tropical areas, where the cooling was not strong enough to produce ice sheets, the change in precipitation is likely to be the principal factor in

causing geomorphic and vegetational responses. As discussed above, pluvial lakes in America, and in several other parts of the world, including the Andes, showed a complex response to the ice ages, with both an increase and decrease in lake levels during the last glacial cycle depending on the region.

Early workers suggested that there was a global increase in precipitation of 25% during ice ages (Charlesworth, 1957). This concept of a pluvial glacial period apparently originated from a mistaken notion that a general increase in the extent of glaciers demanded a general increase in precipitation (Flint, 1957). Field evidence has however now largely disproved the concept of a pluvial ice age. Sand dunes were much more widespread at the LGM than they are today, comprising almost 50% of the land area between 30° N and 30° S (Sarnthein, 1978). Further evidence from lakes, aeolian activity, sea cores and pollen studies in several continents have reinforced the view that there was widespread aridity in both hemispheres during the late Pleistocene (Williams, 1975, Rind and Peteet, 1985). This increased aridity during glacial phases is explained by an increase in "continentality"; with lowered sea levels, and cooler temperatures, oceanic evaporation would decrease, reducing the supply of water vapour to the continents. Despite generalised aridity, regional differences in precipitation patterns remain the rule rather than the exception. In the Edwards Plateau, Texas, humidity was at its highest ever during the LGM (Toomey et al., 1993). Lake levels in Africa experienced dissimilar behaviour during the LGM, some were higher than at present while others were lower (Williams et al., 1993).

About 25% of tropical South America is estimated to have became a sand desert during the LGM (Clapperton, 1993a). However, in the South American Andean lakes, there is evidence of increased moisture at some sites during the last ice age (Clapperton, 1993a). In the lowlands of Brazil, pollen evidence generally agrees that the LGM was characteristically dry (section 6.3.3.3).

This spatial heterogeneity of climate is probably caused by the influence of smaller topographic features on the large-scale atmospheric circulation patterns (Mock and Bartlein, 1995). Such site-to-site differences complicate the general picture of climate change, but are extremely important in providing data that enable testing of the improved high resolution predictions now available from GCM simulations (section 6.8.1).

6.3. PALAEOCLIMATE IN EASTERN BRAZIL

A general review of the palaeoclimate in Brazil will be performed, including sites located away from eastern Brazil, such as in Amazonia. This is justified due to the scarcity of reliable records, and serve to illustrate the regional variations in responses to any given palaeoclimate signal, as well the controversies regarding some areas. For the purpose of this review, Brazil will be divided in two broad zones: the Amazon Basin and the savanna areas which will be dealt with separately

6.3.1. Types and limitations of available palaeoclimate records

Despite the vastness of the Brazilian lowlands, only 24 palaeoclimate records (Fig. 6.1) were considered reliable enough to be included in this review (up to 1998). In addition to these true continental records, I have also considered marine records involving accumulation of continental material (minerals, pollen, etc) offshore. Sea level stands, coral evidence, stratigraphy of river deltas, and deep-sea cores were not included.

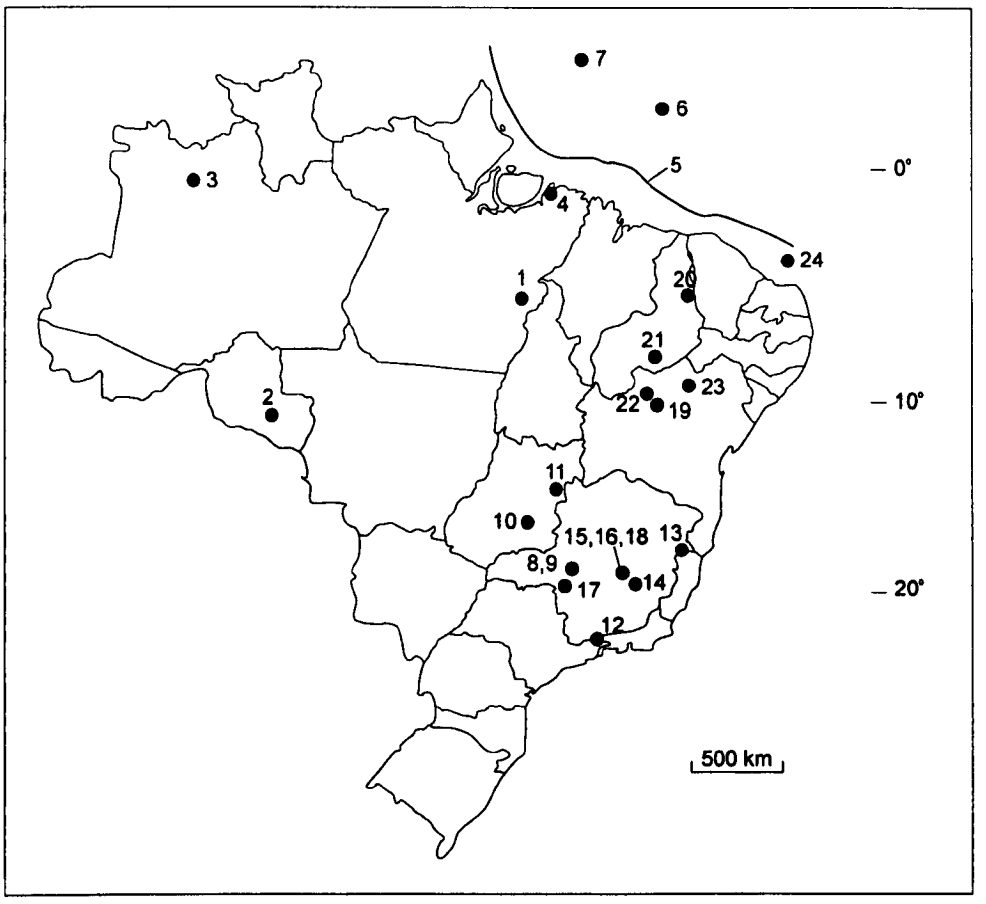

Figure 6.1. Location of palaeoclimate records discussed in the thesis. 1 - Carajás; 2 - Katira; 3 - Pata; 4 - Curuça; 5 - Ocean Core; 6 - Ocean Core at Ceará Rise; 7 - Ocean Core at ODP Site 932; 8 - Salitre; 9 - Serra Negra; 10 - Cromínia; 11 - Águas Emendadas; 12 - Itapeva; 13 - Lago do Pires; 14 - Catas Altas; 15 - Lagoa dos Olhos; 16 - Lagoa Santa; 17 - Tamanduá; 18 - Baú; 19 - Irecê; 20 - Piauí; 21 - São Raimundo Nonato; 22 - Saquinho; 23 - Toca da Boa Vista; 24 - Ocean Core GeoB 3104-1. Record 5 is a composite of several cores along the northern Brazilian coast.

The records fall into two broad groups: Pollen and faunal evidence; and geomorphological evidence. Pollen studies comprise the vast majority of the records. Pollen records from lakes, bogs and swamps (15 records) provide semi quantitative palaeoclimatic information and are based on community shifts as a response to changes in bioclimatic parameters such as elevational temperature gradients or latitudinal precipitation gradients that can directly control vegetation zonation (Markgraf, 1993b). Palaeoclimate information determined from palynological data may be ambiguous and subject to differences in interpretation between different workers, e.g. when only percentage diagrams are used instead of concentration (or influx) pollen

diagrams (Salgado-Labouriau, 1997). Chronological control is provided by dating of organic layers by radiocarbon, and the ages are extrapolated or interpolated for the interval between the dates, assuming constant sedimentation rates (Salgado-Labouriau, 1997). The pitfalls of this procedure have been illustrated by Ledru et al. (1998), changes in sedimentation rates can occur, and a hiatus may pass unnoticed. Furthermore, the radiocarbon technique has its own limitations, including a lower precision near the limit of the method (about 45 ka) and the possibility of contamination by modern carbon.

Pollen has also been studied in marine deposits associated with river mouths (Haberle and Maslin, 1999), dated by palaeomagnetism and AMS radiocarbon. Such deposits are assumed to represent the average pollen runoff from the whole drainage basin. However, questions about the representativeness of these records have been raised because they could reflect reworking of older deposits trapped in terraces or in the oceanic shelf during sea level lowering, or be biased towards riparian forest, underrepresenting savanna areas away from river margins.

Faunal remains comprise fossil deposits of living and extinct species that can provide palaeoenvironmental information. The chronology of the vast majority of these deposits remains uncertain. A few dates, based on radiocarbon (Czaplewski and Cartelle, 1998) and $^{230}Th/^{234}U$ (Piló, 1998) are now available, and further data is presented in this study. A few records of uncertain reliability (Lumley et al., 1987) where $^{230}Th/^{234}U$ ages have been obtained in bone and nuclide migration may have occurred, will not be included in this review.

Geomorphological evidence comprises studies of depositional systems such as sand dunes, river terraces, colluvial deposits, soil horizons and cave sediments. The vast majority of these records also lack chronological control and so their temporal significance is subject to major uncertainty. Only dated evidence will be discussed in this review. Radiocarbon has been used to date river deposits (Turcq et al., 1997) from which past hydrodynamic conditions were inferred. Such study relied in assumptions about the linkage between sediment yield and climate/vegetation changes, which are often complex (see Chapter 7). Radiocarbon dating was also applied to calcite concretions under soil profiles which may represent periods of more humid climate (Dever et al., 1987). Cave sedimentation events have been dated using $^{230}Th/^{234}U$ dating (Piló, 1998). Offshore Brazil, ocean cores have been used to determine variations in the flux of terrigenous material, and have been dated by orbital tuning (Harris and Mix, 1999), radiocarbon (Tintelnot, 1997, Arz et al., 1998) and by foraminifera zonation and accumulation rates (Damuth and Fairbridge, 1970). The same provenance uncertainties described for pollen records in ocean cores apply in these studies.

With one exception, absolute palaeotemperature records are not available in the study area. The exception is a study of noble gases in ground water by Stute et al. (1995), based on the temperature dependent solubility of these gases at the water table. In this study, ages were assigned by radiocarbon dating of the ground water.

The temporal range of the records is largely limited by the heavy dependence on ^{14}C (< 45 ka) dating method. Most records are thought to cover only the last glacial cycle (from 130 ka), the only exception being a study of cave deposits using $^{230}Th/^{234}U$ method. Palaeoclimate data from isotope stage 6 onwards are largely unavailable. Radiocarbon ages reported in the following sections have been calibrated in order to enable a direct comparison with U-series ages (see calibration procedures in section 2.1.3)

6.3.2. Amazon lowlands and the refugia debate

Palaeoclimate in the Amazon lowlands has remained a key issue in biodiversity studies during the last three decades. The Amazon rainforest is the largest continuous forested area in the planet, and holds the greatest biodiversity of any ecosystem in the world. In the late sixties, Haffer (1969) proposed that the forest had been fragmented several times during the Quaternary. He argued that the Amazonian climate during glacial stages was semi-arid, causing the forest to break into isolated forest "islands", surrounded by savannas. These ecological "refuges" would allow evolutionary species divergence, until the next pluvial interglacial phase caused the rainforest to reoccupy the savannas in between. The postulated refugia areas were mapped through topographical and biological criteria (Haffer, 1969, Brown and Ab'Saber, 1979), but the number of areas, and their boundaries remain obscure and are constantly being redefined.

The refugia theory has received both support and criticism from biological and geological evidence and remains a heated and unresolved debate to the present day. Endler (1982) has argued that there is no need to evoke forest fragmentation as sufficient habitat diversity and natural barriers such as major rivers and soil types exist to separate populations which exhibit modern ecological variance. Considerable geomorphological data has been presented to support the idea of a semi-arid Amazonia during glacial phases. Ab'Saber (1982) and Tricart (1985) have interpreted the occurrence of stone lines, the presence of white sands in river divides, the modes of slope dissection and geomorphic features such as inselbergs and duricrusts as evidence of drier climates. All this evidence, however, lacks chronological control, and its interpretation has been questioned (Bush, 1994). Furthermore, Colinvaux (1987) has pointed out that the data on which these reports are based are not readily accessible, so that possible alternative explanations cannot be assessed.

Chronologically constrained records are scarce, and are presented in Fig. 6.2. The Mera site, due to its highly controversial chronology (Heine, 1994, Colinvaux et al., 1996b), will not be reviewed. The evidence from radiocarbon dated pollen records is equivocal. The Carajás site has been interpreted as showing evidence for a dry climate with fragmentation of the rainforest at about 60 ka, 44 ka, and between 28 - 12 ka (Absy et al., 1991, van der Hammen and Absy, 1994), although the older radiocarbon date lies beyond the normal limit of the method and is thus subject to considerable uncertainty. The Carajás lakes are located on a plateau covered by

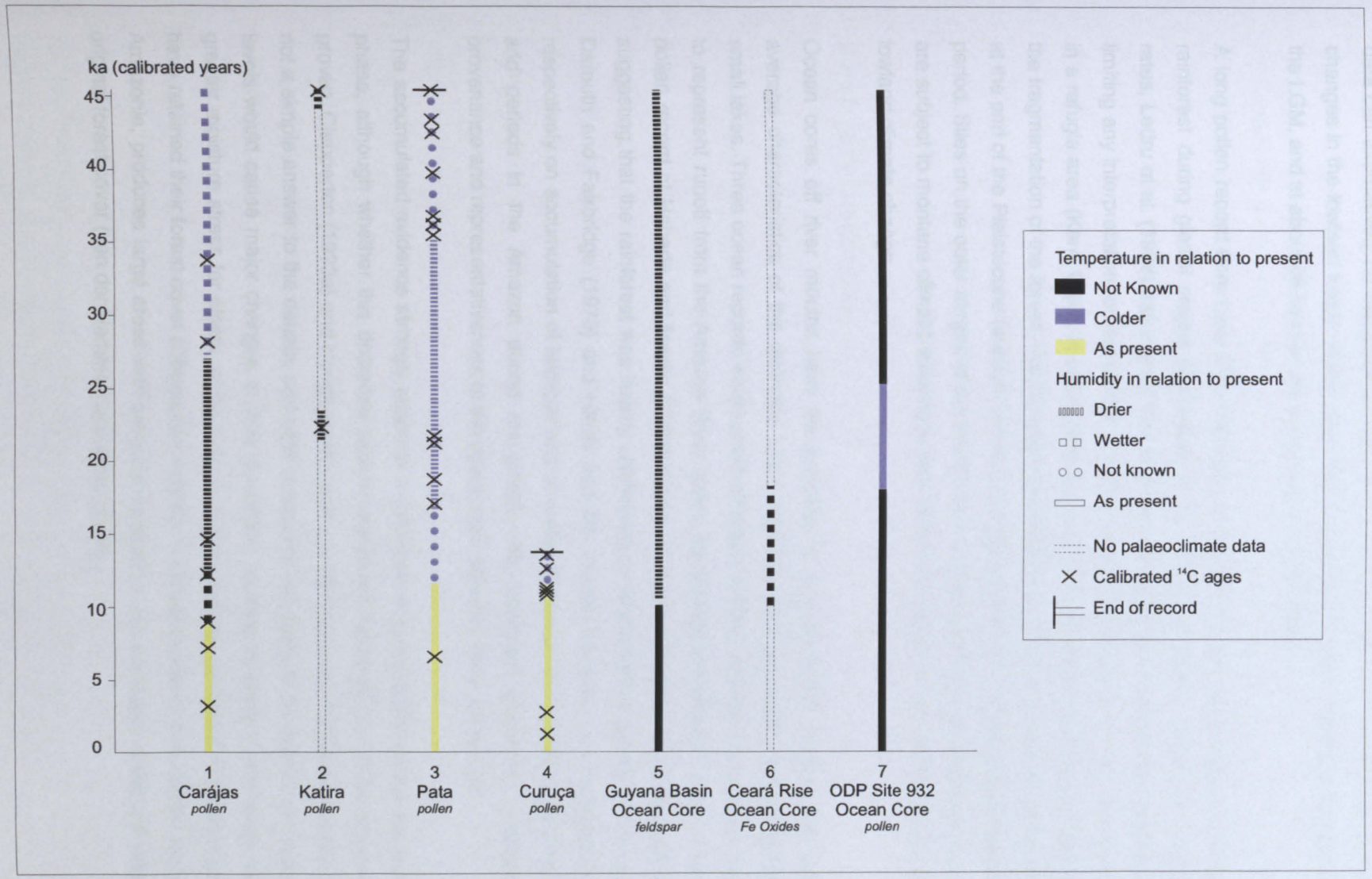

Figure 6.2. Summary of palaeoclimate records for Amazonia. 1 - Absy et al. (1991), Salgado-Labouriau (1997). 2 - Van der Hammen and Absy (1994). 3 - Colinvaux et al. (1996). 4 - Behling (1998). 5 - Damuth and Fairbridge (1970). 6 - Harris and Mix (1999). 7 - Haberle and Marlin (1999). Location of records is shown in Figure 6.1.

savannas, and rainforest occurs in the lowlands surrounding the plateau, tens of kilometres from the cored site (Colinvaux et al., 1996b). Colinvaux et al. (1996b) has stressed that the pollen data can alternatively be explained as reflecting increased aridity on the plateau without major changes in the lowland forest. Pollen data from Katira also suggests savanna vegetation during the LGM, and at about 46 ka (van der Hammen and Absy, 1994).

A long pollen record from Lake Pata has been presented as providing evidence of continuous rainforest during glacial stages (Colinvaux et al., 1996a). However, based on sedimentation rates, Ledru et al. (1998) has argued that a hitherto unrecognised hiatus may exist at the LGM, limiting any interpretation for this period. A further complicating factor is that Lake Pata may be in a refugia area (Kerr, 1996), in which case its record would not add substantial information on the fragmentation of the forest. The Curuça record (Behling, 1998) suggests rainforest is present at the end of the Pleistocene (around 13.4 ka), but the record does not extend into the full glacial period. Sites on the outer fringes of the Andes such as Caquetá (van der Hammen et al., 1992) are subject to montane climatic influences and cannot contribute to this debate on the nature of lowland climate change.

Ocean cores off river mouths have the potential to provide longer records that reflect the average characteristics of the drainage basin, avoiding local signatures typical of records of small lakes. Three ocean records which utilise different climatic indicators have been considered to represent runoff from the Amazon River basin, but agreement between them is poor. The pollen record of Haberle and Maslin (1999) shows no major change in the pollen composition, suggesting that the rainforest was largely unaffected by interglacial to glacial climate changes. Damuth and Fairbridge (1970) and Harris and Mix (1999) however, have suggested, based respectively on accumulation of feldspar and of oxides in terrigenous sediment, that there were arid periods in the Amazon during ice growth. As discussed previously, criticism about provenance and representativeness of the ocean core data has been expressed.

The accumulated evidence strongly supports a decrease in precipitation during the last glacial phase, although whether this decrease caused significant rainforest reduction remains to be proven. Clapperton (1993a) and Hooghiemstra and van der Hammen (1998) believe that there is not a simple answer to the debate, and both viewpoints are likely to be correct. Decreased sea levels would cause major changes in river dynamics, causing lowering of the water table and greater moisture stress for plants, while areas in which humidity remained relatively high would have retained their forest cover (Clapperton, 1993a). A simple model of 40% rainfall reduction in Amazonia, produces large areas with savanna vegetation, but extensive areas still retain their original forest cover (van der Hammen and Absy, 1984).

6.3.3. Palaeoclimate in the lowland savannas of Brazil

Considering that the savannas comprise the largest surface area in tropical South America, there are surprisingly very few radiometrically-constrained palaeoclimate records. Only 11 records of variable quality and resolution have the necessary chronological control to be included in this review (Fig. 6.3). A further 6 records comes from the semi-arid northeast Brazil, and will be treated separately.

6.3.3.1. Marine Isotope Stage 4 and older (> 60 ka)

The only continental record from the penultimate glacial cycle is a $^{230}Th/^{234}U$ dated cave calcite layer from the Lagoa Santa area which suggests a wetter period around 135 ka (Piló, 1998). There are no dated samples from the last interglacial period but a further three U-series dates from the same area yield ages of 80 and 60 ka suggesting wet conditions at the isotope stages 4 and 3 boundary (Piló, 1998).

6.3.3.2. Marine Isotope Stage 3 (60 - 24 ka)

This interval is within the upper limits of the radiocarbon method, and some pollen records are available. At Catas Altas, Behling and Lichte (1997) have inferred a dry and cold climate between > 48 ka and 21.5 ka. Itapeva was also dry and cold during most of this period (Behling, 1997). At Salitre, the climate between 37 - 33 ka was probably wetter than at present (Ledru, 1993), and in nearby Serra Negra it was continuously colder and more humid than at present between > 40 - 12.2 ka (De Oliveira, 1992), although the possibility of a gap between 36.5 - 16.5 ka in this later record cannot be discounted (Behling, 1997, Ledru et al., 1998). In Cromínia, Ferraz-Vicentini and Salgado-Labouriau (1996) and Salgado-Labouriau (1997) have suggested that the period immediately before 37 ka was similar to today's climate, but it became wetter and colder between 32.4 - 22.1 ka. Colder and wetter conditions were also inferred for Aguas Emendadas between approximately 30 - 26 ka (Salgado-Labouriau et al., 1998). The river terrace record from Tamanduá also indicates a wetter climate between 38 - 23.4 ka (Turcq et al., 1997). Overall, with the exception of the Itapeva and Catas Altas records, the data indicates that there was increased moisture in the savanna areas of Brazil during significant parts of the Isotope Stage 3.

6.3.3.3. The last glacial maximum (24 - 18 ka)

Records from the LGM have an added importance, because this was the time period when the climatic conditions departed the furthest from the present conditions. Most records, such as Itapeva (Behling, 1997), Catas Altas (Behling and Lichte, 1997) and Aguas Emendadas (Salgado-Labouriau et al., 1998) point towards colder and drier conditions during this period, although the duration and timing of these conditions vary between records (see Fig. 6.3). On the

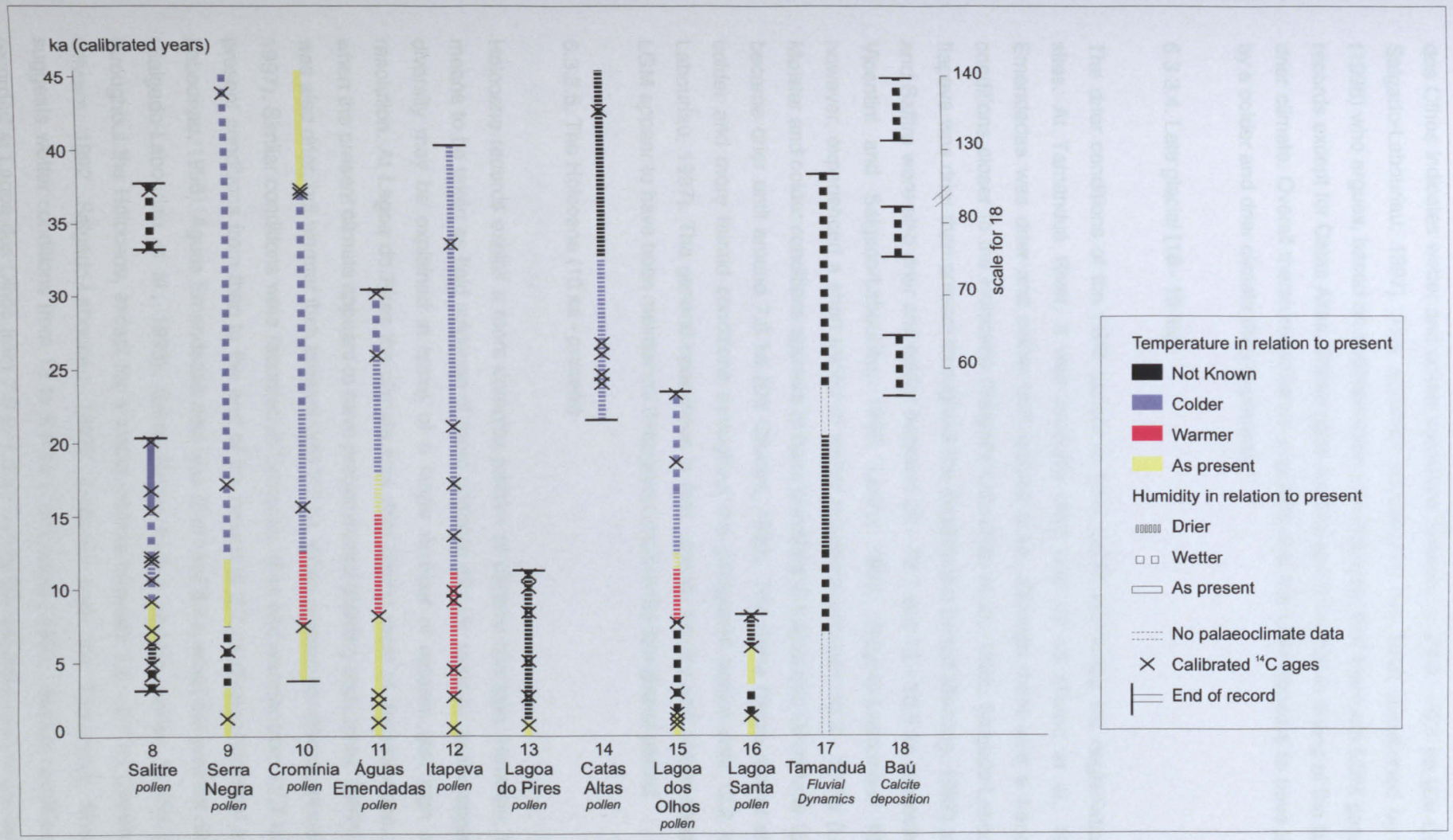

Figure 6.3. Summary of palaeoclimate records of lowland savanna areas of Brazil. 8 - Salgado-Labouriau (1997). 9 - Salgado-Labouriau (1997), Behling (1997), De Oliveira (1992). 10 - Ferraz-Vicentini and Salgado-Labouriau (1996), Salgado-Labouriau (1997). 11 - Salgado-Labouriau et al. (1998), Salgado-Labouriau (1997). 12 - Behling (1997). 13 - Behling and Lichte (1997). 14 - Behling and Lichte (1997). 15 - Salgado-Labouriau (1997), De Oliveira (1992). 16 - Salgado-Labouriau (1997), Parizzi et al. (1998). 17 - Turcq et al. (1997). 18 - Piló (1998). Location of records is shown in Figure 6.1.

other hand, in addition to the record from Serra Negra already mentioned, the record from Lagoa dos Olhos indicates wetter and colder conditions between c. 23.5 - 16.1 ka (De Oliveira, 1992, Salgado-Labouriau, 1997). This apparent discrepancy has been questioned by Ledru et al. (1998) who argues, based on sedimentation rate changes, that there are LGM gaps in all these records except for Catas Altas. These gaps are thought to be due to drying of the lakes due to a drier climate. Overall therefore evidence suggests that the LGM appears to have been marked by a colder and drier climate than at present.

6.3.3.4. Late glacial (18 - 10 ka)

The drier conditions of the LGM appear to have continued during the deglaciation at several sites. At Tamanduá River, it was probably drier until 12 ka (Turcq et al., 1997). Aguas Emendadas was drier and colder until around 8 ka, although there was a trend to warmer conditions closer to the Holocene (Salgado-Labouriau et al., 1998, Salgado-Labouriau, 1997). Itapeva was drier than present throughout the deglaciation period (Behling, 1997) and Cromínia and Salitre were also drier and colder between 22 - 12.7 and 12 - 10.5 ka respectively (Ferraz-Vicentini and Salgado-Labouriau, 1996, Ledru, 1993, Salgado-Labouriau, 1997). Salitre however, experienced a short period of wetter conditons between 15.3 - 12 ka (Ledru, 1993). Moister and colder conditions appears to have prevailed at Lagoa dos Olhos until 16.2 ka, which became drier until around 7.6 ka (De Oliveira, 1992). The Serra Negra record also suggests colder and more humid conditions throughout the postglacial period until 12.2 ka (Salgado-Labouriau, 1997). The general consensus is that, overall, the dry and colder conditions at the LGM appear to have been maintained throughout most of the late glacial period.

6.3.3.5. The Holocene (10 ka - present)

Holocene records exhibit a more complex pattern of climatic changes. However, this is by no means to be taken as field evidence of more unstable climatic regimes as the apparent climatic diversity may be explained in terms of a larger number of records with high chronological resolution. At Lagoa do Pires the climate was drier during most of the Holocene, until 0.8 ka, when the present climate appears to have predominated (Behling and Lichte, 1997). At Itapeva it was also drier, but warmer than present until 2.7 ka, when present conditions prevailed (Behling, 1997). Similar conditions were recorded at Cromínia, drier and warmer from 12.7 to 7.6 ka, with present conditions from then to the end of the record at 3.7 ka (Ferraz-Vicentini and Salgado-Labouriau, 1996). Aguas Emendadas also was drier until 8 ka, when the present climate started (Salgado-Labouriau et al., 1998). Serra Negra had a climate similar to the present one throughout the Holocene, except for a wetter interval between 7.3 - 3.7 ka (Behling, 1997, De Oliveira, 1992, Salgado-Labouriau, 1997). Evidence from the Tamanduá River, however, suggests wetter conditions from 12 to 6.8 ka (Turcq et al., 1997). Wetter conditions were also recorded at Lagoa dos Olhos from 7.6 to 1.3 ka before the establishment of present conditions (Salgado-Labouriau, 1997, De Oliveira, 1992).

The records of Salitre and Lagoa Santa show a more complex Holocene climatic pattern. At Salitre, there were wetter intervals between 10.5 - 9.1 ka and 4.8 - 3.2 ka (Ledru, 1993, Salgado-Labouriau, 1997). There is no record at Salitre after 3.2 ka. The Lagoa Santa record shows drier conditions between 8.2 and 6.4 ka, followed by an interval with climate similar to present (Parizzi, 1993, Parizzi et al., 1998, Salgado-Labouriau, 1997). From 3.3 to 1.3 ka the climate was wetter, before the start of modern climatic conditions (Parizzi, 1993, Salgado-Labouriau, 1997).

6.3.3.6. Regional comparisons

The records discussed above do not entirely agree with each other, and in some cases indicate very different climatic conditions for the same time interval. In such a vast area (see Fig. 6.1) there will clearly be regional climatic differences, caused by topographic features and elevation. Some records, such as Itapeva, Serra Negra and Catas Altas, are located in relatively mountainous areas. The elevation difference for records from the present savanna can range from 1,850 m (Itapeva), to 390 m at Lagoa do Pires. Such elevation and other effects which may give distinct regional patterns must be taken into account when comparing the data.

Some sites lie close together, and therefore, are potentially more suitable for direct comparison. The sites of Serra Negra and Salitre are only a few hundred metres apart, although Serra Negra is approximately 200 m higher. However, the repeated wet and dry cycles that characterise the Salitre record are not present in the Serra Negra record. Ledru et al. (1996) have argued that some of these differences can be explained by the altitudinal contrast, the moisture being higher at Serra Negra, and the existence of a sedimentation gap at Serra Negra during the LGM.

The sites of Lagoa dos Olhos, Lagoa Santa and Catas Altas are also located close together. Lagoa Santa is only a few hundred metres from Lagoa dos Olhos in a low and flat landscape, and Catas Altas is nestled in mountains about 70 km away. Unfortunately the Catas Altas record ends at about 21.5 ka, and a full comparison is not possible. However, at Lagoa dos Olhos, the record starts at about 23.3 ka indicating humid conditions, while the Catas Altas record points towards drier climate until 21.5 ka (Behling and Lichte, 1997, De Oliveira, 1992). The very distinct topographical setting between these sites can account for the difference. However, Lagoa Santa and Lagoa dos Olhos are so close together, that any mismatch between the records cannot be attributed to local climatic factors. The records agree with each other in general terms, but there are some differences. The Lagoa Santa record indicates a drier event between 8.2 - 6.4 ka while Lagoa dos Olhos record indicates continued wet conditions (Parizzi et al., 1998, Salgado-Labouriau, 1997, De Oliveira, 1992). These disagreements may derive from differences in interpretation of the pollen diagrams.

The chronology of some of the records has also been subject to criticism. Sylvestre et al. (1999) have pointed out that the glacial and early Holocene of the Aguas Emendadas record is

represented only by thin (< 10 cm) silty-sand layer interbedded between organic layers dated at 25.7 and 8.1 ka. Similar criticism have been made of the Cromínia record, in which organic layers were assigned a late glacial to Holocene time age span using a single radiocarbon age of 15.5 ka (Sylvestre et al., 1999). Such chronological approximations are also typical of other records. The difficulties in comparing records due to interpolation between ages have been commented by Salgado-Labouriau (1997), and the dangers of overlooking possible gaps were demonstrated by Ledru et al. (1998).

Differences may also arise from the types of evidence being used as palaeoclimatic proxies. The river terrace record of Turcq et al. (1997) takes into account assumptions on fluvial dynamics and sediment yield, and thus is unlikely to precisely reflect the climatic changes derived from pollen influx data.

In the light of the present knowledge of palaeoclimate in the lowland savannas of tropical Brazil, it is still not possible to make generalisations on climate patterns during the late Quaternary. Whether the distinct climatic events recorded in the records reflect true regional and/or local intersite variations or are merely due to interpretation will not be known until a much larger palaeoclimatic database is available. These records should not only be reliably dated, but preferably should be derived by more than one palaeoclimatic technique.

6.3.3.7. The semi-arid Brazilian northeast

The semi-arid zone of northeastern Brazil is distinct from the savanna areas not only because of its dryness, but also because of differences in vegetation and irregularity in precipitation. Arid and semi-arid climates do not favour pollen preservation, and the few records available are based on other palaeoclimate proxies (Fig. 6.4). Early overviews of Brazilian palaeoclimate (Ab'Saber, 1982) extended climatic trends inferred from the savanna areas into the northeast, without taking into consideration the distinct characteristics of this area. It now appears that the semi-arid Brazilian northeast may have responded in a distinctly different way to the Quaternary climatic shifts. Evidence of past wetter climatic regimes abound in the area, being not only of geomorphological nature (to be discussed in Chapter 7) but also derived from biological (Mares et al., 1985) and palaeontological (Cartelle, 1992) data, although there appears also to be evidence, so far undated, for even drier climates in the past (Tricart, 1985).

Arz et al. (1998) have inferred several cycles of increase runoff (and hence increased precipitation) in the area, based on titanium and iron pulses in offshore cores. These pulses correspond approximately to intervals at 68 - 60, 48 - 46, 40 - 38, 30 - 28, 24 - 22 and 20 - 16 ka (Arz et al., 1998). Dever et al. (1987) inferred a wetter period between 26 - 20 ka, based on the isotopic composition of carbonate concretions in soil. Palaeoenvironmental interpretation of a radiocarbon date on a fossil bat also indicates a wetter period around 24 ka (Czaplewsky and Cartelle, 1998). For the period 35 - 10 ka, Stute et al. (1995) inferred a colder period, with a

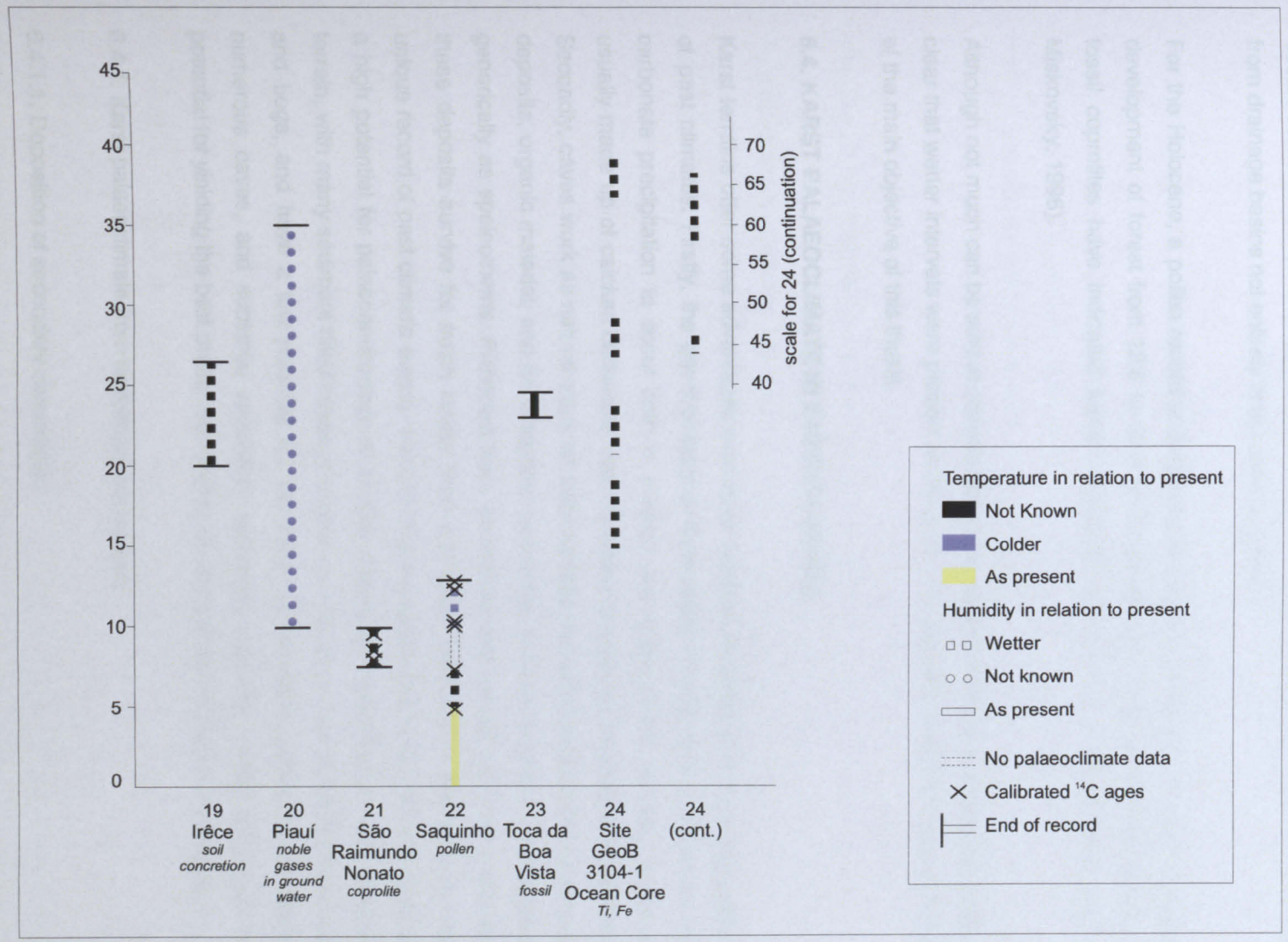

Figure 6.4. Summary of palaeoclimate records for northeastern Brazil. 19 - Dever and Fontes (1987). 20 - Stute et al. (1995). 21 - Chaves and Renault-Miskovsky (1996). 22 - Barreto (1996). 23 - Czaplewski and Cartelle (1998). 24 - Arz et al. (1998). Location of records is shown in Figure 6.1.

5.4°C lowering in temperature during the LGM, based on noble gases in ground water. Overall, there appears to be an agreement that there was increased precipitation in the semi-arid northeast at the LGM, although a much larger database is needed to support this view. Hemming et al. (1998) have also inferred increased rainfall in tropical Brazil from clay peaks in ocean cores drilled off the northeastern coast of Brazil, although there may be a contribution from drainage basins not entirely in the semi-arid area.

For the Holocene, a pollen record at Saquinho by Barreto (1996) shows wetter conditions with development of forest from 12.8 to 10.2 ka thereafter becoming drier. Radiocarbon dates on fossil coprolites have indicated wetter conditions from 9.7 to 8 ka (Chaves and Renault-Miskovsky, 1996).

Although not much can be said at present about the palaeoclimate of the Brazilian northeast, it is clear that wetter intervals were present in the past. The accurate dating of these intervals is one of the main objective of this thesis.

6.4. KARST PALAEOCLIMATE IN EASTERN BRAZIL

Karst terrains offer some advantages over other types of landscapes in providing useful records of past climates. Firstly, the geochemistry of karst water is such that it allows for secondary carbonate precipitation to occur both in surface and underground settings. These deposits, usually made up of calcium carbonate, are important repositories of palaeoclimate information. Secondly, caves work as natural traps for both surface derived material such as gravel, alluvial deposits, organic material, and for autogenic sediments, such as secondary precipitates known generically as speleothems. Protected from weathering and normal external erosional agents, these deposits survive for much longer than equivalent deposits on the surface, providing a unique record of past climatic events. Eastern Brazil is particularly endowed with karst sites with a high potential for palaeoenvironmental studies, because it comprises a very extensive karst terrain, with many sediment filled caves. Furthermore, the dry areas of the northeast lack lakes and bogs, and have a low potential for derivation of non-karst palaeoclimate records. The numerous caves, and subaerial secondary carbonate deposits in this area thus have the potential for yielding the best preserved records of past climate change in the region.

6.4.1. Karst palaeoclimate from secondary carbonates

6.4.1.1. Deposition of secondary carbonates

Secondary carbonates in karst are dominantly of the mineral calcite (and to a much less extent aragonite) which constitute more than 95% of all minerals in caves (Hill and Forti, 1997). In addition to cave speleothems, secondary carbonates can form in a number of surface environments as travertine or tufa (deposits usually associated with spring runoff but also

formed by evaporation in lakes), calcrete or caliche (pedogenic concretions or soil horizons).

Secondary carbonates are usually formed by a three-step process. Rainwater picks up carbon dioxide in the atmosphere and later in the soil zone, becoming acidic. The water then comes in contact with the carbonate rock, dissolving away the limestone:

$$H_2O + CO_2 + CaCO_3 \Leftrightarrow Ca^{2+} + 2HCO_3^- \quad \text{(equation 6.1)}$$

Finally the dissolved $CaCO_3$ is precipitated by a number of alternative processes. The most common of these processes is the degassing of CO_2. As the CO_2-rich water comes in contact with an atmosphere with lower carbon dioxide partial pressure (pCO_2), excess carbon dioxide is released, and calcium carbonate precipitates. In caves, usually because of relatively high pCO_2, where degassing occurs slowly and flow rates are low, dense deposits occur. On the surface and with concentrated flows or in well ventilated caves, degassing can be quite fast, producing massive porous material. A second important precipitation mechanism is evaporation which can occur simultaneously with CO_2 degassing. In some settings such as lakes in drylands or caves in arid regions, evaporation is the dominant process. Evaporation will tend to produce less dense material. Carbonates can also be deposited by less usual processes, such as the common-ion effect, or by changes in pressure or temperature of the saturated solutions (Hill and Forti, 1997).

Because an excess of rainfall over actual evaporation is needed for recharge to occur, secondary carbonate precipitation can be positively correlated with rainfall (although evaporative carbonates such as pedogenic concretions will tend to be associated with drier periods, and thermal subaerial carbonate deposits are not climate dependent). As a general observation, warmer and wetter areas tend to have larger amounts of carbonate precipitates, because of the greater recharge and better developed soils, which give higher soil pCO_2 (Hennig et al., 1983). The simple presence of secondary carbonates in a now arid zone can indicate former periods of greater moisture (Hennig et al., 1983). The deposits can also be associated with floral, faunal or archaeological remains, which may also be palaeoenvironmental indicators. In addition, stable isotope analysis, trace elements, and luminescence studies may yield palaeoclimate data. The potential of secondary carbonates in palaeoclimate studies will be discussed in the next section.

6.4.1.2. Travertines

Travertines are subaerial freshwater carbonate deposits that are widespread on a global basis (Ford and Pedley, 1996). They can be classified according to the geochemistry of their formation into cool (or near ambient temperature) travertines, in which the carbon dioxide originates from the soil or atmosphere (meteogene travertines), and thermal deposits, when the carbon dioxide comes from hypogene sources (Pentecost and Viles, 1994, Ford and Pedley, 1996). A further type of travertine (or tufa) is formed in evaporative lakes (Ford and Pedley, 1996). Only

meteogene travertines will be of interest in this study.

Travertine deposition depends on a supply of both water and elevated levels of soil carbon dioxide, and thus wetter and warmer periods will tend to be associated with more extensive travertine accumulation (Ford and Pedley, 1996). U-series dating of travertine has allowed the definition of past pluvial periods in regions which are now arid (Livnat and Kronfeld, 1985, Szabo, 1990). Carbon and oxygen isotopes in travertines can also yield palaeoclimate information (Andrews et al., 1997) in a similar way as with speleothems (see section 6.4.1.3.2). In many arid regions important archaeological sites occur interstratiphied with travertine deposits (Schwarcz and Blackwell, 1992). The dating of these layers have provided important chronological data for several sites (Harmon et al., 1980, Schwarcz et al., 1979, Blackwell and Schwarcz, 1986).

6.4.1.3. Speleothems

6.4.1.3.1. Frequency and growth phases

Speleothems can only grow when there is infiltration into the cave. In arid areas where actual evapotranspiration exceeds rainfall, there will be no infiltration and therefore no speleothem deposition. The same is true for glacial and permafrost areas, in which the water is locked in frozen state. In northern latitudes therefore, periods of speleothem growth correlate with interglacial periods, with little or no deposition during glacial conditions, as has been demonstrated in Minnesota (Lively, 1983), England (Gordon et al., 1989), and northwest Europe (Baker et al., 1993b). Hennig et al. (1983) applied the same rationale in a world survey of speleothems and travertines, including data from warmer and drier climates, but this cannot be justified as wetter conditions in arid areas may or may not correlate with colder glacial conditions in higher latitudes. Brook et al. (1997) have reported speleothem growth periods in the semi-arid zones of Africa. Baker et at. (1995) also found evidence of a correlation between the timing of growth phases in a British flowstone and the insolation record, and between the duration of the growth phases and the Dansgaard-Oeschger cycles of the ice-core record.

Speleothem frequency and growth rate studies were not performed for this thesis due to laboratory machine constraints. Repeated failures of the alpha spectrometer did not allow critical ages to become available on time for the completion of the thesis.

6.4.1.3.2. Oxygen and carbon stable isotopes

The distribution of ^{18}O between the speleothem and the precipitating water is solely dependent on the temperature if the system is in isotopic equilibrium (Gascoyne, 1992). It has been demostrated by Yonge et al. (1985) that in caves in temperate regions, the oxygen isotopic composition of the recharge water is constant and approximately equal to values in the average annual precipitation. Thus, dated cave deposits can potentially provide information on

palaeotemperature, providing the calcite has been deposited in isotopic equilibrium. This is largely the case in cold caves with humidity approaching 100%, and little ventilation. However, rapid degassing of CO_2, and evaporation due to warm and dry cave atmospheres can cause isotopic fractionation (Harmon et al., 1978), disrupting the temperature-dependent equilibrium between the calcite and the water.

Another problem is that the oxygen isotopic composition of the parent seepage water is not generally known. Fluid inclusions offer some promise in this respect (Schwarcz et al., 1976, Dennis et al., 1996), but fractionation may occur during extraction. Some workers have suggested that an estimate of temperature change can usually be obtained by observing the trends in $\delta^{18}O$ along the speleothem (Gascoyne, 1992). However, the effects of temperature on $\delta^{18}O$ of the calcite may be masked by changes in the $\delta^{18}O$ of the rainfall, which may be opposite in effect (Dorale et al., 1992). Local atmospheric and topographical effects and the temperature change between the ocean and the cave site were also found to affect the oxygen isotopic composition of the precipitation (Gascoyne, 1992). An additional complicating factor in arid and semi-arid lands is that there may be evaporation in the epikarst zone before the water can reach the cave, causing isotopic fractionation (Bar-Matthews et al., 1996).

Carbon isotopic composition in secondary carbonates is believed to reflect: (1) global variations of both $\delta^{13}C$ and partial pressure of atmospheric CO_2 (Coplen et al., 1994), (2) changes in vegetation density and areal distribution (Coplen et al., 1994, Goede et al., 1996) and the relative proportion of C_3 and C_4 plants (Cerling, 1984). Plants with the C_3 Calvin photosynthesis cycle are better adapted to arid conditions while C_4 Hatch-Slack cycle plants include most trees and are more typical of cooler environments. Coplen et al. (1994) have argued that changes in density of plant cover as a direct response to changes in precipitation, control the $\delta^{13}C$ of carbonates in arid zone speleothems from Devils Hole. However, Baker et al. (1997) have warned that possible fractionation in the vadose zone may be significant, limiting the application of this technique to subaerial speleothems.

Despite the limitations posed by carbon and oxygen isotopic interpretations, several studies have successfully inferred past climate and vegetational changes from speleothems (Dorale et al., 1992, Dorale et al., 1998, Holmgren et al., 1995, Hellstrom et al., 1998, Coplen et al., 1992, Harmon et al., 1979, Gascoyne et al., 1980). Oxygen and carbon isotope determinations were planned in a number of speleothems from eastern Brazil, but the calcite was frequently porous, suggesting deposition in non-isotopic equilibrium, and uranium series age inversions along the growth axis suggested that open system conditions were present.

6.4.1.3.3. Luminescence

Some speleothems present microscopic luminescence banding that have been shown to be annual (Baker et al., 1993a). The luminescence is caused by humic and fulvic acids and

appears to be dependent on soil type, plant community variation, speleothem growth rate, metal ion interactions, depth of the aquifer, precipitation and temperature (Baker et al., 1996). Speleothem luminescence studies are still at an early stage, and the banding is by no means present in all samples. However, there appears to be potential for obtaining very high temporal resolution of cyclical climatic oscillations with periodicities ranging from a few days to over 10^5 yr (Shopov et al., 1994), and information on palaeoenvironmental changes, such as soil humification, that can be correlated with broader climate parameters as soil moisture and temperature changes (Baker et al., 1998).

6.4.1.3.4. Trace elements

Gascoyne (1983) was the first to suggest that trace elements in speleothems could be used to provide palaeoclimate information. He found that because of variations of Mg content in the supply water, Mg alone could not be used to determine temperature of deposition, and suggested use of the Mg/Sr ratio, in account of Sr being independent of temperature. Goede and Vogel (1991) and Goede (1994) stressed the palaeoclimate potential of trace elements in speleothem but more recently, Roberts (1997) and Roberts et al. (1998) reported that Mg and Mg/Sr variations were not duplicated in coeval Holocene stalagmites, possibly reflecting differential mixing of geochemically distinct waters in the epikarst zone. Nevertheless, Roberts et al. (1998) found that annual oscillations and longer-term trends in Mg/Ca, Sr/Ca and Ba/Ca ratios are present in speleothems and may provide high-resolution information on palaeoprecipitation.

6.4.1.3.5. Water-table variations

Studies of water-table fluctuations have traditionally concentrated on dating of palaeoshorelines in evaporitic lakes in western United States (Szabo et al., 1996). Similarly, increased precipitation will cause a rise in karst ground water levels. These waters are frequently saturated in $CaCO_3$, and may precipitate subaqueous calcite on cave walls. Three types of calcite deposits can be used to infer past water-table levels in caves: (1) subaqueous coralloids are only formed in phreatic conditions, and will give age and extent of flooded areas, (2) shelfstone and folia indicate former levels of the water-table, and (3) calcite rafts will form on the water surface and if attached to a wall can also indicate minimum past water levels. Surprisingly, despite the abundance of dateable deposits, few studies have been reported. Szabo et al. (1994) have used folia and coralloids to infer fluctuations in the water-table for the Devils Hole area in Nevada, and Ford et al. (1993) have obtained information of the draining history of the Wind Cave aquifer, South Dakota. Calcite rafts and other subaqueous deposits are ubiquitous in Brazilian caves and may provide important evidence on past water table levels.

6.4.1.3.6. Pollen

The extraction of pollen which has become trapped in the speleothem can enable the identification of palaeovegetation, and thus provide palaeoclimate information. This method was pioneered by Bastin (1978, 1982) who successfully derived palaeovegetation information from cave sites in Belgium. Successful pollen studies have been accomplished in a number of karst sites around the world (Bastin and Gewelt, 1986, Brook et al., 1990, Quinif and Bastin, 1994, Lauritzen et al., 1990, Baker et al., 1997).

Pollen can be transported to sites of deposition of speleothems by wind, seepage water or flood water. Because of the possibility of reentrainment of ancient pollen, and filtration of larger grains, only windborne pollen will provide representative palaeovegetation reconstruction. Burney and Burney (1993) have compared modern pollen in traps outside caves with pollen experimentally trapped inside caves and found that caves can indeed provide a reliable index of regional and local vegetation, comparable to more conventional spectra derived from lake sediments. Burney and Burney (1993) also reported that the pollen influx rates decline rapidly away from the cave entrance, leading to the conclusion that sites near large entrances in well ventilated caves are potentially best suited for studies. Such sites are abundant in the study area.

A major problem of pollen studies in caves is the low concentration in most speleothems. At least 200 g of calcite are needed to obtain statistically significant pollen counts. Low pollen counts were found in a set of pilot samples collected for this thesis (P. De Oliveira, pers. comm., 1999), and this avenue of research was not pursued

6.4.1.3.7. Fossil remains

In arid lands, preservation of biotic remains in caves is enhanced because low humidity retards biological degradation (Davis, 1990). For this reason, caves in arid western North America have replaced lakes as the primary source of biotic remains of Quaternary age (Davis, 1990). For centuries, palaeontological and archaeological information have been obtained from caves (Buckland, 1823, Lund, 1840). In semi-arid northeastern Brazil, several important fossil deposits are located in caves (Cartelle, 1995), and have been dated in this study.

U-series dating of fossilised bones has always been problematic. Despite some successful attempts (Rae and Ivanovich, 1986), *post mortem* uranium uptake causes inhomogeneous uranium distribution in the bone, precluding reliable dating (Schwarcz and Blackwell, 1992). Radiocarbon dating is an alternative, but is limited to less than 35 ka and is not possible if calcite has completely replaced the original material. $^{230}Th/^{234}U$ dating of interbedded speleothem layers can thus provide chronological constraints for the fossiliferous sediments and in ideal conditions contemporaneous cementation of fossil bone by speleothem may occur. Gascoyne et al. (1981), Sutcliffe et al. (1985) and Jacobi et al. (1998) have applied this technique to fossiliferous cave

sediments from British caves. Guano and other organic material, when interbedded in calcite, can also be dated by the same approach.

6.5. TRAVERTINES OF THE SALITRE RIVER VALLEY

Along the valley of the Salitre River, a series of previously little described subaerial travertine deposits occur which are often associated with tributary valleys. The Salitre River and its tributaries are ephemeral, running water being present only in very rare high precipitation events. The travertines are relict forms that are being eroded by present day runoff and precipitation. The travertines were first briefly described by Branner (1910) who believed they represented a continuum between the extensive ancient Caatinga Limestone, and present limited soil carbonate deposition. Branner (1910) suggested that both the travertines and the Caatinga Limestone were being formed under the present semi-arid conditions. The travertines and fossil plants found in them were later described by Mello (1938). In this thesis, some of Branner's sites are reexamined, but additional localities are also described for the first time.

6.5.1. Description of the sites

The mapped sites were all in the right bank of the Salitre valley, between the villages of Brejão da Caatinga and Abreus (Fig. 6.5). No sites were found in the adjacent Pacuí valley. It is highly likely that other sites exist as our search was far from exaustive, being limited by availability of roads. Two other sites which have not been mapped were also found: about 50 km upstream from Brejão da Caatinga, where the drainage from Baixa do Ouricuri Farm joins the Salitre valley, and in the nearby Jacaré River valley, some 50 km to the west. It is thus believed that the travertines are depositional features of regional significance.

Six travertine sites were sampled for uranium series dating, and three were surveyed in more detail (Fig. 6.6). Topographical profiles along the travertine slope were obtained by compass, clinometer and tape survey. Photographs were used as an aid in representing the more complex outcrops. In most sites, there has been extensive erosion of the deposits, allowing observation of the inner structure of the deposits. The pattern of layering tends to be extremely complex, and an accurate reproduction of the convoluted patterns observed is outside the scope of this study.

6.5.1.1. Salgadinho travertines

The Salgadinho travertine is the best known of the travertine sites and was probably the occurrence reported by Branner (1910). The main deposit occurs along 200 m of valley side, and forms a bluff containing several shallow caves. It comprises a massive overhanging cascade 16 m high at the highest point, but adjacent to the main cliff a series of low gradient cascades reach the present level of the valley bottom (Fig. 6.6a, 6.7a,b). There are abundant plant remains, such as leaf, tree trunks, and root imprints and casts throughout the deposit.

Upslope from the major cascade, aggraded remains of travertine deposits extend for about 350 m along a low gradient dry tributary. A smaller cascade travertine occurs nearby, behind the farmhouses, but was not inspected in detail.

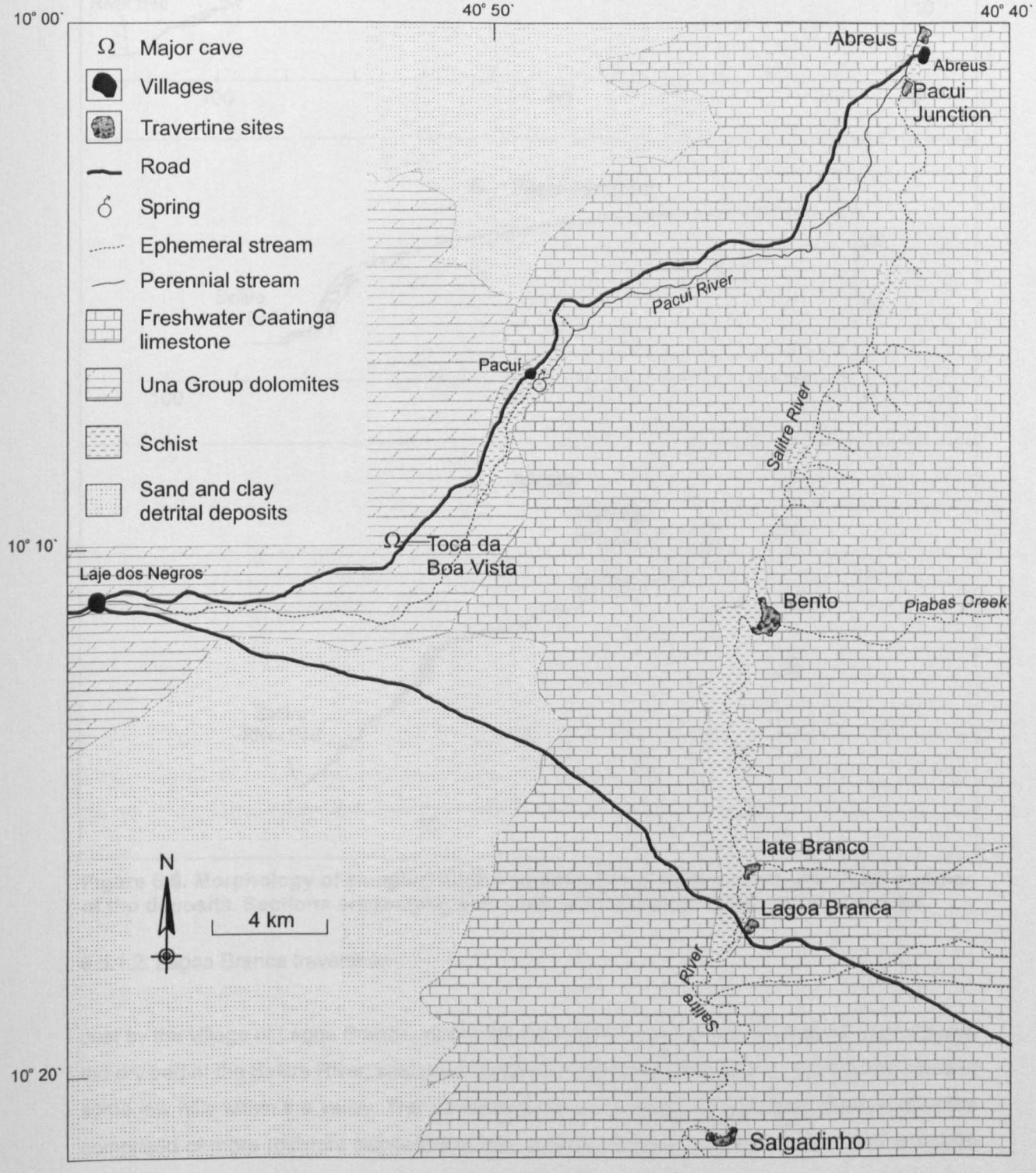

Figure 6.5. Location of travertine sites

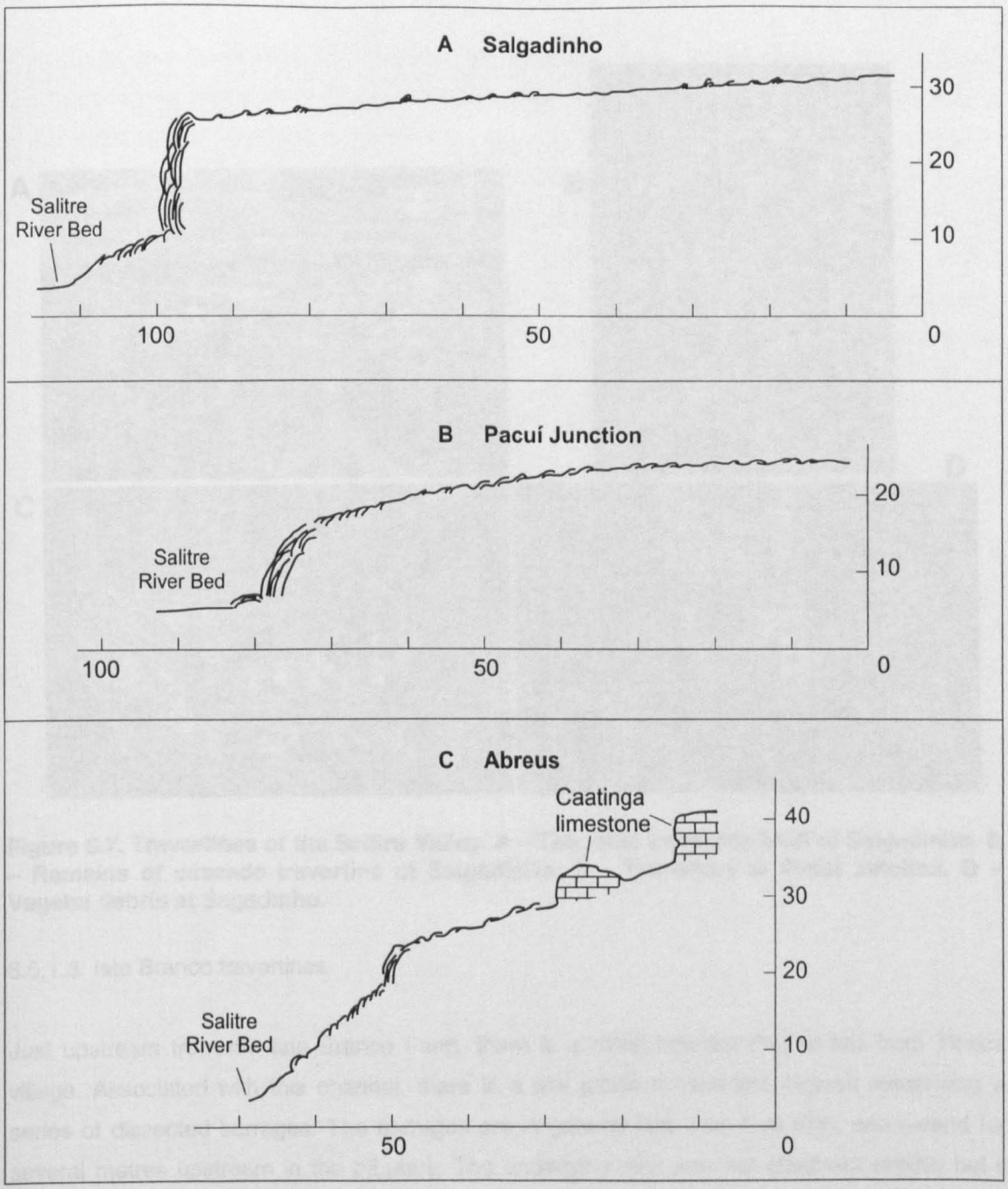

Figure 6.6. Morphology of sampled travertine sites. Survey shows only the distal portion of the deposits. Sections are roughly perpendicular to Salitre Valley. Scale in metres.

6.5.1.2. Lagoa Branca travertines

Just by the village of Lagoa Branca, where the main road from Campo Formoso to Laje crosses the dry bed of the Salitre River, scattered remains of travertine are found on the top and sides of some low hills within the valley. The travertines are not *in situ*, and represent residual deposits comprised of more resistant calcite layers that survived erosion, in clear contrast with the more porous *in situ* deposits mapped elsewhere (such as Salgadinho). The pieces are on average a few centimetres in size and are very hard and dense. Fragments are extremely frequent in some slopes. The deposits probably grew over shales, as the lower portion of the Salitre valley is entirely incised in these rocks at this point. This site was not surveyed.

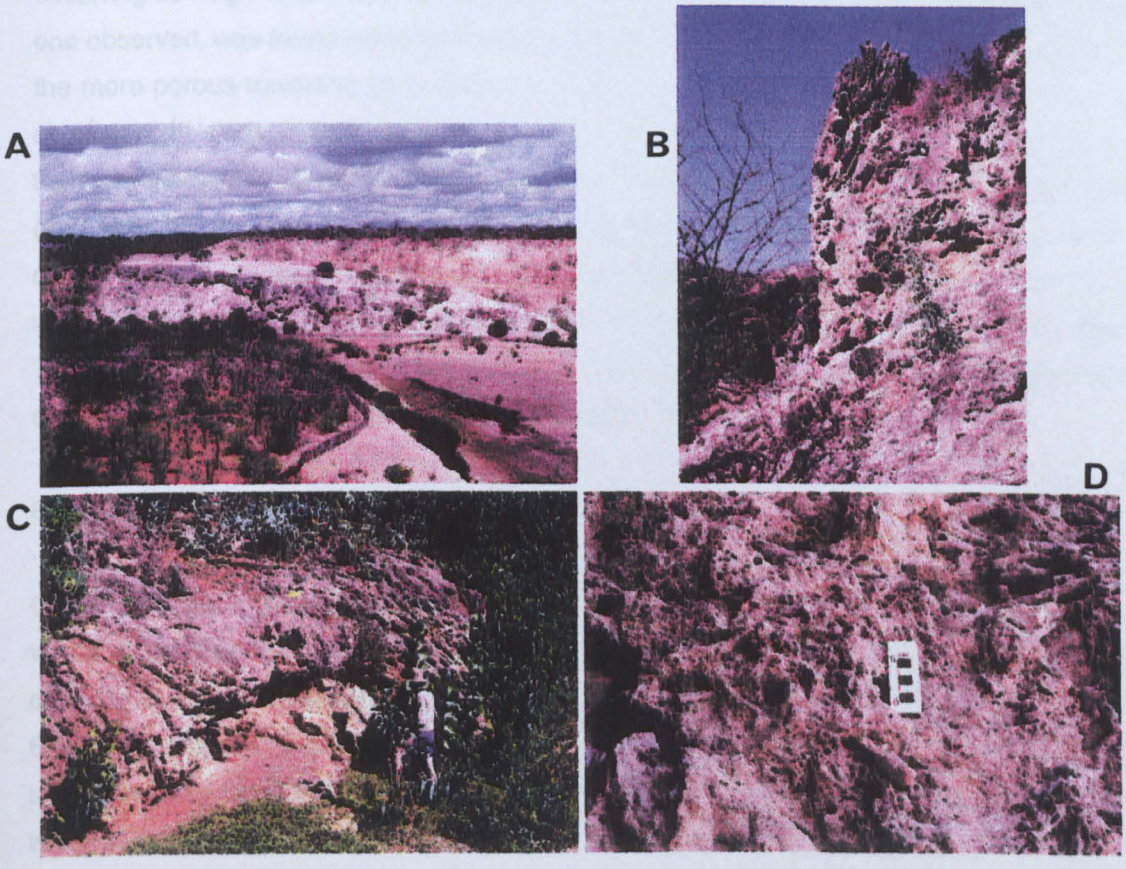

Figure 6.7. Travertines of the Salitre Valley. A – The main travertine bluff of Salgadinho. B – Remains of cascade travertine at Salgadinho. C – Travertine at Pacui junction. D – Vegetal debris at Sagadinho.

6.5.1.3. late Branco travertines

Just upstream from the late Branco Farm, there is a small tributary that comes from Tiririca village. Associated with this channel, there is a low gradient travertine deposit comprising a series of dissected barrages. The barrages are in general less than 2 m high, and extend for several metres upstream in the tributary. The underlying rock was not observed directly but it appears to be shale, since this can be observed in the Salitre riverbed at this location. Widespread remnants of a dense indurated travertine were observed scattered in the flat terrain around the farmhouse, some 10 m above the Salitre riverbed, and somewhat downstream of the main tributary valley.

6.5.1.4. Bento Farm travertines

This is the largest travertine site visited, extending along the river for over one kilometre. It is mainly associated with the tributary that drains from Piabas village, but the deposits appear to be the remains of a once more continuous travertine deposit, now dissected by runoff along the tributary valleys and associated gullies. As at late Branco, a younger *in situ* deposit consisting of barrages and cascades was present, together with remains of a dense indurated variety, largely

occurring as fragments on the upper slopes. An *in situ* deposit of this dense travertine, the only one observed, was found at this site, largely buried under colluvial debris. It is distinguished from the more porous travertine by its darker colour, much more indurated nature, and for occurring at present in slope divides between tributary valleys. The most extensive outcrops of porous travertines are associated with the Piabas creek. They extend upstream for well over 200 metres (and possibly for over a kilometre) into the steep sided narrow valley of the dry creek and contains good examples of barrages and cascades, some over 4 metres high. Plant debris is widespread, and impressive tree trunk casts 30 cm in diameter and leaf imprints were observed. The more porous Bento travertines developed over a chalky unit of the Caatinga Limestone, and are around 5 m thick in one site where the bedrock outcrops.

6.5.1.5. Pacuí junction travertines

On the right bank of the Salitre River, about 60 m upstream from where it joins the active Pacuí valley, there is an important deposit of travertine. The deposit is approximately 250 m wide and consists of a single cascade about 6 m high that drops to the level of the valley bottom (Fig. 6.6b, 6.7c). Isolated travertine outcrops extend upstream for further 350 m as minor outcrops in a progressively flatter terrain. The main deposit appears to be associated with a former tributary which is now largely aggraded, and has little topographic impression. The underlying rock was not observed.

6.5.1.6. Abreus travertines

Downstream from the road bridge, close to the village of Abreus, there is a minor occurrence of travertine. This deposit extends for approximately 50 m along the steep side of the valley. Among the studied sites, this is the only one that is clearly not associated with a tributary, as it appears to have been formed by runoff over the shale on the steep valley side. It consists of cascades, the largest of which is around 4 m high, extending upwards to meet the outcrops of Caatinga Limestone near the top of the slope (Fig. 6.6c).

6.5.2. Morphology and genesis

The travertines occur in two general settings: They are either associated with dry tributary valleys (Salgadinho, Iate Branco, Bento), or developed down the steep side slopes of the Salitre valley (Abreus). Two morphological types predominate, (1) barrage travertines, characterised by arcuate downstream facing dams perpendicular to flow direction, and (2) cascade or waterfall travertines, created at a break of slope of the valley side. Cascade travertine sometimes form overhangings in which shallow caves and speleothems develop. Cascade travertines in the area appear to be gradient controlled, as the more massive deposits occur on the steepest slopes. Similar relationship has been observed by Sancho et al. (1997) in Spanish travertines. Both barrage and cascade travertine types occur together in most of the described sites, and both are

dissected by later runoff and erosion. Most tributary-related travertines form a "fan" type of deposit as they approach the valley slope. Present ephemeral tributaries appear to have been rerouted around the fan. The travertines appear to be rather thin deposits. At most sites they are probably only a few metres thick, while the maximum thickness observed did not exceed 10 m. The travertines are commonly underlain either by impermeable schist or Caatinga Limestone.

The bulk of the travertines comprise a friable and porous calcite precipitated around abundant plant remains (Fig. 6.7d). This type of travertine lacks visible layering and tends to be very impure. A much denser and more compact calcite frequently overlies these layers, and may in most cases represent a later deposit. This second calcite is often brown coloured and serves to protect the more friable inner layers. Similar petrographical characteristics were reported for other travertine sites (Crombie et al., 1997, Schwarcz et al., 1979). Three distinct depositional morphologies proved suitable for sampling in these travertines (Fig. 6.8). The outer laminated travertine layers from cascades were usually sufficiently compact and dense that closed system conditions should have occurred, and thus yielded most of the samples dated. Root and trunks were commonly found embedded in dense concentric calcite layers, the thicker sections of which had enough good calcite for analysis (sample TVT-06). Lastly, some of the caves include speleothems, such as calcite "false floors", or stalactites that can be successfully dated (sample TSG-02).

At least one additional phase of travertine deposition is found. It is represented by *in situ* deposits at Bento, but at two other sites (late Branco and Lagoa Branca) by scattered fragments. This travertine is much more denser than the more abundant travertines, frequently dark brown or even black coloured due to presence of organic material, insoluble residues being generally absent. Interestingly this travertine contains no plant remains. This more indurated travertines do not present any problem in sampling selection since they are invariably dense and compact. Samples were collected at random in three distinct sites. Both dark coloured (organic rich) and clean calcite were observed. Dark calcite tended to show higher contents of detrital thorium.

The travertines of Salitre River were deposited by CO_2 degassing in runoff water rich in calcium carbonate. Two possible mechanisms have been described to explain travertine deposition. The first mechanism evokes release of CO_2 by turbulence of water. The travertine would then tend to grow in breaks of slope, or in the spillways of barrages. This mechanism is believed to predominate in a number of settings, including caves. Carbonate can also precipitate by photosynthetic removal of CO_2 from the water by aquatic plants and mosses (Bischoff et al., 1988a). Both processes have been observed to contribute to carbonate deposition in travertines (Chafetz et al., 1994), and could have occurred in the area.

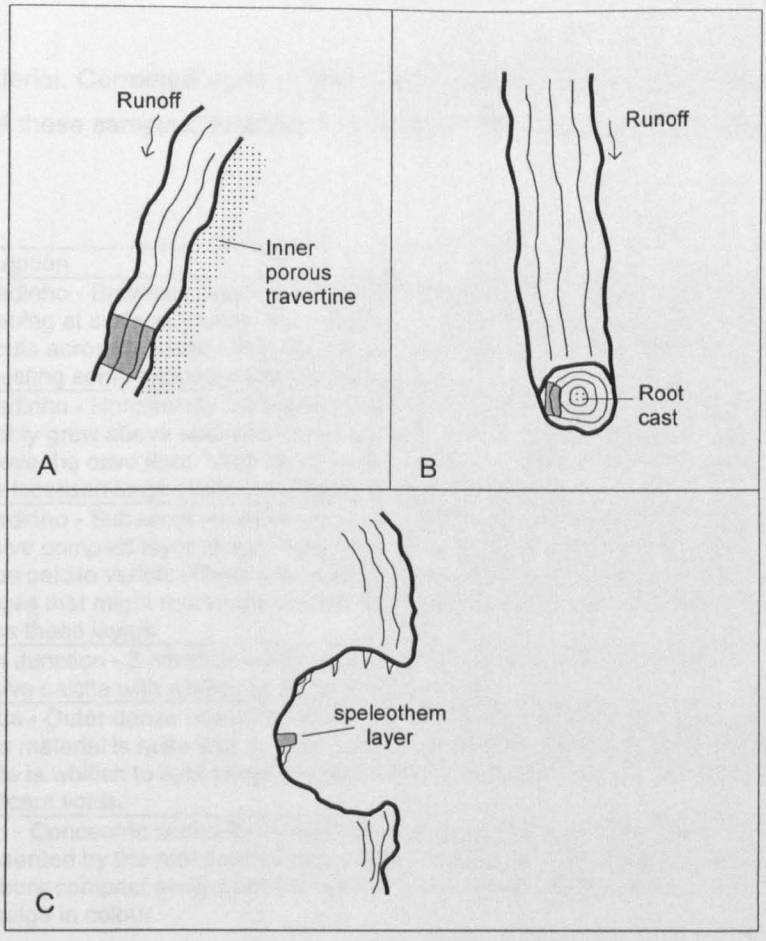

Figure 6.8. Common travertine morphologies sampled for U-series dating A - Outer calcite layer of surface runoff deposit. B - Outer speleothem layer of root or trunk cast. C - Speleothem layer inside caves.

6.5.3. U-series analysis on travertines

Travertine samples analysed are listed in Table 6.1 and the U-series analysis are reported in Table 6.2. Because travertines tend to be more porous than most speleothems, it is important to check for closed system conditions in terms of uranium and thorium mobilisation. Stratigraphical tests cannot be applied to the travertines because the inner layers are invariably porous and friable, and only the outer calcite is suitable for dating. Two samples collected close together at Salgadinho site (TSG-01 and TSG-02), although morphologically distinct, display very similar isotopic values. Furthermore, there appears to be a characteristic initial $^{234}U/^{238}U$ ratio signature for each site, the three samples from Salgadinho having initial $^{234}U/^{238}U$ ratios of 7.3-7.9, while the two samples from late Branco have a much lower ratio (3.8-4.0). Abreus, Bento and Pacuí have similar values intermediate between the two sites described above. If open system conditions had prevailed, such site-specific pattern would probably not be present.

Five of eight younger samples, had $^{230}Th/^{232}Th$ ratios > 20, showing limited detrital Th content. Samples with $^{230}Th/^{232}Th$ ratios below 20, due to its younger ages, yielded significant difference between corrected and uncorrected ages. For the four older samples, only one had $^{230}Th/^{232}Th$ ratios > 20, despite lack of significant insoluble residues, suggesting that ^{230}Th is associated with

organic material. Corrected ages in this case, however, shows little difference because of the older age of these samples, in which the detrital ^{230}Th represents a small proportion of the total Th.

Sample	Description	Location
TSG-01	Salgadinho - Brownish outer layer of subaerial flowstone. Massive with case hardening at surface. Dense layer dated is 1-2 cm thick overlying friable material and cuts across a horizon that appears to have undergone case hardening suggesting some exposure time at the surface.	About 13 m above Salitre valley bed
TSG-02	Salgadinho - Horizontally laminated speleothem layer inside a shallow cave. It probably grew above sediment now removed, and was left overhanging about 3 m above the cave floor. Very dense and indurated, dark brown in colour with some localised large voids but otherwise very compact	About 13 m above Salitre valley bed
TSG-03	Salgadinho - Subaerial flowstone growing on the junction of two runoff channels. Massive compact layer of light beige calcite up to 10 cm thick overlying the porous calcite variety. There are at least three distinct layers, identified by colour changes that might represent distinct depositional events. Dated horizon cuts across these layers	About 16 m above Salitre valley floor.
TVT-02	Pacuí Junction - 3 cm thick outer speleothem layer in subaerial flowstone. Massive calcite with whitish and beige laminations.	About 1 m above Salitre valley floor.
TVT-03	Abreus - Outer dense speleothem layer overlying friable carbonate. Dateable dense material is quite thin (c. 1 cm) and shows some case hardening at surface. Calcite is whitish to light beige, locally porous but mostly compact and free of significant voids.	About 15 m above Salitre valley floor
TVT-06	Bento - Concentric speleothem layer overlying tree root cast. The inner portion, represented by the root itself is very porous and friable. The material gets denser and more compact away from the centre. The dateable layer is about 1 cm thick and beige in colour.	Outcrop overlies chalky Caatinga Limestone. Travertine is about 5 m thick in site.
TVT-07	Iate Branco - 5 cm thick outer layer of outer rim of barrage travertine dissected by tributary erosion. Calcite is brown to light beige and although compact it has a series of radiating voids suggesting some type of recrystallisation.	About 3 m above the Salitre bed, which is filled with 4 m of aggrading sediment.
TVT-08	Iate Branco - Dark brown calcite with outer and inner whitish friable calcite horizons. Only the darkest section was dated, which is 1.5 cm thick. It represents the outer rim of a barrage travertine dissected by erosion.	About 3 m above the Salitre bed which is filled with 4 m of aggrading sediment.
TVT-01	Lagoa Branca - Fragment of indurated travertine scattered over the top of hill between gullies. Dense and well laminated dark brown calcite. Presence of some whitish layers. Material is void free and was collected at random at surface.	About 6 m above the Salitre valley bed.
TVT-04	Bento - *In situ* travertine on top of hill surrounded by gully valleys overlooking the Salitre valley. On the surface of the hill there are a large quantity of fragments of travertine. Blackish calcite with evenly spaced whitish layers. Dense and void free.	About 10 m above the Salitre valley floor.
TVT-05	Bento - Sampled in the same site as TVT-04, it represents one of the fragments scattered at the surface. Clean white calcite, very dense and without visible voids.	About 10 m above the Salitre valley floor.
TVT-09	Bento - Same site as TVT-04 and TVT-05. Blackish variety of the fragments. Presents some light brown speleothem layers. Void free and no evidence of redissolution or recrystallisation.	About 10 m above the Salitre valley floor.

Table 6.1. Description and location of travertine samples dated. All samples represent outer layers of the deposits, except sample TSG-02.

The age data demonstrates clearly that there are two distinct groups of deposits. The younger travertines, corresponding to the vast majority of the *in situ* more porous deposits (first eight samples in Table 6.2) yield ages between the LGM and Holocene. The exception is sample TVT-07 from Iate Branco which may have undergone recrystallisation, because of the porous nature of the calcite, and thus yields an unreliable age. All samples analysed from the younger

Younger travertines								
sample	**site**	**U (ppm)**	**$^{234}U/^{238}U$**	**$^{230}Th/^{234}U$**	**$^{230}Th/^{232}Th$**	**$^{234}U/^{238}U_{t=0}$**	**uncorrected age (ka)**	**corrected age (ka)**
TSG-01	Salgadinho	0.208 ± 0.006	6.94 ± 0.15	0.175 ± 0.004	50.2	7.3	20.4 ± 0.8	-
TSG-02	Salgadinho	0.366 ± 0.006	7.49 ± 0.06	0.183 ± 0.004	63.6	7.9	21.4 ± 0.5	-
TSG-03	Salgadinho	0.194 ± 0.005	7.12 ± 0.12	0.128 ± 0.003	234.1	7.4	14.7 ± 0.5*	-
TVT-02	Pacuí Junction	0.107 ± 0.002	5.11 ± 0.08	0.086 ± 0.002	42.5	5.2	9.7 ± 0.3	-
TVT-03	Abreus	0.031 ± 0.001	4.65 ± 0.23	0.101 ± 0.003	16.7	4.8	11.4 ± 0.9	10.3 ± 0.8*
TVT-06	Bento	0.058 ± 0.002	4.78 ± 0.13	0.094 ± 0.002	20.5	4.9	10.6 ± 0.5*	-
TVT-07	Iate Branco	0.149 ± 0.003	3.28 ± 0.04	0.690 ± 0.017	15.1	4.0	108.0 ± 4.9	101.0 ± 4.7
TVT-08	Iate Branco	0.082 ± 0.002	3.75 ± 0.08	0.101 ± 0.002	7.2	3.8	11.5 ± 0.4	8.9 ± 0.4
Older travertines								
TVT-01	Lagoa Branca	0.045 ± 0.001	1.45 ± 0.03	1.083 ± 0.025	14.4	2.3	394 (+135 –111)	385 (+140 –76)
TVT-04	Bento	0.025 ± 0.001	1.60 ± 0.06	1.114 ± 0.034	6.8	2.8	413 ± inf.	394 (+460 –110)
TVT-05	Bento	0.041 ± 0.001	1.48 ± 0.04	1.079 ± 0.030	42.1	2.4	372 (+125 –109)	-
TVT-09	Bento	0.021 ± 0.001	1.49 ± 0.06	1.204 ± 0.041	7.0	-	>350	

Sample	$^{234}U/^{238}U$ initial (estimated)	$^{234}U/^{238}U$ RUBE age (ka)
TVT-09	2.4	367 (+43 –38)

Table 6.2. U-series analyses for travertine samples, and RUBE age for sample TVT-09. Ages were corrected assuming a $^{230}Th/^{232}Th$ initial ratio of 1.7. Errors are ± 1σ. * denotes samples with U breakthrough in the Th spectrum.

travertine represent a later runoff event, since they tend to grow around the more porous and plant debris rich calcite. Nevertheless, it is likely that these samples are representative of the main period of travertine growth.

The LGM to Holocene samples are characterised by high $^{234}U/^{238}U$ initial activity ratios (> 4), as reported for other travertine sites in France and Spain (Delannoy et al., 1989). The high initial $^{234}U/^{238}U$ ratios show that there has been significant fractionation between these two isotopes during weathering. Samples from the Caatinga Limestone, and from speleothems in caves formed in it display much lower initial $^{234}U/^{238}U$ ratios (Table 2.1). Therefore, dissolution of the Caatinga Limestone cannot account for such high ratios. Significant preferential release of ^{234}U must therefore have occurred during contact with the underlying schists. This finding suggests that on the right bank of the Salitre River, where the travertines are located, runoff occurs predominantly over impermeable schist. On the other hand, on the left bank and in the nearby Pacuí valley, the Caatinga Limestone is probably too thick, favouring infiltration and formation of caves, and limiting runoff and travertine generation. The site specific differences in initial $^{234}U/^{238}U$ ratios could be related to flow path length over schists.

The age of the older travertines is close to the limit of the alpha spectrometric method (last four samples in Table 6.2). They exhibit significantly lower initial $^{234}U/^{238}U$ ratios more compatible with those from the Caatinga Limestone and associated speleothems (Table 2.1) suggesting a hydrological path with considerable less contact with the schists. They also have much lower uranium concentrations, confirming that weathering has occurred predominantly in the less uraniferous Caatinga Limestone.

The high initial $^{234}U/^{238}U$ ratios of the older travertines allow the alpha spectrometry U-series method to be extended a little further from its usual limit of around 350 ka. Furthermore, if we assume that the relatively constant initial $^{234}U/^{238}U$ ratios typical of the samples yielding finite ages are representative, we can use the average initial $^{234}U/^{238}U$ ratio of 2.4 to calculate a RUBE (Regional Uranium Best Estimate) age (Gascoyne et al., 1983) for sample TVT-09. The age derived falls within the limits of the other reported ages. We can thus suggest that the older travertines were deposited before 300 ka, but are probably younger than 600 ka.

6.5.4. Palaeoclimatic implications

Travertines in semi-arid regions are reliable indicators of past pluvial periods (Livnat and Kronfeld, 1985, Kronfeld et al., 1988, Szabo, 1990, Crombie et al., 1997). The travertines of the Salitre River are relict forms, inherited from a former wetter climate. At present they are being eroded by runoff caused by occasional storms, and being buried by slope disaggregation. Branner (1910) believed that river channels in the Salitre basin underwent erosion during periods of enhanced rainfall, and travertine could not be deposited under such situation. He claimed that carbonate precipitation would occur in periods of diminished rainfall, such as the present, when

channel erosion would not take place. Although thin films of evaporitic carbonate are indeed being precipitated in stagnant pools at present, the travertine deposits are clearly inactive and indeed are suffering incision during periods of stream activity. They were formed by precipitation from calcium carbonate rich ground waters during past periods of higher rainfall when persistent ground water flows maintained spring flow from the contact between Caatinga Limestone and underlying schist.

The travertine age data allows the recognition of two past periods of higher rainfall. The younger *in situ* travertines appear to have been deposited between 21-9 ka, during marine isotopic stage 2, comprising the LGM and succeeding deglaciaton period. Travertine growth rates tend to be high (Chafetz et al., 1994), and therefore I believe that even though only the more recent vegetal debris free layer was sampled, the ages determined correspond to the period of major development of the deposits. The conclusion is that isotope stage 2 was a period of increased rainfall in the area (in comparison with the present semi-arid climate). Inactivation of the travertines in the early stages of the Holocene was then due to decreased rainfall as no deposits younger than 8 ka were dated.

Duarte and Nogueira (1983) analysed fossil leaf imprints in similar but undated deposits located in the nearby Jacaré River, and concluded that they represent vegetation characteristic of riparian forest, not related to the present dry Caatinga scrub typical of the area. Barreto (1996) reported higher levels of humidity from 12.8 to around 10.2 ka (calibrated ages) from the pollen record at Saquinho, 250 km to the west with dry conditions then prevailing and caatinga vegetation replacing forest. Fossil data and ocean core terrigenous pulses (Fig. 6.4) also corroborate my conclusions of a wetter climate in the area during isotope stage 2.

The age data also indicates an earlier wetter period between 300-600 ka (centered around 400 ka). Considering that dryness appears to predominate during interglacials in the area, this former period could be assigned to one of the past glacial periods, either to marine isotope stages 10 or more possibly 12. This older phase of travertine deposition appears to have been as widespread as, or even more extensive than the young one, as debris from it is found scattered over large areas presently unrelated to any visible tributary. During deposition of this older travertine, the Salitre valley was shallower than at present, and the remains are now located several metres above the present valley floor. The difference in initial $^{234}U/^{238}U$ ratios between the two phases of travertine discussed in the previous section, supports the notion that valley floor and spring points were at a higher elevation during the deposition of the older travertine.

The absence of travertine deposits belonging to glacial periods between isotope stages 2 and 10 can be explained by a number of factors: (1) sampling was not extensive and degraded and less conspicuous sites belonging to these stages could have been missed; (2) aggradation due to slope disaggregation and erosion by flash runoff is very active in the area during dry periods and

could have either buried or destroyed some of these intermediate age deposits; (3) there was no marked travertine deposition during the intermediate stages as the region did not reach the moisture levels required to promote travertine growth. Further research is needed to test these alternatives.

6.6. WATER TABLE VARIATIONS

6.6.1. Description

In this section I will consider results of U-series dating of subaqueous speleothems from Toca da Boa Vista. Some of the lower passages of this cave are filled with speleothems associated with subaqueous settings, such as cave cones, wall crusts, and extensive raft layers. Furthermore, there is a well defined and laterally extensive calcite shelfstone that marks the upper limit of the water table, subaqueous deposits being largely absent above. No clastic sediments which are frequent in other areas of Toca da Boa Vista are visible in these passages.

Two sites with evidence of past higher water levels have been studied in Toca da Boa Vista (Fig. 6.9). Site 1 is in the northern part of the cave, and is characterised by large chambers with cross sectional areas approaching 150 m^2. Passage walls are smoothly rounded and there are extensive subaqueous deposits. Throughout the passages there is a well marked shelfstone, above which no subaqueous deposits were observed. The shelfstone projects for up to 10 cm from the walls, and is in many places in excess of 5 cm thick with subaqueous deposits adhering to its lower surface. Due to its size it is believed that this shelfstone corresponds to a period when the water level stayed at that level (or close to it) for a relatively long period of time. Samples were obtained both from the shelfstone, and the subaqueous speleothems below it. The latter were sampled at several different levels below the shelfstone, and correspond broadly to two morphological subtypes, "cauliflower" and "grape" shaped coralloids. The present water table can be observed at the bottom of a rift in one of the passages. In August 1998 it stood at 14 metres below the shelfstone level. During other visits to the area, the water level has been observed to rise at least 2 metres above this level due to seasonal rainfall. It is therefore assumed that present water table is at 13 ± 1 m below the past higher stand represented by the shelfstone at Site 1.

Site 2 is more restricted, comprising a series of small low-ceilinged chambers at the northern extremity of the cave. A well marked shelfstone level is present throughout the main chamber, being 10 cm wide and 5 cm thick where sampled. A thick calcite raft, 6 mm in thickness and lying approximately 1 m above the shelfstone was also sampled. This site does not have any passage leading to the present water table, and therefore it is not possible to infer the relative position of this shelfstone in relation to the water table. According to the cave survey data, the shelfstone at Site 2 is 6.8 metres above that of Site 1. However, the cumulative error in surveying with hand held compass, clinometer and tape along kilometres of cave passages is

probably larger than this value, and any inference about the relative elevation between the two shelfstones would be largely speculative.

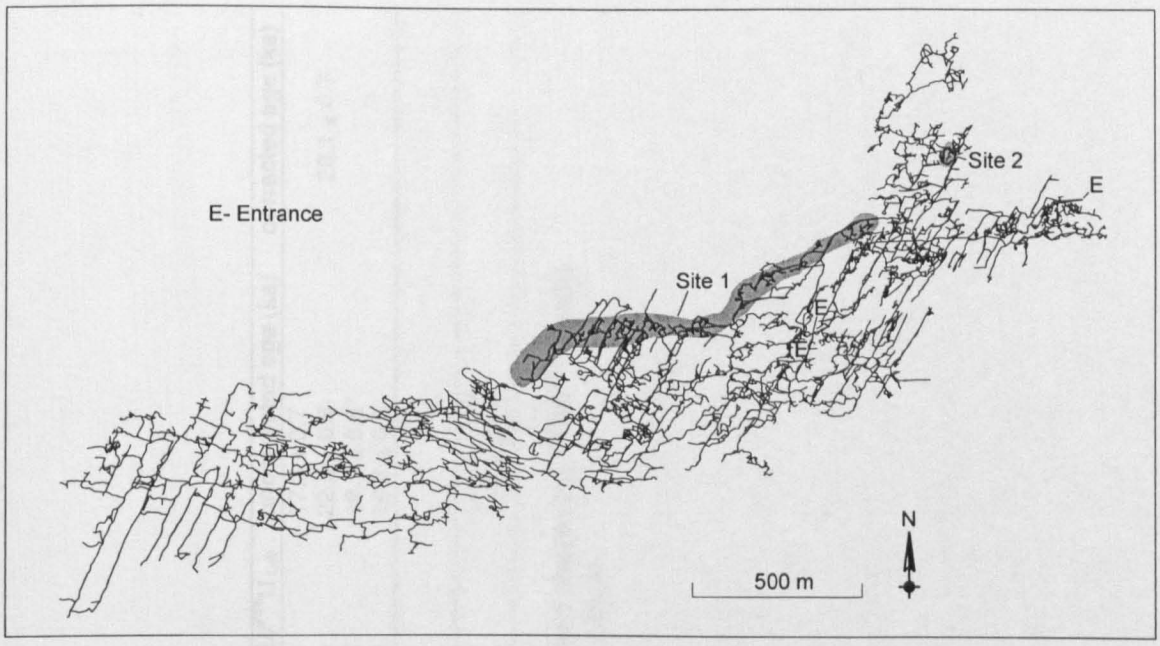

Figure 6.9. Plan of Toca da Boa Vista showing areas of water level calcite.

6.6.2. Chronology of water table high stands

Uranium series analysis data for subaqueous calcite samples are presented in Table 6.3. Only one sample (TBV3-96) has $^{230}Th/^{232}Th < 20$ suggesting it has been affected by detrital contamination. All other samples from Site 1 and Site 2 respectively show a remarkable consistency in initial $^{234}U/^{238}U$ ratios suggesting they have not been affected by post depositional leaching. The data show that there are two distinct episodes of water table high stands at Toca da Boa Vista.

Samples at Site 1 yielded ages which range from 17.3 ± 0.8 to 22.3 ± 0.8 ka, equivalent to the LGM. The subaqueous calcite samples are, as would be expected, roughly synchronous except for shelfstone sample TBV-24 which has yielded a date slightly younger. It is assumed that all ages for Site 1 correspond to the same flooding event, and that the water-table in the region was 13 ± 1 m higher than at present during the LGM.

Only two samples from Site 2 were dated. The isotopic data from samples from both sites (Fig. 6.10) demonstrate that Site 2 samples are not related to Site 1 calcites and correspond to a distinct and older high water table event. The age indicates that they were deposited in the penultimate glacial period, corresponding to marine isotope stage 6. The calcite raft sample TBV-30 predates the shelfstone sample by some 20 ka, although if 2σ errors are adopted, the age ranges overlap. Cave rafts can form very fast, in the range of months (Hill and Forti, 1997), and sample TBV-30 certainly deposited faster than the thick shelfstone (TBV-31) about a metre below it. Therefore, it is suggested that the raft sample represents an older high water-table

Sample	morphology	U (ppm)	$^{234}U/^{238}U$	$^{230}Th/^{234}U$	$^{230}Th/^{232}Th$	$^{234}U/^{238}U_{t=0}$	uncorrected age (ka)	corrected age (ka)
Site 1								
TBV-24	shelfstone	0.096 ± 0.002	3.01 ± 0.07	0.149 ± 0.004	21.9	3.1	17.3 ± 0.7	-
TBV3-96	coralloid	0.067 ± 0.001	2.94 ± 0.06	0.189 ± 0.004	14.8	3.1	22.3 ± 0.8	20.1 ± 0.7
TBV-19	coralloid	0.083 ± 0.001	2.98 ± 0.05	0.163 ± 0.003	92.7	3.1	19.1 ± 0.6*	-
TBV-21	coralloid	0.124 ± 0.001	2.96 ± 0.03	0.169 ± 0.003	120.2	3.1	19.8 ± 0.5	-
Site 2								
TBV-31	shelfstone	1.950 ± 0.028	3.04 ± 0.03	0.823 ± 0.015	984.3	4.1	144.4 ± 5.9	-
TBV-30	raft	0.935 ± 0.018	2.93 ± 0.05	0.889 ± 0.019	1075.4	4.1	167.1 ± 9.7	-

Table 6.3. $^{230}Th/^{234}U$ analyses for subaqueous and water level calcite. Ages corrected assuming $^{230}Th/^{232}Th$ ratio of 1.7. Uncertainties are ± 1σ. * denotes sample with U breakthrough in the Th spectrum.

event that did not last long enough to generate a conspicuous shelfstone line. Whether these two samples represent extremes of the same high water table episode is uncertain. Since the elevation of samples from Site 2 cannot be tied to the present water table, it is not possible to ascertain the amount of water table rise with any confidence. The cave survey data suggest the water table in the area was some 19 m higher than present during the penultimate glacial maximum.

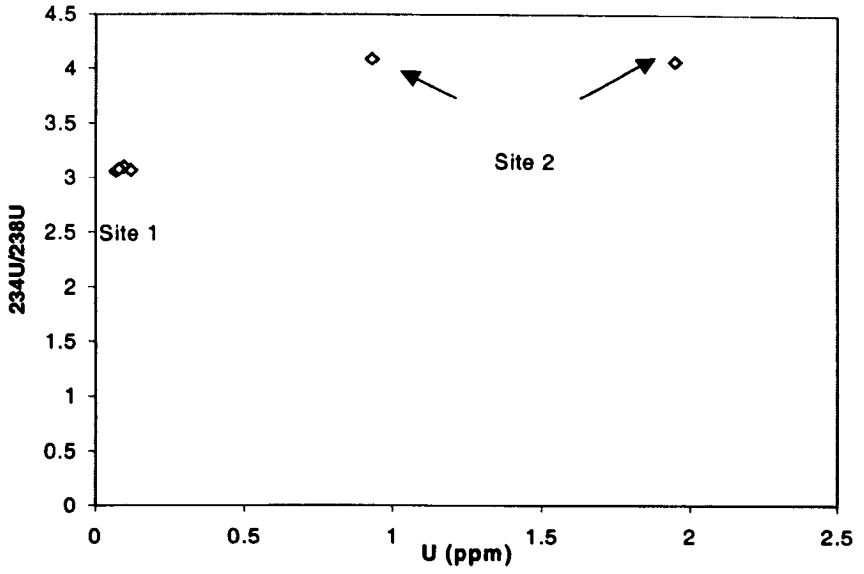

Figure 6.10. Isotopic comparison between Site 1 and Site 2 subaquaeous calcites.

6.6.3. Discussion and palaeoclimatic implications

Hydraulic gradients in mature karst terrains tend to be low, on the order of 0.001 (Worthington, 1991). This is especially true for low relief areas with high cavernous porosity such as the study area. In this situation, the water table can be taken as being essentially horizontal. No sinking streams are known from the surface above the cave, and there is no evidence of significant concentrated recharge to the flooded areas of Toca da Boa Vista. Therefore, it is believed that local point recharge cannot be responsible for the water table rise. Perched ponding levels can occur in caves, and have been observed in Toca da Boa Vista. Such local pools are known as rimstone dams, and can have subaqueous calcite, rafts and shelfstone deposits associated with them. However, some evidence strongly suggests that the major flooded sections of Toca da Boa Vista are not local perched water bodies. (1) The areal extent of the subaqueous calcites is in excess of several kilometres of passages, over two orders of magnitude larger than that of rimstone dams. (2) The water surface at Site 1 was observed to fluctuate by up to 2 m, probably in response to seasonal rainfall. In contrast there is normally no fluctuation in rimstone dams water levels, which are controlled by the elevation of the overflow lip. Therefore it is believed that palaeowater levels of regional significance are preserved as calcite deposits at Toca da Boa Vista.

The water level high stands preserved at sites 1 and 2 were not observed in other areas of the

cave, even though the cave survey elevations appear to indicate that some areas would be within the flood range of such events. Most other low elevation areas in the cave are characterised by extensive clastic sedimentation, with both fine grained material and breakdown. Weathering and masking by such sediments could also have played a role in obscuring such evidence. On the other hand, sampling was not extensive and some other areas with subaqueous speleothems were not visited during this study.

Variations in water level can be attributed to a number of factors. Szabo et al. (1994) discuss the role of regional tectonism affecting the elevation of discharge points, and the water table. None of these processes are possible in the Toca da Boa Vista area, as the region has not undergone any significant tectonic activity during the Quaternary. Water level decline due to normal denudational processes in stable cratonic areas is usually very small, probably below 50 m/Ma (section 5.7.3). A decline of 13 m in the last 20 ka is thus far too large to be explained by regional base level lowering. Ponding of the Salitre River by travertine buildup could account for some of the water table rise but it is unlikely to be of major influence, and in any case indicates wetter conditions than present. Therefore we believe the water level high stands seen in Toca da Boa Vista are associated with periods of higher ground water flow due to higher rainfall. The 13 m decline of the last 20 ka in the study area is comparable to a 10 to 20 m decline/increase in the water level of the aquifer in Wind Cave, Black Hills, USA (Ford et al., 1993) and 9 m oscillation at Devils Hole area (Szabo et al., 1994), interpreted at both sites as being caused by late Quaternary climate changes.

The water level variations inferred from Toca da Boa Vista calcites can be correlated with the subaerial travertine deposits, as both are proxies of past pluvial phases. The major pluvial phase of the LGM is well represented in both records, with major travertine accumulation and areally extensive flooding in the lower levels of Toca da Boa Vista. The penultimate glacial water table rise observed at Site 2 in the cave, was not dated in the travertines sampled. This could be due to later burial, or simply limited sampling. Subaqueous deposits corresponding to the major travertine buildup at around 400 ka were not found at Toca da Boa Vista, but is probably likely that such deposits would be greatly affected by *in situ* breakdown and by weathering of the cave walls which would cause loss of encrusting subaqueous calcite. Further careful survey may however show evidence of such deposits.

6.7. PALAEOENVIRONMENTAL IMPLICATIONS OF CAVE FOSSIL REMAINS

Fossil remains in caves can yield palaeoclimate information in two distinct ways. First, the mode of emplacement of the fossils can be palaeoclimate controlled. Secondly, the presumed habitat and mode of living of the fossil species can yield palaeoenvironmental information. Both possibilities will be discussed in this section.

6.7.1. Vertebrate palaeontology from cave deposits in eastern Brazil

Much of what is known about Quaternary vertebrate palaeontology in eastern Brazil is derived from studies of cave sediments. Over 150 years ago, the Danish naturalist Peter Lund was the first to describe at length numerous species of the now extinct Pleistocene fauna collected from cave deposits in the Lagoa Santa area (Lund, 1838-1842, Lund, 1840, Lutken et al., 1893-1915). Research in caves continued during the present century in the Lagoa Santa area (Paula Couto, 1970, 1975), and in caves in the Bahia State (Cartelle, 1992, 1995). The data obtained from caves, supplemented by that collected in open sites, revealed a fauna characterised by several extinct species usually of large size, mixed with species that have survived to the present day.

Studies of fossil remains in Brazilian caves have had very poor stratigraphic and taphonomic control. Until recent years no radiometric dates had been assigned to the deposits. Based on correlation with similar but better chronologically constrained fauna in Argentina, the deposits have been assigned a late Quaternary age (Paula Couto, 1975). Cartelle (1995) believes that the vertebrate fossils in Brazilian caves were deposited in the transition between the end of the Pleistocene and beginning of the Holocene, in a single synchronous event. Doubts about the timing and spatial correlation between the deposits have however been expressed by other workers (Paula Couto, 1975, Marshall et al., 1984). Cartelle (1992, 1995) has stressed that all fossil cave deposits in Brazil are chronologically synchronous, and result from a palaeoclimate event of regional importance. This interpretation, pending a more precise sedimentological and chronological control, should be regarded with caution.

In more recent times, some radiometric ages for fossil remains in caves have been reported. Lumley et al. (1987) applied the $^{230}Th/^{234}U$ method for bones collected at Toca da Esperança, 170 km southwest from the study area, obtaining minimum ages between 204 - 295 ka. U-series dating of bones is notoriously difficult due to U uptake by the bone (Ayliffe and Veeh, 1988, Bischoff et al., 1988b), and these ages are widely regarded by Brazilian palaeontologists as unreliable (Cartelle, 1992, 1995). Czaplewski and Cartelle (1998) have reported uncalibrated AMS radiocarbon ages of 20 ± 0.29 ka for a humeri of fossil bat from Toca da Boa Vista, and 12.2 ± 0.12 ka for a coprolite attributed to *Nothrotherium* adhering to a cranium of a vampire bat at nearby Gruta dos Brejões. Elsewhere in Brazil, Laming-Emperaire et al. (1975) have reported an uncalibrated radiocarbon age of 9.6 ± 0.2 ka for remains of *Glossotherium* from Lapa Vermelha, and Piló (1998) has reported a U-series age of 77.7 (+3.8 -3.7) ka for a speleothem layer overlying fossiliferous sediment at Gruta do Baú, both in the Lagoa Santa karst area. In western Brazil, Vialou et al. (1995) have dated charcoal in sedimentary layers associated with remains of Mylodontinae by radiocarbon, obtaining an uncalibrated age of 10.1 ± 0.06 ka. These data, although still very limited, suggest that the fossil cave deposits may neither be synchronous nor restricted to the Pleistocene-Holocene transition, as previously believed. New data provided by this thesis will bring fresh evidence concerning this issue.

6.7.2. Modes of fossil emplacement in caves of eastern Brazil

Based on his extensive study of cave fossil deposits from the Lagoa Santa area, Lund (1844) believed that fossil remains could be brought into Brazilian caves by five possible processes: (1) by predators who used caves as a shelter; (2) by the occasional fall of animals in vertical fissures or shafts; (3) by animals entering caves in search of water or protection against the elements, becoming lost and dying; (4) by animals that inhabited the recesses of caves and died in them; (5) by transport by water as runoff into caves. Similar processes are recognised by Simms (1994), although he adopts a different classification of cave deposits.

Most of these processes can introduce bias in the fossil record. In the dry caves of the study area, material brought in by predators seems to be of minor importance, since most deposits are not concentrated near the twilight zone of cave entrances typically used by predators. Animals entering caves in search of water or protection (process 3) will introduce a bias in the fossil record as not every species is likely to enter caves, being limited by the characteristics of cave passages and by the ability to cope with the dark. The large bodied animals of the extinct megafauna could obviously not penetrate far into caves with narrow passages, while species with are better adapted to dark environments, such as some types of rodents or marsupials are more likely to enter and therefore die in caves. Furthermore, the degree of water dependency can vary between species (Behrensmeyer, 1991), introducing a bias on the type of animal that will enter caves in search of water. Process 4 (remains of animals that inhabit caves) will also bring a strong bias to the record as it will largely comprise species that use caves as a roosting site, such as bats, or as hibernacula such as the European fossil bear. Fossil remains brought into caves by water transport (process 5) will go through a hydrodynamic sorting since screening of bones can occur at cave passage restrictions, and heavier bones are less likely to be transported through longer distances than smaller ones (Simms, 1994). Apparently only process 2 (fall of animals in vertical pits) is likely to produce fossil deposits that are truly representative of the fauna existing outside the cave at the time of fossil deposition, although narrow pits can screen out large animals, while smaller more agile animals may be able to avoid the pit. However, bone accumulations at the bottom of vertical passages **inside** caves will carry the bias inherent to processes 3 or 4. The recognition of the process responsible for a particular fossil bone assemblage is essential in explaining the diversity of species present in the deposit and its possible representativeness of the local fauna at time of deposition. Such interpretation has hitherto not been applied to the bone bearing deposits from eastern Brazil and can help explain, at least in part, the apparent distinctiveness of faunas between caves in similar physiographic settings.

Considering the 5 processes discussed above, only transport by enhanced runoff in wetter periods (process 5) could be considered to be directly controlled by palaeoclimate, as will be addressed in section 6.7.5. Fossil deposits related to processes 1 to 4 of Lund's scheme are not strictly dependent on different past climate to explain their accumulation. Cartelle (1992, 1995)

believed that all fossil deposits in Brazilian caves were due to runoff transport and thus could be correlated to a more pluvial period. As will be seen in the following sections, the fossil accumulations studied in this thesis could not have been deposited by flowing water, and thus fossil deposition should not be correlated to any past climatic event. Any fossil-based palaeoclimate interpretation in the area should be focused on the fossil species presumed mode of living and probable palaeohabitat.

6.7.3. Fossil deposits in caves of the study area

A list of all fossil species found in the caves of the study area is presented in Table 6.4. Fossils found at Toca dos Ossos (location in Fig. 5.15), a cave not sampled in this thesis, are also included. The fauna comprise several species that could not have survived in the present caatinga habitat because the dry scrub vegetation would not have provided enough forage. The climate and vegetation in the area must have been very different to support such faunal assemblage.

SPECIES		CAVE
**Caipora bambuiorum*	large monkey	TBV
**Protopithecus brasiliensis*	large monkey	TBV
**Eremotherium laurillardii*	giant ground sloth	TO
**Glossotherium aff. G. lettsomi*	ground sloth	TO
**Scelidodon cuvieri*	ground sloth	TO,TBV
**Nothrotherium maquinense*	ground sloth	TBV
Myrmecophaga tridactyla	anteater	TBV
Tamandua tetradactyla	anteater	TO
Tolypeutes tricinctus	armadillo	TO
**Glyptodon clavipes*	giant armadillo	TO
**Pampatherium humboldtii*	giant armadillo	TO
Coendou sp	porcupine	TBV
Hydrochoerus hydrochaeris	capybara	TO
**Neochoerus sulcidens*	giant capybara	TO
**Myocastor coypus*	rodent	TO
**Protocyon troglodytes*	dog	TBV
**Smilodon populator*	sabre tooth tiger	TO,TBV
Puma concolor	puma	TBV
**Arctotherium brasiliense*	small bear	TBV
**Toxodon platensis*	hypopothamus-like animal	TO
**Trigonodops lopesi*	hypopothamus-like animal	TO
**Haplomastodon waringi*	mastodon	TO
**Equus neogeus*	horse	TBV
**Hippidion principale*	horse	TO
Tayassu tajacu	wild pig	TO,TBV
Lama guanicoi	llama	TBV
**Palaeolama major*	llama	TO
Odocoileus virginianus	deer	TO
Mazama gouazoubira	deer	TO,TBV

Table 6.4. List of vertebrates (except bats) found at Toca dos Ossos (TO) and Toca da Boa Vista (TBV) area, the latter including neighbouring caves as Toca da Barriguda and Toca do Calor de Cima. * indicates an extinct species. Adapted from Cartelle (1995).

6.7.3.1. Description of the studied deposits

6.7.3.1.1. Bone deposits (excluding bats)

With very few exceptions, the fossil deposits at Toca da Boa Vista (TBV) and Toca da Barriguda (TBR) are clearly concentrated around these cave's known entrances (Fig. 6.11), including a former entrance at TBV now blocked with sediment. The fossils are usually on the surface with minimal or no clastic sedimentation on the top of them. Only calcite precipitates, including subaqueous cave rafts, cover some of the bones. Except for a few sites in the bottom of internal pits, there is no marked accumulation of bones. The remains of individual animals are found isolated, their skeleton in either an articulated position, or showing minimal evidence of transport after death. Complete or near complete skeletons have been collected at some sites. The fossil individuals are found in several passage types, and at various elevations, but there appears to be a tendency of finding individuals in passages that contained static water in the past. Cartelle (1995) believed that most of the fossils were carried into the caves by episodic flood runoff events after death in the surface. He suggested that these events were of low energy, since the skeletons had undergone no significant post-depositional disturbance.

The degree of articulation of the skeletons indicates that no post-depositional disturbance has occurred at the majority of the sites. Decompositon and hence disarticulation tends to be rapid in aquatic environments, and any water transport would cause hydrodynamic sorting of this material, with smaller bones being dispersed (Behrensmeyer, 1991). Except for limited runoff in the immediate vicinity of entrances most cave passages appear to have been dry for extended periods of time, there is for instance no evidence of erosion of sediments and the development of graded stream profiles along irregular passage floors. Any major runoff events are also likely to bring clastic sediments into the cave. However, palaeomagnetism analysis of sediments adjacent to some of the fossil remains has demonstrated that some of these passages have been dry at least since the Brunhes/Matuyama reversal at 778 ka. In addition, the small catchment area of the dolines associated with the present cave entrances, and the passage morphology do not show any evidence of significant water input associated with the emplacement of the bones.

I believe that the fossil individuals found at Toca da Boa Vista and Toca da Barriguda entered the cave by their own means (*proprio motu*), in search of a cool atmosphere or water, became lost and died in the cave. Occasional falls into vertical passages inside the caves would result in a few sites with concentrated bone accumulation, but the majority of remains would be of individuals distributed at random within the vicinity of entrances. The absence of larger animals, that could not have wandered though the usually small passages of these caves, gives support to this hypothesis, since water runoff would undoubtedly have carried larger bones into the cave. The fact that several individuals were found in passages that had in the past contained water pools gives further evidence that water could indeed have been the main reason for these

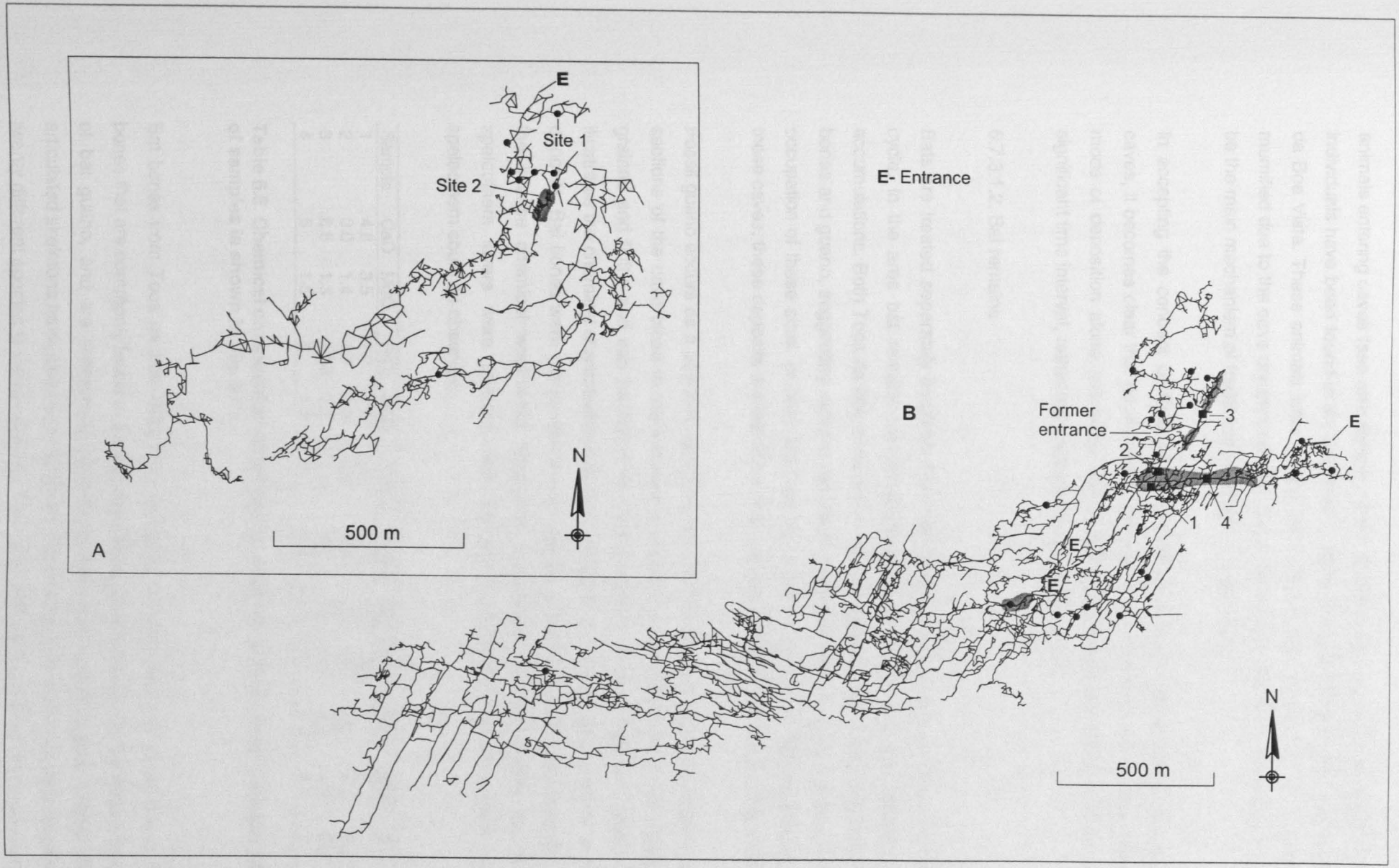

Figure 6.11. Location of fossil deposits at Toca da Barriguda (A) and Toca da Boa Vista (B). Dots indicate vertebrate fossil accumulation. Shaded areas indicate fossil bat guano. Black squares indicate guano samples from Table 4.5.

animals entering caves (see also Simms, 1994). Furthermore, a number of recent non-fossilised individuals have been found in dry passages in several caves in the study area, including Toca da Boa Vista. These animals were clearly not transported by water and are at present largely mumified due to the cave dry atmosphere. They give further support that *proprio motu* seems to be the main mechanism of fossil emplacement in these caves.

In accepting the concept of fossil accumulation via random penetration of animals into the caves, it becomes clear that no immediate palaeoclimatic inference can be made based on the mode of deposition alone, since the age of individual fossils are likely to be spread over a significant time interval, rather than representing a single event.

6.7.3.1.2. Bat remains

Bats are treated separately because these are animals that inhabit caves as part of their life cycle. In the area bat remains can be grouped in two classes, guano deposits and bone accumulations. Both Toca da Boa Vista and Toca da Barriguda show very extensive deposits of bones and guano, suggesting either a very large bat population in the past, a long history of bat occupation of these sites, or both. Because there are no significant bat colonies at present in these caves, these deposits are indicative of a different palaeoenvironment in the past.

Fossil guano occurs as a powdery deposit up to 1 m thick filling the floor of several passages in sections of the cave close to the entrances (Fig. 6.11). The sediment is dark grey, very fine grained and fluffy, and can be stirred into the atmosphere by a slight movement. Table 6.5 illustrates the chemical characteristics of these deposits. No stratigraphy is visible in most of the deposits. Bat bones were not observed, probably because they would have been consumed by the intense chemical weathering processes associated with the guano, but where later speleothem layers were present near the guano, extensive bone deposits overlain by speleothem could be observed.

Sample	CaO	MgO	SiO_2	Al_2O_3	Fe_2O_3	Na_2O	K_2O	P_2O_5	TiO_2	MnO	S	CO_2
1	4.8	3.5	7.7	1.4	2.3	0.3	3.3	10.2	-	-	-	66.5
2	3.0	1.4	1.7	0.5	0.7	0.1	0.4	0.5	0.5	0.1	2.4	89.8
3	6.5	1.3	13.6	3.1	2.9	0.3	0.8	4.8	4.8	0.2	0.6	64.2
4	5	1.5	5	1.5	2	0.5	2.5	3	< 0.1	0.1	2	58

Table 6.5. Chemical composition of bat guano deposits. Values in percentage. Location of samples is shown in Fig. 6.11.

Bat bones from Toca da Boa Vista area comprise accumulations of thousands of intermixed bones that are commonly found at distinct elevations, generally close to the major accumulations of bat guano, and are sometimes covered by later speleothem layers. Lesser deposits or articulated skeletons have also been observed. Czaplewski and Cartelle (1998) identified at least twenty different species in these deposits. The fossil deposit studied by Czaplewski and Cartelle (1998) was associated with cave rafts in a passage that had been flooded in the past, leading

these authors to suppose that the flooding event could have trapped a colony into a chamber, starving them to death. Although this hypothesis could explain this particular deposit, the majority of bat bone accumulations are found in passages well above the water table, that have not seen water for a significant period of time. Bat bone deposits, and guano, are likely to represent *in situ* accumulations, with minimal transport after deposition.

6.7.3.2. Sampling for ^{14}C and U-series dating

Because of the inherent difficulties and uncertainties associated with U-series dating of bones, only speleothems related to the fossil accumulations were analysed. Sampling calcite close to the bones proved impossible without damage, and therefore laterally equivalent calcite layers adjacent to the fossil remains were usually sought. Where this was not possible, material from above or below the bones were collected. Where speleothem from above the bone was sampled, minimum ages for the fossil were obtained, conversely speleothem from below the bone yielded an age interpreted as the maximum for the deposit.

Stalagmites or flowstones were the most common speleothem type associated with fossil bones. However, some skeletons lay on the bottom of rimstone pools, and were covered with a thin veneer of calcite which related to the time when the pool was full of water. A sample of the rimstone dam wall which was considered to be contemporaneous was therefore collected. Similarly, for bones interbedded in cave rafts in dry pools, it was assumed that the rafts which encased the bones were formed by the same event that precipitated more massive subaqueous speleothems or shelfstones, which were sampled in preference as they were larger and tended to be free of detritus.

Bat guano was also sampled for radiocarbon dating. A sample free of detrital material was selected and placed in a closed sterile plastic bag. Samples were kept isolated from any direct atmospheric contact until sent to the laboratory for analysis.

6.7.4. Chronology of the fossil deposits

6.7.4.1. Bone deposits (excluding bats)

U-series and radiocarbon ages for fossil remains at Toca da Boa Vista, Toca da Barriguda and Toca do Calor de Cima are given in Table 6.6. Three sites in Toca da Barriguda yielded ages for fossil skeletons. At site 1 (Fig. 6.12), an almost complete skeleton of the extinct small ground sloth *Nothrotherium maquinense* was found lying inside a rimstone dam, covered by a thin veneer of calcite. This calcite was too thin and dirty to be analysed. Two samples from the edges of the rimstone dam were analysed (TBR-09 and TBR-12). In sample TBR-09, collected about 50 cm from the bones, both the thin layer that covers the bones, and thicker layers below are represented (see insert in Fig. 6.12). The age (20.7 ± 0.7 ka) therefore should bracket a period

sample	fossil	U (ppm)	$^{234}U/^{238}U$	$^{230}Th/^{234}U$	$^{230}Th/^{232}Th$	$^{234}U/^{238}U_{t=0}$	age (ka) uncorrected	age (ka) corrected
TBR-09	*Nothrotherium*	0.093 ± 0.002	2.12 ± 0.04	0.175 ± 0.004	24.5	2.2	20.7 ± 0.7	-
TBR-12	*Nothrotherium*	0.079 ± 0.002	2.26 ± 0.04	0.234 ± 0.005	43.5	2.4	28.4 ± 1.0	-
TBR-10	*Mazama*	0.128 ± 0.002	1.95 ± 0.04	0.368 ± 0.008	9.8	2.1	48.2 ± 1.8	41.4 ± 1.7*
TBR-11A	*Nothrotherium*	0.041 ± 0.001	2.20 ± 0.05	0.205 ± 0.005	31.7	2.3	24.6 ± 1.0	-
TBR-07	*Nothrotherium*	0.037 ± 0.002	2.01 ± 0.14	0.166 ± 0.008	7.6	2.0	19.5 ± 2.2	15.5 ± 1.9
TBR-06	*Nothrotherium*	0.111 ± 0.001	1.69 ± 0.02	0.634 ± 0.012	15.3	1.9	100.4 ± 3.9	93.4 ± 3.7*
TBR-11	*Puma*	0.343 ± 0.004	1.81 ± 0.02	0.599 ± 0.011	12.1	2.0	91.7 ± 2.9	83.2 ± 2.7*
TCC-04	*Smilodon*	0.729 ± 0.010	1.49 ± 0.02	0.926 ± 0.018	752.8	1.9	211.8 (+13.9 -14.2)	-
TBV1-93	unidentified	2.354 ± 0.087	2.36 ± 0.03	0.562 ± 0.022	>1000	2.7	82.2 ± 4.8	-
TBV1-96	bat bones	0.041 ± 0.001	1.79 ± 0.05	0.148 ± 0.004	7.2	1.8	17.3 ± 0.7	13.5 ± 0.6
TBV-18	bat bones	0.209 ± 0.003	1.44 ± 0.02	0.095 ± 0.002	35.6	1.4	10.8 ± 0.3	-
TBV-32	bat bones	0.050 ± 0.001	1.18 ± 0.02	0.962 ± 0.022	23.6	1.4	275.2 (+ 41.0 -38.0)	-
TBR-13	guano	9.307 ± 0.588	3.37 ± 0.11	0.379 ± 0.023	>1000	3.7	49.0 ± 4.3	-

sample	material	lab number	radiocarbon age (ka)	calibrated age (ka)
TBV-1	guano	Beta-103616	16.7 ± 0.1	19.9 ± 0.1

Table 6.6. Uranium series and radiocarbon analyses of fossil remains and guano at Toca da Boa Vista (TBV), Toca da Barriguda (TBR) and Toca do Calor de Cima (TCC). Ages corrected assuming $^{230}Th/^{232}Th$ ratio of 1.7. Errors are ± 1σ. * denotes sample with U breakthrough in the Th spectrum. Radiocarbon age calibrated using the method of Bard et al. (1993). See text for sample details.

of active rimstone calcite deposition, but the bulk age is probably older than the bone itself. Sample TBR-12 is from an outer and higher dam wall that would probably have become dry before the smaller inner dam sampled by TBR-09, and yielded an age of 28.4 ± 1.0 ka. Both ages thus predate the actual time of fossil deposition, but clearly indicate active subaqueous speleothem deposition in the cave.

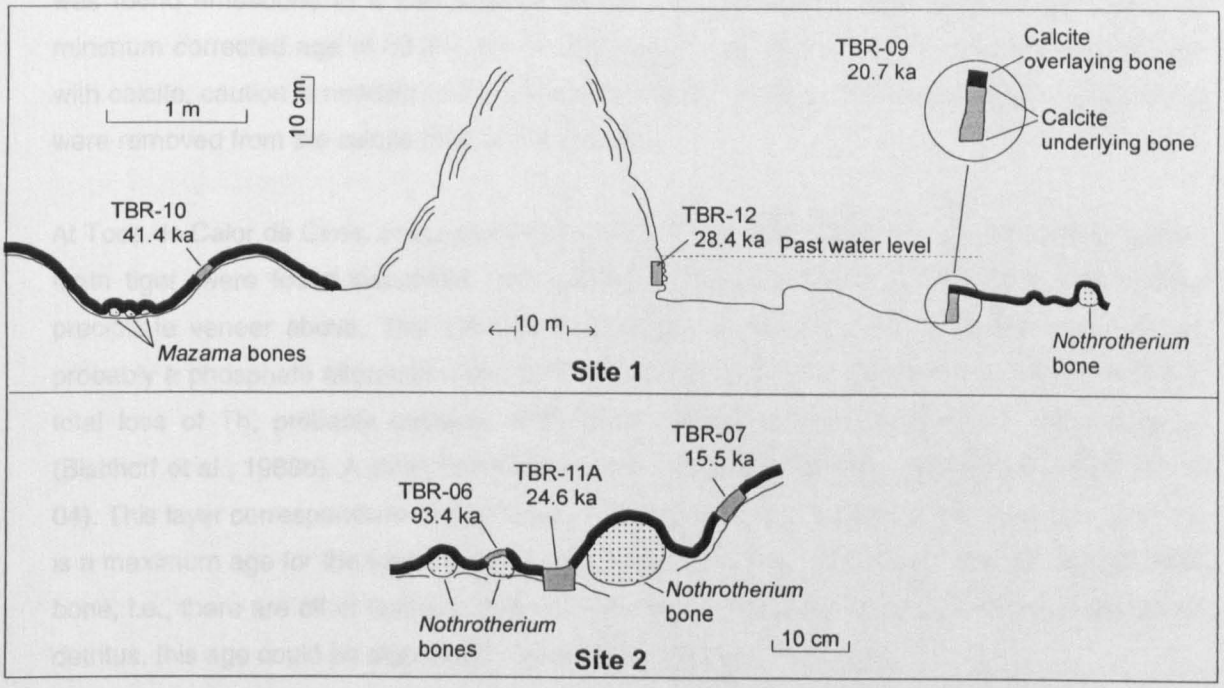

Figure 6.12. Schematic view of fossil sites 1 and 2 at Toca da Barriguda.

About 15 m from the *Nothrotherium* skeleton, remains of the fossil deer *Mazama sp* were found inside a depression in the floor of the cave passage. The fossil was covered by speleothem calcite, and a sample of it (TBR-10) was collected some centimetres from the bones. A corrected age of 41.4 ± 1.7 ka was obtained and should be interpreted as a minimum age for the fossil since most of the dated calcite was deposited after the bone.

Another skeleton of *Nothrotherium maquinense* was studied at site 2 in Toca da Barriguda (Fig. 6.12). This fossil was heavily embedded in flowstone calcite. Three dates were obtained from calcite associated with it. TBR-11A is the cleanest sample, but its calcite represents both the thin layer overlying the bone and the more massive calcite underlying it. The age of 24.6 ± 1.0 ka is probably a maximum age for the deposit. Sample TBR-07 was collected from above a fallen block immediately to the side of the fossil (Fig. 6.12) and is interpreted as corresponding largely to the calcite that overlies the bones. The corrected age of 15.5 ± 1.9 ka is thus believed to represent a minimum age for the deposit, although the sample is low in uranium and detritally contaminated. An additional sample (TBR-06) corresponds to calcite overlying fragments of bones scattered on the floor, which were left from the previous palaeontological excavation. The sample gave a disparate corrected age of 93.4 ± 3.7 ka. Because of the presence of bone material near the calcite sampled, there is the possibility of uranium remobilisation from the bone to the calcite or vice-versa as reported by Bischoff et al. (1988b). The somewhat higher uranium

concentration of this sample when compared with the two others supports this view. This age, therefore, should be regarded as unreliable. This skeleton of *Nothrotherium* was probably deposited between 24 and 15 ka ago.

Elsewhere in Toca da Barriguda, a skeleton of *Puma concolor*, the living South American puma, was found embedded in a thin layer of calcite. The layer was sampled (TBR-11) yielding a minimum corrected age of 83.2 ± 2.7 ka. Because this sample comprises bits of bones mixed with calcite, caution is needed in interpreting this result, although all observable bone fragments were removed from the calcite prior to the analysis.

At Toca do Calor de Cima, some scattered bones of *Smilodon populator*, the Pleistocene sabre-tooth tiger, were found deposited over speleothem calcite, with a very thin later secondary precipitate veneer above. This precipitate is largely composed of a non-carbonate material, probably a phosphate alteration crust derived from bat guano weathering. The analysis showed total loss of Th, probably because phosphates usually interfere with the Th ion exchange (Bischoff et al., 1988b). A clean calcite layer from a nearby stalagmite was also sampled (TCC-04). This layer corresponds to calcite below the bone, and thus the age of 211.8 (+13.9 -14.2) ka is a maximum age for the fossil. Because the sampled calcite layer is not immediately below the bone, i.e., there are other layers inbetween that were not analysed due to the likely presence of detritus, this age could be significantly older than the bone under study.

A stalagmite from Toca da Boa Vista, when sliced showed a broken fragment of bone embedded near its base. The base was dated at 82.2 ± 4.8 ka (TBV1-93), and probably corresponds to the age of the bone emplacement. Unfortunately, the fragmentary nature of the bone does not allow identification of the fossil (C.Cartelle, pers. comm.).

6.7.4.2. Bat remains

Three dates were obtained from calcite overlying thick fossil deposits of intermixed bat bones. Sample TBV1-96 yielded a minimum corrected age of 13.5 ± 0.6 ka. Sample TBV-18 was clean and gave a minimum age of 10.8 ± 0.3 ka. This sample is very porous, and recrystallisation may have occurred, the age should thus be regarded with caution. A further minimum age of 275.2 (+41.0 -38.0) ka (TBV-32) was obtained from a thick flowstone overlying bat bones. This sample includes an outer weathered calcite layer that was removed prior to analysis. The dated calcite is dense and non-recrystallised, and therefore closed system conditions are expected. The large age difference between this sample and those for all other bat remains could therefore indicate a much earlier period of bat bone accumulation.

Stalagmites growing over guano were analysed to provide minimum ages for these deposits. Due to intense weathering related to corrosion by the guano, all but one sample was considered unsuitable for dating. TBR-13 represents the base of a stalagmite growing over the major fossil

guano deposit in Toca da Barriguda. It yielded a minimum age of 49 ± 4.3 ka for this accumulation.

Radiocarbon dating of the guano gave an uncalibrated age of 16.7 ka for one of the accumulations at Toca da Boa Vista. This should be a true age for the deposit, and when calibrated (19.9 ± 0.1 ka) is in agreement with the ages obtained for bat remains. The data thus suggests that there was a vey large bat population in the cave during the last glacial maximum. The older ages obtained from sample TBR-13 and especially TBV-32 suggest that there was more than one episode of bat remains accumulation in the caves, although most of the deposits seem to correspond to marine isotope stage 2.

6.7.5. Discussion and palaeoenvironmental implications

Because the majority of the ages obtained are strictly minimum ages for the fossil deposits, it is difficult to interpret the chronology of the fossil deposits with any confidence, since the lag time between the bone emplacement and the speleothem deposition is unknown and can vary from site to site. However, it can be assumed that in general, speleothem deposition under a wet and somewhat warm climate should be fast enough to preclude a significant amount of time to elapse since bone deposition.

The group of ages obtained in this study is scattered throughout the last glacial period, with only one clear outlier. When considered in conjunction with two calibrated AMS radiocarbon ages reported by Czaplewski and Cartelle (1998) of 24.2 ± 0.2 ka and 14.3 ± 0.1 ka, it becomes clear that the age of fossil remains in the area do not fall into the Pleistocene-Holocene transition as proposed by Cartelle (1995), but spread over an extended period. The same may hold true for deposits from other areas, given a U-series age of 77.7 (+3.8 -3.7) ka for calcite overlying bone remains from the Lagoa Santa Karst reported by Piló (1998). Furthermore, these deposits do not appear to be synchronous, although a tendency of clustering into the last glacial maximum appears to exist. Whether this tendency can be interpreted as reflecting a more abundant fauna on the surface is a matter of debate.

A skeleton of the extinct canidae *Protocyon troglodytes* was found slightly buried in cave rafts associated with a bat bone radiocarbon dated at 24.2 ± 0.2 ka at Toca da Boa Vista (Czaplewski and Cartelle, 1998). The cave rafts are very possibly related to the major water table rise at the last glacial maximum constrained by dating of subaqueous speleothems (section 6.6). The canid skull is likely to have been emplaced at this time. Two complete and very well preserved skeletons of two species of extinct large bodied monkeys were found at one of the subaqueous chambers in Toca da Boa Vista (Hartwig and Cartelle, 1996, Cartelle and Hartwig, 1996). This chamber corresponds to the site where two older dates (144 and 167 ka) were obtained for water level calcite (site 2 in Fig. 6.9). The skeletons were not buried under the calcite rafts (C.Cartelle, pers. comm.), and appear to postdate this earlier (penultimate glaciation) water table

rise. They may therefore also be associated with LGM deposits; further ^{14}C dating is needed.

Since I believe that the vertebrate fossils entered the caves *proprio motu*, no palaeoenvironment can be indicated from the emplacement process itself. I therefore concentrate on the ecological requirements of each fossil species, inferred either from its present day habitat, or from functional morphology and/or relatedness to present-day species (Behrensmeyer, 1991). The small terrestrial ground sloth *Nothrotherium maquinense* is considered to be characteristic of an environment of transition between forest and savanna (Cartelle, 1995). It is believed that this animal was able to climb in trees as is the case for some modern species of small anteaters (Cartelle, 1995). The age of the *Nothrotherium* deposits from Toca da Barriguda suggests a moister environment with savanna and some forested areas during the last glacial period. The deer *Mazama* has survived to the present day, and is found mostly in environments with savannas and forest, although it can also occur in the caatinga. *Mazama* is therefore not an unequivocal palaeoenvironmental indicator. The same is true for *Puma* and possibly for *Smilodon*.

Czaplewski and Cartelle (1998), assuming that all bat remains at Toca da Boa Vista are contemporaneous with the 24 ka old dated bat bone, suggested that the environment in the surroundings of this cave was moister than at present during that period. Our finding that the bat deposits can span a much larger timescale, suggest other periods of increased humidity in the past.

Paula Couto (1970) and Guérin et al. (1990) proposed that the environment in the now semi-arid northeast was wetter in the past and the vegetation was probably of savanna or forest in order to support the extinct fauna. The large bodied, fossil, arboreal monkeys from Toca da Boa Vista led Cartelle and Hartwig (1996) to infer a vegetation with more continuous forest cover in the past. Cartelle (1992, 1995) interpreted the total assemblage of fossil species in the semi-arid northeast as characteristic of a savanna environment containing isolated patches of caatinga, but also areas of forest. In fact, analysis of the modern fauna of the caatinga suggests that the present species reflect an origin in more mesic environments, such as savanna or rainforest (Mares et al., 1985).

The different composition of the fossil fauna from Toca dos Ossos, about 90 km to the south, and those from the caves of Toca da Boa Vista area have been interpreted by Cartelle (1995) as implying a more forested environment at Toca da Boa Vista, compared to Toca dos Ossos where savannas prevailed. However, as discussed earlier, the mode of emplacement can introduce a strong bias in the fossil record derived from caves. Toca dos Ossos represents the swallet of a tributary of the Salitre River, and the fossils there were undoubtedly introduced by runoff from the swallet. Screening of small bones is likely to occur, and could explain the remarkable concentration of large bones in this cave. In contrast, I have suggested that the fossils at Toca da Boa Vista and associated caves were not transported by water, and that the

size of passages, and the habits of the animals would determine which species were more likely to penetrate into the caves. The geology, soil, and present day climate and vegetation of both sites are nearly identical, and therefore the differences in the fossil assemblages are likely to record taphonomical bias and should not be translated in terms of differences in palaeoenvironment.

6.8. CONCLUSIONS

Evidence from travertines, water table calcite and fossil remains suggests that the study area experienced increased humidity during the last glacial maximum. Palaeoclimate evidence is summarised in Fig. 6.13. The palaeoclimate data obtained for this thesis is supported by data from the offshore core of Arz et al. (1998) and from pedogenic calcite (Dever et al.,1987). The area appears to have been much more forested, as indicated by abundant fossil vegetation debris in the travertines and the inferred habitats of the fossil fauna. Further dating is needed to confirm the existence of additional periods of increased precipitation during the last glacial cycle, as suggested by Arz et al. (1998).

A wetter period during the penultimate glacial has been suggested by dating of subaqueous calcite at Toca da Boa Vista, and a further period of increased precipitation is indicated by travertine age, possibly at marine isotope stage 12. The precise delimitation of such periods await more detailed sampling and dating.

A wetter Brazilian northeast during the LGM appears to be in contrast with evidence from most of other lowland areas of Brazil. The bulk of palaeoclimate data for both the Amazon and subhumid savanna areas (see Figs. 6.2 and 6.3) suggests climates drier than present during the LGM. Such departure of humidity conditions in the northeast during the LGM finds an equivalence in modern times, when the present semi-arid climate is atypical for lowland Brazil. It appears that local topographic and atmospheric circulation features may cause the Brazilian northeast to respond to climatic cycles in such constrasting way.

6.8.1. Comparison with General Circulation Models (GCM) simulations

In section 6.2 the discrepancies between CLIMAP results and recent oceanic and terrestrial palaeoclimate records have been discussed. The maintenance of warm conditions in the tropical oceans during the LGM as predicted by CLIMAP are being challenged by a series of records (Guilderson et al., 1994, Thompson et al., 1995, Beck et al., 1997) including a noble gases study in northeastern Brazil (Stute et al., 1995), which predicted a 5.4 °C decrease in the area during the LGM. The response in terms of precipitation is less clear, and it is informative to ascertain how GCM simulations predict the increase in rainfall during the LGM for the now semi-arid Brazilian northeast suggested by this thesis.

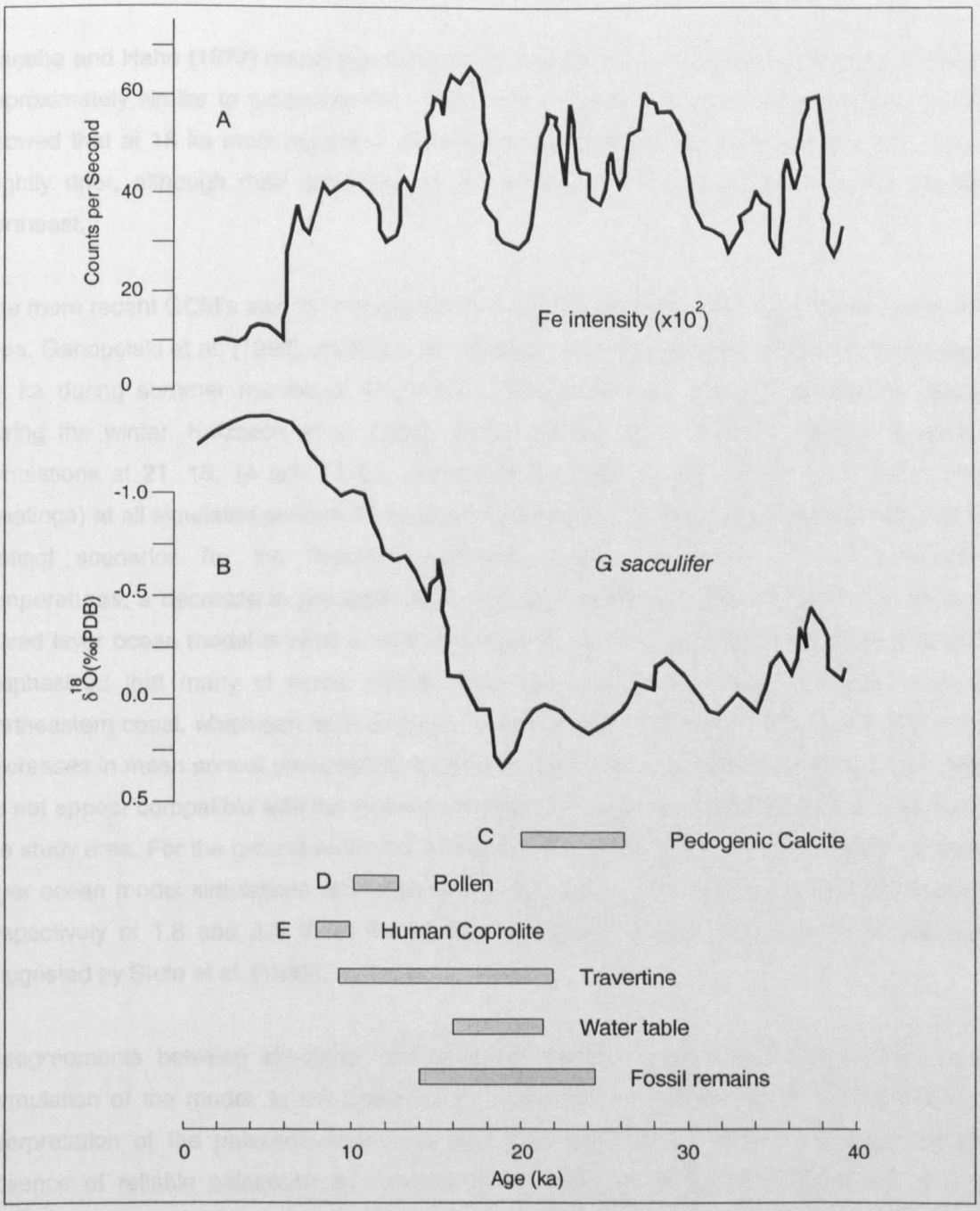

Figure 6.13. Summary of late glacial palaeoclimate data for northeastern Brazil. A - X-ray fluorescence intensity of Fe, and B - δ^{18}O foraminifera record of *G. sacculifer* from ocean cores GeoB 3912-1 and GeoB 3104-1 from Arz et al. (1998). C - From Dever et al. (1987). D - From Barreto (1996). E - From Chaves and Renault-Miskovsky (1996). Travertine, water table fossil remains data from this thesis. Fossil record includes data from Czaplewski and Cartelle (1998). Radiocarbon ages in C, D and E were connected using the procedure in Bard et al. (1993).

In all GCM's precipitation simulations are less reliable than temperature predictions (Ganopolski et al., 1998) and thus must be interpreted with care. While ice age aridity appears to have been the general pattern in the tropics, several departures from this scenario have been detected (section 6.2.1), including the Brazilian northeast. Mock and Bartlein (1985) stress that GCM's tend to have sufficient resolution for predicting large scale variations in the atmosperic circulation, but fail to simulate the smaller scale circulation features and their interaction with topography.

Manabe and Hahn (1977) model predicted P - E (precipitation minus evapotranspiration) levels approximately similar to present at the LGM in the Brazilian northeast while COHMAP (1988) showed that at 18 ka most regions in the tropics had rainfall similar to present levels or were slightly drier, although their database did not have any continental record in the Brazilian northeast.

The more recent GCM's also fail to represent the increased LGM precipitation levels in the study area. Ganopolski et al. (1998) predicts a precipitation decrease of approximately 0.8 mm/day at 21 ka during summer months of December-January-February, and no precipitation change during the winter. Kutzbach et al. (1998) model predicts P - E levels similar to present at simulations at 21, 16, 14 and 11 ka, and shows the maintenance of xerophytic scrub forest (caatinga) at all simulated periods. Pollard and Thompson (1997) global simulation obtained two distinct scenarios for the Brazilian northeast. Using prescribed CLIMAP sea-surface temperatures, a decrease in precipitation of around 5 mm/day is obtained at 21 ka, while if a mixed layer ocean model is used a sligth increase of around 1 mm/day is depicted. It must be emphasized that many of these models take into account the mean precipitation of the northeastern coast, which can be in excess of 1,500 mm/year (Strang, 1972). Some of the large decreases in mean annual precipitation predicted by the model of Pollard and Thompson (1997) do not appear compatible with the present semi-arid climate (annual precipitation of 490 mm) of the study area. For the ground water site of Stute et al. (1995) both the CLIMAP SST and mixed layer ocean model simulations of Pollard and Thompson (1997) predict a temperature cooling respectively of 1.8 and 2.3 °C at the LGM, considerably smaller than the 5.4 °C decrease suggested by Stute et al. (1995).

Disagreements between simulated and observed climates may reflect inadequacies in the formulation of the model, in the specification of boundary conditions, or in the coverage and interpretation of the palaeoenvironmental data (Kutzbach et al., 1998). The near complete absence of reliable palaeoclimate records for northeastern Brazil has represented a major constraint in the modelling of past glacial climates for the Brazilian northeast. The new evidence provided in this thesis will enable the improvement of resolution in GCM simulations.

CHAPTER 7
PALAEOCLIMATE SIGNIFICANCE OF PHASES OF SEDIMENT DEPOSITION AND EROSION IN CAVES IN EASTERN BRAZIL

7.1. INTRODUCTION

Many caves in eastern Brazil show unmistakable evidence of past phases of sediment input and erosion. In many cases, the input phases include not only clastic sedimentation but also chemical precipitation represented by speleothem layers within clastic material. Sediment infill can occur in the phreatic zone as discrete inputs through the roof in flooded passages, as autogenic sedimentation derived from insoluble residues in the bedrock, or as major inputs that lead to filling of most of the passage causing development through paragenesis. Sediment infilling in the phreatic zone has been discussed in Chapter 5 in relation to paragenetic development. In this chapter I will discuss the palaeoclimate related sedimentation phases that take place after the cave passage has reached the vadose zone.

Cave clastic sedimentation can be controlled by a number of factors. Foremost among them is the type of entrance configuration. Many cave entrances lie in the bottom of dolines, and thus are subject to runoff from the doline slope. These dolines may have developed synchronously with the cave, and thus may have behaved as a sediment source throughout the life history of the passage, or may represent a random (and later) feature that brings sediment to a cave passage where allogenic sedimentation was otherwise largely absent. Many caves represent swallet systems, and receive substantial fluvial sedimentation from the river basin. The source area of sediment in this case is much larger than in the doline situation, and may include several tributaries and extensive areas of valley slope. Furthermore, the vertical amplitude of water level rises in caves can be several times higher than on the surface (Gillieson, 1996) due to the "closed" nature of the passage. The fluvial setting is thus likely to represent a much more complex system due to its large extension and combination of slope and river channel settings. These two situations occur in eastern Brazil. Doline fed caves are ubiquitous in the Lagoa Santa and Campo Formoso Karst, and fluvial fed systems, such as Gruta do Convento, have been studied in the Campo Formoso Karst. Sedimentation processes derived from dolines or swallets are likely to respond to climatic changes, and will be studied in detail in this chapter.

Climate changes can also control sedimentation through variations in base level. A water level rise, or aggradation of the base level stream will lead to a decrease in channel gradient inside the cave, causing aggradation. This situation was observed to occur in Clearwater Cave, Sarawak (Farrant et al., 1995). There are, however, non-climate related causes of sediment accumulation/removal in caves. These include passage constrictions (due for instance to ceiling collapse) causing sediment accumulation upstream from the blockage. Conversely, plugging of entrance can restrict sediment influx into the cave, leading to a period of non-deposition preceded by normal sedimentation. Autogenic sedimentation, which includes insoluble residues

of the carbonate and biogenic materials such as guano can also be independent (or not directly related) of climate changes.

Cycles of erosion and sedimentation are commonly observed on the surface associated to hillslopes and fluvial systems, and have been linked to palaeoclimate changes (Bull, 1991). However, such a linkage is not simple because of the complex relationship between vegetation and precipitation, and due to variation of precipitation intensity. Factors that can influence input and removal of sediment include alterations in the density and type of vegetation cover, changes in rates of evapotranspiration, changes in the total amount and intensity of rainfall and its distribution throughout the year (Summerfield, 1991a). Additionally, anthropic landscape modification can also affect rates of sediment flux. The complex responses associated with palaeoclimate changes will control the processes of clastic sedimentation / erosion in hillslopes and fluvial systems.

Caves are subjected to the same palaeoclimate-controlled cycles of clastic sedimentation and erosion as surface terrains, but they also show palaeoclimate related *per descensum* chemical precipitation that does not have an analogue on the surface. Chemical precipitation represents meteoric water that percolates through the soil and bedrock before reaching the cave, and thus is independent of type of entrance or base level control, although in order to precipitate, it requires a substrate where water flow, sedimentation and erosion are absent.

Being isolated from the surface weathering, many cave sediment sequences will be preserved while equivalent surficial deposits will be washed away. Caves are, thus, natural traps of sediment. In addition they contain speleothem phases that can sometimes provide stratigraphical markers within the clastic deposits that can be dated by the U-series method up to 500 ka. Such material is generally absent on the surface, where the chronology is restricted to the short timespan covered by the radiocarbon technique.

7.1.1. Palaeoclimate cycles in caves in stable cratonic settings

Caves in low relief, tectonically stable areas such as the São Francisco Craton, will tend to remain within the range of palaeo water table variations for a more prolonged period than caves in tectonically active areas. This is because of the low rates of base level lowering compared to the recurrent interval of climatic changes, which means that short-term cyclic climatic events may affect caves at a given elevation for over several cycles before the site becomes inactive (Fig. 7.1). If one considers the rates of denudation in the São Francisco Craton reported by Harman et al. (1998) of 30 ± 10 m/Ma, and the water table variation obtained for the last glacial cycle at the Campo Formoso Karst, of 13 ± 1 m, any given fluvial cave passage once above the water table will be affected by at least 3 glacial/interglacial cycles, before being decoupled from direct water input. In tectonically active areas, many fluvial cave passages are drained too quickly to be affected by more than one palaeoclimate cycle. In caves fed by dolines, the

situation appears to be more complex because doline deepening (or aggradation) can depend on local factors, and a given sector in a cave can be under the influence of runoff for a more prolonged period.

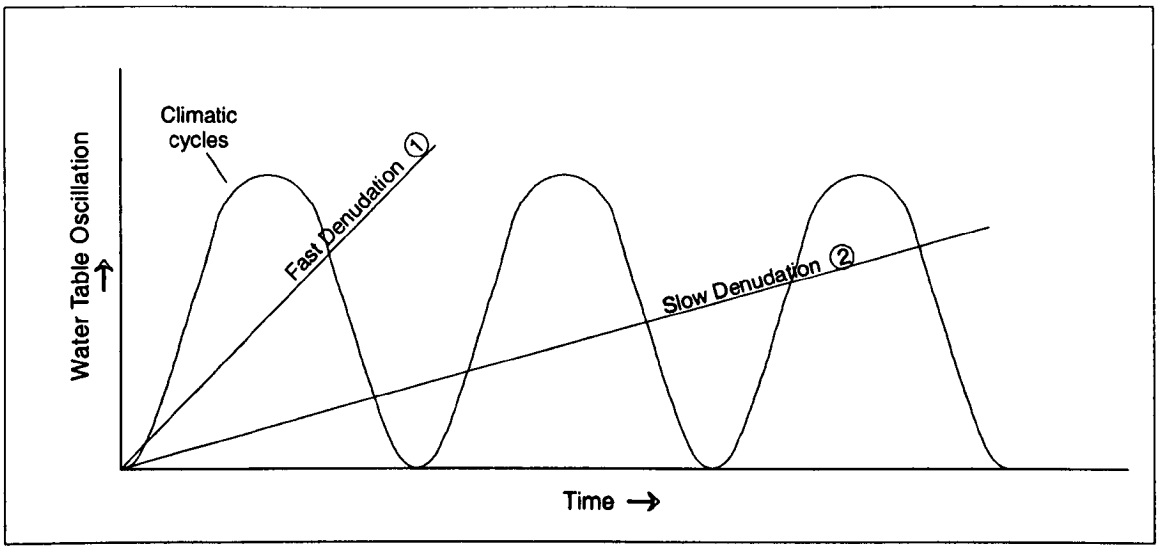

Figure 7.1. Schematic representation of the influence of palaeoclimate related water table oscillations in caves. Caves in areas with rapid denudation (1) will be affected by less climatic cycles than caves in stable cratonic settings (2).

The cratonic area of eastern Brazil presents an excellent opportunity to study the influence of past climatic changes on sedimentary cycles within caves. The climatic gradient between the semi-arid northern sector and the subhumid southern area allows the examination of the influence of the present climate in deposition and erosion of cave sediments and the determination of past periods where similar processes occurred.

7.2. MODES OF SEDIMENT INFLUX INTO CAVES

As discussed previously, the main modes of sediment input into caves are through a slope (or doline), or in a fluvial system via input through the swallet or aggradation of the base level. The slope and fluvial systems of sediment flux into caves will be discussed separately. Human induced changes in the sediment flux (by changes in land use, deforestation or fire) will not be taken into account in the following review.

7.2.1. Slope setting

In a slope system, the amount of sediment remobilised will be related to a balance between rainfall and vegetation. Factors such as soil type, slope gradient and temperature will obviously play a role but because vegetation usually offsets the effects on erosion of the other factors (Selby, 1993) it will be considered in detail.

The relationship between vegetation and sediment erosion is a complex one. Selby (1993) lists at least seven ways in which vegetation can influence soil erosion on slopes: (1) Interception of

rainfall by the vegetation canopy; (2) decrease of runoff velocity and hence the capacity of water to entrain sediment; (3) increase of soil strength, granulation and porosity due to growth of roots; (4) biological activities associated with vegetative growth and their influence on soil porosity; (5) transpiration of water, leading to the subsequent drying out of the soil; (6) insulation of the soil which reduces temperature fluctuations, which can cause cracking; (7) compaction of underlying soil.

There has been a long interest in the erosive response to an increase in precipitation. In what became known as the Huntington Principle (Fairbridge, 1968), Huntington (1907) stated that valley aggradation takes place in dry climates due to increased erosion on the slopes caused by removal of the protective vegetation cover, while valley incision occurs during wetter climates, when slope erosion is minimal. This effect has been demonstrated by Langbein and Schumm (1958) and Schumm (1965). The Langbein-Schumm Rule (Fairbridge, 1968) follows from the Huntington Principle, stating that to a decrease in precipitation corresponds an increase in erosion down to a limit, below which further a decrease in precipitation results in decreasing erosion until both variables reach zero (Fig. 7.2).

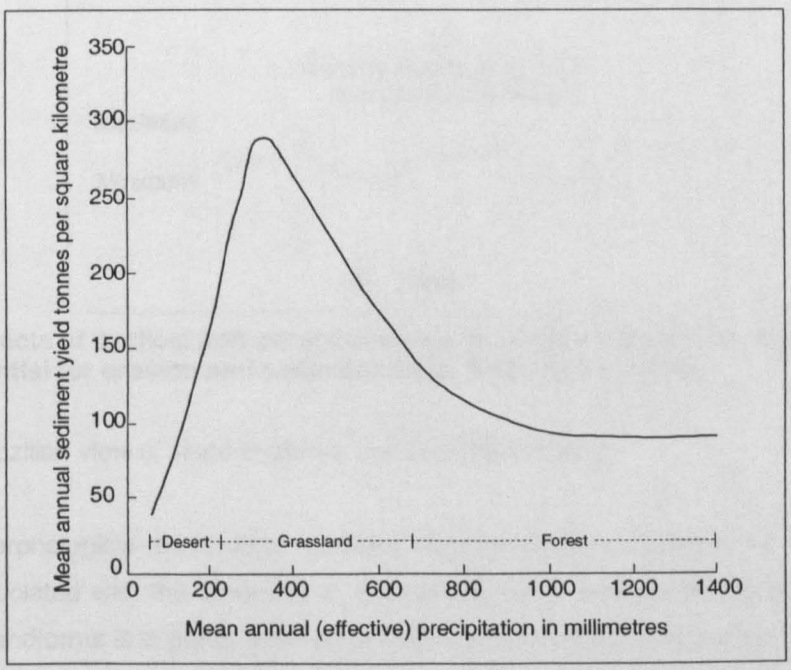

Figure 7.2. Relationship between sediment yield and rainfall in hillslopes as described by the Langbein-Schumm Rule. From Knox (1984).

Abrupt shifts in climatic regimes will also have a marked effect on slope erosion. The greatest instantaneous sediment yields are probably associated with a rapid change from arid to humid climate because the increased precipitation would fall on a surface which is initially unprotected from vegetation (Knox, 1972). Such a large yield should, however, be short lived because of the rapid vegetation response to climatic change (Knox, 1972). The effect of cyclical changes of precipitation on vegetation, slope erosivity and sediment yield are illustrated in Fig. 7.3. Increase in rainfall seasonality can also affect the balance between vegetation and erosion. Such

parameters have been modelled for fluvial systems (Tucker and Slingerland, 1997) and will be discussed in section 7.2.2.

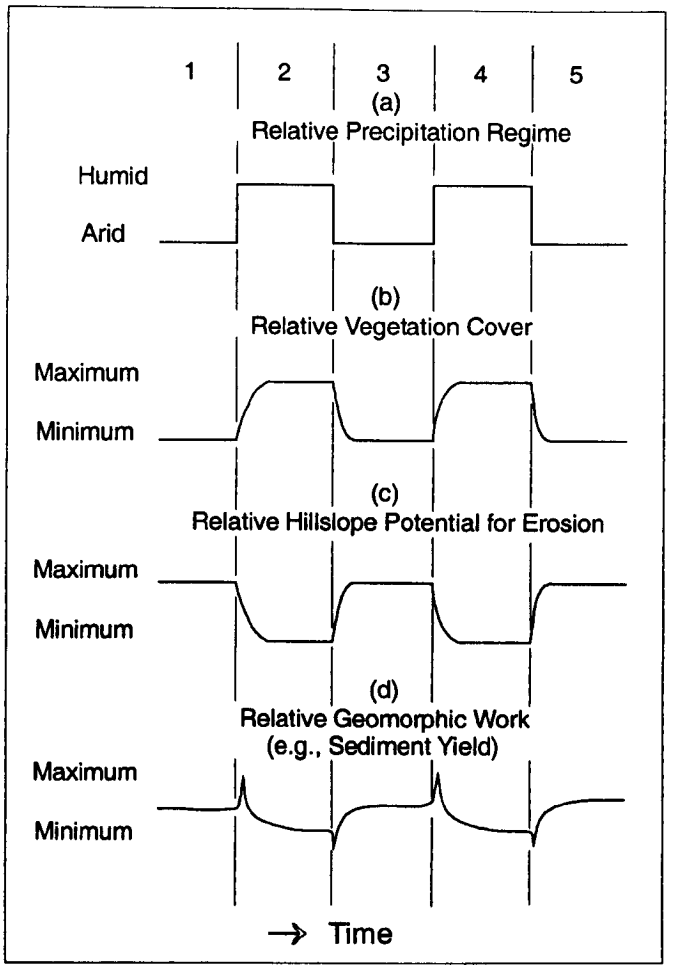

Figure 7.3. Effects of cyclical and abrupt changes in rainfall intensity on vegetation cover, hillslope potential for erosion and sediment yield. From Knox (1972).

7.2.1.1. The Brazilian view of slope evolution due to climate change

Brazilian gemorphologists have long adopted the Huntington Principle in explaining the processes associated with the evolution of tropical slopes. In eastern Brazil, one of the most characteristic landforms is a gently inclined, slightly concave slope (Clapperton, 1993a) with an associated pediment that generally exhibits well marked horizons of pebbles, known as stone lines, covered by fine grained material (Lichte, 1990). Such features have been explained by an evolutionary model (see review in Clapperton, 1993a) that invokes erosion of the slope during semi-arid phases causing pedimentation and development of a lag of residual pebbles (the stone lines), followed by periods of increased moisture where vegetation would shield the soil from erosion and thick weathering mantles would be produced (Bigarella and Ab'Saber, 1964, Bigarella and Andrade, 1965, Bigarella and Mousinho, 1966, Meis and Monteiro, 1979, Bigarella and Andrade Lima, 1982, Ab'Saber, 1982). It has been assumed by these authors that since pedogenesis is occurring during the present subhumid climate, and the stone lines are found

buried under a mantle of soil then they were generated in a previous dry phase, assumed to have occurred during glacial periods.

The palaeoclimatic model inferred by Brazilian geomorphologists, however, lacks rigorous field testing and needs to be chronologically constrained before it can be accepted (Clapperton, 1993a). A possible alternative to this model would be the generation of both stone lines and soil cover during the same climatic phase, in which stone lines would be produced as lag deposits in a dry climate, while high intensity low frequency storms under the same climate would produce a colluvial mantle over the stone lines (Clapperton, 1993a).

7.2.2. Fluvial setting

The dynamics of the sediment flux in fluvial systems are much more complex than in the simpler slope setting. Because the river basin can extend for a considerable area and include many slopes, the response in terms of sedimentation can vary depending on the portion of the drainage basin under consideration. Aggradation and degradation phases can occur simultaneously in different sectors of the system (Tucker and Slingerland, 1997).

The Huntington Principle states that channel aggradation should occur during dry phases due to an increase in sediment flux from side slopes, while river incision would occur during more humid periods when vegetation stabilises the hillslopes reducing runoff, peak discharge and sediment supply. However, a radically different view is offered by Bryan (1928) who argued that greater storm runoff due to loss of vegetation during arid periods would produce channel entrenchment rather than aggradation. Bryan believes that aggradation would occur instead during the transition towards cooler and more humid conditions, as stream energy is reduced. Both Huntington's and Bryan's views have been supported by field studies (see review in Tucker and Slingerland, 1997).

Blum et al. (1994) have stressed that there may be variations in response to climate change along the same drainage basin, either between upstream and downstream reaches or between tributaries and trunk streams. Furthermore, the same climatic change can cause very distinct effects in drainage basins in different physiographic settings due to variations in parameters such as geology (Blum et al., 1994).

Although in general vegetation will tend to shield the slope against erosion and reduce the sediment yield to a fluvial channel, vegetation growth in the channel can trap sediment and cause aggradation as observed in Australia (Prosser et al., 1994). Natural fire can also play a role. Because fire is also associated with dry spells, fire will help remove vegetation and increase the rate of erosion (Meyer et al., 1992). The amount of sediment available for erosion in the upstream reaches of the drainage basin (or in the hillslopes) will also be of paramount importance. If during dry episodes of hillslope erosion the soil supply is exhausted, sediment

yield will be dramatically reduced and intensive runoff over bedrock is likely to cause incision on the fluvial channel (Bull, 1979). In such a situation, the same dry phase is capable of producing both aggradation and erosion of the channel bed.

Base level change can complicate the picture because it can control aggradation and degradation in a similar way to changes in precipitation. Base level rise will lower the stream gradient, resulting in an accumulation of sediment that is thickest downstream and thins upstream (Weninger and McAndrews, 1989). A drop in base level, on the other hand, will initially promote incision, but as the increase in channel gradient diffuses through the system the sediment supply from the upper tributaries increases to the point where the downstream channel is incapable of transporting all the sediment being delivered and aggradation begins (Summerfield, 1991a). The aggradation then extends upstream, reduces channel gradients and leads to a decrease in upstream erosion and sediment supply which allows channel incision to begin again downstream (Summerfield, 1991a).

Attempts to model the complex response of fluvial systems to climatic change have provided interesting new insights into the problem. For instance, Tucker and Slingerland (1997) experimented with changes in the magnitude of runoff events (keeping annual runoff unchanged) and changes in the temporal interval between precipitation shifts. An increase in the magnitude of precipitation events resulted in rapid valley aggradation, followed by slow downstream propagation of erosion when the sediment influx diminished either due to bedrock exposure or gradient reduction (Tucker and Slingerland, 1997). Shortening the period between precipitation changes caused a disequilibrium in the sediment flux in the basin. The catchment will have insufficient time to restore between cyclical changes, and the sediment yield will be reduced in subsequent cycles compared to that from longer period changes (Tucker and Slingerland, 1997). Such short term aggradation/erosion cycles have been observed to occur in nature (Rumsby and Macklin, 1994).

The modelling experiment of Tucker and Slingerland (1997) demonstrates the importance of seasonality in controlling cycles of aggradation and degradation in fluvial systems. Such cycles were observed to occur during a change either to more humid or to more arid conditions (Tucker and Slingerland, 1997). These studies illustrate the complexity of the process and may help explain why both aggradation and erosion have been correlated with the same climatic condition in different parts of the world (Tucker and Slingerland, 1997). Caves fed by fluvial systems may, thus, exhibit a varied and complex sedimentary history during past climatic changes.

7.3. SEDIMENT DEPOSITION AND EROSION IN CAVES

Relatively few studies have been performed on the timing and palaeoclimate significance of episodes of sediment infill and erosion in tropical caves. Many studies lack chronological control and will not be considered in this review. It appears that, although dateable calcite speleothems

are frequent in caves, speleothem units within sediment which allow the depositional sequence to be chronologically constrained are more rare. Five major conditions of clastic and chemical sedimentation/erosion can occur in caves: input of clastic sediment; speleothem deposition; input of sediment intermixed with speleothem; erosion of clastic and chemical sediment; and absence of any type of allogenic sedimentation.

Clastic sediment deposition in caves is usually interpreted as indicating dry conditions, sparse vegetation and intense sediment yield due to runoff (Brook et al., 1997, Brain, 1995a). The majority of such studies, however, are of caves fed by doline slopes. In this situation, the elevation of the sediment fill in the cave is limited by the elevation of the doline upper lip. As infilling proceeds, however, doline slope gradients will tend to decrease, and rates of sediment input should diminish. In the ever wet New Guinea Highlands (rainfall between 3500 - 9000 mm), Gillieson (1986) attributed sediment input into caves to mass movements. Such a process does not appear to play an important role in subhumid tropical environments.

Speleothem deposition has been traditionally interpreted as due to a wet climate, when there is enough water to infiltrate towards the cave. Studies of speleothem frequency in tropical areas (Hennig et al., 1983) demonstrate a relationship between speleothem growth and more humid periods. Thick soil and abundant vegetation will also tend to increase carbonic acid levels in the percolation water, increasing the solutional load available for speleothem precipitation. It should be emphasised, however, that absence of speleothems at a local level does not necessarily imply dry conditions. As pointed out by Frank (1975), high water levels, especially in river caves, can prevent speleothem formation either by erosion, water ponding, or continuous clastic sedimentation. Speleothem deposition is thus likely to reflect not only wet conditions, but also a stable cave environment in which major episodes of clastic sedimentation, erosion, or water table rise are absent.

Speleothem deposition can occur simultaneously with sedimention, creating a carbonate rich sediment, or dirty speleothem. This situation may be due to sediment percolating from the surface through the same joint system that feeds water to the speleothem, or be caused by sediment brought by seasonal flooding to the speleothem depositing site. In both situations, wet conditions are needed. An exception is when *per ascensum* precipitation deposits a carbonate layer on the top of fine grained material, in a similar way as with calcretes under arid conditions in subaerial settings. This process probably occurs in some sites at the Lagoa Santa Karst.

Clastic sediment erosion is probably the least understood of these processes. Most authors (Brook and Nickmann, 1996, Brook et al., 1997, Brain, 1995a) correlate such events with wet periods with well developed vegetation that prevents soil erosion. However, the relationship between such humid conditions and those that cause speleothem growth is less clear. Brook et al. (1997) believe that sediment erosion implies a wetter environment than that associated with speleothem growth, because speleothem erosion takes place in such events. However,

speleothem growth rates increase with effective recharge, provided that the deposition occurs away from the flood range. In early writings, Brook (1982) attributed the erosion of sediment and speleothem to a higher water table, and thus a wetter period. A high water table does not appear to be required, especially in the doline setting, as much of the runoff downslope, even during wet periods, is likely to be associated with a perched water body or vadose streams. Nonetheless, ponding during such phases can occur, preventing sediment erosion.

The last possible scenario is absence of allogenic sedimentation. Caves that do not have an opening to the surface, such as hypogenic caves, will not show clastic sedimentation, except for autogenic deposits. Absence of sedimentation, in this case, cannot be correlated to any climatic episode. Similar effect can be caused by entrance blockage by collapse.

Despite the obvious potential of caves and the ubiquitous presence of large deposits of sediment within them, very little is understood at present about the palaeoclimate significance of such deposits. Lessons can be gained from detailed studies of doline fed archaeological sites in caves in South Africa and Europe. Brain (1995b), when referring to the extremely well detailed stratigraphy of the hominid-bearing cave deposits in South Africa, states that the complexity of the stratigraphy is such that it is impossible to assume adjacent sections of sediment have the same age. Campy and Chaline (1993) in their correlative review of cave archaeological sites in France concluded that: (1) The thickness of any given sediment bed may vary intrasite and intersite, (2) a given climatic change is not always represented by the same sedimentary facies at each site, (3) sedimentation on the bedrock floor of the cave does not always start at the same time, (4) there are depositional breaks in the sedimentation that are diachronous from one site to another. Despite these difficulties, the sediment input / erosion cycles in a number of caves in eastern Brazil were studied. Comparative analysis was performed in caves in the semi-arid Brazilian northeast and in the subhumid southeast, and attempts were made to correlate such events with palaeoclimate changes in the area.

7.4. SEDIMENT CYCLES OF INPUT/EROSION IN CAVES IN EASTERN BRAZIL

Sediment filled passages with associated speleothem layers, or remnants of speleothem layers at different heights in the passage are common features in the caves of eastern Brazil. These features have been noted and described since these caves were first excavated by palaeontologists in the early 19th century (Claussen, 1841, Lund, 1840). Evidence of cycles of sediment input and erosion in caves have been observed throughout the São Francisco Craton, irrespective of present climate. Selected deposits were studied in caves located in the now semi-arid area of the Campo Formoso Karst in northeastern Brazil and in the subhumid area of the Lagoa Santa Karst in southeastern Brazil to determine if distinct phases of sediment infill had occurred, and to assess the extent to which they were determined by palaeoclimate.

7.4.1. Semi-arid northeast

At present the ephemeral fluvial systems in the Campo Formoso area are undergoing aggradation. The floor of the dry Salitre River bed has about 4 m of clastic sediment where observed in a hand dug well, and trees located on the valley sides can be observed to have their trunks buried by over 0.5 m of sediment washed downslope. The aggradation is caused by the sparse caatinga vegetation and the occurrence of brief and violent thunderstorms that allows intense sediment erosion on slopes. The situation appears to have been made worse by anthropic removal of vegetation. Transportation of the sediments accumulated on valley floors or at the slope base is prevented by the near complete absence of active flowing streams in the area. The Pacuí River, the sole perennial stream, is at present an underfit stream running over an alluviated valley floor. The Pacuí River does not appear to be effectively downcutting the alluvial floor of the valley, as there is no major break on the valley floor associated with the active river channel. Valley floors and slope bottoms are thus aggrading at present, and there is no evidence of fluvial channel excavation or sediment removal in the area. No active speleothem deposition is occurring in the caves of the area at present. Sediment sequences were studied in three caves (Tiquara, Convento and Caboclo) where events of sediment infill and erosion can be observed.

7.4.1.1. Slope setting: Toca da Tiquara

Toca da Tiquara is developed in Una Group carbonates and is located a few kilometres from the town of Tiquara, about 50 km to the southeast of Toca da Boa Vista (Fig. 4.12). Toca da Tiquara (Fig. 7.4) is a 1 km long cave that displays hypogenic morphological features similar to many of the caves in the area. The cave has extensive clastic sediments and speleothems, exposed following excavation by saltpeter miners.

The only entrance to Toca da Tiquara lies at the bottom of a shalow doline with a catchment area that do not exceed 1,000 m^2. This doline is considered to be the dominant source of sediments as there are no other entrances at present, and the cave is completely decoupled from any fluvial system. However, it is possible that in the past some sediment was derived from now sealed upper entrances and even by biogenic *in situ* processes, such as bat guano accumulation. The sediments at Toca da Tiquara were clearly deposited under vadose conditions, after the cave had drained as there are abundant speleothem layers buried under the sediment. The bedrock floor is not exposed near the sampling sites at Toca da Tiquara, and sediment thickness may be in excess of 2 m. Five samples were collected for Uranium series dating and the analyses are reported in Table 7.1. Sample locations are shown in Fig. 7.4.

Because the speleothem layers sampled were buried under sediment, detrital contamination was to be expected. However, despite the presence of sediment, the samples are composed of dense non-porous calcite. Three out of the five samples showed $^{230}Th/^{232}Th$ ratios below 20,

indicating presence of significant amounts of detrital thorium. However, three samples collected from correlative calcite horizons (TTQ1-96, TTQ-02, TTQ-05) showed nearly identical ages for one uncorrected and two age corrected samples (Table 7.1), and the three samples from the same sequence (TTQ-03, TTQ-04, TTQ-05) are in correct stratigraphical order, suggesting that the U-series ages obtained are reliable.

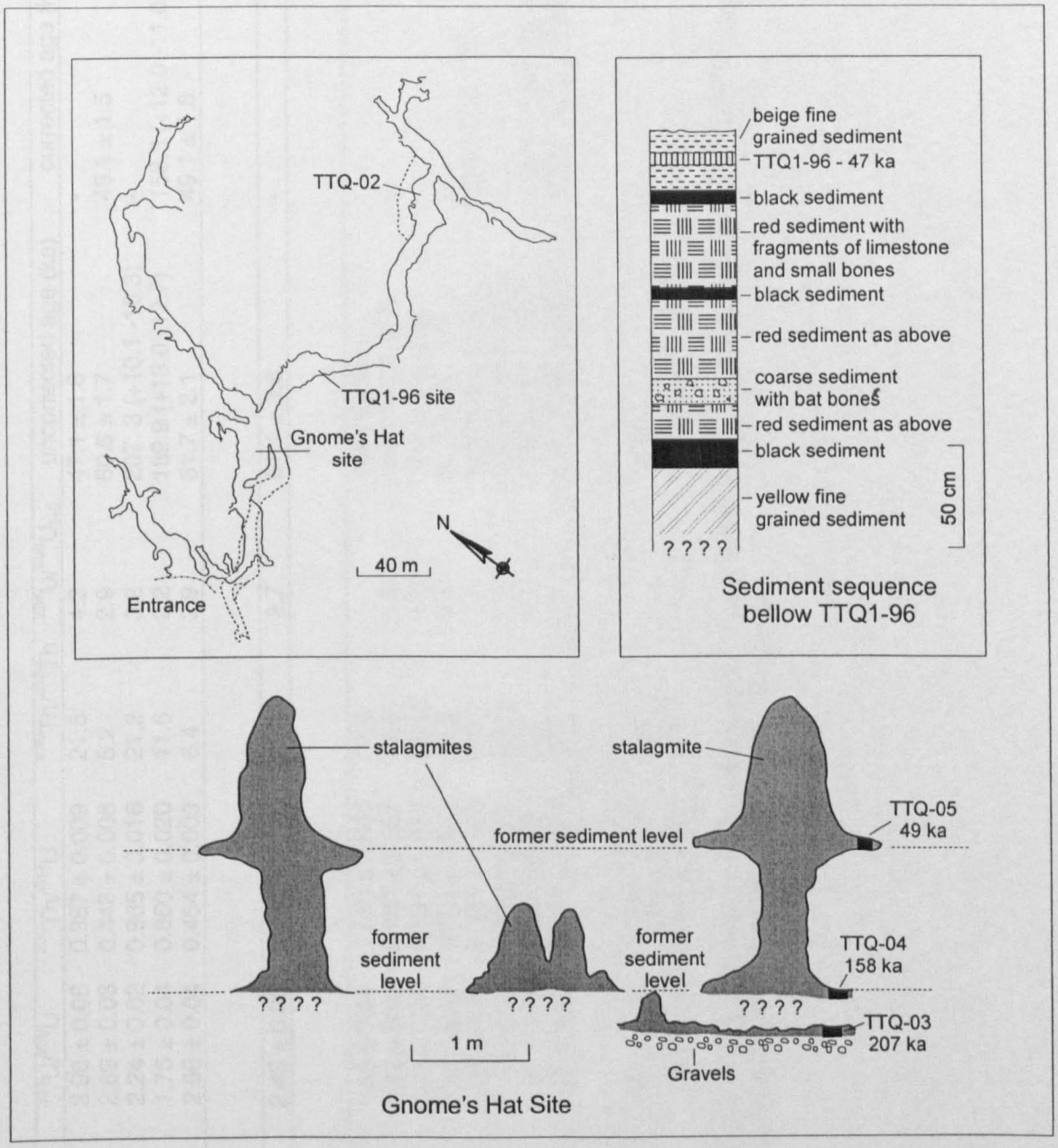

Figure 7.4. Plan of Toca da Tiquara and sketch of sampling sites. Cave survey by Grupo Bambuí de Pesquisas Espeleológicas.

Three samples were collected from the "Gnome's Hat" site, a group of stalagmites that were buried by separate phases of sedimentation (Fig. 7.4). Due to the size and sensitivity of the formation, only the sides of the deposit were sampled. The inner portion, which should represent the older phase of the stalagmite, was not sampled. An initial small stalagmite (TTQ-03) deposited over gravels, yielded a basal age of 207.3 ± 10.3 ka (Table 7.1). This was buried by sediment, and a group of stalagmites and a sloping speleothem layer (the hat "brim", sample

Sample	U ppm	$^{234}U/^{238}U$	$^{230}Th/^{234}U$	$^{230}Th/^{232}Th$	$^{234}U/^{238}U_{t=0}$	uncorrected age (ka)	corrected age (ka)
Toca da Tiquara							
TTQ1-96	0.198 ± 0.004	3.96 ± 0.06	0.367 ± 0.009	21.5	4.3	47.1 ± 1.8	-
TTQ-02	0.066 ± 0.001	2.69 ± 0.03	0.448 ± 0.008	5.2	2.9	60.6 ± 1.7	45.1 ± 1.5
TTQ-03	0.104 ± 0.001	2.24 ± 0.02	0.965 ± 0.016	21.2	3.2	207. 3 (+10.1 -10.3)	-
TTQ-04	0.107 ± 0.002	1.75 ± 0.04	0.860 ± 0.020	11.6	2.2	169.9 (+13.0 -12.7)	158.3 (+12.0 -11.0)*
TTQ-05	0.162 ± 0.003	2.66 ± 0.04	0.454 ± 0.009	6.4	2.9	61.7 ± 2.1	49.1 ± 1.8
Gruta Clovis Saback							
GCS1-96	0.137 ± 0.005	2.43 ± 0.08	0.450 ± 0.014	200.3	2.7	61.1 ± 3.8	-
Gruta do Convento							
GCV1-96	0.063 ± 0.002	1.55 ± 0.04	1.253 ± 0.034	17.6		open system	
GCV-04	0.044 ± 0.001	1.40 ± 0.05	0.627 ± 0.021	28.0	1.5	101.1 (+9.3 -8.7)	-
GCV-07	0.055 ± 0.002	1.24 ± 0.05	0.291 ± 0.011	253.2	1.3	37.2 (+2.6 -2.5)	-
GCV-08B	0.079 ± 0.003	1.22 ± 0.05	0.425 ± 0.017	35.3	1.3	59.3 (+4.7 -4.5)	-
GCV-08T	0.050 ± 0.001	1.33 ± 0.04	0.324 ± 0.010	6.6	1.4	42.0 (+2.4 -2.3)	32.8 (+2.0 -1.9)
GCV-09	0.102 ± 0.002	1.15 ± 0.02	0.992 ± 0.022	250.4	1.4	328.0 (+54.9 -57.6)	-
GCV-10	0.016 ± 0.001	1.66 ± 0.06	0.856 ± 0.027	3.5	1.9	170.8 (+21.4 -19.7)	124.4 (+13.6 -12.1)
GCV-12	0.016 ± 0.001	1.38 ± 0.09	0.916 ± 0.043	5.0	1.6	212.2 (+64.1 -48.4)	179.2 (+45.7 -32.6)
Toca do Caboclo							
TCB-01	0.149 ± 0.002	1.10 ± 0.02	1.107 ± 0.024	9.7	-	>350	
TCB-03	0.510 ± 0.011	1.12 ± 0.01	0.843 ± 0.031	320.0	1.2	189.2 (+18.1 -20.7)	-

Table 7.1. Uranium series analyses of speleothems from the semi-arid northeast Brazil. Ages corrected assuming a $^{230}Th/^{232}Th$ ratio of 1.7. Errors are ± 1σ. * denotes sample with U breakthrough in the Th spectrum.

TTQ-04) grew on the sediment surface. TTQ-04 yielded a detritally corrected age of 158.3 (+13.0 -12.7) ka. Although TTQ-04 was sampled close to the base of the "brim", it is possible that due to either thinning or progradation of layers on the stalagmite side, the sample also contains younger layers. A further major episode of clastic sediment infill over 1 m thick occurred, followed by reactivation of two of the larger stalagmites, and development of another hat brim at the sediment surface (sample TTQ- 05). TTQ-05 is a detritally contaminated sample that yielded a corrected age of 49.1 ± 1.8 ka. This sample is correlative with samples TTQ1-96 and TTQ-02 collected elsewhere in the cave that yield ages respectively of 47.1 ± 1.8 ka and 45.1 ± 1.5 ka, the latter being a detritally corrected age and also showing significant tailing on the Th spectrum. Another clastic sedimentation phase occurred over the speleothem. Removal of the clastic sediment by saltpetre miners has exposed the present sequence.

The Gnome's Hat site shows that at least four sediment infill events occurred in the cave. The first event happened sometime before 207 ka, and is locally represented by small gravels indicating an environment of high energy. The nature of the second fill deposited between 207 and 158 ka is unknown as it was entirely removed by the miners. The third infill phase occurred between 158 and 47 ka, and is represented by a complex sequence composed mostly of fine grained material. Below sample TTQ1-96, the sequence is about 2 m thick and the base of it was not reached by the miners (Fig. 7.4). However, it is not clear if the calcite deposits represented by sample TTQ-04 are locally absent in the TTQ1-96 sequence or were not reached by the excavation. The layers in this sequence are laterally continuous for over 10 m in some trenches. The sediment sequence contains some organic horizons and bone rich sediments, and could therefore be at least partially autogenic. After 47 ka a last episode of fine grained sediment fill, little over 10 cm thick near sample TTQ1-96 occurred.

Toca da Tiquara exhibits phases of chemical and clastic sedimentation but lacks cycles of sediment erosion, common in other caves. Nearby, a small cave by the side of the Campo Formoso-Tiquara road, close to the Clovis Saback Quarry was sampled. This cave, named as Gruta Clovis Saback, contains a well developed speleothem false floor about 10 cm thick that presently hangs about 1 m from the sediment floored passages. The sample (GCS1-96) yielded an age of 61.1 (+3.9 -3.8) ka (Table 7.1), which is to be considered as an average age for the layer, since no depositional breaks were observed. This speleothem layer deposited over sediment that was washed away at a later stage.

7.4.1.2. Fluvial setting: Gruta do Convento

Gruta do Convento is a branchwork cave that receives water from two separate swallets whose catchments extend onto the quartzite terrains (see previous description on section 5.4.3). At present there is no flowing water in the cave, but there are a series of large rimstone dam pools which precipitate calcite cave rafts. A very thick (c. 15 m) sequence of speleothems and fine grained sediments occurs in the main trunk passage of this cave (Fig. 5.19). This sequence (Fig.

7.5) apparently used to prograde across the passage before it was reexcavated by the cave stream. The sediment sequence marks an extended aggradational phase in which the passage was filled with both sediment and speleothems until about 2 m from the ceiling. The clastic sediments in the sequence were probably deposited by the stream, as no opening to the surface is observed in the immediate vicinity of the site.

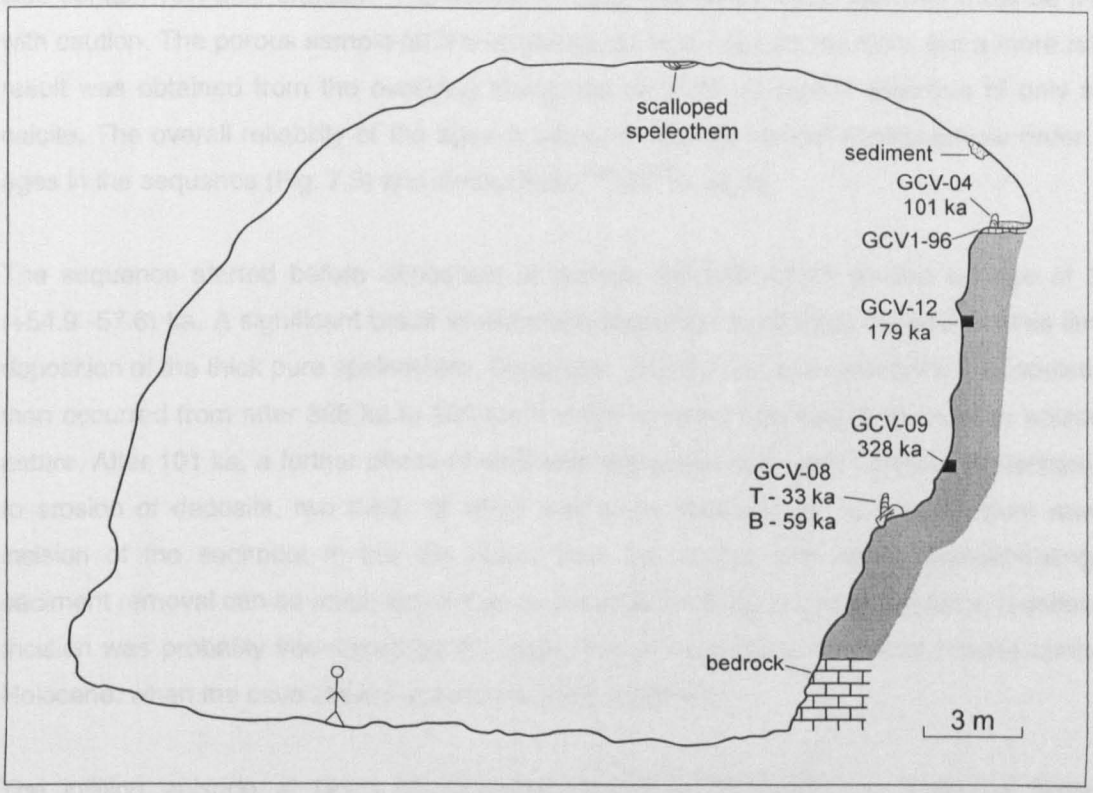

Figure 7.5. Sketch of sediment sequence at Gruta do Convento.

Due to lack of good exposures and access limitations, a detailed description of the sequence could not be made. The base of the sequence is a bench on Caatinga Limestone bedrock some 2 m above the present floor of the passage. The sediments appear to comprise mostly fine grained material with some calcite cement, with a more massive speleothem layer (sample GCV-09) about 7 m from the floor. Above this layer, there are a few more metres of partially cemented clastic material containing impure speleothem layers. Some somewhat cleaner calcite infill voids, and was sampled for dating (GCV-12). Above this sample the sequence continues for 2.6 m comprising mostly fine grained material topped by a speleothem layer. This topmost layer (sample GCV1-96) was very porous and recrystallised. However, better calcite was found in a small stalagmite growing over this layer (GCV-04). Another speleothem layer topping sediment (GCV-10) collected a few metres downstream from the main section is stratigraphically correlative to GCV-04. The upper speleothem layers in the sequence appear to dip into the passage from an alcove in the wall. A thin deposit of fine grained sediment occurs over the topmost speleothem layer, ending the sequence. Remains of sediment can be observed near the ceiling of the passage. Three other speleothem samples (GCV-08B,T and GCV-07) started growing after the incision of the main sequence. GCV-08 is a large stalagmite that grew over

dirty flowstone bedded parallel to the present angle of repose slope of the sequence. GCV-07 is some few metres downstream and also grew over slope caused by the river incision.

Three of the samples analysed for uranium series isotopes contained $^{230}Th/^{232}Th$ ratios below 20, indicating detrital contamination (Table 7.1). Two of these samples (GCV-10 and GCV-12) also contain very little uranium. The corrected ages yielded by these samples must be treated with caution. The porous sample GCV1-96 yielded an open system analysis, but a more reliable result was obtained from the overlying stalagmite GCV-04 by careful selection of only sound calcite. The overall reliability of the ages is demonstrated by correct stratigraphical order of all ages in the sequence (Fig. 7.5) and similar initial $^{234}U/^{238}U$ ratios.

The sequence started before deposition of sample GCV-09 which yielded an age of 328.0 (+54.9 -57.6) ka. A significant break in sediment deposition must have occurred at this time for deposition of the thick pure speleothem. Deposition of sediment and cementation by speleothem then occurred from after 328 ka to 101 ka. It is not known if this was continuous or episodic in nature. After 101 ka, a further phase of sediment deposition occurred. This was completed prior to erosion of deposits, two thirds of which had been removed by 59 ka. Minimum rates for incision of the sediment in the site would thus be around 170 m/Ma, demonstrating that sediment removal can be much faster than water table lowering in cratonic settings (section 3.3). Incision was probably interrupted by the beginning of the present semi-arid climate during the Holocene, when the cave stream acquire its present pattern.

The infilling episode at Gruta do Convento spans at least 200 ka. It seems likely that depositional breaks must exist in the sequence. Much of the deposit shows calcite intermixed with sediment. Similar deposits have been observed at other sites in the cave suggesting that the clastic sediment was derived from the swallet, and not from a local source. Generation of the sequence would require a climate wetter than at present. The apparent dominance of fine grained material (silt and clay) in the sequence is likely to reflect soil stripping from the Caatinga Limestone, rather than sand derived from the quartzite headwaters of the streams that feed the cave. Possibly the climate was wet enough for causing speleothem deposition, but some soil remobilisation was also occurring. Absence of coarse deposits suggest that aggradation may have occurred due to base level (Salitre River) rise or blockage of the passage due to collapse, causing coarser material to be deposited upstream from the site. An alternative explanation is that the sequence could have been formed during a shift from arid to wet conditions, when the soil was not protected by vegetation, and occasional high intensity storms could transport material into the cave. The long timespan represented in the sequence appears to disfavour this hypothesis. At Convento, speleothem and sediment deposition, and erosion occurred under a climate wetter than present.

7.4.1.3. Slope setting: Toca do Caboclo

Toca do Caboclo is a small cave in the Caatinga limestone explored for the first time during field work for this thesis. It occurs on a barren karren field across the Salitre Valley from the village of Abreus (Fig. 4.12). The cave entrance opens up at the foot of a doline about 200 m^2 in area and less than 5 m deep at the cave entrance. After speleogenesis, Toca do Caboclo was filled with at least three generations of speleothem, and was largely reexcavated afterwards. The present pattern of the cave (Fig. 7.6) is due to the last phase of excavation, and most of the lower passages develop entirely on speleothem. At present the cave lacks significant sedimentation. Occasional heavy rains bring limited amounts of fine grained material into the lower levels.

The sequence at Toca do Caboclo is largely devoid of layers of fine grained material. However, most speleothems are heavily intermixed with clastic material, showing that both clastic and chemical deposition occurred simultaneously as at Gruta do Convento. Most of the speleothems are not well layered, and seem to represent more a progradational secondary carbonate sedimentation than more typical drip water deposits. Other small cave nearby shows similar speleothem deposits. Three major speleothem phases can be observed in the vertical fissure that connects the two levels of the cave (Fig. 7.6, cross section B). The oldest (Phase 1) speleothem sequence (TCB-01) can only be seen at one point where the extensive Phase 2 speleothem has been eroded. This Phase 1 speleothem sequence appears to have been largely eroded, before being covered by a massive speleothem of Phase 2 into which the lower level of the cave has subsequently developed. The Phase 2 sequence is dense, but generally contains significant detrital contamination and is not therefore suitable for dating. However, a subaqueous facies composed by thick cave rafts observed only at the top of the vertical fissure was sampled (TCB-03), and corresponds to the upper portion of the Phase 2 speleothem sequence. The Phase 2 sequence is at least 5 m thick, but possibly more since its base lies below the present cave floor level. Massive speleothem of Phase 3 overlies the previous speleothem phases. Phase 3 speleothem is about 1.5 m thick, brown coloured, very impure and lacks visible layering. It is confined to the upper levels of the cave, and was sampled at two separate sites. However, upon dissolving the material for analysis, it was found that the samples were composed of over 50% of insoluble residues (mostly quartz sand), and are thus unsuitable for U-series dating. Following deposition of Phase 3 speleothems, all three sequences were eroded and the present cave was formed. More recent stalactites and stalagmites occur in a few places in the reexcavated cave, but were not sampled.

Only two uranium-series ages were obtained in speleothems from Toca do Caboclo (Table 7.1). Sample TCB-01 has a $^{230}Th/^{232}Th$ ratio below 20, indicating significant contamination by detrital Th. Furthermore this sample lies beyond the limit of the alpha spectrometric U-series technique. Sample TCB-03, on the other hand, is free of impurities and comprises dense, non-porous calcite. The two ages are in correct stratigraphical order.

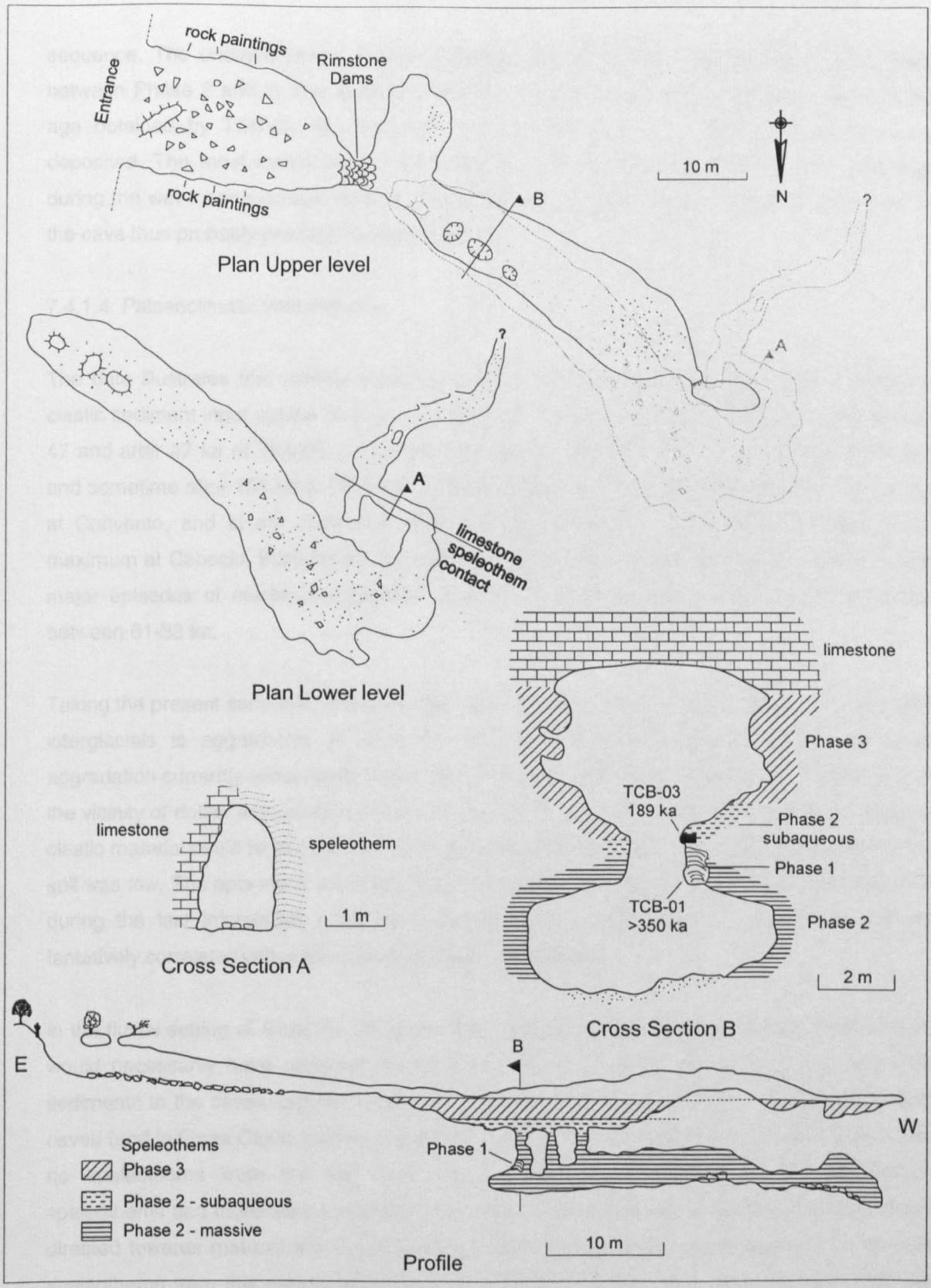

Figure 7.6. Plan and profile of Toca do Caboclo and sketch of sampling site.

The cave obviously predates Phase 1 speleothems and is thus older than 350 ka. After deposition of Phase 1 speleothem, the speleothems were eroded prior to deposition of Phase 2 speleothems, because Phase 2 deposits truncate Phase 1 layers. The Phase 2 event is constrained by a sole U-series age (TCB-03) of 189.2 (+18.1 -20.7) ka, near the top of the

sequence. The undated Phase 3 event followed, but there appears to be no major erosion between Phase 2 and 3. The last and major phase of erosion could significantly postdate the age obtained by TCB-03, but was completed before the most recent speleothems were deposited. The most recent speleothem deposition phase found elsewhere in the area was during the wet marine isotope stage 2. The erosion that generated the present configuration of the cave thus probably predates isotope stage 2.

7.4.1.4. Palaeoclimatic interpretation

The data illustrates that distinct responses appear to have occurred in the caves. Phases of clastic sediment input appear to have occurred prior to 207 ka, between 207-158, between 158-47 and after 47 ka at Tiquara, and intermixed with speleothems prior to 328 and until 101 ka, and sometime after 101 ka at Convento. Erosion of the sediments occurred between 101-60 ka at Convento, and at an unspecified time after 189 ka, but probably before the last glacial maximum at Caboclo. Speleothem deposition follows the age ranges reported in Table 7.1, and major episodes of calcite precipitation appear to have taken place around 189-210 ka and between 61-33 ka.

Taking the present semi-arid interglacial period as a model, the most likely event to occur during interglacials is aggradation at slope bottoms. No speleothem deposition, and no fluvial aggradation currently occur inside caves (due to lack of sediment transport) but sedimentation in the vicinity of doline entrances is evident. This could be the case for Tiquara, where the input of clastic material could have occurred in interglacial semi-arid phases when vegetation retention of soil was low. The episode of sediment input between 158-47 ka at Tiquara could have occurred during the last interglacial while the sediment input episode between 207-158 ka can be tentatively correlated with marine isotope stage 7 interglacial..

In the fluvial setting of Gruta do Convento, the clastic deposition (and associated speleothems) would necessarily have occurred during glacial times, as runoff is needed to transport the sediments to the caves, and the calcite cement suggest moist conditions. Speleothems in both caves (and in Gruta Clovis Saback) suggest a wetter period between 61-33 ka, but surprisingly, no speleothems from the wet last glacial maximum well represented in subaqueous speleothems and travertines (sections 6.6 and 6.7) were found. However, sampling was largely directed towards material that could bracket sedimentation events, and elsewhere in the area speleothems from this period were collected. Therefore, in the fluvial setting of Convento, not only the deposition of the sequence but also the erosion, which occurred in the period between 101-60 ka, took place during glacial periods.

Local factors appear to dominate the signature of erosion events. While both Convento and Caboclo show evidence of major erosion events, no erosion phase was detected at Tiquara. It is possible that the shallow doline at the entrance of Tiquara was largely filled in previous sediment

transport phases and did not allow entry of runoff from the vegetated slope under humid conditions. The present gentle gradient of the doline slope could also explain the lack of significant aggradation during the present interglacial phase. An erosion phase was, however, detected at Gruta Clovis Saback sometime after 61 ka. At Toca do Caboclo the very high percentage of sand in the speleothems, in a cave now located under a totally barren limestone karren pavement, suggests that soil was stripped during the wetter phases responsible for speleothem formation.

7.4.2. Subhumid southeast

The subhumid karst of Lagoa Santa has a very large number of paragenetic caves (section 5.5) that contain abundant chemical and clastic sedimentation. Speleothem layers are ubiquitous in the caves, and stacks of layers can fill passages as much as 20 m high. Extensive removal of sediment from the caves, during the 18th and 19th centuries, first for saltpetre mining, and later for palaeontological work, have led to the exposure of many of those layers. At present, preserved sections of speleothem layers can be observed adhering to cave passage walls, and can often be traced laterally. A few caves that have escaped attention from the miners still retain the original sediment sequences.

The sediment sequences of the Lagoa Santa Karst caves are undoubtedly a later aggradational feature. They could not have been deposited during the phreatic stage of cave genesis due to the frequent occurrence of subaerial speleothem layers which require a vadose setting. The layers appear to be mostly *per descensum* speleothems, because they sometimes show clean calcite with conspicuous layering, and can often be traced to an input point in the cave ceiling. It is possible, however, that some layers were formed by *per ascensum* processes by upward capillary action through the sediment and surface evaporation in the same way as calcrete. Very dirty layers (or carbonate soil horizons) without clear point source, and with no clearly definable upper and lower contact with the sediment may be characteristic of this mode of formation.

Speleothem layers show varied morphology. They can be extremely thin and localised or massive and continuous for several tens of metres. They can be essentially flat, or can dip to various degrees. The complexity of speleothem layer morphology reflects the uneven sediment surface over which they were deposited. Some layers have been observed to undulate in elevation by as much as 5 m along a single passage. The ubiquitous occurrence of speleothem layers that can be up to a metre thick, and the relative scarcity of more common speleothems such as stalactites and stalagmites in the area is intriguing. It is hypothesised that the paragenetic nature of the caves, in which the passages do not tend to follow vertical joints, restrict the infiltration of meteoric water into the caves, and thus drip water speleothems are rare. The few vertical paths from the surface tend to concentrate flow, and favour the formation of laterally extensive layers over sediment. The fact that many caves have been filled with

sediment and subject to cycles of sediment input and removal prevents the occurrence of more common drip type speleothems.

About 35% of the cave entrances in the Lagoa Santa Karst are located inside dolines (Piló, 1988) and may receive runoff from doline slopes. Speleothem layers are frequent in these caves, but also occur in now relict caves that were swallet systems. All caves analysed in this thesis, however, are related to dolines, and belong to the slope setting of sediment input and erosion cycles.

Climate and vegetation in the Lagoa Santa Karst have been briefly discussed in section 5.5. The area was originally covered with low arboreal forest, which has since the 18th century turned into grassland by the European settlers. Dolines, however, tend to retain some of the forest cover, and exposed soil is rare in forested dolines. Many areas, however, are undergoing extensive deforestation, and some dolines are now being subject to soil erosion. The natural hydrological regime in the area under the present climate, appears to have involved little or no sediment transport over doline slopes. The sediments in doline fed caves are at present undergoing erosion. The seasonal climate enable significant runoff to occur during the wet summer months, but because of the well developed vegetation (enhanced during the summer), no soil entrainment occurs. In many caves such as Taquaralzinho or Esquecida, it is possible to observe erosive channels inside caves, and buried speleothems are at present being exhumed. Some recent sediment is being brought into caves, but this seems to represent a small portion of that currently being removed.

7.4.2.1. Doline fed caves of the Lagoa Santa Karst

Over 20 caves were examined for this thesis, 5 of which were described and sampled in detail. Sampling speleothem layers for uranium series dating in the Lagoa Santa Karst is a difficult enterprise. Because these speleothems were originally encased between fine grained sediment, invariably they tend to be porous and detritally contaminated. Furthermore, mining has removed many of the layers, and in many cases it was necessary to resort to small remnants attached to walls. Despite the abundance of speleothem layers in the caves, only a very small proportion of the samples proved suitable for dating. In none of the caves was it possible to obtain a complete chronology for the sequence of layers, as critical horizons proved to be undateable. Table 7.2 summarises the uranium series analyses for the area, including data from Piló (1998).

In addition to problems associated with contamination by terrigenous material, the speleothem layers from the Lagoa Santa area proved to be very difficult to date by the uranium series technique as thorium recoveries were generally very low. Repeated analysis of the same samples showed the problem to be area specific, as speleothems from other sites yielded good isotope recoveries. The problem is not associated with binding of Th into detrital matter, as both clean and dirty calcite yielded equally low Th results. At least six critical samples were discarded

Gruta Marguipegus

sample	U yield (%)	Th yield (%)	U ppm	$^{234}U/^{238}U$	$^{230}Th/^{234}U$	$^{230}Th/^{232}Th$	$^{234}U/^{238}U_{t=0}$	uncorrected age (ka)	corrected age (ka)
GMP-02	31	7	0.089 ± 0.002	1.78 ± 0.04	0.832 ± 0.022	35.8	2.2	158.7 (+12.4 -12.2)	-
GMP-03	22	33	0.039 ± 0.002	1.49 ± 0.07	1.175 ± 0.044	26.3	-	open system	-
GMP-05	66	4	0.102 ± 0.002	1.20 ± 0.02	1.237 ± 0.042	102.1	-	open system	-
GMP-05	55	3	0.101 ± 0.002	1.21 ± 0.01	1.040 ± 0.032	220.0	-	>350	-
Gruta das Escadas									
GES-01	56	70	0.138 ± 0.003	1.64 ± 0.04	0.864 ± 0.022	358.9	2.0	174.6 (+14.9 -14.5)	-
GES-02	6	5	0.076 ± 0.004	1.70 ± 0.10	0.851 ± 0.042	9.1	2.1	167.4 (+33.3 -29.4)	152.5 (+29.9 -23.8)
Gruta Bauzinho de Ossos									
GBO-02	10	13	0.118 ± 0.003	1.06 ± 0.03	1.046 ± 0.034	13.3	-	open system	-
GBO-03	37	10	0.098 ± 0.002	1.08 ± 0.03	1.012 ± 0.030	29.4	-	>350	-
Gruta do Feitiço									
GFE-02	26	71	0.075 ± 0.003	1.48 ± 0.06	0.790 ± 0.029	7.8	1.7	149.3 (+19.6 -17.9)	131.8 (+16.7 -14.4)
GFE-03	28	28	0.085 ± 0.002	1.49 ± 0.05	0.505 ± 0.016	95.3	1.7	73.3 (+4.9 -4.7)	-
Gruta da Escrivania									
GEC-01	52	37	0.163 ± 0.003	1.04 ± 0.01	0.720 ± 0.017	166.4	1.1	136.7 ± 7.4	-

Data reported by Piló (1998) from Gruta do Baú and Gruta dos Macacos

sample	U ppm	$^{234}U/^{238}U$	$^{230}Th/^{234}U$	$^{230}Th/^{232}Th$	$^{234}U/^{238}U_{t=0}$	age (ka)
DT-1	0.254 ± 0.002	1.090 ± 0.012	0.427 ± 0.020	35 ± 14	1.106	59.9 (+3.8 -3.7)
DT-3	0.116 ± 0.001	1.178 ± 0.017	0.730 ± 0.066	26 ±22	1.260	135.0 (+27.7 -22.1)
DT-6	0.187 ± 0.003	1.115± 0.017	0.550 ± 0.023	67 ± 39	1.146	85.0 (+5.6 -5.3)
DT-7	0.239 ± 0.003	1.278 ± 0.017	0.523 ± 0.028	173	1.345	77.7 (+6.1 -5.8)

Table 7.2. U-series analyses of samples from the subhumid Lagoa Santa Karst. Ages corrected assuming a $^{230}Th/^{232}Th$ initial ratio of 1.7. Errors are ±1σ. Samples DT-1, DT-3 and DT-6 from Piló (1998) are from Gruta do Baú. Sample DT-7 is from Gruta dos Macacos.

after initial alpha spectrometric counting showed Th recoveries to be too low to be distinguishable from background. Four of the samples reported in Table 7.2 have low recoveries and the ages reported thus have large associated uncertainties. Open system conditions were also found in samples GMP-03, GMP-04 and GBO-02 due to the porous nature of the calcite. Two of the samples had $^{230}Th/^{232}Th$ ratios below 20, indicating incorporation of significant amounts of detrital thorium. These ages carry uncertainties inherent to the correction procedures. In summary, except for a few analyses, the radiometric data from the Lagoa Santa Karst is generally of poor quality. Some good quality analyses have been reported by Piló (1998), and in conjunction with my analyses allow some palaeoclimatic inferences to be made.

At Gruta Marguipegus (Fig. 7.7), three sites were examined and seven samples were collected. In this cave there is no sediment preserved between the layers. Due to the small size of its entrance, this cave was not excavated by miners or palaeontologists, the sediment being removed by natural processes. At Site 1 there are three phases of calcite deposition. The upper layer A is very flat, and was deposited over a horizontal sediment surface close to the ceiling. This layer could not be reached for sampling. A partially breached, steeply dipping layer, was sampled in two places. The cleanest of the two samples, GMP-01 was analysed twice. The two analyses had near total loss of Th, and were discarded. The lowest speleothem layer, the flowstone that forms the floor of the passages was considered too detritally contaminated to be sampled, but showed evidence of recent calcite deposition.

At Site 2 in Gruta Marguipegus, three generations of now largely breached speleothem layers occur spanning a passage (Fig. 7.7). Remains of the upper layer A attached to the wall were sampled (GMP-02). The analysis showed low Th recoveries and yielded an age of 158.7 (+12.4 -12.2) ka. The intermediate layer B is thin and not very conspicuous, and the small fragments collected were too porous and detritally contaminated to be dated. The lowermost layer C was not sampled due to the lack of clean samples. This layer also shows possible mixing with modern calcite.

At Site 3, two (or possibly three) speleothem layers occur in a sloping passage. The upper layer A is a flat and porous layer that is probably related to layer A at Site 1. Its top is heavily contaminated with silt, and its base, whilst clean calcite, shows a macrocrystalline structure typical of material deposited over sediment. The base of layer A was sampled (GMP-03) but unfortunately represents open system conditions. Layer B slopes towards the middle of the passage. A clean calcite slab, attached to the base of it was sampled (GMP-04) and analysed twice. Both analyses gave total Th loss and were discarded. The morphological affinities of layer C are not clear. It may either be part of layer B, or belong to a lower independent speleothem unit. This layer was analysed twice (GMP-05). The first analysis yielded open system conditions, but a different section yielded and age above 350 ka.

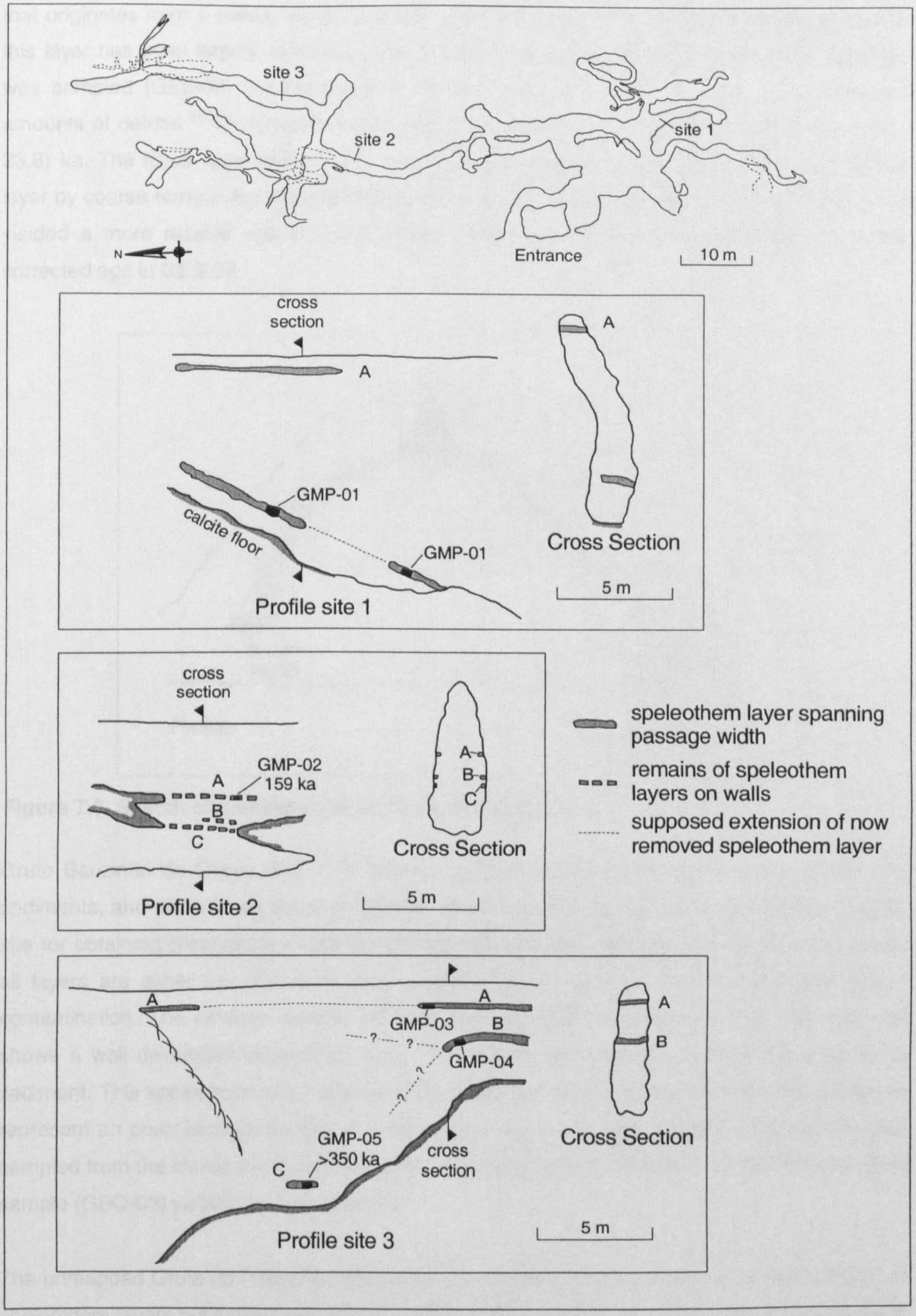

Figure 7.7. Plan of Gruta Marguipegus and sketch of sampling sites. Cave survey by Grupo Bambuí de Pesquisas Espeleológicas.

Gruta das Escadas is located very close to Marguipegus and both were probably part of the same cave before separation occurred due to passage blockage. One site was sampled in Escadas (Fig. 7.8). Two separate layers are found at the site. The upper layer is a massive layer

that originates from a stalagmite and slopes towards the floor of the passage. Sediment below this layer has been largely removed, presumably by natural processes. The base of this layer was sampled (GES-02) but the analysis showed very low U and Th yields, and significant amounts of detrital ^{230}Th. Nevertheless it yielded a low precision corrected age of 152.5 (+29 - 23.8) ka. The lower layer has a more restricted occurrence and is separated from the upper layer by coarse terrigenous material with quartz gravels. The sample collected from it (GES-01) yielded a more reliable age of 174.6 (+14.9 -14.5) ka, which is indistinguishable from the corrected age in GES-02.

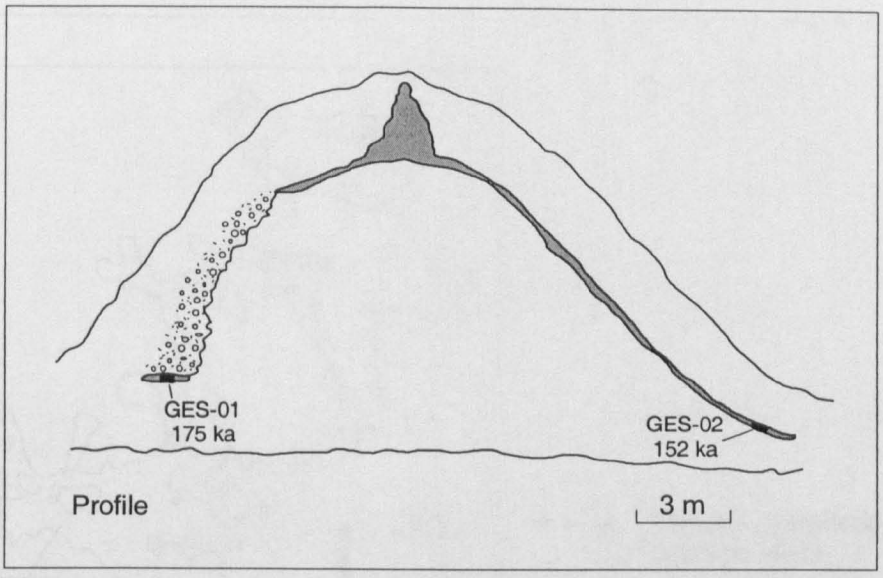

Figure 7.8. Sketch of sampling site at Gruta das Escadas.

Gruta Bauzinho de Ossos (Fig. 7.9) displays excellent sequences of speleothem layers and sediments, and since it has escaped attention from last century miners, it is potentially a good site for obtaining chronological data for speleothem/sediment sequences. Unfortunately, nearly all layers are either too porous to yield reliable U-series data or showed significant detrital contamination. The passage leading off from the main entrance was sampled (Fig. 7.9) and shows a well developed speleothem layer that overlies and is overlain by remains of clastic sediment. This speleothem layer was sampled (GBO-02) but the analysis showed the calcite to represent an open isotopic system in relation to U and Th. A large clast of dense calcite was sampled from the clastic sediments that contain fossil bones and overlie the GBO-02 layer. This sample (GBO-03) yielded an age > 350 ka.

The unmapped Gruta do Feitiço (or Macumba) is a short cave that shows extensive remains of speleothem layers but limited associated sediment. The stratigraphy of the speleothem layers in this cave (Fig. 7.10) is somewhat complex. In the deeper portion of the cave there are at least three generations of layers. The remains of upper layer A lie close to the ceiling and are out of reach for sampling. Layer B is a massive layer whose base comprises two separate speleothem horizons separated by a depositional break. The lower horizon (GFE-02) comprises somewhat porous calcite with some possible recrystallisation. It showed significant detrital ^{230}Th

contamination, and yielded a corrected age of 131.8 (+16.7 -14.4) ka. The top section of this same layer (GFE-03) is very porous and recrystallised and yielded and age of 73.3 (+4.9 -4.7) ka. Although these ages are in correct stratigraphical order, the porous nature of the samples suggests some possible isotopic postdepositional remobilisation. Layer C was sampled but the material was considered too contaminated and porous to be dated. The outer sector of the cave, beyond a gate, shows remains of two layers. It is not clear how these two layers relate to the ones in the inner portion of the cave. Both layers D and E show clean and dense calcite and were collected as samples GFE-04 and GFE-05. Each one of these samples was analysed twice, but for all analyses thorium recoveries were too low to allow an age to be determined.

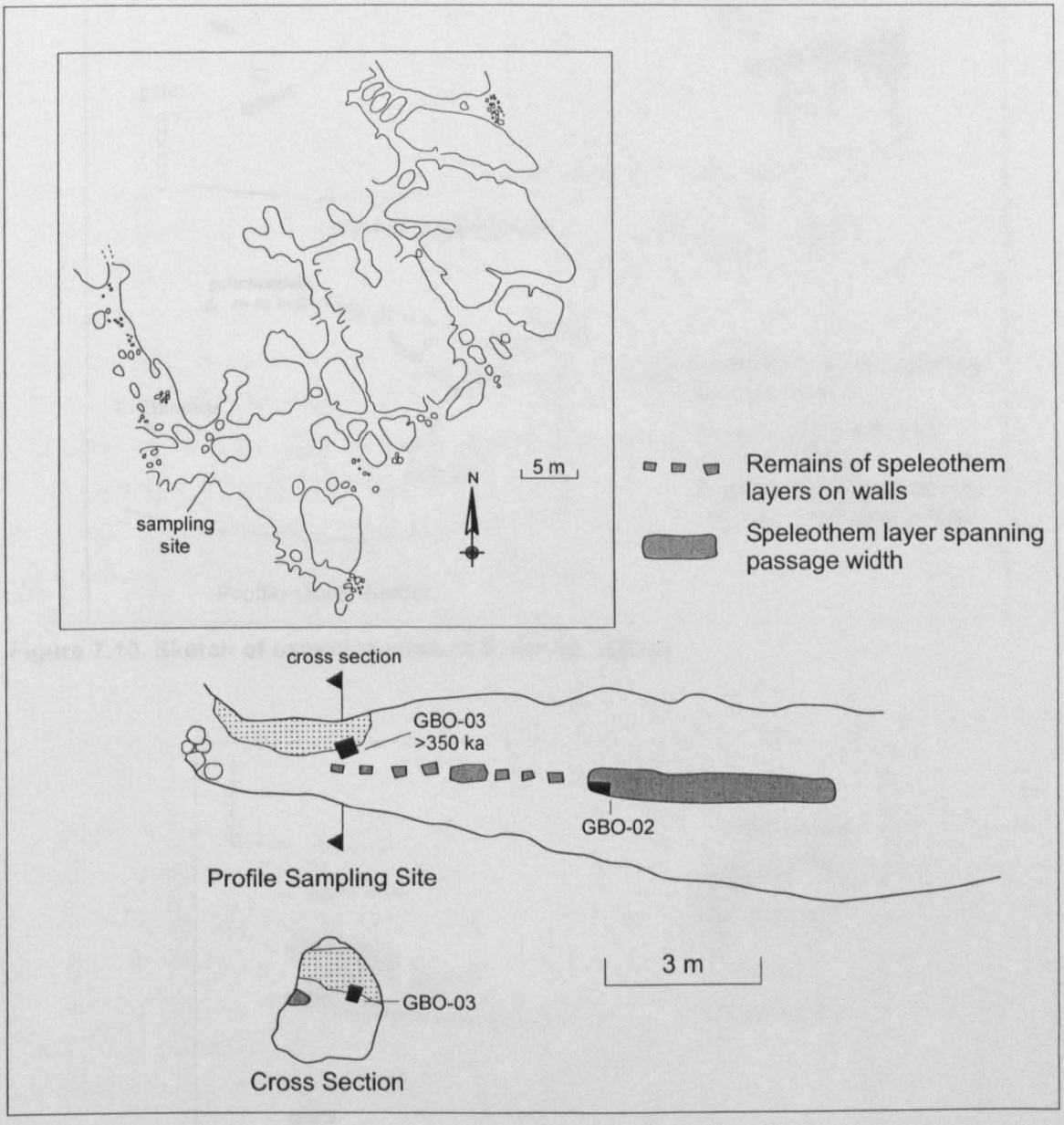

Figure 7.9. Plan of Gruta Bauzinho de Ossos and sketch of sampling site. Cave survey from Piló (1998).

The last cave sampled was one of the several caves in the Escrivania cliff (the one with the largest entrance). It is a very short cave which presents in its lower sector a well developed speleothem layer overlying in situ sediment (Fig. 7.11). The base of this layer is composed of

clean and dense calcite which was sampled (GEC-01) yielding an age of 136.7 ± 7.4 ka. This layer overlies a very indurated sediment which contains syngenetic calcite. This calcite, albeit very dirty, was sampled (GEC-02) but two analyses showed total Th loss. This cave contains higher layers which were not sample due to access difficulties.

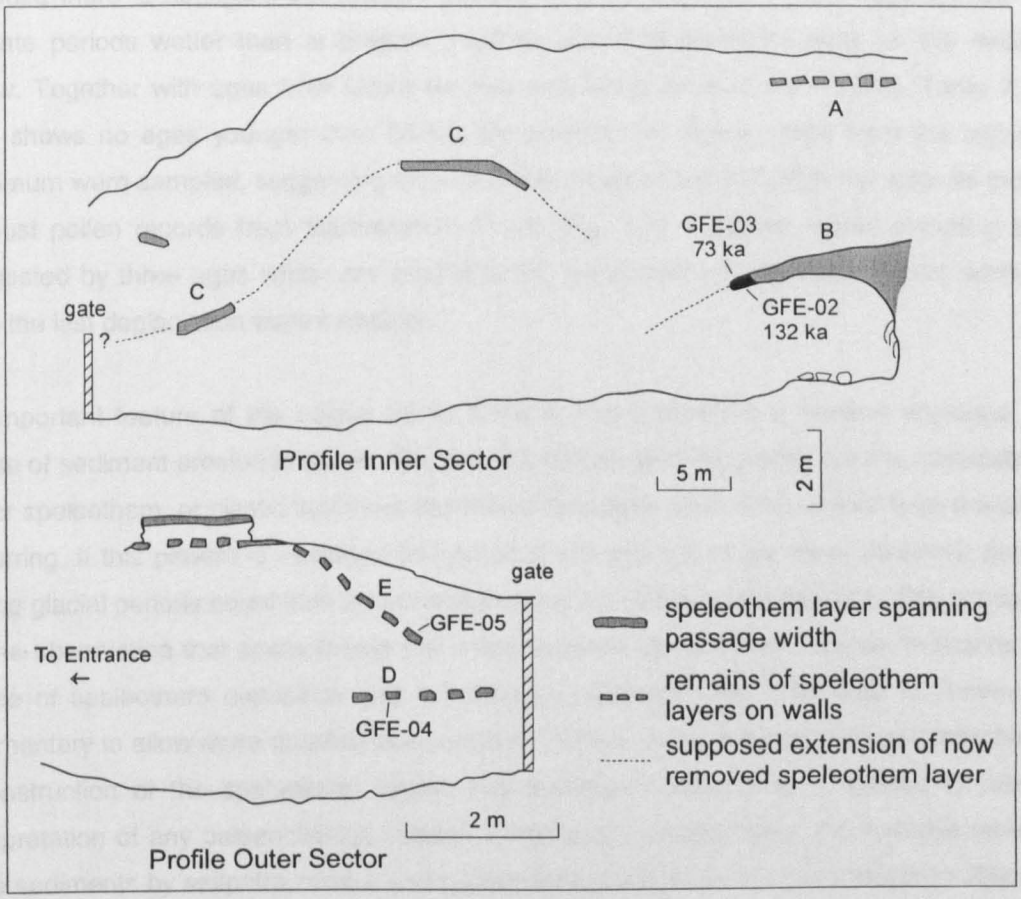

Figure 7.10. Sketch of sampling sites at Gruta do Feitiço.

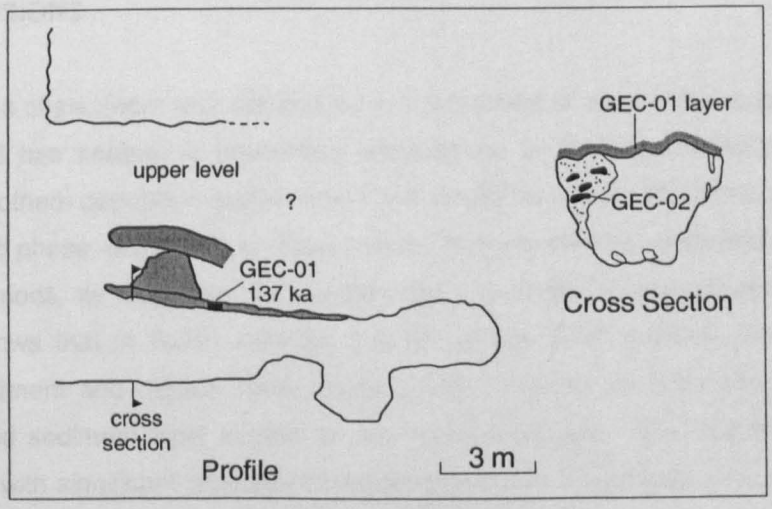

Figure 7.11. Sketch of sampling site at Gruta da Escrivania.

7.4.2.2. Palaeoclimatic interpretation

The poor quality and small number of U-series analyses from the Lagoa Santa Karst allows only a sketchy reconstruction of the timescales of clastic and chemical deposition and erosion. Because there is negligible speleothem deposition at present, the ages of speleothem layers indicate periods wetter than at present, besides providing minimum ages for the sediments below. Together with ages from Gruta do Baú and Macacos from Piló (1998) (Table 7.2) the data shows no ages younger than 59 ka. No speleothem layers dating from the last glacial maximum were sampled, suggesting either sampling bias or a dry LGM in the area, as indicated in most pollen records from southeastern Brazil (Fig. 6.3). However, some sampling bias is suggested by three ages which are related to the penultimate deglaciation period, while none from the last deglaciation were sampled.

An important feature of the Lagoa Santa Karst is that it provides a modern analogue of the phase of sediment erosion in caves. The present climate and vegetation are not associated with either speleothem, or clastic sediment deposition but active sediment removal from the caves is occurring. If this pattern is assumed as typical of interglacials in the area, sediment deposited during glacial periods could then be removed during the following interglacials. This is supported by the observation that speleothems are being exposed by sediment erosion, indicating that a phase of speleothem deposition was followed by sediment input. The data is, however, too fragmentary to allow more detailed interpretation. A more extensive sampling and morphological reconstruction of the speleothem layers and associated sediments is needed to refine the interpretation of any palaeoclimatic phases in this area. Unfortunately, the massive removal of cave sediments by saltpetre miners and palaeontologists make such reconstruction difficult and even impossible in many sites.

7.5. CONCLUSIONS

Study of cycles of sediment removal and input in two areas of contrasting present day climate in eastern Brazil has enabled a preliminary assessment of the palaeoclimate control of these events. Speleothem deposition occurs under wet conditions, but sediment input can be assigned to any climatic phase, depending on local factors. In slope settings, sediment deposition occurs during dry periods, as suggested by the data from Toca da Tiquara. However, the data from Convento shows that in fluvial settings, enough energy (and therefore water) is needed to transport sediment and deposit them inside caves. In Gruta do Convento, both speleothem deposition and sediment input appear to occur simultaneously. The ubiquitous occurrence of speleothems with significant amounts of terrigenous material throughout the area confirms that at least some sediment input occurs during such phases.

The phase of sediment erosion remains the least known part of the sedimentation cycle in caves. Brain (1995a), Brook and Nickmann (1996) and Brook et al. (1997) have correlated this

phase to a wet period in which the vegetation would not allow soil entrainment. Brook et al. (1997) further add that such an event would require a climate wetter than required for speleothem growth because speleothem erosion was also observed to occur. Observations at the Lagoa Santa Karst show this not the case because the present climate is clearly drier than required for extensive speleothem formation. It seems that sediment erosion could in fact occur in the transitions between the wet periods suitable for speleothem growth and the dry phases conducive to soil erosion, although very wet periods could possibly cause both erosion and speleothem deposition in slope setting caves. An alternative explanation for cave sediment erosion phases involves exhaustion of the sediment source. This is not the case in the Lagoa Santa area, because the soil originates from pedogenesis of phyllite layers which used to overlie the limestone (Piló, 1998). Any soil erosion would result in bare doline slopes which would not again be covered by soil. Barren limestone is rare in the area and thus complete removal of soil has not occurred.

Despite the obvious systematic differences between the slope and fluvial settings, specific intersite differences appear to be very important. The complete absence of an erosion phase at Tiquara, and the limited sediment input at Caboclo, in an area which experienced the full transition between a dry and wet climate illustrates that local factors can dominate the processes. Climate seasonality changes could also significantly affect the processes, as demonstrated in the fluvial model of Tucker and Slingerland (1997). The processes of sediment input and erosion and their relationship with climatic patterns appear to be complex and local variables are likely to be of importance at any specific site.

CHAPTER 8
CONCLUSIONS

8.1 SUMMARY FINDINGS

The summary of the major findings in this thesis will be divided in two sections, relating to the geomorphology and palaeoclimate of eastern Brazil.

8.1.1. Karst Geomorphology

The main objective of the study was to develop broad models of cave development in semi-arid areas and in stable cratonic settings. Timescales of karst denudation and cave evolution were obtained through palaeomagnetism and U-series dating.

Denudation rates in the São Francisco Craton were assessed through magnetostratigraphy of cave sediments at Gruta do Padre. A fluvial incision rate of 25-34 m/Ma was obtained, which is compatible with very long term rates reported from apatite fission track studies. The upper (and older) level of Gruta do Padre is at least 1.95 Ma old. Since this level developed under a planation surface now removed by scarp retreat, this age also represents minimum ages for that planation surface. A review of denudation rates in non cratonic settings shows that mountainous and tectonically active areas have denudation rates an order of magnitude higher than in cratonic settings.

The role of sulphuric acid dissolution in the development of the karst on the Una Group carbonates was studied, with emphasis on the semi-arid zone of Campo Formoso. Hydrochemistry and sulphur isotopes suggest that pyrite dissolution is actively occurring in the area, and together with evaporative concentration, is responsible for the high salinity levels of ground water.

The morphology of the caves formed in the Una Group carbonates of the Campo Formoso Karst shows many features in common with deep-seated hypogenic caves such as a ramiform pattern, lack of relationship with the surface and condensation-corrosion processes. This together with the hydrochemical evidence suggests that these caves were generated by sulphuric acid derived from bedrock sulphide oxidation. Nearby caves located in the same climatic setting, but developed in the Caatinga Limestone which does not contain metal sulphide, do not display these features. Palaeomagnetism dating and denudation rates in the São Francisco Craton were applied to constrain the timescales of evolution of Toca da Boa Vista and suggest that the cave and its associated sediments are probably Tertiary in age.

This shallow hypogenic development model probably accounts for the extensive nature and unusual features of the caves, and should predominate in other semi-arid areas of the Una

Group. In the southern wetter portion of the Una Group, the hypogenic component appears to be overwhelmed by normal meteoric processes. This shallow hypogenic model should occur in other pyritiferous carbonate sequences of the world, especially under arid or semi-arid climate.

Cave development processes were assessed by geomorphological studies in three different areas of the São Francisco Craton, the Iraquara, Caatinga, and Lagoa Santa Karsts. In all three areas, phreatic development occurred by paragenesis, this phase ending when the passages reached the water table. Caves were then subject to cyclic phases of sediment removal and emplacement, probably due to palaeoclimate controlled water table, runoff and sediment transport episodes. At Iraquara it is possible that the early paragenetic development was superimposed onto an earlier regional hypogenic phase. Palaeomagnetism and U-series dating in the Iraquara Karst suggest that the draining of Lapa Doce and Torrinha caves occurred within the Brunhes Epoch (since 778 ka).

The freshwhater Caatinga Limestone is probably a palustrine deposit. It has remained open to migration of U and Th, and thus cannot be dated by the U-series technique. A minimum age of 1.3 - 2.6 Ma for the Caatinga Limestone was obtained from U-series dating of travertine and speleothems, and using denudation rates from the São Francisco Craton applied to the incision depth of the Salitre Valley. Despite its relatively young age, the Caatinga Limestone has developed a mature karst landscape, and the caves show the same sequence of development as in swallet/river caves developed in the much older Precambrian carbonates of the Iraquara and Lagoa Santa areas.

The cave passages in the Lagoa Santa Karst usually lack scallops, suggesting that these were too large to be distinguished from the passage bends. The water velocity needed to form such large scallops was very slow and unable to entrain sediment, and thus absence of scallops can probably be used to assess paragenetic conditions at time of cavern genesis at specific points in the cave system. New morphological criteria derived from the Lagoa Santa and Iraquara Karsts that can aid in the identification of paragenesis are: meander junctions at ceiling level occur via an ascending meander; presence of a flat ceiling with no phreatic features such as dissolution pockets; cave development in anastomotic canyon networks; general absence of joint fed speleothems.

Bedding plane anastomoses were not observed in any of the caves examined for this thesis. It is suggested that small scale wide spaced anastomotic channels evolved through paragenesis into paragenetic canyons. Competing anastomotic channels should keep the same hydraulic head if the passage cross section, flow velocities and thus discharge are kept in equilibrium through partial sediment removal on the passage floor, enabling such passages to evolve at similar rates.

A model of cave development for the stable cratonic area of eastern Brazil has been developed based on denudation rates and rates of upward paragenetic conduit migration. Due to low rates of denudation, initial conduits will remain for a long period in the phreatic zone. Sediment is widely available and the passage will evolve by paragenesis, enlarging upwards towards the water table. This model should be applicable to other karst areas in low relief, stable cratonic settings. In mountainous and tectonically active areas, the rates of denudation (and ground water flow velocities) are too high, and the growth of a phreatic passage will tend to be aborted while still a phreatic tube.

The onset of vadose conditions in the paragenetic caves in eastern Brazil will cause total or partial removal of the original paragenetic sediment and establishment of normal vadose conditions with obliteration of many of the original paragenetic features. Paragenetic reactivation can occur during these later phases when "secondary" paragenetic features can develop.

8.1.2. Karst palaeoclimate

This thesis is the first comprehensive attempt to elucidate palaeoclimate for semi-arid northeastern Brazil by systematic study of secondary carbonate deposits which could be reliably dated.

A series of travertine deposits in the Salitre River valley was studied and dated using the U-series method. These non-thermal travertines are reliable indicators of wet climates because they represent runoff from springs, which are inactive under present semi-arid climate. Numerous vegetal debris embedded in the travertine also suggests that during travertine growth the vegetation in the area was much more forested than at present. Two suites of travertine were identified. The youngest deposits yielded ages between 21 - 9 ka while the older travertines were deposited around 400 ka, indicating wetter conditions in the area during the last glacial maximum and succeeding deglaciation period, and at an earlier period (isotope stage 12?). No comparable deposits from the penultimate glacial period were found.

A reconstruction of water table variations in the area was performed through U-series dating of subaqueous speleothems in Toca da Boa Vista. The water table in the cave was 13 ± 1 m above the present level during the last glacial maximum. There is evidence also of another episode of high water stands at the penultimate glacial maximum, although further sampling is needed to reliably constrain such episode.

Vertebrate fossil remains in the caves, including extensive bat guano and bat bone deposits, were studied in order to obtain palaeoenvironmental information. Many of the fossil species modes of living require a much wetter and forested environment than the present one. Speleothem overlying and underlying fossil bones was dated using the U-series method. Results indicate a spread of ages during the last glacial period, indicating that the fossil emplacement

mechanism is not controlled by palaeoclimate as previously supposed. A major episode of bat guano accumulation occurred during the LGM, when it is inferred that the area was more forested.

Overall, the palaeoclimate record obtained for northeastern Brazil suggests increased moisture during the LGM. This is in marked contrast with pollen and ocean records for other areas of Brazil such as the wetter southeast and Amazonia which indicate increased aridity during the LGM. A wet LGM in the semi-arid northeast is not depicted in any of the General Circulation Model simulations reviewed and the data presented in this thesis should contribute to improve the resolution of these models.

Cycles of clastic and chemical sediment accumulation and removal are common in the caves in eastern Brazil, and represent a subsurface response to fluvial and slope sediment transport and runoff. A specific advantage of these deposits is that intercalation of speleothems can be used for dating deposits. The type of input environment, whether through a slope (doline) setting or a fluvial environment was found to affect the response of the cave to palaeoclimate cycles of sedimentation and erosion, with the fluvial setting offering the most complex response.

In the semi-arid northeast, interglacials appear to be characterised by erosion of soil in dolines and cave aggradation, as there is currently neither speleothem deposition nor erosion. However, in the fluvial setting of Gruta do Convento, deposition of speleothems, sediment input, and sediment erosion occurred during glacial periods as water flow (and thus more humid conditions) are needed to allow these processes to remain operative. The major phase of sediment erosion in Convento occurred between 100 - 60 ka.

At the subhumid southeast, sediment and speleothem erosion is occurring under the present climate, with limited cave aggradation and speleothem deposition. No speleothems were obtained from the LGM, suggesting that this period was probably marked by a dry event, as indicated by several pollen records. Overall, intersite differences appear to be significant in controlling the response of cycles of sediment input/erosion in caves in relation to palaeoclimate changes.

8.2. SUGGESTIONS FOR FUTURE WORK

Several avenues for future research exist in the area and should be pursued in the future.

Denudation rates in the area could be refined with additional palaeomagnetism work in other caves. The use of cosmogenic techniques (e.g. ^{26}Al -^{10}Be) could also help constrain the period of sediment emplacement. There are many caves which appear suitable for this type of work, and should yield additional incision rates with implications for the evolution of planation surfaces in the area.

The role of sulphuric acid dissolution in shaping the karst landscape in the area could be further clarified with additional hydrochemical and isotopic work. More detailed ground water sampling in caves and wells should improve understanding of the regional variability in the water chemistry, and enable focus on the specific geochemical issues associated with pyrite oxidation, such as intraregional variabilites related to pyrite abundance and depth zonation of oxidising zone. Additional sampling for sulphur isotopes is also envisaged, including determination of modern values of $\delta^{34}S$ in rainwater in order to better document the variability in sulphur isotope values.

Differentiation between shallow hypogenic caves and their meteoric counterpart is at present largely based on descriptive criteria. There should be an emphasis in trying to quantify cave patterns, including the application of morphometrical analyses that enable the investigation of the relative importance between surface and underground karst development, in order to distinguish between epigenic and hypogenic karst areas.

The denudational model of cave evolution presented in this thesis needs to be tested with field work in other cratonic areas. Karst areas in cratonic sites in Africa and Australia seem to be natural candidates for showing paragenetic caves, and a comparative study is urgently needed. The formulation of less subjective and more quantitative criteria for paragenetic determination should also be a focus of research, in order to eliminate bias in the morphological interpretation of cave genesis.

Palaeoclimate studies in Brazil are still in their early beginnings and much remains to be done. Karst palaeoclimate studies should be expanded to other areas, such as the Amazon, southern and western Brazil. These areas have well developed karst and caves, and should be suitable for such work. In particular, it is important to obtain records beyond the range of the radiocarbon technique, which at present are almost entirely lacking in Brazil.

Many of the secondary carbonates collected for this thesis could be also dated by the Thermal Ionisation Mass Spectrometry (TIMS) technique, allowing a significant improvement in the chronological resolution. Older samples which yielded ages with large errors, such as the older suite of travertines, would particularly benefit from such dating. It was intended to compute speleothem growth frequency curves from alpha spectrometric analyses in this thesis, but delays in counting precluded this. This will be pursued in next year. Speleothem growth periods by TIMS and oxygen and carbon isotope studies are also needed. Luminescence studies should also be pursued since the strong seasonal climate that characterises the area could result in the display of well developed luminescence banding.

Additional sampling of the Salitre River travertine deposits should help better constrain the phases of deposition. Similar deposits have been described from other river valleys in the area,

and should be surveyed. In particular it seems important to establish if the lack of travertines between the two phases sampled in this thesis result from sampling bias, lack of sufficient moisture, or simply surface removal. Pollen and plant macrofossil studies in the travertines seem to be a particularly promising research area, due to the abundant vegetal debris.

The older water table high stand detected at Toca da Boa Vista should be better constrained by more detailed mapping. This cave, and the neighbouring Toca da Barriguda, display other sites with subaqueous speleothems that could yield a more detailed record of water table fluctuations in the area.

The recent discovery of additional fossil remains embedded in speleothem in the caves offers the possibility of additional dating to constrain the ages of deposition of the bones. The abundant bat guano and bone deposits are, at present, constrained by only two radiocarbon dates. More dates should be obtained for such deposits, since they appear to reflect a much more forested environment.

The ubiquitous occurrence of speleothem layers intercalated with clastic deposits in many caves in eastern Brazil provides a future focus for more detailed palaeoclimate work. The preliminary research presented at this thesis hints at the complexity of such deposits and more complete sampling and survey of additional sites should be undertaken. The chronology obtained from the cave deposits should then be linked with the surface deposits, (slope or fluvial deposits) in order to place the cave deposits into a more general landscape context. Correlation with fluvial terraces, lag deposits or soil catenas in slopes should provide an useful complement for the research.

REFERENCES

Ab'Saber, A.N. 1982. The paleoclimate and paleoecology of Brazilian Amazonia. In *Biological Diversification in the Tropics* (Prance, G.T. ed.). Columbia University Press, pp. 41-59.

Absy, M.L.; Cleef, A.; Fournier, M.; Martin, L.; Servant, M.; Sifeddine, A.; Silva, M.F.; Soubies, F.; Suguio, K.; Turcq, B.; van der Hammen, T. 1991. Mise en évidence de quatre phases d'ouverture de la fôret dense dans le sud-est de l'Amazonie au cours des 60 000 dernières années. Première comparaison avec d'autres régions tropicales. *C.R. Acad. Sci. Paris* 312: 673-678.

Acaroglu, E.R.; Graf, W.H. 1968. Sediment transport in conveyance systems. Part 2. *Bull. Int. Assoc. Sci. Hydr.* 13: 123-135.

Adams, G. (Ed.). 1975. *Planation Surfaces.* Benchmark Papers in Geology, Hutchinson and Ross.

Alonso Zarza, A.M.; Calvo, J.P.; Garia del Cura, M.A. 1992. Palustrine sedimentation and associated features - grainification and pseudo-microkarst - in the Middle Miocene (Intermediate Unit) of the Madrid Basin, Spain. *Sedimentary Geology* 76: 43-61.

Amaral, G.; Born, H.; Hadler, J.C.; Iunes, P.J.; Kawashita, K.; Machado Jr., D.L.; Oliveira, E.P.; Paulo, S.R.; Tello, C.A. 1997. Fission track analysis of apatites from São Francisco Craton and Mesozoic alcaline-carbonatite complexes from central and southeastern Brazil. *Journal of South American Earth Sciences* 10: 285-294.

Andrews, J.E.; Riding, R.; Dennis, P.F. 1997. The stable isotope record of environmental and climatic signals in modern terrestrial microbial carbonates from Europe. *Palaeogeography, Palaeoclimatology, Palaeoecology* 129: 171-189.

Arz, H.W.; Patzold, J.; Wefer, G. 1998. Correlated millenial-scale changes in surface hydrography and terrigenous sediment yield inferred from Last Glacial marine deposits off northeastern Brazil. *Quaternary Research* 50: 157-166.

Ashley, R.M.; Verbanck, M.A. 1996. Mechanics of sewer sediment erosion and transport. *Journal of Hydraulic Research* 34: 753-769.

Ashley, R.M.; Wotherspoon, D.J.J.; Goodison, M.J.; McGregor, I.; Coghlan, B.P. 1992. The deposition and erosion of sediment in sewers. *Water Science and Technology* 26: 1283-1293.

Atkinson, T.C.; Harmon, R.S.; Smart, P.L.; Waltham, A.C. 1978. Palaeoclimatic and geomorphic implications of $^{230}Th/^{234}U$ dates on speleothems from Britain. *Nature* 272: 24-28.

Atkinson, T.C.; Rowe, P.J. 1992. Applications of dating to denudation chronology and landscape evolution. In *Uranium Series Disequilibrium. Applications to Earth, Marine and Environmental sciences* (Ivanovich, M.; Harmon, R.S. ed.). Clarendon Press, p. 669-703.

Auler, A.S. 1994. *Hydrogeological and Hydrochemical Characterization of the Matozinhos-Pedro Leopoldo Karst, Brazil.* MSc Thesis, Western Kentucky University.

Auler, A.S. 1995a. Evidências de dissolução por ácido sulfúrico na espeleogênese no Grupo Una, Bahia. *Annals* 8º Simpósio de Geologia de Minas Gerais. SBG MG Boletim 13: 93-94.

Auler, A.S. 1995b. Lakes as a speleogenetic agent in the karst of Lagoa Santa, Brazil. *Cave and Karst Science* 21: 105-110.

Auler, A.S. 1998. Base-level changes inferred from cave paleoflow analysis in the Lagoa Santa Karst, Brazil. *Journal of Cave and Karst Studies* 60: 58-62.

Auler, A.S.; Farrant, A.R. 1996. A brief introduction to karst and caves in Brazil. *Proceedings of the University of Bristol Spelaeological Society* 20: 187-200.

Ayliffe, L.K.; Veeh, H.H. 1988. Uranium-series dating of speleothems and bones from Victoria Cave, Naracoorte, South Australia. *Chemical Geology* 72: 211-234.

Azevedo, A.M.R.; Azevedo, A.E.G. 1991. Paleoclimatic record in carbonates from the semiarid region of Bahia. *Proceedings 2nd International Congress of the Brazilian Geophysical Society*, 2: 1002-1005.

Bahia. 1994. *Mapa Geológico do Estado da Bahia*. Governo Estadual.

Bakalowicz, M.J.; Ford, D.C.; Miller, T.E.; Palmer, A.N.; Palmer, M.V. 1987. Thermal genesis of dissolution caves in the Black Hills, South Dakota. *Geological Society of America Bulletin* 99: 729-738.

Bakalowicz, M.; Sorriaux, P.; Ford, D.C. 1984. Quaternary glacial events in the Pyrenees from U-series dating of speleothems in the Niaux-Lombrives-Sabart caves, Ariege, France. *Norsk Geografisk Tidsskrift* 38: 193-197.

Baker, A.; Caseldine, C.J.; Hatton, J.; Hawkesworth, C.J.; Latham, A.G. 1997. A Cromerian complex stalagmite from the Mendip Hills, England. *Journal of Quaternary Science* 12: 533-537.

Baker, A.; Genty, D.; Smart, P.L. 1998. High resolution records of soil humification and paleoclimate change from variations in speleothem luminescence excitation and emission wavelengths. *Geology* 26: 903-906.

Baker, A.; Smart, P.L.; Edwards, R.L.; Richards, D.A. 1993. Annual growth banding in a cave stalagmite. *Nature* 364: 518-520.

Baker, A.; Smart, P.L.; Ford, D.C. 1993. Northwest European palaeoclimate as indicated by growth frequency variations of secondary calcite deposits. *Palaeogeograhy, Palaeoclimatology, Palaeoecology* 100: 291-301.

Baker, A.; Smart, P.L.; Edwards, R.L. 1995. Paleoclimate implications of mass spectrometric dating of a British flowstone. *Geology* 23: 309-312.

Baker, A.; Barnes, W.L.; Smart, P.L. 1996. Speleothem luminescence intensity and spectral characteristics: signal calibration and a record of palaeovegetation change. *Chemical Geology* 130: 65-76.

Baker, A.; Ito, E.; Smart, P.L.; McEwan, R.F. 1997. Elevated and variable values of ^{13}C in speleothems in a British cave system. *Chemical Geology* 136: 263-270.

Balázs, D. 1984. Exhumált trópusi óskarszt Lapinha videkén (Minas Gerais, Brazília). *Karszt és Barlang* 2: 87-92.

Ball, C.K.; Jones, J.C. 1990. Speleogenesis in the limestone outcrop north of the South Wales Coalfield: The role of microorganisms in the oxidation of sulphides and hydrocarbons. *Cave Science* 17: 3-8.

Bard, E.; Arnold, M.; Fairbanks, R.G.; Hamelin, B. 1993. ^{230}Th-^{234}U and ^{14}C ages obtained by mass spectrometry on corals. *Radiocarbon* 35: 191-199.

Bar-Matthews, M.; Matthews, A.; Ayalon, A. 1991. Environmental controls of speleothem mineralogy in a karstic dolomitic terrain (Soreq Cave, Israel). *Journal of Geology* 99: 189-207.

Bar-Matthews, M.; Ayalon, A.; Matthews, A.; Sass, E.; Halicz, L. 1996. Carbon and oxygen isotope study of the active water-carbonate system in a karstic Mediterranean cave: implications for paleoclimate research in semiarid regions. *Geochimica et Cosmochimica Acta* 60: 337-347.

Barreto, A.M.F. 1996. *Interpretação Paleoambiental do Sistema de Dunas Fixadas do Médio Rio São Francisco, Bahia*. PhD. Thesis, Universidade de São Paulo.

Bastin, B. 1978. L'analyse pollinique des stalagmites: une nouvelle possibilite d'approche des fluctuations climatiques du Quaternaire. *Annales de la Societé Géologique de Belgique* 101: 13-19.

Bastin, B. 1982. Premier bilan de l'analyse pollinique de stalagmites holocènes en provenance de grottes belges. *Revue Belge de Geographie* 106: 87-97.

Bastin, B.; Gewelt, M. 1986. Analyse pollinique et datation ^{14}C de concrétions stalagmitiques holocènes: apports complémentaires des deux méthodes. *Géographie Physique et Quaternaire* 40: 185-196.

Beck, J.W.; Récy, J.; Taylor, F.; Edwards, R.L.; Cabioch, G. 1997. Abrupt changes in early Holocene tropical sea surface temperatures derived from coral records. *Nature* 385: 705-707.

Behling, H. 1997. Late Quaternary vegetation, climate and fire history from the tropical mountain region of Morro de Itapeva, SE Brazil. *Palaeogeography, Palaeoclimatology, Palaeoecology* 129: 407-422.

Behling, H. 1998. Late Quaternary vegetational and climatic changes in Brazil. *Review of Palaeobotany and Palynology* 99: 143-156.

Behling, H.; Lichte, M. 1997. Evidence of dry and cold climatic conditions at glacial times in tropical southeastern Brazil. *Quaternary Research* 48: 348-358.

Behrensmeyer, A.K. 1991. Terrestrial vertebrate accumulations. In *Taphonomy: Releasing the Data Locked in the Fossil Record* (Allison, P.A. and Briggs, D.E.G., ed.). Plenum Press, New York, pp. 291-335.

Bender, M.; Sowers, T.; Dickson, M.L.; Orchardo, J.; Grootes, P.; Mayewski, P.A.; Meese, D.A. 1994. Climate correlations between Greenland and Antarctica during the past 100,000 years. *Nature* 372: 663-666.

Bigarella, J.J.; Ab'Saber, A.N. 1964. Palaogeographische und palaeoklimatische aspekte des kanozoikums in sudbrasilien. *Zeitschrift fur Geomorphologie* 8: 286-312.

Bigarella, J.J.; Andrade, G.O. 1965. Contribution to the study of the Brazilian Quaternary. *Geological Society of America Special Paper* 84: 433-451.

Bigarella, J.J.; Andrade-Lima, D. 1982. Paleoenvironmental changes in Brazil. In *Biological Diversification in the Tropics* (Prance, G.T. ed.), Columbia University Press, pp. 27-40.

Bigarella, J.J.; Mousinho, M.R. 1966. Slope development in southeastern and southern Brazil. *Zeitschrift fur Geomorphologie* 10: 151-160.

Bischoff, J.L.; Julia, R.; Mora, R. 1988a. Uranium-series dating of the Mousterian occupation at Abric Romani, Spain. *Nature* 332: 68-70.

Bischoff, J.L. Rosenbauer, R.J.; Tavoso, A.; Lumley, H. 1988b. A test of uranium-series dating of fossil tooth enamel: results from Tournal Cave, France. *Applied Geochemistry* 3: 145-151.

Bishop, P. 1985. Southeast Australia late Mesozoic and Cenozoic denudation rates: a test for late Tertiary increases in continental denudation. *Geology* 13: 479-482.

Blackwell, B.; Schwarcz, H.P. 1986. U-series analyses of the lower travertine at Ehringsdorf, DDR. *Quaternary Research* 25: 215-222.

Blum, M.D.; Toomey III, R.S.; Valastro, S. 1994. Fluvial response to Late Quaternary climatic and environmental change, Edwards Plateau, Texas. *Palaeogeography, Palaeoclimatology, Palaeoecology* 108: 1-21.

Blumberg, P.N.; Curl, R.L. 1974. Experimental and theoretical studies of dissolution roughness. *Journal of Fluid Mechanics* 65: 735-751.

Bogli, A. 1964. Mischungskorrosion - ein beitrag zum verkarstungsproblem. *Erdkunde* 18: 83-92.

Bond, G.; Broecker, W.; Johnsen, S.; McManus, J.; Labeyrie, L.; Jouzel, J.; Bonani, G. 1993. Correlations between climate records from North-Atlantic sediments and Greenland ice. *Nature* 365: 143-147.

Bottrell, S.H.; Smart, P.L.; Whitaker, F.; Raiswell, R. 1991. Geochemistry and isotope systematics of sulphur in the mixing zone of Bahamian blue holes. *Applied Geochemistry* 6: 97-103.

Brain, C.K. 1995a. The influence of climatic changes on the completeness of the early hominid record in Southern African caves, with particular reference to Swartkrans. In *Paleoclimate and Evolution with Emphasis on Human Origins* (Vrba, E.S.; Denton, G.H.; Partridge, T.C.; Burckle, L.H. ed.), Yale University Press, New Haven, pp. 451-458.

Brain, C.K. 1995b. Understanding the stratigraphic complexity of South African australopithecine cave deposits: the contribution of John T. Robinson. *South African Journal of Science* 91: 435-437.

Branco, J.J.R.; Costa, M.T. 1961. Roteiro da Excursão Belo Horizonte-Brasília. IPR Publ. 15: 1-25.

Branner, J.C. 1910. Aggraded limestone plains of the interior of Bahia and the climatic changes suggested by them. *Geological Society of America Bulletin* 22: 187-206.

Branner, J.C. 1911. The geography of north-eastern Bahia. *Geographical Journal* 38: 139-152, 256-269.

Braun, O.P.G. 1971. Contribuição à geomorfologia do Brasil Central. *Revista Brasileira de Geografia* 32: 3-39.

Bretz, J.H. 1942. Vadose and phreatic features of limestone caverns. *Journal of Geology* 50: 675-811.

Broecker, W. 1986. Oxygen isotope constraints on surface ocean temperatures. *Quaternary Research* 26: 121-134.

Broecker, W.S. 1994. Massive iceberg discharge as triggers for global climate change. *Nature* 372: 421-424.

Broecker, W.S. 1996. Glacial climate in the tropics. *Science* 272: 1902-1904.

Brook, G.A. 1982. Stratigraphic evidence of Quaternary climatic change at Echo Cave, Transvaal, and a paleoclimatic record for Botswana and Northeastern South Africa. *Catena* 9: 343-351.

Brook, G.A.; Burney, D.A.; Cowart, J.B. 1990. Desert paleoenvironmental data from cave speleothems with examples from the Chihuahuan, Somali-Chalbi, and Kalahari deserts. *Palaeogeography, Palaeoclimatology, Palaeoecology* 76: 311-329.

Brook, G.A.; Cowart, J.B.; Brandt, S.A.; Scott, L. 1997. Quaternary climatic change in southern and eastern Africa during the last 300 ka: the evidence from caves in Somalia and the Transvaal region of South Africa. *Zeitschrift fur Geomorphologie* Suppl. Bd. 108: 15-48.

Brook, G.A.; Nickmann, R.J. 1996. Evidence of late Quaternary environments in Northwestern Georgia from sediments preserved in Red Spider Cave. *Physical Geography* 17: 465-484.

Brown, E.T.; Stallard, R.F.; Raisbeck, G.M.; Yiou, F. 1992. Determination of the denudation of Mount Roraima, Venezuela, using cosmogenic ^{10}Be and ^{26}Al. *EOS* 73: 170.

Brown, E.T.; Bourles, D.L.; Colin, F.; Sanfo, Z.; Raisbeck, G.M.; Yiou, F. 1994. The development of iron crust lateritic systems in Burkina Faso, West Africa examined with *in situ*-produced cosmogenic nuclides. *Earth and Planetary Science Letters* 124: 19-33.

Brown, K.S.; Ab'Saber, A.N. 1979. Ice-age forest refuges and evolution in the neotropics: Correlation of paleoclimatological, geomorphological and pedological data with modern biological endemism. *Paleoclimas* 5: 1-30.

Brown, R.W.; Summerfield, M.A.; Gleadow, A.J.W. 1994. Apatite fission track analysis: Its potential for the estimation of denudation rates and implications for models of long-term landscape evolution. *In Process Models and Theoretical Geomorphology* (Kirkby, M.J. ed.). John Wiley and Sons, Chichester, pp. 23-53.

Bryan, K. 1928. Historic evidence on changes in the channel of the Rio Puerco, a tributary of the Rio Grande in New Mexico. *Journal of Geology* 36: 265-282.

Buckland, W. 1823. *Reliquiae Diluvianae*. Oxford.

Bull, P.A. 1981. Some fine-grained sedimentation phenomena in caves. *Earth Surface Processes and Landforms* 6: 11-22.

Bull, W.B. 1979. Threshold of critical power in streams. *Geological Society of America Bulletin* 90: 453-464.

Bull, W.B. 1991. *Geomorphic Responses to Climatic Change*. Oxford University Press, New York.

Burney, D.A.; Burney, L.P. 1993. Modern pollen deposition in cave sites: experimental results from New York state. *New Phytologist* 124: 523-535.

Burton, R.F. 1869. *Explorations of the Highlands of the Brazil*. Tinsley Brothers, London.

Busenberg, E.; Plummer, L.N. 1982. The kinetics of dissolution of dolomite in CO_2-H_2O systems at 1.5 to 65 ºC and 0 to 1 atm P_{CO2}. *American Journal of Science* 282: 45-78.

Bush, M.B. 1994. Amazon speciation: A necessarily complex model. *Journal of Biogeography* 21: 5-17.

Cabral, F.C.F. 1978. *O Uso dos Isótopos Naturais do Carbono no Estudo das Águas Subterrâneas do Calcário Bambuí - Região Central da Bahia*. MSc Thesis, Universidade Federal da Bahia.

Cadier, E. 1996. Hydrologie des petits bassins du Nordeste Brésilien semi-aride: typologie des bassins et transposition écoulements annuels. *Journal of Hydrology* 182: 117-141.

Campy, M.; Chaline, J. 1993. Missing records and depositional breaks in French late Pleistocene cave sediments. *Quaternary Research* 40: 318-331.

Cartelle, C. 1992. *Edentata e Megamamíferos Herbívoros Extintos da Toca dos Ossos (Ourolândia, BA, Brasil)*. Doctoral Thesis, Universidade Federal de Minas Gerais.

Cartelle, C. 1995. *A Fauna Local de Mamíferos Pleistocênicos da Toca da Boa Vista (Campo Formoso, BA)*. Thesis, Universidade Federal de Minas Gerais.

Cartelle, C.; Hartwig, W.C. 1996. A new extinct primate among the Pleistocene megafauna of Bahia, Brazil. *Proc. Natl. Acad. Sci.* USA 93: 6405-6409.

CERB. 1983. *Estudo Hidrogeológico do Plateau de Irecê. Laudo de Análises Químicas das Águas Subterrâneas.* Volume 3, Relatório Final. Companhia de Engenharia Rural da Bahia, Salvador.

Cerling, T.E. 1984. The stable isotopic composition of modern soil carbonate and its relationship to climate. *Earth Planetary Science Letters* 71: 229-240.

Chafetz, H.S.; Srdoc, D.; Horvatincic, N. 1994. Early diagenesis of Plitvice Lakes waterfall and barrier travertine deposits. *Géographie Physique et Quaternaire* 48: 247-255.

Charlesworth, J.K. 1957. *The Quaternary Era.* Edward Arnold, London.

Chaves, S.; Renault-Miskovsky, J. 1996. Paléoethnologie, paléoenvironment et paléoclimatologie du Piauí, Brésil: apport de l'étude pollinique de coprolithes humains recueillis dans le gisement préhistorique de Pedra Furada. *C.R. Acad. Sci. Paris* 322: 1053-1060.

Clapperton, C. 1993a. *Quaternary Geology and Geomorphology of South America.* Elsevier, Amsterdam.

Clapperton, C. M. 1993b. Nature of environmental changes in South America at the Last Glacial Maximum. *Palaeogeography, Palaeoclimatology, Palaeoecology* 101: 189-208.

Claussen, P. 1841. Notes géologiques sur la province de Minas Geraes au Brésil. *Bulletin de la Academie Royale de Bruxelles* 8: 322-343.

Claypool, G.E.; Holser, W.T.; Kaplan, I.R.; Sakai, H.; Zak, I. 1980. The age curves of sulfur and oxygen isotopes in marine sulfate and their mutual interpretation. *Chemical Geology* 28: 199-260.

CLIMAP 1976. The surface of ice-age Earth. *Science* 191: 1131-1137.

COHMAP members 1988. Climatic changes of the last 18,000 years: Observations and model simulations. *Science* 241: 1043-1052.

Colinvaux, P. 1987. Amazon diversity in light of the paleoecological record. *Quaternary Science Reviews* 6: 93-114.

Colinvaux, P.; De Oliveira, P.E.; Moreno, J.E.; Miller, M.C.; Bush, M.B. 1996a. A long pollen record from lowland Amazonia: Forest and cooling in glacial times. *Science* 274: 85-88.

Colinvaux, P.; Liu, K.B.; De Oliveira, P.; Bush, M.B.; Miller, M.C.; Kannan, M.S. 1996b. Temperature depression in the lowland tropics in glacial times. *Climatic Change* 32: 19-33.

Condolios, E.; Chapus, E.E. 1963. Transporting solid materials in pipelines. *Chemical Engineering* 70: 93-98.

Coplen, T.B.; Winograd, I.J.; Landwehr, J.M.; Riggs, A.C. 1994. 500,000-Year stable carbon isotopic record from Devils Hole, Nevada. *Science* 263: 361-365.

Corbel, J. 1957. *Les Karsts du Nord-Ouest de L'Europe et de Quelques Regions de Comparaisons.* Institut des études Rhodaniennes de l'Université de Lyon. Mémoires et Documents 12.

Coutard, J.P.; Kohler, H.C.; Journaux, A. 1978. Memorial descritivo do Mapa do Carste de Lagoa Santa. Université de Caen, France.

Craven, J.P. 1953. The transportation of sand in pipes. I. Full-pipe flow. *State University of Iowa Studies in Engineering Bulletin* 34: 67-76.

Crombie, M.K.; Arvidson, R.E.; Sturchio, N.C.; El Alfy, Z.; Abu Zeid, K. 1997. Age and isotopic constraints on Pleistocene pluvial episodes in the Western Desert, Egypt. *Palaeogeography, Palaeoclimatology, Palaeoecology* 130: 337-355.

Crowley, T.J. 1994. Potential reconciliation of Devils Hole and deep-sea Pleistocene chronologies. *Paleoceanography* 9: 1-5.

Cruz Jr., F.W. 1998. *Aspectos Geomorfológicos e Geoespeleologia do Carste da Região de Iraquara, Centro-Norte da Chapada Diamantina, Estado da Bahia.* MSc Dissertation, Universidade de São Paulo.

Cunningham, K.I.; Northup, D.E.; Pollastro, R.M.; Wright, W.G.; LaRock, E.J. 1995. Bacteria, fungi and biokarst in Lechuguilla Cave, Carlsbad Caverns National Park, New Mexico. *Environmental Geology* 25: 2-8.

Curl, R.L. 1966. Scallops and flutes. *Transactions of the Cave Research Group of Great Britain* 7: 121-160.

Curl, R.L. 1974. Deducing flow velocity in cave conduits from scallops. *National Speleological Society Bulletin* 36: 1-5.

Czaplewksi, N.J.; Cartelle, C. 1998. Pleistocene bats from cave deposits in Bahia, Brazil. *Journal of Mammalogy* 79: 784-803.

Damuth, JE; Fairbridge, R.W. 1970. Equatorial Atlantic deep-sea arkosic sands and ice-age aridity in tropical South America. *Geological Society of America Bulletin* 81: 198-206.

Dansgaard, W.; Johnsen, S.J.; Clausen, H.B.; Dahl-Jensen, D.; Gundestrup, N.S.; Hammer, C.U.; Hvidberg, C.S.; Steffensen, J.P.; Sveinbjornsdottir, A.E.; Jouzel, J.; Bond, G. 1993. Evidence for general instability of past climate from a 250-kyr ice-core record. *Nature* 364: 218-220.

Dardenne, M.A. 1978. Síntese sobre a estratigrafia do Grupo Bambuí no Brasil Central. *Annals* 30th Brazilian Geological Congress, Recife, 2: 597-610.

Davies, T.A.; Hay, W.M.; Southam, J.R.; Worsley, T.R. 1977. Estimates of Cenozoic oceanic sedimentation rates. *Science* 197: 53-55.

Davis, O.K. 1990. Caves as sources of biotic remains in arid western North America. *Palaeogeography, Palaeoclimatology, Palaeoecology* 76: 331-348.

Davis, W.M. 1899. The geographical cycle. *Geographical Journal* 14: 481-504.

Davis, W.M. 1930. Origin of limestone caverns. *Geological Society of America Bulletin* 41: 475-628.

Dawson, A.G. 1992. *Ice Age Earth. Late Quaternary Geology and Climate.* Routledge, London.

Delannoy, J.J.; Guendon, J.L.; Magnin, F.; Quinif, Y. 1989. Datation de travertins. Les exemples de Meyrargues et de Tolox. *Speleochronos* 1: 29-32.

Dennis, P.F.; Rowe, P.J.; Atkinson, T.C. 1996. Isotopic composition of palaeoprecipitation and palaeogroundwaters from speleothem fluid inclusion. In *Climate Change: The Karst Record* (Lauritzen, S.E. ed.), Karst Waters Institute Special Publication 2: 20-22.

De Oliveira, P.E. 1992. *A Palynological Record of Late Quaternary Vegetational and Climatic Change in Southeastern Brazil.* PhD Dissertation, The Ohio State University.

Dever, L.; Fontes, J.C.; Riché, G. 1987. Isotopic approach to calcite dissolution and precipitation in soils under semi-arid conditions. *Chemical Geology* 66: 307-314.

Domenico, P.A.; Schwartz, F.W. 1998. *Physical and Chemical Hydrogeology.* John Wiley and Sons, New York.

Dorale, J.A.; Edwards, R.L.; Ito, E.; González, L.A. 1998. Climate and vegetation history of the midcontinent from 75 to 25 ka: a speleothem record from Crevice Cave, Missouri, USA. *Science* 282: 1871-1874.

Dorale, J.A.; González, L.A.; Reagan, M.K.; Pickett, D.A.; Murrell, M.T.; Baker, R.G. 1992. A high-resolution record of Holocene climate change in speleothem calcite from Cold Water Cave, Northeast Iowa. *Science* 258: 1626-1630.

Drever, J.I. 1997. *The Geochemistry of Natural Waters*. Prentice Hall, Upper Saddle River.

Dreybrodt, W. 1990. The role of dissolution kinetics in the development of karst aquifers in limestone: a model simulation of karst evolution. *Journal of Geology* 98: 639-655.

Dreybrodt, W. 1996. Principles of early development of karst conduits under natural and man-made conditions revealed by mathematical analysis of numerical models. *Water Resources Research* 32: 2923-2935.

Duarte, L.; Nogueira, M.I.M. 1983. Vegetais do Quaternario do Brasil III. Flórula do Morro do Chapéu - BA. In *Coletânea de Trabalhos Paleontológicos do 8º Congresso Brasileiro de Paleontologia*. DNPM : 573-578.

Dublyansky, Y.V. 1995. Speleogenetic history of the Hungarian hydrothermal karst. *Environmental Geology* 25: 24-35.

Durand, R. 1953. Basic relationships of the transportation of solids in pipes. Experimental research. *Int. Assoc. Hydr. Res. Congress* 5: 89-103.

Durov, S.A. 1956. On the question about the origin of the salt composition of karst waters. *Ukranian Chemical Journal* 22: 106-111.

Edmond, J.M.; Palmer, M.R.; Measures, C.I.; Grant, B.; Stallard, R.F. 1995. The fluvial geochemistry and denudation rate of the Guayana Shield in Venezuela, Colombia and Brazil. *Geochimica and Cosmochimica Acta* 59: 3301-3325.

Edwards, R.L.; Chen, J.H.; Wasserburg, G.J. 1986. ^{238}U-^{234}U-^{230}Th-^{232}Th systematics and the precise measurement of time over the past 500,000 years. *Earth Planetary Science Letters* 81: 175-192.

Edwards, R.L.; Cheng, H.; Murrell, M.T.; Goldstein, S.J. 1997. Protactinium-231 dating of carbonates by Thermal Ionization Mass Spectrometry: Implications for Quaternary climate change. *Science* 276: 782-786.

Edwards, R.L.; Gallup, C.D. 1993. Dating of the Devils Hole calcite vein. *Science* 259: 1626.

Egemeier, S.J. 1981. Cavern development by thermal waters. *National Speleological Society Bulletin* 43: 31-51.

Ek, C.; Gewelt, M. 1985. Carbon dioxide in cave atmospheres. New results in Belgium and comparisons with some other countries. *Earth Surface Processes and Landforms* 10: 173-187.

Emiliani, C. 1993. Milankovitch theory verified. *Nature* 364: 583-584.

Endler, J.A.; 1982. Pleistocene forest refuges: fact or fancy? In *Biological Diversification in the Tropics* (Prance, G.T. ed.). Columbia University Press, p. 641-657.

Ewers, R. O. 1985. Patterns of cavern development along the Cumberland Escarpment. In *Caves and Karst of Kentucky* (P.H. Dougherty ed.). Kentucky Geological Survey Special Publication 12: 63-77.

Fairbridge, R.W. 1968. *The Encyclopedia of Geomorphology*. Reinhold Book Corporation, New York.

Fairbridge, R.W.; Finkl, C.W. 1980. Cratonic erosional unconformities and peneplains. *Journal of Geology* 88: 69-86.

Farr, M. 1991. *The Darkness Beckons.* Cave Books.

Farrant, A.R. 1995. *Long-term Quaternary Chronologies from Cave Deposits.* PhD Thesis, University of Bristol.

Farrant, A.R.; Smart, P.L.; Whitaker, F.F.; Tarling, D.H. 1995. Long-term Quaternary uplift rates inferred from limestone caves in Sarawak, Malaysia. *Geology* 23: 357-360.

Ferrari, J.A. 1990. *Interpretação de Feições Cársticas na Região de Iraquara - Bahia.* MSc Dissertation, Universidade Federal da Bahia.

Ferraz-Vicentini, K.R.; Salgado-Labouriau, M.L. 1996. Palynological analysis of a palm swamp in Central Brazil. *Journal of South American Earth Sciences* 9: 207-219.

Finkl, C.W. 1982. On the geomorphic stability of cratonic planation surfaces. *Zeitschrift fur Geomorphologie* 26: 137-150.

Fisher, R.A. 1953. Dispersion on a sphere. *Royal Society of London Proceedings* 217: 295-305.

Flint, R.F. 1957. *Glacial and Pleistocene Geology.* John Wiley and Sons, London.

Ford, D.C. 1973. Development of the canyons of the South Nahanni River, N.W.T. *Canadian Journal of Earth Sciences* 10: 366-378.

Ford, D.C. 1989. Features of the genesis of Jewel Cave and Wind Cave, Black Hills, South Dakota. *National Speleological Society Bulletin* 51: 100-110.

Ford, D.C.; Ewers, R.O. 1978. The development of cave systems in the dimensions of length and depth. *Canadian Journal of Earth Sciences* 15: 1783-1798.

Ford, D.C.; Schwarcz, H.P.; Drake, J.J.; Gascoyne, M.; Harmon, R.S.; Latham, A.G. 1981. Estimates of the age of the existing relief within the southern Rocky Mountains of Canada. *Arctic and Alpine Research* 13: 1-10.

Ford, D.C.; Williams, P.W. 1989. *Karst Geomorphology and Hydrology.* Unwin Hyman, London.

Ford, D.C.; Lundberg, J.; Palmer, A.N.; Palmer, M.V.; Dreybrodt, W.; Schwarcz, H.P. 1993. Uranium-series dating of the draining of an aquifer: the example of Wind Cave, Black Hills, South Dakota. *Geological Society of America Bulletin* 105: 241-250.

Ford, T.D.; Pedley, H.M. 1996. A review of tufa and travertine deposits of the world. *Earth Science Reviews* 41: 117-175.

Frank, R. 1975. Late Quaternary climatic change: evidence from cave sediments in central eastern New South Wales. *Australian Geographical Studies* 13: 154-168.

Freytet, P.; Plaziat, J.C. 1982. Continental carbonate sedimentation and pedogenesis - Late Cretaceous and Early Tertiary of Southern France. *Contributions to Sedimentology 12:* 1-213.

Gac, J.Y. 1980. Géochimie du bassin du Lac Tchad. Bilan de l'alteration, de l'erosion et de la sédimentation. *Travaux et Documents ORSTOM* 123: 1-125.

Galdenzi, S. 1997. Initial geologic observations in caves bordering the Sibari Plain (Southern Italy). *Journal of Cave and Karst Studies* 59: 81-86.

Galdenzi, S.; Menichetti, M. 1995. Occurrence of hypogenic caves in a karst region: examples from central Italy. *Environmental Geology* 26: 39-47.

Gale, S.J. 1992. Long-term landscape evolution in Australia. *Earth Surface Processes and Landforms* 17: 323-343.

Gallagher, K.; Hawkesworth, C.J.; Mantovani, M.S.M. 1994. The denudation history of the onshore continental margin of SE Brazil inferred from apatite fission track data. *Journal of Geophysical Research* 99: 18117-18145.

Ganopolski, A.; Rahmstorf, S.; Petoukhov, V.; Claussen, M. 1998. Simulation of modern and glacial climates with a coupled global model of intermediate complexity. *Nature* 391: 351-356.

Gardner, T.W.; Jorgensen, D.W.; Shuman, C.; Lemieux, C.R. 1987. Geomorphic and tectonic process rates: effects of measured time interval. *Geology* 15: 259-261.

Gascoyne, M. 1977. *Uranium Series Dating of Speleothem: An Investigation of Technique, Data Processing and Precision.* Technical Memo 77-4. McMaster University.

Gascoyne, M. 1983. Trace-element partition coefficients in the calcite-water system and their paleoclimatic significance in cave studies. *Journal of Hydrology* 61: 213-222.

Gascoyne, M. 1992. Palaeoclimate determination from cave calcite deposits. *Quaternary Science Reviews* 11: 609-632.

Gascoyne, M.; Currant, A.P.; Lord, T.C. 1981. Ipswichian fauna of Victoria Cave and the marine palaeoclimatic record. *Nature* 294: 652-654.

Gascoyne, M.; Ford, D.C.; Schwarcz, H.P. 1983. Rates of cave and landform development in the Yorkshire Dales from speleothem age data. *Earth Surface Processes and Landforms* 8: 557-568.

Gascoyne, M.; Latham, A.G.; Harmon, R.S.; Ford, D.C. 1983. The antiquity of Castleguard Cave, Columbia ice fields, Alberta, Canada. *Arctic and Alpine Research* 15: 463-470.

Gascoyne, M.; Schwarcz, H.P.; Ford, D.C. 1978. Uranium series dating and stable isotope studies of speleothems: part 1. Theory and techniques. *Transactions of the Bristish Cave Research Association* 5: 91-111.

Gascoyne, M.; Schwarcz, H.P.; Ford, D.C. 1980. A paleotemperature record for the mid-Wisconsin in Vancouver Island. *Nature* 285: 474-476.

Gat, J.R.; Naor, H. 1979. The relationship between salinity and the recharge/discharge mechanism in arid lowlands. In *The Hydrology of Areas of Low Precipitation.* IAHS Publication 128: 307-312.

Gilchrist, A.R.; Summerfield, M.A. 1990. Differential denudation and flexural isostasy in formation of rifted-margin upwarps. *Nature* 346: 739-742.

Gilchrist, A.R.; Summerfield, M.A. 1991. Denudation, isostasy and landscape evolution. *Earth Surface Processes and Landforms* 16: 555-562.

Gillieson, D. 1986. Cave sedimentation in the New Guinea highlands. *Earth Surface Processes and Landforms* 11: 533-543.

Gillieson, D. 1996. *Caves, Processes, Development, Management.* Blackwell, Oxford.

Goede, A. 1994. Continuous early last glacial palaeoenvironmental record from a Tasmanian speleothem based on stable isotope and minor element variations. *Quaternary Science Reviews* 13: 283-291.

Goede, A.; Harmon, R.S. 1983. Radiometric dating of Tasmanian speleothems - evidence of cave evolution and climate change. *Journal of the Geological Society of Australia* 30: 89-100.

Goede, A.; Vogel, J.C. 1991. Trace element variations and dating of a Late Pleistocene Tasmanian speleothem. *Palaeogeography, Palaeoclimatology, Palaeoecology* 88: 121-131.

Goede, A.; Harmon, R.S.; Atkinson, T.C.; Rowe, P.J. 1990. Pleistocene climatic change in Southern Australia and its effect on speleothem deposition in some Nullarbor caves. *Journal of Quaternary Science* 5: 29-38.

Goede, A.; McDermott, F.; Hawkesworth, C.; Webb, J.; Finlayson, B. 1996. Evidence of Younger Dryas and Neoglacial cooling in a late Quaternary palaeotemperature record from a speleothem in eastern Victoria, Australia. *Journal of Quaternary Science* 11: 1-7.

Goudie, A. 1995. *The Changing Earth. Rates of Geomorphological Processes.* Blackwell, Oxford.

Gordon, D.; Smart, P.L.; Ford, D.C.; Andrews, J.N.; Atkinson, T.C.; Rowe, P.J.; Christopher, N.S.J. 1989. Dating of Late Pleistocene interglacial and interstadial periods in the United Kingdom from speleothem growth frequency. *Quaternary Research* 31: 14-26.

Green, H.S. 1986. The palaeolithic settlement of Wales research project: a review of progress 1978-1985. In *The Palaeolithic of Britain and Its Nearest Neighbours: Recent Trends* (Colcutt, S.N. ed.). Sheffield, p. 36-42.

GRIP members 1993. Climate instability during the last interglacial period recorded in the GRIP ice core. *Nature* 364: 203-207.

Grootes, P.M. 1993. Interpreting continental oxygen isotope records. *In Climate Change in Continental Isotopic Records* (Swart, P.K.; Lohmann, K.C.; Mckenzie, J.; Savin, S. ed.). Geophysical Monograph 78, American Geophysical Union, : 37-46.

Groves, C.G.; Howard, A.D. 1994. Early development of karst systems. 1. Preferential flow path enlargement under laminar flow. *Water Resources Research* 30: 2837-2846.

Guérin, C.; Vogel, M.A.C.; Souza, M.F. 1990. A fauna pleistocênica da região de São Raimundo Nonato (Piauí, Brasil). Implicações paleoecológicas. *Annals* 36º Brazilian Geological Congress 1: 490-500.

Guerra, A.M. 1986. *Processos de Carstificação e Hidrogeologia do Grupo Bambuí na Região de Irecê, Bahia.* Doctoral Thesis, Universidade de São Paulo.

Guilderson, T.P.; Fairbanks, R.G.; Rubenstone, J.L. 1994. Tropical temperature variations since 20,000 years ago: modulating interhemispheric climate change. *Science* 263: 663-665.

Gulden, B. 1999. Long and deep caves of the world. Internet home page.

Gunn, J. 1986. Solute processes and karst landforms. In *Solute Processes* (Trudgill, S.T. ed.), John Wiley and Sons, Chichester, pp. 363-437.

Haberle, S.G.; Maslin, M.A. 1999. Late Quaternary vegetation and climate change in the Amazon Basin based on a 50,000 year pollen record from the Amazon fan, ODP Site 932. *Quaternary Research* 51: 27-38.

Haffer, J. 1969. Speciation in Amazonian forest birds. *Science* 165: 131-137.

Hammil, L.; Bell, F.G. 1986. *Groundwater Resource Development.* Butterworths, London.

Harman, R.; Gallagher, K.; Brown, R.; Raza, A.; Bizzi, L. 1998. Accelerated denudation and tectonic/geomorphic reactivation of the cratons of northeastern Brazil during the Late Cretaceous. *Journal of Geophysical Research* 103: 27091-27105.

Harmon, R.S.; Schwarcz, H.P.; Ford, D.C. 1978. Stable isotope geochemistry of speleothems and cave waters from the Flint Ridge-Mammoth Cave System, Kentucky: implications for

terrestrial climate change during the period 230,000 to 100,000 years B.P. *Journal of Geology* 86: 373-384.

Harmon, R.S.; Schwarcz, H.P.; Ford, D.C.; Koch, D. L. 1979. An isotopic paleotemperature record from late Wisconsinan time in northeast Iowa. *Geology* 7: 430-433.

Harmon, R.S.; Glazek, J.; Nowak, K. 1980. $^{230}Th/^{234}U$ dating of travertine from the Bilzingsleben archaeological site. *Nature* 284: 132-135.

Harris, S.E.; Mix, A.C. 1999. Pleistocene precipitation balance in the Amazon Basin recorded in deep sea sediments. *Quaternary Research* 51: 14-26.

Hartwig, W.C.; Cartelle, C. 1996. A complete skeleton of the giant South American primate *Protopithecus*. *Nature* 381: 307-311.

Harzallah, A.; Aragão, J.O.R.; Sadourny, R. 1996. Interannual rainfall variability in north-east Brazil: Observation and model simulation. *International Journal of Climatology* 16: 861-878.

Heine, K. 1994. The Mera site revisited: ice-age Amazon in the light of new evidence. *Quaternary International* 21: 113-119.

Hellstrom, J.; McCulloch, M.; Stone, J. 1998. A detailed 31,000-year record of climate and vegetation change from the isotope geochemistry of two New Zealand speleothems. *Quaternary Research* 50: 167-178.

Hemming, S.R.; Biscaye, P.E.; Broecker, W.S.; Hemming, N.G.; Klas, M.; Hajdas, I. 1998. Provenance change coupled with increased clay flux during deglacial times in the western equatorial Atlantic. *Palaeogeography, Palaeoclimatology, Palaeoecology* 142: 217-130.

Hennig, G.J.; Grun, R.; Brunnacker, K. 1983. Speleothems, travertines and paleoclimates. *Quaternary Research* 20: 1-29.

Hercman, H.; Bella, P.; Glazek, J.; Gradzinski, M.; Lauritzen, S.E.; Lovlie, R. 1997. Uranium-series dating of sediments from Demanova Ice Cave: a step to age estimation of the Demanova Cave System (The Nizke Tatry Mys., Slovakia). *Annales Societatis Geologorum Poloniae* 67: 439-450.

Herman, J.S.; White, W.B. 1985. Dissolution kinetics of dolomite: Effects of lithology and fluid flow velocity. *Geochimica et Cosmochimica Acta* 49: 2017-2026.

Hill, C.A. 1987. *Geology of Carlsbad Caverns and Other Caves in the Guadalupe Mountains, New Mexico and Texas*. New Mexico Bureau of Mines and Mineral Resources Bulletin 117: 1-150.

Hill, C.A. 1990. Sulfuric acid speleogenesis of Carlsbad Cavern and its relationship to hydrocarbons, Delaware Basin, New Mexico and Texas. *American Association of Petroleum Geologists Bulletin 74*: 1685-1694.

Hill, C.A. 1995. Sulfur redox reactions: hydrocarbons, native sulfur, Mississippi Valley-type deposits, and sulfuric acid karst in the Delaware Basin, New Mexico and Texas. *Environmental Geology* 25: 16-23.

Hill, C.; Forti, P. 1997. *Cave Minerals of the World*. Second Edition, National Speleological Society, Huntsville.

Holmgren, K.; Karlén, W.; Shaw, P.A. 1995. Paleoclimatic significance of the stable isotopic composition and petrology of a late Pleistocene stalagmite from Botswana. *Quaternary Research* 43: 320-328.

Hooghiemstra, H.; van der Hammen, T. 1998. Neogene and Quaternary development of the neotropical rain forest: the forest refugia hypothesis and a literature review. *Earth Science Reviews* 44: 147-183.

Hose, L.D.; Pisarowicz, J.A. 1999. Cueva de Villa Luz, Tabasco, Mexico: Reconnaissance study of an active sulfur spring cave and ecosystem. *Journal of Cave and Karst Studies* 61: 13-21.

Howard, A.D. 1960. Geology and origin of the Crevice Caves of the Iowa, Illinois and Wisconsin lead-zinc district. *Journal of the Yale Speleological Society* 2: 61-95.

Hubbard, D.A.; Herman, J.S.; Bell, P.E. 1990. Speleogenesis in a travertine scarp: observations of sulfide oxidation in the subsurface. In *Travertine-Marl Stream Deposits in Virginia* (Herman, J.D.; Hubbard, D.A. eds.).Virginia Division of Mineral Resources Publication 101: 177-184.

Hughen, K.A.; Overpeck, J.T.; Peterson, L.C.; Trumbore, S. 1996. Rapid climate changes in the tropical Atlantic region during the last deglaciation. *Nature* 380: 51-54.

Huntington, E. 1907. Some characteristics of the glacial period in non-glaciated regions. *Geological Society of America Bulletin* 18: 351-388.

Imbrie, J.; Mix, A.C.; Martinson, D.G. 1993. Milankovitch theory viewed from Devils Hole. *Nature* 363: 531-533.

Ivanovich, M.; Harmon, R.S. 1992. *Uranium-Series Disequilibrium: Applications to Earth, Marine, and Environmental Sciences*. Clarendon Press, Oxford.

Ivanovich, M.; Latham, A.G.; Ku, T.L. 1992. Uranium-series disequilibrium applications in geochronology. In *Uranium-Series Disequilibrium* (Ivanovich, M.; Harmon, R.S. eds). Clarendon Press, Oxford: 62-94.

Ivanovich, M.; Murray, A. 1992. Spectroscopic methods. In *Uranium Series Disequilibrium* (Ivanovich, M.; Harmon, R.S. eds). Clarendon Press, Oxford: 127-173.

Iyer, S.S.; Hoefs, J.; Krouse, H.R. 1992. Sulfur and lead isotope geochemistry of galenas from the Bambuí Group, Minas Gerais, Brazil - Implications for ore genesis. *Economic Geology* 87: 437-443.

Jacobi, R.M.; Rowe, P.J.; Gilmour, M.A.; Grun, R.; Atkinson, T.C. 1998. Radiometric dating of the Middle Palaeolithic tool industry and associated fauna of Pin Hole Cavern, Creswell Crags, England. *Journal of Quaternary Science* 13: 29-42.

James, L.G.; King, B.A. 1984. Predicting sediment deposition patterns in pipes with diminishing flow. *Transactions of the ASAE*: 1758-1762.

Jennings, J.N. 1983. The disregarded karst of the arid and semiarid domain. *Karstologia* 1: 61-73.

Jennings, J.N. 1985. *Karst Geomorphology*. Blackwell, Oxford.

Johnson, R.G.; Wrigth, H.E. 1989. Great basin calcite vein and the Pleistocene time scale. *Science* 246: 262.

Jorgensen, B.B. 1983. The microbial sulphur cycle. In *Microbial Geochemistry* (Krumbein, W.E. ed.). Blackwell. pp. 91-124.

Jouzel, J.; Barkov, N.I.; Barnola, J.M.; Bender, M.; Chappelaz, J.; Genthon, C.; Kotlyakov, V.M.; Lipenkov, V.; Loriud, C.; Petit, J.R.; Raynaud, D.; Raisbeck, G.; Ritz, C.; Sowers, T.; Stievenard, M.; Yiou, F.; Yiou, P. 1993. Extending the Vostok ice-core record of palaeoclimate to the penultimate glacial period. *Nature* 364: 407-412.

Karmann, I. 1994. *Evolução e Dinâmica Atual do Sistema Cárstico do Alto Vale do Rio Ribeira de Iguape, Sudeste do Estado de São Paulo*. Doctoral Thesis, Universidade de São Paulo.

Karmann, I.; Sanchez, L.E. 1979. Distribuição das rochas carbonáticas e províncias espeleológicas do Brazil. *Espeleo-Tema* 13: 105-167.

Kaufman, A. 1992. An evaluation of several methods for determining ^{230}Th/U ages in impure carbonates. *Geochimica et Cosmochimica Acta* 57: 2303-2317.

Kerr, R.A. 1995. Chilly ice-age tropics could signal climate sensitivity. *Science* 267: 961.

Kerr, R.A. 1996. Ice-age rain forest found moist, cooler. *Science* 274: 35-36.

King, L.C. 1956a. A geomorfologia do Brasil oriental. *Revista Brasileira de Geografia* 18: 147-265.

King, L.C. 1956b. A geomorphological comparison between eastern Brazil and Africa (central and southern). *Quarterly Journal of the Geological Society of London* 112: 445-474.

King, L.C. 1967. *The Morphology of the Earth.* Oliver and Boyd, London, 726p.

King, L.C. 1976. Planation remnants upon high lands. *Zeitschrift fur Geomorphologie* 20: 133-148.

King, L.C. 1983. *Wandering Continents and Spreading Sea Floors on an Expanding Earth.* John Wiley and Sons, 232p.

Knox, J.C. 1972. Valley alluviation in Southwestern Wisconsin. *Annals of the Association of American Geographers* 62: 401-410.

Knox, J.C. 1984. Fluvial responses to small scale climatic changes. *In Developments and Applications of Geomorphology* (Costa, J.E.; Fleisher, P.J., ed.), Springer Verlag, Heidelberg, pp. 318-342.

Kohler, H.C. 1989. *Geomorfologia Cárstica na Região de Lagoa Santa-MG.* Doctoral Thesis, Universidade de São Paulo.

Kohn, B.P.; Gleadow, A.J.W.; Cox, S.J.D. 1999. Denudation history of the Snowy Mountains: constraints from apatite fission track thermochronology. *Australian Journal of Earth Sciences* 46: 181-198.

Kronfeld, J.; Vogel, J.C.; Rosenthal, E.; Weinstein-Evron, M. 1988. Age and paleoclimatic implications of the Bet Shean travertines. *Quaternary Research* 30: 298-303.

Krothe, N.C.; Libra, R.D. 1983. Sulfur isotopes and hydrochemical variations in spring waters of southern Indiana, U.S.A. *Journal of Hydrology* 61: 267-283.

Kuhry, P.; Hooghiemstra, H.; van Geel, B.; van der Hammen, T. 1993. The El Abra stadial in the eastern Cordillera of Colombia (South America). *Quaternary Science Reviews* 12: 333-343.

Kutzbach, J.; Gallimore, R.; Harrison, S.; Behling, P.; Selin, R.; Laarif, F. 1998. Climate and biome simulations for the past 21,000 years. *Quaternary Science Reviews* 17: 473-506.

Kyle, J.R.; Misi, A. 1997. Origin of Zn-Pb-Ag sulfide mineralization within Upper Proterozoic phosphate-rich carbonate strata, Irecê Basin, Bahia, Brazil. *International Geology Review* 39: 383-399.

Laming-Emperaire, A.; Prous, A.; Morais, A.V.; Beltrão, M. 1975. Grottes et abris de la region de Lagoa Santa, Minas Gerais, Brésil. *Cahiers d'Archéologie d'Amerique du Sud* 1. Paris, 185 p.

Lanari, C.U. 1909. Ossadas humanas fósseis encontradas numa caverna calcarea das vizinhanças do Mocambo. *Annaes da Escola de Minas* 11: 15-35.

Langbein, W.B.; Schumm, S.A. 1958. Yield of sediment in relation to mean annual precipitation. *American Geophysical Union Transactions* 39: 1076-1084.

Laureano, F.V. 1998. *O Registro Sedimentar Clástico Associado aos Sistemas de Cavernas Lapa Doce e Torrinha, Município de Iraquara, Chapada Diamantina (BA).* MSc Dissertation, Universidade de São Paulo.

Lauritzen, S.E. 1982. The paleocurrents and morphology of Pikhaggrottene, Svartisen, North Norway. *Norsk Geogr. Tiddskr.* 36: 183-209.

Lauritzen, S.E.; Bottrell, S.H. 1994. Microbiological activity in thermoglacial karst springs, South Spitzbergen. *Geomicrobiology Journal* 12: 161-173.

Lauritzen, S.E.; Lauritsen, A. 1995. Differential diagnosis of paragenetic and vadose canyons. *Cave and Karst Science* 21: 55-59.

Lauritzen, S.E.; Lovlie, R.; Moe, D.; Ostbye, E. 1990. Paleoclimate deduced from a multidisciplinary study of a half-million-year-old stalagmite from Rana, northern Norway. *Quaternary Research* 34: 306-316.

Ledru, M.P. 1993. Late Quaternary environmental and climatic changes in Central Brazil. *Quaternary Research* 39: 90-98.

Ledru, M.P.; Bertaux, J.; Sifeddine, A.; Suguio, K. 1998. Absence of last glacial records in lowland tropical forests. *Quaternary Research* 49: 233-237.

Ledru, M.P.; Braga, P.I.S.; Soubies, F.; Fournier, M.; Martin, L.; Suguio, K.; Turcq, B. 1996. The last 50,000 years in the Neotropics (Southern Brazil): evolution of vegetation and climate. *Palaeogeography, Palaeoclimatology, Palaeoecology* 123: 239-257.

Liais, E. 1872. *Climats, Geologie, Faune et Geographie Botanique du Brésil.* Garnier Freres, Paris.

Lichte, M. 1990. Stonelines as a definite cyclic feature in Southeast Brazil: a geomorphological and pedological case study. *Pedologie* 40: 101-109.

Lively, R.S. 1983. Late Quaternary U-series speleothem growth record from southeastern Minnesota. *Geology* 11: 259-262.

Livnat, A.; Kronfeld. J. 1985. Paleoclimatic implications of U-series dates for lake sediments and travertines in the Arava Rift Valley, Israel. *Quaternary Research* 24: 164-172.

Lovlie, R.; Ellingsen, K.L,; Lauritzen, S.E. 1995. Palaeomagnetic cave stratigraphy of sediments from Hellemofjord, northern Norway. *Geophys. J. Int.* 120: 499-515.

Lowe, D.J. 1992. *The Origin of Limestone Caverns: An Inception Horizon Hypothesis.* PhD Thesis, Manchester Metropolitan University.

Lowe, D.J.; Gunn, J. 1995. The role of strong acid in speleo-inception and subsequent cave development. *Acta Geographica* 34: 33-60.

Lowell, T.V.; Heusser, C.J.; Andersen, B.G.; Moreno, P.I.; Hauser, A.; Heusser, L.E.; Schluchter, C.; Marchant, D.R.; Denton, G.H. 1995. Interhemisperic correlation of late Pleistocene glacial events. *Science* 269: 1541-1549.

Lowry, D.C.; Jennings, J.N. 1974. The Nullarbor Karst, Australia. *Zeitschrift fur Geomorphologie* 18: 35-81.

Lumley, H.; Lumley, M.A.; Beltrão, M.C.M.C.; Yokoyama, Y.; Labeyrie, J.; Danon, J.; Delibrias, G.; Falgueres, C.; Bischoff, J.L. 1987. Présence d'outils taillés associés a une faune Quaternaire datée du Pleistocène Moyen dans la Toca da Esperança, région de Central, état de Bahia, Brésil. *L'Antropologie* 91: 917-942.

Lund, P.W. 1838-1842. Blyk paa Brasiliens Dyreverden for den sidste Jordomvaeltning I. Copenhagen.

Lund, P.W. 1840. View of the fauna of Brazil previous to the last geological revolution. *Magazine of Natural History* 4: 1-8; 49-57; 105-112; 153-161; 207-213; 251-259; 307-317; 373-89.

Lund, P.W. 1844. Letter to C.C. Rafn, secretary of the Societé Royale des Antiquaires du Nord.

Lutken, C.F. et al. 1893-1915. *E Museo Lundii.* Vol 1 to 5. Copenhagen.

Mabesoone, J.M.; Castro, C. 1975. Desenvolvimento geomorfológico do nordeste brasileiro. *Boletim do Núcleo Nordeste da SBG* 3: 5-36.

Mabesoone, J.M.; Rolim, J.L.; Castro, C. 1977. Late Cretaceous and Cenozoic history of Northeastern Brazil. *Geologie en Mijnbouw* 56: 129-139.

Malott, C.A. 1937. Invasion theory of cavern development. *Proceedings of the Geological Society of America*: 323.

Manabe, S.; Hahn, D.G. 1977. Simulation of the tropical climate of an ice age. *Journal of Geophysical Research* 82: 3889-3911.

Mankinen, E.A.; Dalrymple, G.B. 1979. Revised geomagnetic polarity time scale for the interval 0-5 m.y. B.P. *Journal of Geophysical Research* 84: 615-626.

Mares, M.A.; Willig, M.R.; Lacher, T.E. 1985. The Brazilian caatinga in South American zoogeography: tropical mammals in a dry region. *Journal of Biogeography* 12: 57-69.

Markgraf, V. 1989. Palaeoclimates in Central and South America since 18,000 BP based on pollen and lake-level records. *Quaternary Science Reviews* 8: 1-24.

Markgraf, V. 1993a. Younger Dryas in southernmost South America - an update. *Quaternary Science Reviews* 12: 351-355.

Markgraf, V. 1993b. Climatic history of Central and South America since 18,000 yr BP: Comparison of pollen records and model simulations. In *Global Climates Since the Last Glacial Maximum* (Wright et al., ed.). Minnesota University Press : 357-385.

Marshall, L.G.; Berta, A.; Hoffstetter, R.; Pascual, R.; Reig, O.A.; Bombim, M.; Mones, A. 1984. Mammals and stratigraphy: Geochronology of the continental mammal-bearing Quaternary of South America. *Paleovertebrata, Mémoire Extraordinaire*, Montpellier: 1-76.

Martini, J.E.J.; Marais, J.C.E. 1996. Grottes hydrothermales dans le Nord-Ouest de la Namibia. *Karstologia* 28: 13-18.

Martins, M.R. (ed.). 1986. *Avaliação dos Recursos Hídricos das Bacias Hidrográficas do Estado da Bahia - Bacia do Rio Salitre.* Centro de Estatística e Informações, Salvador.

Mayerle, R.; Nalluri, C.; Novak, P. 1991. Sediment transport in rigid bed conveyances. *Journal of Hydraulic Research* 29: 475-495.

Meiman, J.; Groves, C.G. 1997. Magnitude/frequency analysis of cave passage development in the Central Kentucky Karst. *Journal of Cave and Karst Studies* 59: 168.

Meis, M.R.M.; Monteiro, A.M.F. 1979. Upper Quaternary "rampas": Doce River Valley, Southeastern Brazilian plateau. *Zeitschrift fur Geomorphologie* 23: 132-151.

Melhorn, W.N.; Edgar, D.E. 1975. The case for episodic, continental scale erosion surfaces: a tentative gedynamic model. In *Theories of Landform Development* (Melhorn, W.N.; Flemal, R.C. eds.). Allen and Unwin, London, pp. 243-275.

Mello, J.L. 1938. *Geologia e Hidrologia do Noroeste da Bahia.* Serviço Geológico e Mineralógico, DNPM, Boletim 90.

Meyer, G.A.; Wells, S.G.; Balling Jr., R.C.; Jull, A.J.T. 1992. Response of alluvial systems to fire and climate change in Yellowstone National Park. *Nature* 357: 147-150.

Misi, A. 1979. O Grupo Bambuí no estado da Bahia. In: *Geologia e Recursos Minerais do Estado da Bahia* (H.A.V. Inda ed.). SME, CPM, Salvador, pp. 120-154.

Misi, A.; Kyle, J.R. 1994. Upper Proterozoic carbonate stratigraphy, diagenesis, and stromatolitic phosphorite formation, Irecê Basin, Bahia, Brazil. *Journal of Sedimentary Research* A64: 299-310.

Misi, A.; Veizer, J. 1998. Neoproterozoic carbonate sequences of the Una Group, Irecê Basin, Brazil: chemostratigraphy, age and correlations. *Precambrian Research* 89: 87-100.

Mock, C.J.; Bartlein, P.J. 1995. Spatial variability of Late-Quaternary palaeoclimates in the western United States. *Quaternary Research* 44: 425-433.

Morehouse, D.A. 1968. Cave development via the sulfuric acid reaction. *National Speleological Society Bulletin* 30: 1-10.

Moses, C.O.; Nordstrom, D.K.; Herman, J.S.; Mills, A.L. 1987. Aqueous pyrite oxidation by dissolved oxygen and by ferric iron. *Geochimica et Cosmochimica Acta* 51: 1561-1571.

Nakai, N.; Jensen, M.L. 1964. Kinetic isotope effect in the oxidation and reduction of sulphur. *Geochimica et Cosmochimica Acta* 28: 1893-1912.

Nalluri, C.; Ab Ghani, A.; El-Zaemey, A.K.S. 1994. Sediment transport over deposited beds in sewers. *Water Science and Technology* 29: 125-133.

Nascimento, J.G.C. 1990. *Caracterização Geoespeleológica do Complexo Caverna do Padre.* Report, Museu Geológico, Salvador, 37p.

Nascimento, J.G.C. 1992. *Mapeamento Ecodinâmico Aplicado ao Uso e Ocupação do Solo: um Exemplo no Complexo Caverna do Padre.* MSc dissertation, Universidade Federal da Bahia, 99p.

Negrão, F.I. 1987. *Caracterização Hidrogeoquímica e Vulnerabilidade do Sistema Hidrogeológico Cárstico da Região de Irecê, Bahia.* MSc Dissertation, Universidade de São Paulo.

Nicholson, R.V.; Gillham, R.W.; Reardon, E.J. 1988. Pyrite oxidation in carbonate-buffered solutions: 1. Experimental kinetics. *Geochimica et Cosmochimica Acta* 52: 1077-1085.

Niewolt, S. 1977. *Tropical Climatology.* John Wiley and Sons, London.

Noel, M. 1986. The palaeomagnetism and magnetic fabric of cave sediments from Pwll y Gwynt, South Wales. *Physics of the Earth and Planetary Interiors* 44: 62-71.

Noel, M.; Shaw, R.P.; Ford, T.D. 1984. A palaeomagnetic reversal in early Quaternary sediments in Masson Hill, Matlock, Derbyshire. *Mercian Geologist* 9: 235-242.

Nott, J. 1995. The antiquity of landscapes on the North Australian Craton and the implications for theories of long-term landscape evolution. *Journal of Geology* 103: 19-32.

Ollier, C. 1985. Morphotectonics of passive continental margins: Introduction. *Zeitschrift fur Geomorphologie Suppl. Bd.* 54: 1-9.

Ollier, C. 1991. *Ancient Landforms.* Belhaven Press, London.

Ollier, C.; Pain, C. 1996. *Regolith, Soils and Landforms.* John Wiley and Sons, Chichester.

Osmond, J.K.; Cowart, J.B. 1992. Ground water. In *Uranium-Series Disequilibrium* (Ivanovich, M.; Harmon, R.S., ed.). Clarendon Press, Oxford: 290-333.

Palmer, A.N. 1975. The origin of maze caves. *National Speleological Society Bulletin* 37: 56-76.

Palmer, A.N. 1984. Geomorphic interpretation of karst features. In *Groundwater as a Geomorphic Agent* (LaFleur, R.G. ed.). Allen and Unwin, Boston: 173-209.

Palmer, A.N. 1987. Cave levels and their interpretation. *National Speleological Society Bulletin* 49: 50-66.

Palmer, A.N. 1989. Geomorphic history of the Mammoth cave system. In *Karst Hydrology - Concepts from the Mammoth Cave area* (White, W.B.; White, E.L. ed.) Van Norstrand Reinhold, p. 317-337.

Palmer, A.N. 1990. Groundwater processes in karst terranes. In *Groundwater Geomorphology* (Higgins, C.G.; Coates, D.R. eds.). Geological Society of America Special Paper 252: 177-209.

Palmer, A.N. 1991. Origin and morphology of limestone caves. *Geological Society of America Bulletin* 103: 1-21.

Palmer, A.N.; Palmer, M.V. 1989. Geologic history of the Black Hills Caves, South Dakota. *National Speleological Society Bulletin* 51: 72-99.

Palmer, A.N.; Palmer, M.V. 1991. Replacement mechanisms among carbonates, sulfates, and silica in karst regions: some Appalachian examples. In *Appalachian Karst* (Kastning, E.; Kastning, K. eds.). National Speleological Society, Huntsville, pp. 109-115.

Palmer, A.N. 1998. Dissolution of karst systems closed to carbon dioxide. In *Friends of Karst, IGCP 379 Proceedings.* Western Kentucky University, Bowling Green, pp.16.

Parizzi, M.G. 1993. *A Gênese e a Dinâmica da Lagoa Santa, com Base em Estudos Palinológicos, Geomorfológicos e Geológicos de sua Bacia.* MSc Dissertation, Universidade Federal de Minas Gerais.

Parizzi, M.G.; Salgado-Labouriau, M.L.; Kohler, H.C. 1998. Genesis and environmental history of Lagoa Santa, southeastern Brazil. *The Holocene* 8: 311-321.

Partridge, T.C.; Maud, R.R. 1987. Geomorphic evolution of southern Africa since the Mesozoic. *South African Journal of Geology* 90: 179-208.

Pasini, G. 1967. Nota preliminare sul ruolo speleogenetico dell'erosione "antigravitativa". *Le Grotte d'Italia* 4(1): 75-88.

Pasini, G. 1975. Sull'importanza speleogenetica del "erosione antigravitativa". *Le Grotte d'Italia* 4(4): 297-322.

Paula Couto, C. 1970. Paleontologia da região de Lagoa Santa, Minas Gerais, Brasil. *Boletim do Museu de História Natural* 1: 1-21.

Paula Couto, C. 1975. Mamíferos fósseis do Quaternário do sudeste brasileiro. *Boletim Paranaense de Geociências* 33: 89-132.

Pease, P.P.; Gomez, B.; Schmidt, V.A. 1994. Magnetostratigraphy of cave sediments, Wyandotte Ridge, Crawford County, Indiana: towards a regional correlation. *Geomorphology* 11: 75-81.

Penha, A.E.P.P. 1994. *O Calcário Caatinga de Ourolândia, Bahia: Feições Diagnósticas, Gênese e Evolução de um Perfil Calcrete.* MSc Thesis, Universidade Federal da Bahia.

Pentecost, A.; Viles, H. 1994. A review and reassessment of travertine classification. *Géographie Physique et Quaternaire* 48: 305-314.

Perrusquía, G.S. 1992. An experimental study on the transport of sediment in sewer pipes with a permanent deposit. *Water Science and Technology* 25: 115-122.

Piló, L.B. 1988. *Contribuição ao Estudo do Carste na Microregião de Belo Horizonte.* Unpublished report.

Piló, L.B. 1998. *Morfologia Cárstica e Materiais Constituintes: Dinâmica e Evolução da Depressão Poligonal Macacos-Baú - Carste de Lagoa Santa, MG.* Doctoral Thesis, Universidade de São Paulo.

Platt, N.H. 1992. Fresh-water carbonates from the Lower Freshwater Molasse (Oligocene, western Switzerland): sedimentology and stable isotopes. *Sedimentary Geology* 78: 81-99.

Pollard, D.; Thompson, S.L. 1997. Climate and ice-sheet mass balance at the last glacial maximum from the Genesis version 2 global climate model. *Quaternary Science Reviews* 16: 841-863.

Polyak, V.J.; McIntosh, W.C.; Guven, N.; Provencio, P. 1998. Age and origin of Carlsbad Cavern and related caves from $^{40}Ar/^{39}Ar$ of alunite. *Science* 279: 1919-1922.

Prosser, I.P.; Chappell, J.; Gillespie, R. 1994. Holocene valley aggradation and gully erosion in headwater catchments, South-eastern Highlands of Australia. *Earth Surface Processes and Landforms* 19: 465-480.

Quinif, Y. 1989. La datation uranium-thorium. *Speleochronos* 1: 3-22.

Quinif, Y.; Bastin, B. 1994. Datation uranium/thorium et analyse pollinique d'une séquence stalagmitique du stade isotopique 5 (Galerie des Verviétois, Grotte de Han-sur-Lesse, Belgique). *C.R. Acad. Sci. Paris* 318: 211-217.

Rae, A.M.; Ivanovich, M. 1986. Successful application of uranium series dating of fossil bone. *Applied Geochemistry* 1: 419-426.

Ramos, R.P.L. 1975. Precipitation characteristics in the Northeast Brazil dry region. *Journal of Geophysical Research* 80: 1665-1678.

Renault, P. 1958. Éléments de spéléomorphologie karstique. *Annales de Spéléologie* 13: 23-47.

Renault, P. 1968. Contribution a l'etude des actions mécaniques et sédimentologiques dans la spéleogenèse. *Annales de Spéléologie* 23: 529-596.

Ribeiro, A.F.; Garrido, I.A.; Brito, R.S.C.; Nonato, I.F. 1993. *Geologia e Potencialidades para Mineralizações de Ouro e Sulfetos da Faixa Rio Salitre, Juazeiro-Bahia.* CBPM, Salvador. Série Arquivos Abertos 3: 1-9.

Richards, D.A. 1995. *Pleistocene Sea Levels and Palaeoclimate of the Bahamas Based on Th-230 Ages of Speleothems.* PhD Thesis, University of Bristol.

Rightmire, C.T.; Pearson, F.J.; Back, W.; Rye, R.O.; Hanshaw, B.B. 1974. Distribution of sulphur isotopes in groundwaters from the principal artesian aquifer of Florida and the Edwards Aquifer of Texas, United States of America. In *Isotope Techniques in Groundwater Hydrology.* IAEA, vol. 2: 191-207.

Rind, D. 1990. Puzzles from the tropics. *Nature* 346: 317-318.

Rind, D.; Peteet, D. 1985. Terrestrial conditions at the last glacial maximum and CLIMAP sea-surface temperature estimates: Are they consistent? *Quaternary Research* 24: 1-22.

Roberts, M.S. 1997. *Trace Elements in Speleothem Calcite: the Potential for Terrestrial Palaeoclimate Studies.* PhD Thesis, University of Bristol.

Roberts, M.S.; Smart, P.L.; Baker, A. 1998. Annual trace element variation in a Holocene speleothem. *Earth Planetary Science Letters* 154: 237-246.

Robinson, M.P.; Graf, W.H. 1972. Pipelining of low-concentration sand-water mixtures. *Journal of the Hydraulics Division* 98: 1221-1241.

Roucou, P.; Aragão, J.O.R.; Harzallah, A.; Fontaine, B.; Janicot, S. 1996. Vertical motion changes related to north-east Brazil rainfall variability: a GCM simulation. *International Journal of Climatology* 16: 879-891.

Rowe, P.J.; Austin, T.; Akinson, T.C. 1989. The Quaternary evolution of the South Pennines. *Cave Science* 16: 117-121.

Rumsby, B.T.; Macklin, M.G. 1994. Channel and floodplain response to recent abrupt climate change: the Tyne Basin, Northern England. *Earth Surface Processes and Landforms* 19: 499-515.

Rye, R.O.; Back, W.; Hanshaw, B.B.; Rightmire, C.T.; Pearson, F.J. 1981. The origin and isotopic composition of dissolved sulfide in groundwater from carbonate aquifers in Florida and Texas. *Geochimica et Cosmochimica Acta* 45: 1941-1950.

Sacks, L.A.; Herman, J.S.; Kauffman, S.J. 1995. Controls on high sulfate concentrations in the Upper Floridan aquifer in southwest Florida. *Water Resources Research* 31: 2541-2551.

Sancho, C.; Peña, J.L.; Melendez, A. 1997. Controls on Holocene and present-day travertine formation in the Guadalaviar River (Iberian Chain, NE Spain). *Zeitschrift fur Geomorphologie* 41: 289-307.

Salgado-Labouriau, M.L. 1997. Late Quaternary palaeoclimate in the savannas of South America. *Journal of Quaternary Science* 12: 371-379.

Salgado-Labouriau, M.L.; Barberi, M.; Ferraz-Vicentini, K.R.; Parizzi, M.G. 1998. A dry climatic event during the late Quaternary of tropical Brazil. *Review of Palaeobotany and Palynology* 99: 115-129.

Sarbu, S.M.; Lascu, C. 1997. Condensation corrosion in Movile Cave, Romania. *Journal of Cave and Karst Studies* 59: 99-102.

Sarnthein, M. 1978. Sand deserts during glacial maximum and climatic optimum. *Nature* 272: 43-46.

Sasowksy, I.D.; Granger, D.E.; Coons, D.; Kambesis, P. 1998. Revised age for Xanadu Cave, Tennessee, and implications for river incision in the Cumberland Plateau Escarpment. *Journal of Cave and Karst Studies* 60: 189.

Sasowsky, I.D.; White, W.B.; Schmidt, V.A. 1995. Determination of stream-incision rate in the Appalachian plateaus by using cave-sediment magnetostratigraphy. *Geology* 23: 415-418.

Schmidt, V.A. 1982. Magnetostratigraphy of sediments in Mammoth Cave, Kentucky. *Science* 217: 827-829.

Schmidt, V.A.; Jennings, J.N.; Haosheng, B. 1984. Dating of cave sediments at Wee Jasper, New South Wales, by magnetostratigraphy. *Australian Journal of Earth Sciences* 31: 361-370.

Schobbenhaus, C. (ed.). 1984. *Geologia do Brasil.* Departamento Nacional da Produção Mineral, Brasília.

Schobbenhaus, C.; Campos, D.A. 1984. A evolução da Plataforma Sul Americana no Brasil e suas principais concentrações minerais. In *Geologia do Brasil* (Schobbenhaus et al. Eds.), DNPM, Brasilia, pp. 9-53.

Schumm, S.A. 1965. Quaternary paleohydrology. In *The Quaternary of the United States* (Wrighy, H.E.; Frey, D.G., ed.), Princeton University Press, Princeton, pp. 783-794.

Schwarcz, H.P. 1980. Absolute age determination of archaeological sites by uranium series dating of travertines. *Archaeometry* 22: 3-24.

Schwarcz, H.P.; Blackwell, B.A. 1992. Archaeological applications. In *Uranium Series Disequilibrium* (Ivanovich, M.; Harmon, R.S. eds.). Clarendon Press, Oxford, p. 513-552.

Schwarcz, H.P.; Blackwell, B.; Goldberg, P.; Marks, A.E. 1979. Uranium series dating of travertine from archaeological sites, Nahal Zin, Israel. *Nature* 277: 558-560.

Schwarcz, H.P.; Harmon, R.S.; Thompson, P.; Ford, D.C. 1976. Stable isotope studies of fluid inclusions in speleothems and their paleoclimatic significance. *Geochimica et Cosmochimica Acta* 40: 657-665.

Selby, M.J. 1993. *Hillslope Materials and Processes.* Oxford University Press, Oxford.

Selfridge, R.J. 1986. What's so interesting about mud? (Bone-Normal systems). *The Netherworld News* 36: 25-29.

Servant, M.; Maley, J.; Turcq, B.; Absy, M.L.; Brenac, P.; Fournier, M.; Ledru, M.P. 1993. Tropical forest changes during the Late Quaternary in African and South American lowlands. *Global and Planetary Change* 7: 25-40.

Shackleton, N.J. 1993. Last interglacial in Devils Hole. *Nature* 362: 596.

Shackleton, N.J.; Opdyke, N.D. 1973. Oxygen isotope and palaeomagnetic stratigraphy of equatorial Pacific core V28-238: oxygen isotope temperatures and ice volumes on a 10^5 and 10^6 year scale. *Quaternary Research* 3: 39-55.

Shackleton, N.J.; Berger, A.; Peltier, W.R. 1990. An alternative astronomical calibration of lower Plestocene timescale based on ODP Site 677. *Royal Society of Edinburgh Transactions, Earth Sciences* 81: 51-261.

Shoemaker, E. M. et al. 1990. Ages of Australian meteorite craters - a preliminary report. *Meteoritics* 25: 409.

Shopov, Y.Y.; Ford, D.C.; Schwarcz, H.P. 1994. Luminescent microbanding in speleothems: high-resolution chronology and paleoclimate. *Geology* 22: 407-410.

Siemers, J.; Dreybrodt, W. 1998. Early development of karst aquifers on percolation networks of fractures in limestone. *Water Resources Research* 34: 409-419.

Simms, M.J. 1994. Emplacement and preservation of vertebrates in caves and fissures. *Zoological Journal of the Linnean Society* 112: 261-283.

Siqueira, A.F. 1978. *O Uso dos Dados Isotópicos e Químicos como Indicadores de Origem das Águas e Sais Dissolvidos no Aquífero Calcário Bambuí, Irecê, Bahia.* MSc Thesis, Universidade Federal da Bahia.

Skipworth, P.J.; Tait, S.J.; Saul, A.J. 1996. Laboratory investigations into cohesive sediment transport in pipes. *Water Science and Technology* 33: 187-193.

Smart, P.L. 1986. Origin and development of glacio-karst closed depressions in the Picos de Europa, Spain. *Zeitschrift fur Geomorphologie* 30: 423-443.

Smart, P.L.; Andrews, J.N.; Batchelor, B. 1984. Implications of uranium-series dates from speleothems for the age of landforms in north-west Perlis, Malaysia: a preliminary study. *Malaysian Journal of Tropical Geography* 9: 59-68.

Smart, P.L.; Smith, B.W.; Chandra, H.; Andrews, J.N.; Symons, M.C.R. 1988. An intercomparison of ESR and uranium series ages for Quaternary speleothem calcites. *Quaternary Science Reviews* 7: 411-416.

Smith, D.I.; Atkinson, T.C. 1976. Process, landforms and climate in limestone regions. In *Geomorphology and Climate* (Derbyshire, E. ed.). Wiley, New York, pp. 367-409.

Springer, G.S.; Kite, J.S.; Schmidt, V.A. 1997. Cave sedimentation, genesis, and erosional history in the Cheat River Canyon, West Virginia. *Geological Society of America Bulletin* 109: 524-532.

Strang, D.M.D. 1972. *Climatological Analysis of Rainfall Normals in Northeastern Brazil.* Report IAE-M-02/72, Centro Técnico Aeroespacial, São José dos Campos.

Strauss, H. 1993. The sulfur isotopic record of Precambrian sulfates: new data and a critical evaluation of the existing record. *Precambrian Research* 63: 225-246.

Stuiver, M.; Becker, B. 1993. High-precision decadal calibration of the radiocarbon time scale, AD1950-6000BC. *Radiocarbon* 35: 35-65.

Stute, M.; Forster, M.; Frischkorn, H.; Serejo, A.; Clark, J.F.; Schlosser, P.; Broecker, W.S.; Bonani, G. 1995. Cooling of tropical Brazil (5º C) during the last glacial maximum. *Science* 269: 379-383.

Suguio, K.; Barcelos, J.H.; Matsui, E. 1980. Significados paleoclimáticos e paleoambientais das rochas calcárias da Formação Caatinga (BA) e do Grupo Bauru (MG/SP). *Proceedings* XXXI Brazilian Geological Congress, 1: 607-617.

Summerfield, M.A. 1991a. *Global Geomorphology.* Longman, Harlow.

Summerfield, M.A. 1991b. Sub-aerial denudation of passive margins: regional elevation versus local relief models. *Earth and Planetary Science Letters* 102: 460-469.

Summerfield, M.A.; Hulton, N.J. 1994. Natural controls of fluvial denudation rates in major world drainage basins. *Journal of Geophysical Research* 99: 13871-13883.

Sutcliffe, A.J.; Lord, T.C.; Harmon, R.S.; Ivanovich, M.; Hess, J.W. 1985. Wolverine in Northern England at about 83,000 yr BP: faunal evidence for climatic change during Isotope Stage 5. *Quaternary Research* 24: 73-86.

Swayne, D.J.; Schneider, J.L. 1971. The Geochemistry of Underground Water. In *Salinity and Water Use* (Talsma, T.; Philip, J.R. eds.). Macmillan, London, pp. 3-23.

Sweeting, M.M. 1972. *Karst Landforms.* Macmillan, London.

Sylvestre, F.; Servant, M.; Servant-Vildary, S.; Causse, C.; Fournier, M.; Ybert, J.P. 1999. Lake-level chronology on the southern Bolivian Altiplano (18 - 23º S) during late-Glacial time and the early Holocene. *Quaternary Research* 51: 54-66.

Szabo, B.J. 1990. Ages of travertine deposits in eastern Grand Canyon National Park, Arizona. *Quaternary Research* 34: 24-32.

Szabo, B.J.; Bush, C.A.; Benson, L.V. 1996. Uranium-series dating of carbonate (tufa) deposits associated with Quaternary fluctuations of Pyramid Lake, Nevada. *Quaternary Research* 45: 271-281.

Szabo, B.J.; Kolesar, P.T.; Riggs, A.C.; Winograd, I.J.; Ludwig, K.R. 1994. Paleoclimatic inferences from a 120,000-Yr calcite record of water-table fluctuation in Browns Room of Devils Hole, Nevada. *Quaternary Research* 41: 59-69.

Talbot, M.R. 1990. A review of the palaeohydrological interpretation of carbon and oxygen isotopic ratios in primary lacustrine carbonates. *Chemical Geology* 80: 261-279.

Talma, A.S.; Netterberg, F. 1983. Stable isotope abundances in calcretes. In *Residual Deposits: Surface Related Weathering Processes and Materials* (Wilson, R.C.L., ed.). Blackwell, p. 221-233.

Tarling, D.H. 1983. *Palaeomagnetism: Principles and Applications in Geology, Geophysics and Archaeology*. Chapman and Hall, London.

Tarhule-Lips, R.F.A.; Ford, D.C. 1998. Condensation corrosion in caves on Cayman Brac and Isla de Mona. *Journal of Cave and Karst Studies* 60: 84-95.

Tauxe, L.; Herbert, T.; Shackleton, N.J.; Kok, Y.S. 1996. Astronomical calibration of the Matuyama-Brunhes boundary: Consequences for magnetic remanence acquisition in marine carbonates and the Asian loess sequences. *Earth and Planetary Science Letters* 140: 133-146.

Tavares, G.A. 1983. *Estudos Isotópicos e Hidroquímicos em Águas na Bacia do Rio Verde*. MSc Dissertation, Universidade Federal da Bahia.

Taylor, K.C.; Lamorey, G.W.; Doyle, G.A.; Alley, R.B.; Grootes, P.M.; Mayewski, P.A.; White, J.W.C.; Barlow, L.K. 1993. The "flickering switch" of late Pleistocene climate changes. *Nature* 361: 432-436.

Thompson, L.G.; Mosley-Thompson, E.; Davis, M.E.; Lin, P.N.; Henderson, K.A.; Cole-Dai, J.; Bolzan, J.F.; Liu, K.B. 1995. Late glacial stage and Holocene tropical ice core records from Huascarán, Peru. *Science* 269: 46-50.

Thunnel, R.; Anderson, D.; Gellar, D.; Miao, Q. 1994. Sea-surface temperature estimates for the tropical western Pacific during the last glaciation and their implication for the Pacific warm pool. *Quaternary Research* 41: 255-264.

Tintelnot, M. 1997. Holocene and Late Pleistocene climate changes and sea-level fluctuations in tropical northeastern Brazil - Evidence from marine clay mineral records. In *Beitrage zur Jahrestagung 1996* (Wolf, D.; Starke, R.; Kleberg, R. Ed.), DTTG : 72-88.

Todd, D.K. 1980. *Groundwater Hydrology*. John Wiley and Sons, New York.

Toomey, R.S.; Blum, M.D.; Valastro, S. 1993. Late Quaternary climates and environments of the Edwards Plateau, Texas. *Global and Planetary Change* 7: 299-320.

Toran, L.; Harris, R.F. 1989. Interpretation of sulfur and oxygen isotopes in biological and abiological sulfide oxidation. *Geochimica et Cosmochimica Acta* 53: 2341-2348.

Trewartha, G.T. 1961. *The Earth's Problem Climates*. The University of Wisconsin Press.

Tricart, J. 1985. Evidence of Upper Pleistocene dry climates in northern South America. In *Environmental Change and Tropical Geomorphology* (Douglas, I.; Spencer, T. Ed.). George Allen and Unwin, pp. 197-217.

Trombe, F. 1952. *Traité de Spéléologie*. Payot, Paris.

Tucker, G.E.; Slingerland, R. 1997. Drainage basin responses to climatic change. *Water Resources Research* 33: 2031-2047.

Tuller, M.P.; Ribeiro, J.H.; Danderfer, A. 1992. *Mapeamento Geológico da Área do Projeto VIDA*. CPRM, Belo Horizonte. Unpublished Report.

Turcq, B.; Pressinotti, M.M.N.; Martin, L. 1997. Paleohydrology and paleoclimate of the past 30,000 years at the Tamanduá River, Central Brazil. *Quaternary Research* 47: 284-294.

Valadão, R.C. 1998. *Evolução de Longo-Termo do Relevo do Brasil Oriental*. Doctoral Thesis, Universidade Federal da Bahia.

Valero Garcés, B.L.; Aguilar, J.G. 1992. Shallow carbonate lacustrine facies models in the Permian of the Aragon-Bearn Basin (Western Spanish-French Pyrenees). *Carbonates and Evaporites* 7: 94-107.

van Breemen, N. 1988. Redox processes of iron and sulfur involved in the formation of acid sulfate soils. In *Iron in Soils and Clay Minerals* (Stucki, J.W. ed.). D. Reidel. pp. 825-841.

van Everdingen, R.O.; Shakur, M.A.; Krouse, H.R. 1985. Role of corrosion by H_2SO_4 fallout in cave development in a travertine deposit - Evidence from sulfur and oxygen isotopes. *Chemical Geology* 49: 205-211.

van der Hammen, T.; Absy, M.L. 1994. Amazonia during the last glacial. *Palaeogeography, Palaeoclimatology, Palaeoecology* 109: 247-261.

van der Hammen, T.; Duivenvoorden, J.F.; Lips, J.M.; Urrego, L.E.; Espejo, N. 1992. Late Quaternary of the middle Caquetá River area (Colombian Amazonia). *Journal of Quaternary Science* 7: 45-55.

Vialou, A.V.; Aubry, T.; Benabdelhadi, M.; Cartelle, C.; Figuti, L.; Fontugne, M.; Solari, M.E.; Vialou, D. 1995. Découverte de Mylodontinae dans un habitat préhistorique daté du Mato Grosso (Brésil): l'abri rupestre de Santa Elina. *C.R. Acad. Sci. Paris* 320: 655-661.

Waltham, A.C. 1986. Valley excavation in the Yorkshire Dales karst. In *New Directions in Karst* (Paterson, K.; Sweeting, M.M. ed.). Geobooks, p. 541-550.

Webb, J.A.; Fabel, D.; Finlayson, B.L.; Ellaway, M.; Shu, L.; Spiertz, H.P. 1992. Denudation chronology from cave and river terrace levels: the case of the Buchan karst, southeastern Australia. *Geological Magazine* 129: 307-317.

Weninger, J.M.; McAndrews, J.H. 1989. Late Holocene aggradation in the lower Humber River valley, Toronto, Ontario. *Canadian Journal of Earth Sciences* 26: 1842-1849.

White, E.L.; White, W.B. 1968. Dynamics of sediment transport in limestone caves. *National Speleological Society Bulletin* 30: 115-129.

White, W.B. 1977. The role of solution kinetics in the development of karst aquifers. In *Karst Hydrogeology* (Tolson, J.S.; Doyle, F.L. eds.). International Association of Hydrogeologists Memoir 12: 503-517.

White, W.B. 1984. Rate processes: chemical kinetics and karst landform development. In *Groundwater as a Geomorphic Agent* (LaFleur, R.G. ed.). Allen and Unwin, Boston, pp. 227-248.

White, W.B. 1988. *Geomorphology and Hydrology of Karst Terrains*. Oxford University Press, Oxford.

Williams, M.A.J. 1975. Late Pleistocene tropical aridity synchronous in both hemispheres? *Nature* 253: 617-618.

Williams, M.A.J.; Dunkerley, D.L.; De Decker, P.; Kershaw, A.P.; Stokes, T. 1993. *Quaternary Environments*. Edward Arnold, London.

Winograd, I.J.; Szabo, B.J. 1988. Water-table decline in the south-central Great Basin during the Quaternary: implications for toxic waste disposal. In *Geologic and Hydrologic Investigations of a Potential Nuclear Waste Disposal Site at Yucca Mountain, Southern Nevada*. (Carr, M.D., Younts, J.C. ed.). U.S. Geological Survey Bulletin 1790: 147-152.

Winograd, I.J.; Coplen, T.B.; Landwehr, J.M.; Riggs, A.C.; Ludwig, K.R.; Szabo, B.J.; Kolesar, P.T.; Revesz, K.M. 1992. Continuous 500,000-year climate record from vein calcite in Devils Hole, Nevada. *Science* 258: 255-260.

Winograd, I.J.; Landwehr, J.M.; Ludwig, K.R.; Coplen, T.C.; Riggs, A.C. 1997. Duration and structure of the past four interglaciations. *Quaternary Research* 48: 141-154.

Wolff, T.; Mulitza, S.; Arz, H.; Patzold, J.; Wefer, G. 1998. Oxygen isotopes versus CLIMAP (18 ka) temperatures: A comparison from the tropical Atlantic. *Geology* 26: 675-678.

Worthington, S.R.H. 1991. *Karst Hydrogeology of the Canadian Rocky Mountains.* PhD thesis, McMaster University.

Worthington, S.R.H.; Ford, D.C. 1995. High sulfate concentrations in limestone springs: An important factor in conduit initiation? *Environmental Geology* 25: 9-15.

Wright, V.P.; Platt, N.H. 1995. Seasonal wetland carbonate sequences and dynamic catenas: a re-appraisal of palustrine limestones. *Sedimentary Geology* 99: 65-71.

Wright, V.P.; Tucker, M.E. 1991. *Calcretes.* International Association of Sedimentologists.

Yonge, C.J.; Krouse, H.R. 1987. The origin of sulphates in Castleguard Cave, Columbia Icefields, Canada. *Chemical Geology* 65: 427-433.

Yonge, C.J.; Ford, D.C.; Gray, J.; Schwarcz, H.P. 1985. Stable isotope studies of cave seepage water. *Chemical Geology* 58: 97-105.

Young, R.W. 1992. Structural heritage and planation in the evolution of landforms in the East Kimberley. *Australian Journal of Earth Sciences* 39: 141-151.

APPENDIX 1

Ground water analyses of the Una carbonate aquifer and Chapada Diamantina quartzites. Values in mg/l. Si – Siqueira (1978), cerb – CERB (1983), UNA – this study, Sali – (Martins, 1986), Iraq – CERB (unpublished data). Original code refers to the sample number in the original publication or field log.

Carbonate ground waters

Sample	Original code	SO_4^{2-}	Cl^-	HCO_3^-	Ca^{+2}	Mg^{+2}	Na^+	K^+	NO_3^-
Si-1	IR-15	118.0	178.0	405.2	174.6	79.4	52.0	28.0	-
Si-2	IR-24	234.6	93.2	286.2	29.0	104.9	83.0	5.6	-
Si-3	IR-29	75.0	641.6	402.1	235.3	91.4	42.0	11.4	-
Si-4	IR-32	194.8	1882.4	481.4	1113.0	307.7	380.0	3.7	-
Si-5	IR-33	24.0	37.9	335.0	51.5	22.2	21.0	2.4	-
Si-6	IR-71	33.0	36.9	505.9	52.1	47.2	22.0	2.8	-
Si-7	IR-74	38.1	354.5	452.8	158.4	55.2	46.0	3.4	-
Si-8	IR-78	25.5	47.8	399.7	140.8	37.3	12.8	4.9	-
Si-9	IR-80	208.4	249.6	431.4	186.0	110.9	87.0	13.0	-
Si-10	IR-209	32.6	113.4	555.3	118.8	74.9	43.0	5.6	-
Si-11	IR-233	82.6	327.2	544.3	116.2	121.4	102.0	1.0	-
Si-12	IR-241	300.7	63.4	474.7	197.6	58.4	30.0	21.5	-
Si-13	IE	41.4	112.0	350.9	71.8	36.1	42.0	1.8	-
Si-14	JR-06	146.7	336.8	547.3	253.1	129.4	92.0	6.7	-
Si-15	CA-03	22.4	134.7	78.1	117.4	19.0	52.0	36.0	-
Si-16	CA-07	2.8	21.3	183.7	44.1	26.1	8.7	4.7	-
Si-17	BM-Q	1.8	76.6	37.8	24.3	4.9	36.0	1.0	-
Si-18	BM-S	19.1	85.4	331.1	82.6	33.2	59.0	6.7	-
Si-19	CE-05	46.8	274.7	323.4	184.0	56.7	74.0	6.1	-
Si-20	CN-02	96.9	210.9	339.3	133.8	54.3	87.0	8.2	-
Si-21	CN-24	6.4	129.7	286.2	128.0	28.2	27.0	11.5	-
Si-22	PD-01	32.4	196.4	216.0	117.2	51.0	43.0	3.8	-
Si-23	SR	1.9	26.6	173.9	33.3	26.6	10.4	12.2	-
cerb-1	002	189	690	265	267	95	136	2.8	39.3
cerb-2	003	312	595	336	370	132	180	13.6	60
cerb-3	008	260	545	293	325	97	113	2.1	58
cerb-4	011	87	850	217	415	66	55	5.4	28.6
cerb-5	013	712	290	550	244	132	292	32	0.7
cerb-6	014	59	185	308	220	15	16	1.4	22
cerb-7	017	53	295	228	232	27	63	1.4	45
cerb-8	023	340	350	332	259	118	90	7.6	0.58
cerb-9	029	441	1430	308	605	152	551	2.7	72.9
cerb-10	047	170	355	246.9	202	58	98	3.7	10.6
cerb-11	051	454	585	276	190	167	319	8.2	5.8
cerb-12	057	185	317	280	179	72	94	8.1	18
cerb-13	062	43	112	135.6	150	10	36	1.7	22
cerb-14	067	51	325	180	141	52	83	2.8	31.4
cerb-15	077	329	2075	201	698	246	458	3.5	80
cerb-16	078	63	242	175	250	33	40	1.1	45
cerb-17	079	320	2275	110	767	234	467	8.7	78
cerb-18	080	87	755	118	432	37	124	2.5	59
cerb-19	081	110	372	163	39	38	213	2.2	0.9
cerb-20	082	112	695	112.5	349	47	135	2.4	69
cerb-21	084	61	450	205	279	68	72	3.9	0.55
cerb-22	116	154	1700	240	815	121	141	5.7	132
cerb-23	122	269	570	163	139	145	143	8.5	163

cerb-24	124	306	415	344	179	144	161	10	44.5
cerb-25	133	57	342	161.7	198	39	35	4	19
cerb-26	202	110	765	263	324	75	164	1.2	64.5
cerb-27	203	105	195	312	212	46	41	2.3	24.6
cerb-28	213	215	505	237.4	302	72	193	2.7	61
cerb-29	245	57	695	268	422	67	70	2.7	31
cerb-30	317	70	175	408	208	50	52	1.9	11
cerb-31	350	89	695	368	408	78	81	3.9	39.6
cerb-32	374	20	62	376	88	48	17	4.2	2.7
cerb-33	382	99	297	203.4	189	57	53	6.1	24
cerb-34	393	35	87	402	123	62	30	29	22
cerb-35	411	225	870	264	560	42	157	1.6	76.6
cerb-36	415	157	335	416	302	73	79	8	31.5
cerb-37	421	547	705	328	428	136	211	3.4	48.7
cerb-38	428	51	39	454	153	31	16	5.3	0.5
cerb-39	429	272	1030	221.4	418	141	226	3.4	38
cerb-40	431	48	20	248	82	10	28	4.2	10
cerb-41	438	93	285	312	179	49	45	3	13.5
cerb-42	440	53	415	304	302	66	69	5.2	21.5
cerb-43	443	454	160	376	225	89.4	50	10	2
cerb-44	453	432	840	300	421	108	219	5.9	0.05
cerb-45	456	102	227	258.9	193	38	69	2	14
cerb-46	458	289	285	484	212	90	108	7.8	0.51
cerb-47	460	61	137	302.5	172	45	46	8.5	33.5
cerb-48	462	6	41	249	53	30	16	6.9	1.5
cerb-50	467	233	345	356	224	74	198	4.2	24.4
cerb-51	547	76	262	348	273	46	44	3.7	30.6
cerb-52	578	87	232	382	189	58	47	3.6	26
cerb-53	579	74	132	248	177	57	40	4.6	55
cerb-54	597	42	138	289	128	50	48	1.9	14.5
cerb-55	603	100	380	296	234	48	84	4	12
cerb-56	607	115	535	277	197	83	205	2.6	40
cerb-57	609	177	217	430	177	57	127	4.7	21.6
cerb-58	613	251	97	349	146	60	49	4.4	0.25
cerb-59	614	118	194	292	165	26	77	7.4	28
cerb-60	625	170	495	428	232	117	131	5.2	13.5
cerb-61	626	131	207	299	149	53	56	2.7	5.6
cerb-62	635	12	46	329	116	21	8	3.9	0.5
cerb-63	647	76	60	447	141	47	13	2.2	1
cerb-64	648	178	266	396	209	72	86	3.7	0.3
cerb-65	700	112	242	404	206	64	114	1.6	41.6
cerb-66	702	133	278	192	191	64	29	3.4	10
cerb-67	704	190	345	268	316	68	61	3	45
cerb-68	709	116	214	351	189	60	65	2.9	9.9
cerb-69	714	652	740	276	367	168	160	3.4	5
cerb-70	720	101	150	375	165	47	23	1.8	3.7
cerb-71	723	211	101	272	134	54	67	5.4	3.5
cerb-72	728	53	75	332	146	42	13	2.3	2.4
cerb-73	729	156	166	320	183	50	94	4.3	36
cerb-74	733	92	178	352	42	15	185	2.7	0.2
cerb-75	735	118	118	300	114	57	44	5.8	0.02
cerb-76	736	180	760	180	264	52	215	4	7.3
cerb-77	739	87	138	275	154	16	45	5.3	3.5
cerb-78	740	70	115	348	158	20	46	1.9	37.8
cerb-79	748	170	370	304	235	70	55	2.8	19.3
cerb-80	750	564	770	116	400	148	228	7.2	0.02
cerb-81	751	190	122	310	115	67	35	3.4	1.7

cerb-82	754	376	425	336	372	76	101	7	2
cerb-83	756	120	110	434	136	76	16	9	2.9
cerb-84	759	227	710	310	381	119	88	3.6	31
cerb-85	760	34	55	328	109	32	6.4	1.8	13
cerb-86	762	259	735	308	368	67	146	6.6	55
cerb-87	763	788	340	364	288	155	112	7.8	1.12
cerb-88	764	882	48	256	326	92	21	3.6	0.3
cerb-89	766	47	94	220	122	51	17	1.2	4.3
cerb-90	767	294	337	404	302	108	99	7.5	0.02
cerb-91	800	88	275	244	263	62	61	2.7	76
cerb-92	802	260	225	336	131	89	143	3.9	2.7
cerb-93	803	16	51	241	110	36	43	2.2	16
cerb-94	805	147	198	364	175	68	103	4.5	59.4
cerb-95	807	127	485	164	267	60	135	2.8	49
cerb-96	808	50	76	330	324	74	96	3.9	50
cerb-97	810	17	72	384	158	27	32	3.6	28.5
cerb-98	812	47	154	430	165	55	52	1.4	22
cerb-99	817	54	57	420	156	43	34	5.9	40.6
cerb-100	819	47	178	284	141	50	48	2.8	31.6
cerb-101	822	421	565	256	319	136	172	6.5	21.5
cerb-102	828	60	29	332	109	44	11	2.6	0.5
cerb-103	830	83	57	280	97	37	13	2.9	3.2
UNA-01	-	12.1	33.8	-	34.7	14.5	9.0	1.3	0.7
UNA-02	-	4.1	17	-	24.8	25.7	9.5	3.4	0
UNA-03	-	8.5	31.4	-	32	28.3	15.1	3.1	0
UNA-04	-	4.7	18.5	-	36.4	28.1	9.7	3.1	0
UNA-05	-	76.9	115.8	-	40.8	56.7	39.8	5.4	2.3
UNA-06	-	4.7	14.6	-	28.4	22.5	7.8	3.1	0
UNA-07	-	416.3	103.9	-	106.5	100.2	27.9	4.0	14.9
UNA-08	-	13.6	33	-	38.2	31.8	12.4	4.9	0.8
UNA-09	-	9.4	28.7	-	25.8	8.7	10.3	2.3	4.3
UNA-10	-	130.1	201.8	-	53.2	99.9	40.9	9	7.2
UNA-11	-	164.9	185.1	-	78.0	91.0	36.8	3.9	48.3
UNA-12	-	198.3	278.9	-	119.9	106.8	66.5	3.6	37.5
UNA-13	-	125.9	316.9	-	177.0	97.7	80.4	3.4	151.5
UNA-14	-	365.1	424.8	-	97.7	161.2	155.6	6.8	8.2
UNA-15	-	66.1	45.4	-	43.0	22.4	26.8	1.4	13.1
UNA-16	-	20.8	52.9	-	40.3	24.1	24.0	3.0	2.4
UNA-17	-	187.8	392.9	-	92.7	121.4	127.5	4.7	14.4
UNA-18	-	95.4	226.1	-	185.3	47.8	55.3	1.9	145
UNA-19	-	66.3	208.8	-	144.0	59.1	70.2	4.7	178.8
UNA-20	-	62.9	276.1	-	211.7	74.7	48.3	2.3	199.9
UNA-21	-	153.3	411.6	-	116.3	80	216.8	21.6	243.1
UNA-22	-		27.5	-	37.2	30.7	13.4	3.5	0
UNA-23	-	347.1	838.1	-	924	592.5	372.9	110.4	3678.5
UNA-24	-	1982.1	19000	-	9949.8	7128.2	8681.9	652.4	12000
sali-1	09	137	264	380	192	63	141.5	21.2	24.9
sali-2	10	383	1380	340	400	146	451	16.2	10.7
sali-3	11	19	50	404	97	42	20.9	4.2	3.5
sali-4	15	49	110	421	184	41.3	37.3	5.1	20
sali-5	16	113	360	340	122	58	276.5	8.8	21.2
sali-6	19	128	256	420	162	71	157.4	19.2	26.7
sali-7	20	163	240	323	89.7	62	190.6	3.2	0.45
sali-8	22	235	980	316	239	129	316	30	16.4
sali-9	23	30	26	184	44	22	46	7.5	0.3
sali-10	24	12	96	235	72	32	29	4.2	0.04
sali-11	25	33	90	311	47	38	97.1	14.2	5

sali-12	28	1170	308	199	288	132	217	23	0.04
sali-13	29	326	784	404	199	126	403.4	7.5	52
sali-14	34	58	1216	198	256.3	174.9	273	25	4
sali-15	36	67	300	330	68	31.6	209	47.5	0.26
sali-16	37	40	720	219	136	120	183.5	22	2.5
sali-17	38	7	26	166	33.6	17.5	11.7	7.8	0.07
sali-18	39	156	2250	355	400	364	575	153	0.5
sali-19	14	113	284	420	120	104	149.5	15.4	54.8
sali-20	30	177	672	300	261	69	244.7	15.4	30.6
Iraq-1	2-1147/92	188	28.7	104.38	93.84	39.07	-	-	0.013
Iraq-2	1-5486/93	5.2	19.86	151.63	61.67	15.82	-	-	0.016
Iraq-3	1-2393/84	18.4	68.37	188.52	204.94	28.9	-	-	2.72
Iraq-4	251/83	35	261.4	51.96	421.73	35.03	-	-	4.32
Iraq-5	1-1555/83	8	21.84	121.94	94.53	82.32	-	-	0.01
Iraq-6	1-1524/83	114	324.93	301.95	450.63	338.47	-	-	26.43
Iraq-7	1-1521/83	88	24.08	195.93	174.84	119.57	-	-	0.001
Iraq-8	1-1365/82	270	550.78	416.02	581.62	513.94	-	-	0.001
Iraq-9	1-1202/81	55	810	79	630	92.38	-	-	18.1
Iraq-10	1-827/79	493	4	193	174.3	49.9	-	-	0.21
Iraq-11	1-815/79	70	208	69	109.3	16.9	-	-	6.8
Iraq-12	1-3151/85	138	237.16	286.56	606.08	36.97	-	-	0.0001
Iraq-13	2-782/85	2.6	12.67	70	79.07	4.94	-	-	0.0001
Iraq-14	2-858/85	8.8	17.55	207.99	203.6	27.2	-	-	0.0001
Iraq-15	2-886/86	9	38.39	179.38	132.49	25.14	-	-	1.07
Iraq-16	1-5103/92	6.6	25.97	181.29	186.73	10.47	-	-	7.45
Iraq-17	1-5520/93	58	21.84	230.94	250.94	33.73	-	-	0.039
Iraq-18	1-5608/94	20	136.4	130.65	285.6	17.42	-	-	0.0001
Iraq-19	1-5636/94	2.2	18.77	121.94	100.8	21.52	-	-	0.0001
Iraq-20	1-5669/94	130	513.97	115.4	462.91	87.85	-	-	18.75
Iraq-21	1-5785/94	65	62.65	229.38	320.91	17.07	-	-	1.4
Iraq-22	1-778/78	257.5	260	352	149.3	81.9	-	-	0.0001

Quartzite ground waters

Sample	Original code	SO_4^{2-}	Cl^-	HCO_3^-	Ca^{+2}	Mg^{+2}	Na^+	K^+	NO_3^-
sali-1	05	5	26	33	8.8	2.4	11.5	7.2	0.43
sali-3	08	18	184	164	80	24.3	50.2	10.6	1.5
sali-4	18	13	340	220	94	42	98.7	16.5	0.04
sali-7	35	148	1300	254	424.5	131.2	324	18.8	40.3
sali-2	06	5	20	26	6.4	0.48	12.6	1.2	0.04
sali-5	31	71	168	284	128	33	79.6	16.7	25.7
sali-6	33	5	18	8	4	1.2	7	1.5	0.04
Tareco	080	6	29	148	41	19	11	8.5	0.5
L.cerc	831	5	25	148	39	15	8	3.5	1
Iraq-1	1-5139/92	3.4	76.64	16.62	22.22	2.71	-	-	0.46
Iraq-2	1-4907/90	37.6	226.9	118.3	192.8	10.96	-	-	0.022
Iraq-3	1-4908/90	2	19.44	18.35	7.94	3.23	-	-	0.657
Iraq-4	1-4914/90	72	285.6	28.63	58.97	30.27	-	-	0.0001
Iraq-5	1-5097/91	3.2	14.35	38.38	13.26	7.72	-	-	0.0001
Iraq-6	1-5105/92	5.2	57.02	10.95	8.34	2.8	-	-	0.26
Iraq-7	1-5129/92	6.2	28.89	0	39.65	3.72	-	-	0.04
Iraq-8	1-5135/92	2.8	57.76	18.99	24.24	3.94	-	-	1.72
Iraq-9	1-5692/94	7.4	26.59	40.62	41.15	4.52	-	-	0.015
Iraq-10	1-5824/95	29	186.86	21.79	74.64	24.54	-	-	4.268
Iraq-11	1-5812/95	0.6	23.76	6.88	8.47	3.75	-	-	0.943
Iraq-12	1-6107/96	16.6	120.97	48.17	64.05	28.29	-	-	0.015
Iraq-13	1-5831/95	0.2	64.81	71.12	90	15.5	-	-	0.005